THE UNIVERSITY *of* EDINBURGH

Bioactive Scaffolds for Potential Bone Regenerative Medical Applications

Duncan M^{c}Neill Craig Sharp, M.Eng. M.A. (*CANTAB.*)

A thesis submitted for the degree of Doctor of Philosophy

The University of Edinburgh

2011

Thesis Abstract

Fracture non-unions and bone defects represent a recalcitrant problem in the field of orthopaedic surgery. Although the current gold-standard treatment, autologous bone grafting, has a relatively high success rate, the technique is not without serious problems. The emerging field of regenerative medicine may have the potential to provide an alternative treatment. One promising strategy involves the delivery of both cells and multiple growth factors with different release profiles.

A range of scaffolds was developed from Poly(ε-caprolactone) (PCL), Poly(lactide-co-glycolide) (PLGA), and two blends of PCL (M_n 42,500) and PLGA. The scaffolds were manufactured utilising a novel modified fused deposition modelling system, using polymer/dichloromethane solutions. The scaffolds were found to have pore sizes suitable for bone regenerative medical applications (373±9.5 μm in the Y-direction and 460±13 μm in the X-direction). However, the scaffolds were found to be only 52±3 μm in height. This means that the two-layer scaffolds were relatively flat. This was undesirable, as direct control of the complete 3D geometry was the favoured strategy, though it may not be a necessary requirement.

Five scaffold coatings were also developed from alginate, chitosan (crosslinked using sodium hydroxide or tripolyphosphate), Type-I collagen and Type-A gelatin. The scaffold coatings were screened *in vitro* for their cell-compatibility with human marrow stromal cells (hMSCs), human osteoblasts and MG63 cells. This was assessed using an assay for cell death, and assessing total cell counts. From these studies, Type-I collagen was found to be the optimum coating. For hMSCs, their death rates were found to be 19.1±6.3% for alginate, 5.3±3.6% and 2.9±1.4% for chitosan crosslinked with tripolyphosphate and sodium hydroxide respectively, compared to 0.11±0.07% for Type-I collagen, and 0.15±0.13% and 0.16±0.12% for 0.1% and 0.2% gelatin respectively. Type-I collagen was found to be the most cell-compatible coating, as it was consistently associated with higher cell counts than Type-A gelatin.

Similarly, PCL scaffolds vacuum dried for 1 hr were found to be cell-compatible. No detectable clinically significant difference was found in either total cell counts, or the proportion of cell death in; hMSCs exposed to PCL scaffolds processed with dichloromethane, hMSCs either exposed to scaffolds known to be biocompatible, or hMSCs cultured in the absence of scaffolds. When cell morphology was compared, scaffolds vacuum dried for 1 hr or more were found to have a similar morphology to the cells cultured in the absence of scaffolds. It was therefore concluded that a vacuum drying time of 1 hr was sufficient for cell-compatibility.

The scaffold materials were screened both for their encapsulation efficiencies and release characteristics using the model drug, methylene blue. The encapsulation efficiency was found to be both relatively high and consistent for both M_n 42,500 and 80,000 PCL as well as PCL:PLGA 66:33, at 71±6%, 71±5%, and 78±10% respectively, relative to the low efficiencies recorded for both PCL:PLGA 66:33 and PLGA: 57±5% and 38±10% respectively.

The release rate of methylene blue from PCL (M_n 42,500), was found to be relatively slow, controlled, and consistent between batches (between 21±2% and 20±3% released in the first 24 hr). Despite the release rate being consistent for PCL (M_n 80,000), the release rate was thought to be too high, since between 29±3% and 39±5% of the test compound was released in the first 24 hr period. The release rate of methylene blue from the PCL/PLGA blends (between 17±2% – 30±7% and 18±4% – 31±6% in the first 24 hr) and PLGA (between 7.1±3.4% – 9.3±2.9% in the first 24 hr) were found to be inconsistent, and low in the case of PLGA, even taking the different loading efficiencies into account. Therefore, PCL (M_n 42,500) was selected as the favoured candidate scaffold material.

The loading content and release profiles from methylene blue loaded collagen scaffold coatings were also evaluated. The drug loading capacity was found to be suitable for use as a drug delivery system (65±5 μg/g of methylene blue per unit scaffold mass). The release of methylene blue was observed to be rapid (between

54±10% – 70±17% in the first 24 hr), which was thought to be desirable for the coating delivery system.

Recombinant human bone morphogenetic protein-7 (rhBMP-7) was used as a representative growth factor of interest for bone regenerative medical applications. It was loaded in collagen scaffold coatings ($Coat_{BMP\ 1.25}$) and encapsulated within PCL (M_n 42,500) scaffolds ($Scaff_{BMP\ 1.25}$). Control coatings and scaffolds were designated $Coat_{PBS}$ and $Scaff_{PBS}$ respectively. Both delivery systems were found to release detectable quantities of rhBMP-7 (releasing 2.8±0.2 μg/g and 87±7 ng/g respectively in the first 24 hr), even after 14 days. The release rate of the growth factor from the scaffold coating was higher than that from the encapsulating scaffolds. However, the cumulative release profiles were found to deviate from the desired ideal release profiles, and burst release was observed from both delivery systems. Although differences were observed for the two delivery systems, this difference may not be of clinical significance.

Nevertheless, scaffolds with less than ideal delivery properties may still be of potential clinical use. The bioactivity of the rhBMP-7 released from the test scaffolds was therefore assessed by quantifying the area of normalised ALP staining of hMSCs. The release of rhBMP-7 from the collagen coating of the PCL (M_n 42,500) scaffolds ($Coat_{BMP\ 1.25}Scaff_{PBS}$) was capable of statistically significantly increasing hMSC normalised ALP expression, although the actual differences were often relatively small. Therefore, at least a proportion of the growth factor released is likely to have been bioactive. The release from scaffolds encapsulating rhBMP-7 ($Coat_{PBS}Scaff_{BMP\ 1.25}$) did not have this effect on the hMSCs, indicating that either the concentration released was too low, or the growth factor released was no longer bioactive.

However, when the cells were seeded directly onto the scaffolds, the activity of ALP, normalised by a DNA assay, was statistically significantly increased for the $Coat_{PBS}Scaff_{BMP\ 1.25}$ scaffolds, in hMSCs from all three test patient donors (by 35±10% on the control). ALP activity was also significantly increased in hMSCs

from two of the three patients seeded onto $Coat_{BMP\ 1.25}Scaff_{BMP\ 1.25}$ scaffolds (by 39±10% on the control). ALP activity was only statistically significantly increased for one of the hMSC patients when seeded onto $Coat_{BMP\ 1.25}Scaff_{PBS}$ scaffolds (by 35±14% on the control).

The functional osteoinductive capacity of Type-I collagen coated PCL (M_n 42,500) scaffolds loaded with rhBMP-7 was assessed using C2C12 cells seeded onto the scaffolds, and quantified using qRT-PCR. The genes of interest were; Type-I collagen (Col1), osteopontin (OP), ALP, osteocalcin (OC) and runt related transcription factor 2 (Runx2). The $Coat_{BMP\ 1.25}Scaff_{PBS}$ scaffolds had an early osteoinductive effect on the C2C12 cells, as ALP, OC and Runx2 were elevated during the first 2 days only, compared to the control (*e.g.* by 44±12%, 128±42%, 60±25% and 46±25% respectively at the 24 hr mark).

The $Coat_{PBS}Scaff_{BMP\ 1.25}$ scaffolds also had an osteoinductive effect on the cells, which was more sustained than that observed for the $Coat_{BMP\ 1.25}Scaff_{PBS}$ group. While OP, ALP and Runx2 were up-regulated in the first 24 hr compared to the control (by 38±10%, 208±82% and 72±31% respectively), statistically significant up-regulation of the late marker OC was delayed until the 48 hr mark (by 73±49%). The effect was found to be sustained until day 7, when OC and Runx2 were both statistically significantly up-regulated compared to the control (by 151±91% and 93±27% respectively).

The $Coat_{BMP\ 1.25}Scaff_{BMP\ 1.25}$ scaffolds were found to combine the early effect of the $Coat_{BMP\ 1.25}Scaff_{PBS}$ scaffolds, with the more sustained effect of the $Coat_{PBS}Scaff_{BMP\ 1.25}$ scaffolds. ALP, OC and Runx2 were all up-regulated at the 24 hr mark (by 312±56%, 329±39% and 96±25% respectively). This osteoinductive effect was sustained until day 7 when Col1, ALP and Runx2 were still up-regulated compared to the control (by 174±78%, 72±24% and 178±78% respectively).

These data suggest that the scaffolds containing rhBMP-7 have a weak osteoinductive effect on the cells seeded onto them. The different delivery systems

were found to affect the cells differently. The clinical significance of this was not assessed in these studies.

1,25-dihydroxyvitamin D_3 ($1,25(OH)_2D_3$) was used as a model drug to assess the feasibility of releasing lipid-soluble active factors from the scaffolds. This was assessed by quantifying the area of normalised ALP staining of hMSCs. The release of $1,25(OH)_2D_3$ from the loaded collagen scaffold coatings and the encapsulating scaffolds significantly increased ALP expression compared to the control scaffold groups (by 115±28% and 69±25% respectively). Furthermore, ALP expression was significantly increased when the two delivery systems were used together, when compared to either delivery system on its own.

These data suggest that the delivery of lipid-soluble active factors is feasible from collagen coated PCL scaffolds, and that the coating and encapsulating delivery systems are mutually compatible.

Declaration

I hereby declare that this thesis has been composed by myself and is the result of my own work. I was assisted through the donation of cellular material, as clearly indicated throughout the text of the thesis. The cell characterisation detailed in Appendix G was undertaken by a team of scientists of which I was part. Particular contributions were made by Dr Aimee Reynolds and Miss Kate Cameron. This work has not been submitted for any other degree.

Duncan Sharp
2011

Acknowledgements

I do not have the words to express my thanks to all those who have helped me over the years. However, special mention must be given to the following: my supervisors, Prof Brendon Noble and Prof Hamish Simpson; my friends, Caroline Adam, Brian Atkinson, Sarah Brown, Fiona Buchan, Kate Cameron, Lewis Downie, Christian Felgemacher, Ruth Harrison, Dr Christina Huber, Laura Moore, Dr Seth Racey, Dr Aimee Reynolds, Antonello Spadaccino, Amy Stockwell, Dr Sarah Thackray, Dr Antiopi Voultsiadou, Robert Ward, and Poppy Wilson; my girlfriend, Kristen Atkins; and most of all my patents, Dorothy Sharp and Professor Emeritus Craig Sharp.

To my mother, Dorothy Sharp

Contents

Figures

Tables

Abbreviations Prefixes and Units

Abbreviations

$1,25(OH)_2D_3$	1,25-dihydroxyvitamin D_3
3D	Three dimensional
+ve	Positive
–ve	Negative
$\alpha_{j,x}$	Area of ALP staining per cell in well *j* in group *x*
aFGF	Acidic FGF
A_i	Area of ALP staining in field *i*
ALK	Activin receptor-like kinase
ALP	Alkaline phosphatase
ANOVA	One-way analysis of variance
APC	Adenomatosis polyposis coli
bFGF	Basic FGF
BMPs	Bone morphogenetic proteins
BRUs	Bone remodelling units
BSA	Bovine serum albumin
$Coat_{PBS}$	Coating with PBS
$Coat_{BMP\ 0.63}$	Coating with low rhBMP-7 dose
$Coat_{BMP\ 1.25}$	Coating with high rhBMP-7 dose
$Coat_{ethanol}$	Coating with ethanol
$Coat_{1,25(OH)2D3}$	Coating with $1,25(OH)_2D_3$
Ca^{2+}	Calcium ions
$CaCl_2$	Calcium chloride
CAD	Computer aided design
$CaHPO_4$	Dibasic calcium phosphate
Calcein-AM	Calcein-acetoxymethyl
CAM	Computer aided manufacture
Cbfa1	Core binding factor alpha1
CBP/p300	CREB-binding protein
cDNA	Complementary deoxyribonucleic acid
CFU-F	Fibroblastic colony-forming cells

CK1α	Casein kinase-1α
C_{MB}	Concentration of Methylene Blue (µg/ml)
$C_{MB,A}$	Apparent concentration of Methylene Blue (µg/ml)
CO_2	Carbon dioxide
Col1	Type 1 Collagen
$C_{rhBMP-7}$	Concentration of rhBMP-7 (pg/ml)
D_{AB}	Diffusivity of A in B (m^2/s)
DAPI	4',6-diamino-2-phenylindole
DBM	Demineralised bone matrix
DCM	Dichloromethane
dH_2O	Distilled water
Dlx5	Distal-less homeobox-5
Dkk	Dickkopf
DMEM	Dulbecco's Modified Eagle's Medium
DNA	Deoxyribonucleic acid
Dvl	Dishevelled
ECM	Extracellular matrix
ELISA	Enzyme-linked immunosorbent assay
ERK	Extracellular-signal-regulated kinase
FAK	Focal adhesion kinase
FCS	Foetal calf serum
FDM	Fused deposition modelling
FGF	Fibroblast growth factor
FZD	Frizzled
GAPDH	Glyceraldehyde 3-phosphate dehydrogenase
GSK-3β	Glycogen synthase kinase-3β
HA	Hydroxyapatite
HCl	Hydrochloric acid
hESCs	Human embryonic stem cells
Hh	Hedgehog
HLA	Human leukocyte antigen

hOB	Human osteoblast
hPL	Human platelet lysine
HBSS	Hanks' balanced salt solution
IGF	Insulin-like Growth Factor
Ihh	Indian hedgehog
IL-1	Interleukin-1
IL-6	Interleukin-1
IMS	Industrial methylated spirit
iPSCs	Induced pluripotent stem cells
${}_{V}J_{A}$	Molar flux of A with respect to mean volume velocity (mol/[m^2s])
JNK	c-Jun N-terminal kinase
LRP	Low-density lipoprotein receptor-related Protein
MAP	Mitogen-activated protein
Msx2	Msh homeobox 2
M_t/M_∞	Fraction of drug released
Na^+	Sodium ions
NaCl	Sodium chloride
NaOH	Sodium hydroxide
NC	Numerical control
$N_{C,i}$	Number of calcein positive cells in field *i*
N_i	Number of cells in field *i*
$N_{P,i}$	Number of PI positive cells in field *i*
MCSF	Macrophage Colony Stimulating Factor 1
$MgCl_2$	Magnesium Chloride
MSCs	Marrow stromal cells
OC	Osteocalcin
OD	Optical density (-)
ON	Osteonectin
OP	Osteopontin
OPG	Osteoprotegerin

Osx	Osterix
PBS	Phosphate buffered saline
PBT	Poly(butylene terephthalate)
PCL	Poly(ε-caprolactone)
PDGF	Platelet derived growth factor
PEGT	Poly(ethylene glycol)-terephthalate
PGA	Poly(glycolic acid)
PI	Propidium iodide
PLA	Poly(lactic acid)
PLGA	Poly(lactide-co-glycolide)
pNP	Para-nitrophenol
pNPP	Para-nitrophenylphosphate
PTH	Parathyroid hormone
PDGF	Platelet derived growth factor
qRT-PCR	Quantitative reverse transcription polymerase chain reaction
Ptch1	Patched1
RGD	Arginine glycine aspartic acid
RNA	Ribonucleic acid
Runx2	Runt related transcription factor 2
$Scaff_{PBS}$	Scaffold encapsulating PBS
$Scaff_{BMP\ 0.63}$	Scaffold encapsulating low rhBMP-7 dose
$Scaff_{BMP\ 1.25}$	Scaffold encapsulating high rhBMP-7 dose
$Scaff_{ethanol}$	Scaffolds encapsulating ethanol
$Scaff_{1,25(OH)2D3}$	Scaffolds encapsulating $1,25(OH)_2D_3$
SEM	Standard error of the mean
Smad	Mothers against decapentaplegic homolog
Smo	Smoothened
SOST	Sclerostin
Sox9	SRY (sex determining region Y)-box 9
t	Time (hr)
T0	Time zero

TC	Treated tissue culture
TCP	Tricalcium phosphate
TGF-β	Transforming growth factor-β
TNF-α	Tumour necrosis factor-α
TPP	Tripolyphosphate
USFDA	United States Food and Drug Administration
VEGF	Vascular endothelial growth factor

Prefixes

μ	Micro ($\times 10^{-6}$)
G	Giga ($\times 10^{9}$)
k	Kilo ($\times 10^{3}$)
M	Mega ($\times 10^{6}$)
m	Milli ($\times 10^{-3}$)
p	Pico ($\times 10^{-12}$)
rh	Recombinant human

Units

bar	Pressure in bar
°C	Temperature in degrees Celsius
K	Temperature in degrees Kelvin
M	Concentration in moles per litre
m	Length in metres
mol	Quantity in moles
Pa	Pressure in Pascals
% (v/v)	Percent, volume by volume
% (w/v)	Percent, weight by volume

Chapter 1 : General Introduction

1.1. Problems in Orthopaedics

1.1.1. Bone Biology

1.1.1.1. Introduction

The skeletal system, which consists of bone and cartilage tissue, is a complex organ which fulfils a variety of different functions (Karsenty, 2003). The primary functions of bone are: to support locomotion by providing sites for muscle attachment; to protect the vital organs of the body such as the brain, spinal cord, heart, lungs, and bone marrow; and to produce cells of the haematopoietic lineage (Baron, 1996; Harada and Rodan, 2003). As a secondary function, bone acts as a store for calcium and phosphate ions that participate in serum homeostasis (Felsenfeld and Rodriguez, 1999).

Despite its static appearance, bone is a dynamic tissue. Throughout life, it is continually remodelled, both to adapt to mechanical stimuli, and to remove damaged areas of matrix resulting from everyday use (Wolff, 1892; Turner, 1992). The local balance between osteoclastic bone resorption, and osteoblastic bone formation is subject to a number of controls aimed at maintaining homeostasis (**Figure 1.1**).

1.1.1.2. Bone Structure

Calcified bone contains about 25% organic matrix, including cells (2 – 5%), 5% water, and 70% hydroxyapatite crystals (Philipson, 1965; Sommerfeldt and Rubin, 2001). The organic component of bone is made up of approximately 85 – 90% Type-I collagen (Carter *et al.*, 1991; Baron, 1996). The remainder may be involved in signalling functions, or play a role during mineralisation.

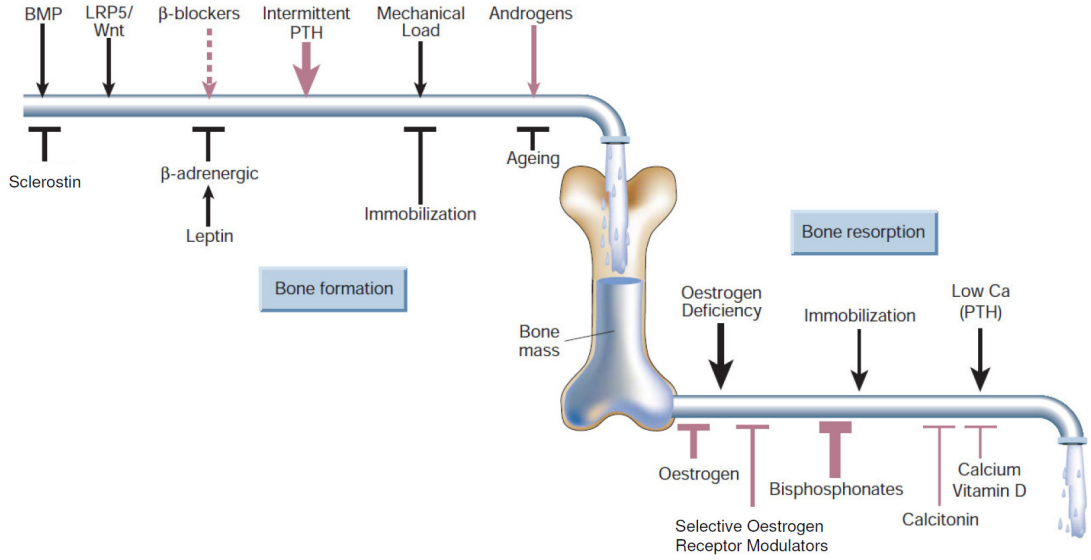

Figure 1.1: Determinants of skeletal homeostasis and bone mass.

A schematic representation of the factors affecting bone homeostasis. Stimulators are represented by arrows, whereas inhibitors are shown by blunt arrows. The thickness of the arrow is approximately proportional to the impact of the factor. (Adapted from Harada and Rodan, 2003).

Anatomically there are two main types of bones: flat bones, such as the skull, mandible, and scapula, and long bones such as the femur, tibia, and radius (Dempster *et al.*, 2006). The long bones consist of a shaft (the diaphysis), which gradually increases in diameter at either end to form the metaphyses, culminating in the epiphyses (**Figure 1.2**). At the joints, these are capped with articular cartilage. Except for the joints, bones are covered by a membrane: the periosteum. This fibrous tissue contains adult mesenchymal progenitor cells, osteoblasts, fibroblasts, blood vessels and sympathetic nerves (Shapiro *et al.*, 1977; Allen *et al.*, 2004).

The long bones are composed of cortical and trabecular (or cancellous) bone (**Figure 1.2**). Cortical bone has a dense structure of irregular branching channels known as osteons, which are orientated in the direction of maximal stress (Einhorn, 1996; Miller *et al.*, 2002). Each osteon contains a blood vessel enclosed in a Harversian canal, surrounded by concentric lamellae and interstitial bone.

On a macroscopic level, cancellous bone is a honeycomb-like network of interconnected trabecular plates and bars, surrounded by bone marrow (Dempster *et al.*, 2006). The trabeculae themselves are also made from osteons, and are arranged to resist mechanical loading (Weiner *et al.*, 1999; Sikavitsas *et al.*, 2001). Due to its porous structure, cancellous bone is able to deform and thereby distribute mechanical loading from the articular cartilage (Keaveny and Yeh, 2002).

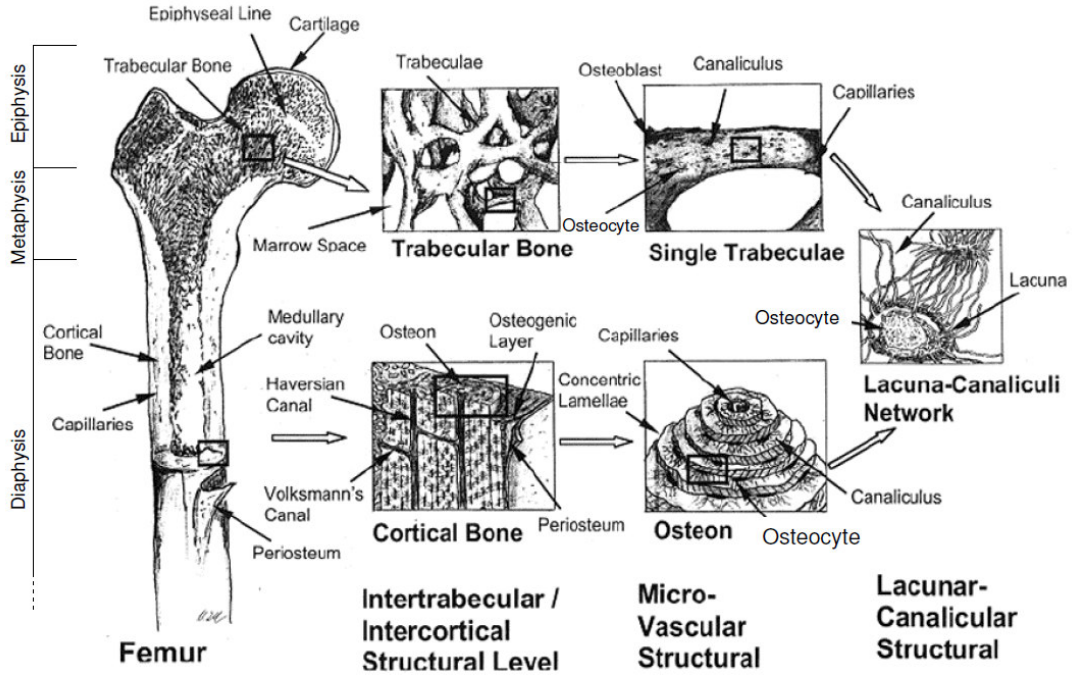

Figure 1.2: Schematic of bone anatomy.

A schematic diagram of bone anatomy. The macroscopic anatomy of a human femur is shown, along with the microstructure of both cortical and cancellous bone (Adapted from: Liebschner and Wettergreen, 2003)

1.1.1.3. Bone Modelling

Modelling is the process by which bones are either shaped or re-shaped. It occurs when bone formation by osteoblasts is out of balance with bone resorption by osteoclasts. Although the majority of modelling occurs during growth, it can also occur in normal adult bone, primarily as a result of mechanical loading (Pead *et al.*, 1988; Burr *et al.*, 1989; Dempster *et al.*, 2006).

There are two forms of bone formation, the first being intramembranous ossification (Ogden *et al.*, 1975). This happens when marrow stromal cells (MSCs) differentiate into osteoblasts (Brighton and Hunt, 1991). These osteoblasts deposit collagen fibres in a disorganised fashion. The matrix quickly mineralises to form woven bone, which is eventually remodelled into mature lamellar bone (Hawke and Jahn, 1975; Bernard, 1969; Baron, 1996; Sikavitsas *et al.*, 2001). Growth of the flat bones, and increases in girth of the long bones occurs by intramembranous ossification.

The second type of modelling is endochondral ossification (Ogden *et al.*, 1975). In this case, MSCs differentiate into chondroblasts, which secrete cartilaginous matrix (Brighton and Hunt, 1986b). In the growth plate, the chondroblasts become encased in their own matrix, becoming chondrocytes. As the proliferation zone progresses on, the chondrocytes become larger and the matrix calcifies. After chondrocyte apoptosis, this matrix is first remodelled into woven bone, before being further remodelled to lamellar bone (Brighton *et al.*, 1973; Baron, 1996; Weiner and Wagner, 1998; Carter *et al.*, 1996). Endochondral ossification is responsible for the longitudinal growth of the long bones.

1.1.1.4. Bone Remodelling

"The stability and immutability of dry bones and their persistence for centuries, and even millions of years after the soft tissues have turned to dust, give us a false impression of bone during life. Its fixity after death is in sharp contrast to its ceaseless activity during life." (Cooke, 1955).

The ceaseless activity referred to by Cooke (1955), is bone remodelling (Dempster *et al.*, 2006). In healthy bone, this process involves the two major cell lineages in bone,

osteoclasts and osteoblasts, working in balance in groups of cells termed bone remodelling units (BRUs) (Frost, 1969). The function of the BRUs is to replace old or damaged bone with new bone.

Exactly what initiates the remodelling cycle is unclear, though it is possible that signalling caused by osteocyte apoptosis, in response to microcrack formation, may fulfil this role (Noble *et al.*, 2003; Verborgt *et al.*, 2000). Mononucleated osteoclast precursors then bind to the bone surface, and fuse to form multinucleated osteoclasts (Baron *et al.*, 1986; Kurihara *et al.*, 1990). The osteoclasts then digest both the mineral and organic bone matrix before undergoing apoptosis (Hughes *et al.*, 1995; Hill, 1998).

Afterwards, osteoblast precursors populate the cavities formed by the osteoclasts. This process is tightly coupled to bone resorption, though the exact stimulus is currently unknown (Andersen *et al.*, 2008). The osteoblasts then secrete collagenous matrix, which they then mineralise, in part, by releasing matrix vesicles (Bianco *et al.*, 1993, Zaidi, 2007). After matrix formation, the majority of osteoblasts die by apoptosis. The remainder either become embedded in their own matrix, becoming osteocytes, or stay on the surface, becoming bone-lining cells (Hill, 1998).

1.1.1.5. Bone cells

Osteoclasts form from haematopoietic precursors from either the bone marrow or peripheral blood (Husheem *et al.*, 2005; Vaananen and Laitala-Leinonen, 2008). Their function has previously been discussed in §1.1.1.4. Osteoclast formation, activation and activity are governed by local factors such as RANKL/osteoprotegerin (OPG), interleukins -1 and -6 (IL-1 and IL-6), and Macrophage Colony Stimulating Factor 1 (MCSF), as well as the systemic hormones such as 1,25-dihydroxyvitamin D_3 ($1,25(OH)_2D_3$) (Udagawa *et al.*, 1990; Yasuda *et al.*, 1998; Lacey *et al.*, 1998; Boyle *et al.*, 2003).

Osteoblasts are of mesenchymal origin (see **Figure 1.3**), and were thought to derive exclusively from MSCs (Castro-Malaspina *et al.*, 1980; Friedenstein *et al.*, 1987; Aubin *et al.*, 1995; Ducy *et al.*, 2000). However, in recent years, this has been

complicated by the discovery of marked phenotypic plasticity in the stromal system (Bianco and Robey, 2000). *In vitro*, adipocytes or chondrocytes may regress, enabling them to differentiate towards osteoblasts (Song and Tuan, 2004). MSCs play a prominent role in bone modelling, remodelling and fracture healing, as discussed in §1.1.1.3, §1.1.1.4, and §1.1.2 respectively.

Osteoblast formation and function are influenced by systemic hormones, such as parathyroid hormone (PTH), oestrogens, glucocorticoids, and $1,25(OH)_2D_3$ (Krishnan *et al.*, 2003; McCarthy *et al.*, 2003; Zhou *et al.*, 2006; Smith and Frenkel, 2005; Bouillon *et al.*, 2008; Marie, 2008), as well as local signals, including; bone morphogenetic proteins (BMPs), transforming growth factor-β (TGF-β), and platelet derived growth factor (PDGF) (Chen *et al.*, 1991; Ryoo *et al.*, 2006; Cheng *et al.*, 2003a; Kells *et al.*, 1995; Chandrasekhar and Harvey, 1996; Fiedler *et al.*, 2002) (see **Figure 1.3**). The primary function of osteoblasts is to secrete new bone matrix. In so doing, they express such genes as; Type-I collagen, alkaline phosphatase (ALP), osteopontin, and osteocalcin (Liu *et al.*, 1994). Collagen expression is an early event in osteoblastic differentiation, occurring after proliferation of pre-osteoblasts. This is followed by ALP expression, which reaches its maximum before mineralisation (Yoon *et al.*, 1987; Zaidi, 2007) (see **Figure 1.3**).

After forming new bone matrix, some osteoblasts remain behind on the bone surface, becoming bone-lining cells. Under conditions of increased mechanical stimulation, there is some evidence that they can revert back to osteoblasts (Chow *et al.*, 1998). They may create specialised compartments on cancellous bone in which remodelling can be initiated (Hauge *et al.*, 2001).

Osteocytes, by far the most numerous cell Type-In bone, are the non-proliferative, terminally differentiated endpoint of the osteoblast lineage (Noble, 2008). During modelling or remodelling, between 10 – 20% of osteoblasts become entombed in their own matrix to become osteocytes (Aubin and Turksen, 1996). Their exact function has not been well defined, but it is possible that these cells play a role in the sensing of microcracks, and the initiation of remodelling (see §1.1.1.4).

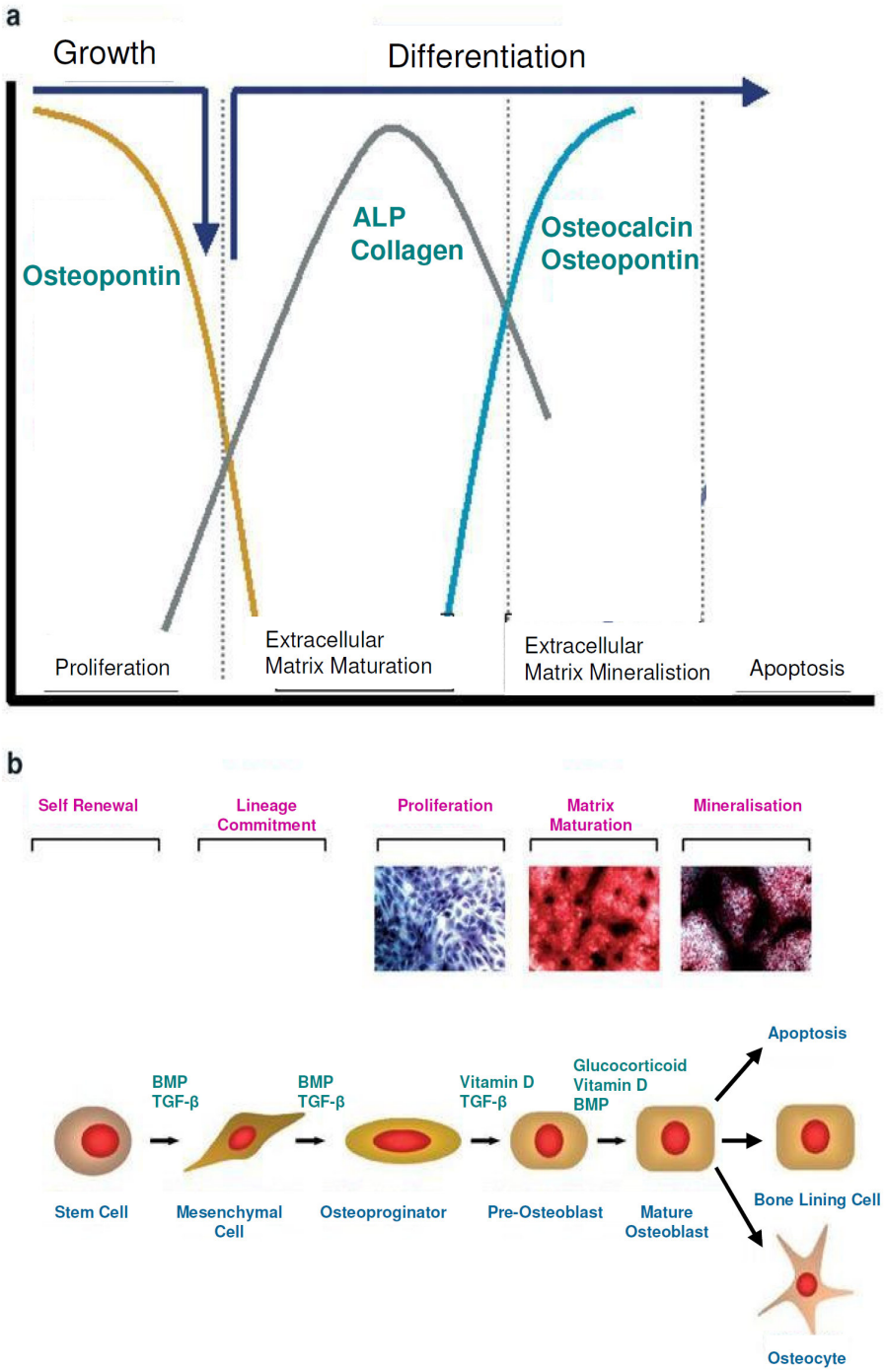

Figure 1.3: The Osteoblast Lineage.

Cartoon of growth and differentiation of osteoblast lineage cells. A) Various marker genes are up-regulated (shown in green) by runt related transcription factor 2 (Runx2). B) Progression through the osteoblast lineage from multipotent MSCs to mature osteocytes is regulated by physiological signals. (Adapted from Stein *et al.*, 2004).

1.1.2. Fracture Healing

Unlike many other tissues in the adult body that heal with the formation of poorly organised scar tissue, bone fracture healing can largely restore the properties of the original bone (Einhorn, 1998). Although the macroscopic processes of fracture healing are well understood, particularly in the murine model, less is known about the regulation of these events (Reed *et al.*, 2002).

Histologically, fracture healing is divided into primary (or direct) healing and secondary (or indirect) healing. Primary healing occurs when BRUs remodel bone across the fracture site, thus re-establishing cortical continuity. This form of healing is comparatively rare, as it requires rigid internal fixation (Phillips, 2005). Secondary healing is much more common, and is a coordinated response of the bone marrow, the cortex, the periosteum, and the adjacent soft tissue. In contrast to primary healing, it is stimulated by micromotion of the fracture (McKibbin, 1978).

1.1.2.1. Secondary Healing

The first stage in secondary healing is the formation of a haematoma, caused by the bleeding from the medullary cavity and periosteum, as well as from tearing of the adjacent soft tissue (Wraighte and Scammell, 2006). The haematoma itself releases signalling molecules which may initiate cellular cascades crucial to fracture healing. These include IL-1, IL-6, TGF-β, and PDGF (Bolander, 1992; Einhorn *et al.*, 1995). A fibrin mesh forms within the haematoma, as the latter is replaced by granulation tissue.

In secondary healing, new bone forms by both endochondral and intramembranous ossification. MSCs from the marrow, trapped in the haematoma, and from the periosteum adjacent to the fracture site, differentiate to chondrocytes and form cartilage (Bielby *et al.*, 2007). This is termed the soft or cartilaginous callus. The soft callus stabilises the fracture fragments, and provides early bridging across the fracture. In a similar process to that which occurs in growth plates, chondrocytes stop proliferating and become hypertrophic. They also participate in calcifying their matrix (Brighton and Hunt, 1986a). Once the cartilage is calcified, the chondrocytes

undergo apoptosis, and the soft callus becomes a target for the ingrowth of blood vessels (Carano and Filvaroff, 2003).

MSCs, chiefly from the periosteum a few millimetres from the fracture site, also differentiate to osteoblasts and form woven bone directly by intramembranous ossification (Nikolaou and Tsiridis, 2007). This is termed the hard callus.

Bony union is restored across the fracture as the soft callus is remodelled to woven bone. It undergoes further remodelling to form mechanically competent lamellar bone, largely restoring the properties of the original tissue (Einhorn, 1998).

Locally acting signalling molecules as well as systemic agents are thought to play a major role in the coordination of the fracture healing process (Nikolaou and Tsiridis, 2007). These can be further classified into; pro-inflammatory cytokines, growth factors, and hormones.

1.1.2.2. Pro-Inflammatory Cytokines

Pro-inflammatory cytokines IL-1, IL-6, and tumour necrosis factor-α (TNF-α) are signals thought to be secreted by macrophages and other inflammatory cells (Kon *et al.*, 2001). In murine models, they are known to be up-regulated during the first three days of fracture healing, and during the bone remodelling phase (Prisell *et al.*, 1993). In the early stages of fracture healing, they are thought to be chemotactic for inflammatory cells, to encourage extracellular matrix production, and to stimulate angiogenesis (Nikolaou and Tsiridis, 2007).

1.1.2.3. Bone Morphogenetic Proteins

The existence of BMPs was first hypothesised in 1965 by Urist (1965). Since then, at least 14 isoforms have been identified. Of these, BMP-2, -4, -6, and -7 are thought to be the most important in bone (Westerhuis *et al.*, 2005). They are pleiotropic morphogens, and are members of the TGF-β superfamily. They are produced by MSCs, osteoblasts and chondrocytes, and play a crucial role in the regulation of growth, differentiation and apoptosis for various cell types, including MSCs, osteoblasts and chondroblasts (Sakou, 1998; Kloen *et al.*, 2003).

BMPs have a variety of functions. In animal knockout models, BMP-2 deficient mice were found to be non-viable due to developmental cardiac defects (Zhang and Bradley, 1996). BMP-7 knockout mice died shortly after birth because of kidney abnormalities. Development of the eyes was also affected, as well as skeletal patterning (Luo *et al.*, 1995). However, in the adult body, the primary function of BMPs appears to be in bone and cartilage formation (Kang *et al.*, 2004; Bessa *et al.*, 2008). Indeed, *in vitro* they are known to stimulate both osteogenic and chondrogenic differentiation of MSCs (Knippenberg *et al.*, 2006; Edgar *et al.*, 2007)

The BMPs do, however, have different roles and different temporal expression patterns during fracture healing. For example, in murine models BMP-2 is expressed throughout the first 21 days of fracture healing, while BMP-7 is up-regulated from days 14 – 21 (Cho *et al.*, 2002). They may also act at different points as MSCs differentiate to osteoprogenitors, osteoblasts, and finally osteocytes (Cheng *et al.*, 2003a).

Both BMP-2 and BMP-7 are members of the TGF-β superfamily and have signalling pathways according to the general TGF-β signalling pathway for MSCs (see **Figure 1.4**). Once the BMPs bind to BMP receptors types I (BMPR-IA and BMPR-IB) and II (BMPR-II), BMP-7 is thought to phosphorylate the receptor-regulated mothers against decapentaplegic homologs (Smads)-1 and -5, whereas BMP-2 also phosphorylates Smad-8 (Aoki *et al.*, 2001). This process is thought to be inhibited by Smad-6 and Smad-7 (Itoh *et al.*, 2001a). The activated Smads then bind to Smad-4 (Shen *et al.*, 2002). The resulting complex translocates to the nucleus, where it influences the expression of target genes including Dlx5, which in turn induces the expression of runt related transcription factor 2 (Runx2) (Miyama *et al.*, 1999; Lee *et al.*, 2003b; Holleville *et al.*, 2007).

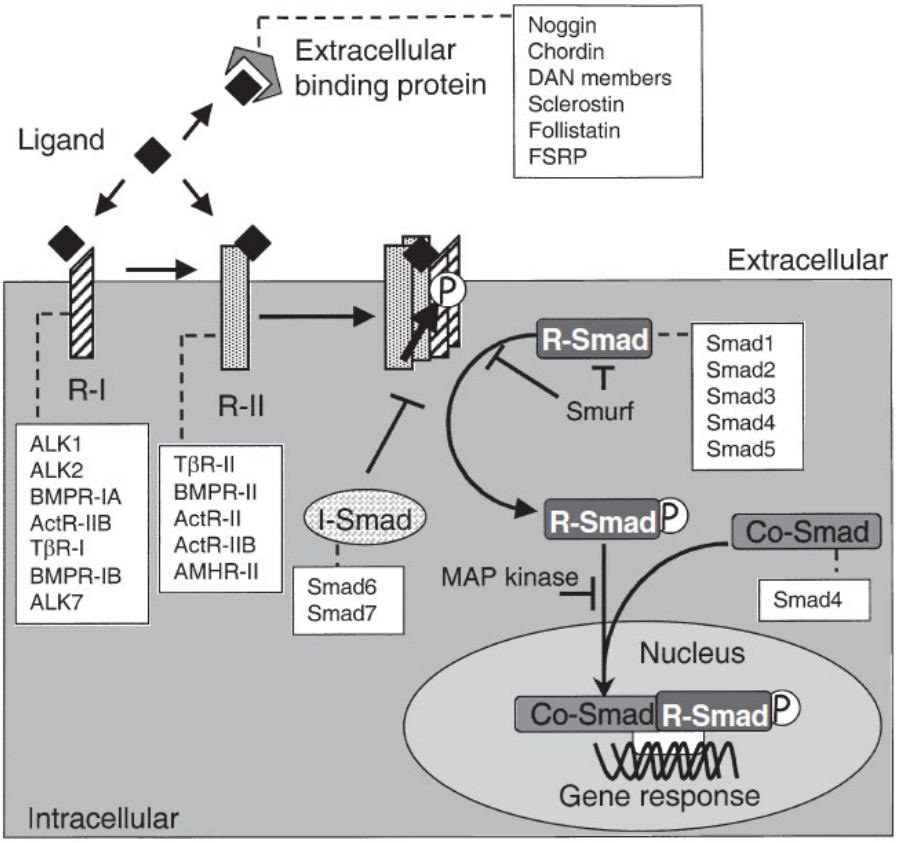

Figure 1.4: TGF-β Superfamily Signalling Pathway.

Ligand binding-induced heteromerisation of Type-II and Type-I receptors leads to Type-I receptor phosphorylation by the Type-II receptor followed by R-Smad phosphorylation by Type-I receptors. A complex is formed of phosphorylated R-Smad with the Co-Smad, and this complex translocates to the nucleus where it regulates transcription. The components of extracellular binding proteins, Type-I receptors, Type-II receptors, and Smad proteins are indicated. (From Roelen and Dijke (2003)).

Recombinant human BMPs (rhBMPs) are now used clinically for fracture healing. This is discussed in §1.1.6.6.

1.1.2.4. Transforming Growth Factor-β

The five TGF-β isoforms form a subset of the larger TGF-β superfamily. They are thought to be released by platelets after the clot forms at the time of fracture (Robey *et al.*, 1987). Although the TGF-βs are known to inhibit the activity of the osteogenic transcription factor Runx2 *in vitro* (Kang *et al.*, 2005), they are also known to stimulate formation of new bone *in vivo* (Sumner *et al.*, 1995; Baylink *et al.*, 1993).

This apparent paradox may be explained as the TGF-βs are thought to have a potent chemotactic effect on MSCs, and to stimulate MSC, chondrocyte and osteoblast proliferation (Lieberman *et al.*, 2002). Hence the pool of cells available for endochondral and intramembranous ossification is increased. TGF-βs may also enhance bone formation in indirect ways, such as stimulating the synthesis of BMPs (Bostrom, 1998) and inhibiting RANKL production by osteoblasts and thereby decreasing bone removal (Fox and Lovibond, 2005).

In terms of differentiation, it is thought that TGF-β1 may be involved in chondrogenesis and early osteogenesis (Lieberman *et al.*, 2002). TGF-β3 has been found to stimulate chondrogenesis (Jin *et al.*, 2006; Miyanishi *et al.*, 2006; Tang *et al.*, 2009) in mesenchymal cells. TGF-β2 and TGF-β3 may be primarily involved in chondrogenesis, though they may also play a role in endochondral ossification (Thorp *et al.*, 1992).

In endothelial cells, both TGF-β1 and -β3 bind to activin receptor-like kinase (ALK) -1 and ALK5 (which act as Type-I receptors) and TβR–II to activate Smad-1 and -5 for ALK1, and Smad-2 and -3 for ALK5 (Goumans *et al.*, 2002; Pen *et al.*, 2008). These form a complex with Smad-4, which translocates to the nucleus and affects the expression of target genes. It is thought that the Smad-1/5 pathway (which is only activated by TGF-βs in endothelial cells) stimulates endothelial cell migration and proliferation, whereas the Smad-2/3 pathway induces angiogenesis. Particularly with

TGF-β1, this is thought to occur in a dose-dependant manner, with low doses activating the Smad-1/5 pathway whereas higher doses stimulate the Smad-2/3 pathway (Goumans *et al.*, 2002).

For MSCs the TGF-βs follow the general TGF-β Superfamily signalling pathway (see **Figure 1.4**). TGF-βs 1, 2 and 3 bind to the receptors TβR-I and TβR -II, which leads to the activation of Smad-2 and -3. Again, these form a complex with Smad-4, which translocates to the nucleus and affects the expression of target genes. In cells of the osteoblast lineage, Smad-3 appears to inhibit osteogenic differentiation by physically interacting with Runx2, and inhibiting its function (Alliston *et al.*, 2001). Additionally, Smad-3 forms a complex with SRY (sex determining region Y)-box 9 (Sox9) and CREB-binding protein (CBP/p300) to activate genes for chondrogenesis (Furumatsu *et al.*, 2005; Furumatsu *et al.*, 2009). Smad -3 is also thought to be important for the maintenance of articular cartilage by preventing chondrocytes from undergoing terminal hypertrophic differentiation (Yang *et al.*, 2001). Hence TGF-βs are thought to be important in early chondrogenic differentiation (Song *et al.*, 2009).

1.1.2.5. Other Growth Factors in Fracture Healing

PDGF is thought to be released by degranulating platelets, macrophages, and monocytes during the early stages of the fracture healing process (Andrew *et al.*, 1995). *In vitro* studies have indicated that it is mitogenic for osteoblasts, however its role in fracture healing has yet to be clearly defined (Canalis *et al.*, 1989; Lieberman *et al.*, 2002). Recent studies have found that PDGF-AA can be release by hMSCs (Salazar *et al.*, 2009), potentially this may have an effect on their ability to stimulate bone formation *in vivo*.

Fibroblast growth factor (FGF) is also involved in fracture healing. In the FGF family, there are at least nine structurally related proteins, the most abundant in normal adult tissue being FGF-1 and -2 (Lieberman *et al.*, 2002). These are also called acidic FGF (aFGF) and basic FGF (bFGF), respectively. Both proteins are released early in fracture healing, and are associated with angiogenesis as well as chondrocyte and osteoblast activation (Radomsky *et al.*, 1998). FGF signalling is discussed in §1.1.3.5.

The insulin-like growth factor (IGF) family has two members, namely IGF-I and -II. *In vitro*, IGF-I is known to stimulate osteoblast activity and chemotaxis (Panagakos, 1993). IGF-I has also been found to induce proliferation and chondrogenic differentiation in MSCs (Longobardi *et al.*, 2006). During fracture healing, IGF-II is known to play a role in endochondral ossification by stimulating Type-I collagen production, cartilage matrix synthesis, and chondrocyte proliferation (Prisell *et al.*, 1993; Nikolaou and Tsiridis, 2007).

IGF-I in particular has been examined as a potential therapeutic agent for fracture healing. However, studies using animal fracture models have yielded inconsistent results, and more work needs to be done to reveal its true therapeutic potential (Carpenter *et al.*, 1992; Aspenberg *et al.*, 1989; Bak *et al.*, 1990; Thaller *et al.*, 1993).

Vascular endothelial growth factor (VEGF) was first discovered on 1989, and since then has been described as playing a cornerstone role in the angiogenesis component of fracture healing (Keramaris *et al.*, 2008). Indeed the potent angiogenic activity of human fracture haematoma is thought to be predominantly due to VEGF (Street *et al.*, 2000), and it may be involved in the tight coupling of angiogenesis and osteogenesis during bone repair (Peng *et al.*, 2002). VEGF production is known to be stimulated by other growth factors, such as FGF-2 and BMP-2, and may mediate their angiogenic action (Claffey *et al.*, 2001; Deckers *et al.*, 2002). Interestingly, recent studies have found that hMSCs have the ability to secrete VEGF. This may enhance their ability to repair tissue *in vivo* (Zisa *et al.*, 2009), although the precise mechanism for this is currently unknown (Wang *et al.*, 2009c).

1.1.3. Signal Cascades

Sections §1.1.3.1 – §1.1.3.5 below, outline simplified summaries of the current knowledge of some of the signal cascades thought to be important in bone biology. However, it should be noted that, although the protein interactions are becoming

clearer, in this emerging field, it is possible that some of the conclusions in the literature may have been premature.

1.1.3.1. Smad-Dependent Pathways

As discussed in §1.1.2.3 BMPs -2 and -7 are thought to stimulate the expression of distal-less homeobox-5 (Dlx5) (Lee *et al.*, 2003b; Holleville *et al.*, 2007). This transcription factor has been found to increase osteocalcin expression and mineralisation (Miyama *et al.*, 1999; Tadic *et al.*, 2002). Dlx5 is thought to stimulate Runx2 and Osterix (Lee *et al.*, 2003b; Lee *et al.*, 2003c).

The transcription factor Runx2 is thought to act as a "master switch" during the commitment of mesenchymal stem cells to the osteoblastic lineage (Ducy *et al.*, 1997). As discussed below in §7.3, Runx2 binding sites have been found in the promoter region of many genes associated with osteogenesis, including osteocalcin (Ducy and Karsenty, 1995; Ducy *et al.*, 1997), Type-I collagen (Kern *et al.*, 2001) and osteopontin (Ducy *et al.*, 1997).

More recently, the transcription factor Osterix (Osx) has been identified as being necessary for bone formation, and is thought to act down-stream of Runx2 (Nakashima *et al.*, 2002), however Osx expression may not be entirely dependant on Runx2 (Matsubara *et al.*, 2008) (see **Figure 1.5**). Osx has been found to have an inhibitory effect on the Wnt signalling pathway, thereby inhibiting osteoblast proliferation and stimulating differentiation (Zhang *et al.*, 2008). Although it should be noted that Wnt signalling may have a positive role in the commitment of osteochondroprogenitors to the osteoblastic lineage (Day *et al.*, 2005; Hill *et al.*, 2005) (see §1.1.3.3). It is possible that Osx interacts with Runx2 to activate osteoblastic markers, as Osx-null mouse embryos, which express near wild-type levels of Runx2, have been found to lack expression of Type 1 collagen and osteocalcin (Nakashima *et al.*, 2002). It has also been hypothesised that Osx mainly acts during terminal osteoblastic differentiation (Nakashima *et al.*, 2002; Ryoo *et al.*, 2006).

In addition to the Smad pathways leading to chondrogenesis for TGF-βs described in §1.1.2.4, Msh homeobox 2 (Msx2) is thought to be a target for TGF-β signalling (Hosokawa *et al.*, 2007) (see **Figure 1.5**). Some studies have also found that BMP-2 treatment also results in elevated levels of Msx2 in human osteoprogenitors (Osyczka *et al.*, 2004). While Msx2 is known to be important in osteogenesis and skeletal development (Satokata *et al.*, 2000; Wilkie *et al.*, 2000), the method of action is currently unclear. Some studies have suggested Msx2 has a pro-proliferative effect on osteoprogenitors and suppresses their differentiation (Dodig *et al.*, 1999; Kim *et al.*, 2004). It has been hypothesised that this effect could be due to antagonism of Dlx5 (Ryoo *et al.*, 2006). However, other studies have suggested Msx2 has a positive effect on osteoprogenitor differentiation, independent of Runx2, potentially acting through Osx (Cheng *et al.*, 2003b; Ichida *et al.*, 2004; Matsubara *et al.*, 2008) (see **Figure 1.5**).

As yet, the Smad-dependant pathways are not fully understood. Although the protein interactions are becoming clearer, further work may be needed to elucidate these pathways more fully.

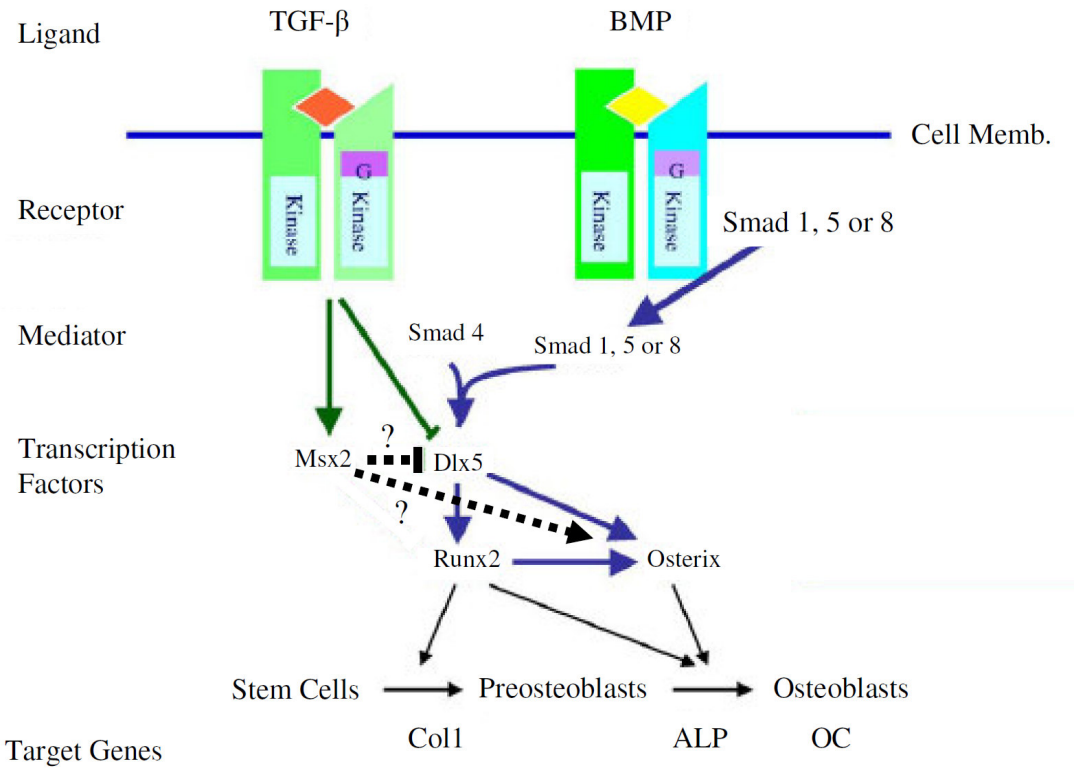

Figure 1.5: Smad Pathways.

A cartoon showing a working model of the molecular switches involved in Smad-dependent BMP-induced osteoblastic differentiation. The dashed lines indicate possible effects that are yet to be fully substantiated (adapted from Ryoo *et al.* (2006)).

1.1.3.2. MAP Kinase Pathway

Although the Smad-dependent signalling pathways are thought to be the major signalling pathways involved in BMP-induced osteogenesis, Smad- independent pathways are also thought to be important. During osteoblastic differentiation, BMP-2 has been found to activate the mitogen-activated protein (MAP) kinases; extracellular-signal-regulated kinase (ERK), c-Jun N-terminal kinase (JNK), and P38 (Guicheux *et al.*, 2003; Lai and Cheng, 2002; Ulsamer *et al.*, 2008) (see **Figure 1.6**). In the case of P38 and JNK, this may be through PKD (see **Figure 1.6**). In turn, Dlx5 is activated via these MAP kinases, leading to osteoblastic differentiation through Runx2 and Osx as described in §1.1.3.1. However, it should be noted ERK has also been found to mediate FGF-2 and TGF-β stimulated proliferation in human osteoblastic cells (Lai *et al.*, 2001).

Interestingly, the MAP Kinase pathway may be one of the most important pathways involved in mechanosensing by osteoblasts (Kapur *et al.*, 2003). Bone is known to respond to increased mechanical loading by increasing bone formation, and suppressing resorption (Hillam and Skerry, 1995). The converse is also thought to be true (Bikle and Halloran, 1999).

Integrins have been suggested as candidates for mediating mechanical strain and ERK activation (Schmidt *et al.*, 1998; Zhang *et al.*, 2003a). One potential model of the mechanism of osteoblast mechanosensing involves the activation of focal adhesion kinase (FAK) by the stimulation of integrins (Hanks *et al.*, 1992), although this activation may not act directly (Gao *et al.*, 1997). The activation of FAK is thought to lead to the binding of Src family kinases (Calalb *et al.*, 1995). Together with Grd2, FAK-Src is thought to lead to the activation of ERK2 (Schlaepfer *et al.*, 1994; Boutahar *et al.*, 2004), which in turn, may enhance osteoblast proliferation and differentiation (Lai *et al.*, 2001). It should be noted however, that even if correct, this is unlikely to be the only pathway connected to mechanosensing in osteoblasts

As yet, the MAP Kinase pathway is not fully understood. Although the protein interactions are becoming clearer, further work may need to be undertaken before firm conclusions can be made.

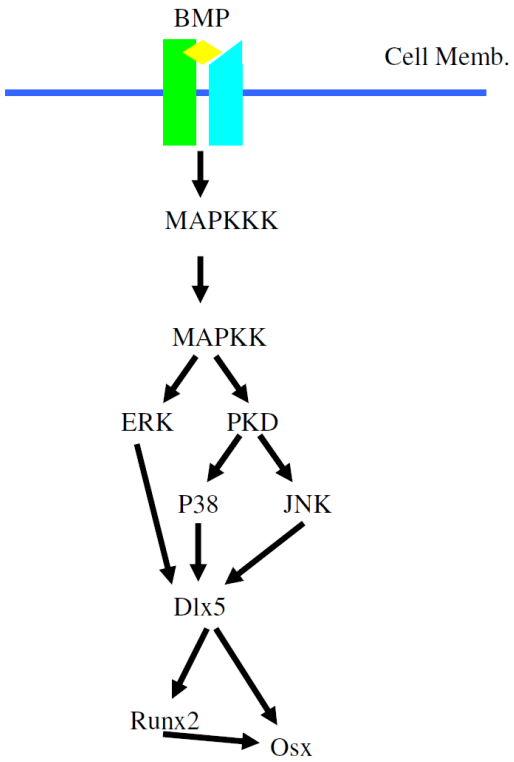

Figure 1.6: MAP Kinase Pathway.

A cartoon showing a working model of the molecular switches involved in MAP Kinase BMP-induced osteoblastic differentiation.

1.1.3.3. Canonical Wnt Signalling

Wnts are a family of secreted glycoproteins. Although Wnt signalling is involved in many different aspects of cell biology, canonical Wnt signalling is thought to be particularly important in bone (Day *et al.*, 2005;).

Canonical Wnt signalling begins with the binding of Wnt to cell surface receptor complexes consisting of frizzled (FZD) and low-density lipoprotein receptor-related protein (LRP)5 or LRP6 (Bhanot *et al.*, 1996; Yang-Snyder *et al.*, 1996; Wehrli *et al.*, 2000) (see **Figure 1.7**). A signal is then thought to be generated through dishevelled (Dvl) (Hay *et al.*, 2005), which is thought to disrupt a protein complex which may contain, amongst others, glycogen synthase kinase-3β (GSK-3β), casein kinase-1α (CK1α), adenomatosis polyposis coli (APC) and Axin (Behrens *et al.*, 1998; Itoh *et al.*, 1998; Hamada *et al.*, 1999). There is also evidence that Axin can bind to LRP5/6 in a Wnt dependant manner, facilitating the disruption of the complex (Mao *et al.*, 2001; Tolwinski *et al.*, 2003; Tamai *et al.*, 2004).

Consequently, GSK-3β no longer phosphorylates β-catenin. This is thought to stabilise it, leading to its accumulation (Salic *et al.*, 2000) (see **Figure 1.7**). β-catenin translocates to the nucleus, where it is thought to interact with, amongst others, TCF (Tolwinski and Wieschaus, 2004). β-catenin is thought to displace Groucho, which may convert TCF into a transcription factor (Daniels and Weis, 2005), which then activates or represses a considerable number of target genes, a list of which may be found at (http://www.stanford.edu/~rnusse/pathways/targets.html).

Members of sclerostin (SOST) and Dickkopf (Dkk) are thought to inhibit the canonical Wnt signalling pathway by binding LRP5/6 (Semenov *et al.*, 2005; Mao *et al.*, 2002). Mutations to the Dkk1 gene have been found to increase the proliferation of osteoblastic cells in mice (Morvan *et al.*, 2006). Furthermore, overexpression of Dkk1 appears to decrease the number of osteoblasts (Li *et al.*, 2006b). Studies such as these have led to the hypothesis that Wnt signalling has a positive effect on the proliferation of osteoblast progenitors (Zhang, 2010). Wnt signalling may also facilitate bone formation by playing a role in the commitment of

osteochondroprogenitors to the osteoblastic lineage (Day *et al.*, 2005; Hill *et al.*, 2005), and by inhibiting osteoclast formation (Glass *et al.*, 2005).

It should be noted that the full complexity of canonical Wnt signalling is not fully understood. It is therefore, likely that Wnt has further effects in bone outwith those described in the simplified description detailed above.

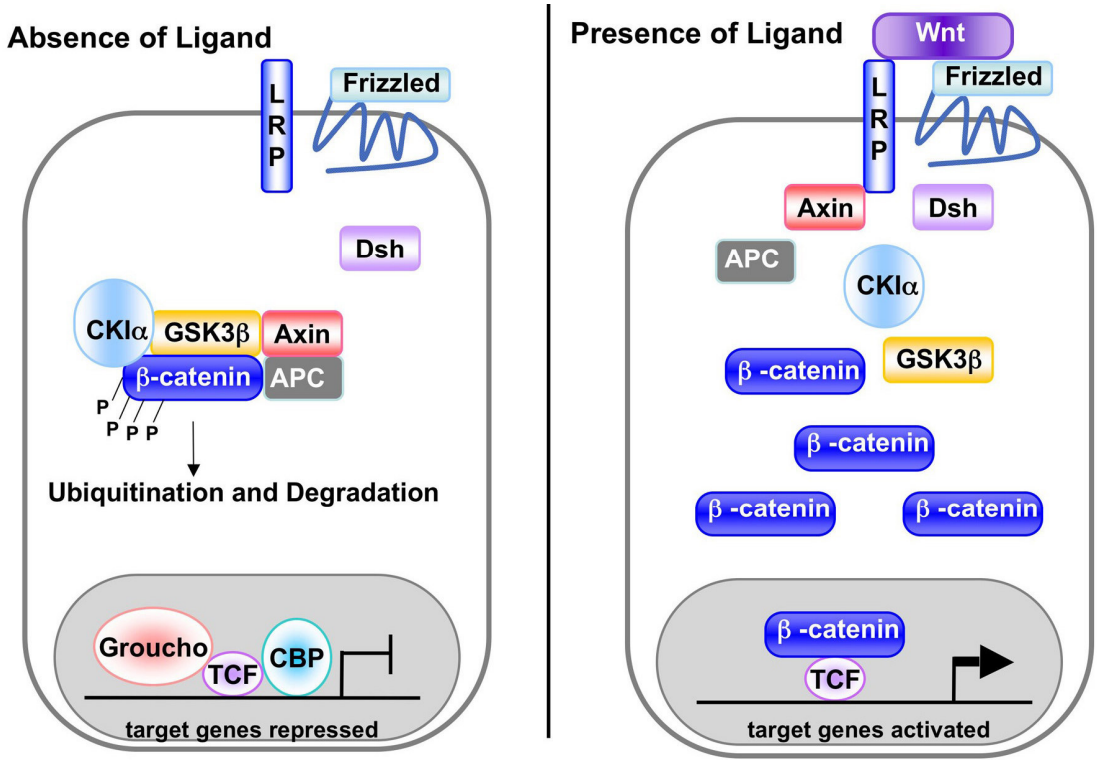

Figure 1.7: Canonical Wnt Signalling Pathway.

A cartoon showing a simplified model of the canonical Wnt signalling pathway, showing two states: in the absence and presence of Wnt (from Eisenmann (2005)).

1.1.3.4. Hedgehog Signalling

Two multipass transmembrane proteins, Smoothened (Smo) and Patched1 (Ptch1) are thought to be involved in hedgehog (Hh) signalling (Marigo *et al.*, 1996; Stone *et al.*, 1996; Taipale *et al.*, 2002). Ptch1 is thought to act as an inhibitor of Smo, however Hh is able to bind to Ptch which remove the inhibition of Smo (Taipale *et al.*, 2002) (see **Figure 1.8**). Once activated, Smo is thought to increase the transcription of Ptch1 (Goodrich *et al.*, 1996), Gli1 (Bai *et al.*, 2002) and Hip1 (Chuang and McMahon, 1999).

There is evidence that the Hh signalling pathway is important in bone. For example, mice lacking Indian hedgehog (Ihh), show an absence of expression of the transcription factor Runx2 (Razzaque *et al.*, 2005). Other studies have indicated that Hh signalling plays a role in osteogenic differentiation, particularly in the early stages, potentially through, and upstream, of Wnt signalling (Hu *et al.*, 2005). Ihh signalling may also be necessary for endochondral bone formation (St-Jacques *et al.*, 1999).

Again, further work may need to be undertaken to investigate the full complexity of this pathway.

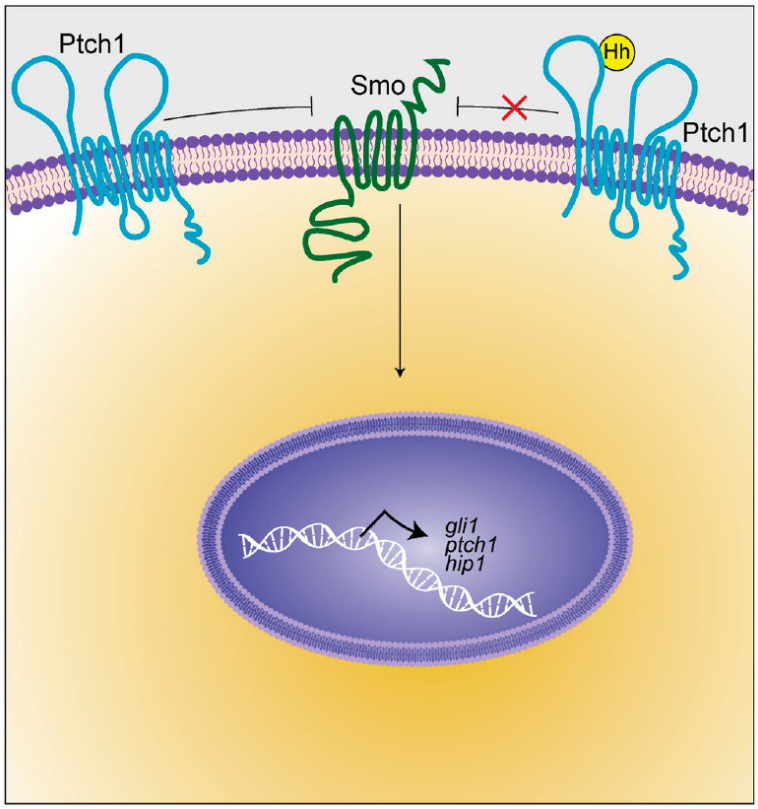

Figure 1.8: Hedgehog Signalling Pathway.

A cartoon showing a simplified model of the hedgehog signalling pathway (from Day and Yang (2008)).

1.1.3.5. FGF Signalling

FGFs are thought to influence intramembranous ossification, by acting through their receptors (Fgfr1 – Fgfr4) to activate ERK and p38 in osteoblasts (Hurley *et al.*, 1996; Chaudhary and Avioli, 1997; Kozawa *et al.*, 1999; Tokuda *et al.*, 2000; Xiao *et al.*, 2002) and this in turn influences osteogenesis through the MAP kinase pathway (see §1.1.3.2) (see **Figure 1.9**). There is also some evidence that FGF signalling stimulates expression of Runx2 through PKC (Kim *et al.*, 2003b) (see **Figure 1.9**). However, this effect on cells of the osteoblastic lineage, appears to act in the early stages of differentiation, as FGF signalling may inhibit the transition from immature to mature osteoblasts (Jacob *et al.*, 2006).

Furthermore, deletion of FGF-2 has also been found to lead to a loss of trabecular bone volume in mice (Montero *et al.*, 2000), while studies investigating mice lacking FGF-9 and -18, found delayed ossification during mid-gestation skeletogenesis (Colvin *et al.*, 1999; Liu *et al.*, 2002; Ohbayashi *et al.*, 2002).

FGF signalling may also play a role in endochondral ossification. The receptor Fgfr3 is expressed in proliferating chondrocytes and Fgfr1 is expressed in prehypertrophic and hypertrophic chondrocytes (Peters *et al.*, 1992; Peters *et al.*, 1993; Deng *et al.*, 1996). In addition, mice lacking FGF-18 showed decreased endochondral and intramembranous ossification (Liu *et al.*, 2002).

As with the other pathways discussed in this section, FGF signalling is not currently fully understood. Further work may need to be done to clarify the full complexity of this pathway.

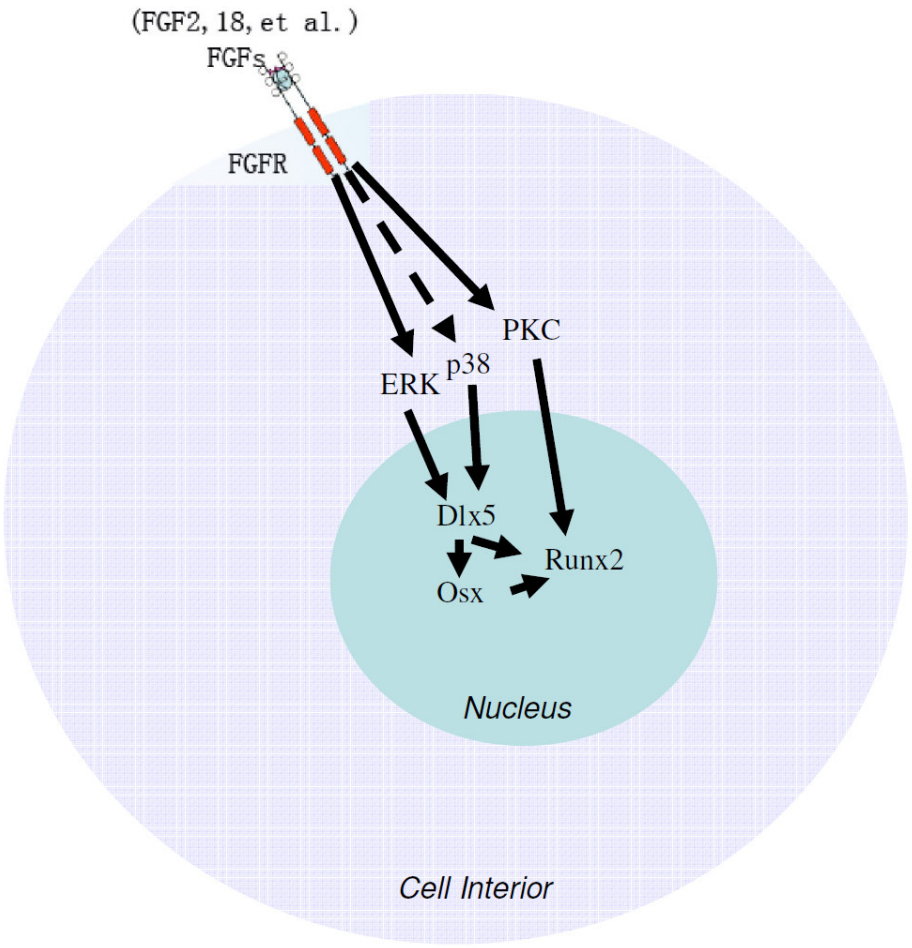

Figure 1.9: FGF Signalling Pathway.

A cartoon showing a simplified model of the FGF signalling pathway in cells of the osteoblastic lineage (adapted from Huang *et al*. (2007)).

1.1.4. Fracture Non-Union

The treatment of fracture non-union is a serious challenge in orthopaedic surgery. Sufferers often endure multiple operations, prolonged hospitalisation, and years of disability and pain, before either union is achieved or the limb is amputated (Phieffer and Goulet, 2006). Although definitions of this condition vary, the United States Food and Drug Administration (USFDA) defines it as: a fracture with a minimum age of nine months, that has not shown radiographic signs of progression towards healing for three consecutive months (USFDA, 1988).

While there are many different classification systems (Weber and Cech, 1976; McKee, 2000; Paley *et al.*, 1989), fracture non-unions are traditionally classified as being hypertrophic, oligotrophic or atrophic (LaVelle, 1998) (see **Figure 1.10**). They may be further categorised as; stiff or mobile, septic or aseptic, and open or closed (Panagiotis, 2005).

Hypertrophic non-unions have a large callus and an adequate blood supply. Similarly, oligotrophic and stiff atrophic non-unions have a sufficient blood supply although their fracture callus is considerably smaller (Reed *et al.*, 2002; Reed *et al.*, 2003). For these types of fracture, the primary cause of non-union is thought to be inadequate fixation. Once properly immobilised, they are thought not to require additional biological solutions to achieve union (Phieffer and Goulet, 2006; Olson and Hahn, 2006).

In contrast, mobile atrophic non-unions lack a fracture callus, and bone resorption is present at the fracture site (**Figure 1.10**). In this case, both mechanical and biological solutions must be employed to achieve union. This is because such fractures have a deficient biologic healing process (Phieffer and Goulet, 2006). This is usually thought to be caused by deficient blood supply, due to their avascular appearance in bone scintigrams (Frölke and Patka, 2007).

While much is understood about the process of normal fracture healing, comparatively little is known about how these mechanisms are regulated, and still less about what causes them to fail (Reed *et al.*, 2002). There are multiple causes of non-union, and a number of risk factors are known to be important (Gaston and Simpson, 2007). Some of the more important risk factors are summarised in **Table 1.1**.

The prevalence of fracture non-union of the long bones was estimated by Phieffer and Goulet (2006) to be 2.5%. This result was derived from 22 studies, with a total of 5517 fractures which were predominantly closed, low energy fractures of the tibia. This figure rises to 13-16% for open fractures (Clancey and Hansen, 1978; Velazco *et al.*, 1983). Dickson *et al*. (1994) even found that the incidence of non-union was as high as 35%, when there was a vascular injury associated with the fracture.

Donaldson *et al*. (2008) estimated there are approximately 1.0 long bone fractures per year per 100 people in England. Assuming this is true for Scotland, Northern Ireland and Wales, this would mean that there are approximately 15,000 long bone fracture non-unions in the UK every year. Furthermore, there are some 150,000 wrist, vertebral, and hip fractures due to osteoporosis, annually costing the National Health Service £17 billion (Dawson and Oreffo, 2008; Jordan and Cooper, 2002).

There is a range of treatment options available to orthopaedic surgeons. These are reviewed in §1.1.6.

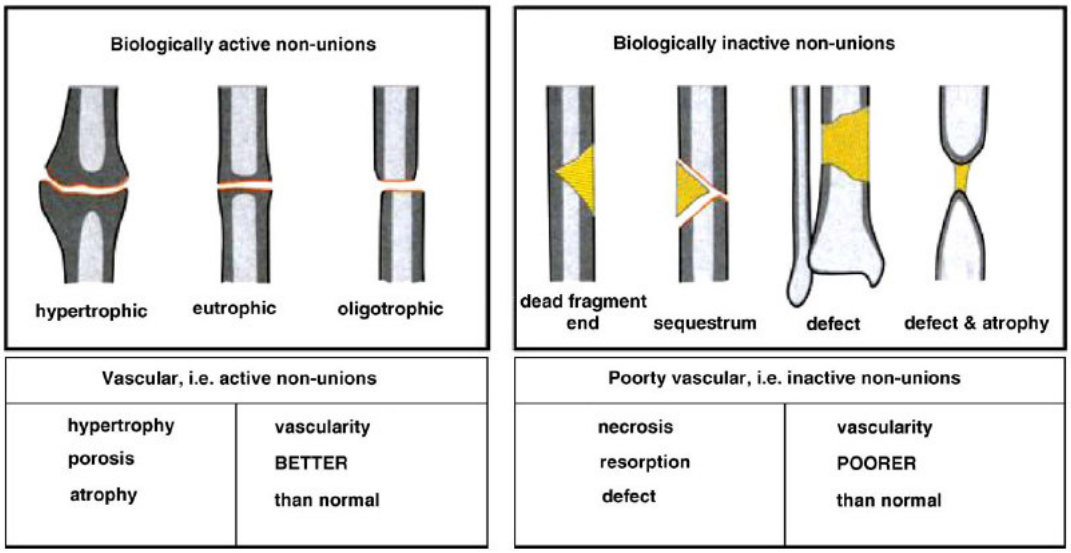

Figure 1.10: The Weber and Cech classification of fracture non-unions.

Both biologically active and inactive non-union classifications are illustrated. (From Olson and Hahn, 2006)

Table 1.1: Risk factors for fracture non-unions.

Risk Factor	References
Patient Effects	
Malnutrition	Phieffer and Goulet, 2006
Smoking	Phieffer and Goulet, 2006
Old Age	Panagiotis, 2005
Cachexia	Panagiotis, 2005
Medication (anti-inflamatories, anticoagulants, and steroids)	Panagiotis, 2005
Diabetes	Perumal and Roberts, 2007
Local Effects	
High Energy Fracture	Phieffer and Goulet, 2006
Open Fracture	Panagiotis, 2005
Infection	Olson and Hahn, 2006
Limitation of Blood Supply	Phieffer and Goulet, 2006
Periosteal Stripping	Phieffer and Goulet, 2006
Burns	Panagiotis, 2005
Radiation	Panagiotis, 2005
Insufficient Mechanical Stability	Frölke and Patka, 2007
Poor Bone Contact	Perumal and Roberts, 2007

1.1.5. Bone Defects

Bone defects are often classified as a subset of biologically inactive fracture non-unions (Weber and Cech, 1976) (see **Figure 1.10**). However, some authors regard them as a separate classification in their own right (Phieffer and Goulet, 2006).

True fracture non-unions result when the normal mechanisms of repair are either compromised or absent. Bone defects commonly occur when large sections of bone are removed during tumour excision, or during the surgical debridement after a high energy fracture (Paley and Maar, 2000).

1.1.6. Current Treatments

1.1.6.1. Stabilisation

All fracture non-unions require adequate fixation, in terms both of alignment and mechanical stability, in order to achieve union. Indeed, as previously stated, this may be the only treatment required in the case of hypertrophic, oligotrophic and stiff atrophic non-unions.

Reamed intramedullary nailing is the most common form of fixation for non-unions with no history of infection. The autologous graft created by the reamer appears to stimulate bone repair (Phieffer and Goulet, 2006). It is also more mechanically stable then intramedullary nailing without reaming. Reamed nailing can yield high success rates. For example Claucey *et al*. (1982) found that out of 48 patients, 46 achieved union without any further treatment.

External fixation is often used where there is a history of infection, or in the case of serious grade-II and -III open fractures. The Ilizarov technique (a type of external fixation) may also be successful in treating non-unions, particularly when other methods of stabilisation have failed, or when correct alignment of the fracture is difficult to achieve (Phieffer and Goulet, 2006). This technique is thought to be particularly useful in the treatment of bone defects (Paley and Maar, 2000).

Although effective stabilisation of the fracture site is a prerequisite for the healing of non-unions, additional biological treatments are often necessary. This is especially true for mobile atrophic non-unions and bone defects. The remainder of this section will focus on the most commonly used biological treatments.

1.1.6.2. Bone Autografts

Autologous bone grafting remains the 'Gold Standard' treatment for the biological problems associated with both fracture non-unions and bone defects (Phieffer and Goulet, 2006; De Long *et al.*, 2007; Sen and Miclau, 2007). Of these techniques, cancellous bone grafting from the iliac crest into the defect site is the most common. Indeed it is the standard to which all biological solutions are usually compared (Sen and Miclau, 2007).

Autografting has been found to have a high success rate. For stabilised atrophic, aseptic non-unions of the long bones, clinical studies report the success rate as being 87 – 100% (Babhulkar *et al.*, 2005; Finkemeier and Chapman, 2002; Goulet *et al.*, 1997). For non-unions with a history of infection, the success rate has been reported as being 53 – 72% after the first operation, and 95 – 100% after further surgical intervention (Cove *et al.*, 1997; Ueng *et al.*, 1999).

Cancellous autografts are thought to be so successful because they are osteogenic, osteoinductive and osteoconductive. Even though the majority of the transplanted cells die shortly after implantation by necrosis due to ischemia or apoptosis, many survive. Among the cells most resistant to ischemia are primitive mesenchymal cells and the progenitors of endothelial cells. The ability of these cells to form new vascularised bone makes autografts osteogenic (Bauer and Muschler, 2000). Autografts also have the ability to attract host MSCs to the defect site and cause them to differentiate into osteoblasts. This is achieved by proteins, such as the BMPs, and other chemotaxic factors which are released from the matrix of the graft (Phieffer and Goulet, 2006). This makes them osteoinductive. Finally, the large surface area of cancellous bone grafts provides an ideal structure on which new bone can form. Hence, they are also osteoconductive (Goldberg and Stevenson, 1987).

Despite the high success rate of the technique, it is not without problems. The supply and quality of donor bone is often limited (Arrington *et al.*, 1996; Hall *et al.*, 1991). There is often substantial bone morbidity at the donor site (Ahlmann *et al.*, 2002; Younger and Chapman, 1989) sometimes leading to pelvic instability or fracture. However, the most common complaint associated with the donor site is pain. Goulet *et al*. (1997) found that 37.9% of patients reported pain six months postoperatively. This dropped to 18.7% two years after surgery. Rarer, but nonetheless serious, complications include; nerve damage (Guha and Poole, 1983), vascular injury including pseudoaneurysm of the pelvic vasculature (Goulet *et al.*, 1997), and small bowel herniation through the donor defect (Arrington *et al.*, 1996).

1.1.6.3. Bone Allografts

Currently the dominant alternative to autografting is the use of allogeneic bone. This is where a patient receives bone tissue from a donor. It can be used either in large structural sections (often called massive bone allografts), or in small cancellous or cortico-cancellous chips (Marsh, 2006).

Massive bone allografts are often used to treat bone defects caused by tumour excision, where there is insufficient material available for bone autografting. They also have an advantage over autografts, as there is no need to harvest bone from the patient. Hence there is no donor site to suffer from morbidity.

The allogeneic bone is usually lyophilised or deep frozen before implantation (Finkemeier, 2002). Allografts can provide mechanical support, and are osteoconductive. They are, however, only weakly osteoinductive. They also lack the cells of autologous grafts, hence they are not osteogenic. This is thought to be the reason why allograft incorporation is slower than of autografts (Bauer and Muschler, 2000).

Allografts of this type, typically have a success rate of approximately 57% after one operation, and 72% after two or more (Donati *et al.*, 2005). Despite this success, they are never fully remodelled by the host. Even five years after surgery, the graft

remains distinguishable from the host bone by the grain of the osteons, and the centre of the graft remains necrotic and acellular (Enneking and Mindell, 1991).

As stated above, allogeneic bone may be prepared as bone chips. After lyophilisation, they too are osteoconductive and provide some mechanical support in compression. They may be used to pack bone defects or to supplement autografts when the supply of autologous bone is limited (Finkemeier, 2002).

As with all transplanted tissue, there is a small risk of disease transmission. This risk is minimised as much as possible by the bone banks that collect the tissue. Members of high risk groups are excluded from becoming donors, as are those who are found to have occult disease during autopsy. The grafts are also screened for HIV, bacterial contamination, syphilis, and hepatitis B and C (Buck and Malinin, 1994).

Allografts inevitably provoke an immune response from the host. Indeed many studies in animals have found that optimum graft incorporation is achieved when histocompatibility differences are minimised or when the grafts are treated to reduce their immunogenicity (Bauer and Muschler, 2000). For example, the immunogenicity of allografts may be reduced by deep-freezing or lyophilisation (Yu *et al.*, 2007). A strong host immune response may lead to the failure of the graft.

Apart from the local effects, sensitisation to an expanded pool of human leukocyte antigen (HLA) may result. Although the production of broadly reactive HLA antibodies may not have a significant effect on the graft itself (Ward *et al.*, 2008), this may make further transplantation of other tissue more difficult (Lee *et al.*, 1997a).

1.1.6.4. Demineralised Bone Matrix

Demineralised bone matrix (DBM) is now widely commercially available in the form of powders, pastes or putties. It is prepared from allogeneic bone which is first crushed or pulverised, before being demineralised in hydrochloric acid, and finally washed in sterile water, ethanol and ethyl ester (Finkemeier, 2002).

Although it offers no mechanical support, DBM is osteoconductive and osteoinductive. This biological activity has been attributed to growth factors and various other proteins which are made available by the demineralisation process (Wildemann *et al.*, 2007; Bae *et al.*, 2006).

DBM, especially when used in conjunction with bone marrow aspirate, can be successful in the treatment of fracture non-union and bone defects (Tiedeman *et al.*, 1995; Lindsey *et al.*, 2006). Although promising, there has been a lack of large scale randomised controlled studies examining the treatment's effectiveness (Finkemeier, 2002). DBM also suffers from all the disadvantages of potential disease transmission and immunogenicity as bone allografts (see §1.1.6.3).

1.1.6.5. Ceramics

Almost all calcium phosphate biomaterials can be classified as polycrystalline ceramics. They are constructs of individual crystals of highly oxidised substances that have been fused together at the grain boundaries by a high temperature process know as sintering (Jarcho, 1981). Both hydroxyapatite (HA) [$Ca_{10}(PO_4)_6(OH)_2$], and tricalcium phosphate (TCP) [$Ca_3(PO_4)_2$] are widely commercially available to orthopaedic surgeons as blocks, powders or cements.

In general, they are osteoconductive, and do not appear to produce an immune response when implanted (Schildhauer *et al.*, 2000). While calcium phosphate ceramics compare favourably to cortical bone in terms of compressive strength, they have poor tensile strength and are very brittle (Jarcho, 1981; Kim *et al.*, 2008). Indeed, when implanted, they need to be protected from shear stresses by fixation (Bucholz *et al.*, 1987).

Although TCP has been used clinically, there are concerns about its unpredictable biodegradation profile. Moreover, TCP biodegradation within bone defects was found not to be routinely accompanied by bone formation (Hollinger *et al.*, 1996).

HA blocks have been successfully used to treat tibial plateau fractures (Bucholz *et al.*, 1989), yielding similar functional outcomes to the autograft control group. However, its brittleness and slow *in vivo* resorption rate have caused concern among clinicians (De Long *et al.*, 2007). Consequently, HA is seldom used alone.

More recently, a composite material of HA, TCP and Type-I and III collagen, has been developed (Collagraft®, Zimmer), which can be combined with autologous bone marrow aspirate. In a prospective, randomized comparison with autologous bone grafting, Chapman *et al.* (1997) reported that it can be effective in the treatment of traumatic bone defects in long bones. After 24 months, union was achieved in 130 of 132 patients for the collagen-ceramic grafts, compared to 122 of 126 for the autograft treatment group. No statistically significant difference between the treatment groups was found. Although initially promising, more data need to be gathered to assess the true efficacy of this bone graft substitute.

1.1.6.6. Recombinant Human Bone Morphogenetic Proteins

As discussed in §1.1.2.3, BMPs are thought to play a crucial part in natural fracture healing. Clinical trials by Govender *et al.* (2002) and Friedlaender *et al.* (2001) were instrumental in the granting of USFDA approval for the application of rhBMP-2 and -7 respectively, for the treatment of delayed and non-union fractures (USFDA, 2004; USFDA, 2001). Both use collagen sponges as delivery systems, and both are now used clinically under the names INFUSE® Bone Graft and OP-1™ Implant.

Nevertheless, some aspects of these trials have been questioned (Sen and Miclau, 2007). The study by Friedlaender *et al.* (2001), compared the rhBMP-7 implant against bone autografting in the treatment of tibial fracture non-unions. The authors found no difference between the groups, and concluded that the rhBMP-7 implant was an effective alternative to autografting. However, reamed intramedullary nailing was used to stabilise all the fractures. As discussed in §1.1.6.1, this technique introduces autologous bone, and possibly BMPs, to the defect site. It is therefore unclear whether it was the surgical procedures or the administered rhBMP-7 that contributed most to healing (Sen and Miclau, 2007). Similar criticisms have been made of other clinical trials using rhBMP-7 such as those of Dimitriou *et al.* (2005).

Govender *et al.* (2002) used both reamed and unreamed nailing in their study. Despite admitting that reaming could make a positive difference to the healing of delayed union fractures, they still used a significantly higher proportion of reamed nailing in the rhBMP-2 groups than the control group.

However, the delivery of rhBMPs and other growth factors may prove to be a powerful strategy for augmenting fracture healing (Simpson *et al.*, 2006). This strategy is currently limited by the lack of a satisfactory delivery system (Dawson and Oreffo, 2008). Hence the development of growth factor delivery systems is an important area of orthopaedic research.

1.2. Regenerative Medicine

1.2.1. Introduction

The need for alternatives for organ transplantation extends beyond the field of orthopaedics. In the UK, as well as many developed countries, the waiting list for kidney, pancreas, heart, lung and liver transplants continues to increase, while the number of donor organs available remains relatively static (NHS, 2008) (see **Figure 1.11**).

The increasing shortfall between the number of patients requiring transplant, and the number of operations performed, has motivated the development of the relatively new field: regenerative medicine. Regenerative medicine has been described as:

"–an umbrella term given to varied strategies of repairing or replacing damaged or diseased tissues." (Petit-Zeman, 2001)

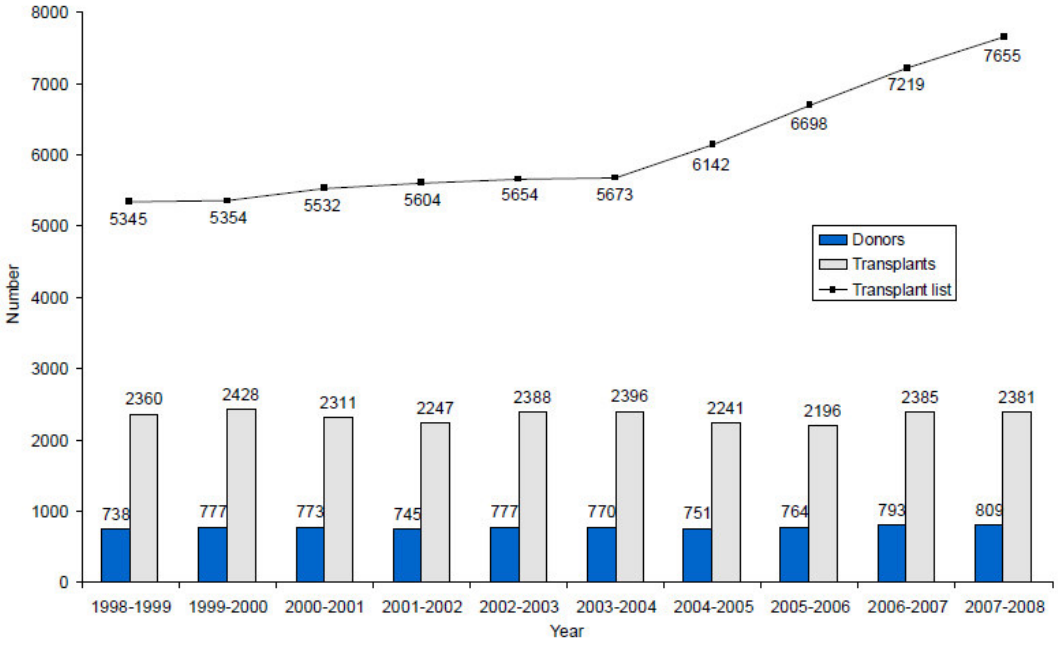

Figure 1.11: UK Transplant and waiting list statistics

The number of deceased donors and transplants in the UK (1st April 1998 – 31st March 2008), and of patients on the active transplant list on 31st March. (From NHS, 2008).

Potential regenerative medical solutions have been investigated for most major organs in the body, including; small intestine (Gupta *et al.*, 2006), trachea (Kobayashi *et al.*, 2006), smooth muscle (Rodriguez *et al.*, 2006), liver and kidney (Leclerc *et al.*, 2006), heart valves (Mendelson and Schoen, 2006), and bone (Fisher and Reddi, 2003). Indeed, since bone has the highest potential for regeneration of any tissue, bone regenerative medicine is expected to form the vanguard of advances in the field (Fisher and Reddi, 2003).

1.2.2. Strategy and Scaffold Design Criteria

It has been stated that successful regenerative medical constructs must comprise three elements: cells, growth factors, and a scaffold (Lavik and Langer, 2004; Fisher and Reddi, 2003; Barron and Pandit, 2003). This strategy has been termed the combined approach (see **Figure 1.12**).

Although in-growth of host cells into a scaffold following implantation is possible (Ellis and Yannas, 1996), in most cases a host or donor derived cell source is necessary (Lavik and Langer, 2004). Several groups have stated that it is critical to create the correct chemical environment for the cells, including growth factors (Babensee *et al.*, 2000; Elisseeff *et al.*, 2001, Kaigler *et al.*, 2003), particularly in the hostile environment of defect sites, where the cells may be further from blood vessels than the oxygen diffusion limit of 100 – 200 μm (Carmeliet and Jain, 2000).

Scaffolds are necessary to act as a delivery system for both the cells and growth factors. They are also essential for providing a tailored environment for the cells (Langer and Vacanti, 1993; Lavik and Langer, 2004). Since the scaffolds are required to act in a multifunctional capacity, their engineering design criteria are very demanding (Lavik and Langer, 2004; Barron and Pandit, 2003; Stock and Vacanti, 2001), namely:

1) Scaffolds must be biocompatible, including being non-toxic, with non-toxic breakdown products.

2) Scaffolds must not produce an adverse effect, such as an immune response, or induce neoplasia.
3) Scaffolds should provide the correct three-dimensional (3D) geometry.
4) Scaffolds should be sufficiently porous such that nutrients can diffuse to the cells, and cell waste products can be removed.
5) Scaffolds should have appropriate surface chemistry to allow cell attachment, proliferation and differentiation.
6) Scaffolds should degrade at a rate comparable to extracellular matrix production.
7) Scaffolds should have the ability to release bioactive growth factors.
8) Scaffolds should have similar mechanical properties to the surrounding tissue to avoid damage to either.
9) Scaffolds should be manufactured in a simple and cost-effective manner.

During the relatively short life of the field of regenerative medicine, a variety of both materials and fabrication methods have been employed to meet as many of the above design criteria as possible. How these materials and methods relate to bone regenerative medicine is discussed in §1.2.5 and §1.2.6.

In the combined approach, the choices of the cell source and of the bioactive compounds released from the scaffolds, are also very important. The options available for bone regenerative medicine are discussed in §1.2.3 and §1.2.4 respectively.

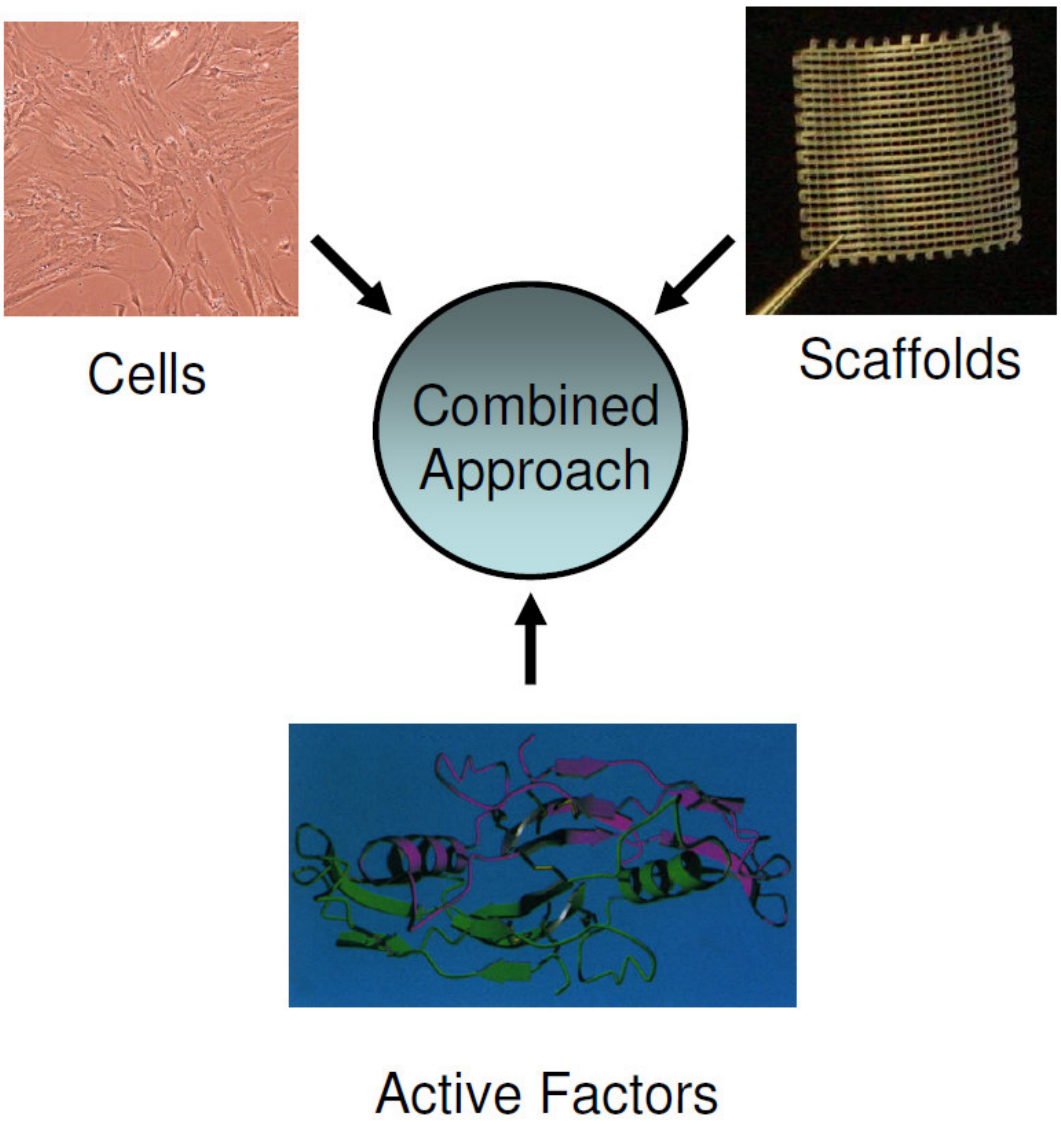

Figure 1.12: The Combined Approach

The combined approach in regenerative medicine utilises cells, active factors, and scaffolds to form regenerative medicine constructs. The active factor represented here is BMP-7 (BMP-7 voxel rendered image from Griffith *et al.* (1996)).

1.2.3. Cell Sources

1.2.3.1. Embryonic Stem Cells

Embryonic stem cells from mice were first isolated in 1981 independently by Martin (1981) and Evans and Kaufman (1981). The dual capacities of mouse embryonic stem cells for unlimited *in vitro* expansion and multilineage differentiation provoked interest in establishing similar cell lines of human origin (Smith, 2001). Human embryonic stem cells (hESCs) were first identified in 1998 (Shamblott *et al.*, 1998; Thomson *et al.*, 1998).

hESCs could have great potential for bone regenerative medical applications. They have already been shown to be capable of forming neo-tissues, including blood vessels which can integrate with the blood vessels of the host (Levenberg *et al.*, 2002). Theoretically they could provide an almost unlimited source of cells, in marked contrast to either autologous adult stem cells or differentiated cells (Levenberg *et al.*, 2003). hESCs can also undergo osteogenic differentiation in a similar way to MSCs (Tremoleda *et al.*, 2008).

However, there are problems in using hESCs clinically. Apart from ethical considerations, it is necessary to ensure that the cells are successfully differentiated before implantation. Failure to do this could result in teratoma formation (Smith, 2001). For a therapy based on hESCs to be approved by the USFDA, it would need to be demonstrated that the number of partially differentiated or undifferentiated cells is below an as yet undefined threshold (Baker, 2008). However, the USFDA has recently approved the use of hESCs in a Geron funded clinical trial to investigate their potential in the treatment of spinal cord injury (Pollack, 2009). Nevertheless there are numerous technical challenges to be overcome in the development of this technology.

1.2.3.2. Induced Pluripotent Stem Cells

Induced pluripotent stem cells (iPSCs) may provide an alternative cell source for regenerative medicine in the future. These cells can be created by retrovirus-

mediated induction of four transcription factors (Oct3/4, Sox2, c-Myc, and Klf4) of adult fibroblasts (Takahashi and Yamanaka, 2006). These cells have many of the properties of embryonic stem cell including proliferative capacity, teratoma formation, and the ability to form adult chimaeras (Okita *et al.*, 2007).

Ultimately, iPSCs may prove to be a superior alternative to hESCs. Since they could be formed from patients' own somatic cells, the ethical problems with hESCs, as well as the possibility of immune rejection, could be overcome (Okita *et al.*, 2007). However, human iPSCs have only recently been produced (Park *et al.*, 2008), and further work needs to be undertaken before this cell source can be used clinically.

1.2.3.3. Marrow Stromal Cells

1.2.3.3.1. General Properties

Cell sources for regenerative medical applications must strike a balance between ethical issues, safety and efficacy (Langer and Vacanti, 1993). For orthopaedic regenerative medicine, the cells must have high osteogenic potential, and should be easily expanded and maintained *in vitro* for long periods of time, in order to produce a therapeutically relevant number of cells. Taking these requirements into account, hMSCs are thought to be a promising potential solution (Salgado *et al.*, 2006; Ringe *et al.*, 2002; Jorgensen *et al.*, 2004a), particularly as they are involved in the process of normal fracture healing, as discussed in §1.1.2.1.

Marrow stromal cells have alternatively been termed mesenchymal stem cells and mesenchymal stromal cells, all with the acronym MSC. They are capable of differentiating along the mesenchymal (adipocytic, osteoblastic and chondrocytic) lineages (Pittenger *et al.*, 1999, Keating, 2006). To varying degrees, they are also capable of neuronal (Sanchez-Ramos *et al.*, 2000), hepatic (Weng *et al.*, 2003), and myocytic (Toma *et al.*, 2002) differentiation.

These multipotent cells are commonly isolated from bone marrow (Beresford *et al.*, 1994), but similar cells can also be isolated from adipose tissue (Zuk *et al.*, 2002), and umbilical cord (Sarugaser *et al.*, 2005). In particular, the osteogenic potential of

bone marrow derived hMSCs has been well characterised (Liao *et al.*, 2008). There are, however, a number of concerns regarding their use in clinical therapies.

1.2.3.3.2. Characterisation

Research into hMSCs biology has been impaired by the lack of a universally acknowledged characterisation protocol. In part this is due to the lack of a specific surface marker (Horwitz *et al.*, 2005). hMSC characterisation is further complicated by the heterogeneous nature of hMSC cultures (Sengers *et al.*, 2010).

Since hMSCs are relatively rare cells in bone marrow, they would need to undergo considerable *in vitro* amplification in order to achieve sufficient numbers. Some studies have demonstrated that a subset of fibroblast colony-forming cells (CFU-F) isolated from bone marrow, are capable of generating bone from a single cell when transplanted *in vivo* (Kuznetsov *et al.*, 1997; Muraglia *et al.*, 2000; Sacchetti *et al.*, 2007). However, it is thought that their ability to proliferate and differentiate is progressively lost over time *in vitro* (McCulloch *et al.*, 1991; Banfi *et al.*, 2000; Gregory *et al.*, 2005). This may be due to different sub-populations contributing at different degrees to the population-level phenotype emerging over time and passage (Sengers *et al.*, 2010).

Therefore, for studies aimed at investigating hMSC biology, characterisation of the cells is important. Apart from plastic adherence and the ability to undergo osteogenic, chondrogenic and adipogenic differentiation, expression of surface markers is also thought to be important.

The surface marker Stro-1 has been found to be associated with CFU-F in human bone marrow (Simmons and Torok-Storb, 1991). Selecting for Stro-1 positive cells in bone marrow aspirates has been found to increase the proportion of CFU-F isolated, and the proportion of cells able to undergo osteogenic differentiation (Gronthos *et al.*, 1994; Howard *et al.*, 2002). Stro-1 positive cells from bone marrow have also been found to be relatively undifferentiated (Stewart *et al.*, 1999). Stro-1 has, therefore, been used to characterise MSCs in a number of studies (Wang *et al.*, 2003; Tuli *et al.*, 2003; Coipeau *et al.*, 2009; Zhang *et al.*, 2009).

Another surface marker of interest in MSC characterisation is CD105. A common source of contamination in MSC cultures are cells of haematopoietic origin. CD105 is thought to be expressed by MSCs, but not cells of the haematopoietic lineage (Haynesworth *et al.*, 1992b), furthermore CD105 expression is thought to disappear upon differentiation (Barry *et al.*, 1999; Goussetis *et al.*, 2005). CD105, also called endoglin, is thought to form part of the TGF-β signalling system (Cheifetz *et al.*, 1992). It is, however, not specific to MSCs, as it has also been detected in endothelial cells (Gougos and Letarte, 1990). Nevertheless, in conjunction with other markers, CD105 has been widely used in characterisation processes for MSCs (Keating, 2006; Meinel *et al.*, 2004; Kotobuki *et al.*, 2005; Harting *et al.*, 2008; Liu *et al.*, 2008a).

The surface marker CD73 has also been found on MSCs (Barry *et al.*, 2001). Early studies indicated that antibodies for CD73 (SH-3 and SH-4) were specific for MSCs, and did not react with other cells present in the bone marrow, including cells of the haematopoietic lineage (Haynesworth *et al.*, 1992a). However, CD73 is thought to be expressed by a number of cell types, including lymphocytes (Yamashita *et al.*, 1998). CD73 has also been widely used in characterisation processes for MSCs (Dominici *et al.*, 2006; Liu *et al.*, 2008a; Harting *et al.*, 2008; Coipeau *et al.*, 2009).

CD90, alternatively called Thy-1, is another surface marker thought to be expressed by MSCs, indeed it is one of the surface markers specified by the International Society for Cellular Therapy in their definition of MSCs (Dominici *et al.*, 2006). CD90 expression has also been found to correlate with the proliferative potential of MSCs (Campioni *et al.*, 2008). The expression of this surface marker is, however, not restricted to MSCs, as it is also expressed by hepatic progenitor cells (Masson *et al.*, 2006), and neurons in humans (Kemshead *et al.*, 1982). CD90 has also been widely used in characterisation processes for MSCs (Dominici *et al.*, 2006; Harting *et al.*, 2008; Liu *et al.*, 2008a; Campioni *et al.*, 2009).

The surface marker CD34, also called MY10, is thought to be expressed by haematopoietic progenitor cells (Civin *et al.*, 1984; Katz *et al.*, 1985). HLA-DR is also expressed by haematopoietic progenitor cells (Civin *et al.*, 1987), as well as the more mature myeloid and erythroid progenitors (Robinson *et al.*, 1981). CD45, also called leukocyte-common antigen is thought to be expressed by B- and T-lymphocytes (Kincade, 1987; Hathcock *et al.*, 1992; Lefrancois and Goodman, 1987; Spickett *et al.*, 1983), and endothelial cells (Forsyth *et al.*, 1993). It is, therefore, generally recognised that MSCs should lack CD34, CD45 and HLA-DR expression (Dominici *et al.*, 2006). These markers have been used in studies characterising MSCs to test for the presence of cells of the haematopoietic lineage (Kotobuki *et al.*, 2005; Campioni *et al.*, 2006; Liu *et al.*, 2008a).

The surface marker CD14 is thought to be expressed on a number of cell types including; macrophages, monocytes, polymorphonuclear neutrophils, chondrocytes, dendritic cells and B-lymphocytes (Tobias and Ulevitch, 1993; Verhasselt *et al.*, 1997; Schumann *et al.*, 1994). CD11b is thought to be expressed on monocytes, granulocytes, macrophages and natural killer cells (Coxon *et al.*, 1996; Ding *et al.*, 1999; Solovjov *et al.*, 2005). CD79 is thought to be expressed on B-cells (Mason *et al.*, 1992). CD19, also termed B4 antigen, is also thought to be expressed on B-cells and dendritic cells (Nadler *et al.*, 1983; Tedder and Isaacs, 1989). Hence, MSCs are thought to lack any of these markers (Dominici *et al.*, 2006), and have been used to test for the presence of cells of the haematopoietic lineage (Liu *et al.*, 2008a; Sudres *et al.*, 2006; Mansilla *et al.*, 2006).

Recently, the International Society for Cellular Therapy attempted to ameliorate the situation by publishing minimum criteria for defining hMSCs (Dominici *et al.*, 2006);

1) Plastic-adherent under standard culture conditions.
2) Express CD105, CD73, and CD90. Lack CD45, CD34, CD14 or CD 11b, CD79 or CD19, and HLA-DR.
3) Differentiate into osteoblasts, adipocytes and chondroblasts *in vitro*.

It should be noted, however, that MSC characterisation is an evolving field of research, and that other markers such as Stro-1, may be included in future attempts to define MSCs, whereas other markers may ultimately prove to be less important.

1.2.3.3.3. Application in Regenerative Medicine

Outwith the issues associated with hMSC isolation, there are other potential problems connected to hMSC expansion in culture. Currently, hMSCs are routinely cultured in media containing foetal calf serum (FCS). This carries the risks of prion and zoonotic transmission, as well as the possibility of activation of the host immune system by the introduction of foreign molecules (Lepperdinger *et al.*, 2008).

Alternatives to FCS are currently being tested, including freshly frozen plasma and platelets, and human platelet lysate (hPL). Recent studies comparing hPL to FCS, have found that hPL enhances proliferation without changing morphology, immunophenotype or differentiation capacity, and does not induce any obvious genetic abnormalities (Doucet *et al.*, 2005; Lange *et al.*, 2007).

It is also feared that hMSCs may undergo spontaneous transformation during the expansion process. This concern is mostly based on the rapid accumulation of chromosomal abnormalities in cultures of murine MSCs, resulting in sarcoma formation when implanted (Miura *et al.*, 2006). However, this has not been reported to be the case for hMSCs (Bernardo *et al.*, 2007). Although transformation of hMSCs is thought to be an exceptional event, the matter is still debated (Lazennec and Jorgensen, 2008).

Of all the cell sources currently being considered for bone regenerative medicine, hMSCs are possibly the closest to being used therapeutically. Bone marrow aspirates, containing hMSCs, have been used to treat fracture non-unions by injecting them at the defect site (Goel *et al.*, 2005; Hernigou *et al.*, 2005). Indeed, Hernigou *et al.* (2005) found that the efficacy of the treatment was related to the number of progenitor cells injected. hMSCs have also been successfully used in other branches of regenerative medicine, including the repair of a human trachea (Macchiarini *et al.*,

2008). They are, therefore, the current cell of choice for bone regenerative medical applications.

Direct injection of hMSCs is, however, not the preferred option in bone regenerative medicine. As discussed previously in §1.2.2, cells are thought to perform best when supported on scaffolds (Stock and Vacanti, 2001): providing the cells with the correct 3D geometry and retaining the cells at the defect site. Co-delivery with bioactive factors is also thought to be desirable to provide the correct chemical environment (Babensee *et al.*, 2000). The various options available in bone regenerative medicine in terms of active factors and scaffolds are discussed in §1.2.4 and §1.2.5 respectively.

1.2.4. Bioactive Compounds

1.2.4.1. Growth factors

As discussed in §1.1.2, growth factors perform important functions during the normal processes of fracture healing. As a consequence, they are thought to have the potential to increase greatly the efficacy of regenerative medical constructs.

Due to their importance in normal fracture healing (§1.1.2.3), and their approval for use in a clinical setting (§1.1.6.6), rhBMP-7 and particularly rhBMP-2 have been used to augment the osteogenic capacity of a large number of potential regenerative medical constructs. When used in animal bone defect models, rhBMP-2 has been found to improve bone mineralisation and repair significantly (Chen *et al.*, 2007; Schmoekel *et al.*, 2005; Kamakura *et al.*, 2004). Similar results have been observed for rhBMP-7 (Donati *et al.*, 2008; Springer *et al.*, 2005; Makino *et al.*, 2005). Both these growth factors show great potential in bone regenerative medical applications.

The role of the five TGF-β isoforms in normal fracture healing is briefly reviewed above (§1.1.2.4). Although most often used for cartilage regenerative medical applications, rhTGF-β1 has been used in preclinical studies and was found to promote scaffold bone in-growth (Vehof *et al.*, 2002; Szivek *et al.*, 2005). While ineffective on its own, rhTGF-β3 was found to enhance ectopic bone formation

within a scaffold in a rat model, when combined with rhBMP-2 (Simmons *et al.*, 2004). In general, it seems that the TGF-β isoforms have potential for bone regenerative medicine, especially in combination with other osteoinductive growth factors.

The roles of other growth factors, such as FGF and VEGF, in normal fracture healing are outlined in §1.1.2.5. They have also been the subject of preclinical studies.

Of the FGF family, FGF-2 is thought to be particularly potent. Studies involving the delivery of rhFGF-2 to rabbit, beagle dog and baboon fracture models have shown increases in callus volume and mineral content, MSC proliferation, and final mechanical bone strength (Kato *et al.*, 1998; Nakamura *et al.*, 1998; Radomsky *et al.*, 1999).

The therapeutic potential of rhVEGF has been examined in animal fracture models. Recently it has been found to increase the number of blood vessels at the fracture site (Kleinheinz *et al.*, 2005), and to help unite fracture non-union models (Eckardt *et al.*, 2005).

There are, therefore, several growth factors which are capable of a number of *in vivo* functions. rhBMP-2 and -7, however, remain the only growth factors licensed by the USFDA for use in cases of open fracture and fracture non-union. The most successful regenerative medical constructs are likely to employ a number of different active factors working in synergistic combination (Cartmell, 2008).

1.2.4.2. Other Active Factors

Recently, *in vitro* studies have led to a number of non-protein based active factors being considered for possible bone regenerative medical applications.

Bisphosphonates, also called diphosphonates, are known to suppress osteoclast mediated bone resorption (van Beek *et al.*, 1999). Hence, their therapeutic potential for the treatment of bone diseases has been examined. Zoledronate has been used to stabilise orthopaedic implants in osteoporotic rats (Peter *et al.*, 2006), and has been

found to improve bone ingrowth into scaffolds in a canine fracture model (Tanzer *et al.*, 2005).

Cathepsin K is the most abundant cysteine protease expressed by osteoblasts, and is thought to be necessary for osteoclast bone resorption. Cathepsin inhibitors are, therefore, thought to be promising future drugs for the treatment of a number of bone diseases such as osteoporosis (Wang and Bromme, 2005; Stoch and Wagner, 2008). The *in vivo* activity of cathepsin inhibitors released from scaffolds has yet to be demonstrated.

1,25-dihydroxyvitamin D_3 is known to play a key role in calcium and bone homeostasis. It is also active in muscle tissue, the cardiovascular system, the immune system, and may also play a role in cancer suppression (Bouillon *et al.*, 2008). *In vitro*, it is capable of inducing osteoblastic differentiation of hMSCs (Zhou *et al.*, 2006). The osteogenic effects of $1,25(OH)_2D_3$ may be further enhanced by the addition of TGF-β (Bosetti *et al.*, 2007; Liu *et al.*, 1999).

Hence, $1,25(OH)_2D_3$ has become a promising active factor for bone regenerative medical applications. Indeed a recent study, used critical-sized intercalated bone defects in rabbit femurs, to test scaffolds loaded with $1,25(OH)_2D_3$ (Yoon *et al.*, 2007). After 10 weeks, the bony callus had increased more than 80% for the $1,25(OH)_2D_3$ loaded group, compared to 40% with the scaffold alone.

As discussed above, a number of non-protein based active factors are of interest in the field of bone regenerative medicine. Potentially they could prove to be superior to growth factors, both in terms of cost, and their ability to maintain their bioactivity in harsher biochemical environments. They are, however, largely untested in animal fracture models.

1.2.5. Scaffold Materials

1.2.5.1. Ceramics

Ceramics, such as HA and TCP, are a widely used class of biomaterials. Scaffolds made from these materials are commercially available, and are used clinically. They are discussed above in §1.1.6.5.

Hench *et al.* (1971) were the first to develop another class of ceramics for use in orthopaedic surgery, which was found to be capable of bonding to bone *in vivo*, without becoming surrounded with scar tissue. This was a soda lime phosphosilicate glass, termed Bioglass 45S5®, consisting of; 45% silicon dioxide, 24.5% sodium oxide, 24.5% calcium oxide and 6% phosphorous dioxide. It has USFDA approval as a middle ear prosthesis, and as an implant for the maintenance of the endosseous ridge. It has also been reported that it is capable of up-regulating genes associated with osteogenic differentiation in human osteoblasts (hOBs), including; ALP, Type-I collagen, osteopontin, osteocalcin and Runx2 (Jell and Stevens, 2006).

Bioglasses have therefore been suggested potential materials for bone regenerative medical applications (Bosetti and Cannas, 2005; Dorea *et al.*, 2005).

1.2.5.2. Natural Polymers

A number of natural materials are now available for use in bone regenerative medicine. In general, they have the advantage of being bioactive, biocompatible and biodegradable. There are, however, common disadvantages including the difficulty in altering their chemical and mechanical properties, as well as their degradation rates (Dawson *et al.*, 2008). Some of the most commonly used natural polymers in bone regenerative medicine are described below.

1.2.5.3. Alginate

Alginate is an anionic copolymer of β-D-mannuronic acid and α-L-guluronic acid residues, extracted from brown algae (see **Figure 1.13a**). Chain length varies depending on the species used as the source, for example varying from 80 kDa in *Azotobacter vinelandii* to 290 kDa in *Pseudomonas aeruginosa* (Martinsen *et al.*,

1991). It can be dissolved in aqueous solutions of sodium chloride. Monovalent cations and magnesium ions do not induce gelation, however divalent cations such as strontium, barium and calcium induce gelation of sodium alginate (Clark and Ross-Murphy, 1987). This is primarily achieved by the exchange of sodium ions from the α-L-guluronic acid residues with the divalent cations, and the formation of "egg-box" structures (Rees, 1981). The alginate chains can then dimerise, causing the formation of gel networks (Rees and Welsh, 1977) (see **Figure 1.13b**). The mechanical properties of the resulting gels vary depending on the proportion and relative positions of β-D-mannuronic acid and α-L-guluronic acid residues. Higher proportions of α-L-guluronic acid residues adjacent to each other, producing the stiffest gels (Smidsrød, 1973).

Alginate has been used to deliver bioactive growth factors in regenerative medical applications (Simmons *et al.*, 2004; Mierisch *et al.*, 2002). However, since alginate can inactivate growth factors such as TGF-β1 through charge interactions, additives such as polyacrylic acid may be necessary (Mumper *et al.*, 1994). Since mammalian cells do not have receptors for alginate polymers, cellular interaction and adhesion are relatively poor. To a certain extent, this can be alleviated by the covalent attachment of the fibronectin-derived adhesion peptide arginine glycine aspartic acid (RGD) (Augst *et al.*, 2006).

When used in *in vivo* studies, alginate has been found to be biodegradable and to elicit little in the way of tissue reaction (Wee and Gombotz, 1998). Calcium alginate gels do not degrade by hydrolysis, but are thought to degrade enzymatically or by the action of chelating agents (Perka *et al.*, 2000). However, like all hydrogels, alginate's mechanical properties are thought to be insufficient for use alone in bone regenerative medicine.

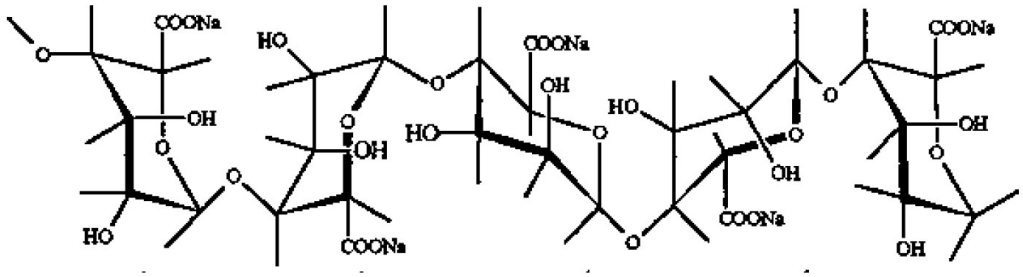

a)

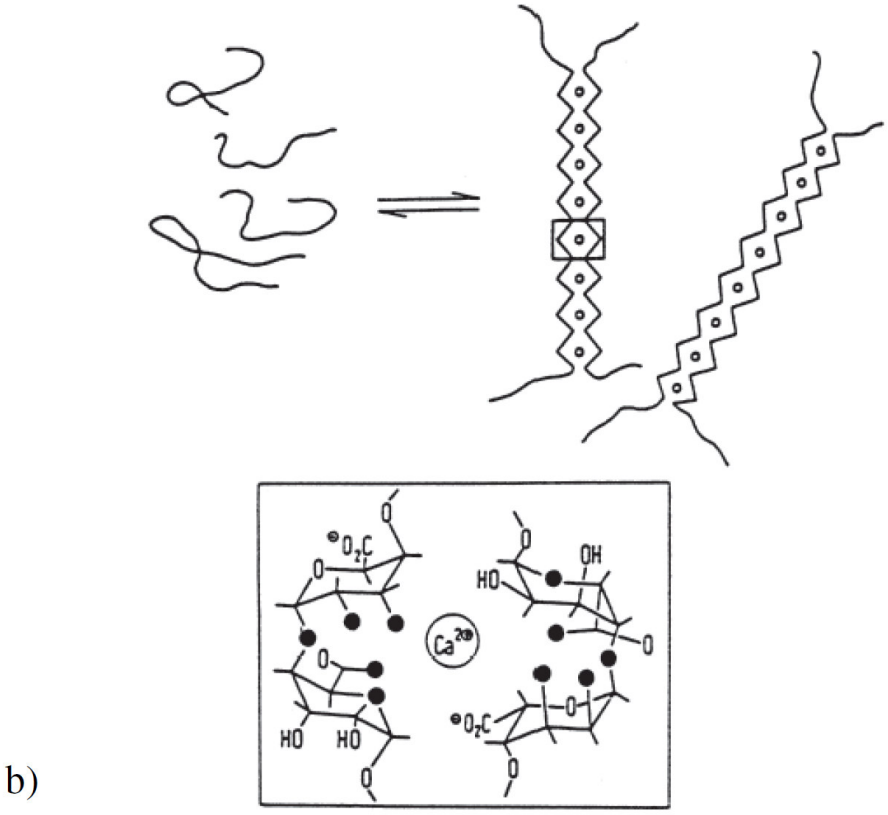

b)

Figure 1.13: Chemical structure of alginate.

Figure a) shows the chemical structure of alginate polymer chains (adapted from Phillips *et al.* (1990)). Figure b) shows the chemical interaction between alginate polymer chains upon gelling, via the interaction of Ca^{2+} ions with α-L-guluronic acid residues (adapted from Rees *et al.* (1981)).

1.2.5.4. Chitosan

Chitosan is a cationic aminopolysaccharide, composed of glucosamine and N-acetyl glucosamine linked in a β(1-4) manner; the glucosamine/ N-acetyl glucosamine ratio being referred to as the degree of deacetylation (Di Martino *et al.*, 2005) (see **Figure 1.14b**). It is manufactured by deacetylating chitin (see **Figure 1.14a**). Interestingly, cell adhesion has been found to correlate with the degree of deacetylation of the chitosan (Mao *et al.*, 2004). Chitosan is able to be degraded by lysozyme by hydrolysis, and the rate of degradation is thought to be affected by the degree of deacetylation (Hirano *et al.*, 1989). It is, therefore, biodegradable (Dhanikula and Panchagnula, 2004).

The deacetylation enables chitosan to dissolve in aqueous solutions with a low pH, which is facilitated by the protonation of the amino groups (Di Martino *et al.*, 2005). Hydrogels of chitosan can be formed in a number of different ways, however the two most important methods for regenerative medical applications are formed by pH changes or ionic crosslinking (see **Figure 1.14c**). If the solution is neutralised, chitosan becomes insoluble, causing the tangling of the polymer chains, forming a gel (Berger *et al.*, 2004b). Alternatively, a species of anion may be added, such as tripolyphosphate (TPP) forming ionically crosslinked networks (Berger *et al.*, 2004a). This induces the chains to bond together by the electrostatic interactions between the amino groups and the polyanions (Shu and Zhu, 2002).

Chitosan is particularly useful in cartilage regenerative medicine because of its structural similarity to, and interaction with, a variety of glycoaminoglycans. It is also thought to be biocompatible (VandeVord *et al.*, 2002). When used for bone regenerative medical applications, it is frequently used in combination with calcium phosphate (Zhang *et al.*, 2003b). Like alginate, its principal function in regenerative medicine is often to deliver bioactive growth factors (Lee *et al.*, 2004b; Mattioli-Belmonte *et al.*, 1999).

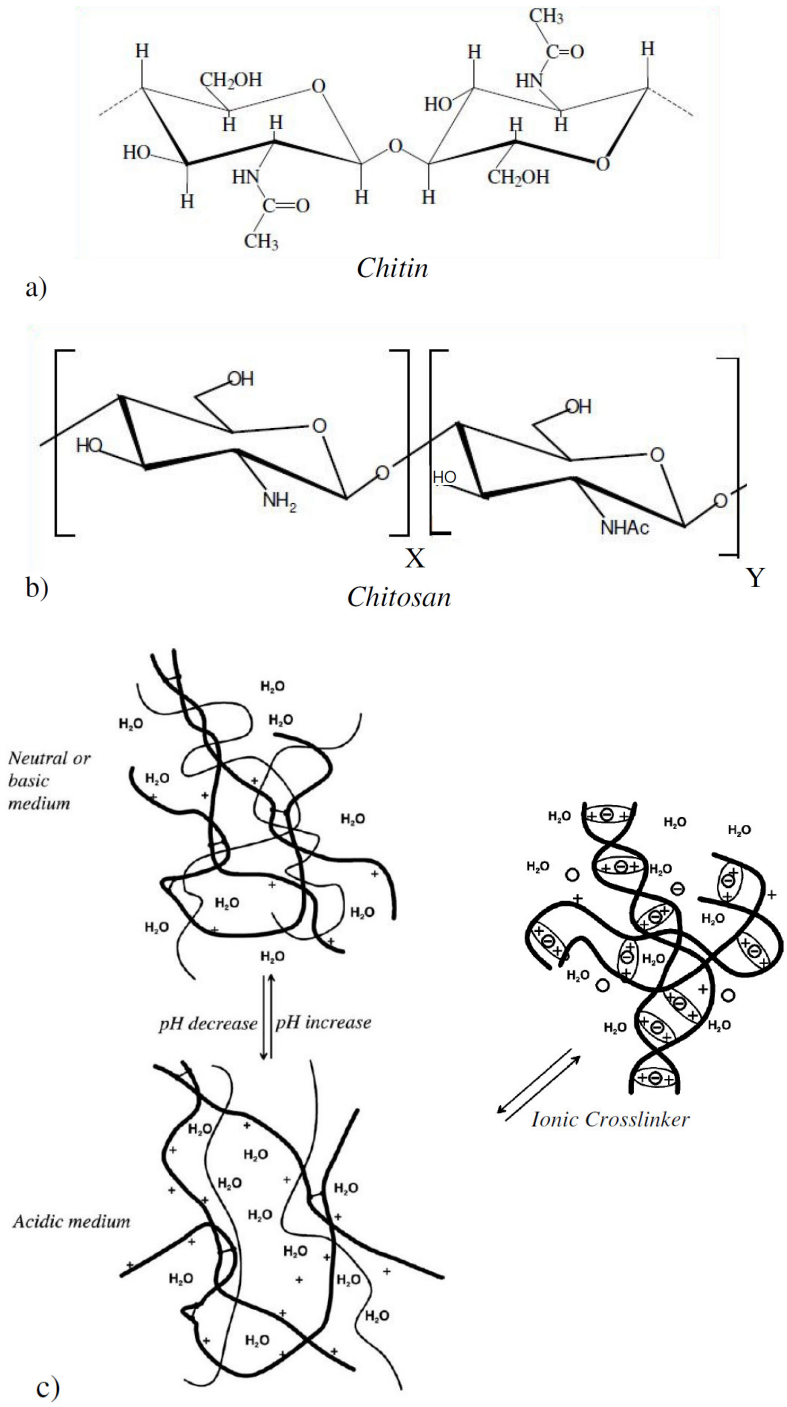

Figure 1.14: Chemical structures of chitin and chitosan.

Figure a) shows the chemical structure of chitin. Figure b) shows the chemical structure of chitosan (adapted from Di Martino *et al.* (2005)). Figure c) shows the charge interactions involved in chitosan gelation, either by increases in pH, or by the addition of an ionic crosslinker (adapted from Berger *et al.* (2004b)).

1.2.5.5. Collagen

Collagens are abundant in mammalian extracellular matrix (ECM), indeed they comprise approximately 25% of the total protein mass in most mammals (Drury and Mooney, 2003). There are at least 19 types of collagen, however Type-I is most commonly used in bone regenerative medical applications, as it makes up the majority of the organic component of bone (Baron, 1996).

Type-I collagen chains, which are approximately 1000 residues in length, are capable of self-assembly to form triple helices (see **Figure 1.15a**) which in turn aggregate to form fibrils which again in turn bond together to form fibres (Piez, 1984; Vitagliano *et al.*, 1995; Brodsky and Ramshaw, 1997). The collagen chains are formed from repeating sequences of glycine-X-Y, where X and Y are frequently proline and hydroxyproline (Hofmann *et al.*, 1980). Glycine is thought to repeat, as it is the only residue capable of fitting in the interior of the helix (Stryer, 1995). On the ends of the chains, there are 9 – 25 residues, which are thought to play a role in the formation of fibrils from triple helices (Helseth and Veis, 1981) (see **Figure 1.15b**). Although hydrogen bonding is absent from within the chains, in the triple helix, the different chains are held together by hydrogen bonds (Stryer, 1995).

Fibrillogenesis occurs both *in vivo* and *in vitro*. The length of the fibrils is approximately 67 nm in length, however the diameters have been found to vary (Chapman, 1989).

One common approach for using Type-I collagen for regenerative medical applications is to prepare it as a gel. Collagen fibres and fibrils may be decomposed using acetic acid, to produce small aggregates of collagen monomers dispersed in the acid solution (Rajan *et al.*, 2006; Achilli and Mantovani, 2010). These aggregates are capable of self-assembly at pH 7, forming fibrils (Silver *et al.*, 2003). There is, however, a loss of structural organisation which leads to relatively poor mechanical properties, making it unsuitable for regenerative medical applications without support (Atala and Lanza, 2002).

Type-I collagen has a number of favourable properties. It is non-antigenic (once purified), biodegradable and bioreabsorbable, biocompatible, and is synergistic with many bioactive compounds (Itoh *et al.*, 2001b; Lee *et al.*, 2001). Unlike the majority of hydrogels, most cells have receptors for collagen and can easily adhere to it. Indeed there is some evidence that Type-I collagen specific binding mediates the osteogenic response of hMSCs (Yang *et al.*, 2004; Mizuno *et al.*, 2000). In contrast, many other hydrogels are used as post-operative adhesion barriers (West *et al.*, 1996).

Collagen may be treated using a variety of methods to make it suitable as part of an regenerative medical construct. These include crosslinking with glutaraldehyde, formaldehyde or carbodiimide, or by physical treatments such as UV-radiation, drying or heating (Drury and Mooney, 2003). It is capable of releasing bioactive growth factors, and is currently used clinically to deliver rhBMP-2 and -7, as discussed in §1.1.6.6.

As a biomaterial, collagen does also have disadvantages. It is relatively expensive, and has relatively poor mechanical properties (Lee and Mooney, 2001). The use of chemical crosslinking agents may also be unsuitable for regenerative medical applications, due to their high toxicity. Any residual crosslinking agent release could have detrimental effects on the surrounding tissue (van Luyn *et al.*, 1992). These problems may be partially overcome by using collagen in combination with other biomaterials.

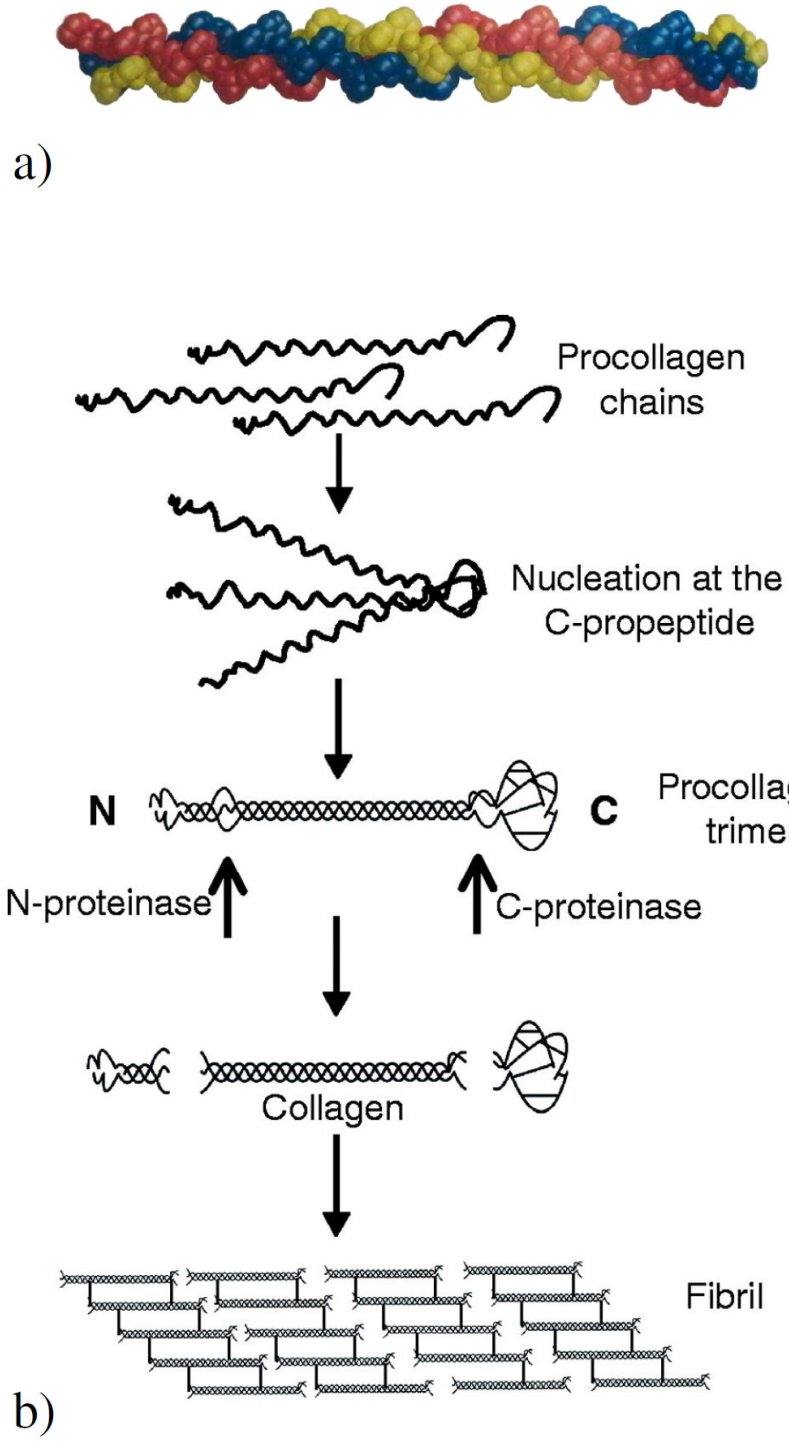

Figure 1.15: Type-I collagen structure.

Figure a) shows a space-filling model of the collagen triple helix. The three strands are shown in different colours (from Stryer 1995). Figure b) shows the hierarchy of collagen structure (Canty and Kadler, 2005).

1.2.5.6. Gelatin

There are two types of gelatin; both are produced by denaturing collagen. Type-A involves acid treatment of the collagen, followed by thermal denaturation. Type B is denatured using a base (Lee and Mooney, 2001). In both cases, the triple helix ordered structure is broken down into random single strands. It is also interesting to note that the mechanical properties of gelatin have been related to the degree of renaturation, *i.e.* the triple helix content (Bigi *et al.*, 1998).

Aqueous solutions can be formed by heating above 40°C. Gels can then easily be formed by cooling or drying the solution. On gelling, the gelatin molecules undergo a conformational disorder-order transition and partly regenerate the collagen triple-helix structure (Pezron *et al.*, 1991; Ross-Murphy, 1992). In this case, thermoreversible networks are formed, with the helices being held together by hydrogen bonds in the junction zones (Bigi *et al.*, 2004). Although chemically similar, gelatin gels are less stable than collagen gels as not all the strands undergo renaturation. This problem can be alleviated by covalent crosslinking with substances such as glutaraldehyde (Bigi *et al.*, 2001), however, as with collagen, these substances may be unsuitable for regenerative medical applications due to residual toxicity (van Luyn *et al.*, 1992).

Gelatin retains the biocompatibility of the original collagen and is capable of releasing bioactive growth factors. Hence it has been used in a number of potential regenerative medical growth factor delivery systems (Liu *et al.*, 2007; Kempen *et al.*, 2008; Komura *et al.*, 2008).

The major disadvantage of gelatin for bone regenerative medicine is its poor mechanical properties (Lee and Mooney, 2001). Therefore, gelatin is usually used alongside other biomaterials.

1.2.5.7. Synthetic Polymers

In bone regenerative medicine, the most commonly used synthetic polymers are; poly(lactic acid) (PLA), poly(glycolic acid) (PGA), and their co-polymer

poly(lactide-co-glycolide) (PLGA) (Sokolsky-Papkov *et al.*, 2007). Poly(ε-caprolactone) (PCL) is also thought to be a promising biomaterial (Hutmacher, 2000). For their chemical structures, see **Figure 1.16**.

With synthetic polymers, there is considerable scope for altering their physical properties such as; mechanical properties, surface and bulk chemistry, and degradation rate (Dawson *et al.*, 2008). Synthetic polymers experience less batch variation than natural polymers, and are often easier to purify and sterilise. However, synthetic polymers are often less biocompatible than their natural counterparts, and have the potential to release harmful breakdown products on degradation.

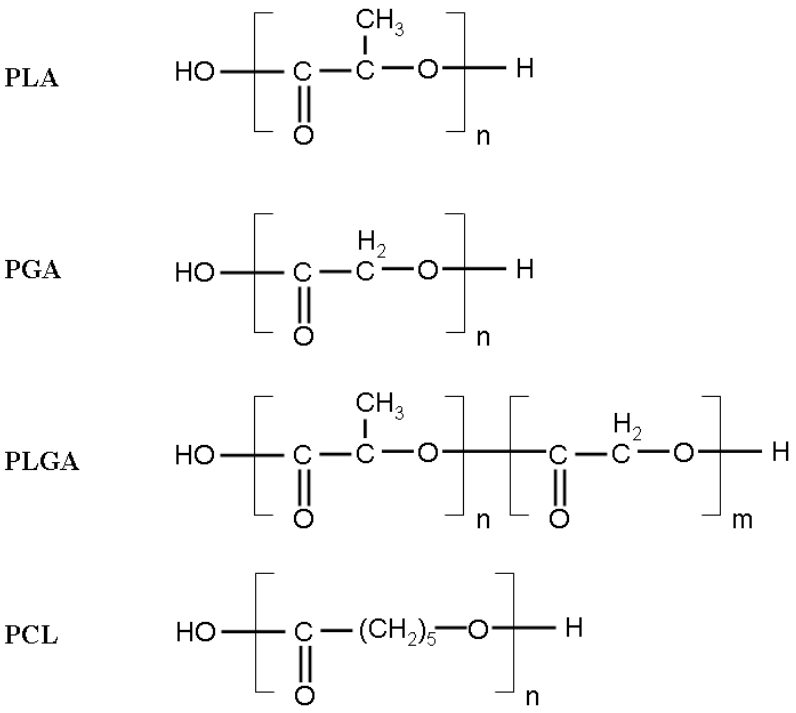

Figure 1.16: The chemical structures of PLA, PGA, PLGA and PCL.

The structural formulae of PLA, PGA, PLGA and PCL. Each of the polymers is made up of repeating units, indicated by the parenthesise, which occur at frequencies n and m.

1.2.5.8. Poly(ε-caprolactone)

PCL is a biocompatible, bioresorbable, semicrystaline, aliphatic polyester (Hutmacher *et al.*, 2001). It is relatively hydrophobic, caused by the long saturated carbon chains in the molecules (see **Figure 1.16**). When fabricated into regenerative medical scaffolds, the compressive modulus and yield strength values have been reported as ranging from 52 – 67 MPa and 2.0 – 3.2 MPa respectively, lying within the lower range of properties for human trabecular bone (Williams *et al.*, 2005).

PCL degrades by hydrolysis under physiological conditions (Pitt *et al.*, 1981), although it can also be degraded enzymatically (Pitt *et al.*, 1984). In addition, it has been found that fragments of PCL can be degraded intra-cellularly by macrophages (Woodward *et al.*, 1985). However, the *in vivo* degradation time has been found to be of the order of two years (Ma *et al.*, 2006), although the addition of other polymers with higher degradation rates has been found to shorten the degradation time (Middleton and Tipton, 2000).

As PCL has a glass transition temperature of approximately -60°C, and a melting point of approximately 60°C, at physiological temperatures it exists in a "rubber-like" state (Engelberg and Kohn, 1991). This is thought to increase the permeability of PCL, enabling the diffusive release of many therapeutic drugs (Pitt *et al.*, 1987).

Because of the relative ease with which it can be processed into regenerative medical scaffolds, it has been used as the base for a number of regenerative medical constructs (Rai *et al.*, 2005; Williams *et al.*, 2005; Kim *et al.*, 2006). A relatively small number of studies has shown that PCL is capable of releasing proteins (Cao and Shoichet, 1999; Goodwin *et al.*, 1998; Ginty *et al.*, 2008). It has also been used as part of a USFDA approved drug delivery device (Hunter *et al.*, 1998).

The degradation time of PCL is relatively long: of the order of two years (Ma *et al.*, 2006). This is possibly longer than is desirable for bone regenerative medicine. However, the degradation time could potentially be cut by adding other materials with higher degradation rates such as DL-lactide (Middleton and Tipton, 2000).

1.2.5.9. PLGA, PLA and PGA

PLA, PGA and particularly PLGA are the most commonly used synthetic polymers in bone regenerative medicine. Scaffold manufacture from these materials is relatively easy, and there is scope for tailoring their degradation rates to suit the particular situation. The degradation rate of PLGA can be altered by altering the molecular weight, and the copolymer ratio (Sokolsky-Papkov *et al.*, 2007): the more lactide units, the longer the degradation time. PLA, PGA and PLGA are also less hydrophobic than PCL due to the higher concentration of carbon to oxygen double bonds in the chemical structure, hence increasing its polarity (see **Figure 1.16**). Indeed adding PLGA to PCL has been found to increase its hydrophilicity (Tang *et al.*, 2005).

PGA, which is a linear aliphatic polyester made from glycolic acid monomer units, has a semicrystaline structure at room temperature. However, crystallinity may be lost at physiological temperatures, as the glass transition temperature is approximately 35°C (Engelberg and Kohn, 1991). PGA is relatively hydrophilic and has a tendency to lose its mechanical strength between 2-4 weeks after implantation *in vivo*. Hence it has been used in the manufacture of biodegradable surgical sutures (Reed and Gilding, 1981).

PLA, another linear aliphatic polyester, made from lactic acid monomer units, is thought to be more hydrophobic than PGA because of the additional methyl group (see **Figure 1.16**) (Engelberg and Kohn, 1991). Additionally, the rate of degradation of PLA by hydrolysis is lower than that of PGA (Reed and Gilding, 1981).

Unlike glycolic acid, lactic acid is a chiral molecule. Hence four different morphologically distinct polymers are possible (Engelberg and Kohn, 1991). D-PLA and L-PLA are stereoregular polymers. DL-PLA is the racemic polymer derived from D- and L-lactic acid. Meso-PLA can be derived from DL-PLA. D-PLA and L-PLA have semicrystaline structures whereas DL-PLA is amorphous. The glass transition temperature of PLA varies from 50 – 60°C. L-PLA is favoured for use in medical devices where mechanical strength is important, due to its crystal structure (Leenslag

et al., 1987). Conversely, DL-PLA is favoured for drug delivery devices as its amorphous structure increases the permeability of drugs (Delgado *et al.*, 1996).

Interestingly, copolymers of lactic and glycolic acid do not show a linear relationship between the ratio of monomer units and their physico-mechanical properties (Engelberg and Kohn, 1991). Changes in morphology caused by altering the ratio have been found to alter the rates of hydration and hydrolysis. In addition, PLGAs tend to degrade more rapidly than pure PLA or PGA (Leenslag *et al.*, 1987; Gilding and Reed, 1979).

There are disadvantages to using these materials. On their degradation by hydrolysis, they release acidic breakdown products. Some authors have found this to reduce osteogenesis significantly in the healing bone surrounding the scaffold, during polymer erosion (Martin *et al.*, 1996). The breakdown of scaffolds from these materials is potentially self-accelerating, as the localised drop in pH could catalyse the hydrolysis of the ester bonds (Sokolsky-Papkov *et al.*, 2007). These polymers are also considerably more expensive than other polyesters such as PCL.

However, PLGA has USFDA approval for use in the fixation of bone fractures (USFDA, 2008), and has been used in a large number of studies as either a regenerative medical scaffold or a drug delivery device, usually in the form of microparticles. The bioactive factors delivered include; rhTGF-β1 (DeFail *et al.*, 2006), rhPDGF (Wei *et al.*, 2006), rhVEGF (Patil *et al.*, 2007), rhBMP-7 (Wei *et al.*, 2007), rhBMP-2 (Woo *et al.*, 2001), and rhFGF-2 (Perets *et al.*, 2003).

1.2.6. Scaffolds as Delivery Systems

1.2.6.1. Controlled Delivery

As discussed in §1.2.4.1, growth factors have the potential to be potent therapeutic agents for bone regenerative medicine. Although growth factors can be delivered systemically, this is not the preferred delivery method. For a therapeutic dose to be delivered to the defect site by systemic delivery, it has been suggested that there could be side effects in other tissues (Chen and Mooney, 2003). This is because all

growth factors are active in more than one tissue. For example, BMP-7 is active during the development of the kidneys and eyes (Luo *et al.*, 1995). Hence, delivery must be locally applied to the defect site.

How the growth factors are presented, both in terms of the concentration and the timing, is thought to be extremely important (Chen and Mooney, 2003). For example, simple infusion of rhVEGF failed to stimulate angiogenesis for the treatment of myocardial ischemia (Henry *et al.*, 2003). Therefore bone regenerative medicine has concentrated on the controlled delivery of growth factors to the defect site. The most promising scaffold manufacture and growth factor delivery strategies are discussed below in §1.2.6.2, §1.2.6.3 and §1.2.6.3.4.

1.2.6.2. Structural Delivery Systems and Scaffolds

1.2.6.2.1. Solvent Casting/Particulate Leaching

Solvent casting is a widely used technique for scaffold manufacture in bone regenerative medicine. Typically, it involves dissolving synthetic polymers, such as PLGA and PCL, in an organic solvent (*e.g.* chloroform or dichloromethane) dispersed with water-soluble particles. The solution is placed in a mould, where the solvent is removed by evaporation. The scaffold is then washed with an aqueous solution to remove the particulates, hence creating porosity.

This technique is usually used to produce purely structural scaffolds (Vaquette *et al.*, 2008; Shin *et al.*, 2008; Kim *et al.*, 2007a), but they are also capable of delivering bioactive factors such as; human growth hormone (Goodwin *et al.*, 1998), $1,25(OH)_2D_3$ (Yoon *et al.*, 2007) and a combination of ascorbic acid and dexamethasone (Kim *et al.*, 2003a).

This manufacturing technique does, however, have limitations. The distribution of the soluble salt, and hence the pores, is heterogeneous. This is caused by differences in the density between the salt particles and the liquid polymer/solvent solution (Liao *et al.*, 2002). Also, since the salt particles are completely surrounded by the polymer solution, the salt particles cannot be easily removed by washing (Liao *et al.*, 2002).

In addition, dense layers often form on the outer surface of the polymer as the solvent is removed. This increases the difficulty of the salt removal step (Nam and Park, 1999). Due to these factors, scaffolds produced by this technique have usually been limited to thicknesses of between 500 – 2000 µm (Liao *et al.*, 2002).

In addition, the organic solvents used in the scaffold fabrication must be carefully extracted to meet USFDA standards, as they are toxic (Howard *et al.*, 2008).

1.2.6.2.2. Supercritical Carbon Dioxide Gas Foaming

A supercritical fluid is a state of matter existing above both the critical pressure and temperature. While it can expand to fill its container, it has a density similar to a liquid. Carbon dioxide (CO_2) has a critical point of 73.8 bar, and 304.1 K, and is capable of solubilising synthetic polymers such as PLGA or PLA. Scaffolds can be fabricated by reducing the pressure on the solution. This results in solidification of the polymer. Pores in the scaffold are formed by the foaming of the gaseous CO_2.

Such scaffolds can be manufactured at low temperatures and at mild chemical conditions. Hence they are capable of encapsulating and releasing bioactive growth factors such as rhVEGF (Kanczler *et al.*, 2007) and rhBMP-2 (Yang *et al.*, 2004). Supercritical CO_2 is easier to remove completely than organic solvents, which theoretically could make the scaffolds toxic if they were not removed sufficiently.

This technique may have great potential for the future, though it does have some problems. There is no direct control over the scaffold porosity, or indeed pore sizes, shapes or orientations, although the pore sizes may be influenced by altering the rate of depressurisation. Slower depressurisation has been found to lead to smaller pores (Howdle *et al.*, 2001). The pores are also often not completely connected to one another (Mathieu *et al.*, 2006). Also, suitable porosity for regenerative medical applications has been found to be difficult to achieve in polymers that are not amorphous (Mooney *et al.*, 1996).

The encapsulation efficiency of this technique may also be relatively low. Murphy *et al.* (2000) estimated the encapsulation efficiency of rhVEGF in their PLA scaffolds to be 44±9%.

1.2.6.2.3. Electrospinning

Electrospinning is another commonly used technique to manufacture scaffolds. This involves a needle dispensing a fine fibre of a charged polymer solution. A high voltage is applied to the strand, influencing the direction it falls. The strands harden as the solvent evaporates. This gradually forms a 3D scaffold (Yoshimoto *et al.*, 2003).

Electrospinning is usually applied to synthetic polymers such as PCL and PLGA, dissolved in an organic solvent such as chloroform. However, it has also been used with fibres of gelatin and silk. This technique is capable of delivering bioactive growth factors such as rhBMP-2 (Li *et al.*, 2006a; Nie *et al.*, 2008). Although the pores of electrospun scaffolds are interconnected, there is no direct control over the internal architecture of the scaffolds. In addition, it is difficult to build up significant 3D structures using this technique, and the scaffolds are very time-consuming to produce (Yan *et al.*, 2009; Teo and Ramakrishna, 2006). This technique also often utilises organic solvents, which are toxic if not extracted carefully (Howard *et al.*, 2008).

1.2.6.2.4. Sintering

Scaffolds manufactured from ceramics such as HA and TCP, are usually fabricated by sintering, as discussed in §1.1.6.5. Scaffolds such as these are currently commercially available for the treatment of bone defects.

Ceramic scaffolds are capable of being loaded directly with growth factors, such as bovine BMP, rhBMP-2, rhBMP-4, rhFGF-2 and rhVEGF, by adsorption, due to the high affinity of ceramics for proteins (Noshi *et al.*, 2000; Ziegler *et al.*, 2002). There is often a burst of release in the first few hours of non-adsorbed protein followed by slower release due to desorption. However, ceramic sintered scaffolds cannot protect the adsorbed proteins, which are constantly exposed to the hostile chemical

environment on the surface. Hence protein degradation is almost complete within the first three days of release (Ziegler *et al.*, 2002). Structures with interconnected pores are also very difficult to achieve with this technique.

Sintered calcium phosphate scaffolds are biocompatible and osteoinductive (Schildhauer *et al.*, 2000) and have favourable mechanical properties for bone regenerative medicine in compression. However, they have poor tensile strength, are very brittle, and have a long degradation time *in vivo* (Jarcho, 1981; Kim *et al.*, 2008). Indeed, when implanted, they need to be protected from shear stresses by fixation (Bucholz *et al.*, 1987).

1.2.6.2.5. Rapid Prototyping

Rapid prototyping, also called free-formed fabrication, describes a range of computer-aided techniques of scaffold manufacture. Unlike the methods described above, rapid prototyping techniques provide direct control over scaffold architecture and porosity. Indeed, scaffolds can be custom made to fit the 3D shape of the tissue defects (Leong *et al.*, 2003).

To manufacture a scaffold, the desired 3D shape is generated by a computer-aided design (CAD) program. The 3D computer model is then interpreted by a computer-aided manufacture (CAM) system. The CAM system then directs the manufacture of the scaffold, building up 3D structure one layer at a time. The main rapid prototyping techniques used are described in §1.2.6.2.6, §1.2.6.2.7 and §1.2.6.2.8.

1.2.6.2.6. Selective Laser Sintering

Selective laser sintering uses a CO_2 laser beam to sinter selectively powders of polymers or polymer/ceramic composites together to form layers of solid material (Leong *et al.*, 2003). Therefore 3D geometry can by built up layer by layer from powder beds. In addition, since layers are supported by the powder bed during manufacture, there is a great flexibility in the geometric control of the scaffolds.

The high temperatures used during conventional laser sintering preclude the incorporation of many bioactive factors. However a relatively new process, termed

surface-selective laser sintering, which involves the melting of the particles at the surface only, may have the potential to release bioactive growth factors in the future (Antonov *et al.*, 2004).

Scaffolds for bone regenerative medicine are usually primarily composed of calcium phosphate, hence scaffolds fabricated using this technique tend to be brittle (Leong *et al.*, 2003). Other limitations include shrinking and warping of the scaffold structure during the sintering process, which may reduce control over the final scaffold geometry (Lee and Barlow, 1994; Vail *et al.*, 1994).

1.2.6.2.7. 3D Printing

3D printing involves ink jet printing technology to dispense solvents or adhesives into a powder bed. Again, 3D geometry can then by built up in layers (Park *et al.*, 1998). This is an extremely versatile technique, as it can be applied to a variety of materials including synthetic polymers (Park *et al.*, 1998), ceramics (Seitz *et al.*, 2005) and even metals (Li *et al.*, 2006c). Like laser sintering, there is great flexibility in the scaffold geometries that can be achieved. Due to the support of the powder bed, features like overhanging struts, can easily be achieved.

Recent work has shown that, potentially, growth factors could be selectively attached at different concentrations to the surfaces of 3D printed scaffolds. Miller *et al.* (2006) were able to print rhFGF-2 immobilised on fibrin, in patterns onto a fibrin substrate. Cells, from the human osteoblast-like cell line MG-63, seeded on top, showed increased proliferation compared to the non-loaded areas. Subject to future development, this could potentially be a powerful tool for bioactive factor delivery.

Although this technique appears to be very promising for the future, there are some limitations. Currently it is difficult to form scaffolds with complex internal geometry, partly because of the particle sizes of the powders, limiting the layer thickness to between 80 and 250 μm (Hutmacher *et al.*, 2004). Additionally, the capital cost of 3D printers is currently high, costing as much as $100,000 (Vance, 2010).

1.2.6.2.8. Fused Deposition Modelling

Fused deposition modelling (FDM) involves the extrusion of a material from a nozzle. Variables such as the nozzle's 3D position and velocity, as well as the dispensing pressure of the gas, used to extrude the material, are controlled by the CAM system. The extruded material may be solidified by chemical crosslinking, non-solvent-induced phase separation (which involves the precipitation of a polymer by immersion in a non-solvent) or freezing polymer melts (Quaglia, 2008) (see **Figure 1.17**). Hence a 3D structure can be built up, with fully interconnected pores.

This technique is, however, often difficult to apply in practice. Many materials are unsuitable for this technique because of their physical or chemical properties. For example, the liquids to be extruded must have viscosities within a certain range to prevent the strands spreading out (Hutmacher *et al.*, 2004). The extruded strands must also solidify quickly to support the next layer laid down on top of them. Also, not all geometries may be manufactured due to need for the preceding layer to support the next layer. For example, for FDM, overhangs are very difficult to achieve, in contrast to both selective laser sintering and 3D printing (Ahn *et al.*, 2002).

FDM has been applied to create scaffolds out of a number of materials, including; alginate (Khalil *et al.*, 2005), chitosan/HA blends (Ang *et al.*, 2002), and PCL (Hutmacher *et al.*, 2001; Zein *et al.*, 2002; Rai *et al.*, 2005). Conventional FDM, relying on extrusion of polymer melts, is thought to be incapable of incorporating bioactive growth factors directly, due to the necessary high processing temperatures. However, Rai *et al.* (2004; 2005) have successfully released bioactive rhBMP-2 from a coating of fibrin on PCL scaffolds. Hydrogel scaffolds plotted using this technique are thought to have the potential to deliver bioactive factors, though they may lack sufficient mechanical strength for bone regenerative medicine (Landers *et al.*, 2002).

Of all the rapid prototyping techniques, adaptations of conventional FDM are thought to have the greatest scope for creating scaffolds directly encapsulating bioactive factors, suitable for bone regenerative medical applications.

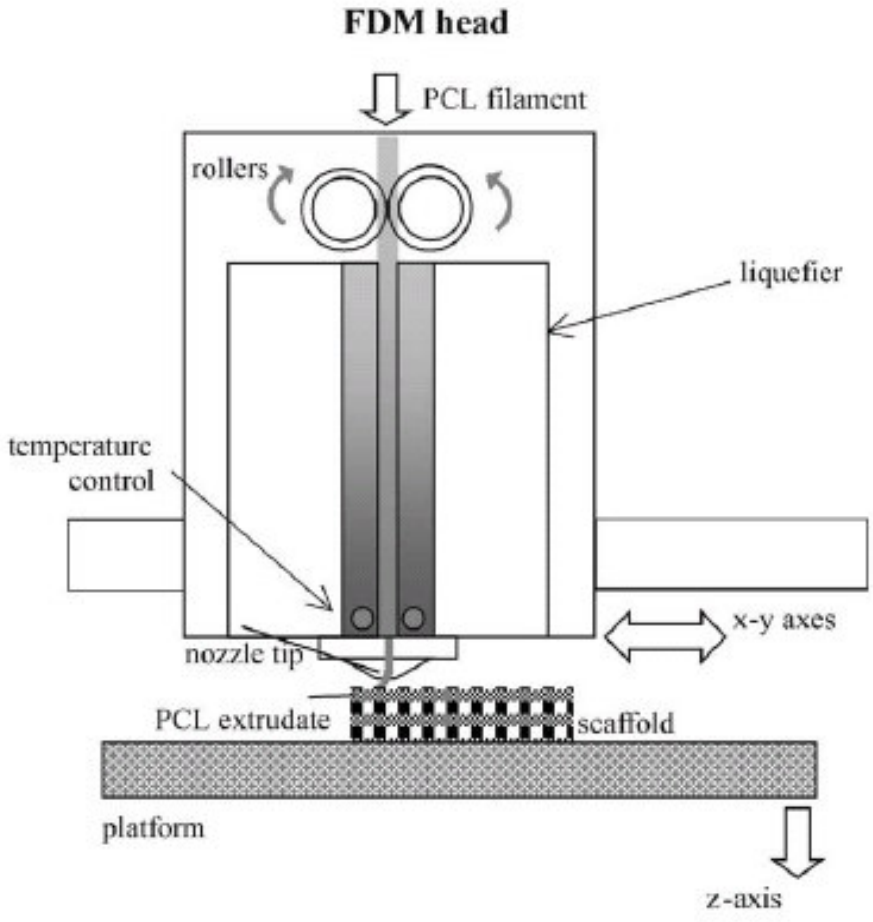

Figure 1.17: Schematic Representation of FDM.

Schematic representation of traditional FDM based on extrusion of PCL melt (From Zein *et al.*, 2002).

1.2.6.3. Non-Structural Delivery Systems

1.2.6.3.1. Sponges

Absorbable sponges of collagen are currently used clinically for the delivery of rhBMP-2 and -7, for the treatment of fracture delayed union and non-union (see §1.1.6.6). They are a useful delivery system for bioactive factors, however because of their relatively poor mechanical properties, usually some degree of support is needed. For example, the company Stryker manufactures OP-1™ Putty, which consists of bovine Type-I collagen, loaded with rhBMP-7 in a putty of carboxymethylcellulose. This product has received USFDA approval for use in spinal fusion operations (USFDA, 2003).

However sponges tend to undergo rapid degradation, and consequently release of growth factors from sponges tends to be very rapid. For example, Ueda *et al.* (2002) found that over 25% of the TGF-β1 loaded in collagen sponges was released in the first hour of exposure to the release media. Ueda *et al.* (2002) also found that approximately 75% of the collagen sponges had degraded 10 days after implantation in rabbit calvarial defect models.

1.2.6.3.2. Hydrogels

Hydrogels are a class of highly hydrated polymer networks with a water content of ≥ 30% by mass. Many hydrogels are hydrophilic, biodegradable, biocompatible and have similar structural and mechanical properties to ECM. For the purposes of regenerative medicine, hydrogels may be formed from a variety of material including; poly(ethylene oxide), poly(vinyl alcohol), poly(acrylic acid), poly(propylene furmarate-co-ethylene glycol), alginate, chitosan, collagen and hyaluronic acid (Drury and Mooney, 2003).

In general regenerative medicine, they are often used as space fillers, and cell delivery systems. They are often applied as *in situ*-forming injectable matrices. In certain situations, this strategy can eliminate the need for scaffold implantation, using more invasive surgical techniques (Quaglia, 2008). Hydrogels are also capable of

delivering bioactive growth factors. For example, chitosan has been used to deliver rhFGF-1, -2, rhVEGF, and epidermal growth factor (Ishihara *et al.*, 2003; Alemdaroglu *et al.*, 2006), whereas alginate can deliver rhFGF-2, rhVEGF, and rhTGF-β1 (Lee *et al.*, 2003a; Mierisch *et al.*, 2002).

However, the mechanical properties of hydrogels are ill suited to bone regenerative medical applications (Seal *et al.*, 2001) typically having a tensile strength of between 300 and 50 kPa (Lee *et al.*, 1997b; Johnson *et al.*, 2004), indeed they are more commonly used for cartilage regenerative medicine (Liu *et al.*, 1998; Kim *et al.*, 2003c). Hence, for this application of regenerative medicine, they require support from a structural scaffold. In addition, cells do not have receptors to many hydrogels, indeed they have been used as post-operative adhesion barriers (West *et al.*, 1996).

1.2.6.3.3. Microparticles

Microparticles are a commonly used method for the delivery of bioactive growth factors. Generally, they are used in conjunction with a structural scaffold to prevent their migration away from the defect site and into surrounding tissues. The material of choice for this technique is often PLGA, which is capable of encapsulating growth factors by the double emulsion technique. A number of examples may be found in §1.2.5.9.

They are popular as it is believed that the release properties could be altered to match any desired drug release profile, simply by altering the degradation rate of the polymer. This could be achieved without the need to alter the manufacturing parameters of the scaffold itself (Quaglia, 2008).

This is based on the assumption that the primary method of release is by degradation of the microparticles. However, unless there is a strong charge interaction, or the growth factors are covalently bonded to the polymer, the primary mode of release has been reported to be diffusion (Wada *et al.*, 1995). Hence the scope for releasing active factors on longer time scales may be limited, as geometric factors (*i.e.* the radii of the microparticles) may play a key role (see **Equation 1.1** and **Equation 1.2**).

Microparticles also commonly release a substantial burst of drug in the first few hours of use, which is very difficult to control.

Equation 1.1

$$\frac{M_t}{M_\infty} = 6\sqrt{\frac{D_{AB}t}{\pi r^2}} - \frac{3D_{AB}t}{r^2} \qquad \text{(where } M_t/M_\infty < 0.4\text{)}$$

Equation 1.2

$$\frac{M_t}{M_\infty} = 1 - \frac{6}{\pi^2}\exp\left(-\frac{\pi^2 D_{AB}t}{r^2}\right) \qquad \text{(where } M_t/M_\infty > 0.6\text{)}$$

The above equations represent the rate of release of encapsulated drugs from microparticles (from Wada *et al.*, 1995). Where M_t/M_∞ is the fraction of drug released , t is time, and D_{AB} represents the diffusivity of species A in media B.

Microparticles are commonly supported on scaffolds (Liebschner and Wettergreen, 2003). This is both to provide the necessary mechanical support, and to localise the microparticles to the defect site.

1.2.6.3.4. Dual Delivery Systems

As discussed in §1.2.4.1, since different growth factors perform different functions, it could be advantageous for bone regenerative medical constructs to release two or more. In addition, since the timing of growth factor delivery is thought to be important, it may also be advantageous for the release to be from different delivery systems, so that the release kinetics of the two factors can be altered independently of each other.

There are surprisingly few examples of scaffolds capable of dual delivery in bone regenerative medicine. However, virtually all dual delivery scaffolds in the literature (see **Table 1.2**) release the growth factors from the same delivery system. Hence the release kinetics cannot be adjusted individually.

Table 1.2: Examples of dual growth factor delivery for bone regenerative medicine.

Factors Released	Scaffold	Animal Model	Reference
rhTGF-β1, rhBMP-2	Gelatin hydrogel	Rat tibial segmental defect	Srouji *et al.*, 2004
rhTGF- β3, rhBMP-2	Alginate	Ectopic SCID mouse	Simmons *et al.*, 2004
rhTGF- β3, rhBMP-2	Alginate coating on PLA scaffold	Rat tibial segmental defect	Oest *et al.*, 2007
rhVEGF, rhBMP-2	Gelatin microparticles on poly(propylene fumatate) scaffold	Rat cranial critical size defect	Patel *et al.*, 2008

There are at least three examples of scaffolds capable of releasing proteins, utilising independent delivery systems. Ginty *et al*. (2008) presented a scaffold with the potential to do this. They were able to release the model drugs, RNase and horseradish peroxidase, from both a PLA scaffold, fabricated using super critical CO_2, and from alginate fibres crosslinked with calcium and barium chloride. The choice of barium chloride as a crosslinking agent is also possibly a questionable one, as barium chloride is toxic. Their system utilising PLA scaffolds and PCL microparticles may have greater potential for bone regenerative medical applications. However, as yet these systems have not demonstrated their biocompatibility or ability to release bioactive growth factors.

Sohier *et al*. (2006) were able to coat a scaffold of poly(ethylene glycol)-terephthalate (PEGT) and poly(butylene terephthalate) (PBT) with successive coatings of the same material. The coatings of PEGT/PBT were formed by a water-in-oil emulsion, using chloroform as the solvent. The release kinetics of the model drugs, myoglobin and lysozyme, could be altered by varying the combination of the

PEGT/PBT blend. However, the biocompatibility of the system and the bioactivity of released growth factors is yet to be demonstrated.

In an elegantly designed study by Richardson *et al.* (2001) PLGA scaffolds, produced by $scCO_2$ gas foaming, and microparticles delivery systems were combined, and used to deliver bioactive VEGF and PDGF. However, release from the microparticle delivery system presented, was either virtually identical to the release from the scaffold, or was too slow to be of clinical significance. In addition, such $scCO_2$ gas foaming scaffolds, encapsulating growth factors, have been found to have a relatively poor encapsulation efficiency (Murphy *et al.*, 2000).

Therefore, it would seem that there is scope for the development of a scaffold capable of releasing bioactive growth factors from two (or more) separate delivery systems.

1.3. Summary and Thesis Hypothesis

Both fracture non-unions and bone defects pose a recalcitrant problem to orthopaedic surgeons. The current gold standard treatment is autologous bone grafting, despite the potential problems of morbidity of the donor site, uncontrolled bone resorption, and the limited supply and quality of donor bone. The emerging field of regenerative medicine could provide an alternative treatment.

A scaffold able to deliver both multiple bioactive growth factors, and human marrow stromal cells, could be advantageous. However, a satisfactory scaffold delivery system for achieving this has yet to be developed. This thesis describes the development of a scaffold potentially capable of accomplishing this, and meeting the demanding design criteria for regenerative medicine constructs.

The following hypothesis was tested: *It is possible to manufacture cell-compatible scaffolds, with sufficient porosity for the diffusion of cellular nutrients and waste products, incorporating two delivery systems, each capable of releasing a bioactive growth factor with clinically significantly different release profiles.*

1.4. Experimental Procedure and Rationale

1.4.1. Ideal Scaffold Release

As discussed in §1.2.6.3.4, the dual delivery of growth factors with different temporal release profiles may be advantageous, yet few examples exist. Ideally one or more growth factors should be released relatively quickly to stimulate angiogenesis, and host osteoblast progenitor chemotaxis and proliferation (see **Figure 1.18**). Ideally this should be followed by later, and perhaps more sustained, delivery of growth factors to induce osteogenic differentiation of osteoprogenitors (see **Figure 1.18**).

As discussed in §1.1.2.5 and §1.2.4.1, VEGF has shown promise in stimulating angiogenesis. However, direct injection of VEGF has been found to fail to stimulate angiogenesis *in vivo* (Henry *et al.*, 2003). In contrast, release over the course of approximately 14 days from scaffolds, has been found to increase blood vessel numbers *in vivo* (Kanczler *et al.*, 2007). VEGF may, therefore, be a promising candidate for early delivery as shown in **Figure 1.18**.

Isoforms of TGF-β are thought to have a potent chemotactic effect on MSCs, and to stimulate MSC, chondrocyte and osteoblast proliferation (Lieberman *et al.*, 2002). In normal healing, the TGF-β isoforms are released early from the platelets after the clot forms at the time of fracture (Robey *et al.*, 1987). Hence, growth factors such as TGF- β1 may be another potential candidate for early release.

Growth factors such as BMP-2 and -7 are thought to induce the differentiation of osteoprogenitors (see §1.1.2.3 and §1.1.6.6). They are therefore promising candidates for more sustained release. In normal fracture healing in mice, expression of both BMP-2 and -7 is sustained for the first 21 days (Cho *et al.*, 2002; Bostrom, 1998; Nikolaou and Tsiridis, 2007). Therefore, a more sustained release profile may be desirable for these growth factors. Ideally, however, there should be a delay in the initial release of these factors, in order not to interfere with any pro-proliferative effect on osteoprogenitors, caused by the release of other growth factors from the scaffold.

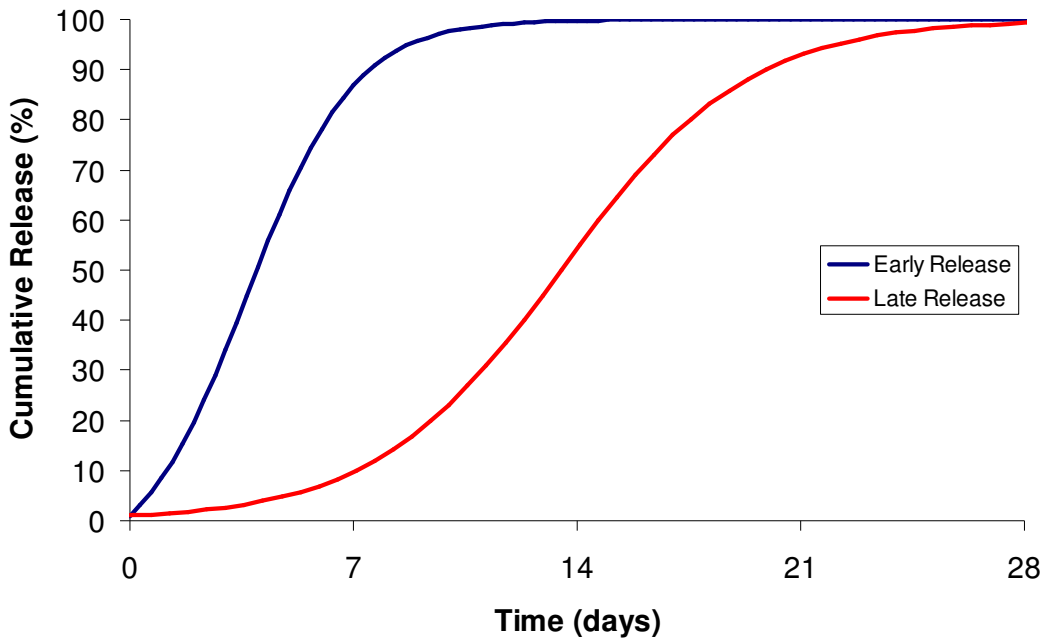

Figure 1.18: Ideal Growth Factor Release Profiles from Scaffolds.

This figure represents the ideal release profiles of growth factors from scaffolds for bone regenerative medical applications. The blue line represents the ideal release of growth factors intended to stimulate angiogenesis or MSC chemotaxis and proliferation. The red line represents the ideal release of growth factors intended to stimulate osteogenic differentiation of osteoprogenitors.

1.4.2. Material Selection

1.4.2.1. Design Philosophy

As discussed in §1.4.1, an ideal scaffold should have the potential to release different growth factors with different temporal release profiles. It was thought that this would be easiest to achieve with two different delivery systems; the first releasing rapidly, and the second releasing over a longer period of time (see **Figure 1.18**).

It was thought that early release could be best achieved by release from a scaffold coating. Since the thickness of the coating would be thinner than the scaffold strands and since the coating is on the outer surface, the diffusive release from the coating is likely to be higher (Ritger and Peppas, 1987a; 1987b).

It was also thought that the release from within the scaffold would be relatively slow, when compared both to the coating, and to microparticles which are a commonly used drug delivery system in regenerative medicine. This was thought to be the case, in part, as the different geometry should slow the diffusive release from the scaffold (Ritger and Peppas, 1987a; 1987b; Wada *et al.*, 1995).

1.4.2.2. Coating Material Selection

The scaffold coating must meet a number of design criteria, though the coating must perform two functions in particular. First, it acts as the primary cell-scaffold interface, and second, it must act as a drug delivery device. The coating materials must, therefore, be biocompatible, biodegradable and be capable of releasing bioactive growth factors. Ideally, the coating materials should also be osteoconductive.

As discussed in §1.2.5.3, alginate is thought to be biocompatible (Schuh *et al.*, 1996), biodegradable (Blaine, 1947), and capable of releasing bioactive growth factors (Mierisch *et al.*, 2002; Simmons *et al.*, 2004). Although alginate is not osteoconductive, it was thought to be a suitable to be evaluated as a potential coating material.

Chitosan is also thought to be biocompatible (VandeVord *et al.*, 2002), biodegradable (Dhanikula and Panchagnula, 2004), and capable of releasing bioactive growth factors (Lee *et al.*, 2004b; Mattioli-Belmonte *et al.*, 1999) (see §1.2.5.4). Again, chitosan is not thought to be osteoconductive, however, it was considered as a potential scaffold coating material.

Type-I collagen was also considered as a potential coating material. It is biodegradable, bioresorbable, biocompatible, and has been used as part of USFDA approved devices capable of delivering bioactive rhBMP-2 and -7 (Lee *et al.*, 2001; Itoh *et al.*, 2001b; Govender *et al.*, 2002; Friedlaender *et al.*, 2001) (see §1.2.5.5). In fact there is some evidence that Type-I collagen specific binding mediates the osteogenic response of hMSCs (Yang *et al.*, 2004; Mizuno *et al.*, 2000).

Type-A gelatin was the final potential scaffold coating material selected. Type-A gelatin has been found to retain the biocompatibility and biodegradability of the collagen from which it is manufactured (Link *et al.*, 2008), and is capable of releasing bioactive growth factors (Liu *et al.*, 2007; Kempen *et al.*, 2008; Komura *et al.*, 2008) (see §1.2.5.6).

1.4.2.3. Scaffold Material Selection

The scaffold materials must meet a number of design criteria (see §1.2.2), though in particular, the scaffold materials must be; biocompatible, biodegradable, capable of delivering bioactive growth factors, and have suitable mechanical properties.

As discussed in §1.2.5.8, PCL is; biocompatible, bioresorbable, capable of releasing bioactive growth factors, and has mechanical properties which lie within the lower range of properties for human trabecular bone (Hutmacher *et al.*, 2001; Pitt *et al.*, 1981; Cao and Shoichet, 1999; Goodwin *et al.*, 1998; Ginty *et al.*, 2008; Williams *et al.*, 2005). PCL scaffolds have also been fabricated into scaffolds by fused deposition modelling (Vadillo, 2009). PCL was therefore thought to be a suitable potential scaffold material.

PLGA is also biocompatible, biodegradable, and has sufficient mechanical properties to be used in bone regenerative medical scaffolds (Kim *et al.*, 2007a; Martin *et al.*, 1996) (see §1.2.5.9). PLGA has also been widely used to release a variety of bioactive growth factors (DeFail *et al.*, 2006; Wei *et al.*, 2007; Woo *et al.*, 2001). Like PCL, PLGA has also previously been used to fabricate fused deposition modelling (Vadillo, 2009). PLGA was therefore investigated as a potential scaffold material. PLGA 50:50 is more commonly used in growth factor releasing microspheres (DeFail *et al.*, 2006; Wei *et al.*, 2007), however PLGA 75:25 was used in an attempt to slow growth factor release. Additionally, this is the ratio successfully employed by Vadillo (2009) to fabricate scaffolds for bone regenerative medical applications.

Blends of the two polymers PLGA and PCL were also used as scaffold materials. It was hypothesised that altering the ratio of the two polymers in the blend would have an effect on the drug release rate from the resulting scaffolds.

Dichloromethane (DCM) was selected as the organic solvent. DCM is capable of dissolving both PCL and PLGA. Many previous studies have shown that bioactive factors can be delivered by microparticles of synthetic polymers, processed with DCM using the double emulsion technique (Bodde *et al.*, 2008; Kim and Park, 2004; Phillips *et al.*, 2006a; Wei *et al.*, 2004; Wei *et al.*, 2007; Yang *et al.*, 2006). DCM has yet to be used in the manufacture of scaffolds fabricated by rapid prototyping that have been shown to be capable of bioactive growth factor release. However, DCM was thought to be a suitable solvent for the production of scaffolds capable of releasing bioactive growth factors.

1.4.2.4. Active Factors

As discussed in §1.1.2 and §1.2.4, a plethora of growth factors are involved in normal fracture healing, hence many different options are available for bone regenerative medical applications. rhBMP-7 was chosen both as a representative growth factor, and as a compound of interest in its own right. Like many other growth factors of interest in the field of bone regenerative medicine, including FGF-2, PDGF, and BMP-2, BMP-7 is positively charged at physiological conditions and

has a similar molecular weight (Quaglia, 2008) (see **Figure 4.1**). Therefore the release profile of rhBMP-7 is likely to be similar to other growth factors of interest.

rhBMP-7 was also chosen, being of interest in its own right, as it is one of only two growth factors to be given USFDA approval for use in the treatment of fracture non-unions (see §1.1.6.6).

In addition, $1,25(OH)_2D_3$ was used as a model drug to assess the feasibility of releasing hydrophobic lipid-soluble active factors for the scaffolds. For example, many cathepsin K inhibitors are hydrophobic (Wang *et al.*, 2004). However, as discussed in §1.2.4.2, $1,25(OH)_2D_3$ has also been considered as a potential compound of interest for bone regenerative medicine, particularly in combination with an isoform of TGF-β (Bosetti *et al.*, 2007).

1.4.3. Outcome Measures/Experimental Procedure

1.4.3.1. Chapter 2

A feasibility study was conducted to assess whether scaffolds could be fabricated from the materials selected in §1.4.2.3, while encapsulating aqueous solutions. The outcome measures for this study were; the regularity of scaffold geometry, and the scaffold porosity (see **Figure 1.19**). The latter is thought to be particularly important to allow the diffusion of nutrients in, and waste products out, and to allow tissue ingrowth (Karageorgiou and Kaplan, 2005).

A second feasibility study was undertaken to assess whether the materials selected in §1.4.2.2 were capable of coating the scaffolds. The outcome measures were; the uniformity of coating coverage, and the preservation of the original scaffold porosity (see **Figure 1.19**).

1.4.3.2. Chapter 3

As discussed in §1.2.2, one of the most important design criteria for materials used in regenerative medicine is biocompatibility. However, this is very difficult to test without using animal models. Nevertheless, *in vitro* methods of studying cell-

compatibility are widely accepted for the purpose of primary screening, before preclinical trials are undertaken (Wang *et al.*, 2009a; Carinci *et al.*, 2007; Paul and Sharma, 2007). They also have the advantage of giving good control over the variables, and their sensitivity is thought, by some authors, to be at least equal to that of *in vivo* studies (Ho *et al.*, 2008).

In the context of bone regenerative medicine, cell-compatibility is commonly taken to mean the lack of cytotoxicity, as well as osteoconductivity. Many methods exist to assess cell-compatibility, including MTT or MTS assays (Sgouras and Duncan, 1990). However, imaging of cells stained to reveal whether they are viable or necrotic (using calcein-acetoxymethyl and propidium iodide respectively) was thought to yield the most information (Lichtenfels *et al.*, 1994; Roden *et al.*, 1999; Goodell *et al.*, 1996; McKeague *et al.*, 2003). First, this assay is capable of detecting even very low levels of cell death. Second, the number of cells can be calculated. Third, the morphology of the cells can be examined.

For the selection of the optimum coating material, the coatings were exposed to three cell types. First hMSCs, which, as discussed in §1.2.3.3 are a promising cell type for bone regenerative medicine. Second hOBs, which would also come into contact with the scaffold *in vivo*, either formed from the hMSCs delivered with the scaffold, or by host in-growth. Third MG63 to represent more proliferative cells. The selection of the optimum coating material was done using this assay as the coating was the primary cell-scaffold interface (see **Figure 1.19**).

While cell-compatibility was thought to be less important than that of the coating, it was important to confirm that sufficient dichloromethane had been removed to avoid the release of the cytotoxic organic solvent from the scaffolds. The live/dead assay was therefore performed on the optimum scaffold (as determined from the release studies in Chapter 4, see **Figure 1.19**) using hMSCs. In this case, the hMSCs were seeded primarily on the tissue culture plastic rather than the scaffold material. This enabled accurate quantification of the numbers of viable and dead cells. This would not have been possible for cells seeded onto the scaffolds directly because of the

effect the scaffold 3D structure would have had on the microscope field of focus. The optimum scaffolds were compared to scaffolds already known to be biocompatible as a positive control for cell-compatibility (Vadillo, 2009).

1.4.3.3. Chapter 4

Since both PCL and PLGA were known to be biocompatible materials (see §1.2.5.8 and §1.2.5.9), selection of the optimum scaffold material was made on the basis of release profiles and encapsulation efficiency (see **Figure 1.19**).

This was achieved using the model drug, methylene blue. A model drug was used, both because of economic considerations, and the ease of quantification. In addition, methylene blue may not undergo significant degradation in the release media, in contrast to active factors. Methylene blue has previously been used as a model drug (De and Robinson, 2003; Wu *et al.*, 1996; Tu *et al.*, 2005). Although the molecular weight is relatively low (320 Da), since the mode of release and the charge interactions were very similar, scaffolds releasing methylene blue more rapidly would similarly release rhBMP-7 more rapidly according to the laws of Fickian diffusion (Fick, 1855; Ritger and Peppas, 1987a). It should be noted that this would not be the case if the model drug's molecular weight was identical to the growth factor, but had a different charge. Methylene blue was, therefore, used to assess the scaffold materials based on the release profiles and encapsulation efficiencies.

While the optimum scaffold coating material had previously been selected on the basis of cell-compatibility, it was important to assess the coating's drug loading capacity to ensure it was adequate, as well as its release profile to ensure it was consistent with the design philosophy of the thesis. This was achieved using methylene blue.

While model drugs may be effective for the purposes of preliminary testing and screening, it is thought to be necessary to confirm the actual *in vitro* release profile using growth factors themselves (Wang *et al.*, 2009b). Such release profiles are normally investigated using either radioactively labelled forms of the growth factors (Wei *et al.*, 2007; Hosseinkhani *et al.*, 2007; Bodde *et al.*, 2008), or by using an

appropriate enzyme-linked immunosorbent assay (ELISA) (Kim and Valentini, 2002; Moioli *et al.*, 2006; Jaklenec *et al.*, 2008). This was achieved using rhBMP-7 as a representative growth factor (see §1.4.2.4), detected using an ELISA.

1.4.3.4. Chapter 5

The release profiles of rhBMP-7 had previously been assessed using an ELISA (see **Figure 1.19**). However immuno-reactivity does not necessarily show that active factor release remained bioactive. Since the antibodies used in ELISAs only bind to a small region of the complete protein structure, the proteins detected may only have been deactivated fragments of the original active factors (Bae *et al.*, 2006).

It was therefore necessary to assess whether the rhBMP-7 released was capable of affecting cells. This is commonly achieved employing cell lines, using changes in such properties as cell proliferation or ALP expression as outcome measures (Meager, 1991; Garrigue-Antar *et al.*, 1995; Parker *et al.*, 2002). However, such assays, which often employ transformed non-human cells, yield little information on how primary human cells would behave or what dose of active factor is most appropriate.

It was also thought to be important to use human cells to assess their reaction to a range of rhBMP-7 concentrations. Currently, the majority of *in vitro* studies have been conducted using mouse or rat MSCs, however the response of these cells to rhBMP-7 has been found to differ from that of human MSCs (Diefenderfer *et al.*, 2003). Therefore, the optimum concentration for human cells cannot be deduced from these studies. Nevertheless, there is broad agreement that MSC expression of ALP, an early marker for osteogenic differentiation, is increased in response to rhBMP-7 in the range 10 – 100 ng/ml (Knippenberg *et al.*, 2006; Edgar *et al.*, 2007; Tsiridis *et al.*, 2007).

Normalised ALP expression in hMSCs was therefore used as the main outcome measure for assessing which rhBMP-7 dose was most appropriate, and whether the rhBMP-7 release from the scaffolds was capable of affecting the target cell type (see **Figure 1.19**).

The feasibility of releasing hydrophobic active factors was also assessed using a similar assay (see **Figure 1.19**). As discussed in §1.4.2.4, $1,25(OH)_2D_3$ was chosen as a representative active factor. The sensitivity of the assay for $1,25(OH)_2D_3$ was increased by the addition of TGF-β3 to the cell media, as isoforms of TGF-β were known act synergistically with $1,25(OH)_2D_3$ to enhance osteogenic differentiation (Bosetti *et al.*, 2007).

For both assays, the cells were seeded on tissue culture plastic rather than the scaffolds themselves. This was to enable the study of the release from the scaffolds independently from cell-scaffold interactions. Hence the potential confounding factor of variations in scaffold topography was removed, as surface topography is known to influence the behaviour of cells of the osteoblast lineage (Dalby *et al.*, 2002).

1.4.3.5. Chapter 6

The rhBMP-7 loaded scaffolds were then tested for their ability to induce osteogenic differentiation in hMSCs *in vitro*. As discussed in §1.1.1.5, ALP expression and matrix mineralisation are well established indicators of osteogenic differentiation. Therefore, quantification of ALP activity and calcium deposition, normalised to the quantity of DNA present, were used as the main outcome measures. Such assays have been used previously to assess the osteogenic differentiation of cells on scaffolds (Bjerre *et al.*, 2008; Liu *et al.*, 2008b; Moreau and Xu, 2009; Holtorf *et al.*, 2005; Vadillo, 2009; Dadsetan *et al.*, 2008).

Colourimetric assays for ALP activity and calcium deposition were used, as quantitative photographic techniques were unsuitable for use on the scaffolds.

1.4.3.6. Chapter 7

The ability of the rhBMP-7 loaded scaffolds to induce osteogenic differentiation was further assessed by examining the expression of a number of genes associated with osteogenesis. Gene expression was investigated using quantitative reverse transcription polymerase (qRT-PCR).

The genes selected were; Runx2, Type 1 collagen (Col1), osteocalcin (OC), osteopontin (OP), and ALP. The transcription factor Runx2 is thought to be essential for osteoblastic differentiation (Komori *et al.*, 1997; Otto *et al.*, 1997). Col1 expression is an early maker of osteoblastic differentiation and is first expressed by osteoprogenitor cells, as is OP (Liu *et al.*, 1994). ALP mRNA expression is also a marker of immature osteoblasts, but is thought to occur later than osteopontin (Liu *et al.*, 1994). It is one of the few genes thought to be specific to osteoblasts and odontoblasts (Desbois *et al.*, 1994). Osteocalcin is thought to play a role in mineralisation and calcium homeostasis, as well as being a marker of mature osteoblasts (Liu *et al.*, 1994).

The cell type selected for these studies was the murine myoblast cell line C2C12. This was because previous studies have shown that the differentiation pathway can be shifted from myoblastic to osteoblastic in the presence of either rhBMP-2 (Lee *et al.*, 1999; Katagiri *et al.*, 1994; Kim *et al.*, 2009) or rhBMP-7 (Gu *et al.*, 2004b; Yeh *et al.*, 2002; Tou *et al.*, 2003).

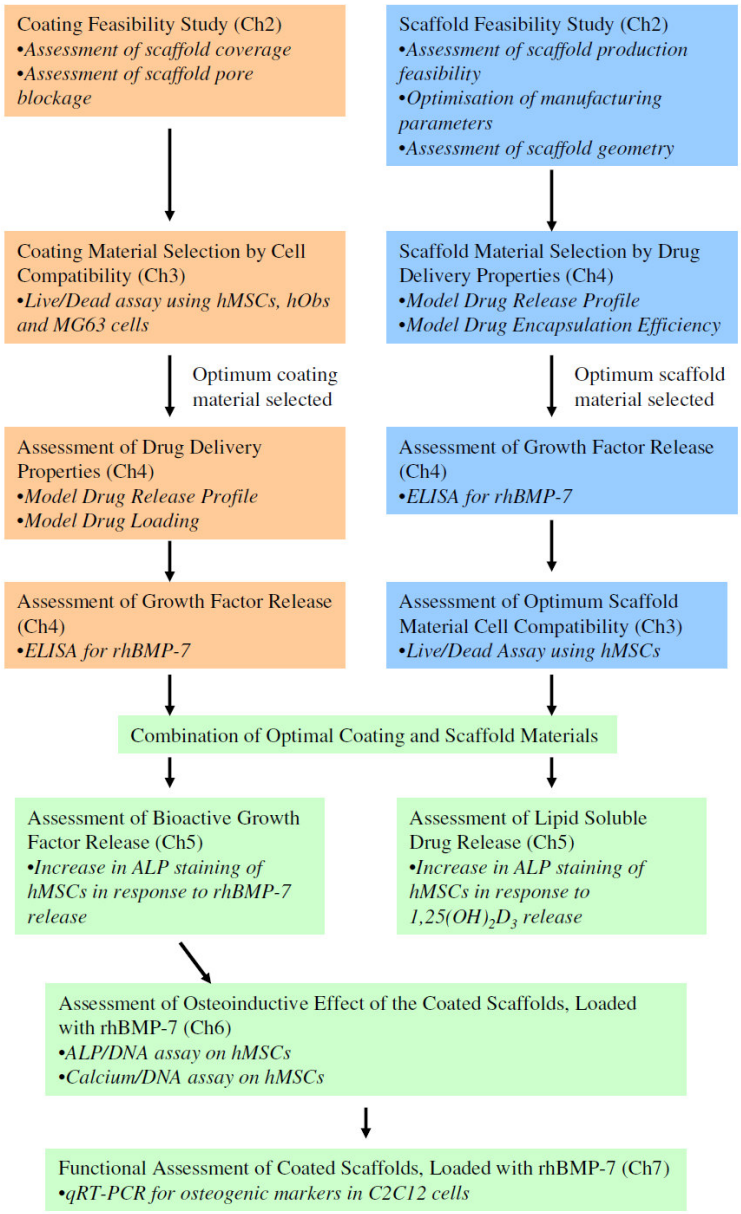

Figure 1.19: Flow diagram of experimental sequence.

This figure represents a flow diagram of the sequence of experiments conducted in this thesis. The experiments coloured brown were concerned with the selection of the optimum coating material by cell-compatibility, and its testing for its suitability as a drug delivery system. The experiments coloured blue were concerned with the selection of the optimum scaffold material by its suitability as a delivery system, and subsequent evaluation for cell-compatibility. The experiments coloured green investigated the ability of both delivery systems to deliver active factors and to induce osteogenic differentiation in hMSCs and C2C12 cells.

Chapter 2 : Scaffold Development

2.1. Abstract

In bone regenerative medicine, it may be necessary to deliver different bioactive factors with different temporal release profiles. There is however, a near complete absence of such dual delivery systems in the literature. The purpose of the studies described in this chapter, was to find the optimum manufacturing parameters for a range of scaffolds and scaffold coatings. Each scaffold and coating was thought to have the potential to act as an independent delivery system for bioactive growth factors.

Two-layer scaffolds were manufactured from poly(ε-caprolactone) (PCL) (both M_n 42,500 and M_n 80,000), poly(lactide-co-glycolide) (PLGA), as well as two blends of PCL and PLGA. It was found that aqueous solutions could be incorporated into the scaffolds, making it potentially possible to release bioactive factors from them. The pore size of PCL (M_n 42,500) scaffolds manufactured in house, was found to be suitable for bone regenerative medical applications: allowing the diffusion of nutrients and waste produces to and from the cells. The four potential scaffold materials were subjected to screening based on their drug delivery properties in Chapter 4.

It was found that PCL (M_n 42,500) scaffolds could be coated with alginate, chitosan, Type 1 collagen and Type-A gelatin, without compromising the porosity of the resulting regenerative medical construct. The five potential scaffold coating materials were subjected to screening based on their cell-compatibility to determine the optimum material, as discussed in Chapter 3.

2.2. Introduction

The Bioplotter™ is a versatile computer aided design/manufacture rapid prototyping system, for the manufacture of regenerative medical scaffolds. The computer aided manufacture system controls the three dimensional (3D) position and velocity of a pneumatic syringe. The dispensing pressure can be set manually, and is maintained and controlled by a regulator. Scaffold material extruded from the needle of the syringe may be solidified using a number of techniques, depending on the material used.

This system has been used in scaffold manufacture from a number of materials. Ang *et al*. (2002) produced scaffolds using a solution of chitosan and hydroxyapatite (HA), by dispensing into a bath of sodium hydroxide solution, followed by freeze drying.

Fedorovich *et al*. (2008) used the Bioplotter™ to fabricate scaffolds of hydrogels containing bone marrow derived goat MSCs. The hydrogels used were; Matrigel, Lutrol, alginate and agarose. The alginate scaffolds, which were manufactured from 2% (w/v) sodium alginate extruded in a bath of calcium chloride ($CaCl_2$), showed no significant decrease in viability of cells within the scaffold, over a seven day period.

Malda *et al*. (2005) produced scaffolds from a poly(ethylene glycol)-terephthalate / poly(butylene terephthalate) molten blend. The strands of the scaffold were formed as the melt cooled and solidified. The scaffolds were seeded with bovine chondrocytes, and transplanted into subcutaneous pockets in nude mice. The authors found that the mass of glycosaminoglycan, normalised against the mass of deoxyribonucleic acid (DNA), was significantly higher than for the similar scaffolds manufactured using moulding and particulate leaching.

Extensive studies using the Bioplotter™ have also been conducted in-house. Vadillo (2009) manufactured scaffolds using; alginate, chitosan, gelatin, PLGA and PCL. It was found that the system had a dispensing accuracy of 10 μm. Alginate scaffolds

were fabricated from solutions of 3% (w/v) alginate in 0.9% (w/v) sodium chloride (NaCl), plotted in a bath of 0.1 M $CaCl_2$. Chitosan was used at a concentration of 3% (w/v) in 2% (v/v) acetic acid. This solution was plotted in a bath of 1% (w/v) sodium hydroxide (NaOH) and ethanol in a ratio of 7:3, followed by treatment with 2% (w/v) TPP and lyophilisation. Gelatin constructs were produced from a heated 20% (w/v) solution, crosslinked with glutaraldehyde or transglutaminase.

The most successful scaffolds fabricated by Vadillo (2009), in terms of the scaffold mechanical properties, and the extent of control of 3D geometry, were made from PCL and PLGA. Both were plotted at a concentration of 30% (w/v) in glacial acetic acid, where the plotting medium was industrial methylated spirit (IMS). Good control over the scaffold 3D geometry was achieved. The PCL scaffolds were seeded with hMSCs and transplanted into critical-sized defects in the skulls of mice (Martin *et al.*, 2008). The scaffolds aided the healing of the defect, and it was found that calcium was deposited directly onto the PCL strands. This shows the biocompatibility and osteoconductivity of the PCL scaffolds. The direct encapsulation of growth factors in scaffolds such as these is thought to be inappropriate, since the harsh chemical environment caused by the glacial acetic acid, would denature encapsulated proteins.

Biocompatible PCL scaffolds have also been fabricated using a rapid prototyping technique very similar to the Bioplotter™, based on polymer melts (Rai *et al.*, 2005, Zein *et al.*, 2002). The relatively high temperatures (120°C) used in processing these scaffolds, preclude encapsulating growth factors.

As discussed previously (§1.2.5), scaffolds made from natural polymers tend not to possess the mechanical properties necessary for bone regenerative medicine. However, synthetic polymer scaffolds such as those described above, have traditionally been unsuitable for direct encapsulation, because of the harsh processing conditions used to produce 3D structure.

In contrast to melting or the use of glacial acetic acid, processing with the organic solvent dichloromethane (DCM) is relatively mild. Many studies have shown that bioactive factors can be delivered by microparticles of synthetic polymers, processed with DCM using the double emulsion technique (Bodde *et al.*, 2008; Kim and Park, 2004; Phillips *et al.*, 2006a; Wei *et al.*, 2004; Wei *et al.*, 2007; Yang *et al.*, 2006). However DCM has yet to be used in the manufacture of scaffolds fabricated by rapid prototyping that have been shown to be capable of bioactive growth factor release.

In this study, a range of scaffolds and scaffold coatings was developed, each with the potential to release bioactive growth factors. Structural scaffolds, processed using DCM, were manufactured from the synthetic polymers; PCL (M_n 42,500 and 80,000), PLGA, and blends of the two. Coating protocols, based on the natural polymers; alginate, chitosan, collagen and gelatin, were developed.

2.3. Materials and Methods

2.3.1. General Bioplotting Procedure

The Bioplotter™ (Envisiontec GmbH, Germany) is controlled by two distinct computer software programs, namely; PrimCAM (Primus Data, Switzerland) and PrimCNC (Primus Data, Switzerland). PrimCAM is capable of importing 3D computer aided design (CAD) files, and combining this with user inputs such as; strand spacing in the X and Y axes, strand offset, patterning and the plotting spacing between layers in the Z axis. From this information, PrimCAM produces a numerical control (NC) code programme file. This can be read by PrimCNC, which in turn controls the Bioplotter™. Alternatively, the user may write the NC code programme directly. The latter option was chosen for use in all studies described in this thesis.

After loading the NC code programme, a nitrogen gas cylinder was connected to the Bioplotter™ via the pressure regulator (see **Figure 2.1**). The Bioplotter™ itself was housed in a class-two tissue culture hood, to reduce the possibility of contaminating the scaffolds with airborne pathogens during manufacture. To reach the syringe (Engineered Fluid Dispensing™, UK), the nitrogen first had to pass through a sterile filter (see **Figure 2.1**), preventing infectious agents in the nitrogen from contaminating the plotting solution. The regulator was then set to the desired plotting pressure.

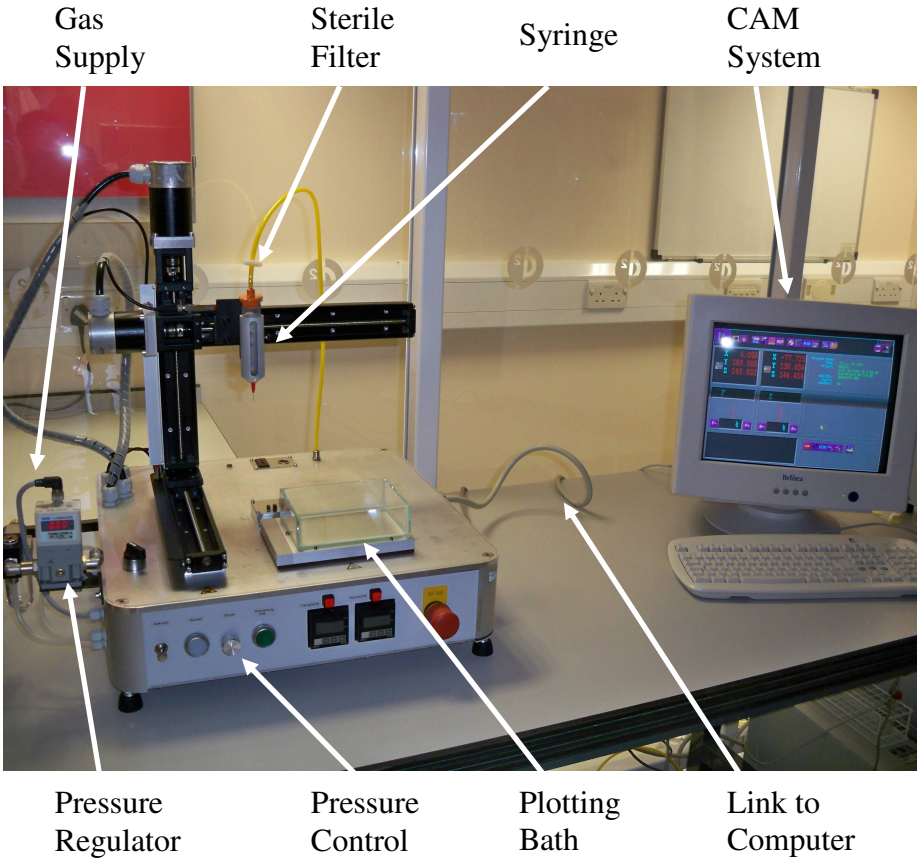

Figure 2.1: The Bioplotter™.

An annotated photograph of the Bioplotter™ and CAM system, showing the subcomponents of the scaffold manufacturing system.

After a blunt needle was attached, the plotting solution was loaded into the syringe. The syringe was then fixed securely into the holder, and was connected to the gas supply (see **Figure 2.1**). The position of the needle was determined using two light gate sensors. The plotting height was manually set to approximately 0.5 mm above a glass slide in the plotting bath, which acted as the plotting surface. After the plotting speed was set using the PrimCNC interface, scaffold plotting could then be initiated.

2.3.2. Scaffolds of Synthetic Polymers

2.3.2.1. PCL (M_n 42,500) Scaffold Fabrication

2.3.2.1.1. Optimisation of Plotting Parameters

Polycaprolactone (M_n 42,500) (Sigma, UK) was dissolved in DCM (dichloromethane for peptide synthesis, ≥ 99.8%) (Fluka, UK) at concentrations of 25 and 30% (w/v) (i.e. 1.0 or 1.2 g PCL added to 4 ml of DCM). The solutions were left to dissolve in an orbital incubator (Stuart S150), set to 120 rpm (orbital diameter: 1.5 cm) and 37°C, for 24 hours. The 30% (w/v) was incubated under the same conditions for a further 48 hours. An NC code programme was written to produce two-layer scaffolds with a strand spacing of 0.80 mm in both the X and Y axes (with the dimensions 20 × 20 mm), and a Z spacing of 0.14 mm, see **Appendix A**. The starting plotting speed was 140 mm/min. The 25% (w/v) PCL/DCM solution was then used to manufacture scaffolds as described in the general protocol in §2.3.1, using blunt needles (inner diameter: 0.26 mm), 12.7 mm in length (Engineered Fluid Dispensing™, UK). The plotting surfaces used were glass slides (76 × 26 mm, Menzel-Gläser, Germany). Five minutes after plotting, the scaffolds could easily be removed from the glass slides using a scalpel. The plotting speed and pressure were optimised by direct experimentation. Afterwards, the scaffolds were vacuum dried using a freeze dryer (Alpha 1-4, Christ, Germany) set to 75 mbar of absolute pressure for 60 min.

The plotting parameters were also optimised for scaffolds manufactured using the same manufacturing procedure as above, but with the addition of plotting solutions. Two plotting solutions were used, namely; 100% industrial methylated spirit (IMS)

(Fisher), and 70% IMS, 30% distilled water (dH_2O). Approximately 250 ml of plotting solution were added to the plotting bath (see **Figure 2.1**).

Representative scaffolds were then examined using a dissecting microscope (Zeiss, Stemi 2000-C). Images were taken at × 2 magnification using a mounted camera (Nikon, DXM1200).

2.3.2.1.2. Incorporation of Aqueous Solutions

The purpose of these experiments was to determine whether scaffolds could be produced which encapsulated aqueous solutions.

Phosphate buffered saline (PBS) (Oxoid, UK) was added to 25% (w/v) solutions of PCL/DCM, prepared as in §2.3.2.1.1, at concentrations of; 5, 2, and 1% (v/v), in a 15 ml centrifuge tube (Corning, UK). Methylene blue (Sigma) aqueous solutions (5 mg/ml) were also added at 1% (v/v) to 25% (w/v) solutions of PCL/DCM. This facilitated the examination of the distribution of the aqueous solution in the PCL/DCM solution, and in the resulting scaffolds.

Once added, emulsions were created by vigorous manual mixing using sterile 3 ml transfer pipettes (Fisher, UK) for approximately 30 seconds. The resulting emulsions were loaded into the syringe of the Bioplotter™. Scaffolds were then manufactured, with no plotting media, using the optimised plotting parameters determined in §2.4.1.1.1, and then vacuum dried at 75 mbar (absolute pressure) for 60 min.

To determine scaffold pore sizes and strand thickness, three scaffolds were randomly selected from three different scaffold batches of eight. The batches were manufactured from separate 25% (w/v) PCL/DCM solutions encapsulating 1% (v/v) PBS. The scaffolds were then photographed using an inverted microscope (Axio Observer, Carl Zeiss Ltd., Germany) at × 10 magnification. The pore sizes and strand thicknesses in both the X and Y axes were measured for three randomly selected fields of view for each scaffold.

The thickness of the scaffolds used above was also measured directly. Three measurements of scaffold thickness were made for each of the scaffolds using Vernier callipers (Farnell Inone, UK).

2.3.2.1.3. Plotting More Than Two-Layers

An NC code programme was written to produce 16 layer scaffolds with a strand spacing of 0.80 mm in both the X and Y axes (with the dimensions 20 × 20 mm), and a Z spacing of 0.14 mm, see **Appendix C**. Solutions of 25% (w/v) PCL/DCM were produced as described in §2.3.2.1.1. Scaffolds were then manufactured with either no plotting media or IMS, using the optimised plotting parameters determined in §2.4.1.1.1.

2.3.2.2. PCL (M_n 80,000) Scaffold Fabrication

Polycaprolactone (M_n 80,000) (Sigma, UK) was dissolved in DCM at concentrations of 25% (w/v). The solutions were left to dissolve in an orbital incubator (Stuart S150), set to 120 rpm and 37°C, for 24 hours. The NC code programme was the same as that used in §2.3.2.1.1, using a strand spacing of 0.80 mm in both the X and Y axes (with the dimensions 20 × 20 mm), and a Z spacing of 0.14 mm, see **Appendix A**.

The starting plotting speed was 140 mm/min, and blunt needles (inner diameter: 0.26 mm), 12.7 mm in length were used. Methylene blue aqueous solutions at a concentration of 5 mg/ml were added to the PCL/PLGA solutions at 1% (v/v). Once added, emulsions were created by vigorous manual mixing using sterile 3 ml transfer pipettes for approximately 30 seconds. The resulting emulsions were loaded into the syringe of the Bioplotter™.

The PCL/DCM solutions were used to manufacture scaffolds as described in the general protocol in §2.3.1. Glass slides were used as the plotting surfaces. After plotting, the scaffolds were vacuum dried at 75 mbar (absolute pressure), for 60 min. The plotting speed and pressure were optimised by direct experimentation.

2.3.2.3. PLGA Scaffold Fabrication

Poly(lactide-co-glycolide) (lactide: glycolide 75:25, M_w 66,000 – 107,000) (Sigma) was dissolved in dichloromethane at concentrations of 25%, and 30% (w/v). The solutions were left to dissolve in an orbital incubator (Stuart S150), set to 120 rpm and 37°C, for 6 hours. Two NC code programmes were used to produce two-layer scaffolds. The 30% (w/v) solutions were plotted with a strand spacing of 0.80 mm in both the X and Y axes (with the dimensions 20 × 20 mm), and a Z spacing of 0.14 mm, see **Appendix A**. The starting plotting speed was 140 mm/min, and blunt needles (inner diameter: 0.26 mm), 12.7 mm in length (Engineered Fluid Dispensing™, UK) were used. The solutions of 25% (w/v) were plotted with an X-Y strand spacing of 1.00 mm (with the dimensions 20 × 20 mm), and a Z spacing of 0.14 mm, see **Appendix B**. The starting plotting speed was 560 mm/min, and blunt needles (inner diameter: 0.21 mm), 12.7 mm in length (Engineered Fluid Dispensing™, UK) were used.

The PLGA/DCM solutions were used to manufacture scaffolds as described in the general protocol in §2.3.1. The plotting surfaces used were glass slides (76 × 26 mm, Menzel-Gläser, Germany). After plotting, the scaffolds were either left on the bench to dry, or vacuum dried at 75 mbar (absolute pressure), for 1, 2, 3 or 24 hr. The plotting speed and pressure were optimised by direct experimentation.

Methylene blue aqueous solutions at a concentration of 5 mg/ml were also added at 1% (v/v) to 25% (w/v) solutions of PLGA/DCM. Once added, emulsions were created by vigorous manual mixing using sterile 3 ml transfer pipettes for approximately 30 seconds. The resulting emulsions were loaded into the syringe of the Bioplotter™. Scaffolds were formed using the optimised plotting parameters as determined in §2.4.1.3.

Representative scaffolds were then examined using a dissecting microscope (Zeiss, Stemi 2000-C). Images were taken using a mounted camera (Nikon, DXM1200).

2.3.2.4. PCL/PLGA Scaffold Fabrication

Two different PCL/PLGA blends were made. The mass ratios of PCL:PLGA were 66:33 and 33:66. The plastic blends were dissolved in DCM at 25% (w/v).

For both blends, the NC code programme used was that used in §2.3.2.1.1 to produce scaffolds from 25% (w/v) PCL/DCM, see **Appendix A**. The starting plotting speed was 140 mm/min, and blunt needles (inner diameter: 0.26 mm), 12.7 mm in length (Engineered Fluid Dispensing™, UK) were used. Methylene blue aqueous solutions at a concentration of 5 mg/ml were added to the PCL/PLGA/DCM solutions at 1% (v/v). Once added, emulsions were created by vigorous manual mixing using sterile 3 ml transfer pipettes for approximately 30 seconds. The resulting emulsions were loaded into the syringe of the Bioplotter™.

The PCL/PLGA/DCM solutions were used to manufacture scaffolds as described in the general protocol in §2.3.1. The plotting surfaces used were glass slides. After plotting, the 66:33 blend scaffolds were vacuum dried at 75 mbar (absolute pressure) for 60 min, whereas the 33:66 blend scaffolds were left on the bench, at room temperature, to dry for 72 hr. The plotting speed and pressure were optimised by direct experimentation.

2.3.3. Scaffold Coatings

2.3.3.1. Alginate Coating

PCL scaffolds were manufactured as described in §2.3.2.1.1, with no plotting media, using the optimised plotting parameters determined in §2.4.1.1.1. A stock solution of alginate (Alginic Acid Sodium salt from Brown Algae, Sigma, UK) was dissolved at 3% (w/v) in an aqueous solution of 0.5 M sodium chloride (Sigma, UK). The alginate stock was incubated at room temperature for three days before being autoclaved. A 1.5% (w/v) alginate solution in 0.5 M NaCl was then made up by diluting the stock alginate solution.

PCL scaffolds (20 × 20 mm) were cut into four approximately equal (10 × 10 mm) parts. Three of these scaffolds were wetted by immersing them in IMS for 10 min.

They were washed with dH_2O, then PBS and then immersed in PBS for 5 min. After they had been quickly blotted with a dry medical wipe (Kimberly Clark, UK), the scaffolds were immersed in the 1.5% (w/v) alginate solution for 10 min.

Afterwards, the scaffolds were removed and quickly blotted to remove excess alginate, using dried medical wipes (Kimberly Clark, USA). The scaffolds were then placed in 15 ml of dH_2O in a 30 ml universal container for 5 min (inverting five times) before being immersed in 0.1 M aqueous calcium chloride (Sigma, UK) solution for 30 min.

From preliminary experiments, it had previously been determined that 0.5% (w/v) safranin-o (Sigma, UK) in a 0.1 M sodium acetate (Sigma, UK) aqueous buffer (pH 4.6) could vividly stain calcium alginate red. Therefore the alginate coated scaffolds were immersed in safranin-o solution for 30 min. Afterwards they were washed five times with 10 ml of distilled water (dH_2O), and incubated overnight in dH_2O. Subsequently the scaffolds were blotted and photographed using an inverted microscope (Nikon Eclipse TS 100) at × 10 magnification using a mounted camera (Nikon, DXM1200).

2.3.3.2. Chitosan Coating

PCL scaffolds were manufactured as described in §2.3.2.1.1, with no plotting media, using the optimised plotting parameters determined in §2.4.1.1.1. A stock solution of chitosan (Chitosan from Crab Shells, minimum 85 % deacetylated, Sigma, UK) was dissolved at 3% (w/v) in an aqueous solution of 0.5% (v/v) acetic acid (Fluka, Germany). The chitosan stock was incubated at room temperature for three days before being autoclaved. A 1.5% (w/v) chitosan solution in 0.5% (v/v) acetic acid was then made up by diluting the stock chitosan solution.

PCL scaffolds (20 × 20 mm) were cut into four approximately equal (10 × 10 mm) parts. Three of these scaffolds were wetted by immersing them in IMS for 10 min. They were washed in dH_2O, then PBS and then immersed in PBS for 5 min. After they had been quickly blotted with a dry medical wipe (Kimberly Clark, UK), the scaffolds were immersed in the 1.5% (w/v) chitosan solution for 10 min.

Afterwards, the scaffolds were removed and quickly blotted to remove excess chitosan. The scaffolds were then placed in 15 ml of dH_2O in a 30 ml universal tube for 5 min (inverting five times) before being immersed in 2% (w/v) aqueous TPP (sodium tripolyphosphate, Sigma, UK) solution for 30 min.

From preliminary experiments, it had previously been determined that 0.15% (w/v) light green SF yellowish (Sigma, UK) in 0.2% (v/v) aqueous acetic acid, could vividly stain chitosan green. Therefore the chitosan coated scaffolds were immersed in light green SF yellowish solution for 30 min. Then they were washed five times with 10 ml of dH_2O, and incubated overnight in dH_2O. Afterwards the scaffolds were blotted and photographed using an inverted microscope (Nikon Eclipse TS 100) at × 10 magnification using a mounted camera (Nikon, DXM1200).

2.3.3.3. Collagen Coating

PCL scaffolds were manufactured as described in §2.3.2.1.1, with no plotting media, using the optimised plotting parameters determined in §2.4.1.1.1. Methylene blue aqueous solution (5 mg/ml) was added at 1% (v/v) to 1 mg/ml Type-I collagen (rat tail, Sigma, UK) in 0.1 M aqueous acetic acid. This coloured the solution and facilitated the later examination of the distribution of the collagen on the scaffolds, even though methylene blue was not a direct stain for collagen.

PCL scaffolds (20 × 20 mm) were cut into four approximately equal (10 × 10 mm) parts. Twelve of these scaffolds were wetted by immersing them in IMS for 10 min. They were washed in dH_2O, then PBS and then immersed in PBS for 5 min. They were then immersed in the collagen/methylene blue solution for 5 min. Afterwards, the scaffolds were removed, and allowed to air dry for 4 hr at room temperature.

Once dry, the scaffolds were photographed using an inverted microscope at × 10 magnification using a mounted camera. They were also photographed using a hand held digital camera (M1033 Kodak, USA).

2.3.3.4. Gelatin Coating

PCL scaffolds were manufactured as described in §2.3.2.1.1, with no plotting media, using the optimised plotting parameters determined in §2.4.1.1.1. Methylene blue aqueous solution (5 mg/ml) was added at 1% (v/v) to 2% (w/v) aqueous gelatin (Type-A, Sigma, UK). This coloured the solution and facilitated the later examination of the distribution of the gelatin on the scaffolds, even though methylene blue was not a direct stain for gelatin.

PCL scaffolds (20 × 20 mm) were cut into four approximately equal (10 × 10 mm) parts. Twelve of these scaffolds were wetted by immersing them in IMS for 10 min. They were washed dH_2O, then PBS and then immersed in PBS for 5 min. The scaffolds were then immersed in the gelatin/methylene blue solution for 5 min. After which time, they were removed, and allowed to air dry for 4 hr at room temperature.

Once dry, the scaffolds were photographed using an inverted microscope at × 10 magnification using a mounted camera. They were also photographed using a hand held digital camera (M1033 Kodak, USA).

2.3.4. Statistical Treatment of Results

All results are expressed as the sample means ± standard error of the mean (SEM).

2.4. Results

2.4.1. Scaffolds of Synthetic Polymers

2.4.1.1. PCL Scaffold Fabrication

2.4.1.1.1. Optimisation of Plotting Parameters

The 25% (w/v) PCL/DCM mixture dissolved to a homogeneous solution within 24 hr. In contrast, the 30% (w/v) PCL/DCM mixture was still heterogeneous even after 72 hr. What is more, by the end of this period, evaporation of DCM became significant. The 25% (w/v) PCL/DCM solutions were therefore chosen for use in further work.

A plotting pressure of 1.00 bar of gauge pressure was selected, and the optimum plotting speed was found by direct experimentation. The initial plotting speed of 140 mm/min was found to be too low with the result that scaffold porosity was lost (see **Figure 2.2a**). When the plotting speed was increased by 40% to 196 mm/min, defects in the scaffold formed when the second layer was plotted (see **Figure 2.2b**). However, scaffold porosity was retained, and no defects formed, when the plotting speed was set to 168 mm/min, an increase of 20% on the initial plotting speed (see **Figure 2.2e**).

When the plotting pressure was varied, scaffold porosity was partially lost when the pressure was increased to 1.20 bar (gauge pressure) (see **Figure 2.2c**). Plotting defects in the second layer were again observed when the pressure was decreased to 0.80 bar (gauge pressure).

Therefore, the optimum plotting speed was found to be 168 mm/min when the plotting pressure was set to 1.00 bar (gauge pressure). It was found that scaffolds could be manufactured using a plotting media of IMS (see **Figure 2.3b**). However, using plotting solutions of 70% IMS 30% dH_2O, caused the PCL/DCM solution to detach from the plotting surface, and coalesce into droplets (see **Figure 2.3a**).

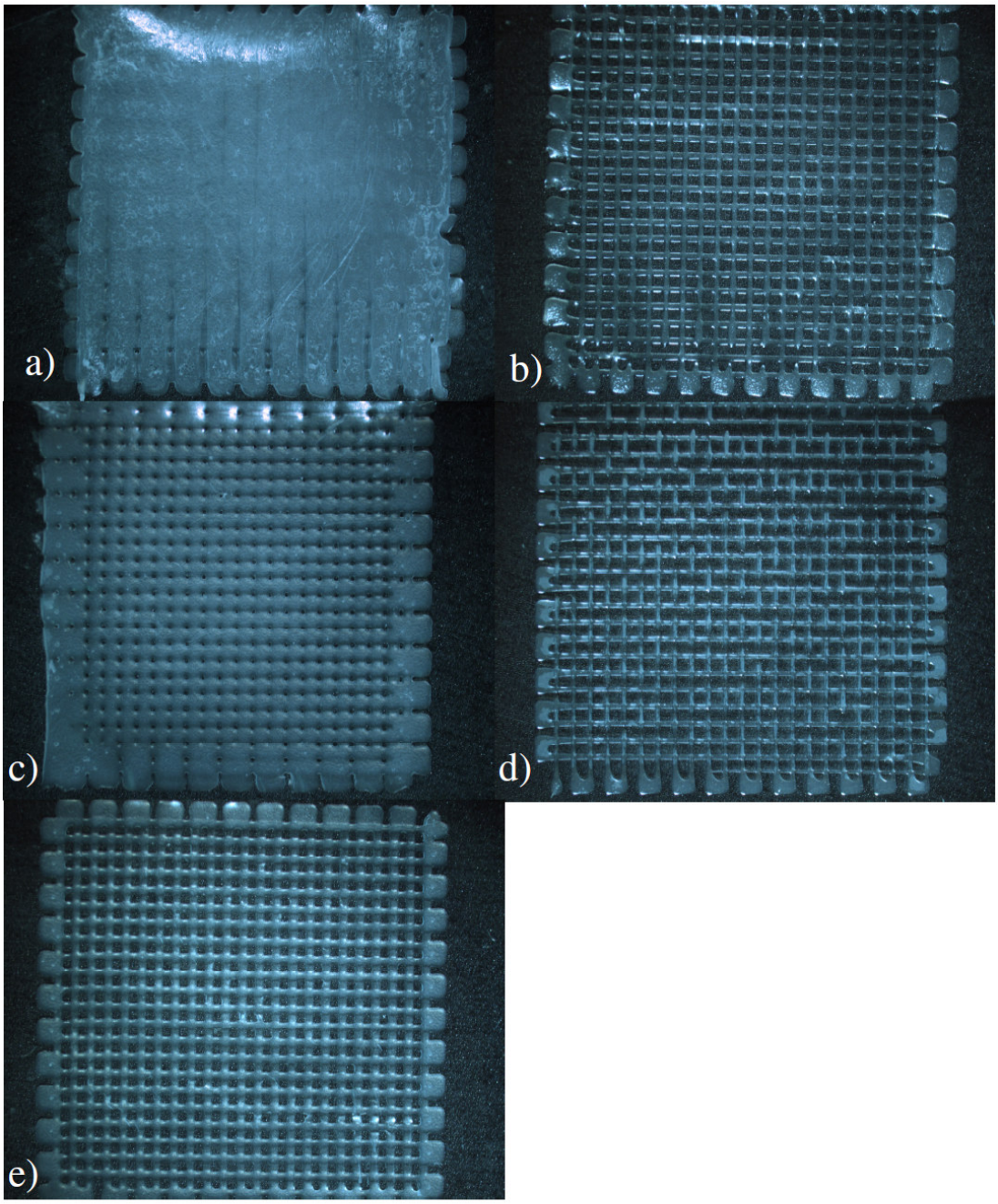

Figure 2.2: Optimisation of PCL plotting parameters

Scaffold images taken using a dissecting microscope. The plotting parameters were a) speed = 140 mm/min, pressure = 1.00 bar (gauge pressure), b) speed = 196 mm/min, pressure = 1.00 bar (gauge pressure), c) speed = 168 mm/min, pressure = 1.20 bar (gauge pressure), d) speed = 168 mm/min, pressure = 0.80 bar (gauge pressure), e) speed = 168 mm/min, pressure = 1.00 bar (gauge pressure). The bar represents 20 mm.

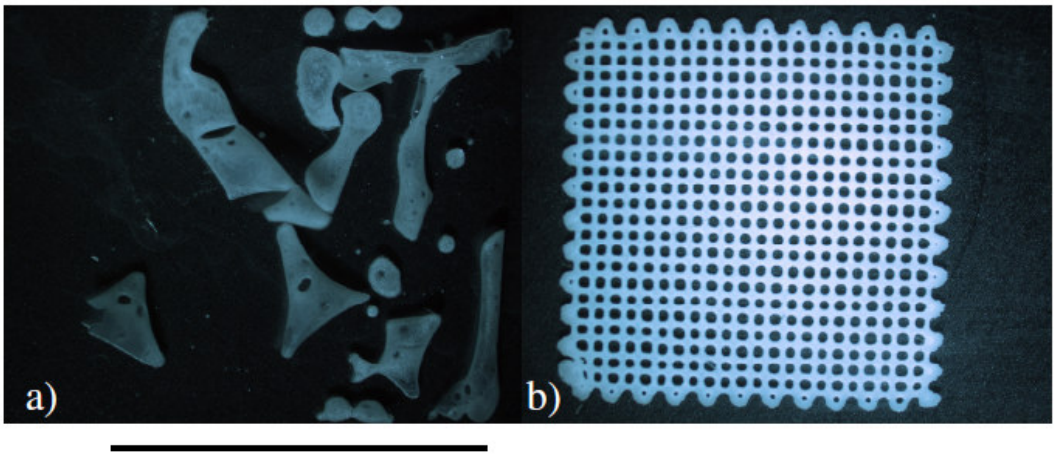

Figure 2.3: Addition of plotting media.

Scaffolds plotted in plotting solutions of a) 70% IMS 30% dH_2O, b) 100% IMS. The bar represents 20 mm.

2.4.1.1.2. Incorporation of Aqueous Solutions

As can be seen in **Figure 2.4**, emulsions of aqueous solutions could be formed by manual mixing with transfer pipettes. The aqueous methylene blue solution was found to be distributed throughout the organic phase of PCL/DCM.

Attempts to manufacture scaffolds with a 5% (v/v) aqueous solution were unsuccessful, since serious disruption of geometry occurred even in the first layer (see **Figure 2.5a**). Fabricating scaffolds with 2% (v/v) solutions was similarly unsuccessful, although the geometrical disruption was less severe (**Figure 2.5b** and **Figure 2.5c**).

In contrast, scaffolds could be formed with 1% (v/v) aqueous solutions while preserving the structure of the scaffold (see **Figure 2.5d** and **Figure 2.5e**). Using 1% (v/v) solutions of methylene blue, it was found that aqueous droplets, of various sizes, were distributed throughout the resulting scaffold (see **Figure 2.5f**).

The mean strand diameters and pore thicknesses were measured by image analysis (see **Figure 2.6**). The results can be found in **Table 2.1**.

Table 2.1: Mean PCL scaffold pore and strand thicknesses.

The mean values for three scaffolds were used in each case.

Y-direction strand diameter (µm)	X-direction strand diameter (µm)	Y-direction pore thickness (µm)	X-direction pore thickness (µm)
353±9.7	444±3.5	373±9.5	460±13

The mean thickness of the two-layer scaffolds was found to be 52±3 µm.

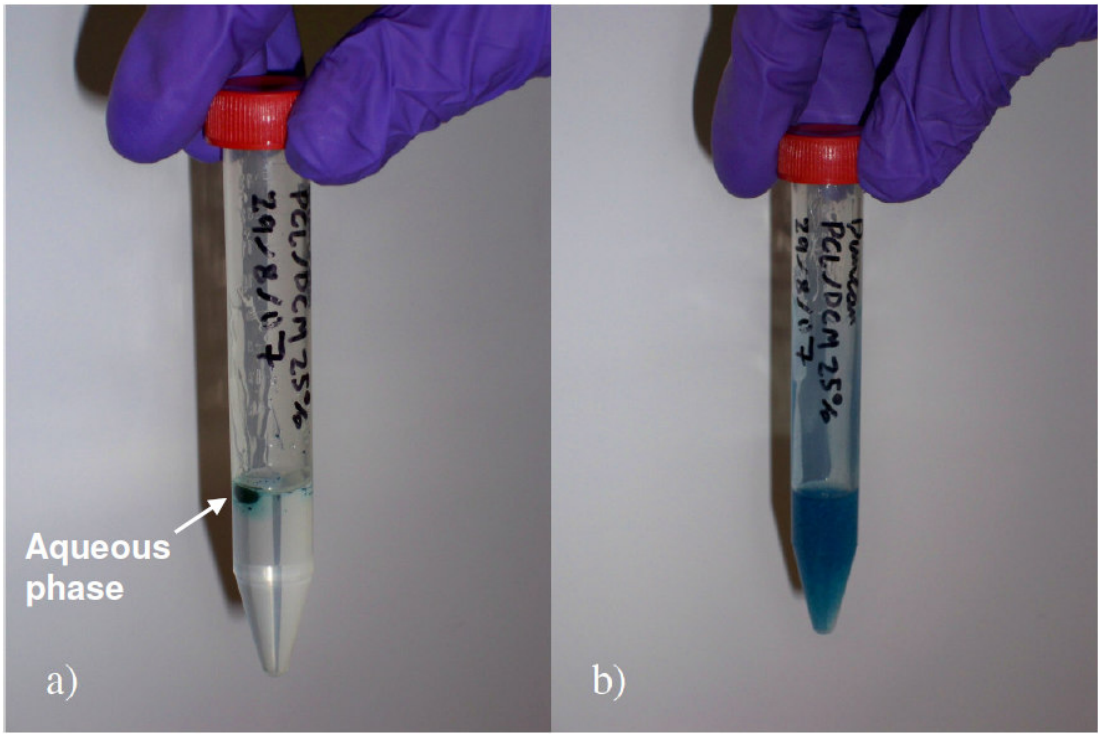

Figure 2.4: Distribution of aqueous methylene blue solution in 25% (w/v) PCL/DCM solution.

The distribution of the aqueous phase, as shown by methylene blue a) before mixing, and b) after mixing.

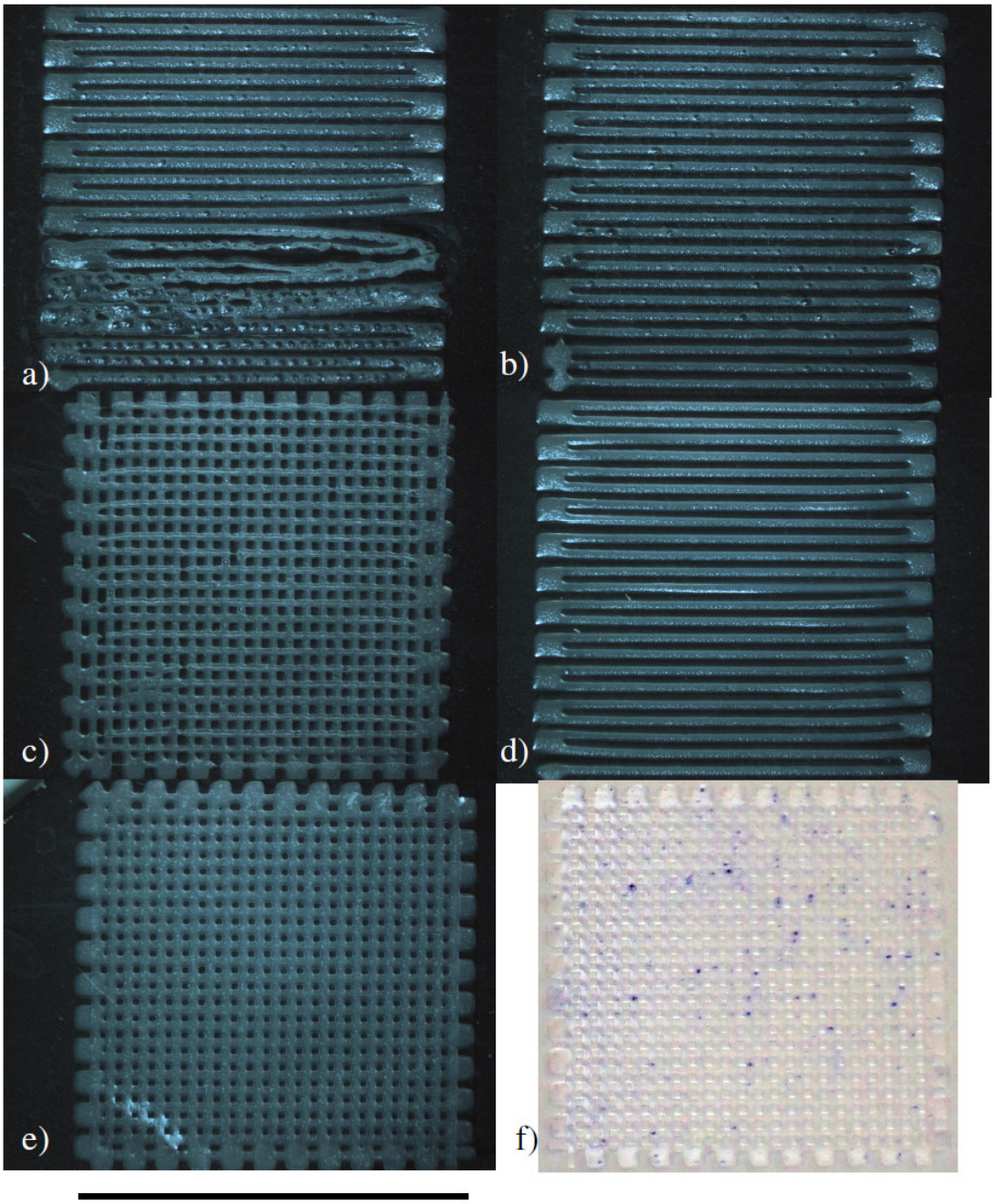

Figure 2.5: PCL scaffolds plotted encapsulating aqueous solutions.

PCL scaffolds manufactured with various different concentrations of aqueous solutions; a) 5% (v/v), one layer, b) 2% (v/v), one layer, c) 2% (v/v), two layers, d) 1% (v/v), one layer, e) 1% (v/v), two layers, f) 1% (v/v), two layers on a light background, demonstrating the distribution of methylene blue, indicated by the blue stain within the scaffold. The bar represents 20 mm.

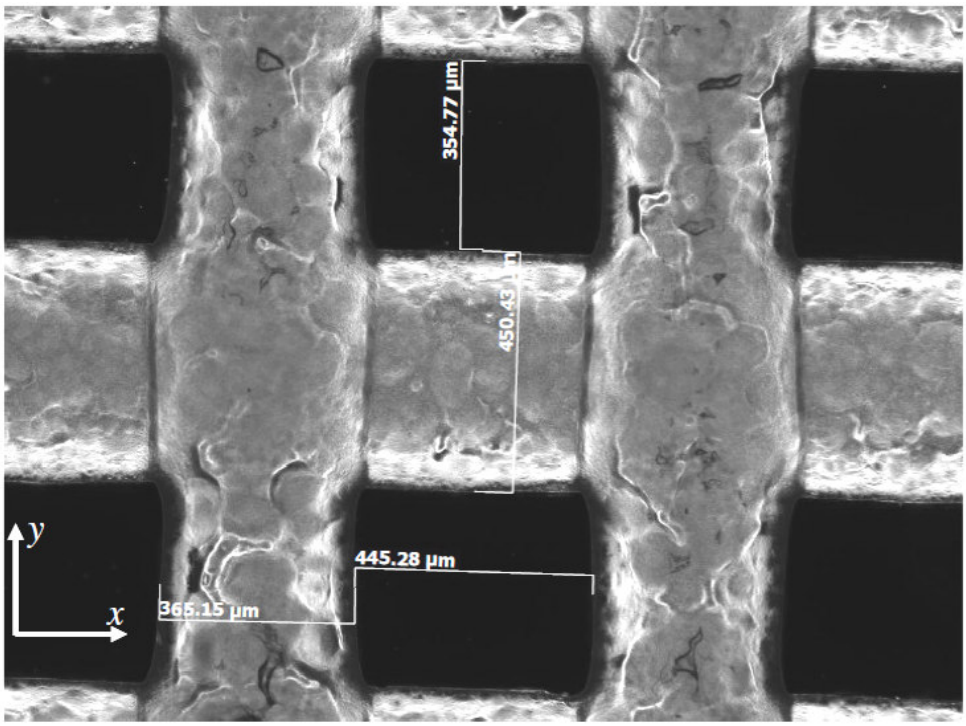

Figure 2.6: Measurement of scaffold pore and strand thickness.

A representative negative image of the PCL scaffolds. The lengths shown were measured using Zeiss image analysis software.

2.4.1.1.3. Plotting More Than Two-Layers

Attempts at fabricating scaffolds, from 25 % (w/v) PCL (M_n 42,500)/DCM, greater than two-layers in height were unsuccessful. As the successive layers were plotted, the layers underneath were re-dissolved. Therefore all the layers fused together, and flattened out across the glass slide plotting surface, eliminating all porosity. This effect was, however, less pronounced when IMS was used as plotting medium.

2.4.1.2. PCL (M_n 80,000) Scaffold Fabrication

The 25% (w/v) solution dissolved to a homogeneous solution within 24 hr of mixing. The resulting solutions, especially when mixed with the aqueous solution, were found to be more viscous than solutions of PCL (M_n 42,500). Hence, for a speed of 168 mm/min, the optimum plotting pressure was found to be 1.5 bar (gauge pressure).

The resulting scaffolds could easily be removed from the plotting surface with a scalpel approximately 5 min after manufacture (see **Figure 2.7**).

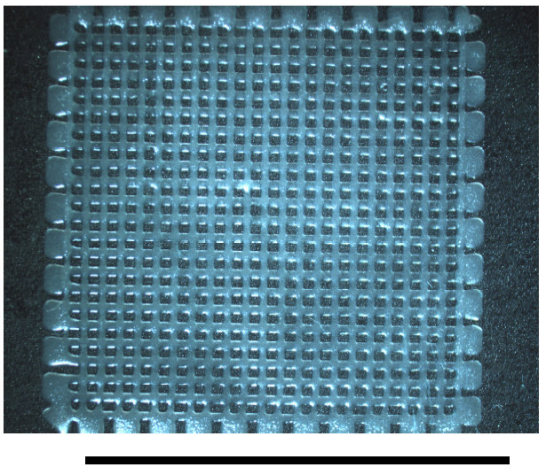

Figure 2.7: PCL (M_n 80,000) Scaffold.

PCL (M_n 80,000) scaffold manufactured from 25% (w/v) PCL/DCM, with an XY strand spacing of 0.8 mm. The bar represents 20 mm.

2.4.1.3. PLGA Scaffold Fabrication

The 30 and 25% (w/v) PLGA/DCM mixtures dissolved to homogeneous solutions within 6 hr. It was observed that the viscosity of the solutions was less than that of 25% (w/v) PCL/DCM.

For the 30% (w/v) solution, using a plotting pressure of 1.00 bar (gauge pressure) as a starting point, the optimum speed of the needle was found to be 210 mm/min. It was found that the struts merged together at the end of each row and column (see **Figure 2.8a**). Large bubbles also formed during the drying process which further compromised scaffold geometry (see **Figure 2.8a**). Once plotted, the scaffolds required a setting time on the bench of approximately 72 hr. After which time, the scaffolds could be removed, although with difficulty, from the glass slides using a scalpel.

The starting pressure for the 25% (w/v) solution was 0.70 bar (gauge pressure). This yielded an optimum speed of 672 mm/min. For these scaffolds, the merging of the struts at the edges was limited to approximately 1 mm (see **Figure 2.8b**). Bubbles, which were a severe problem for the more viscous 30% (w/v) solution, were not evident.

The scaffolds required approximately 72 hr to set before they could be removed from the plotting surface. It was found that vacuum drying for 1, 2, 3 or 24 hr had no measureable effect on the ultimate scaffold setting time.

When aqueous solutions of methylene blue were added at a concentration of 1% (v/v) to 25% (w/v) PLGA/DCM, evenly dispersed emulsions could be achieved. Methylene blue dispersion was also observed in the resulting scaffolds (see **Figure 2.8c**). The optimum plotting parameters were found to be identical to those for the original 25% (w/v) PLGA/DCM solution.

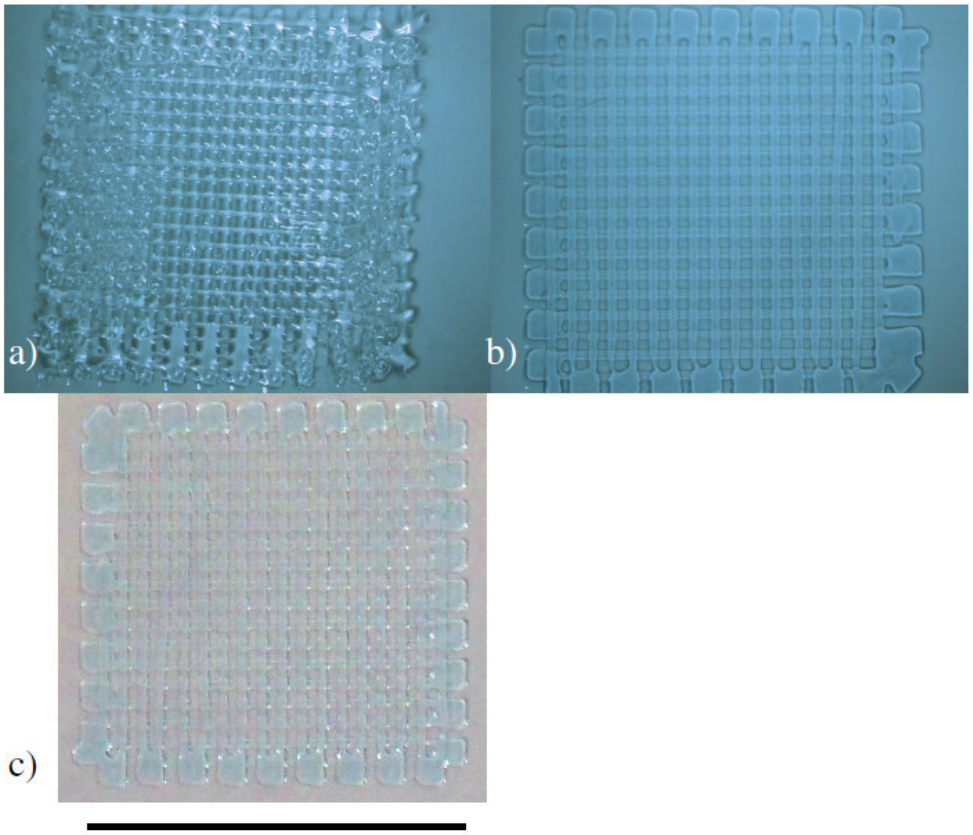

Figure 2.8: PLGA Scaffolds.

PLGA scaffolds manufactured from a) 30% (w/v) PLGA/DCM, with an XY strand spacing of 0.8 mm, b) 25% (w/v) PLGA/DCM, with an XY strand spacing of 1.0 mm, and c) 25% (w/v) PLGA/DCM, encapsulating 1% (v/v) methylene blue solution. The bar represents 20 mm.

2.4.1.4. PCL/PLGA Scaffold Fabrication

Both 66:33 and 33:66, 25% (w/v) PCL:PLGA/DCM solutions dissolved to homogeneous solutions within 24 hr.

For the 66:33 (PCL rich) blend, for a plotting pressure of 1.5 bar (gauge pressure), the optimum plotting speed was 168 mm/min. The XY strand spacing used was 0.8 mm. The resulting scaffolds could be easily removed from the plotting surface with a scalpel approximately 5 min after manufacture (see **Figure 2.9a**). The scaffolds were also found to encapsulate the methylene blue solution (see **Figure 2.9c**).

The optimum plotting parameters for the 33:66 (PLGA rich) blend were; 1.4 bar (gauge pressure) for the plotting pressure, and 266 mm/min for the plotting speed. The XY strand spacing used was 0.8 mm. In contrast to the PCL rich blend, the scaffolds required a setting time of approximately 72 hr, though they were also capable of encapsulating the methylene blue solution (see **Figure 2.9b**).

In both cases, the porosity in the XY plain was preserved. The geometry of the scaffolds was not disrupted by bubbles.

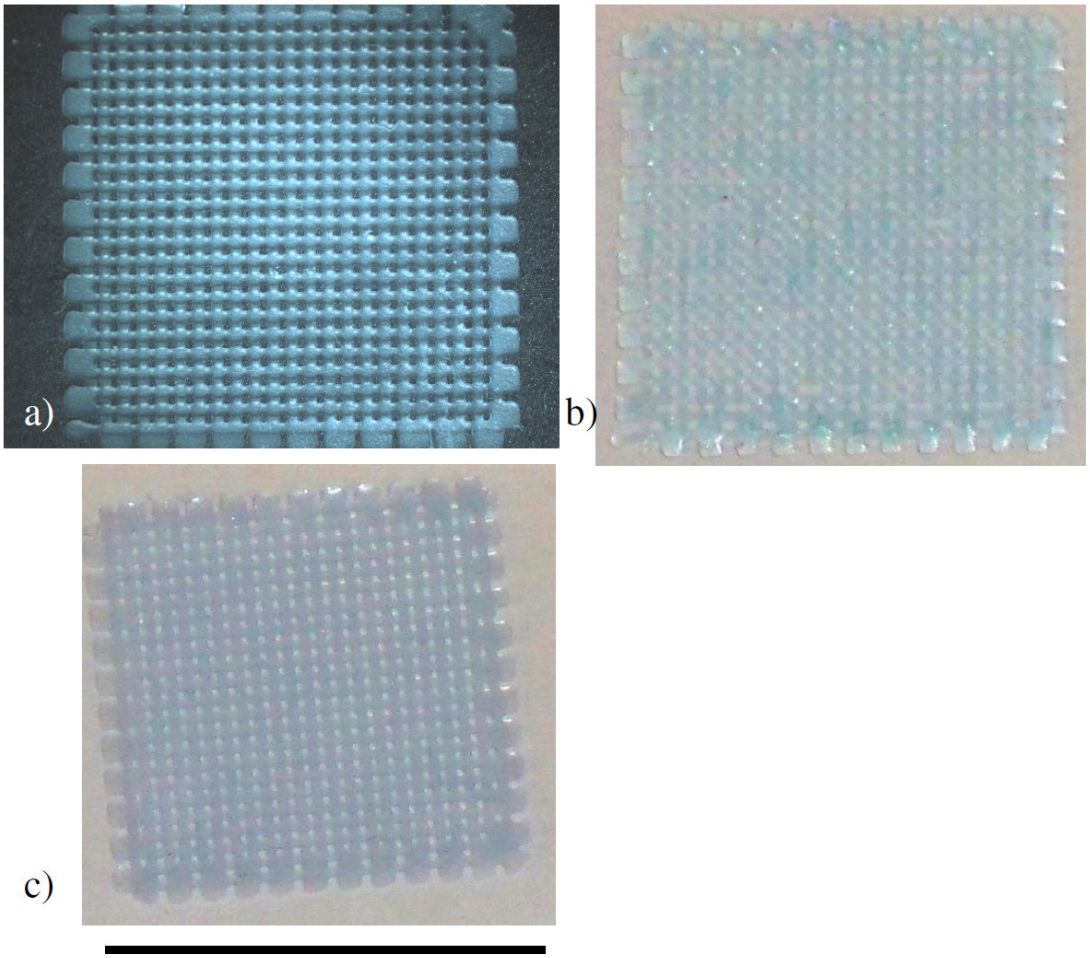

Figure 2.9: Scaffolds of PCL/PLGA Blends.

Scaffolds manufactured from a) 66:33 PCL/PLGA blend, 25% (w/v) PCL/PLGA/DCM, with an XY strand spacing of 0.8 mm, and b) 33:66 PCL/PLGA blend 25% (w/v) PCL/PLGA/DCM, with an XY strand spacing of 0.8 mm, encapsulating methylene blue. c) 66:33 PCL/PLGA blend, 25% (w/v) PCL/PLGA/DCM, with an XY strand spacing of 0.8 mm, encapsulating methylene blue. The blue colour observed within the scaffolds, indicates the presence of methylene blue. The bar represents 20 mm.

2.4.2. Scaffold Coatings

2.4.2.1. Alginate Coating

Vivid red staining (by safranin-o) was observed to cover all the scaffolds, indicating the presence of alginate, as previously the safranin-o had been shown to stain alginate but not PCL. On examination with the inverted microscope, it was found that all the scaffold pores had been blocked (see **Figure 2.10a**). However, pores of the scaffolds which were washed before the crosslinking step were unobstructed (see **Figure 2.10b**).

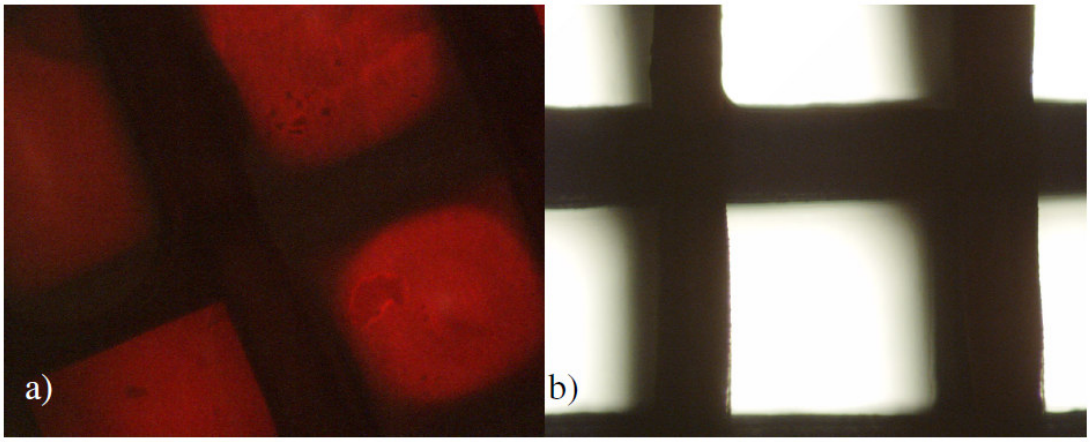

Figure 2.10: PCL Scaffolds Coated with Alginate.

PCL Scaffolds with an XY strand spacing of 0.8 mm coated with alginate 1.5% (w/v) a) crosslinked with $CaCl_2$ and b) washed to remove excess alginate before being crosslinked with $CaCl_2$. The bar represents 0.8 mm.

2.4.2.2. Chitosan Coating

Vivid green staining (by light green SF yellowish solution) was observed to cover all the scaffolds, denoting the presence of chitosan as previously the light green SF yellowish solution had been shown to stain chitosan but not PCL. On examination with the inverted microscope, it was found that all the scaffold pores had been blocked (see **Figure 2.11a**). However, pores of the scaffolds which were washed before the crosslinking step were unobstructed (see **Figure 2.11b**).

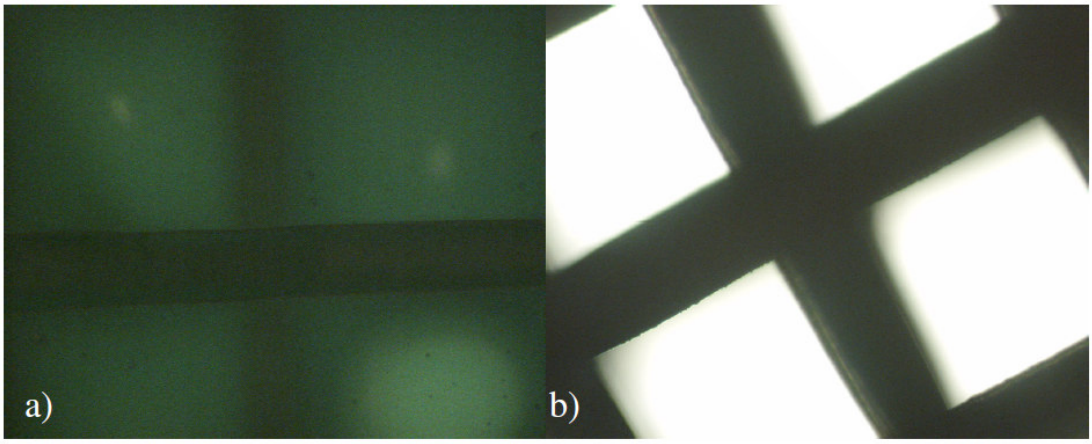

Figure 2.11: PCL Scaffolds Coated with Chitosan.

PCL Scaffolds with an XY strand spacing of 0.8 mm coated with chitosan 1.5% (w/v) a) crosslinked with TPP and b) washed to remove excess chitosan before being crosslinked with TPP. The bar represents 0.8 mm.

2.4.2.3. Collagen Coating

The scaffolds were found to be evenly coated with a blue colour, demonstrating the presence of collagen (see **Figure 2.12a**). This was because methylene blue was co-dissolved in the collagen coating solution. On examination with the inverted microscope, the scaffold pores were found to be almost completely unobstructed (see **Figure 2.12b**).

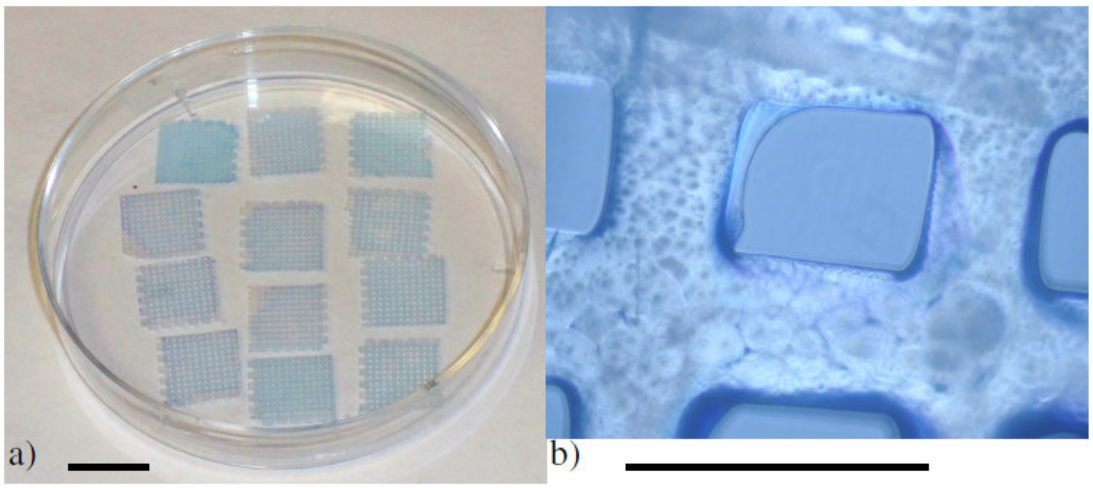

Figure 2.12: PCL Scaffolds Coated with Collagen.

PCL Scaffolds with an XY strand spacing of 0.8 mm coated with collagen. a) macroscopic view, the bar represents 10 mm. b) × 10 magnification, the bar represents 0.8 mm.

2.4.2.4. Gelatin Coating

The scaffolds were found to be evenly coated with a blue colour, demonstrating the presence of gelatin (see **Figure 2.13a**). This was because methylene blue was co-dissolved in the gelatin coating solution. On examination with the inverted microscope, the scaffold pores were found to be almost completely unobstructed (see **Figure 2.13b**).

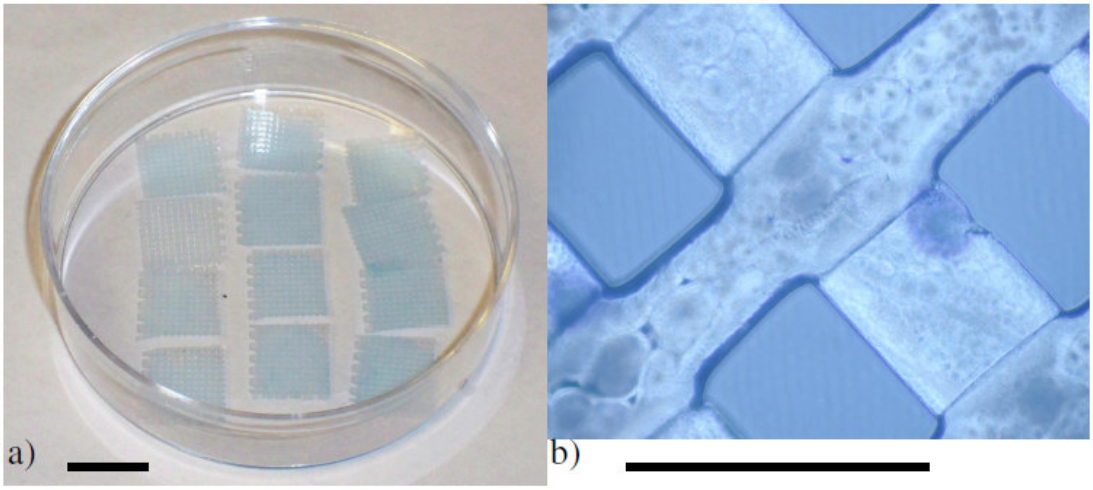

Figure 2.13: PCL Scaffolds Coated with Gelatin.

PCL Scaffolds with an XY strand spacing of 0.8 mm coated with gelatin. a) macroscopic view, the bar represents 10 mm. b) × 10 magnification, the bar represents 0.8 mm.

2.5. Discussion

As outlined in §1.2.6.3.4, few studies have reported regenerative medical constructs capable of releasing growth factors by two independent delivery systems, and even these are in their early stages of development (Sohier *et al.*, 2006; Ginty *et al.*, 2008). However, the ability to deliver different growth factors with different release profiles is thought to be highly desirable.

A promising dual delivery strategy was thought to be: encapsulating growth factors both within a scaffold, and in a scaffold coating. The purpose of the studies described in this chapter was to determine the feasibility of manufacture of a range of scaffolds and scaffold coatings which have the potential to be used as growth factor delivery systems.

2.5.1. Scaffolds of Synthetic Polymers

2.5.1.1. PCL Scaffold Fabrication

PCL was the first potential scaffold material to be investigated. As discussed in §1.2.5.8, PCL is biocompatible and has formed part of a USFDA approved drug delivery device (Hutmacher *et al.*, 2001; Hunter *et al.*, 1998). Therefore PCL components of a regenerative medical construct are unlikely to fail design criteria 1 (non-toxic) and 2 (producing no adverse effects) (see §1.2.2). These "tight design criteria" preclude scaffolds which are not biocompatible or are likely to produce an adverse reaction, such as an immune response, or induce neoplasia.

PCL may not completely meet the loose design criterion, number 6 (scaffold degradation rate matching the rate of extracellular matrix production) (see §1.2.2). The degradation time of approximately two years (Ma *et al.*, 2006) is likely to be longer than is desirable. However many current clinical treatments also do not fully meet this standard. For example, bone allografts are not fully remodelled even five years after surgery (Enneking and Mindell, 1991). Failure to fully meet design criterion 6 is unlikely to be a significant disadvantage of the final product.

Design criterion 8 (similar scaffold mechanical properties to the surrounding tissue) (see §1.2.2) is likely to be satisfied by PCL. Williams *et al*. (2005) reported that the mechanical properties of their PCL scaffolds were within the lower range for human trabecular bone. Finally, PCL is known to be relatively inexpensive, and scaffolds have previously been fabricated from it (Martin *et al.*, 2008; Hutmacher *et al.*, 2001). Therefore scaffolds fabricated from this material are likely to satisfy design criterion 9 (scaffold manufacture should be simple and cost-effective).

Hence, PCL was thought to be a near-ideal potential scaffold material.

2.5.1.1.1. Optimisation of Plotting Parameters

Experiments were conducted to determine whether it was possible to manufacture PCL scaffolds using DCM. Previously, PCL scaffolds have been manufactured by rapid prototyping techniques either by extruding polymer melts (Hutmacher *et al.*, 2001, Rai *et al.*, 2005) or by dissolving the polymer in glacial acetic acid (Martin *et al.*, 2008).

Although the melting point of PCL is approximately 60°C, the polymer melt must be processed at 120°C (Hutmacher *et al.*, 2001). This effectively precludes the incorporation of biologically active factors (Brown *et al.*, 1990). Similarly, since glacial acetic acid is fully miscible with water (O'Neil, 2006), the solvent is free to interact and denature any bioactive factors present in the polymer solution. In contrast, DCM is largely immiscible with water, having a solubility of only 13g/l (O'Neil, 2006). Hence there is much less scope for the DCM to interact with growth factors dissolved in an aqueous solution. Indeed, a plethora of growth factor delivery systems in regenerative medicine rely on DCM as the solvent for synthetic polymers, as is discussed in §1.2.6.3.3 and §2.2. Since DCM is known be a solvent for PCL (Luong-Van *et al.*, 2007), this was thought to be a promising system for scaffold manufacture.

It was found that scaffolds could be produced in a practical fashion from solutions of 25% (w/v) PCL/DCM, using the optimised parameters described in §2.4.1.1.1. Scaffold porosity and strand regularity were also found to be maintained whether a

plotting solution of 100% IMS was used or not (see **Figure 2.2e** and **Figure 2.3b**). With the improvements made to both the NC code programme and the plotting surface from those used by Vadillo (2009), the optimised plotting procedure had a very low failure rate, and required little in the way of user input or skill. Thus, practical two-layer regenerative medical scaffolds were manufactured.

2.5.1.1.2. Incorporation of Aqueous Solutions

It was of great importance that the scaffolds could be manufactured containing aqueous solutions without disrupting their geometry or porosity. The presence of aqueous solutions within the scaffolds could enable the encapsulation and release of water soluble drugs, such as growth factors.

As can be seen in **Figure 2.5e** and **f**, aqueous solutions of 1% (v/v) could be successfully encapsulated within the scaffolds without any significant disruption to the geometry or porosity.

The porosity of regenerative medical scaffolds is known to be vital to allow host cell infiltration into the scaffold, as well as allowing nutrients and cell waste products to flow in and out respectively. Studies using computational fluid dynamics have indicated that scaffolds with pores of the size range 96 – 350 µm, are capable of being pervaded with fluids in bioreactor systems (Jungreuthmayer *et al.*, 2008). Robinson *et al.* (1995) tested PLA scaffolds with pore diameters of 100, 200 and 350 µm in rabbit calvarial defect models. They found that the scaffolds with pores of 350 µm allowed the greatest amount of bone ingrowth. Indeed, Karageorgiou and Kaplan (2005) noted that smaller pores favour endochondral ossification, whereas larger pores promote vascularisation, and therefore favour intramembranous ossification. They therefore recommend pore sizes greater than 300 µm in diameter.

It was found in §2.4.1.1.2 that the mean pore diameters in the X and Y-directions were 373±9.5 µm and 460±13 µm respectively. Therefore, the pore sizes were thought to be suitable for bone regenerative medical applications.

The scaffolds were found to be only 52±3 µm in height, whereas the strand thicknesses were found to be 444±3.5 µm and 353±9.7 µm in the X and Y-directions respectively. This means that the two-layer scaffolds were relatively flat. This is in contrast to scaffolds manufactured by Vadillo (2009) and Hutmacher (2001), where the strand diameters were approximately the same in the X, Y, and Z directions.

2.5.1.1.3. Plotting More Than Two-Layers

It was found that 3D geometry was difficult to fabricate using the process developed in §2.4.1.1.1 and §2.4.1.1.2. This was undesirable, as direct control of the complete 3D geometry was the favoured strategy (see design criterion 3, §1.2.2) (van Griensven *et al.*, 2008; Zhang and Ma, 2004), though it may not be a necessary requirement (Karp *et al.*, 2003).

3D geometry, however, could be created from two-layer scaffolds, either by binding them together using an adhesive, or by packing them into the defect site. The latter is possibly the preferred option, and has two distinct advantages over custom built 3D scaffolds. First, the scaffolds would not need to be individually tailored to the defect site. The scaffolds could, therefore, form part of an "off-the-shelf" product, which is likely to be both quicker and cheaper to manufacture. Second, it is known that the even seeding of cells onto 3D regenerative medical scaffolds is extremely challenging technically. Indeed it may require the continuous circulation of media in a bioreactor system (Sodian *et al.*, 2002; Carrier *et al.*, 1999). This problem could be largely eliminated by using multiple two-layer scaffolds, each of which could be seeded statically under identical conditions.

It was concluded that such two-layer scaffolds could form the basis of an regenerative medical construct. Therefore, these scaffolds were subjected to further testing and refinement, as described in chapters 3, 4, 5, and 6 of this thesis.

2.5.1.2. PCL (M_n 80,000) Scaffold Fabrication

PCL (M_n 80,000) was investigated as a possible alternative scaffold material to PCL (M_n 42,500). It was thought that the difference in the number average molar mass would affect the diffusivity of the scaffold, and influence the release rate of

encapsulated drugs. This has been found to be the case for other synthetic polymers such as PLGA (Wei *et al.*, 2007). This was investigated in Chapter 4.

It was found that it was feasible to manufacture scaffolds from PCL (M_n 80,000). The scaffolds closely resembled the PCL (M_n 42,500) scaffolds described in §2.4.1.1.2, though the same degree of rigour in characterisation was not applied to them. This was because, after testing in Chapter 4, the PCL (M_n 80,000) scaffolds were found to be inferior to those manufactured from PCL (M_n 42,500). They were therefore not subjected to further testing.

2.5.1.3. PLGA Scaffold Fabrication

As discussed in §1.2.5.9, PLGA is a widely used material in bone regenerative medicine. PLGA is thought to be biocompatible (Shive and Anderson, 1997), and has been used extensively in drug delivery devices (Oldham *et al.*, 2000; Ruhe *et al.*, 2003; Wei *et al.*, 2004). However, there is some evidence that PLGA is less biocompatible than PCL, due to the release of acidic breakdown products (Sung *et al.*, 2004; Ignatius and Claes, 1996; Linhart *et al.*, 2001). Nevertheless, it has gained USFDA approval for use in the fixation of bone fractures (USFDA, 2008). Therefore, components of PLGA in regenerative medical constructs are unlikely to cause the failure of design criteria 1 (non-toxic) and 2 (producing no adverse reaction) (§1.2.2).

The degradation rate of PLGA is substantially higher than of PCL. For example, one study found that PLGA microparticles degraded completely by hydrolysis within two months in PBS (Zhu *et al.*, 2008). The rate of degradation may also be altered by varying the ratio of lactide to glycolide subunits (Sokolsky-Papkov *et al.*, 2007). Hence, PLGA scaffolds are likely to meet design criterion 6 (favourable degradation rate) (§1.2.2).

In terms of mechanical properties, PLGA is thought to be sufficient for bone regenerative medical applications. It has been reported that the elastic modulus of the bulk is approximately 1.31 GPa, although when manufactured as a scaffold, this can fall to 1.6 MPa (Leung *et al.*, 2008). PLGA is significantly more expensive than

PCL (by approximately 76-fold), but not prohibitively so for a medical device material.

Therefore, it was concluded that PLGA showed great promise as a potential scaffold material. It was found that scaffolds could be manufactured from PLGA containing aqueous solutions, using the optimised parameters in §2.4.1.3, see **Figure 2.8b**.

Although, qualitatively, the scaffolds were found to resemble the PCL scaffolds manufactured closely in §2.4.1.1.2, the same degree of rigour in characterisation was not applied to them. This was because, after testing in Chapter 4, the PLGA scaffolds were found to be inferior to those manufactured from PCL (M_n 42,500). They were therefore not subjected to further testing.

2.5.1.4. PCL/PLGA Scaffold Fabrication

Physical blends of PCL and PLGA have been investigated as scaffold materials in the regenerative medicine of nerve, skin, and bone (Panseri *et al.*, 2008; Ng *et al.*, 2004; Marra *et al.*, 1999). Since they are physical rather then chemical (co-polymer) blends, it is likely that scaffolds of PCL/PLGA blends will not necessarily fail design criteria 1, 2, 6, 8 and 9 (non-toxic, producing no adverse reactions, having favourable degradation rates and mechanical properties, and being cost-effective and simple to manufacture) (§1.2.2).

PCL/PLGA blends have previously been employed as they offer scope for tuning the mechanical properties and the degradation rates (Panseri *et al.*, 2008). Similarly, it was thought that there was scope for altering the release profiles of encapsulated drugs. This hypothesis was tested in the studies described in Chapter 4 of this thesis.

It was found that scaffolds could be manufactured using two different polymer blends (see **Figure 2.9**). Again, although the scaffolds appeared to be similar to the PCL scaffolds as manufactured in §2.4.1.1.2, they were not characterised further. This was because, after testing in Chapter 4, the PCL/PLGA scaffolds were found to be inferior to those manufactured from PCL (M_n 42,500) alone. They were therefore not subjected to further testing.

2.5.2. Scaffold Coatings

The primary purpose of the scaffold coating in the strategy used in the studies detailed in this thesis, was to act as a second growth factor delivery system. Four materials, which are known to be capable of growth factor release, were selected. Each material was examined to determine whether they could feasibly be employed as scaffold coatings without compromising scaffold porosity.

In addition to acting as a drug delivery system, it is also important that the scaffold coating should facilitate cell-scaffold interaction. This aspect of the scaffold coatings was examined in the studies reported in Chapter 3.

2.5.2.1. Alginate Coating

Alginate is most commonly used in regenerative medical applications as a void filler and in cell delivery systems (see §1.2.6.3.2), particularly in cartilage regenerative medicine (Yamaoka *et al.*, 2006). Though it also has USFDA approval for use in wound dressing for ulcers and 2nd degree burns (USFDA, 2006). Additionally, it has also been used as a growth factor delivery system (Gu *et al.*, 2004a; Mumper *et al.*, 1994; Lee *et al.*, 2003a). $CaCl_2$ was used as the crosslinking solution, as $CaCl_2$ is compatible with bioactive growth factor release, and it is non-toxic. The concentration chosen was that used by Mumper (1994).

It was found that alginate was capable of forming a coating on PCL scaffolds. However, a wash step was found to be necessary to unblock the scaffold pores (see **Figure 2.10**). While the alginate coating was found to be feasible, it was thought that the wash step could have a detrimental effect on the encapsulation efficiency if growth factors were added in the coating. However, as a feasible coating, alginate was subjected to further testing in Chapter 3.

2.5.2.2. Chitosan Coating

As with alginate, chitosan has been used in a number of regenerative medical applications (Di Martino *et al.*, 2005). Additionally, chitosan has USFDA approval for use in haemostatic dressing for severely bleeding wounds (USFDA, 2009). It is also capable of releasing bioactive growth factors (Lee *et al.*, 2004c; Kim *et al.*,

2003c; Mattioli-Belmonte *et al.*, 1999), and was therefore considered to be a suitable scaffold coating material. It was decided to crosslink the chitosan using TPP, as it was thought to have less potential to denature the encapsulated growth factors than the alternative method of using strong alkaline solutions. A 2% (w/v) solution of TPP was used, as the mechanical properties of chitosan crosslinked with this solution were found to be superior to that crosslinked with 1% (w/v), as recommended by Shu and Zhu (2002).

Also, like alginate, chitosan coatings were found to be feasible, but to require a wash step prior to crosslinking. Again, this is likely to have a detrimental effect on the efficiency of encapsulation of the final product. Nevertheless chitosan was subjected to further testing in Chapter 3.

2.5.2.3. Collagen Coating

As discussed in §1.1.6.6, collagen is used in USFDA approved devices for the delivery of rhBMP-2, and -7. Collagen has also been shown to support mineralisation more than either PCL or PLGA used alone (Phillips *et al.*, 2006b). Indeed there is evidence which suggests that Type-I collagen is more capable of retaining the osteogenic differentiation potential of hMSCs compared to tissue culture plastic alone (Mauney *et al.*, 2006). Type-I collagen was therefore thought to be a near-ideal choice for a scaffold coating material.

Collagen was found to be capable of coating the PCL scaffolds evenly, without leaving the pores blocked (see **Figure 2.12**). It was thus considered to be a feasible coating material, and was therefore subjected to further testing in chapters 3, 4, 5, and 6.

2.5.2.4. Gelatin Coating

Gelatin is also known to retain much of the biocompatibility of the original collagen from which it was derived, and has been used in a number of growth factor delivery systems (see §1.2.5.6). It is known that many growth factors of interest in bone regenerative medicine, including PDGF, VEGF, TGF-β, BMP-2, and -7, have isoelectric points greater than 7 (Quaglia, 2008). Since a fast release profile from the

scaffold coating was desired, Type-A gelatin was selected. Since Type-A gelatin has an isoelectric point of between 7 and 9 (Cole, 2000), it was thought that there would be little attractive charge interaction with growth factors, which might slow the release.

Gelatin was found to be a feasible coating material, as it was also found to coat the PCL scaffolds evenly without blocking the pores (see **Figure 2.13**). Therefore, Type-A gelatin was subjected to further testing in Chapter 3.

2.6. Conclusion

A range of scaffolds and scaffold coatings was developed from different materials. Scaffolds were manufactured from PCL (both M_n 42,500 and M_n 80,000), PLGA, as well as two blends of PCL and PLGA. The pore size of PCL (M_n 42,500) scaffolds, was found to be suitable for bone regenerative medical applications. Each of the scaffolds was thought to have the potential to release bioactive growth factors. The five potential scaffold materials were subjected to screening based on their drug delivery properties in Chapter 4.

Coatings protocols using alginate, chitosan, Type 1 collagen and Type-A gelatin, were developed. All the coatings were thought to have the potential to release bioactive growth factors, and were found not to compromise PCL (M_n 42,500) scaffold porosity. The four potential scaffold coating materials were subjected to screening based on their biocompatibility in Chapter 3.

Chapter 3 : Primary Screening

3.1. Abstract

Biocompatibility is an essential property which all bone regenerative medical constructs must possess. The purpose of the studies described in this chapter, was to quantitatively and qualitatively assess the toxicity and cell-compatibility of the scaffolds and scaffold coatings. This was achieved using live/dead assays, based on the staining of test cells with calcein-acetoxymethyl, a marker of cell viability, and propidium iodide, used to determine cell death.

The biocompatibility of the potential scaffold coatings noted in Chapter 2 was assessed using cell cultures of human marrow stromal cells (hMSCs), human osteoblasts (hOBs), and MG63 cells. The cells were grown to 80% confluency and subsequently challenged with well coatings of alginate, chitosan, gelatin and Type-I collagen. At the end of the 72 hr test period, cell viability and death was assessed. It was found that the hydrogels alginate and chitosan (crosslinked with tripolyphosphate and sodium hydroxide) were associated with reduced total cell numbers (5.0±1.1%, 39±13% and 39±11% relative to the hMSC TC plastic control respectively), and increased cell death (absolute values: 19.1±6.3%, 5.3±3.6%, and 2.9±1.4% respectively), compared to the TC plastic control (0.048±0.011%). In contrast, gelatin (0.1% and 0.2%) and collagen coatings led to similar or increased cell numbers (101±8%, 104±14%, and 115±13% for hMSCs relative to the control respectively), and comparable cell death (absolute values: 0.11±0.07%, 0.15±0.13%, and 0.16±0.12% for hMSCs), compared to the TC plastic control. Since the Type-I collagen groups achieved consistently high cell numbers, and low percentages of cell death, this material was selected as the most cell-compatible potential scaffold coating. PCL scaffolds coated with collagen were therefore subjected to testing in chapters 4, 5, 6 and 7 of this thesis.

From the studies described in Chapter 4, scaffolds of poly(ε-caprolactone) (PCL) (M_n 42,500) manufactured with dichloromethane (DCM) were found to be the optimum scaffold design from the perspective of controlled drug release. However, it was essential to ascertain whether a vacuum drying time of 1 hr was satisfactory to

remove sufficient DCM for biocompatibility. The scaffolds were therefore compared against similar PCL scaffolds, manufactured with acetic acid, which were known to be biocompatible.

Although similar total cell numbers were present at the end of the test period in all of the test scaffold and control groups, there were differences in the very low amount of cell death seen in all groups. The groups with scaffolds processed with acetic acid either unprocessed or vacuum dried for 24 hrs showed statistically significant increases in hMSC cell death (0.92±0.02% and 1.75±0.66% respectively) compared to the treated tissue culture (TC) plastic (0.28±0.08%) control for at least two out of three patients tested, although cell death remained below 4% in all treatment groups. While these differences were statistically significant, they were thought to not be of physiological significance.

In contrast, no significant elevation in cell death was observed for the DCM processed scaffolds, at any of the vacuum drying times tested, compared to the TC plastic control.

It was observed that the groups with scaffolds processed with acetic acid, as well as the non-dried PCL/DCM scaffolds showed abnormal hMSC morphology. It was found that normal morphology was restored when the PCL/DCM scaffolds were vacuum dried for 1 hr or more, thus a vacuum drying time of 1 hr was deemed adequate to remove enough DCM for cell-compatibility. Such scaffolds were therefore subjected to further testing as described in chapters 5, 6 and 7.

3.2. Introduction

As discussed in §1.2.2, the two most important design criteria for materials used in regenerative medicine are; biocompatibility, and the lack of potential to produce adverse effects, such as an immune response, or the induction of neoplasia. The latter is very difficult to test without using animal models. However, *in vitro* methods of studying biocompatibility are widely accepted for the purpose of primary screening, before preclinical trials are undertaken (Wang *et al.*, 2009a; Carinci *et al.*, 2007; Paul and Sharma, 2007). They also have the advantage of giving good control over the variables, and their sensitivity is thought, by some authors, to be at least equal to that of *in vivo* studies (Ho *et al.*, 2008).

Although there are several definitions of the term "biocompatible", it has recently been eloquently defined as:

"…the ability of a biomaterial to perform its desired function with respect to a medical therapy, without eliciting any undesirable local or systemic effects in the recipient or beneficiary of that therapy, but generating the most appropriate beneficial cellular or tissue response in that specific situation, and optimising the clinically relevant performance of that therapy." (Williams, 2008).

In the context of bone regenerative medicine, the biocompatibility of materials is commonly taken to mean the lack of cytotoxicity, as well as osteoconductivity. Cytotoxicity is commonly measured using; MTT or MTS assays (Sgouras and Duncan, 1990; Ignatius and Claes, 1996), lactate dehydrogenase assays (Unger *et al.*, 2007; Serrano *et al.*, 2004) or calcein-acetoxymethyl (calcein-AM) in combination with a dye such as propidium iodide (PI) (Papadopoulos *et al.*, 1994; Curran *et al.*, 2005; Wang *et al.*, 1993; Adhirajan *et al.*, 2009; Giacomello *et al.*, 1999).

Calcein-AM is a widely used dye in cell viability assays (Lichtenfels *et al.*, 1994; Roden *et al.*, 1999). The dye is well retained in the viable cell targets, and it is relatively insensitive to pH. There is also no stain transfer between cells (Papadopoulos *et al.*, 1994). Calcein-AM is lipid-soluble and can therefore diffuse passively across cell membranes. Inside viable cells, it is converted by esterases to fluorescent calcein, which is lipid-insoluble (see **Figure 3.1**) (Neri *et al.*, 2001).

PI is a dye commonly used for fluorescent deoxyribonucleic acid (DNA) and ribonucleic acid (RNA) staining. It fluoresces red when excited at either 568 or 488 nm (Suzuki *et al.*, 1997). It is incapable of diffusing across intact cellular plasma membranes, hence it can be used in a number of studies to stain cells that are either necrotic, or in the final stages of apoptosis (Palma *et al.*, 2008; McKeague *et al.*, 2003; Goodell *et al.*, 1996).

As described in the previous chapter, a number of potential scaffold coatings were developed. Since these would potentially form the primary cell-scaffold interface, it was very important to assess the biocompatibility of each coating. Therefore, in the work of this chapter, the cell-compatibility of each of the potential coatings was assessed by the addition of both calcein-AM and PI to the cultures of test cells.

The optimum scaffold base material was first assessed on the basis of drug encapsulation efficiency and desirability of the release profile, in Chapter 4. However, it was also important to assess whether the optimum scaffold for drug release had a cytotoxic effect. Here, this was assessed by culturing staining test cells exposed to the scaffold materials with calcein-AM and PI.

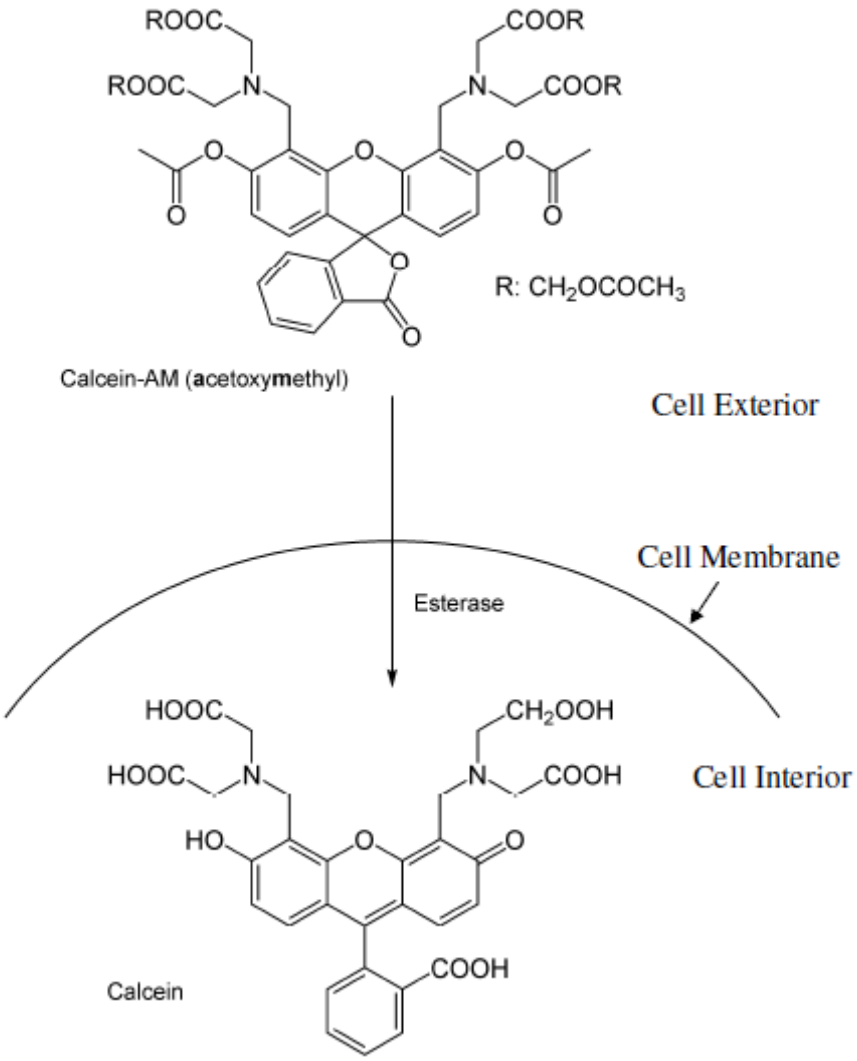

Figure 3.1: Mode of action of calcein-AM.

A cartoon of the viable cellular response to calcein-AM. The dye diffuses across the cell membrane, and is converted to fluorescent calcein by esterases present in viable cells (adapted from http://commons.wikimedia.org/wiki/File:Calcein-AM.png).

3.3. Materials and Methods

Unless otherwise stated, all reagents were purchased from Sigma, UK. All the techniques described below were conducted in a sterile cell culture environment, using sterilised equipment.

3.3.1. Cell Culture

The media referred to as 'growth media' consists of Dulbecco's Modified Eagle's Medium – high glucose (DMEM), supplemented with 10% (v/v) FCS (Autogen Bioclear, UK), L-glutamine (2 mM) (Gibco, UK), penicillin (100 IU/ml) and streptomycin (100 µg/ml) (Gibco, UK).

3.3.1.1. Human MSC Isolation and Culture

After written consent from the patients and approval from the local ethical committee (Lothian local research ethics committee), human femoral head tissue was obtained from patients who had undergone elective arthroplasty. Tissue was collected from a total of three patients; a 68 year-old male (542), a 66 year-old male (544), and a 61 year-old female (549). The tissue samples were allocated an anonymous number based on the chronological order of the sample collection.

The samples were stored at 4°C in sterile phosphate buffered saline (PBS) (Oxoid, UK) directly after surgery. The hMSC isolation protocol used was as previously described by Tremoleda *et al.* (2008) and with minor modifications from Gronthos *et al.* (1998) and Gundle *et al.* (1995), was started less than 4 hr after surgery.

Using bone cutters, the trabecular bone was removed from the femoral head and placed in a 30 ml conical-bottomed universal container. Then 9 ml of growth media was added to the bone chips, and the mixture was stirred vigorously for approximately 1 min with a 5 ml pipette (Corning, USA). Afterwards the bone material was allowed to settle to the bottom of the universal container and the supernatant, containing cells, was transferred to a new 30 ml universal. This process was repeated twice using 7 ml of growth media. The supernatants were then combined.

The majority of the 21 ml of media was transferred to a 75 cm^2 tissue culture flask (Corning, USA), leaving behind the layer of fat (approximately 1 ml) at the top of the media. The cells were maintained in a humidified air incubator at 37°C with 5% (v/v) carbon dioxide (CO_2), undisturbed for 4 days. At this time, non-adherent cells were removed by washing with 10 ml of PBS, before 10 ml of fresh growth media was added to the flasks.

Primary isolates were incubated at 37°C with 5% (v/v) CO_2. The growth media was refreshed at regular intervals three times every 7 days. When the cells were approximately 80% confluent, they were washed three times with PBS, and passaged by adding 1 ml of trypsin solution (2.5 mg/ml) in PBS (Invitrogen, UK). After 15 min incubation at 37°C, 9 ml of growth media were added to the flasks. Then 5 ml of cell suspension and 5 ml of fresh growth media were added to new tissue culture flasks (75 cm^2). The flasks were then incubated and refreshed with new growth media as before. The hMSCs underwent routine characterisation as described in **Appendix G**.

3.3.1.2. Human Osteoblasts

After written consent from the patients and approval from the local ethical committee (Lothian local research ethics committee), human femoral head tissue was obtained from a patient who had undergone elective arthroplasty. Tissue was collected from a 52 year-old male (431).

The samples were stored at 4°C in sterile PBS directly after surgery. The human osteoblast (hOB) isolation protocol, which included minor modifications from the techniques previously described by Gallagher (2003) and Bland *et al.* (1999), was started less than 4 hr after surgery.

After the majority of the trabecular bone had been removed from the femoral head as described in §3.3.1.1, the tissue sample was wrapped in plastic. It was then broken open with a 1 kg steel mallet. The resulting bone chips were cut into smaller pieces using bone cutters, and placed in a 30 ml universal container. The chips were

washed four times with 15 ml of Hanks' balanced salt solution (HBSS) to remove non-adherent marrow-associated cells, which were then discarded.

The bone fragments were then incubated with 2 ml of trypsin, and agitated for 10 min at 37°C, before being washed with 9 ml of growth media. The bone chips were then incubated with Collagenase (2 ml, 1 mg/ml) in HBSS at 37°C for 3 hr. After washing with HBSS, the bone fragments were transferred to a tissue culture flask (75 cm^2) with 20 ml of growth media.

The tissue culture flask was maintained in a humidified air incubator at 37°C with 5% (v/v) CO_2, undisturbed for 4 days. After which time, non-adherent cells were removed by washing with 10 ml of PBS, before 10 ml of fresh growth media was added to the flask.

Primary isolate was incubated at 37°C with 5% (v/v) CO_2. The growth media was refreshed at regular intervals three times every seven days. When the cells were approximately 80% confluent, they were washed three times with PBS, and passaged by adding 1 ml of 2.5 mg/ml trypsin solution in PBS. After 15 min incubation at 37°C, 9 ml of growth media were added to each flask. Then 5 ml of cell suspension and 5 ml of fresh growth media were added to new tissue culture flasks (75 cm^2). The flasks were then incubated and refreshed with new growth media as before.

3.3.1.3. MG63

The osteosarcoma-derived osteoblast-like cell line MG63 (European Tissue Culture Agency, UK) (Heremans *et al.*, 1978) was cultured with minor modifications as from Lincks *et al.* (1998). MG63 cells were cultured in growth media, in tissue culture flasks (75 cm^2), incubated at 37°C with 5% (v/v) CO_2. The growth media was refreshed at regular intervals three times every seven days. When the cells were confluent, they were washed three times in PBS, and passaged by adding 1 ml of 2.5 mg/ml trypsin solution in PBS. After 5 min incubation at 37°C, 9 ml of growth media were added to each of the flasks. Then 1 ml of cell suspension was added to new tissue culture flasks (75 cm^2). An additional 9 ml of fresh growth media were

then added to each new flask. The flasks were then incubated and refreshed with new growth media as before.

3.3.2. Test Coatings

For the experiments involving hMSCs, six wells were used per group for each patient tissue isolate. For the experiments using hOBs and MG63 cells, three wells were used per group.

3.3.2.1. Alginate

A 3% (w/v) stock solution of alginate (Alginic Acid Sodium salt from Brown Algae) was dissolved in an aqueous solution of 0.5 M sodium chloride (NaCl). The alginate stock was incubated at room temperature for three days, to dissolve, before being autoclaved. A 1.5% (w/v) alginate solution in 0.5 M NaCl was then made up by diluting the stock alginate solution.

200 µl of 1.5% (w/v) alginate solution were added per well of 48-well tissue culture (TC) plastic plates (Corning, USA). Excess alginate was aspirated off, and 400 µl of 0.1 M aqueous calcium chloride solution were added for 30 min, to crosslink the hydrogel. Each well was then washed three times with PBS (Oxoid, UK). The PBS was aspirated off and discarded. The coated wells were then ready for cell seeding.

3.3.2.2. Chitosan

A stock solution of chitosan (Chitosan from Crab Shells, minimum 85 % deacetylated) was dissolved at 3% (w/v) in an aqueous solution of 0.5% (v/v) acetic acid (Fluka, Germany). The chitosan stock was incubated at room temperature for three days before being autoclaved. A 1.5% (w/v) chitosan solution in 0.5% (v/v) acetic acid was then made up by diluting the stock chitosan solution.

200 µl of 1.5% (w/v) chitosan solution were added per well of tissue culture (TC) plastic (Corning, USA). Excess chitosan was aspirated off, and 400 µl of either 2% (w/v) aqueous sodium tripolyphosphate (TPP) or 1 M aqueous sodium hydroxide (NaOH) solution was added for 30 min, to crosslink the hydrogel. Each well was

then washed three times with PBS. The PBS was aspirated off and discarded. The coated wells were then ready for cell seeding.

3.3.2.3. Collagen and Gelatin

Type-I collagen solution (1 mg/ml) in 0.1 M aqueous acetic acid, and Type-A aqueous gelatin solutions (1% and 2% (w/v)) were used to coat wells of 48-well non-TC plastic plates (ultra-low binding, Corning, USA). The two solutions were filter sterilised using 0.22 µm filters (Millipore, UK).

50 µl of the solutions were added to the wells. The plates were agitated to distribute the solutions evenly over the well surfaces. After 10 min, the excess liquid was removed from each well. The plates were then left to dry at room temperature for 4 hr. The coated wells were then ready for cell seeding.

3.3.3. Test Scaffold Manufacture

PCL (M_n 42,500) scaffolds were manufactured using two methods, utilising two different solvents: DCM and acetic acid.

3.3.3.1. Scaffolds Made Using DCM

Scaffolds were manufactured using the protocol with no plotting media, described in §2.3.2.1.1, with a plotting speed and pressure of 168 mm/min and 1.00 bar (gauge pressure). The following modifications were made:

The NC code used was written to produce two-layer scaffolds with a strand spacing of 1.6 mm in both the X and Y axes (with the dimensions 20 × 20 mm), and a Z spacing of 0.14 mm, see **Appendix D**. These scaffolds were either not dried, or vacuum dried for 1 or 24 hr at 75 mbar (absolute pressure), using a freeze dryer (Alpha 1-4, Christ, Germany). They were then frozen at -80°C.

3.3.3.2. Scaffolds Made Using Acetic Acid

Scaffolds were manufactured using the protocol with 100% IMS as the plotting media, described in §2.3.2.1.1, with a plotting speed and pressure of 168 mm/min

and 1.00 bar (gauge pressure). The following modifications were made to produce scaffolds similar to those described by Vadillo, (2009):

The plotting solution was 30% (w/v) PCL in glacial acetic acid, which had previously been dissolved in an orbital incubator (Stuart S150), set to 120 rpm (orbital diameter: 1.5 cm) and 37°C, for 72 hr. The NC code used was that used in §3.3.3.1, see **Appendix D**. These scaffolds were either not dried, or vacuum dried for 1 or 24 hr at 75 mbar (absolute pressure), using a freeze dryer (Alpha 1-4, Christ, Germany). They were then frozen at -80°C.

3.3.4. Live/Dead Assay

3.3.4.1. Test Coatings

Tissue culture flasks (75 cm^2) containing confluent hMSCs (passage 2), hOBs (passage 4), and MG63 (passage 20) were washed three times in PBS, and the cells were detached from the flask using trypsin and growth media, as described in §3.3.1. The cell density of the suspensions was measured using a haemocytometer. After appropriate dilution with growth media, the cells were added to the coated wells (described in §3.3.2) at a density of 10,000 cells/well (in 400 µl of media). Cells at the same density were also added to uncoated TC plastic and non-TC plastic 48-well cell culture plates. For the hMSCs, six wells were used per group. For the hOBs and MG63s, three wells were used for each group. Extra wells of cells on TC plastic were set aside to be fixed to act as positive (+ve) controls for PI. The experiment was repeated using cells from three different patients.

The cells were maintained in a humidified air incubator at 37°C with 5% (v/v) CO_2. After 3 days, the cells set aside for the +ve PI control were fixed in 4% (w/v) paraformaldehype in PBS for 10 min. The wells were washed with PBS (twice) and dH_2O (once): 2 min per wash. The wells were left to dry for 4 hr. Since none of the cells would be viable, and all the cell membranes would be permeated after such treatment, this group acted as a positive and negative control for PI and calcein AM staining, respectively.

The media was then completely changed to growth media containing 2 µM calcein AM and 2 µg/ml PI. The cells were incubated in the dark at 37°C with 5% (v/v) CO_2 for 5 min. Afterwards, the wells were washed three times with PBS for 2 min each. After the washes were discarded, 200 µl of PBS were added to each well. The plates were then photographed using a mounted camera (Nikon, DXM1200) on an inverted microscope (Nikon, Eclipse TS 100) set for fluorescence, at × 10 magnification. Three randomly selected fields of view were photographed per well, representing 6.0% of the growth area of the wells.

The number of calcein and PI +ve cells were counted with the aid of ImageJ (National Institute of Health, USA) using a batch image processing macro (see **Appendix E**). A manual count of randomly selected images was used to confirm the accuracy of the ImageJ counts (six images per patient). The percentage differences between the manual and automated counts were calculated.

3.3.4.2. Test Scaffolds

The scaffolds, manufactured as described in §3.3.3, were de-frosted and cut into four approximately equal (10 × 10 mm) parts. The scaffolds were immersed in IMS for 10 min. They were washed with dH_2O, then PBS and then immersed in PBS for 5 min. Afterwards, the scaffolds were placed flat at the bottom of 48-well TC plates.

Tissue culture flasks (75 cm^2) containing confluent hMSCs (passage 2) were washed three times in PBS, and the cells were detached from the flask using trypsin and growth media, as described in §3.3.1. The cell density of the cell suspensions was measured using a haemocytometer. After appropriate dilution with growth media, the cells were added to the wells containing scaffolds at a density of 10,000 cells/well (in 400µl of media). Cells at the same density were also added to TC plastic wells which did not contain scaffolds. Six wells were used for each patient's tissue per group. Extra wells of cells on TC plastic were set aside to be fixed to act as positive (+ve) controls for cell membrane disruption and PI staining.

The cells were maintained in a humidified air incubator at 37°C with 5% (v/v) CO_2. After 3 days, the cells cultured to act as the +ve PI control were fixed in 4% (w/v)

paraformaldehyde in PBS for 10 min. The wells were washed with PBS (twice) and dH_2O (once): 2 min per wash. The wells were left to dry for 4 hr.

After the test incubation period of 3 days, the media and scaffolds were removed from the wells and discarded. Growth media containing 2 µM calcein AM and 2 µg/ml PI was added. The cells were incubated in the dark at 37°C with 5% (v/v) CO_2 for 5 min. After which time the wells were washed three times with PBS for 2 min each. After the washes were discarded, 200 µl of PBS were added to each well. The plates were then photographed using a fluorescent inverted microscope at × 10 magnification. Three randomly selected fields of view were photographed per well.

The number of calcein (N_C) and PI (N_P) +ve cells in field i was counted with the aid of ImageJ (National Institute of Health, USA) using a batch image processing macro (see **Appendix E**). A manual count of randomly selected images was used to confirm the accuracy of the ImageJ counts (six images per patient).

The total cell count and percentage of PI +ve cells were determined for each well using **Equation 3.1** and **Equation 3.2** respectively. The average for each group was found by taking the mean of the cell counts, and percentages of PI +ve cells, for all the wells in that group.

Equation 3.1

$$\text{Cell Count in well } j = \frac{1}{3}\sum_{i=1}^{3} N_{C,i} + N_{P,i}$$

Equation 3.2

$$\text{Percentage of PI +ve cells in well } j = \frac{1}{3}\sum_{i=1}^{3} \frac{N_{P,i}}{N_{C,i} + N_{P,i}} \times 100\%$$

3.3.5. Statistical Analysis

All data were analysed using the statistical software package SPSS 14.0 for Windows.

The data on the test coatings were found not to satisfy Levene's test for homogeneity of variance, even after the use of mathematical transformations. Parametric tests, such as one-way analysis of variance (ANOVA), were therefore unsuitable. Hence, the non-parametric test Kruskal-Wallis was used to test for statistical significance for each data set. The statistical significance between the groups was found using the Mann-Whitney U test (Zar, 1984; Petrie and Sabin, 2005).

The statistical difference in the cell numbers between the collagen and gelatin groups was calculated using the Wilcoxon Signed Ranks test.

The data on the test scaffolds were found to be normally distributed using the Kolmogorov-Smirnov test. Levene's test was applied to confirm homogeneity of variance for the cell counts. The percentage of PI +ve cells required transformation. The square root of each percentage was transformed into its arcsine. Levene's test was again applied to confirm homogeneity of variance. The parametric test ANOVA was then employed. This was followed by using the Tukey-Kramer *post hoc* test, to determine the statistical differences between the groups (Zar, 1984; Petrie and Sabin, 2005). $p < 0.05$ was considered to be statistically significant.

The mean was used throughout, and all results are expressed as the sample means ± standard error of the mean (SEM).

3.4. Results

3.4.1. Test Scaffold Manufacture

Test scaffolds made from PCL (M_n 42,500) were successfully manufactured using either DCM or acetic acid as the processing solvent. Using a strand spacing of 1.6 mm in the XY plane, a more open porous structure was achieved (see **Figure 3.2**).

3.4.2. Live/Dead Assay

Under normal tissue culture conditions, virtually all the cells stained positive for calcein, and only very few stained positive with PI (see **Figure 3.3**). In contrast, on cells which had previously been fixed with 4% (w/v) paraformaldehyde, all the cells stained positive with PI and negative for calcein (see **Figure 3.3**). Randomly chosen manual counts showed an average deviation from the automated ImageJ counts of 0.66±0.2%.

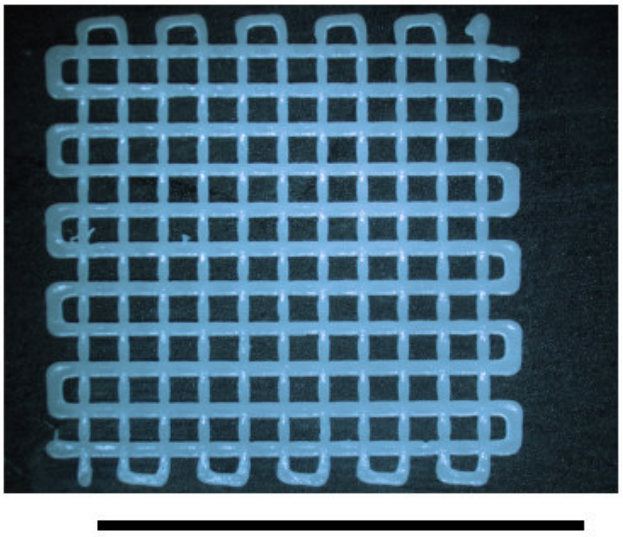

Figure 3.2: Test Scaffold.

A representative of the test scaffolds, with an XY strand spacing of 1.6 mm. This particular scaffold was made from 30% (w/v) PCL/acetic acid solution, with a plotting solution of 100% IMS. The bar represents 20 mm.

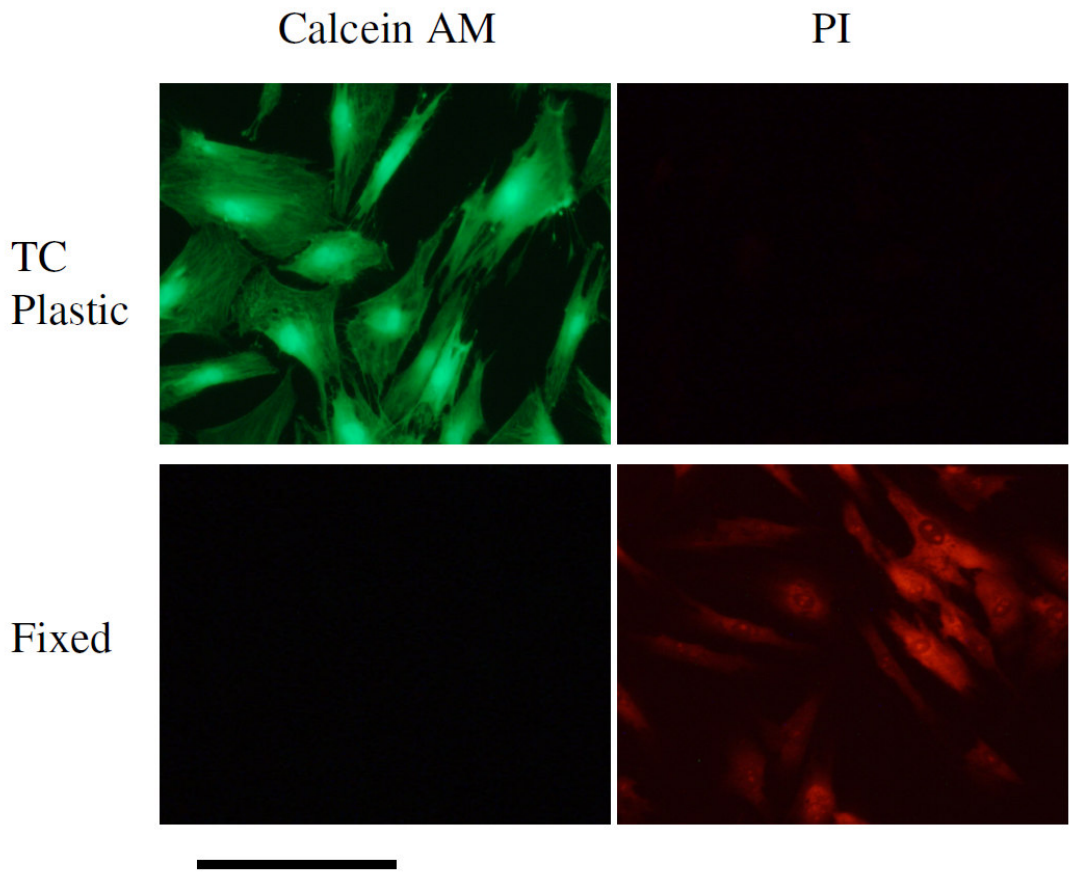

Figure 3.3: Controls for Live/Dead Assay

Representative images of hMSCs on TC plastic, both fixed with 4% (w/v) paraformaldehyde, and un-fixed, stained with both calcein AM and PI. Viable cells were stained green with calcein, whereas cells with non-intact plasma membranes were stained red with PI. The bar represents 50 µm.

3.4.2.1. Test Coatings

For the test coatings of alginate, chitosan (TPP crosslinked) and chitosan (NaOH crosslinked), significantly lower cell counts were observed compared to TC plastic for all hMSC test patients, as well as for the hOBs and MG63 cells (see **Figure 3.4**, **Figure 3.6a** and **Figure 3.7a**). Similarly, there was a statistically significant increase in the percentage of dead (PI +ve) cells in the alginate groups for the hOBs and MG63 cells, and for one of the three hMSC patients (see **Figure 3.5**, **Figure 3.6b** and **Figure 3.7b**). Chitosan, whether crosslinked with TPP or NaOH, statistically significantly increased the percentage of PI +ve cells compared to TC plastic, for all the cells tested.

In contrast, the cell counts for the collagen and gelatin groups were statistically significantly higher than the non-TC plastic controls, for all the hMSC patient isolates tested as well as for the MG63 cells (see **Figure 3.4** and **Figure 3.7a**). Indeed, the cell counts for the collagen and gelatin groups were comparable to the TC plastic control for all hMSC and hOB experiments. It should be noted that higher cell counts were observed in the collagen groups than in the gelatin groups, in all the experiments conducted on test coatings ($21 \pm 3\%$, $p = 0.043$).

It was also found that a statistically significantly lower percentage of PI +ve cells was observed in the collagen and gelatin groups compared to the non-TC control in two out of three hMSC patient isolates (see **Figure 3.5**). However, this difference may not be physiologically relevant since the cell death in the non-TC control was relatively low. The values obtained were found to be comparable to the TC plastic control.

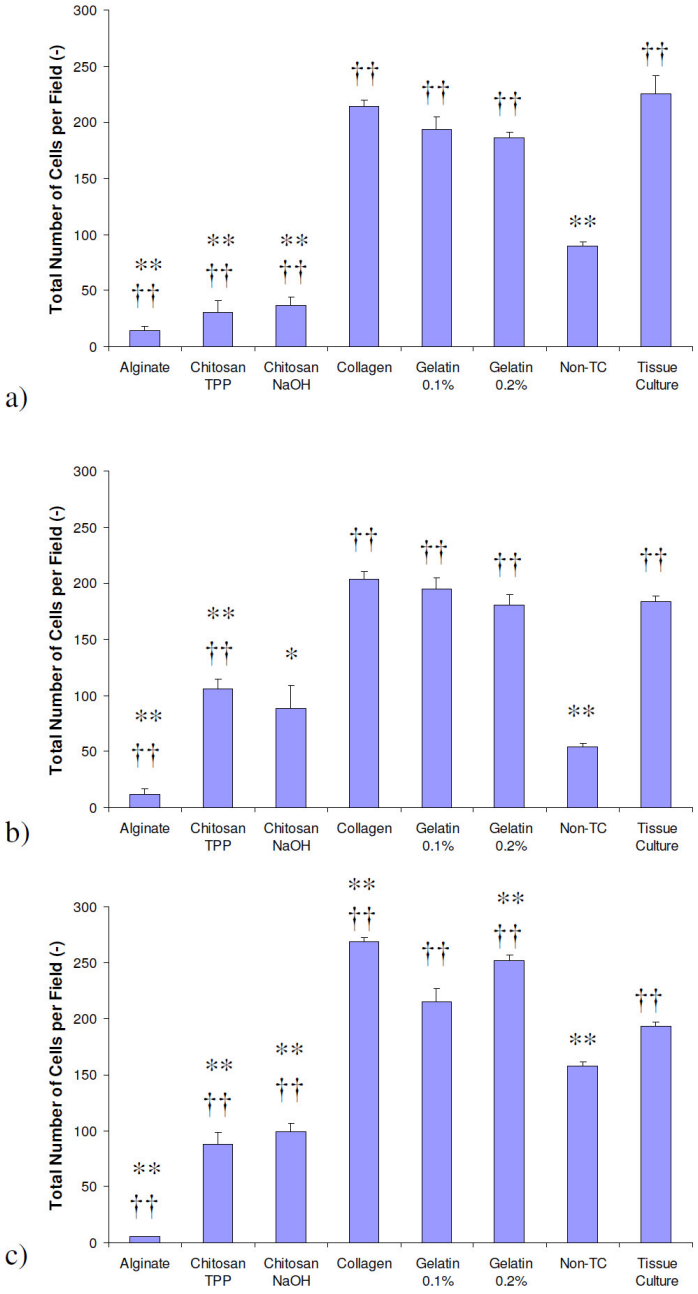

Figure 3.4: hMSCs total counts on coating materials.

The average total cell counts per field of view for hMSCs seeded onto different coating materials. Each figure represents data from a different patient a) 542, b) 544, and c) 549. The error bars represent the SEM, n = 6 in each case. * and † denote $p < 0.05$, and ** and †† denote $p < 0.01$ compared to the TC and non-TC controls respectively.

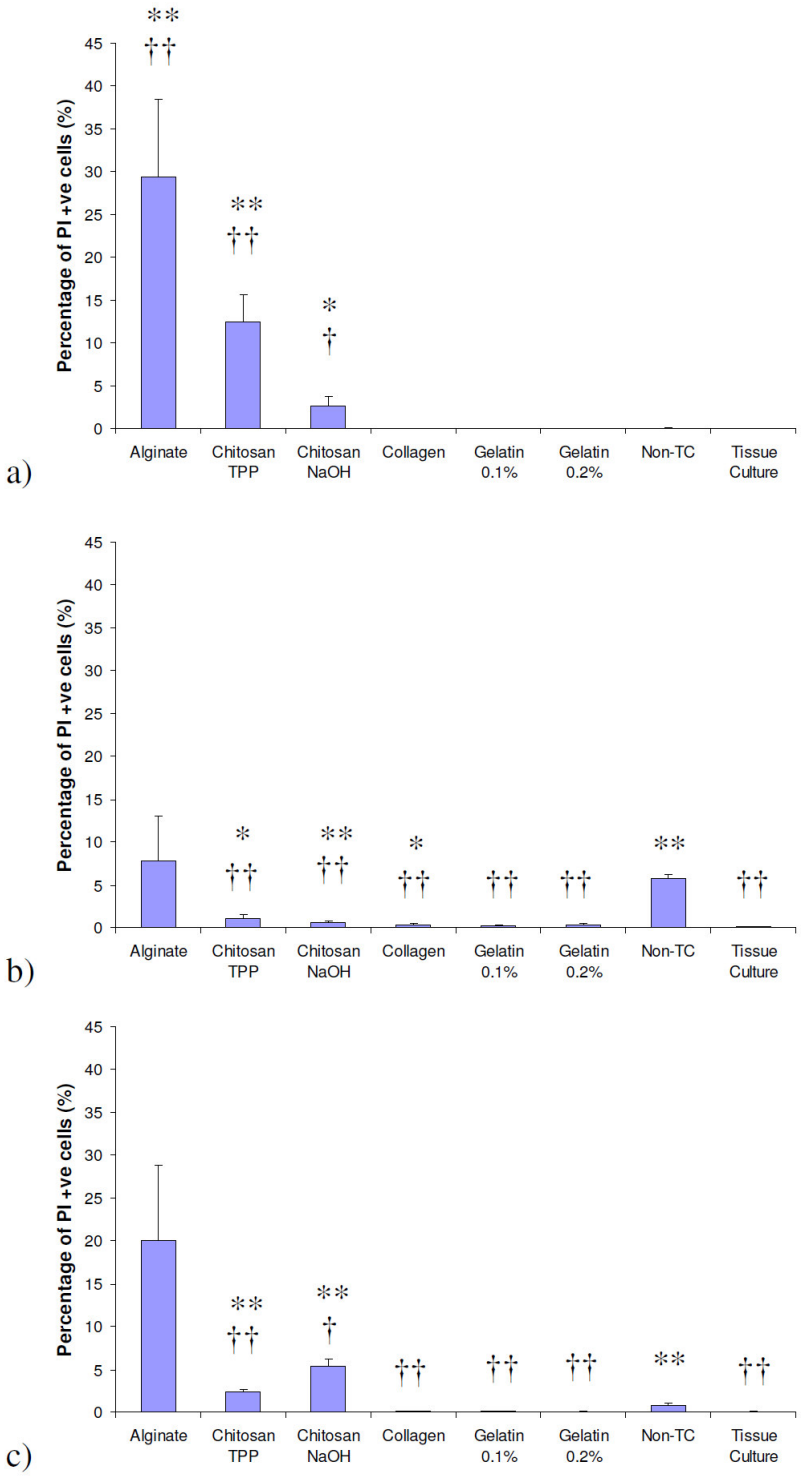

Figure 3.5: hMSCs percentage of PI +ve cells on coating materials.

The average percentages of PI +ve hMSCs on different coating materials. Each figure represents data from a different patient a) 542, b) 544, and c) 549. The error bars represent the SEM, n = 6 in each case. * and † denote $p < 0.05$, and ** and †† denote $p < 0.01$ compared to the TC and non-TC controls respectively.

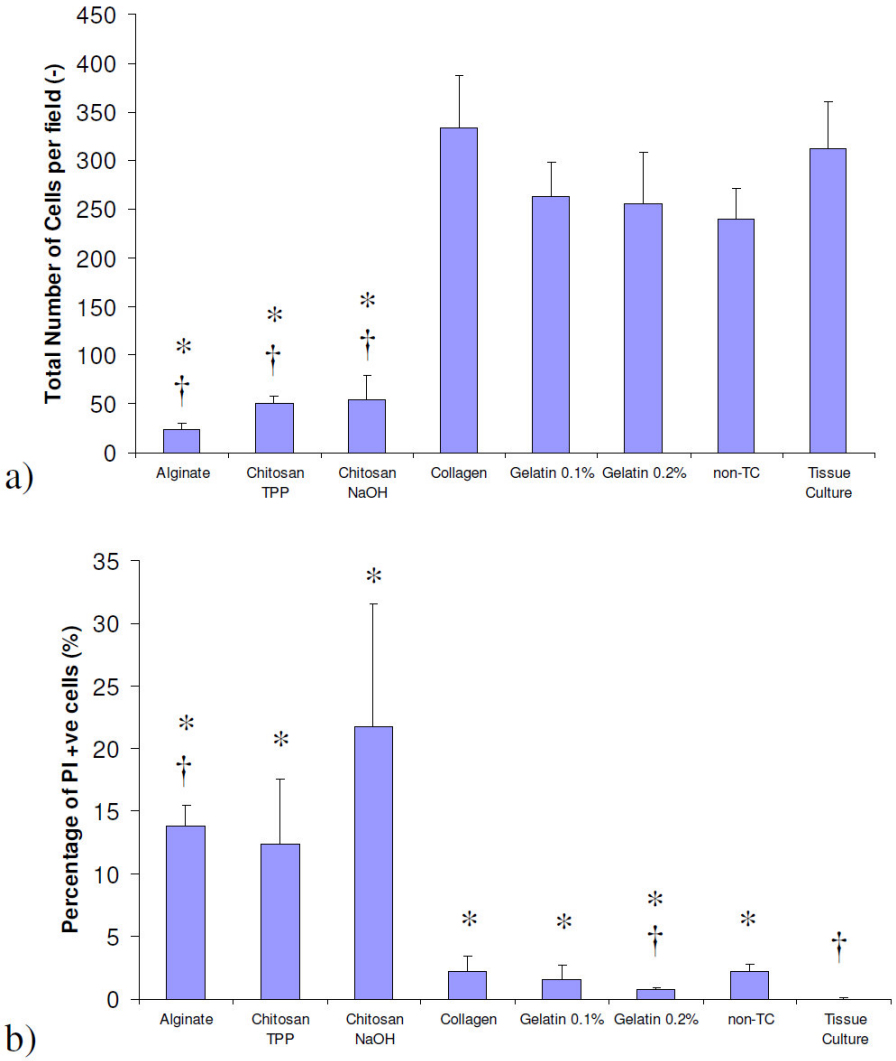

Figure 3.6: hOBs on coating materials.

a) The average total cell counts per field of view for hOBs seeded onto different coating materials. The error bars represent the SEM, n = 3 in each case. b) The average percentage of PI +ve hOBs on different coating materials. The error bars represent the SEM, n = 3 in each case. * and † denote $p < 0.05$, and ** and †† denote $p < 0.01$ compared to the TC and non-TC controls respectively.

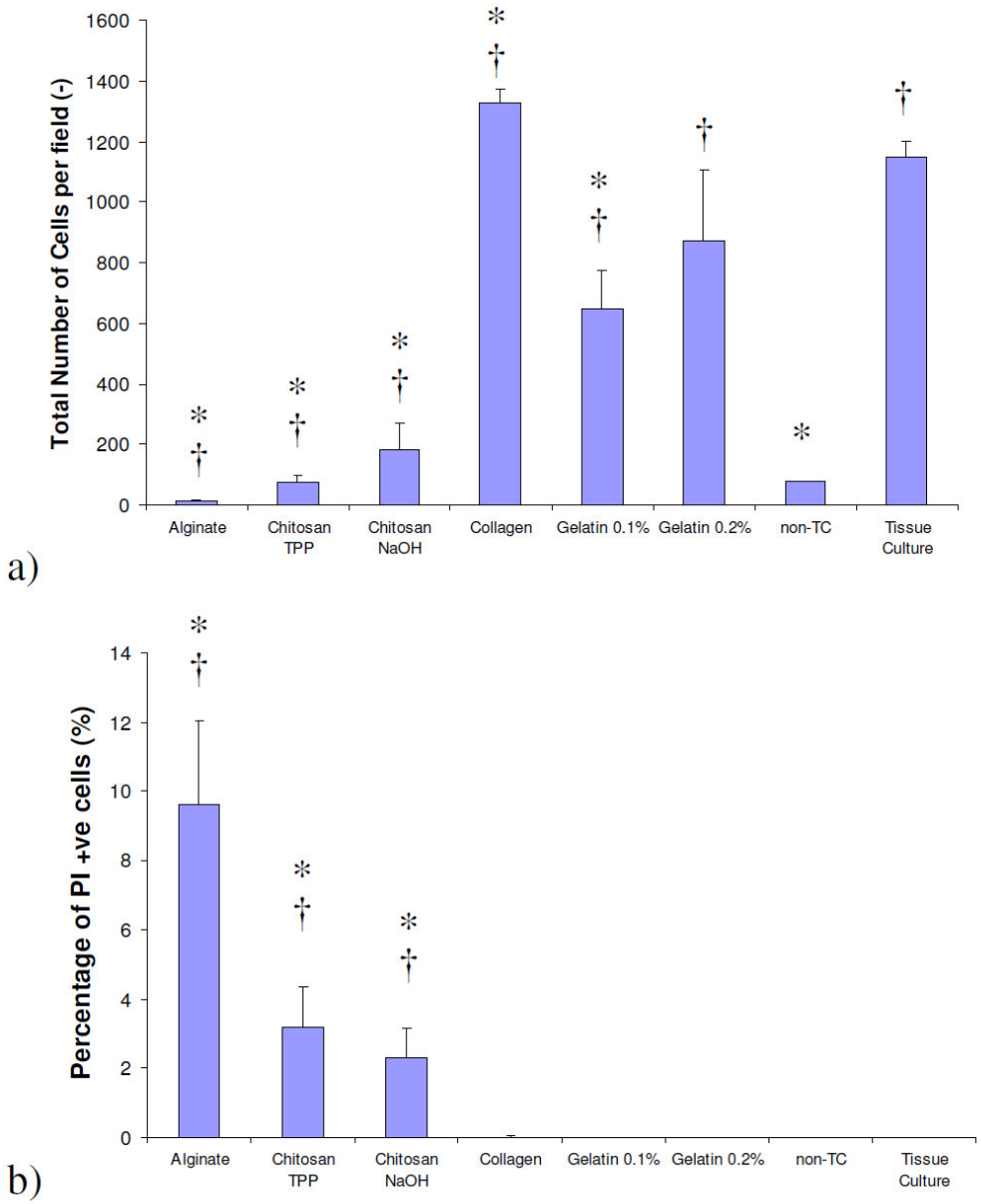

Figure 3.7: MG63 cells on coating materials.

a) The average total cell counts per field of view for MG63 cells seeded onto different coating materials. The error bars represent the SEM, n = 3 in each case. b) The average percentage of PI +ve MG63 cells on different coating materials. The error bars represent the SEM, n = 3 in each case. * and † denote $p < 0.05$, and ** and †† denote $p < 0.01$ compared to the TC and non-TC controls respectively.

Qualitatively, there were marked differences in morphology of the cells seeded onto the different surfaces (see **Figure 3.8**). The cells on alginate were found to be rounded, and often clumped together. The morphology of cells seeded onto chitosan, crosslinked with either TPP and NaOH, were found to be very similar to each other. The cells were rounded, though many had developed cellular processes or dendrites. The dendrites were particularly evident in the hMSCs seeded onto chitosan crosslinked with NaOH, where more than 10 cellular processes were observed on many of the cells (see **Figure 3.8**).

For the gelatin coating, there was a visible difference between the two concentrations used. At the higher concentration, the hMSCs had a more elongated, fibroblastic appearance than the more rounded cells on the lower concentration (see **Figure 3.8**).

All the different cell types seeded onto the collagen coating, had a very similar morphology to that on TC plastic. This was in marked contrast to the morphology of the cells on non-TC plastic, the material over which the collagen was coated. The hMSCs seeded onto the collagen were observed to have an elongated, fibroblastic morphology (see **Figure 3.8**).

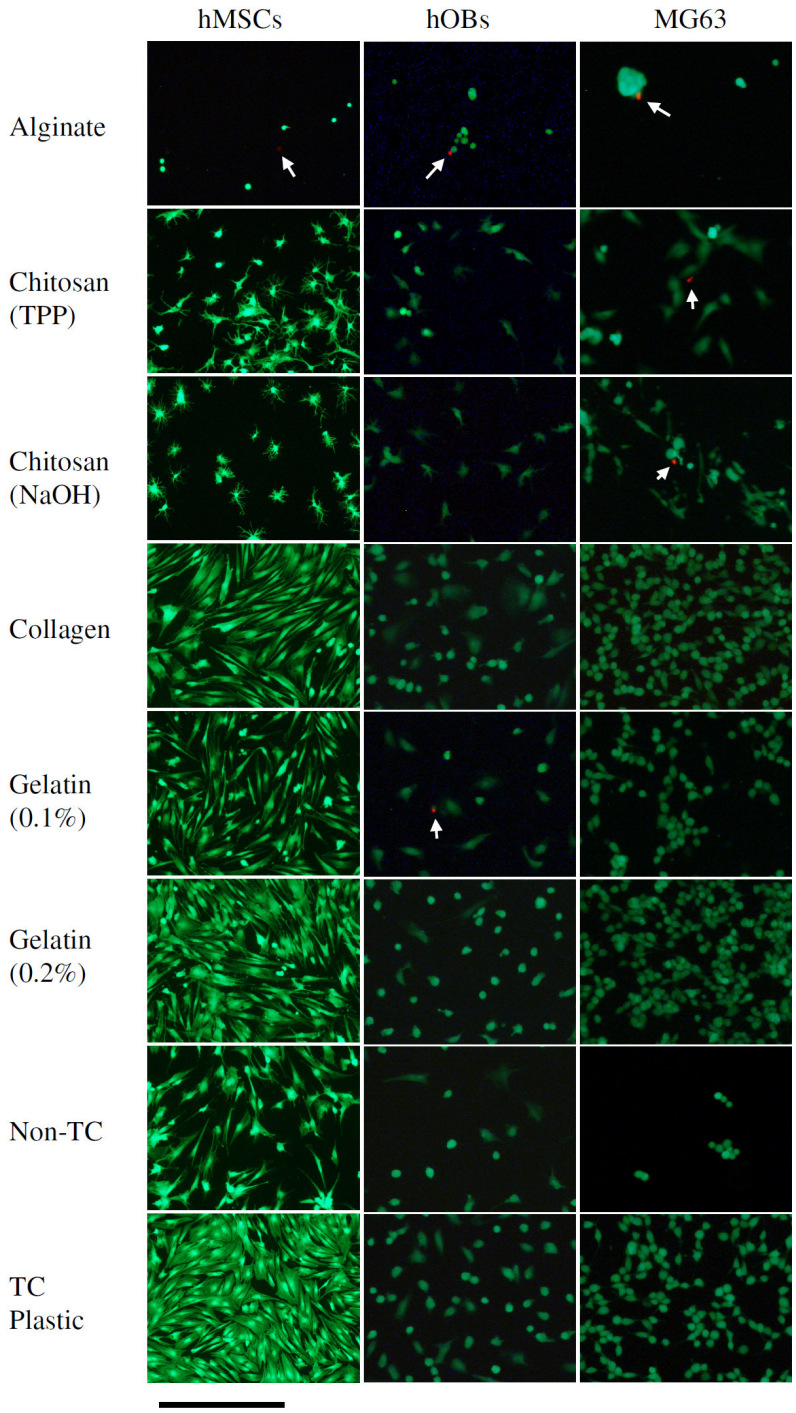

Figure 3.8: Cells on the test coating materials.

Combined bright-field and fluorescence images of hMSCs, hOBs and MG63 cells on the test coating materials. Viable cells were stained green with calcein, whereas cells with non-intact plasma membranes were stained red with PI. The arrows indicate PI +ve cells. The bar represents 100 µm.

3.4.2.2. Test Scaffolds

The cell counts of the hMSCs exposed to the test scaffolds, showed no consistent statistical differences compared to the growth media controls (see **Figure 3.9**). Indeed, no consistently significant effect was observed for the different test scaffold vacuum drying times (see **Figure 3.9**).

However, this was not the case for the percentages of PI +ve cells. There was a consistent, though small, increase in the PI +ve percentages for all the acetic acid processed scaffolds (the positive control for scaffold cell-compatibility), compared to the growth media control (see **Figure 3.10**). This difference was statistically significant in two ($p = 0.013, 0.031$), one ($p = 0.002$) and three ($p = 0.001, 0.001, 0.027$) patient isolates for the non-dried, 1 hr dried and 24 hr dried scaffolds respectively. In contrast, no statistically significant change in the percentage of PI +ve cells was observed for the DCM scaffolds, compared to the growth media control (see **Figure 3.10**). However, it should be noted that the proportions of cell death were relatively low. For the test scaffold groups, the highest percentage of PI +ve cells was found to be less than 3.5%.

For the data on percentages of PI +ve cells, no consistent trend was observed between scaffolds processed with the same solvent and vacuum dried for different times. However, differences could be observed in the morphology of the cells. hMSCs exposed to non-dried scaffolds, processed with either solvent, were found to be more rounded and dendritic compared to the growth media control (see **Figure 3.11**). For the DCM processed scaffolds, a drying time of 1 hr was found to be sufficient to maintain the normal morphology of the hMSCs. However, this was not the case for the acetic acid processed scaffolds, as the abnormal morphology was present even for a scaffold drying time of 24 hr (see **Figure 3.11**).

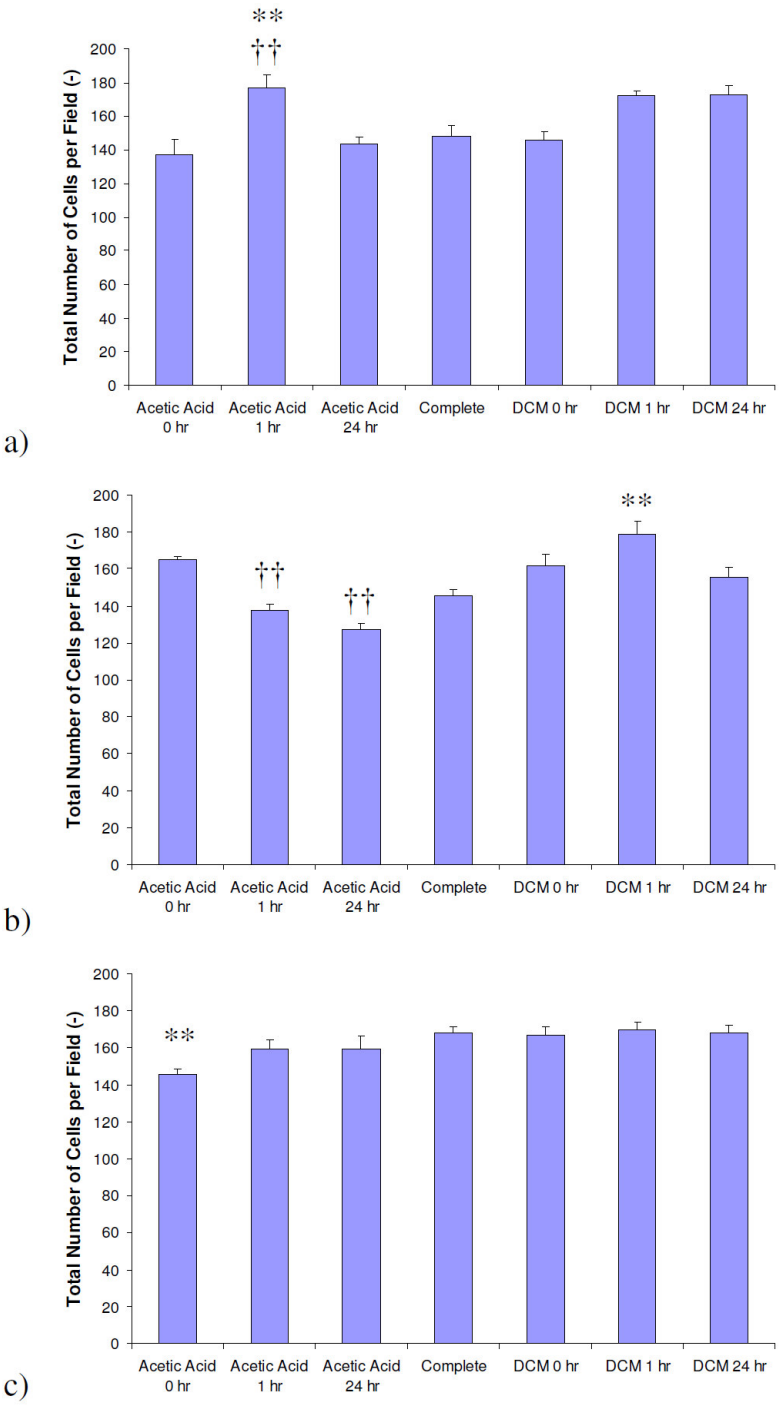

Figure 3.9: hMSC total counts exposed to test scaffolds.

The average total cell counts per field of view for hMSCs exposed to differently prepared scaffolds. Each figure represents data from a different patient isolate a) 542, b) 544, and c) 549. The error bars represent the SEM, n = 6 in each case. * and † denote $p < 0.05$, and ** and †† denote $p < 0.01$ compared to the growth media and corresponding non-dried controls respectively.

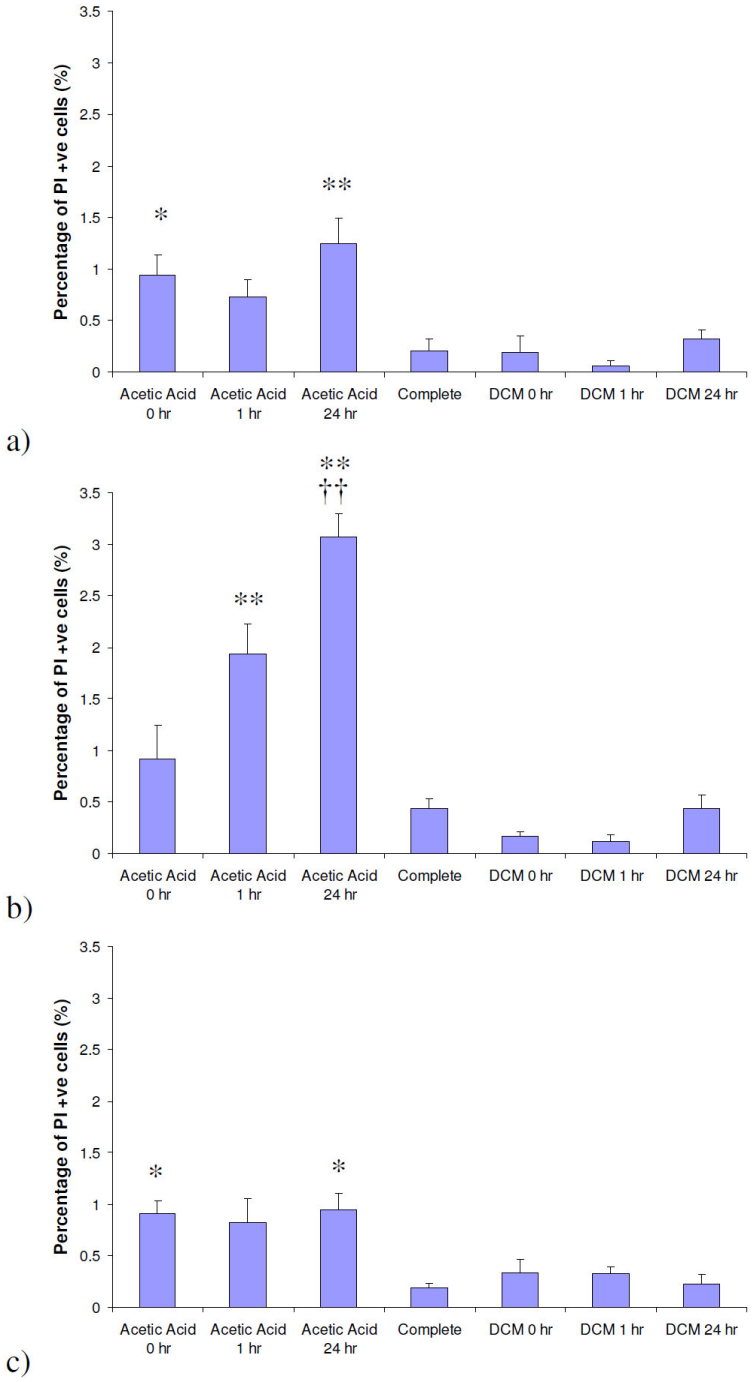

Figure 3.10: hMSC percentage of PI +ve cells exposed to test scaffolds.

The average percentages of PI +ve hMSCs exposed to differently prepared scaffolds. Each figure represents data from a different patient isolate a) 542, b) 544, and c) 549. The error bars represent the SEM, n = 6 in each case. * and † denote $p < 0.05$, and ** and †† denote $p < 0.01$ compared to the growth media and corresponding non-dried controls respectively.

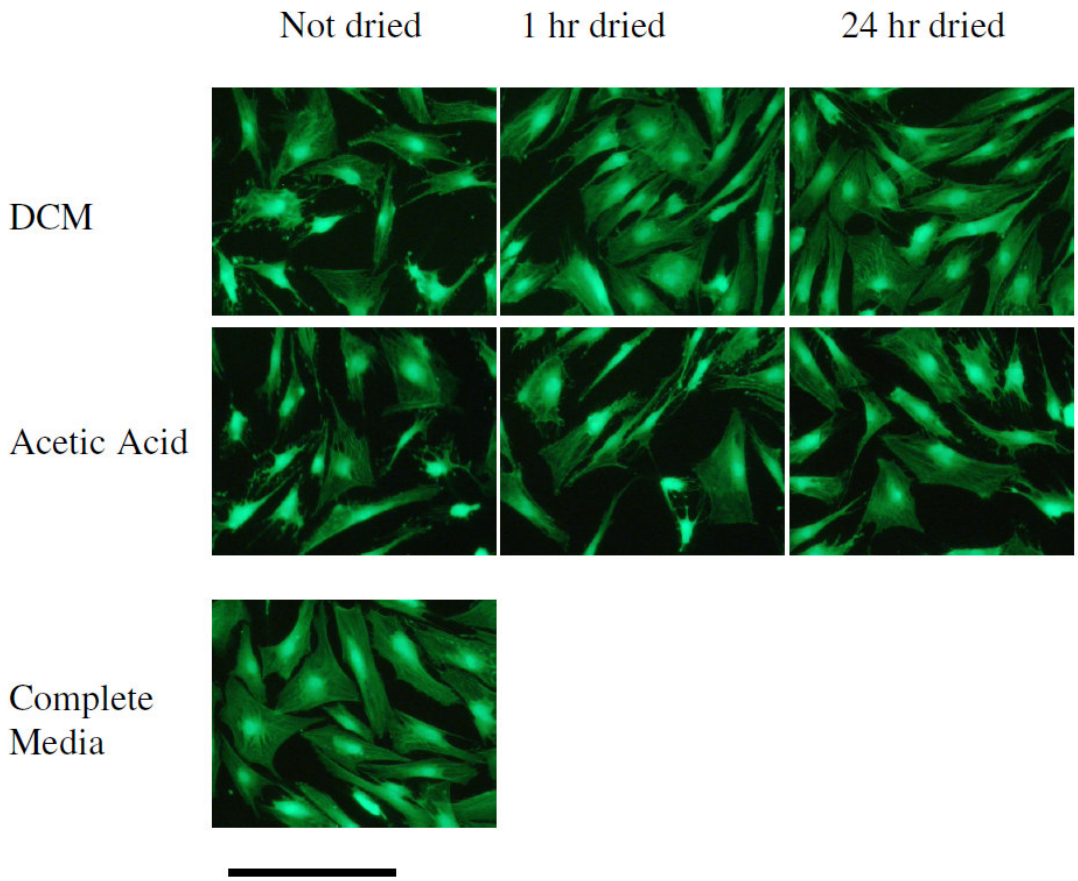

Figure 3.11: hMSCs exposed to test scaffolds.

Combined calcein and PI fluorescence images of hMSCs exposed to differently processed scaffolds. Viable cells were stained green with calcein. The bar represents 50 µm.

3.5. Discussion

As outlined in §1.2.2 and §3.2, it was imperative that both the potential scaffolds and scaffold coatings, developed as discussed in Chapter 2, should be as compatible with cell survival and growth as possible. To this end, the aims of the experiments described in the current chapter were; to select the most cell-compatible coating, and to determine the necessary scaffold vacuum drying time for sufficient removal of DCM. It was also important to assess whether the final combination of scaffold and coating were capable of supporting cellular differentiation. This was examined in the studies described in Chapter 6 and Chapter 7.

In order to compare the different scaffolds and scaffold coatings, a quantitative system was thought to be necessary. As discussed in §3.2, both calcein AM and PI are widely used to test for cell viability and death. They were, therefore, considered to be a suitable quantitative system to determine the cell-compatibility of test materials.

Since over 1900 images were taken for the experiments described in this chapter, an automated approach to cell counting was necessary. The image analysis package ImageJ has previously been used for such applications (Sieuwerts *et al.*, 2008; Collins, 2007), and automated counts were found to give good agreement with the randomly chosen manual counts.

3.5.1. Coating Assessment

Many studies have individually shown the biocompatibility of alginate (Choi *et al.*, 2007), chitosan (Risbud *et al.*, 2002), gelatin (Unger *et al.*, 2005) and collagen (Sandeman *et al.*, 2000). However, to the knowledge of the author, no direct comparison has been made of the biocompatibility of these materials.

Since hMSCs are thought to be the most promising current cell source for bone regenerative medical applications (see §1.2.3), they were used as possibly the most important test cell types. In addition it was recognised that *in vivo*, the scaffold

would also come into contact with osteoblasts, either formed from the hMSCs delivered with the scaffold, or by host cell in-growth. Hence, hOBs were used as an additional, more differentiated, test group. MG63 cells were used as the final test group to represent more proliferative cells. This cell line has previously been used to test the cell-compatibility of a variety of materials (Amaral *et al.*, 2008; Barron *et al.*, 2007; Takagishi *et al.*, 2006; Carinci *et al.*, 2004).

It is interesting to note that the cell densities of the MG63 cells were higher than those of hMSCs and hOBs. This is consistent with the findings of previous studies (Billiau *et al.*, 1977). It has been found that accumulation of hyaluronan matrix decreases contact inhibition of cell growth (Itano *et al.*, 2002), and MG63 cells are thought to have an abundant hyaluronan-rich cell associated matrix (Hosono *et al.*, 2007).

A higher proportion of cell death was observed for the more differentiated hOBs than for the relatively undifferentiated hMSCs in the collagen, gelatine and non-TC plastic groups, although the rates of cell death were comparable for the alginate and chitosan groups. It is possible that this was due to the higher sensitivity of hOBs to the lack of cell-cell adhesion. Expression of the cell-cell adhesion proteins E-cadherin and N-cadherin is thought to be higher in hOBs than hMSCs (Marie, 2002; Hay *et al.*, 2000). These proteins are known to play a role in the protection of hOBs from apoptosis (Marie, 2002). Hence, this may explain the elevated cell death for this cell type, and the inversely proportional relationship between the cell density and the death rate observed for all the cell types (see **Figure 3.4**, **Figure 3.5**, **Figure 3.6** and **Figure 3.7**). However, testing this hypothesis would require further study.

It was found that the total cell counts for the hydrogels alginate and chitosan were significantly reduced compared to the TC plastic controls for all cell types tested (see **Figure 3.4**, **Figure 3.6** and **Figure 3.7**). The percentage of PI +ve cells was also higher in these groups, indicating elevated levels of cell death (see **Figure 3.5**, **Figure 3.6** and **Figure 3.7**), although for alginate this was statistically significant for one of the three hMSC patients.

The precise mechanism for this result is unclear. The decreased cell counts could have been due to; reduced proliferation, increased cell death, low cell adhesion, or any of these factors in combination. Nevertheless, whichever hypothesis is correct, it would appear that alginate and chitosan do not have sufficient cell-compatibility to be used as effective scaffold coatings. However, it is possible that these data may be explained by the cell adhesion characteristics of the hydrogels. Mammalian cells are thought to lack receptors for either alginate or chitosan. Indeed this has led some authors to covalently attach RGD sequences to the polymers in an attempt to alleviate this problem (Augst *et al.*, 2006; Ho *et al.*, 2005). The predominantly round morphology of the cells on the hydrogels may indicate that the level of cell-hydrogel interaction was relatively low (Watanabe *et al.*, 2002). This lack of cell adhesion may have resulted in the relatively high observed rates of cell death, by anoikis (Benoit *et al.*, 2007).

In contrast, for collagen and both concentrations of gelatin, hMSC and MG63 cell counts were comparable to the TC plastic control, and significantly higher than the non-TC plastic control (see **Figure 3.4** and **Figure 3.7**). Also, both coating materials statistically significantly reduced the apparent cell death for two of the three hMSC patients tested, compared to the non-TC plastic control (see **Figure 3.5**). Indeed the coatings reduced the apparent cell death on non-TC plastic to the level of the TC plastic control for all cell types tested. Although it should be noted that the percentage of cell death in the non-TC plastic group was still relatively low (2.2±1.8%). The level of hMSC death on tissue culture plastic was found to be comparable to that found in previous studies (Santiago *et al.*, 2009). It was concluded that coatings of collagen and gelatin were more cell-compatible than the hydrogels alginate and chitosan.

These data are consistent with the hypothesis that both collagen and gelatin improve cell adhesion to the non-TC plastic. Integrin binding and focal adhesion assemblies are known to be critical to cell attachment. Type-I collagen has been found to up-regulate integrin expression in hMSCs (Chen *et al.*, 2008). In addition, Type-I

collagen has been found to enhance the adhesion, spreading and proliferation of rat osteoblasts (Cowles *et al.*, 2000; Geissler *et al.*, 2000). This is thought to be due to the binding of its specific motif, GFOGER, to integrin (Knight *et al.*, 2000). Although integrin binding to gelatin is thought to be compromised by the denaturation process used in its manufacture (Zaman, 2007), cellular integrin binding is still possible (Davis, 1992). As stated above, this is likely to reduce the rate of cell death by anoikis in these groups.

Of the two gelatin concentrations assessed, the 0.2% (w/v) coating consistently produced higher cell counts than the 0.1% (w/v) coating. This effect was particularly pronounced for the MG63 cells (see **Figure 3.7**). However, Type-I collagen consistently produced the highest cell counts of all the test coatings. Furthermore, a very low incidence of cell death was observed in the collagen coated test wells. Thus it was reasoned that Type-I collagen was the most cell-compatible potential scaffold coating of the materials tested.

Hence, Type-I collagen coated scaffolds were subjected to further testing as described in Chapters 4, 5, 6 and 7.

3.5.2. Scaffold Assessment

While DCM is considered to be, chemically, a relatively mild solvent from the viewpoint of retaining growth factor bioactivity, it can be cytotoxic. Indeed, the USFDA has set an upper limit for the presence of DCM residue of 600 parts per million for clinical treatments (Howard *et al.*, 2008). DCM is, however, highly volatile, making it relatively easy to extract.

Previous studies have employed either vacuum drying or freeze drying to remove residual DCM from regenerative medical constructs (Wei *et al.*, 2007; DeFail *et al.*, 2006). Consequently, this was thought to be a potentially useful strategy for processing the scaffolds made with DCM to a biocompatible state.

Clearly it is difficult to assess whether sufficient DCM had been removed, without employing an animal model. However, it was possible to compare the scaffolds processed with DCM, with very similar scaffolds which were known to be biocompatible. Vadillo (2009) and Martin *et al.* (2008) found that PCL scaffolds, processed using acetic acid as the solvent and 100% IMS as the plotting medium, were biocompatible, using a calvarial defect model in NOD/SCID mice. The DCM-processed scaffolds were therefore tested against scaffolds similar to those used by Vadillo (2009) and Martin *et al.* (2008), using calcein AM and PI to stain the test cells. The acetic acid-processed scaffolds would, therefore, act as a positive control for cell-compatibility.

For this test, the XY strand distance of the scaffolds was increased, to allow more cells to fall through the pores to the TC plastic beneath. It was decided to study the cells on TC plastic rather than on the scaffolds. This avoided complicating the experimental system, by potentially adding the additional variables of differences in scaffold geometry and surface topography.

Surprisingly it was found that, despite the presence of the scaffolds in the wells, all the cell counts were comparable with the TC plastic control. It would seem that the

cells were capable of filling the gaps left in the cell seeding by the scaffold. No consistent difference was found between any of the test scaffold groups and the TC plastic control (see **Figure 3.9**). Similarly, no consistent differences were observed between the scaffold groups manufactured using different solvent, and dried for different times.

However, the percentages of PI +ve cells, indicating cell death, were consistently higher for all the scaffolds groups processed with acetic acid compared to the TC plastic control, although the actual differences in cell death were very small. The level of hMSC death on tissue culture plastic was found to be comparable to that found in previous studies (Santiago *et al.*, 2009). In contrast, no statistically significant difference was found between any of the DCM processed scaffolds and the control (see **Figure 3.10**). These data suggest that the PCL scaffolds processed using DCM were at least comparable to the acetic acid-processed scaffolds, which were used as the positive control for cell-compatible scaffolds. Hence, since there was no physiologically significant difference between the DCM-processed scaffolds and the scaffolds known to be biocompatible (Martin *et al.*, 2008; Vadillo, 2009), it was concluded that these findings do not preclude the DCM-processed scaffolds from use in bone regenerative medical applications on the grounds of cell-compatibility.

It should be noted that although cell death was elevated in the acetic acid groups, it remained relatively low (> 3.5%). Hence the elevated death rate was not sufficient to prevent the hMSCs from becoming confluent by the end of the test period.

Interestingly, no evidence was obtained from either the data on the cell counts, or the +ve PI percentages, to suggest that vacuum drying had any impact on the cell-compatibility of the scaffolds. Nevertheless, it was found that there were marked differences in cell morphology between the groups (see **Figure 3.11**). The groups of PCL/DCM scaffolds which had not been dried, as well as all PCL/acetic acid scaffolds, contained a large number of rounded or dendritic hMSCs. This morphology is thought to be one of the most ubiquitous characteristics of cell death,

regardless of the stimulus (Bortner and Cidlowski, 2003; Doonan and Cotter, 2008). Since it is known that cells of the osteoblastic lineage are very sensitive to even small changes in pH, even in the range of pH 7.37 – pH 7.29 (Brandao-Burch *et al.*, 2005), it is possible that the residual acetic acid within the scaffolds was capable of deceasing the pH sufficiently to induce a slight increase in the rate of apoptosis. This was in contrast to the control, and the groups containing PCL/DCM scaffolds which had been dried for 1 and 24 hr. In these groups, the hMSC morphology was similar to that described by Gronthos *et al.* (1998) and Tremoleda *et al.* (2008), with very few rounded or dendritic hMSCs. This evidence indicates that a vacuum drying time of a least 1 hr is required for the PCL/DCM scaffolds to obtain the required level of cell-compatibility.

PCL (M_n 42,500) scaffolds processed with DCM and vacuum dried for 1hr, were therefore subjected to further testing as described in chapters 5, 6 and 7.

3.6. Conclusion

A quantitative system, based on the use of calcein AM and PI, was used to assess the relative cell-compatibility of coatings of alginate, chitosan, gelatin and Type-I collagen, based on cell viability and morphology in both progenitor (hMSCs) and differentiated human cells (hOBs and MG63 cells) of the osteoblastic lineage. The hydrogels alginate and chitosan were found to perform poorly compared to gelatin and collagen. This was in terms of decreased total cell counts, increased proportions of apparent cell death, and a morphology more associated with apoptosis. Type-I collagen was found to be the most cell-compatible coating, as it was found to be consistently superior to gelatin in terms of the total cell count. Type-I collagen coated scaffolds were therefore subjected to further testing, as described in chapters 4, 5, 6 and 7 of this thesis.

PCL scaffolds, processed using DCM as the solvent, and vacuum dried for different times, were also quantitatively and qualitatively assessed for their cell-compatibility. This was done relative to PCL/acetic acid scaffolds, which have previously been shown, by others, to be biocompatible in an animal model. This was achieved by

incubating hMSCs, which had been exposed to the scaffolds, with calcein AM and PI. The morphology of the cells was also examined to test for abnormalities.

From the data on the total cell counts, and the proportion of apparent cell death, it was found that the PCL/DCM scaffolds were at least comparable in terms of cell-compatibility to the PCL/acetic acid scaffolds, which had been used as a positive control for cell-compatibility. From the morphology studies, it was concluded that a vacuum drying time of 1 hr was sufficient for satisfactory DCM removal.

Having shown their cell-compatibility, such scaffolds were subjected to further examination, as discussed in chapters 4, 5, 6 and 7 of this thesis.

Chapter 4 : Quantitative Release

4.1. Scaffold Nomenclature

$Coat_{PBS}$	Collagen coating with PBS (rhBMP-7 control)
$Coat_{BMP\ 1.25}$	Collagen coating with rhBMP-7 (1.25 µg/ml)
$Scaff_{PBS}$	Scaffold encapsulating PBS (rhBMP-7 control)
$Scaff_{BMP\ 1.25}$	Scaffold encapsulating rhBMP-7 (1.25 µg/ml)

4.2. Abstract

For all regenerative medical drug delivery devices, it is important to assess the potential drug loading capacity, the drug release profiles, and the consistency between batches. In this chapter, the model drug methylene blue was used to select the optimum scaffold material, from those developed during the studies described in Chapter 2. Once identified in this way, the favoured candidate scaffold material, and the collagen coating, were loaded with recombinant human bone morphogenetic protein-7 (rhBMP-7). The release of this growth factor was confirmed using an enzyme-linked immunosorbent assay (ELISA).

The encapsulation efficiency of scaffold made from poly(ε-caprolactone) (PCL) (M_n 42,500 and 80,000), poly(lactide-co-glycolide) (PLGA), and blends of PCL (M_n 42,500) with PLGA, were assessed. The efficiency was found to be both relatively high and consistent for both M_n 42,500 and 80,000 PCL as well as PCL:PLGA 66:33, at 71±6%, 71±5%, and 78±10% respectively, relative to the low efficiencies recorded for both PCL:PLGA 66:33 and PLGA: 57±5% and 38±10% respectively. It was also found that PCL (M_n 42,500) scaffold, made using a plotting medium of IMS, did not contain detectible levels of the model drug.

The release rate of methylene blue from PCL (M_n 42,500), was found to be relatively slow, controlled, and consistent between batches (between 21±2% and 20±3% released in the first 24 hr). Despite the release rate being consistent for PCL (M_n 80,000), the release rate was thought to be too high, since between 29±3% and 39±5% of the test compound was released in the first 24 hr period. The release rate of methylene blue from the PCL/PLGA blends (between 17±2% – 30±7% and

18±4% – 31±6% in the first 24 hr) and PLGA (between 7.1±3.4% – 9.3±2.9% in the first 24 hr) were found to be inconsistent, and low in the case of PLGA, even taking the different loading efficiencies into account. Therefore, PCL (M_n 42,500) was selected as the favoured candidate scaffold material.

The loading content and release profiles from methylene blue loaded collagen scaffold coatings were also evaluated. The drug loading capacity was found to be suitable for use as a drug delivery system (65±5 µg/g of methylene blue per unit scaffold mass). The release of methylene blue was observed to be rapid (between 54±10% – 70±17% in the first 24 hr), which was thought to be desirable for the coating delivery system, if, for example, a dual temporal mode of release is favoured using one or more compounds.

The growth factor rhBMP-7 was loaded in collagen scaffold coatings and encapsulated within PCL (M_n 42,500) scaffolds. Both delivery systems were found to release detectable quantities of rhBMP-7 (releasing 2.8±0.2 µg/g and 87±7 ng/g respectively in the first 24 hr), even after 14 days. The release rate of the growth factor from the scaffold coating was higher than that from the encapsulating scaffolds. However, the cumulative release profiles were found to deviate from the desired ideal release profiles, and burst release was observed from both delivery systems. Although differences were observed for the two delivery systems, this difference may not be of clinical significance. Nevertheless, scaffolds with less than ideal delivery properties may still be of potential clinical use.

Evidence was also obtained that while the primary mode of release from the encapsulating scaffolds was diffusion, degradation may play a significant role in the release from the scaffold coatings.

The scaffolds were therefore found to be capable of releasing immuno-reactive rhBMP-7. The bioactivity of this release was investigated in the studies described in Chapter 5.

4.3. Introduction

As discussed in §1.2.6.3.4, the delivery of various bioactive factors, with different release profiles, may be necessary for the success of some regenerative medical constructs. The drug delivery strategy chosen for the studies described in this thesis, was to release bioactive factors from two separate delivery systems: the scaffold and the scaffold coating. It was intended that release from the scaffold coating would be rapid, whereas release from the encapsulating scaffolds would be more prolonged.

To assess both the encapsulation efficiency and the *in vitro* release profiles from potential drug delivery devices, it is common practice to conduct preliminary experiments using model drugs. There are two main reasons for this. First, the model drugs may be easy to detect, and may not undergo significant degradation in the release media, in contrast to active factors. Second, the cost of both the model drugs themselves, and the methods used for their detection, may be several orders of magnitude less than for the active factors.

However, care must be taken when choosing a model drug. Factors such as electrostatic charge and molecular weight are known to affect their diffusivity and therefore the profile of release (Weadock *et al.*, 1987; Simon *et al.*, 1999; Fredenberg *et al.*, 2005; Lee *et al.*, 2007).

4.3.1. Model Drug Rational

In general terms, two modes of drug release exist for drug delivery devices for regenerative medical applications: diffusion and degradation (Wada *et al.*, 1995; Tabata *et al.*, 1999). In reality, both methods of release will operate simultaneously, however one mode is usually dominant in a given situation and timepoint.

Where there is a strong charge interaction between the drug and the drug delivery device, release by degradation is usually the dominant mode of release. For example, Lee *et al.* (2004a) achieved the release of a growth factor (TGF-β1) from a hydrogel (chitosan) with the same charge. However, Lee *et al.* (2004a) failed to

achieve release from TGF-β1 from alginate by diffusion, where there is significant charge interaction. Similarly, Tabata *et al.* (1999) varied the release of bFGF from oppositely charged gelatin by altering the degradation properties of the carrier.

In contrast, where there is no charge interaction and the degradation time of the carrier is relatively long, diffusion is likely to be the dominant mode of release (Ritger and Peppas, 1987a; Ritger and Peppas, 1987b; Wada *et al.*, 1995).

While drug release by degradation is thought to be proportional to the degradation of the carrier, release by diffusion, where there is no strong charge interaction, is governed by the principles first investigated by Fick (1855). Fick's first law, see **Equation 4.1**, relates flux of a component ($_VJ_A$) to its composition gradient (dc_A/dz) employing a constant of proportionality called diffusivity (D_{AB}) (Fick, 1855; Perry *et al.*, 1997).

Equation 4.1

Fick's First Law of diffusion in one dimension: $$_V J_A = -D_{AB}\frac{dc_A}{dz}$$

In solving the equation for three dimensions, the "shape" of the release curves is affected by the geometry of the carrier. Examples are shown in **Equation 1.1**, **Equation 1.2** and **Equation 4.2**.

Equation 4.2

Release from a slab of thickness l (Ritger and Peppas, 1987a): $$\frac{M_t}{M_\infty} = 4\sqrt{\frac{D_{AB}t}{\pi l^2}}$$

It is thought that diffusivity varies approximately inversely with the cube root of the molecular weight of the compound (Goodhill, 1997). However, altering the molecular weight does not affect other aspects of the theoretical release profiles (Ritger and Peppas, 1987a; Ritger and Peppas, 1987b; Wada *et al.*, 1995). Although altering the molecular weight will alter the rate of release, this effect should be the

same across different carrier materials, assuming the geometry is similar. That is to say: if the release rate from carrier *X* is faster than carrier *Y*, for drug *A*, the release of *X* should theoretically be faster than carrier *Y* for drug *B* (assuming *A* and *B* have similar charges but different molecular weights). In contrast, as stated above, altering the charge interactions has been found to alter the mode of release (Lee *et al.*, 2004a)

The protein bovine serum albumin (BSA) has been employed as a model drug for a variety of potential drug delivery devices (Ginty *et al.*, 2008; Ho *et al.*, 2008; Habraken *et al.*, 2008). This is primarily because the molecular weight of BSA (66.4 kDa) is similar to many growth factors commonly used for regenerative medical applications (see **Figure 4.1**). However, in the physiological pH range of 7.35 – 7.45 (Waugh *et al.*, 2006), BSA is negatively charged (Lee *et al.*, 2007; Blanco and Alonso, 1998). This is in contrast to many growth factors of interest for bone regenerative medical applications, such as; fibroblast growth factor-2 (FGF-2), platelet derived growth factor (PDGF), bone morphogenetic protein-2 (BMP-2) and bone morphogenetic protein-7 (BMP-7), which carry a net positive charge (see **Figure 4.1**). Potentially, this difference in charge could mean that the release kinetics would be very different to the growth factors listed above. BSA may not, therefore, be an appropriate model drug for bone regenerative medical applications.

Methylene blue is another commonly used model drug (De and Robinson, 2003; Wu *et al.*, 1996; Tu *et al.*, 2005). It is a positively charged aromatic compound, hence it has the same charge as many growth factors under physiological conditions. Although the molecular weight is relatively low (320 Da), the mode of release, though not the rate, is likely to be similar to positively charged growth factors, as discussed above. Therefore, the model drug methylene blue is thought to be a useful model drug to evaluate potential bone regenerative medical drug delivery devices (Wu *et al.*, 1996).

4.3.2. Growth Factor Release

While model drugs may be effective for the purposes of preliminary testing and screening, it is thought to be necessary to confirm the actual *in vitro* release profile using growth factors themselves (Wang *et al.*, 2009b). Such release profiles are normally investigated using either radioactively labelled forms of the growth factors (Wei *et al.*, 2007; Hosseinkhani *et al.*, 2007; Bodde *et al.*, 2008), or by using an appropriate enzyme-linked immunosorbent assay (ELISA) (Kim and Valentini, 2002; Moioli *et al.*, 2006; Jaklenec *et al.*, 2008).

As indicated in Chapter 2, a number of potential scaffolds were developed. In the studies described in the current chapter, these were evaluated based on their encapsulation efficiencies and release profiles of methylene blue. The scaffold coating Type-I collagen, which was found to be the most cell-compatible of the potential coatings developed, was evaluated in a similar fashion. The release profile of rhBMP-7 was then evaluated from both the favoured candidate scaffold and scaffold coating, using an ELISA.

Growth factor superfamilies	Growth factor and relevant isoforms	Molecular weight (kDa)[a]	Isoelectric point
Epidermal growth factor (EGF)	EGF	6	5.3–5.5
	Heparin-binding EGF-like growth factor (HB-EGF)	22	7.2–7.8
Fibroblast growth factor (FGF)	Acid-FGF (aFGF or FGF-1)	18	6.5
	Basic-FGF (bFGF or FGF-2)	17	9.6
Platelet derived growth factor (PDGF)[b]	PDGF-AB	25	10.2
	PDGF-BB	25	10.5
	Vascular endothelial growth factor-121 (VEGF-121)	30	Acid
	Vascular endothelial growth factor-165 (VEGF-165)	45	8.5
Insuline-like growth factor (IGF)	IGF-1	8	8.3
	IGF-2	8	5.1
Transforming growth factor-β(TGF-β)	TGF-β1 TGF-β2 TGF-β3	25	8.9[c]
	BMP-2	15	8.8
	BMP-7	16	7.9
Neurotrophins and neurokines	Nerve growth factor (NGF)[d]	30	–
	Ciliary neurotrophic factor (CNTF)	23	4.8

[a] Referred to quaternary structure.
[b] Dimeric glycoprotein composed of A or B chains.
[c] Referred to TGF-β1.
[d] Referred to β-NGF.

Figure 4.1: Growth factor chemical properties.

The molecular weights and isoelectric points of growth factors commonly employed in regenerative medical applications (taken from Quaglia (2008)).

4.4. Materials and Methods

Unless otherwise stated, all reagents were purchased from Sigma, UK.

4.4.1. Encapsulation Efficiency

4.4.1.1. Methylene Blue Phase Partition

A methylene blue stock aqueous solution of 5 mg/ml was diluted with distilled water (dH_2O) to a concentration of 62.5 µg/ml. This solution was serially diluted with dH_2O to produce concentrations of 31.3, 15.6, 7.81, 3.91, 1.95 and 0.98 µg/ml. Each of the diluted solutions as well as a dH_2O blank (150 µl) were added to dichloromethane (DCM) (1.5 ml) in 15 ml centrifuge tubes (Corning, UK). Three replicates were used for each methylene blue concentration.

The tubes were placed in an orbital incubator (Stuart S150), set to 120 rpm (orbital diameter: 1.5 cm) and 37°C. After 4 hr, 100 µl of the aqueous solution were aspirated from each tube, and added to the wells of a 96-well plate (Corning, UK). The optical densities of the test wells, along with a calibration curve of aqueous methylene blue (62.5, 31.3, 15.6, 7.81, 3.91, 1.95, 0.98 and 0 µg/ml) were then measured using an automated 96-well plate reader (Cytofluor multiwall reader, Series 4000) set at 630 nm. The apparent methylene blue concentrations were then derived using the data from the calibration curve.

4.4.1.2. Scaffold Encapsulation Efficiency

Scaffolds were manufactured from PCL (both M_n 42,500 and M_n 80,000), and PLGA, as well as two blends of PCL and PLGA. Scaffolds were also fabricated from PCL (M_n 42,500) using a plotting medium of 100% IMS. The protocols for scaffold manufacture were as previously stated in §2.3.2.1.2, §2.3.2.2, §2.3.2.3 and §2.3.2.4 (see **Table 4.1**), except that the scaffolds were not vacuum dried. This was necessary to ensure the methylene blue remained in solution. The scaffolds encapsulated methylene blue as described in Chapter 2: methylene blue stock solution (5 mg/ml), encapsulated at 1% (v/v) in the 25% (w/v) polymer/DCM solutions.

Table 4.1: Scaffold plotting parameters.

	Plotting Material				
	PCL (42,500)	**PCL (80,000)**	**PCL:PLGA 66:33**	**PCL:PLGA 33:66**	**PLGA**
Pressure (bar)	1.0	1.5	1.5	1.4	0.7
Speed (mm/min)	168	168	168	266	672
XY Spacing (mm)	0.8	0.8	0.8	0.8	1.0

Two batches of each scaffold formulation were manufactured. The masses were determined for four scaffolds from each batch. These scaffolds were then completely immersed in DCM (3 ml) in 15 ml centrifuge tubes, then 300 µl dH_2O were added to each tube. The tubes were placed in an orbital incubator, set to 120 rpm and 37°C. After 4 hr, 200 µl of the aqueous solution were aspirated from each tube, and added to the wells of a 96-well plate (100 µl per well). The optical densities of the test wells, along with a calibration curve of aqueous methylene blue (62.5, 31.3, 15.6, 7.81, 3.91, 1.95, 0.98 and 0 µg/ml) were then measured using an automated 96-well plate reader set at 630 nm.

The apparent methylene blue concentrations were then calculated using the data from the calibration curve, after which the results were corrected to take into account the phase partition of the methylene blue from the results reported in §4.5.1.1. The mass of methylene blue per scaffold, normalised against the scaffold mass, was then calculated.

4.4.1.3. Scaffold Coating Encapsulation Efficiency

PCL (M_n 42,500) scaffolds were manufactured and then coated with Type-I collagen (rat tail) containing methylene blue, as described in §2.3.3.3. Two separate scaffold batches were fabricated, with four scaffolds randomly selected from each batch.

After the mass of each scaffold had been measured, the scaffolds were cut into four approximately equal parts. The scaffolds were then completely immersed in 1 ml of 0.1 M aqueous acetic acid in 1.5 ml Eppendorf tubes. The tubes were placed in an orbital incubator, set to 120 rpm (orbital diameter: 1.5 cm) and 37°C. After 4 hr, 200 µl of the aqueous was aspirated from each solution, and added to the wells of a 96-well plate (100 µl per well). The optical densities of the test wells, along with a calibration curve of methylene blue in 0.1 M aqueous acetic acid (62.5, 31.3, 15.6, 7.81, 3.91, 1.95, 0.98 and 0 µg/ml) were then measured using an automated 96-well plate reader set at 630 nm. The apparent methylene blue concentrations were then found using the data from the calibration curve. The mass of methylene blue per scaffold, normalised against the scaffold mass, was then calculated.

4.4.2. Methylene Blue Release

Four scaffolds from each of the batches manufactured for the experiments described above in §4.4.1.2 and §4.4.1.3, were either vacuum dried for 1 hr at 75 mbar (absolute pressure) using a freeze dryer (Alpha 1-4, Christ, Germany) or air dried for 4 hr, respectively. The mass of each scaffold was then determined. The scaffolds which were not coated in collagen, were immersed in IMS for 10 min before being washed with dH_2O (5 min) and PBS (Oxoid, UK) (5 min) in order to approximate the scaffold sterilisation process.

Every scaffold was then cut into 16 approximately equal parts before being placed in 0.5 ml Eppendorf tubes, along with 250 µl of PBS. Care was taken that all the scaffold parts were completely immersed in the PBS. The tubes were then sealed and placed in an orbital incubator, set to 120 rpm and 37°C.

After 1, 2, and 3 days, all the PBS was aspirated from the tubes and retained, before 250 µl of fresh PBS were added to each tube. After 4 days, all the PBS was removed from each tube and retained. All the PBS which had previously been in contact with the scaffolds was stored at 4°C in sealed 0.5 ml Eppendorf tubes.

The following day, 200 µl of the supernatant containing released methylene blue, was aspirated from each solution, and added to the wells of a 96-well plate (100 µl per well). The optical densities of the test wells, along with a calibration curve of aqueous methylene blue solutions in PBS (62.5, 31.3, 15.6, 7.81, 3.91, 1.95, 0.98 and 0 µg/ml) were then measured using an automated 96-well plate reader set at 630 nm. The apparent methylene blue concentrations were then calculated using the data from the calibration curve. The mass of methylene blue released in each 24 hr period was then calculated and normalised against the scaffold masses and encapsulation efficiencies.

4.4.3. rhBMP-7 Release

All of the dH_2O and phosphate buffered saline (PBS) used in the experiments described in this section, was filter sterilised using 0.22 µm filters (Millipore, UK). The scaffold manufacture and coating steps described in §4.4.3.1 were conducted in a sterile environment, using sterilised equipment. Sterile conditions were used so that the same procedure could be used to manufacture sterile scaffolds for studies involving cells (see Chapter 5, Chapter 6 and Chapter 7).

4.4.3.1. rhBMP-7 Release from Scaffolds

A stock solution of 1 mg/ml rhBMP-7 was diluted with PBS to a concentration of 25 µg/ml. This was added at 1% (v/v) to 25% (w/v) solutions of PCL (M_n 42,500)/DCM. This yielded a final mass ratio of rhBMP-7 to PCL of 1.00 µg/g or 1.25 µg/ml for the PCL/DCM solution (allowing for evaporation).

Once the plotting solutions were prepared, emulsions were created by vigorous manual mixing, using sterile 3 ml transfer pipettes (Fisher, UK), for approximately 30 seconds. The resulting emulsions were loaded into the syringe of the Bioplotter™. Scaffolds were then manufactured, with no plotting medium, using the optimised

plotting parameters determined in §2.4.1.1.1, and then vacuum dried at 75 mbar (absolute pressure) for 60 min. These scaffolds were designated $Scaff_{BMP\ 1.25}$.

Scaffolds were also manufactured in a similar fashion, replacing the 25 µg/ml rhBMP-7 solution with PBS. These scaffolds were designated $Scaff_{PBS}$.

All the scaffolds were immersed in industrial methylated spirit (IMS) for 10 min before being washed with dH_2O (5 min) and PBS (Oxoid, UK) (5 min). The stock solution of rhBMP-7 (1 mg/ml) was then added to 1 mg/ml Type-I collagen (rat tail) in 0.1 M aqueous acetic acid, to yield a final concentration of 1.25 µg/ml. The equivalent volume of PBS was added to a similar solution of Type-I collagen.

All the scaffolds were then immersed for 5 min in one of the collagen solutions either containing or lacking rhBMP-7. The scaffolds were designated with the prefixes $Coat_{BMP\ 1.25}$ or $Coat_{PBS}$ respectively. Afterwards, the scaffolds were removed, and allowed to air dry for 4 hr at room temperature. Once dry, the scaffolds were stored at -80°C.

The above protocol was conducted a total of three times using separate batches of materials. For each batch, three scaffolds were in each of the groups ($Coat_{PBS}Scaff_{PBS}$, $Coat_{BMP\ 1.25}Scaff_{PBS}$, $Coat_{PBS}Scaff_{BMP\ 1.25}$, $Coat_{BMP\ 1.25}Scaff_{BMP\ 1.25}$). After the scaffolds had been defrosted, the mass of each scaffold was measured. Every scaffold was then cut into 16 approximately equal parts before being placed in 0.5 ml Eppendorf tubes, along with 250 µl of 0.1% (w/v) BSA in PBS. Care was taken that all the scaffold parts were completely immersed in the solution. The tubes were then sealed and placed in an orbital incubator, set to 120 rpm (orbital diameter: 1.5 cm) and 37°C.

Over the next 14 days, the 250 µl of BSA/PBS solution was removed from the individual tubes and replaced with fresh BSA/PBS every 24 hr. The conditioned solutions, which were aspirated from each of the tubes, were retained in new 0.5 ml Eppendorf tubes, and labelled to enable identification of the sample source. The

tubes were immediately sealed and frozen at -80°C. The concentration of the rhBMP-7 was then measured for the samples collected on days 1, 2, 3, 4, 7 and 14. This was achieved using the ELISA protocol, as described in §4.4.3.2. It should be noted that samples for $Coat_{BMP\ 1.25}Scaff_{PBS}$ and $Coat_{BMP\ 1.25}Scaff_{BMP\ 1.25}$ for days 1 and 2 were diluted 100-fold with 0.1% (w/v) BSA in PBS. This was necessary to reduce the concentration to within the range of the ELISA concentration curve. The calculated concentrations of these samples were later adjusted to take the degree dilution into account.

4.4.3.2. rhBMP-7 ELISA Procedure

The rhBMP-7 concentrations were quantified using a DuoSet human BMP-7 ELISA kit (R&D Systems, USA). The protocol was followed according to the manufacturer's instructions. Briefly, EIA 96-well plates (Costar, USA) were coated with the Capture Antibody (100 µl per well) (R&D Systems, USA) overnight. The plate was washed with Wash Buffer (0.05% (v/v) Tween 20, in PBS), before being blocked with Reagent Diluent (300 µl per well) (R&D Systems, USA) for 1 hr.

After washing with Wash Buffer, 100 µl of test samples and standards for the calibration curve were added to the wells for 2 hr. The concentrations of the standards used were 4000, 2000, 1000, 500, 250, 125, 62.5 and 0 pg/ml. Two wells were used per standard. After washing the plate, the Detection Antibody (R&D Systems, USA) was added to each well (100 µl). After 2 hr, the plate was washed again.

Following 2 hr of incubation at room temperature, the plate was washed before Streptavidin-HRP (R&D Systems, USA) was added to each well (100 µl). After incubating for 20 min in the dark, the plate was re-washed. Then, Substrate Solution (R&D Systems, USA), containing hydrogen peroxide and tetramethylbenzidine, was added to each well (100 µl). Following 20 min of incubation in the dark, Stop Solution (1 M sulphuric acid) was added to each well (50 µl).

The optical densities of the wells was then read using an automated 96-well plate reader set at 540 nm, using a reference filter of 750 nm. The apparent rhBMP-7

concentrations were then calculated using the data from the calibration curve. The mass of rhBMP-7 released in each 24 hr period was then calculated and normalised against the scaffold masses.

4.4.4. Statistical Analysis

The mean was used throughout, and all results are expressed as the sample means ± standard error of the mean (SEM). All correlations were derived from calibration curves using Excel 2003. All correlations used, had R^2 values greater than 0.99.

The data were found not to satisfy Levene's test for homogeneity of variance, even after the use of mathematical transformations as the p-values obtained were less than 0.05. Parametric tests, such as one-way analysis of variance (ANOVA), were therefore unsuitable. Hence, the non-parametric test Kruskal-Wallis was used to test for statistical significance for each data set. The statistical significance between the groups was found using the Mann-Whitney U test (Zar, 1984; Petrie and Sabin, 2005). $p < 0.05$ was considered to be statistically significant, as calculated using the statistical software package SPSS 14.0 for Windows.

4.5. Results

4.5.1. Encapsulation Efficiency

4.5.1.1. Methylene Blue Phase Partition

In the range of methylene blue concentrations (C_{MB}) examined, a linear relationship between the concentration and the optical density (OD) at 630 nm, was found. Linear correlations were therefore calculated by linear regression. Unknown methylene blue concentrations were calculated using such correlations (see **Figure 4.2a**).

For the encapsulation efficiency experiments, it was necessary to determine what quantity of methylene blue was lost to the DCM phase. As can be seen in **Figure 4.2b**, the loss of methylene blue to the DCM phase was measureable, and was most pronounced at low methylene blue concentrations. The apparent methylene blue concentrations ($C_{MB,A}$) were compared to the standards of known methylene blue concentrations, and a correlation, taking into account the methylene blue lost to the DCM phase, was derived (see **Figure 4.2c**).

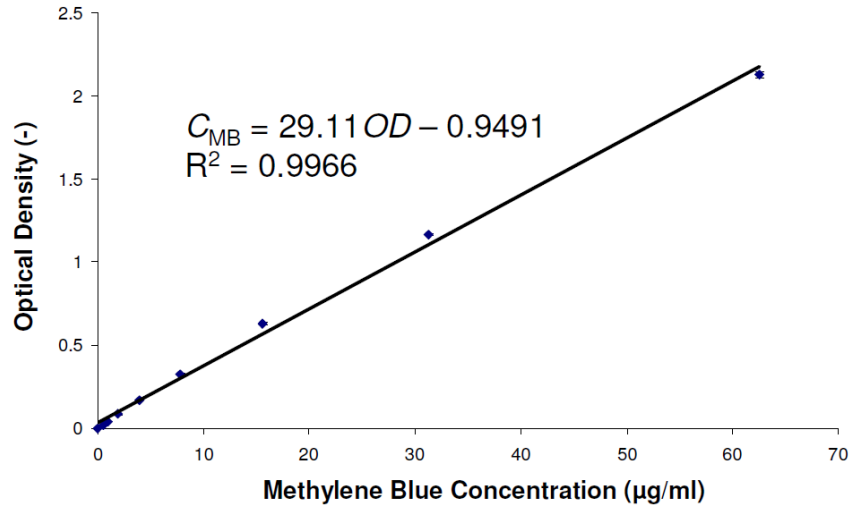
$C_{MB} = 29.11\,OD - 0.9491$
$R^2 = 0.9966$
Optical Density (-)
Methylene Blue Concentration (µg/ml)

a)

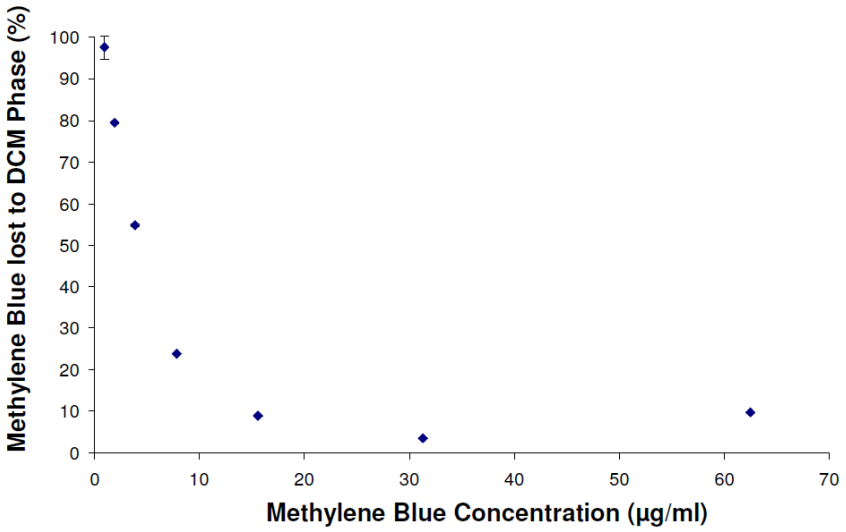
Methylene Blue lost to DCM Phase (%)
Methylene Blue Concentration (µg/ml)

b)

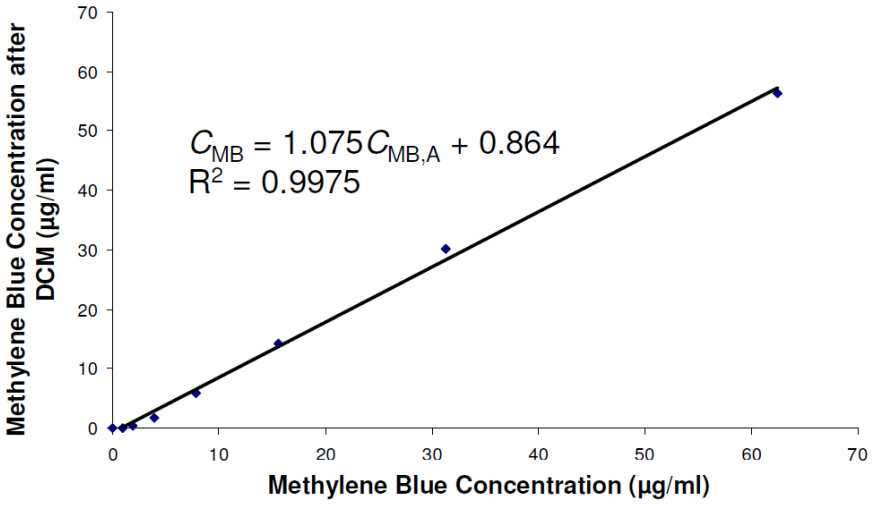
$C_{MB} = 1.075\,C_{MB,A} + 0.864$
$R^2 = 0.9975$
Methylene Blue Concentration after DCM (µg/ml)
Methylene Blue Concentration (µg/ml)

c)

Figure 4.2: Methylene blue phase separation.

Figure a) shows a representative calibration curve, relating the optical density at 630 nm to the concentration of methylene blue. Figure b) shows the proportion of methylene blue lost to the DCM phase under the same conditions as the encapsulation efficiency protocol. Figure c) shows the correction necessary to find the total methylene blue concentration in the aqueous/DCM system, from the apparent methylene blue concentration in the aqueous phase. This takes into account the methylene blue lost to the DCM phase. Each data point represents the mean of three repeats.

4.5.1.2. Encapsulation Efficiency

The methylene blue content for two separate batches of methylene blue encapsulating scaffolds made from PCL (M_n 42,500 and 80,000) and PLGA, as well as from blends of PCL (M_n 42,500) and PLGA, was determined (see **Figure 4.3**). In each case the methylene blue lost to the DCM phase was taken into account, using the results from §4.5.1.1. Similarly, the methylene blue content of methylene blue loaded collagen coatings, on PCL (M_n 42,500) scaffolds, was assessed. Again, two separate batches were assessed (see **Figure 4.3**). Although the methylene blue encapsulation efficiency percentage of PCL (M_n 42,500), plotted with IMS, was measured, all the results were below the limit of detection of the assay (data not shown).

It was found that the scaffolds made from PCL, of both molecular weights (M_n 42,500 and 80,000), as well as the PCL:PLGA 33:66 blend, had both a high and a relatively consistent methylene blue content (157±20 – 126±11 µg/g, 155±12 – 131±16 µg/g, and 193±30 – 120±6 µg/g between batches respectively). In contrast, the methylene blue of the PCL:PLGA 66:33 blend was found to be inconsistent between batches (130±5 – 96±15 µg/g). Although the methylene blue content of PLGA scaffolds was consistent between batches, the total encapsulation was approximately half that of the PCL scaffolds (89±39 – 64±8 µg/g) (see **Figure 4.3**). The methylene blue content of the collagen coating on PCL scaffolds was found to be relatively consistent between batches. The mass of methylene blue per unit mass of scaffold was found to be comparable to the results obtained for the encapsulating scaffolds (see **Figure 4.3**).

The encapsulation efficiencies were calculated, based on the maximum theoretical encapsulation of 200 µg/g (see **Table 4.2**).

Table 4.2: Encapsulation efficiencies of polymer scaffolds.

Polymer	PCL (42,500)	PCL (80,000)	PCL:PLGA 66:33	PCL:PLGA 33:66	PLGA
Encapsulation Efficiency (%)	71±6	71±5	57±5	78±10	38±10

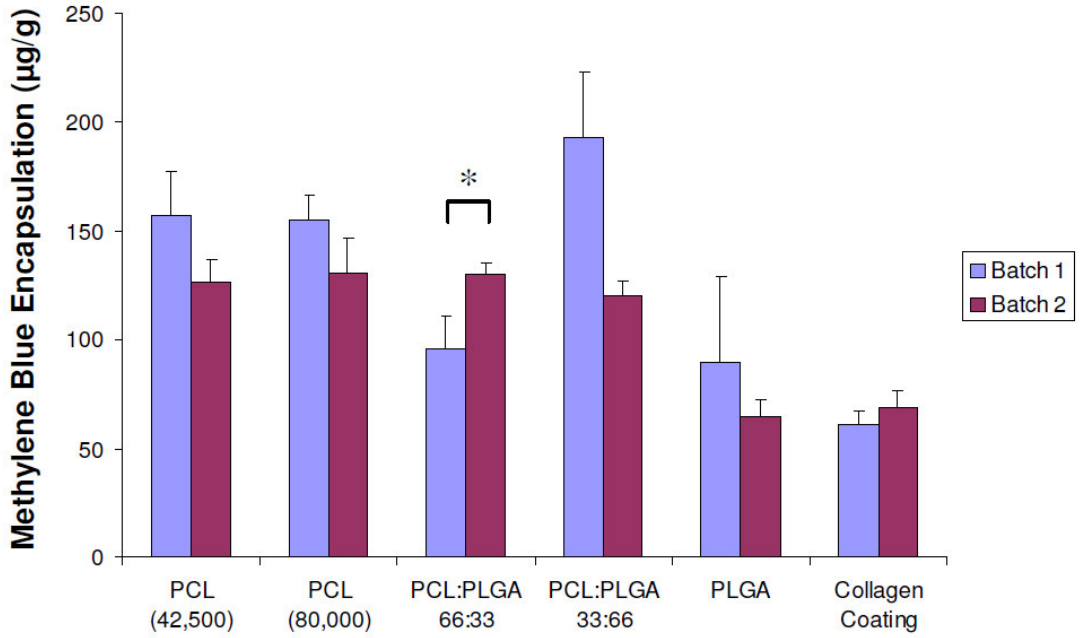

Figure 4.3: Methylene blue content of different scaffold preparations.

These figures show the apparent methylene blue content of scaffolds prepared from different polymers, or polymer blends, as well as scaffolds coated with Type 1 Collagen. Data from two separate batches are shown. Each data point represents the mean of four repeats. * denotes $p < 0.05$ between the groups indicated.

4.5.2. Methylene Blue Release

The release of methylene blue from scaffolds was quantified for each 24 hr period. This was normalised against the total theoretical methylene blue content of the scaffolds for each batch, as calculated from the results in **Table 4.2** (see **Figure 4.4** and **Figure 4.5**). The release of methylene blue from scaffolds of PCL (M_n 42,500) was found to be relatively consistent between batches as no significant difference was observed between them at any time point (see **Figure 4.5a).** The cumulative release profiles were also found to be relatively consistent (see **Figure 4.4a**). The release from the PCL (M_n 80,000) was higher than that from PCL (M_n 42,500) (by 66.9±0.1% in the first 24 hr period), however release from the two different batches were calculated to differ significantly from each other at all time points tested (see **Figure 4.5b**). Differences in the cumulative release profiles between the two different batches were also observed (see **Figure 4.4b**).

Although relatively consistent within batches, the release of methylene blue from scaffolds of the two blends of PCL (M_n 42,500) with PLGA, statistically significant differences between the batches were observed (see **Figure 4.5c** and **d**). This was also reflected in the cumulative release profiles (see **Figure 4.4c** and **d**). In contrast, the variability of release from the PLGA scaffolds within the same batch was relatively large, while no statistically significant differences were observed between different batches. For the two PCL/PLGA blends, the mean normalised release rates were found to be similar to those of PCL (M_n 42,500). In contrast, even taking into account the reduced encapsulation efficiency, the release rates from the PLGA scaffolds were considerably lower than those of PCL (M_n 42,500) (see **Figure 4.5**e). Again, this was reflected in the cumulative release profiles (see **Figure 4.4e**).

The methylene blue release rates from scaffolds coated with methylene blue loaded collagen, were found to be high. The release was observed to be relatively consistent, both in the same batch and between batches (see **Figure 4.5f** and **Figure 4.4f**).

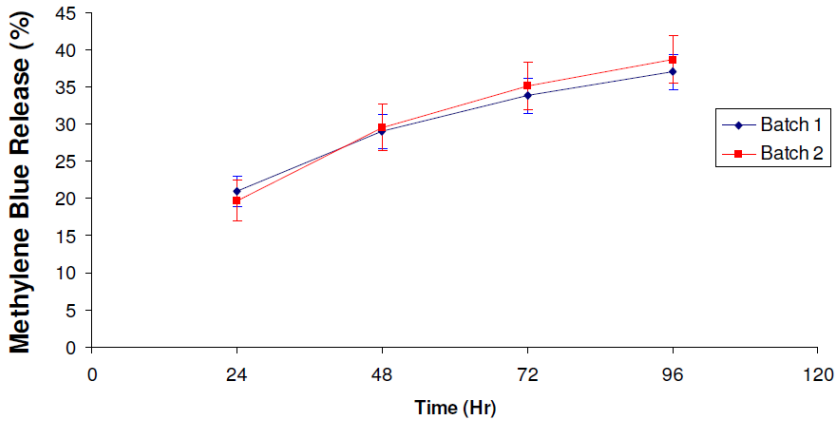

PCL (42,500)

a)

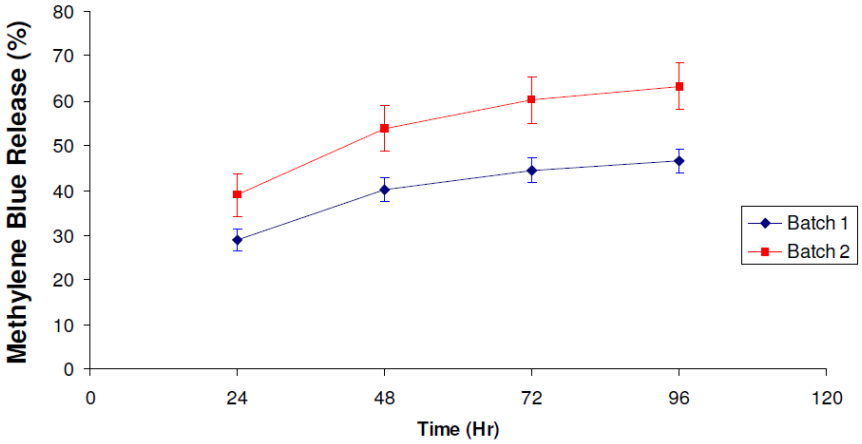

PCL (80,000)

b)

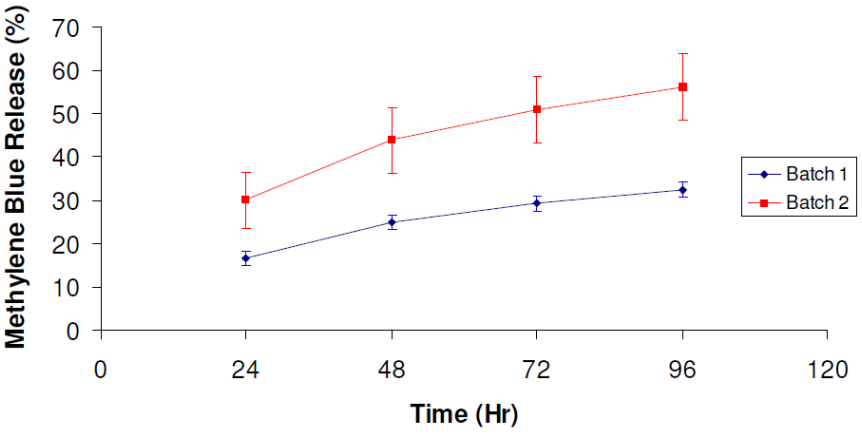

PCL:PLGA 66:33

c)

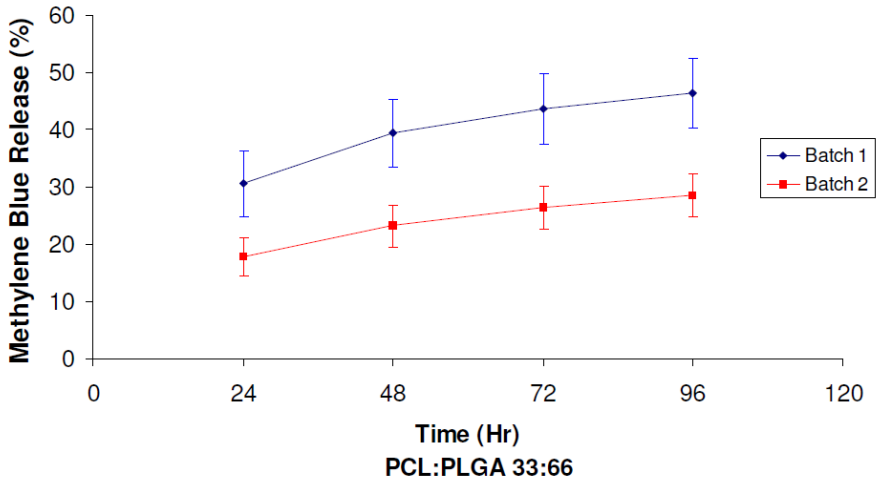
Methylene Blue Release (%)
60
50
40
30
20
10
0
0
24
48
72
96
120
Time (Hr)
Batch 1
Batch 2
PCL:PLGA 33:66

d)

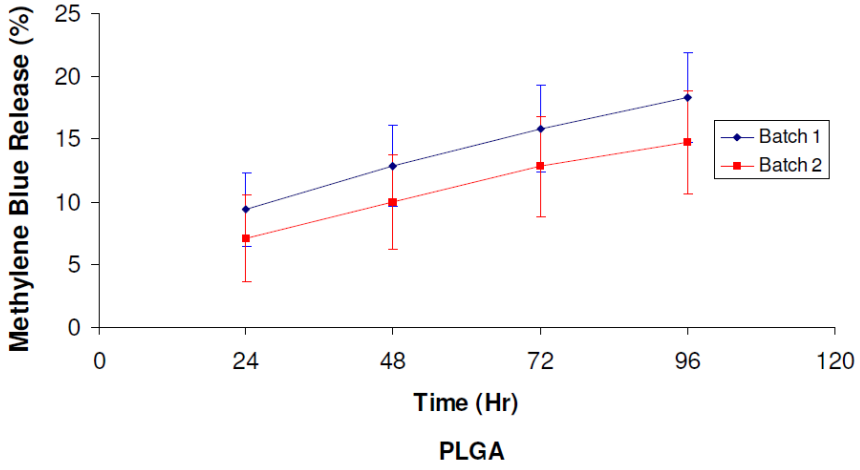
Methylene Blue Release (%)
25
20
15
10
5
0
0
24
48
72
96
120
Time (Hr)
Batch 1
Batch 2
PLGA

e)

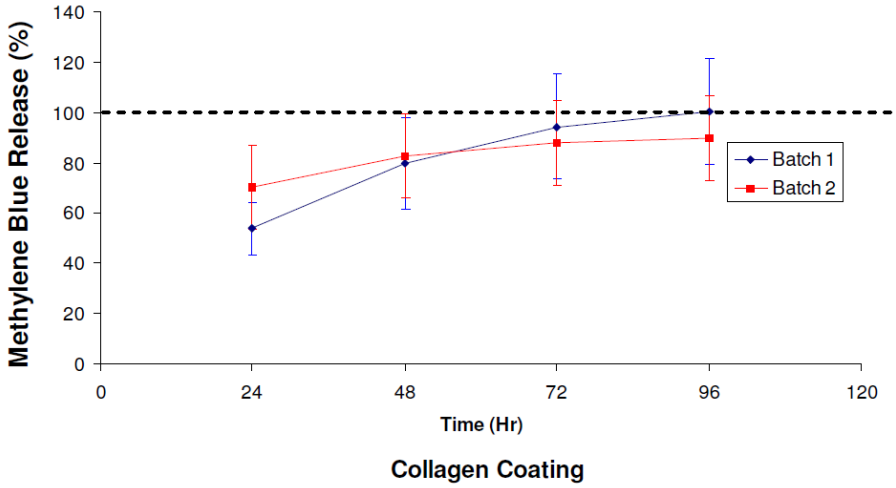
Methylene Blue Release (%)
140
120
100
80
60
40
20
0
0
24
48
72
96
120
Time (Hr)
Batch 1
Batch 2
Collagen Coating

f)

Figure 4.4: Cumulative methylene blue release from scaffolds.

These figures represent the cumulative release of methylene blue from encapsulating scaffolds manufactured from; a) PCL 42,500, b) PCL 80,000, c) PCL:PLGA 66:33, d) PCL:PLGA 33:66, and e) PLGA. Figure f) represents the release of methylene blue from the collagen coating on PCL 42,500 scaffolds. The results were normalised against the encapsulation efficiency for each scaffold batch. Each data point represents the mean of four repeats.

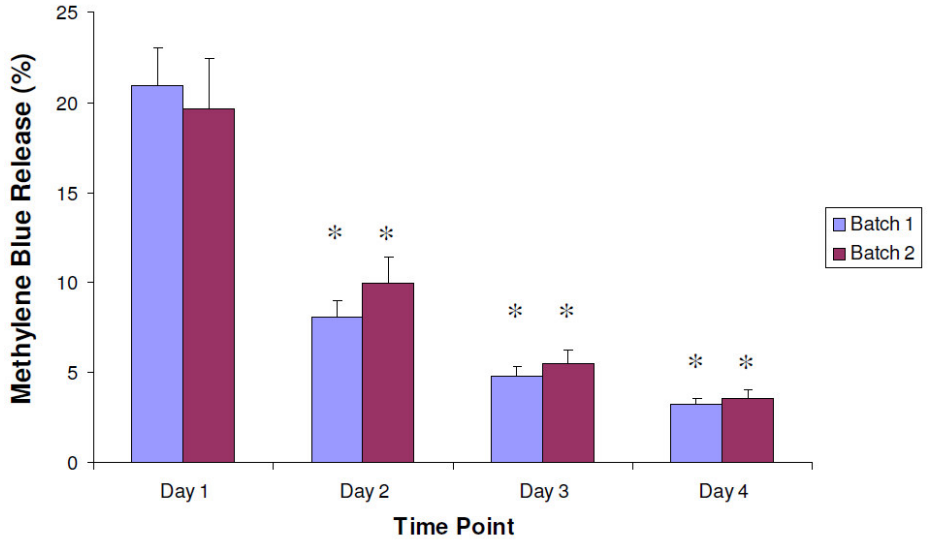
Methylene Blue Release (%)
25
20
15
10
5
0
Day 1
Day 2
Day 3
Day 4
Time Point
Batch 1
Batch 2
*

a)

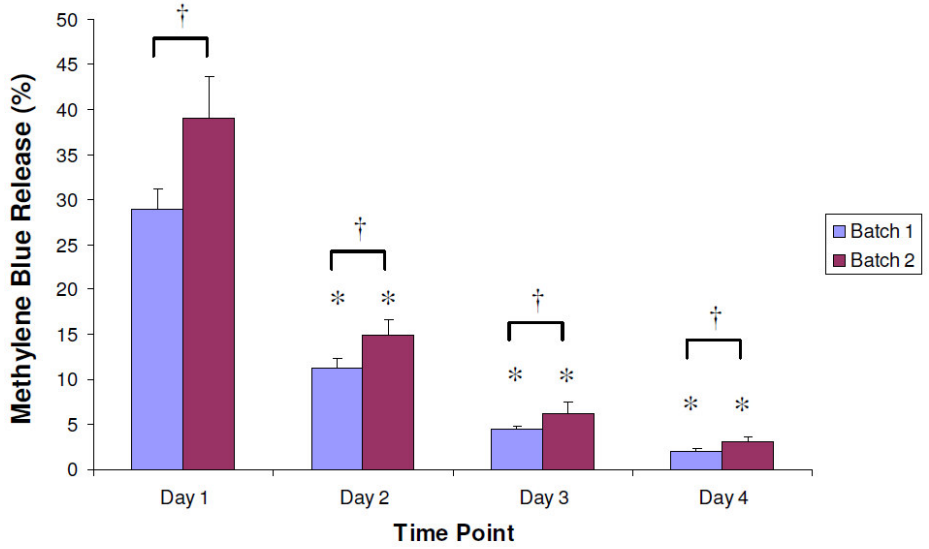
Methylene Blue Release (%)
50
45
40
35
30
25
20
15
10
5
0
Day 1
Day 2
Day 3
Day 4
Time Point
Batch 1
Batch 2
*
†

b)

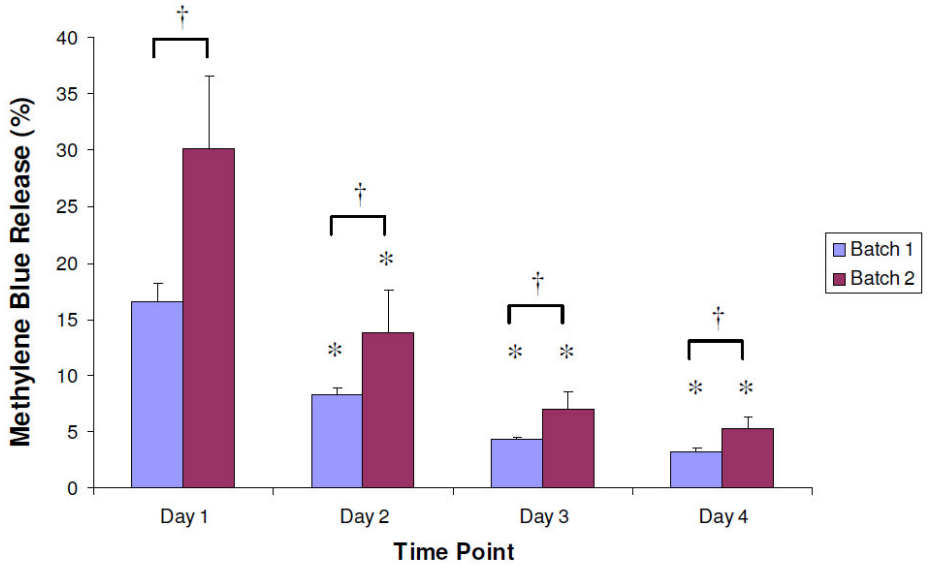
Methylene Blue Release (%)
40
35
30
25
20
15
10
5
0
Day 1
Day 2
Day 3
Day 4
Time Point
Batch 1
Batch 2
*
†

c)

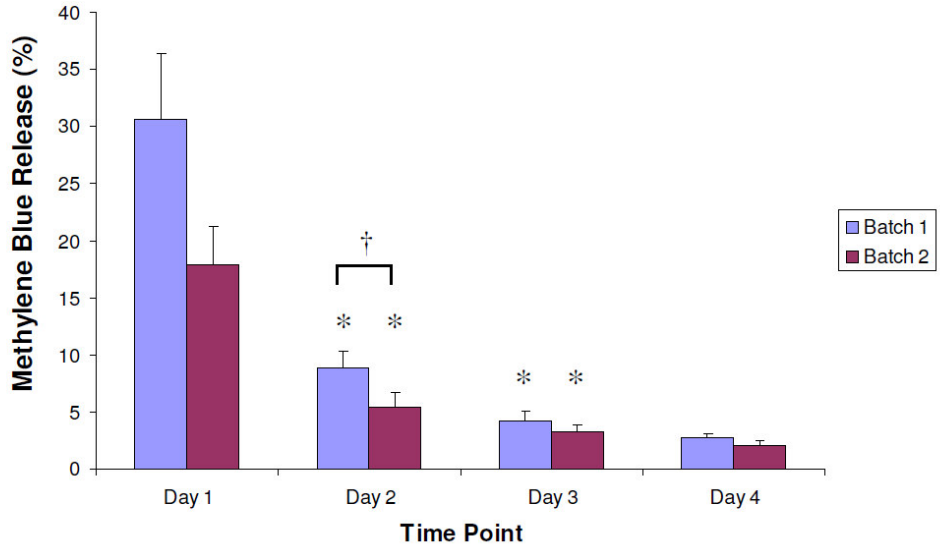
Methylene Blue Release (%)
40
35
30
25
20
15
10
5
0
Day 1
Day 2
Day 3
Day 4
Time Point
Batch 1
Batch 2
†
*
*
*
*

d)

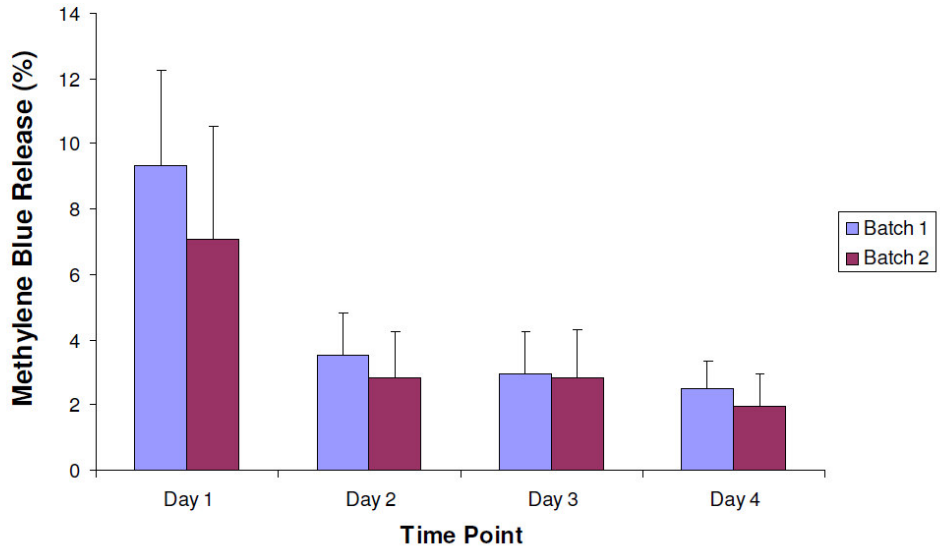
Methylene Blue Release (%)
14
12
10
8
6
4
2
0
Day 1
Day 2
Day 3
Day 4
Time Point
Batch 1
Batch 2

e)

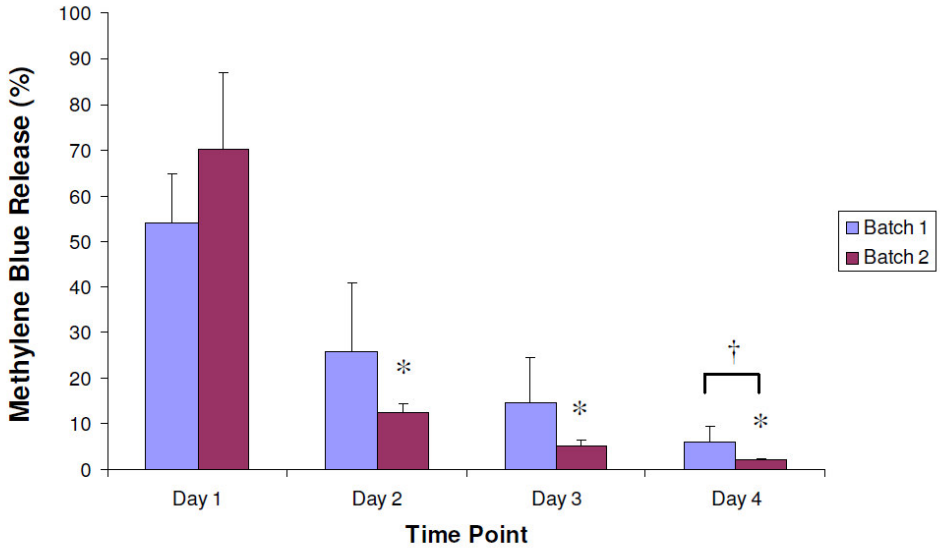
Methylene Blue Release (%)
100
90
80
70
60
50
40
30
20
10
0
Day 1
Day 2
Day 3
Day 4
Time Point
Batch 1
Batch 2
*
*
†
*

f)

Figure 4.5: Methylene blue release from scaffolds.

These figures represent the release of methylene blue from encapsulating scaffolds manufactured from; a) PCL 42,500, b) PCL 80,000, c) PCL:PLGA 66:33, d) PCL:PLGA 33:66, and e) PLGA. Figure f) represents the release of methylene blue from the collagen coating on PCL 42,500 scaffolds. The results were normalised against the encapsulation efficiency for each scaffold batch. Each data point represents the mean of four repeats. * denotes $p < 0.05$ between the group indicated, and the previous 24 hr period. † denotes $p < 0.05$ between the different batches as indicated.

4.5.3. rhBMP-7 Release

Following the manufacturer's instructions, log-log plots were graphed for all the calibration curves for the rhBMP-7 ELISA. As can be seen from the representative calibration curve in **Figure 4.6**, the log-log plots yielded a linear relationship between the optical density and the concentration of rhBMP-7 ($C_{\text{rhBMP-7}}$). Correlations, derived from log-log plots of the calibration curves, were used to find the apparent rhBMP-7 concentrations throughout this section.

For each batch tested, the control $Coat_{PBS}Scaff_{PBS}$ scaffolds, which were manufactured without rhBMP-7, were found not to give a false positive ELISA reading (see **Figure 4.8a**). In contrast, rhBMP-7 was observed to have been released from all the scaffolds loaded with the growth factor.

The rate of release of rhBMP-7 from the $Coat_{PBS}Scaff_{BMP\ 1.25}$ scaffolds, normalised by scaffold mass, was found to decrease statistically significantly with time between each consecutive time point (see **Figure 4.8b**) (for example, decreasing from 86.9±6.5 ng/g to 21.5±2.1 ng/g [p = 0.001] in the first and second 24 hr periods respectively). The release profile was similar to that obtained using the model drug methylene blue. The release of rhBMP-7 was found to be consistent, both within and between batches. Detectable levels of rhBMP-7 were measured from each batch of scaffolds on each 24 hr period tested, even after 14 days in the BSA/PBS solution. The cumulative release from the $Coat_{PBS}Scaff_{BMP\ 1.25}$ scaffolds showed that 12.2±0.9% of the theoretical rhBMP-7 was released in the first 24 hour period, and by day 4 17.8±0.4% had been released (see **Figure 4.7a**).

Similar to the results for the model drug, the release rate of rhBMP-7 from the scaffold coating ($Coat_{BMP\ 1.25}Scaff_{PBS}$) was considerably higher than that for $Coat_{PBS}Scaff_{BMP\ 1.25}$ (see **Figure 4.8c**). However, the release profile was observed to "tail off" more quickly towards a release rate of zero. The release of rhBMP-7 was found to be consistent, both within and between scaffold batches. Detectable levels of rhBMP-7 were measured from each batch of scaffolds on each 24 hr period tested,

even after 14 days. The cumulative release from the *Coat* $_{BMP\ 1.25}$*Scaff*$_{PBS}$ scaffolds showed that 23±2% of the theoretical rhBMP-7 was released in the first 24 hour period, and by day 4 28.8±0.4% had been released (see **Figure 4.7b**).

The release profiles from the *Coat*$_{BMP\ 1.25}$*Scaff*$_{BMP\ 1.25}$ scaffolds were very similar to those from the *Coat*$_{BMP\ 1.25}$*Scaff*$_{PBS}$ scaffolds (see **Figure 4.8d**). Since the release rate from the coating was much greater than the release from the encapsulating scaffold, it is unsurprising that this effect would dominate the release profiles. However, the release of rhBMP-7 was less consistent between batches, as significant differences between batches were observed. Again, detectable rhBMP-7 concentrations were measured at each time point tested.

Log-log plots of cumulative growth factor release against time were graphed for *Coat*$_{PBS}$*Scaff*$_{BMP\ 1.25}$ and *Coat*$_{BMP\ 1.25}$*Scaff*$_{PBS}$ scaffolds. The purpose of this was to assess the mode of rhBMP-7 release. The values of R^2 for the linear model for the *Coat*$_{BMP\ 1.25}$*Scaff*$_{PBS}$ scaffolds, were found to be relatively low (the mean being 0.927±0.020), indicating a statistically significant deviation from the linear model (see **Figure 4.9a**). In contrast, the *Coat*$_{PBS}$*Scaff*$_{BMP\ 1.25}$ showed good agreement with the linear model, the mean R^2 being 0.988±0.003 (see **Figure 4.9b**).

4.5.3.1. Scaffold Loading Capacity

From the methylene blue studies, the encapsulation efficiency of scaffold delivery system was 71±6%. Therefore the loading of rhBMP-7 in *Scaff*$_{BMP\ 1.25}$ scaffolds, was calculated to be 710 ng/g.

The methylene blue loading capacity in the coating delivery system was 65±5 µg/ml, using a methylene blue stock solution of 5 mg/ml. Since the rhBMP-7 stock solution was 1 mg/ml, the rhBMP-7 loading capacity in *Coat*$_{BMP\ 1.25}$ scaffolds was calculated to be 12,500 ng/g.

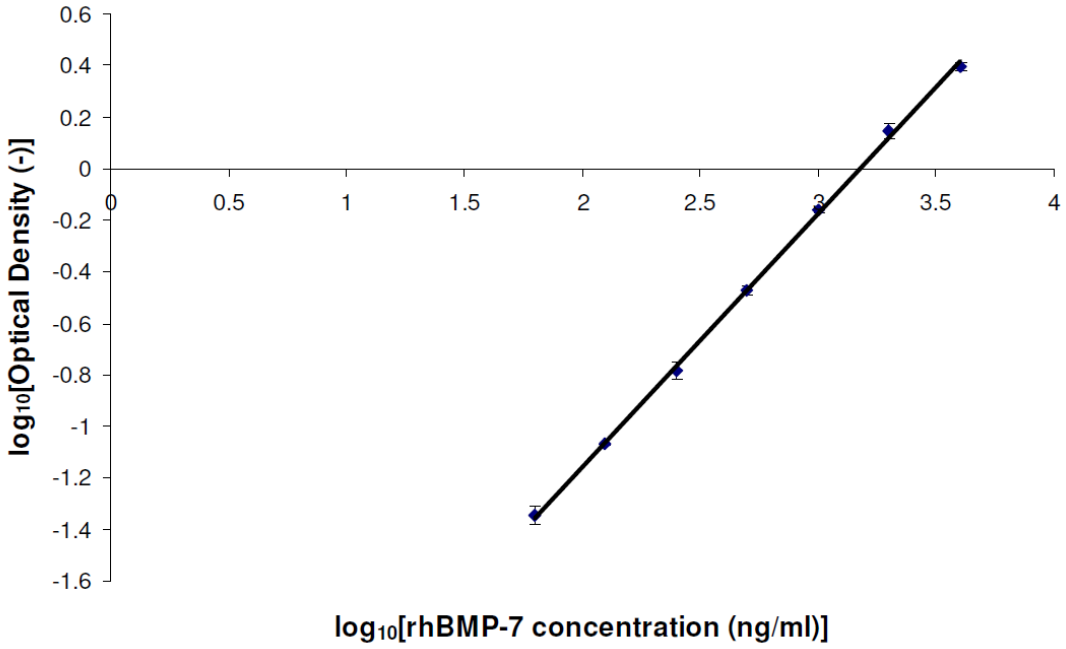

Figure 4.6: rhBMP-7 calibration curve.

A representative calibration curve relating the concentration of rhBMP-7 with the optical density. From this calibration curve, the correlation $\log_{10}[C_{\text{rhBMP-7}}] = 1.018 \times \log[OD] + 3.177$ ($R^2 = 0.9992$) was derived. Each data point represents the average of two repeats.

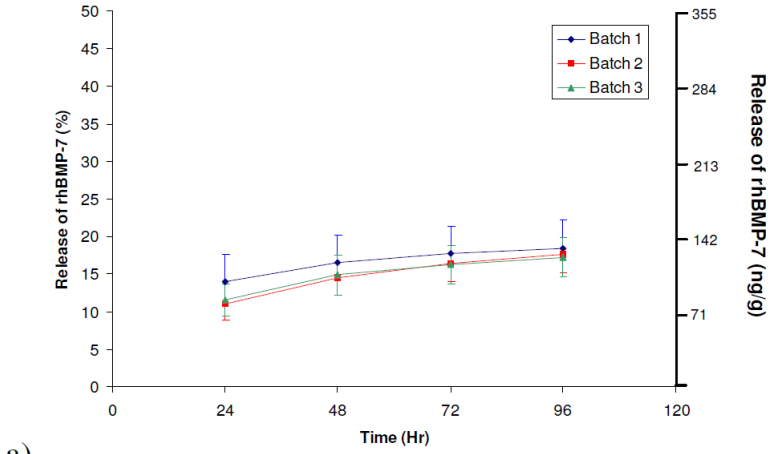

a) $Coat_{PBS}Scaff_{BMP\ 1.25}$

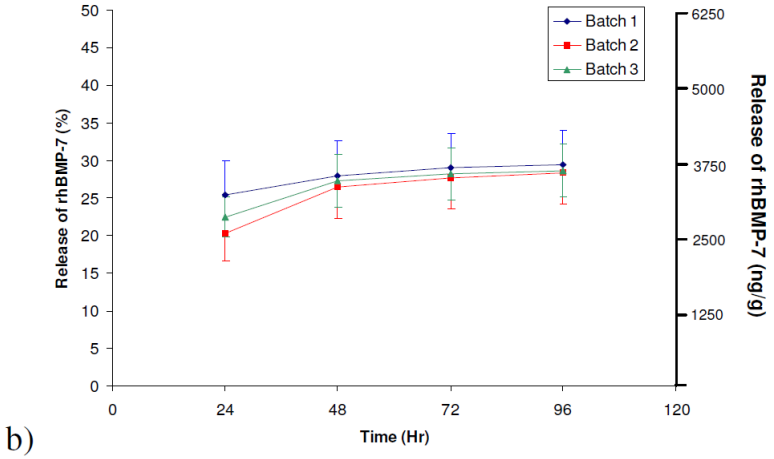

b) $Coat_{BMP\ 1.25}Scaff_{PBS}$

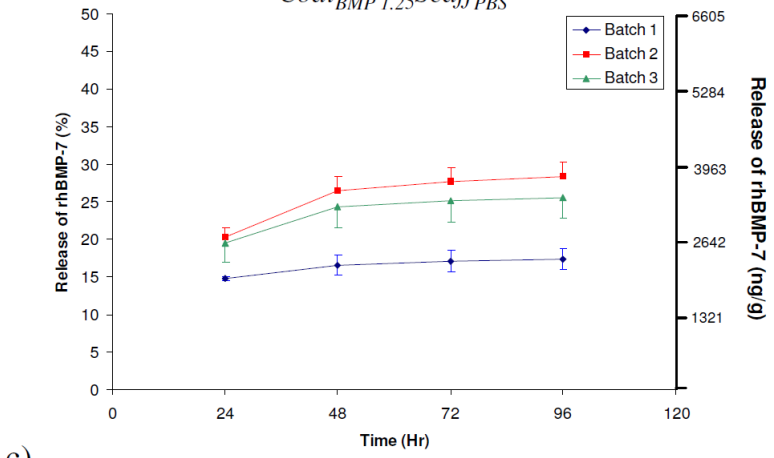

c) $Coat_{BMP\ 1.25}Scaff_{BMP\ 1.25}$

Figure 4.7: rhBMP-7 cumulative release from scaffolds.

These figures represent the cumulative release of rhBMP-7 from three batches of scaffolds loaded as a) $Coat_{PBS}Scaff_{BMP\ 1.25}$, b), $Coat_{BMP\ 1.25}Scaff_{PBS}$ and c) $Coat_{BMP\ 1.25}Scaff_{BMP\ 1.25}$.

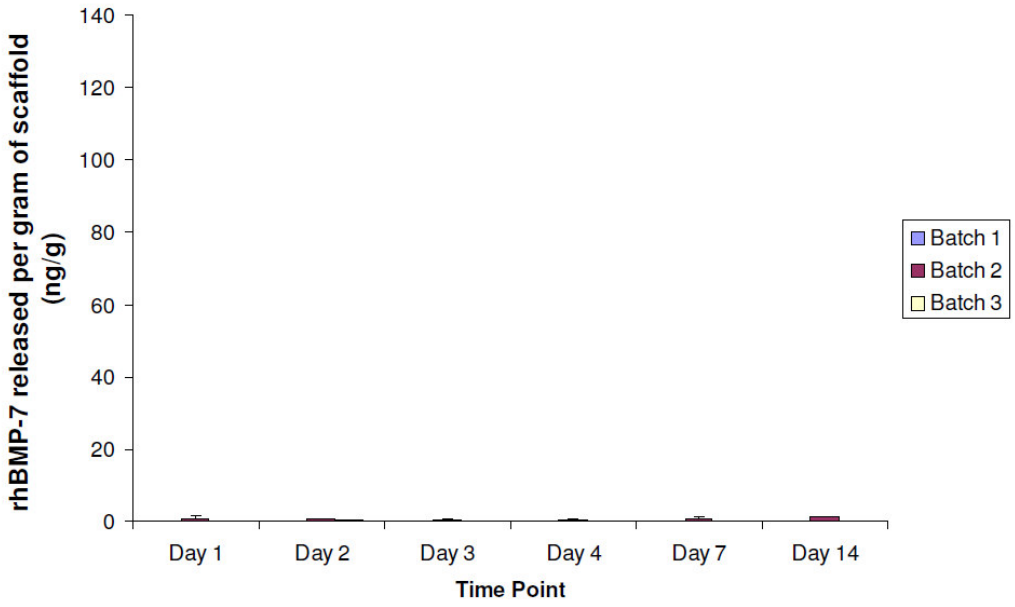
rhBMP-7 released per gram of scaffold (ng/g)
140
120
100
80
60
40
20
0
Day 1
Day 2
Day 3
Day 4
Day 7
Day 14
Time Point
Batch 1
Batch 2
Batch 3

a)

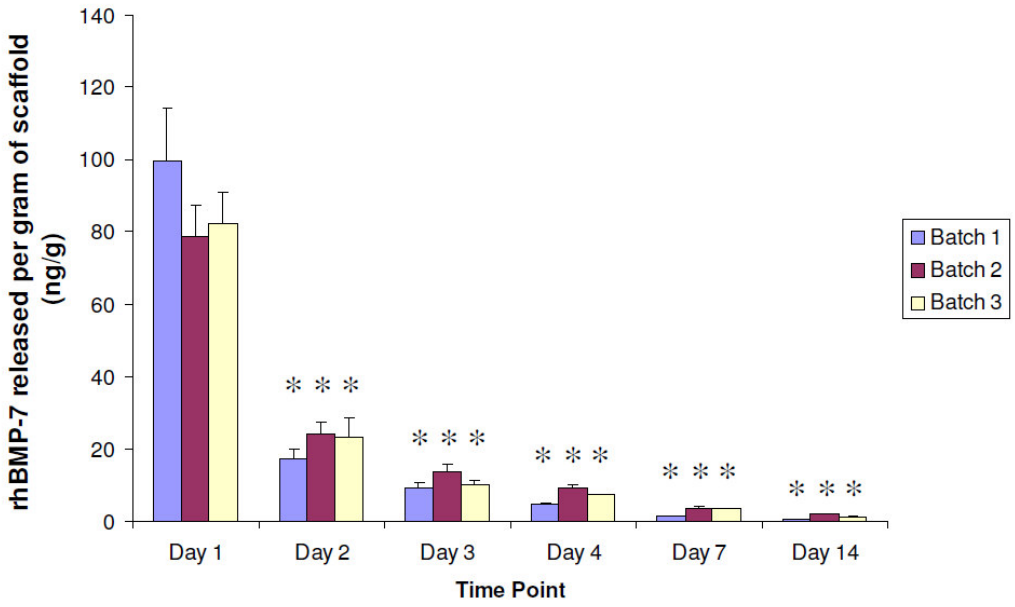
rhBMP-7 released per gram of scaffold (ng/g)
140
120
100
80
60
40
20
0
* * *
Day 1
Day 2
Day 3
Day 4
Day 7
Day 14
Time Point
Batch 1
Batch 2
Batch 3

b)

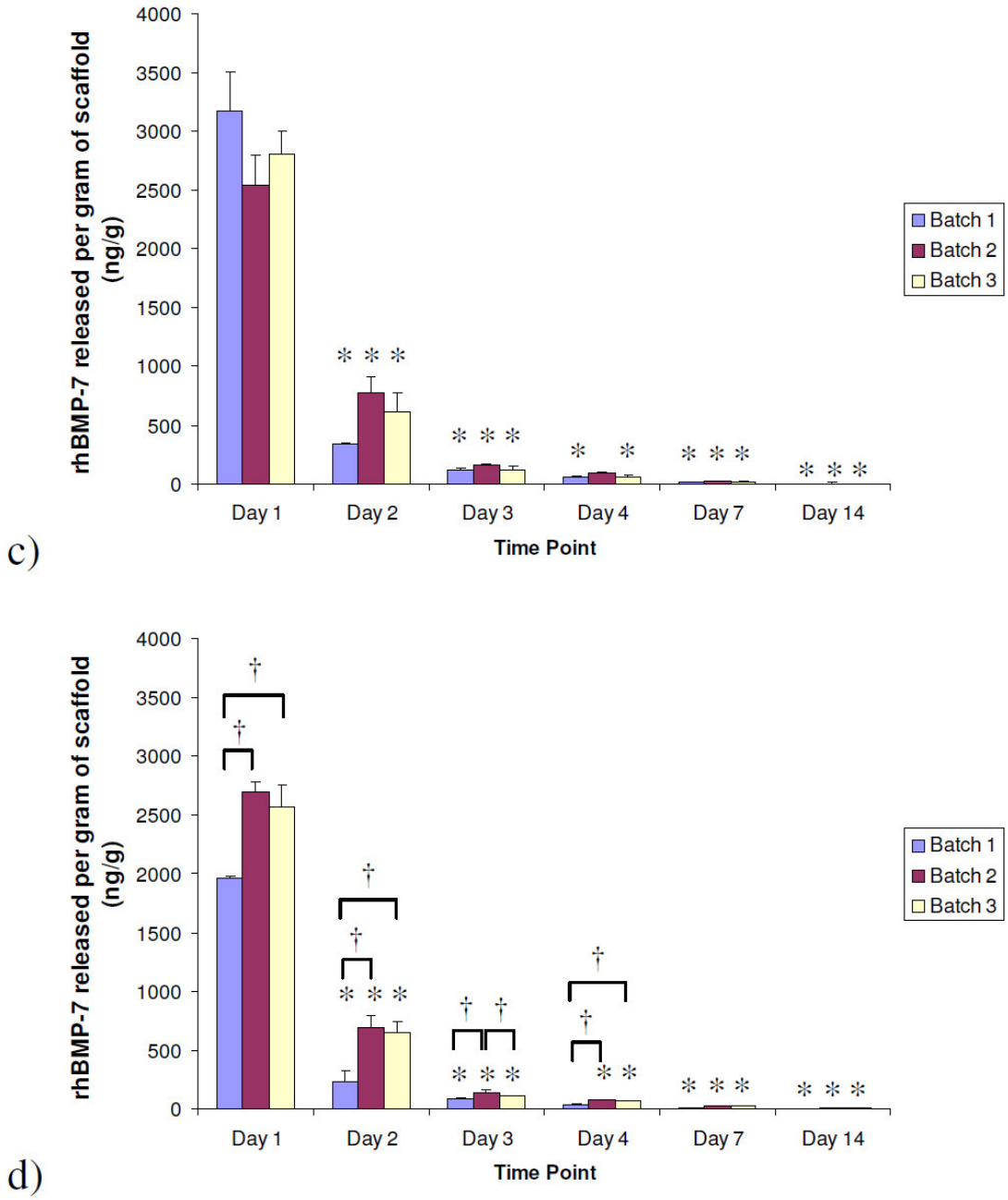

Figure 4.8: rhBMP-7 released from scaffolds.

These figures represent the release of rhBMP-7 from three batches of rhBMP-7 encapsulating scaffolds manufactured with different formulations; a) $Coat_{PBS}Scaff_{PBS}$, b) $Coat_{PBS}Scaff_{BMP\ 1.25}$, c) $Coat_{BMP\ 1.25}Scaff_{PBS}$, d) $Coat_{BMP\ 1.25}Scaff_{BMP\ 1.25}$. The results were normalised against the scaffold mass in each case. Each data point represents the mean of three repeats. * denotes $p < 0.05$ between the group indicated, and the previous 24 hr period. † denotes $p < 0.05$ between the different batches as indicated.

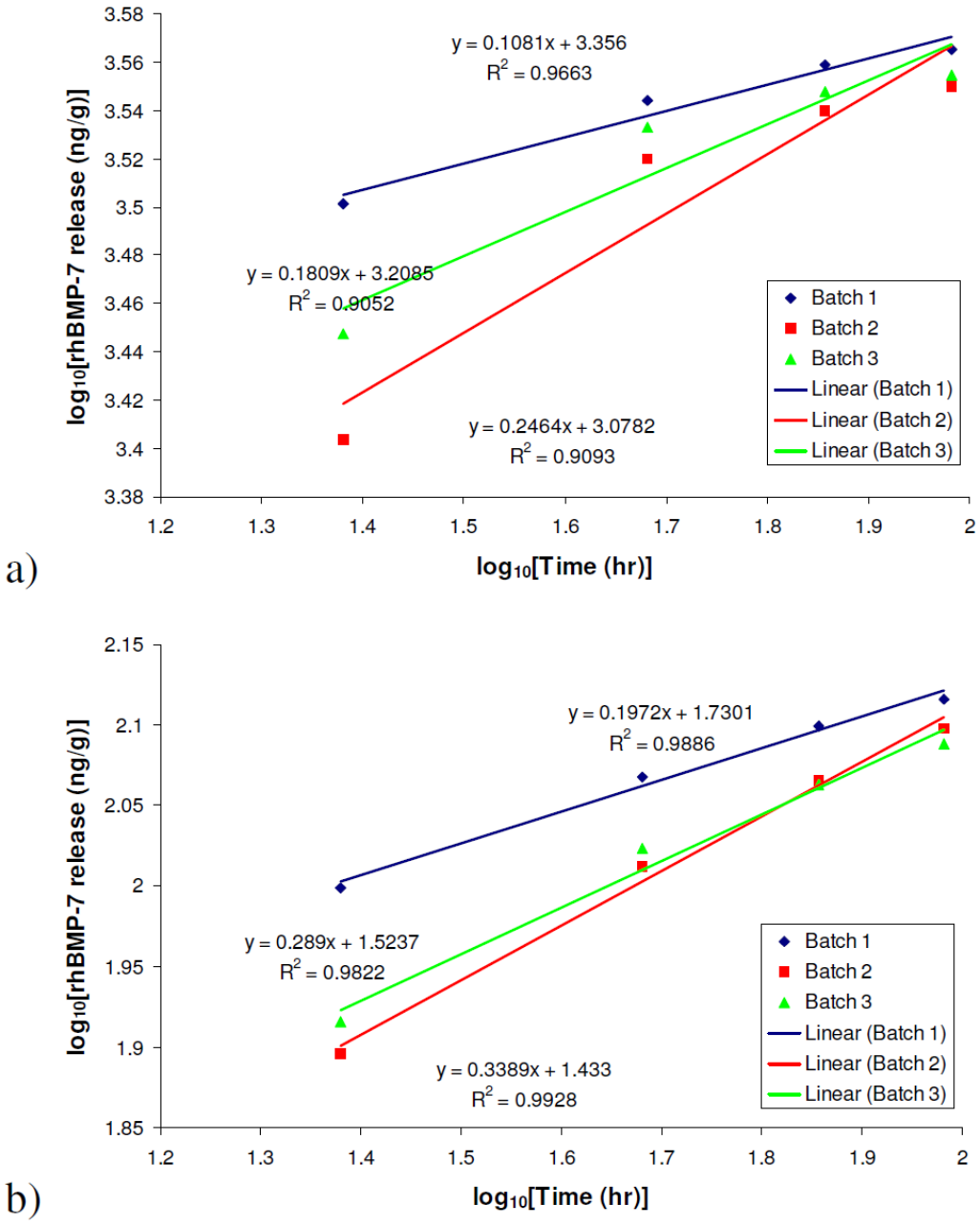

Figure 4.9: Log-log plots of rhBMP-7 cumulative release from scaffolds.

These figures represent log-log plots of the cumulative release of rhBMP-7 from three batches of scaffolds loaded as a) $Coat_{BMP\ 1.25}Scaff_{PBS}$, b) $Coat_{PBS}Scaff_{BMP\ 1.25}$. Lines of linear regression are displayed for each batch, along with the equations of the lines and their R^2 values. Each data point represents the mean of three repeats.

4.6. Discussion

4.6.1. Encapsulation Efficiency

Methylene blue was chosen as the model drug to measure the encapsulation capacity of the different scaffold materials, as well as the collagen scaffold coating. The reasons for employing a model drug to study these systems include; favourable model drug stability, ease of detection, and economic cost (see §4.3).

In particular, methylene blue was an almost ideal choice for the encapsulation efficiency studies. This is because methylene blue is hydrophilic, hence the majority of the methylene blue encapsulated in scaffolds was successfully recovered after dissolving them in DCM. A similar method was employed by Cao and Shoichet (1999). However, as such systems reach equilibrium, inevitably some of the methylene blue was lost to the DCM phase. The phase partition of methylene blue between dH_2O and DCM was difficult to predict theoretically (Perry *et al.*, 1997, Sandler, 1999), therefore there was a need to find it experimentally.

As can be seen from **Figure 4.2b**, the proportion of methylene blue lost to the DCM phase was more pronounced at lower concentrations. After the DCM phase became saturated, a linear correlation was applied to take this loss of methylene blue mass into account (see **Figure 4.2c**). This correlation was used to adjust for the loss of methylene blue in all the encapsulation experiments using DCM.

The methylene blue content of the scaffolds was found. For the encapsulating polymer scaffolds, these data were compared against the theoretical methylene blue loading of 200 μg/g (see **Table 4.2**). The encapsulation efficiency of the PCL scaffolds, for both M_n 42,500 and 80,000, was calculated to be 71±6% and 71±5% respectively. The encapsulation efficiency was found to be relatively consistent, both between and within batches. This loading efficiency was found to be similar to other potential drug delivery devices (Rai *et al.*, 2005; Silva *et al.*, 2006).

In contrast, the methylene blue content of the PCL (M_n 42,500) plotted in IMS was found to be below the detection limit of the methylene blue assay. The use of such scaffolds was therefore discontinued, as they were found to be an extremely inefficient potential drug delivery system. This was an unfortunate result, as it limited the scope for the manipulation of the three dimensional (3D) geometry. However, as discussed in §2.5.1.1.3, the building up of 3D geometry may not be necessary for the creation of an effective bone regenerative medical treatment.

The PCL:PLGA 33:66 encapsulation efficiency was the highest measured (78±10%) and although variation within the batches was relatively high, no significant difference was found between the batches. Both the PCL:PLGA 66:33 blend and the PLGA encapsulation efficiencies were found to be relatively low at 57±5% and 38±10%. Furthermore, a statistically significant difference between the PCL:PLGA 66:33 batches was found. Therefore, of the polymers tested, PCL of either molecular weight and the PCL:PLGA 33:66 blend were the most promising materials regarding encapsulation efficiency.

It is possible that the differences in encapsulation efficiency were due to the differences in both the viscosities and densities of the polymer solutions. This would affect the rate at which the aqueous droplets would rise to the top of the solution in the syringe during the scaffold manufacturing process. In principle, the encapsulation efficiencies could be increased by increasing the polymer concentration in the solution, thus increasing the viscosity of the solution. However, as investigated in Chapter 2, this would be difficult to achieve.

The encapsulation efficiency for the collagen coated scaffolds could not be calculated in the same way as for the encapsulating polymer scaffolds, as the quantity of coating on the scaffolds was difficult to determine directly. However, in terms of the model drug content, this drug delivery system was found to be comparable to the encapsulating scaffolds (see **Figure 4.3**). The coating was therefore thought to be acceptable regarding model drug encapsulation.

4.6.2. Methylene Blue Release

Despite the similarities in the encapsulation efficiencies, there were differences in the methylene blue release profiles from the two molecular weights of PCL. It is interesting to note that the release rate from PCL (M_n 80,000) was higher than that from PCL (M_n 42,500) (for example by 1.7±0.1 fold in the first 24 hr period) (see **Figure 4.5a** and **b**).

Fick's first law, see **Equation 4.1**, relates flux of a component to its composition gradient, employing a constant of proportionality called diffusivity (Fick, 1855; Perry *et al.*, 1997). It is also known that the diffusivity of PCL decreases as the molecular weight increases (Gilmore *et al.*, 1980). Therefore it was hypothesised that the release rate of the model drug from the higher molecular weight of PCL would be less than for the lower molecular weight PCL. The fact that this is not the case, implies that the microstructure of the scaffolds may be different. Since a slow release rate, consistent between batches, was desired for the scaffolds, PCL (M_n 42,500) was thought to be the better option of the two.

It was observed that the release profiles of methylene blue from scaffolds of both the PCL/PLGA blends as well as PLGA were relatively inconsistent (see **Figure 4.5c**, **d** and **e**, and **Figure 4.4c**, **d** and **e**). Also, it was found that there was relatively little scope for adjusting the release profile by altering the proportions of PCL and PLGA. Furthermore, the addition of PLGA considerably increases the capital cost of the scaffolds.

Therefore, since no significant benefit was observed over PCL (M_n 42,500), either in terms of the release profiles or the encapsulation efficiency, PCL (M_n 42,500) was considered to be the favoured candidate material tested. Therefore, scaffolds manufactured from PCL (M_n 42,500) were subjected to further testing as described and discussed in §4.4.3, §4.5.3, and §4.6.3, as well as chapters 5, 6 and 7.

The release rate of methylene blue from the collagen coating was found to be relatively high (see **Figure 4.5f**). The burst release in the first 24 hr period, was

similar to that observed for most formulations of microparticles (Wei *et al.*, 2007; Holland *et al.*, 2003). Release from the coating was found to have reached approximately 100% by the 96 hr mark (see **Figure 4.4f**).

It was thought to be desirable that the release profiles of the scaffold and scaffold coating should be different. This would allow the early release of one active factor, and the more controlled release of a second factor. It was believed that this aim would be best achieved using the scaffold coating as a fast delivery system, while employing the scaffold itself as a more controlled one. The results from collagen as a scaffold coating, and PCL (M_n 42,500) scaffolds, were therefore thought to be compatible with the design philosophy of this study (see §1.4.2.1).

4.6.3. rhBMP-7 Release

As discussed in §1.2.4, there is a variety of active factors which are thought to have the potential for therapeutic use in bone regenerative medicine. It is currently unclear which combination of active factors will ultimately provide the most effective treatment for fracture non-unions. Indeed it is possible that this may vary from patient to patient. In the absence of this information, and since measuring the release profiles of each potential active factor was not economically feasible, a growth factor was chosen as a representative of the group.

rhBMP-7 was selected as the representative growth factor, for two main reasons. First, its charge and molecular weight are similar to many other active factors of potential therapeutic application (Quaglia, 2008), including; FGF-2, PDGF, TGF-β1, -β2, -β3, and BMP-2 (see **Figure 4.1**). Second, rhBMP-7 is one of only two growth factors currently licensed by the USFDA for the treatment of fracture non-unions (USFDA, 2001).

It was observed that the release profiles of rhBMP-7 obtained using the ELISA were similar in form to those found using the model drug methylene blue. This provides some evidence to justify both the choice of methylene blue as the model drug, and the conclusions on material selection based upon it, as discussed in §4.6.1 and §4.6.2.

As predicted by the methylene blue model, it was found that the release rate of rhBMP-7 from the collagen coating was considerably higher than that from the encapsulating scaffolds (see **Figure 4.8**). The release from the collagen coating was also found to "tail off" more quickly. This was consistent with the design philosophy employed in this thesis. Potentially, active factors encouraging angiogenesis or cell proliferation could be released early on from the coating. Whereas, factors encouraging osteogenic differentiation could be released in a more controlled fashion, and for a longer amount of time, from within the scaffold.

It was found that the release of rhBMP-7 from the $Coat_{BMP\ 1.25}Scaff_{PBS}$ and $Coat_{PBS}Scaff_{BMP\ 1.25}$ scaffolds was relatively consistent both within and between the batches (see **Figure 4.8b** and **c**). Whereas, $Coat_{BMP\ 1.25}Scaff_{BMP\ 1.25}$ scaffolds showed small, but statistically significant, differences in release rate between batches (see **Figure 4.8d**). Consistency between different scaffolds is an obvious precondition for therapeutic application. In this respect, these data would seem not to preclude these scaffold designs from clinical use.

Based on the laws of Fickian diffusion, Ritger and Peppas (1987a; 1987b) derived a general relation between the fraction of drug released (M_t/M_∞) and time (t), using the constants k and n (see **Equation 4.3**). In order to determine the primary mode of release, log-log plots of cumulative drug release against time were graphed (see **Figure 4.9**). Since M_t/M_∞ is likely to be proportional to the normalised mass of drug released, if the release profile fits the diffusion model, such plots should yield a straight line.

Equation 4.3

Ritger and Peppas' equation relating diffusive drug release with time: $\frac{M_t}{M_\infty} = kt^n$

It was found that the release profile of rhBMP-7 from the $Coat_{PBS}Scaff_{BMP\ 1.25}$ scaffolds fitted the diffusion model with a mean R^2 value of 0.988±0.003. This

indicates that diffusion was the primary mode of release from these scaffolds. In contrast, the release profile from $Coat_{BMP\ 1.25}Scaff_{PBS}$ scaffolds deviated more from the diffusion model. In this case, the mean R^2 value was 0.927±0.020. This might indicate that degradation played a role in the mode of growth factor release from the coating.

In the studies described in this chapter, the release of the immuno-reactive form of rhBMP-7 from the scaffolds was confirmed. Despite some studies which claim to use ELISAs to confirm bioactivity (Douglas *et al.*, 2008), it is currently unknown whether the bioactive and immuno-reactive forms of growth factors are identical. Therefore, studies were conducted to confirm the bioactivity of the rhBMP-7 released (see Chapter 5).

4.6.3.1. Comparison to Ideal Release Profile

The rhBMP-7 release profiles (see **Figure 4.7**) were found to differ from the ideal release profiles detailed in §1.4.1 and **Figure 1.18**.

From **Figure 4.7b**, it would appear that approximately 30% of the rhBMP-7 theoretically loaded into the scaffold coating was available for release. 23±2% of the theoretical loading capacity was released in the first 24 hr period. This represents approximately 77% of the total available rhBMP-7 available for release. Therefore the burst release from the coating, which appeared to be largely exhausted in the first 72 hr did not match the ideal "rapid" release profile detailed in **Figure 1.18**.

From **Figure 4.7a**, it would appear that the release of rhBMP-7 from the $Scaff_{BMP\ 1.25}$ delivery system tended towards a maximum release of approximately 20% of the growth factor theoretically encapsulated, after approximately 96 hr. Five potential explanations why only 20% of rhBMP-7 was available for release are as follows. First, loosely bound rhBMP-7 may be lost during the scaffold sterilisation process, before the collagen coating. Second, a proportion of rhBMP-7 may have been degraded during the scaffold manufacturing process. Third, a proportion of rhBMP-7 may have been unavailable for diffusive release, and may have only been available upon degradation, similar to the findings of Wei *et al.* (2007), in the release of

rhBMP-7 from PLGA 50:50 (64 kDa). Fourth, a proportion of the rhBMP-7 may have degraded in the release media once released from the scaffolds. Five, a proportion of the rhBMP-7 may have become bound to the collagen coating after diffusing from the PCL scaffold base.

Although 12.2±0.9% of the theoretical rhBMP-7 loading was released in the first 24 hr period, this represents approximately 60% of the rhBMP-7 seemingly available for release. Hence this burst release was inconsistent with the ideal release profile detailed in **Figure 1.18**, where a delay to facilitate the action of the "rapidly" delivered growth factor was desired. In addition, the majority of the release was found to occur in the first 4 days, rather than between days 7 and 28 which was detailed in the ideal release profile (see **Figure 1.18**).

Hence ideal release was not achieved from either delivery system. In addition, although the release profiles were found to be different, this difference may not be of clinical significance. However, delivery systems with less than ideal release kinetics may still be of potential clinical use. For example, scaffolds loaded with rhBMP-7 were capable of inducing ectopic bone formation in rats in 6 weeks when implanted subcutaneously (Wei *et al.*, 2007). This was despite *in vitro* release kinetics with indicated that ~50% of all the rhBMP-7 released in the first 6 weeks occurred in the first 24 hr. The scaffolds were therefore tested further in studies described in chapter 5, 6 and 7.

4.7. Conclusion

Scaffolds manufactured from PCL (M_n 42,500 and 80,000), PLGA, as well as blends of PCL (M_n 42,500) and PLGA, were evaluated using the model drug methylene blue. The encapsulation efficiencies, and the release profiles of methylene blue, were quantitatively assessed.

It was found PCL (M_n 42,500) scaffolds had high encapsulation efficiencies, and released the methylene blue at a controlled rate. The results were found to be consistent between different batches. While the encapsulation efficiency was

similarly high for PCL (M_n 80,000), significant differences in the release from different scaffold batches were observed. In addition, the rate of methylene blue release was thought to be too high for the encapsulating delivery system.

The PLGA, and PCL/PLGA blends were found to perform poorly. The methylene blue release rates from the PCL/PLGA blends were found to be relatively inconsistent between batches. The encapsulation efficiencies of PLGA and PCL:PLGA 66:33 were also relatively low. PCL (M_n 42,500) scaffolds, made without plotting media, were therefore considered to be the favoured candidate scaffold material.

The drug loading potentials, as well as model drug release profiles from collagen coatings on PCL (M_n 42,500) scaffolds, were similarly assessed. The fast methylene blue release rate, and methylene blue content of the scaffolds, were found to be compatible with the design philosophy employed in this thesis.

The release profiles of the growth factor rhBMP-7, from both encapsulating scaffolds and loaded collagen scaffold coatings, were measured using an ELISA. As with the methylene blue results, the collagen coating was found to release rhBMP-7 at a faster rate than the encapsulating PCL (M_n 42,500) scaffolds. The release profiles were found to deviate from the desired ideal release profiles, and burst release was observed from both delivery systems. Although differences were observed for the two delivery systems, this difference may not be of clinical significance.

Nevertheless, having shown that the encapsulating PCL (M_n 42,500) scaffolds, and the loaded collagen scaffold coatings, were capable of releasing detectable amounts of rhBMP-7 for up to 14 days, the bioactivity of this release was then assessed as described in Chapter 5.

Chapter 5 : Bioactive Release

5.1. Scaffold Nomenclature

$Coat_{PBS}$	Collagen coating with PBS (rhBMP-7 control)
$Coat_{BMP\ 0.63}$	Collagen coating with low rhBMP-7 dose (0.63 µg/ml)
$Coat_{BMP\ 1.25}$	Collagen coating with high rhBMP-7 dose (1.25 µg/ml)
$Coat_{ethanol}$	Collagen coating with ethanol ($1,25(OH)_2D_3$ control)
$Coat_{1,25(OH)2D3}$	Collagen coating with $1,25(OH)_2D_3$
$Scaff_{PBS}$	Scaffold encapsulating PBS (rhBMP-7 control)
$Scaff_{BMP\ 0.63}$	Scaffold encapsulating low rhBMP-7 dose (0.63 µg/ml)
$Scaff_{BMP\ 1.25}$	Scaffold encapsulating high rhBMP-7 dose (1.25 µg/ml)
$Scaff_{ethanol}$	Scaffolds encapsulating ethanol ($1,25(OH)_2D_3$ control)
$Scaff_{1,25(OH)2D3}$	Scaffolds encapsulating $1,25(OH)_2D_3$

5.2. Abstract

It is essential that all regenerative medical drug delivery devices have the ability to release active factors which are still bioactive. It is also important to identify the range of concentrations of the released bioactive factors which have the desired effect on the target cells.

The range of recombinant human bone morphogenetic protein-7 (rhBMP-7) concentrations capable of stimulating the osteogenic differentiation of human marrow stromal cells (hMSCs) was investigated. This was achieved by quantitatively assessing the area of alkaline phosphatase (ALP) staining, normalised against the cell count. Although the increase was relatively slight, normalised ALP expression was statistically significantly elevated for each of the test concentrations (5, 20, and 50 ng/ml), in hMSCs from at least three of the four test patients. No universal optimum concentration was found, and each test concentration appeared to have very similar osteoinductive potential.

As before, rhBMP-7 was used as a clinically relevant model drug to assess the feasibility of releasing water-soluble growth factors from the scaffolds. The bioactivity of the rhBMP-7 released from the test scaffolds was assessed by

quantifying the area of normalised ALP staining of hMSCs. It was found that the release of rhBMP-7 from the collagen coating of the poly(ε-caprolactone) (PCL) (M_n 42,500) scaffolds was capable of statistically significantly increasing hMSC normalised ALP expression, although the actual differences were often relatively small. Therefore, at least a proportion of the growth factor released is likely to have been bioactive. The release from scaffolds encapsulating rhBMP-7 did not have this effect on the hMSCs, indicating that either the concentration released was too low, or the growth factor released was no longer bioactive.

However, the cells were likely to experience a different environment and growth factor concentration when seeded directly onto the scaffolds. Therefore, this was assessed in the studies described in Chapter 6 and Chapter 7.

1,25-dihydroxyvitamin D_3 ($1,25(OH)_2D_3$) was used as a model drug to assess the feasibility of releasing lipid-soluble active factors from the scaffolds. Concentrations of 10 nM were found to significantly stimulate normalised ALP expression of hMSC compared to the base media. Similarly, the release of $1,25(OH)_2D_3$ from the loaded collagen scaffold coatings and the encapsulating scaffolds significantly increased ALP expression compared to the control scaffold groups (by 115±28% and 69±25% respectively). Furthermore, ALP expression was significantly increased when the two delivery systems were used together, when compared to either delivery system on its own.

These data suggest that the delivery of lipid-soluble active factors is feasible from collagen coated PCL scaffolds, and that the coating and encapsulating delivery systems are mutually compatible.

5.3. Introduction

In Chapter 4 it was found that PCL (M_n 42,500) scaffolds, and scaffold coatings of Type-I collagen, were capable of releasing immuno-reactive rhBMP-7. However, immuno-reactivity does not necessarily show that active factor released remained bioactive. Since the antibodies used in enzyme-linked immunosorbent assays (ELISAs) only bind to a small region of the complete protein structure, the proteins detected may only have been deactivated fragments of the original active factors (Bae *et al.*, 2006).

For all potential regenerative medical drug delivery devices, it is important to assess whether the active factors released are capable of affecting cells. Traditionally this has been achieved using an appropriate bioassay (DeFail *et al.*, 2006; Premaraj *et al.*, 2006; Partridge *et al.*, 2002). This is commonly achieved employing cell lines, using changes in such properties as cell proliferation or ALP expression as outcome measures (Meager, 1991; Garrigue-Antar *et al.*, 1995; Parker *et al.*, 2002). However, such assays, which often employ transformed non-human cells, yield little information on how primary human cells would behave or what dose of active factor is most appropriate.

Expression of ALP is not restricted to bone, as it is also found in both liver and kidney tissue (Tylzanowski *et al.*, 2001; Fernandez and Kidney, 2007; Martins *et al.*, 2001). However, it is commonly used in assays for osteogenesis (Hoemann *et al.*, 2008; Tsiridis *et al.*, 2006). This is because, in cells of the osteoblastic lineage, it is considered to be an early marker for osteogenic differentiation (Yoon *et al.*, 1987; Zaidi, 2007), see **Figure 1.3**.

Although there is debate in the literature about whether rhBMP-7 primarily causes chondrogenic or osteogenic differentiation of MSCs *in vitro*, there is broad agreement that ALP expression is increased (Knippenberg *et al.*, 2006; Edgar *et al.*, 2007; Tsiridis *et al.*, 2007). Similarly, as discussed in §1.2.4.2, $1,25(OH)_2D_3$ is known to induce osteogenic differentiation of MSCs cultured *in vitro*, in the presence

of growth media supplemented with ascorbic acid and β-glycerophosphate (Zhou *et al.*, 2006). This effect is further enhanced by the addition of TGF-β (Bosetti *et al.*, 2007; Liu *et al.*, 1999).

rhBMP-7 and 1,25$(OH)_2D_3$ were used as hydrophilic and hydrophobic model drugs (respectively) to investigate the feasibility of releasing water-soluble and lipid-soluble active factors from both loaded scaffolds and scaffold coatings. During the studies described in this chapter, the dose of rhBMP-7 necessary to induce osteogenic differentiation of hMSCs was investigated. The bioactivity of rhBMP-7 released from both rhBMP-7 encapsulating PCL (M_n 42,500) scaffolds and loaded Type-I collagen scaffold coatings, were evaluated. Similar studies were also conducted using 1,25$(OH)_2D_3$ containing scaffolds.

5.4. Materials and Methods

Unless otherwise stated, all reagents were purchased from Sigma, UK. All the techniques described below were conducted in a sterile environment, using sterilised equipment.

5.4.1. hMSC Isolation and Culture

After written consent from the patients and approval from the local ethical committee (Lothian local research ethics committee), human femoral head tissue was obtained from patients who had undergone elective arthroplasty. Tissue was collected from a total of seven patients (see **Table 5.1**). The tissue samples were allocated an anonymous number based on the chronological order of the sample collection. The hMSCs were isolated and cultured as described in §3.3.1.1. The hMSCs underwent routine characterisation as described in **Appendix G**.

Table 5.1: hMSC patient details.

In-House Patient Number	496	506	513	518	542	544	549
Patient Age	51	76	79	74	68	66	61
Patient Sex	Male	Male	Male	Male	Male	Male	Female

5.4.2. rhBMP-7 Release

5.4.2.1. Scaffold Manufacture

A stock solution of 1 mg/ml rhBMP-7 (Stryker, USA) was diluted with phosphate buffered saline (PBS) (Oxoid, UK) to concentrations of 25 µg/ml and 12.5 µg/ml. These solutions were added at 1 % (v/v) to 25% (w/v) solutions of PCL (M_n 42,500)/dichloromethane (DCM). This yielded final mass ratios of rhBMP-7 to PCL of 1.00 µg/g or 0.50 µg/g respectively.

Once added, emulsions were created by vigorous manual mixing, using sterile 3 ml transfer pipettes (Fisher, UK), for approximately 30 seconds. The resulting

emulsions were loaded into the syringe of the Bioplotter™. Scaffolds were then manufactured, with no plotting medium, using the optimised plotting parameters determined in §2.4.1.1.1, and then vacuum dried at 75 mbar (absolute pressure) for 60 min. Each scaffold was then cut by scalpel into four approximately equal parts. The scaffolds with an rhBMP-7 to PCL mass ratio of 1.00 µg/g or 0.50 µg/g were designated $Scaff_{BMP\ 1.25}$ and $Scaff_{BMP\ 0.63}$ respectively.

Control scaffolds were also manufactured in a similar fashion, replacing the rhBMP-7 solutions with PBS. These scaffolds were designated $Scaff_{PBS}$.

All the scaffolds were immersed in IMS for 10 min before being washed with distilled water (dH_2O) (5 min) and PBS (5 min). The stock solution of rhBMP-7 (1 mg/ml) was added to 1 mg/ml Type-I collagen in 0.1 M aqueous acetic acid, to yield final concentrations of 1.25 µg/ml and 0.63 µg/ml respectively. The equivalent volume of PBS was added to a similar solution of Type-I collagen.

The scaffolds were immersed in one of the collagen solutions either lacking rhBMP-7, or containing it at 1.25 µg/ml or 0.63 µg/ml. The scaffolds were designated with the prefixes $Coat_{PBS}$, $Coat_{BMP\ 1.25}$ or $Coat_{BMP\ 0.63}$ respectively. The resulting scaffold types were; $Coat_{PBS}Scaff_{PBS}$, $Coat_{BMP\ 0.63}Scaff_{PBS}$, $Coat_{BMP\ 1.25}Scaff_{PBS}$, $Coat_{PBS}Scaff_{BMP\ 0.63}$, and $Coat_{PBS}Scaff_{BMP\ 1.25}$. Afterwards, the scaffolds were removed, and allowed to air dry for 4 hr at room temperature. Once dry, the scaffolds were stored at -80°C.

The above protocol was conducted twice to produce two separate scaffold batches. Batch 1 was used for the experiments involving hMSC patients 496 and 506. Batch 2 was used with hMSC patients 513 and 518.

5.4.2.2. hMSC Reaction to rhBMP-7

Tissue culture flasks (75 cm^2) containing confluent hMSCs (passage 2) from patients 496, 506, 513, and 518 (in separate flasks), were washed three times in PBS, and the cells were detached from the flasks using trypsin solution (2.5 mg/ml) in PBS (Invitrogen, UK) and growth media, as described in §3.3.1. The cell density of the

suspensions was measured using a haemocytometer. After appropriate dilution with growth media, the cells were added to wells of 48-well treated tissue culture (TC) plastic plates (Corning, USA) at a density of 8,000 cells/well (in 400 µl of media). For each patient's tissue used, 60 wells were seeded. The plates were then maintained in a humidified air incubator at 37°C with 5% (v/v) CO_2, for 3 days, to become confluent.

Once the cells had become confluent, fresh cell media was prepared. Growth media (see §3.3.1) was supplemented with β-glycerophosphate disodium hydrate (10 mM), L-ascorbic acid-2-phosphate (50 µM, from a 10 mM stock solution in PBS). This media was designated OS-D media. A portion of OS-D media was supplemented with dexamethasone (100 nM, from a 1 mM stock solution in ethanol). This media was designated OS media. rhBMP-7 was also added to OS-D media at three concentrations (5, 20 and 50 ng/ml).

All the old media was aspirated from the cells. The wells were divided into groups of six. Growth media, OS media, and rhBMP-7 at each concentration in OS-D media, were added to one group of wells for each patient (400 µl/well). OS-D media was added to six groups (of six wells) for each patient (400 µl/well) (see **Figure 5.1**).

The scaffolds were thawed by incubation at room temperature for 30 min. The quarter scaffolds were then added directly to wells containing hMSCs in OS-D media. Each scaffold type was added to one group of wells per patient. One scaffold was added per well, and care was taken such that the scaffolds were fully immersed in the media, without being in direct contact with the cells at the bottom of the wells (see **Figure 5.1**). The empty wells were then filled with growth media (see **Figure 5.1**).

The plates were then maintained in a humidified air incubator at 37°C with 5% (v/v) carbon dioxide (CO_2). The media was replaced with fresh media, of the same composition as the original experimental media, at regular intervals three times every 7 days. After 14 days, the scaffolds and media were removed from the wells before

the cells were fixed in 4% (w/v) paraformaldehyde in PBS for 10 min. The wells were washed with PBS (twice) and dH_2O (once): 2 min per wash. The wells were left to dry for 4 hr before being stored at 4°C. The plates were then stained for ALP as described in §5.4.4.

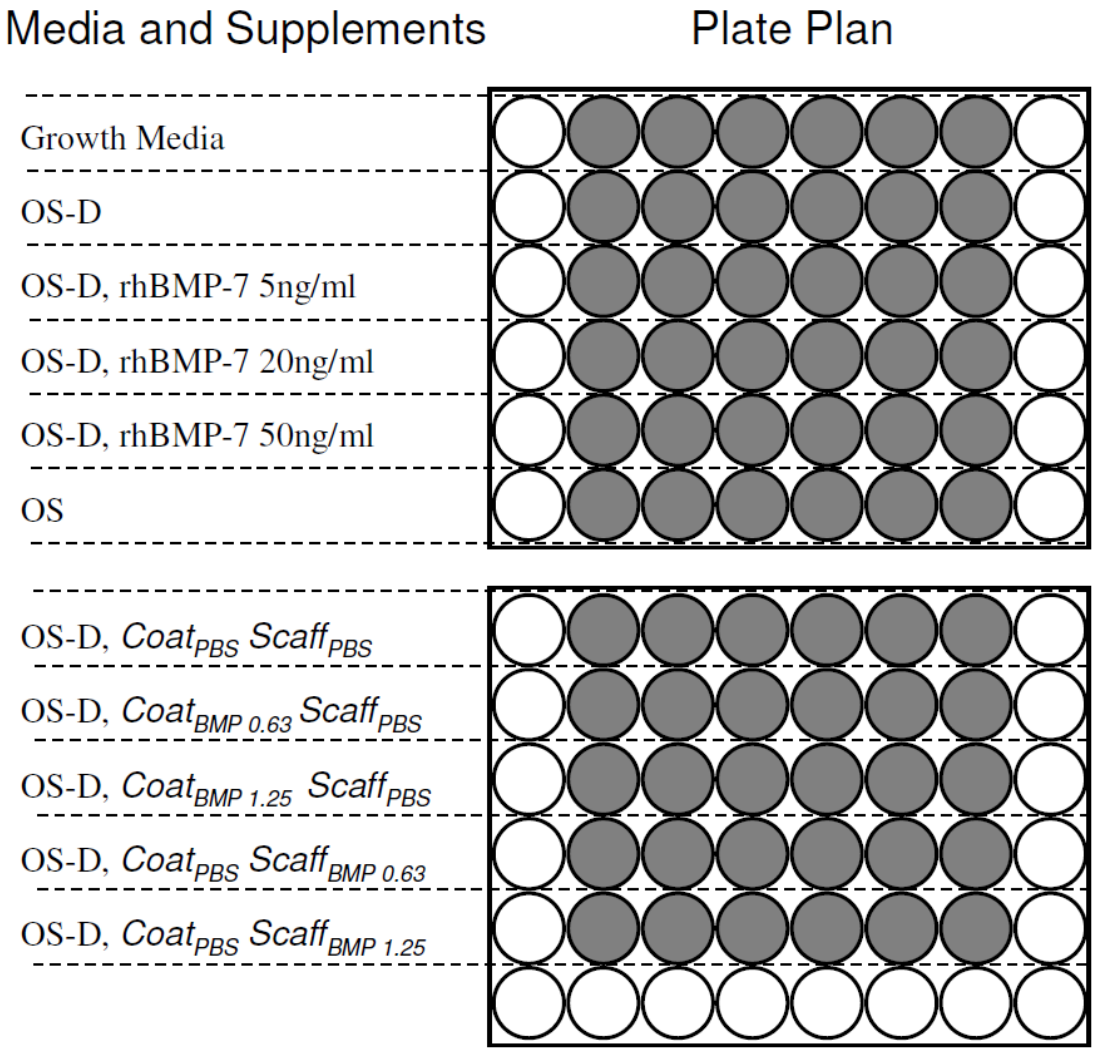

Figure 5.1: Plate plan for experiments involving rhBMP-7.

A cartoon showing the plate plan of the 48-well plates used for the experiments involving rhBMP-7. The media composition, and either scaffold or media supplements are indicated. The shaded wells indicate the test well, containing hMSCs used during the experiments. The white wells indicate wells containing growth media only. This plate plan was used for each of the four hMSC test patients.

5.4.3. $1,25(OH)_2D_3$ Release

5.4.3.1. Scaffold Manufacture

A stock solution of 24 μM (10 mg/ml) 1,25-dihydroxyvitamin D_3 ($1,25(OH)_2D_3$) was made up in ethanol. This solution was added at 5% (v/v) to 25% (w/v) solutions of PCL (M_n 42,500)/DCM. This yielded a final moles/mass ratio of $1,25(OH)_2D_3$ to PCL of 4.8 nmoles/g.

Once added, the two miscible solutions were mixed together, using sterile 3 ml transfer pipettes, for approximately 30 seconds. The resulting emulsions were loaded into the syringe of the Bioplotter™. Scaffolds were then manufactured, with no plotting medium, using the optimised plotting parameters determined in §2.4.1.1.1, and then vacuum dried at 75 mbar (absolute pressure) for 60 min. Each scaffold was then cut into four approximately equal parts, using a scalpel. These scaffolds were designated $Scaff_{1,25(OH)2D3}$.

Control scaffolds were also manufactured in a similar fashion, replacing the $1,25(OH)_2D_3$ solution with ethanol. The ethanol was added at 5% (v/v) to the plotting solution of 25% (w/v) PCL (M_n 42,500)/DCM. The resulting scaffolds were designated $Scaff_{ethanol}$.

All the scaffolds were immersed in IMS for 10 min before being washed with dH_2O (5 min) and PBS (5 min). The stock solution of $1,25(OH)_2D_3$ (24 μM) was added to 1 mg/ml Type-I collagen in 0.1 M aqueous acetic acid, to yield a final concentration of 3.6 μM. The equivalent volume of ethanol was added to a similar solution of Type-I collagen.

The scaffolds were immersed in one of the collagen solutions either containing or lacking $1,25(OH)_2D_3$. The scaffolds were designated with the prefixes $Coat_{1,25(OH)2D3}$ and $Coat_{ethanol}$ respectively. Afterwards, the scaffolds were removed, and allowed to air dry for 4 hr at room temperature. Once dry, the scaffolds were stored at -80°C.

5.4.3.2. hMSC Reaction to $1,25(OH)_2D_3$

Tissue culture flasks (75 cm^2) containing confluent hMSCs (passage 2) from patients 542, 544 and 549, were washed three times in PBS, and the cells were detached from the flask using trypsin and growth media, as described in §3.3.1. The cell density of the suspensions was measured using a haemocytometer. After appropriate dilution with growth media, the cells were added to wells of 48-well TC plastic plates (Corning, USA) at a density of 8,000 cells/well (in 400 µl of media). For each patient's tissue used, 48 wells were seeded. The plates were then maintained in a humidified air incubator at 37°C with 5% (v/v) CO_2, for 3 days, to become confluent.

Once the cells had become confluent, new cell media was prepared. OS media was supplemented with recombinant human transforming growth factor-β3 (rhTGF-β3) (R&D Systems, USA) at 10 ng/ml. This media was designated OST media. $1,25(OH)_2D_3$ was also added to OST media at three concentrations (0.1, 1 and 10 nM).

All the media was aspirated from the cells and discarded. The wells were divided into groups of six. Growth media and $1,25(OH)_2D_3$, at each concentration in OST media, were added to one group of wells for each patient (400 µl/well). OST media was added to four groups for each patient (400 µl/well) (see **Figure 5.2**).

The scaffolds were thawed by incubation at room temperature for 30 min. The quarter scaffolds were then added directly to wells containing hMSCs in OST media. Each scaffold type was added to one group of wells per patient. One scaffold was added per well, and care was taken such that the scaffolds were fully immersed in the media, without being in direct contact with the cells at the bottom of the wells (see **Figure 5.2**). The empty wells were then filled with growth media (see **Figure 5.2**).

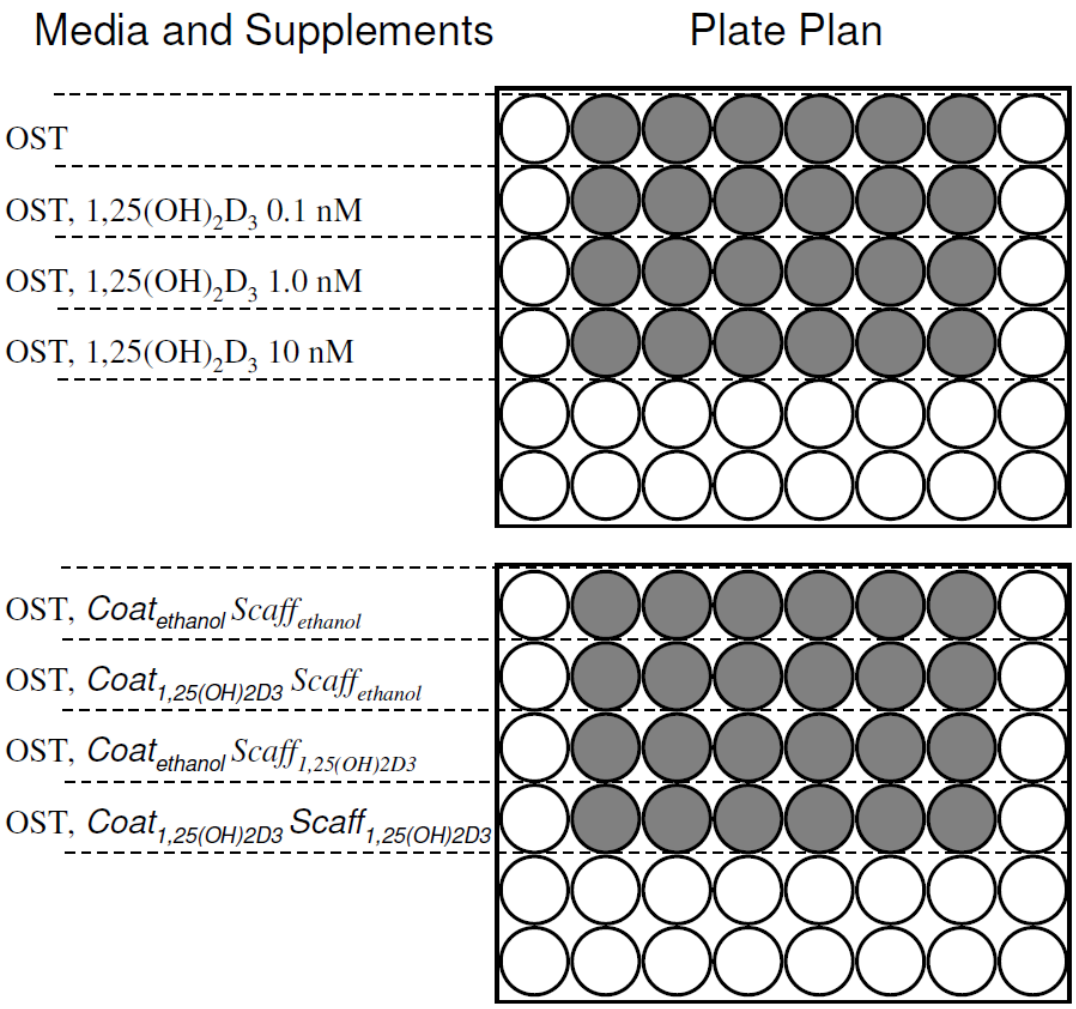

Figure 5.2: Plate plan for experiments involving $1,25(OH)_2D_3$.

A cartoon showing the plate plan of the 48-well plates used for the experiments involving $1,25(OH)_2D_3$. The media composition, and either scaffold or media supplements are indicated. The shaded wells indicate the test well, containing hMSCs used during the experiments. The white wells indicate wells containing growth media only. This plate plan was used for each of the three hMSC test patients.

The plates were then maintained in a humidified air incubator at 37°C with 5% (v/v) CO_2. The media was replaced with fresh media, of the same composition as the original experimental media, at regular intervals three times every 7 days. After 14 days, the scaffolds and media were removed from the wells before the cells were fixed in 4% (w/v) paraformaldehyde in PBS for 10 min. The wells were washed with PBS (twice) and dH_2O (once): 2 min per wash. The wells were left to air dry for 4 hr before being stored at 4°C. The plates were then stained for ALP as described in §5.4.4.

5.4.4. Cell Staining

The cells, prepared as described in §5.4.2.2 and §5.4.3.2, were stained for ALP using an Alkaline Phosphatase kit. The protocol was followed according to the manufacturer's instructions. Briefly, 250 µl of sodium nitrate solution (0.1 M) were added to 250 µl of Fast Blue Base-Alkaline Solution (5 mg/ml). The mixture was inverted and allowed to stand at room temperature. After 2 min, 11.25 ml of dH_2O and 250 µl of Naphthol AS-BI Alkaline Solution (4mg/ml) were added. After mixing, 180 µl of this solution were added to each of the wells in the 48-well plates.

The plates were then incubated in the dark at room temperature for 15 min, before each well was washed with PBS. The cells prepared in §5.4.2.2 were then stained with 2 µg/ml propidium iodide (PI) (180 µl/well). Similarly, the cells prepared in §5.4.3.2 were stained with 2 µg/ml 4',6-diamino-2-phenylindole (DAPI) (180 µl/well). The cells were incubated in the staining solutions in the dark for 15 min, before being washed twice with PBS. After the washes were discarded, 200 µl of dH_2O were added to each well. The plates were then photographed using a mounted camera (Nikon, DXM1200) on an inverted microscope (Nikon, Eclipse TS 100) set for both bright-field and fluorescence, at × 10 magnification. Three randomly selected fields were photographed per well, with both bright-field and fluorescence.

The area of +ve ALP staining was quantified with the aid of ImageJ (National Institute of Health, USA) using a batch image processing macro (see **Appendix F**). A similar method was used by Zhu *et al*. (2006). The number of either PI or DAPI

+ve cells was also counted using a batch image processing macro (see **Appendix E**) for ImageJ. A manual count of randomly selected images was used to confirm the accuracy of the ImageJ counts.

For each well, the mean area of ALP staining per cell was calculated from the areas of +ve ALP staining (A_i), and the cell count (N_i), in field i (see **Equation 5.1**). The normalised area of staining was then found for each group by dividing the mean areas of staining per cell, with that found for the appropriate base media, for the same patient (see **Equation 5.2**).

Equation 5.1

Area of ALP staining per cell in well j in group x ($\alpha_{j,x}$) $\equiv \frac{1}{3}\sum_{i=1}^{3}\frac{A_i}{N_i}$

Equation 5.2

Normalised area of ALP staining in well j in group $x \equiv \frac{\alpha_{j,x}}{\frac{1}{6}\sum_{j=1}^{6}\alpha_{j,\text{base media}}}$

5.4.5. Statistical Analysis

All data were analysed using the statistical software package SPSS 14.0 for Windows.

The data collected for the rhBMP-7 release experiments were found not to satisfy Levene's test, even after mathematical transformations. Parametric tests, such as one-way analysis of variance (ANOVA), were therefore unsuitable. Hence, the non-parametric Kruskal-Wallis test was used to test for statistical significance for each data set. The statistical significance between the groups was found using the Mann-Whitney U test (Zar, 1984; Petrie and Sabin, 2005). $p < 0.05$ was considered to be statistically significant.

All the data collected for the $1,25(OH)_2D_3$ studies required the transformation of $\log_{10}$ to satisfy Levene's test and that of Kolmogorov-Smirnov. ANOVA was then applied, followed by the Tukey-Kramer *post hoc* test to determine the statistical differences between the groups.

The mean was used throughout, and all results were expressed as the sample means ± standard error of the mean (SEM).

5.5. Results

5.5.1. rhBMP-7 Release

Positive ALP staining of the hMSCs, prepared as described in §5.4.2.2 and §5.4.4, was observed in all the groups tested. Although differences in the staining were observed visually (see **Figure 5.3**), it was necessary to quantify the staining through image analysis using ImageJ.

This was achieved by "thresholding" the images to discard areas of staining below a certain intensity (see **Figure 5.4**). For each patient, a range of images from the growth media (–ve ALP control) and the OS media (+ve ALP control). The threshold was selected such that areas judged to be ALP +ve were included, whereas areas of ALP –ve shadow were excluded.

Similarly, a range of PI images were examined for each patient. Both the threshold and the size range were adjusted such that all visually identified cells were counted, and all objects identified as artefacts were excluded. The numbers of cells per field were then counted using the images of PI stained cells (see **Figure 5.5**). Randomly chosen manual cell counts, from the PI stained images, showed a mean deviation from the automated ImageJ counts of 0.98±0.24%. It should be noted that, due to a fungal contamination, some of the groups of rhBMP-7 coated and encapsulating scaffolds were lost. These groups were; $Coat_{PBS}Scaff_{BMP\ 0.63}$ and $Coat_{PBS}Scaff_{BMP\ 1.25}$ from patient 496, and $Coat_{BMP\ 0.63}Scaff_{PBS}$ and $Coat_{BMP\ 1.25}Scaff_{PBS}$ from patient 513.

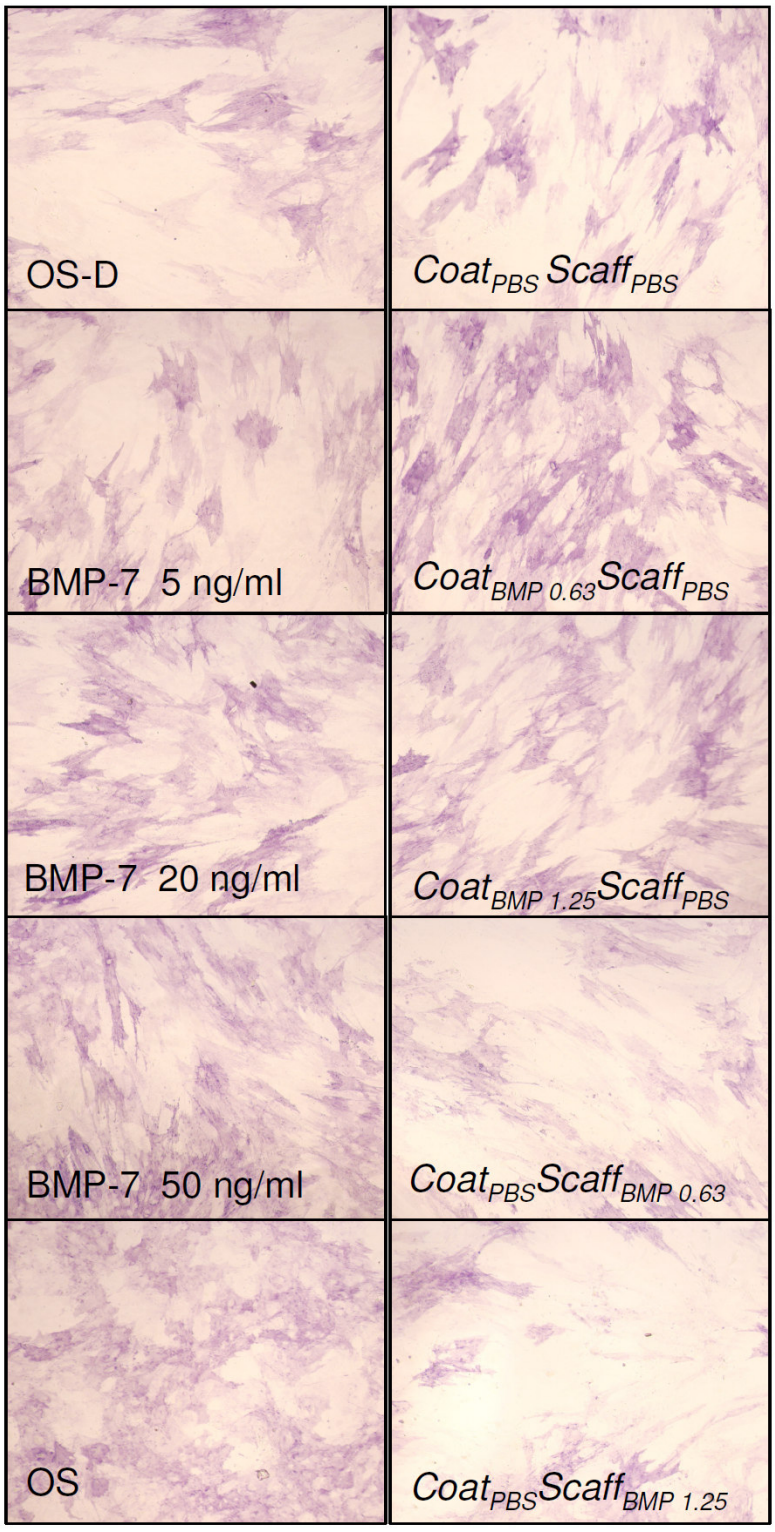

Figure 5.3: ALP staining for the rhBMP-7 release experiments.

Bright-field images of hMSCs stained for ALP in response to various test media and scaffolds. These representative images were taken at × 10 magnification, of tissue from patient 518. The bar represents 100 µm.

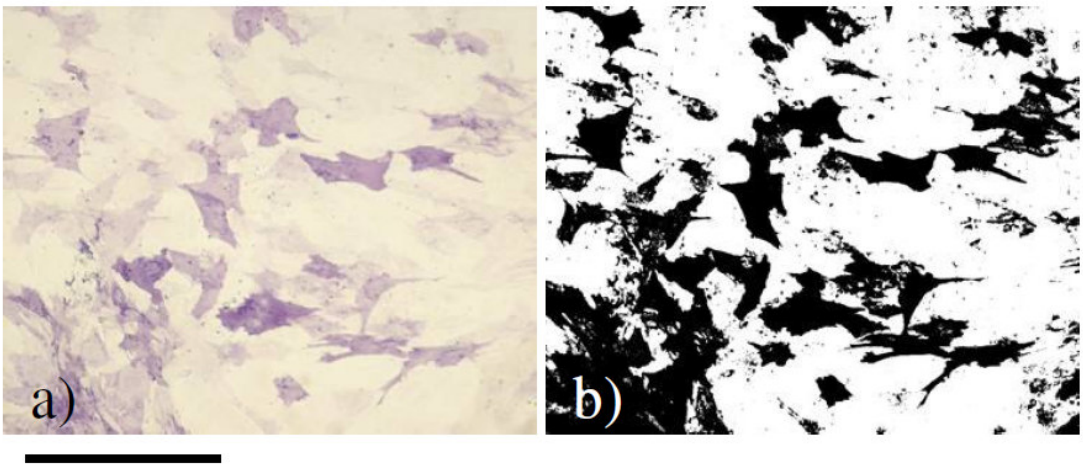

Figure 5.4: Area of ALP staining quantification.

Figure a) shows a representative bright-field image of the ALP stained hMSCs, at × 10 magnification. The threshold of these images was taken, to produce images such as that shown in figure b). The areas of shading were then quantified using ImageJ. In the case of figure b), the shaded area was found to be 27.4%. The bar represents 100 µm.

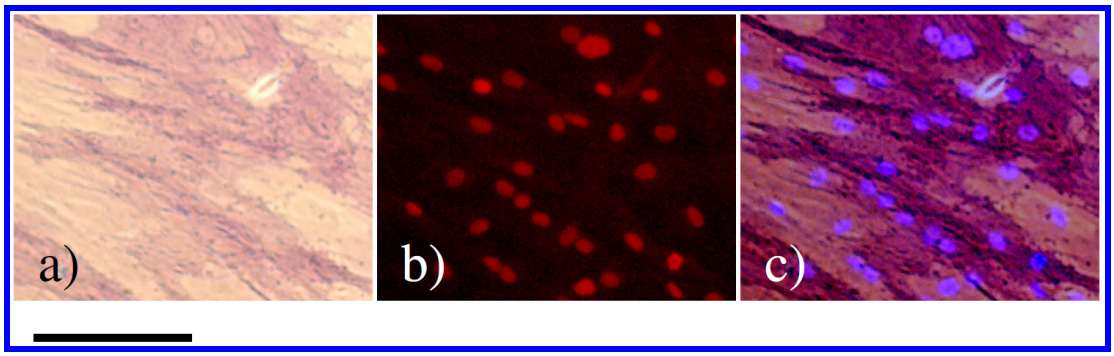

Figure 5.5: hMSC cells stained for ALP and PI.

A representative field of hMSCs treated with OS-D media, photographed at × 10 magnification. In this case, the cells were exposed to a $Coat_{BMP\ 1.25}Scaff_{PBS}$ scaffold. The hMSC patient was 496. Figure a) shows a bright-field view of ALP staining. Figure b) shows the PI image of the same field. Figure c) shows a combined image of the two fields. The bar represents 50 µm.

It was found that there was considerable patient variability in both the area of ALP staining, and the cell counts (see **Figure 5.6** and **Figure 5.7**). However, more consistent results were observed between patients when the ALP staining was normalised against both the cell count and the results for the base media (see **Figure 5.8**).

For cells maintained in OS media, both ALP and normalised ALP staining were significantly higher than the base media for all patients tested. OS media was also associated with a significant decrease in the observed cell density in two of the four patients (decreases of 32±3%, $p < 0.01$, and 18±1%, $p < 0.01$).

Normalised ALP staining was statistically significantly increased, from the base media, for at least one concentration of rhBMP-7 for each patient (see **Figure 5.6** and **Figure 5.8**). However, the rhBMP-7 concentration associated with the highest normalised ALP staining varied from patient to patient. In addition, no threshold rhBMP-7 concentration was observed above which ALP staining was consistently enhanced. No consistent difference in the cell density was measured for any concentration of rhBMP-7 compared to the base media.

For the scaffolds containing rhBMP-7 in the collagen coating, normalised ALP staining was significantly increased, compared to the control scaffolds, for two out of three of the patients tested ($p < 0.01$). The average increases in normalised ALP staining compared to the control scaffolds were 290±250% for the low rhBMP-7 dose, and 210±170% for the high dose. However this trend was not observed for the rhBMP-7 encapsulating scaffolds (see **Figure 5.8**).

For the test scaffolds groups, no obvious trend in the cell densities was observed, except for the $Coat_{PBS}Scaff_{BMP\ 1.25}$ group. For these scaffolds, the mean cell densities were significantly reduced, compared to the control scaffold group, for two of the three patients tested (see **Figure 5.7b**).

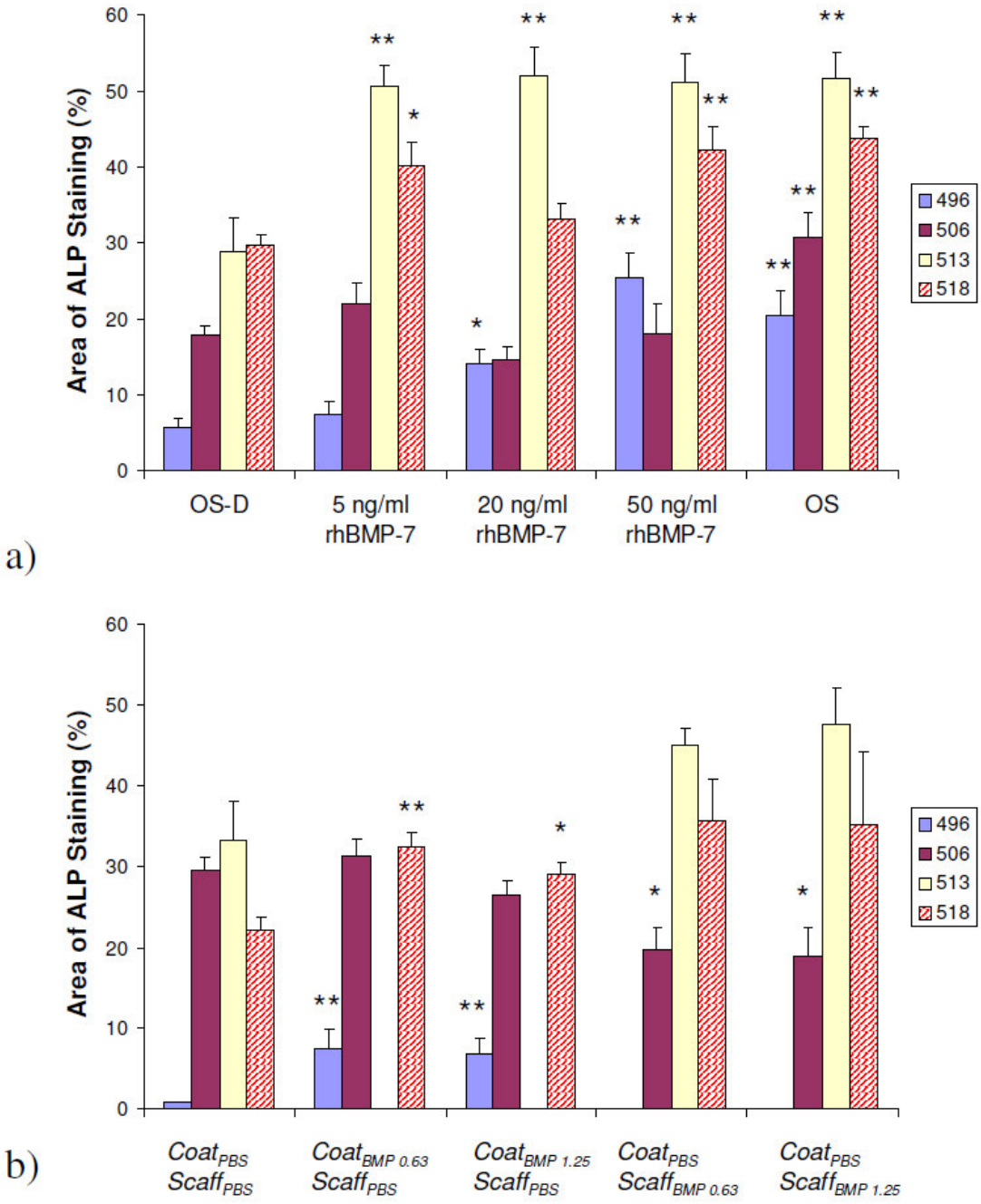

Figure 5.6: Areas of ALP staining of hMSCs.

The mean areas of +ve ALP staining of hMSCs. Figure a) shows the data for the cells exposed to rhBMP-7 and other test media, with no scaffold present. * and ** denote $p < 0.05$ and 0.01 respectively, compared to the base OS-D media. Figure b) shows the data for the cells exposed to the test scaffolds in OS-D media. * and ** denote $p < 0.05$ and 0.01 respectively, compared to the control $Coat_{PBS}Scaff_{PBS}$ group. The error bars represent the SEM, n = 6 in each case.

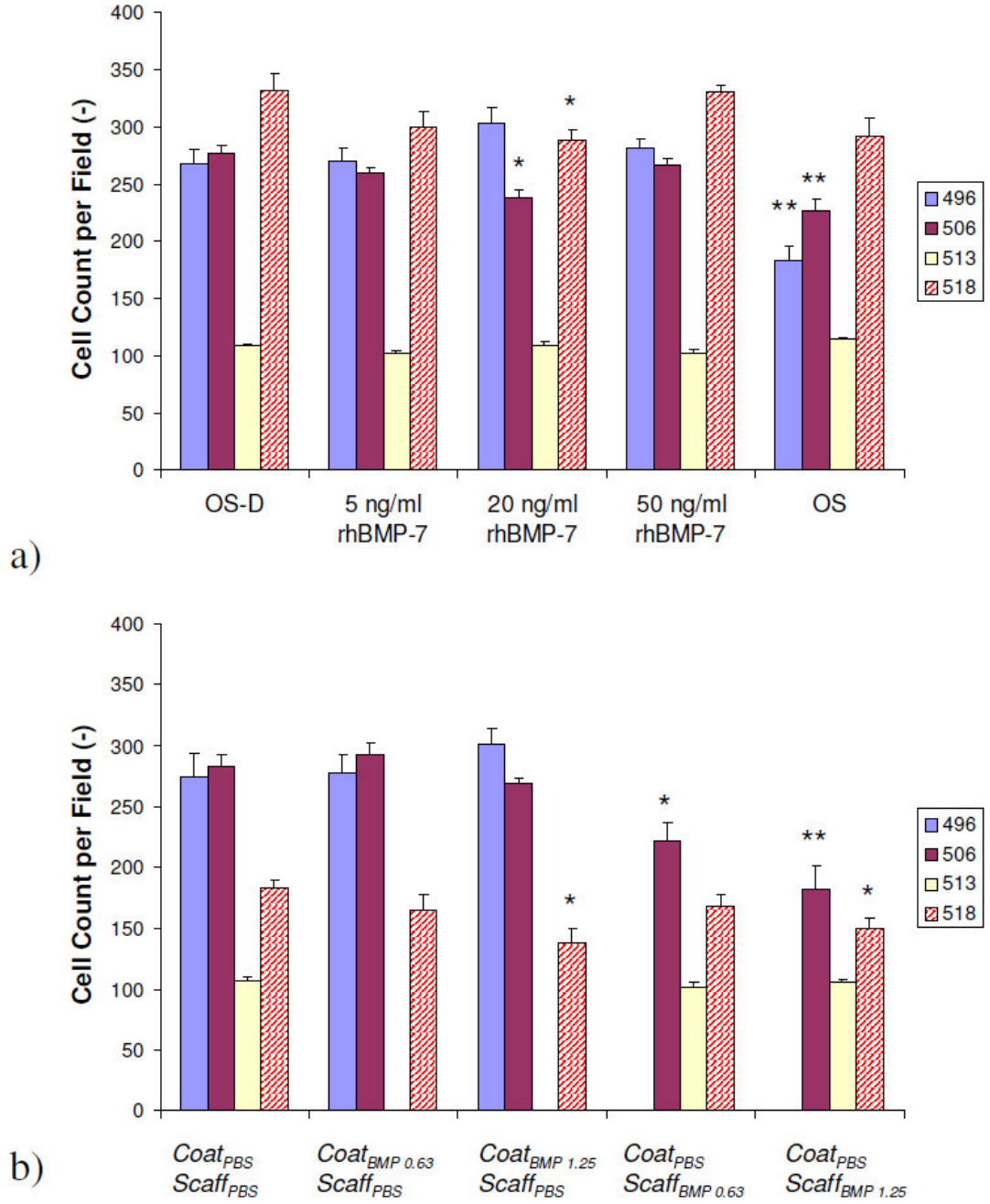

Figure 5.7: Cell counts of hMSCs.

The mean cell densities of hMSCs. Figure a) shows the data for the cells exposed to rhBMP-7 and other test media, with no scaffold present. * and ** denote $p < 0.05$ and 0.01 respectively, compared to the base OS-D media. Figure b) shows the data for the cells exposed to the test scaffolds in OS-D media. * and ** denote $p < 0.05$ and 0.01 respectively, compared to the control $Coat_{PBS}Scaff_{PBS}$ group. The error bars represent the SEM, n = 6 in each case.

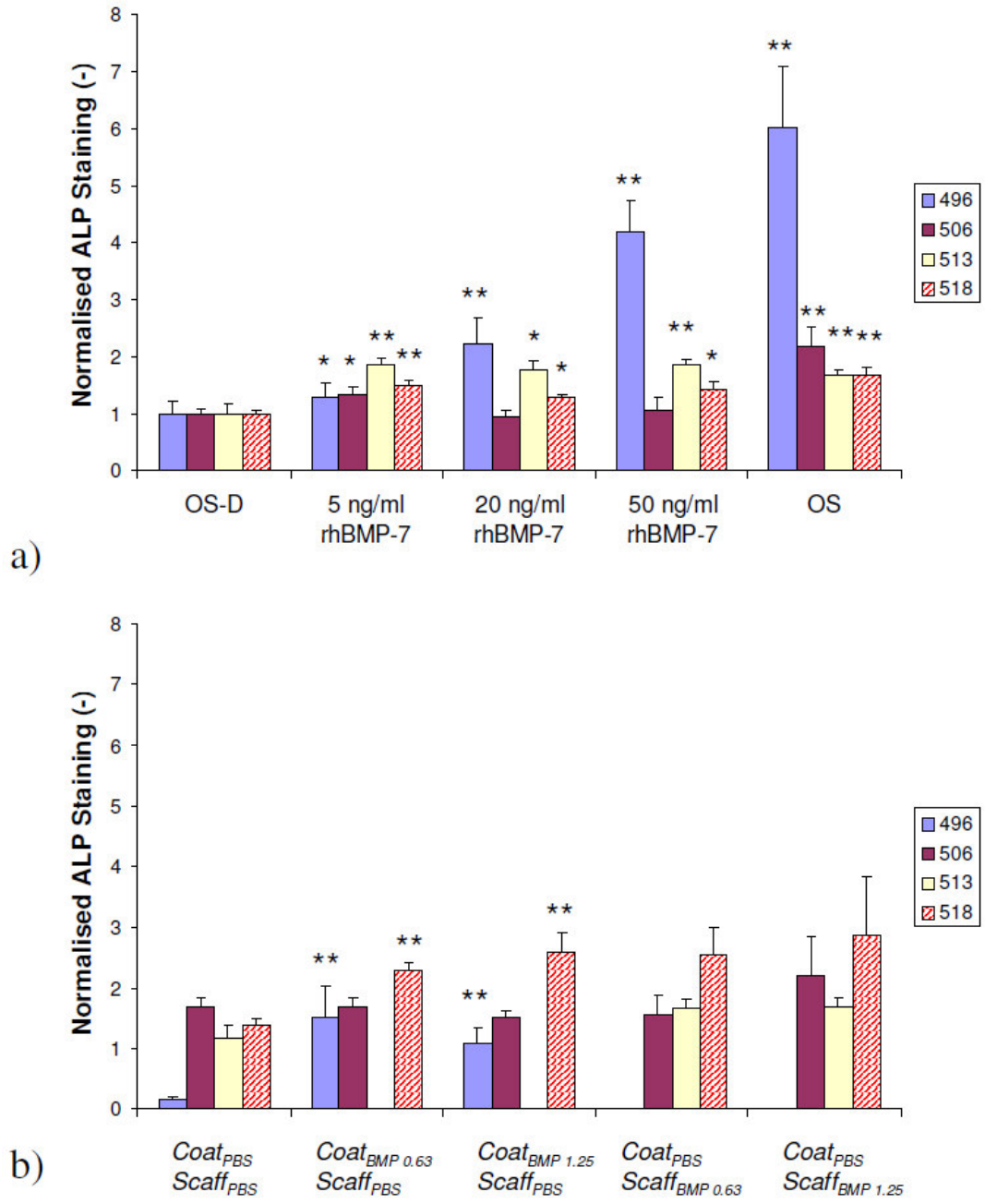

Figure 5.8: Normalised areas of ALP staining of hMSCs.

The average areas of +ve ALP staining of hMSCs per cell, normalised against the OS-D group. Figure a) shows the data for the cells exposed to rhBMP-7 and other test media, with no scaffold present. * and ** denote $p < 0.05$ and 0.01 respectively, compared to the base OS-D media. Figure b) shows the data for the cells exposed to the test scaffolds in OS-D media. * and ** denote $p < 0.05$ and 0.01 respectively, compared to the control $Coat_{PBS}Scaff_{PBS}$ group. The error bars represent the SEM, n = 6 in each case.

5.5.2. $1,25(OH)_2D_3$ Release

5.5.2.1. Scaffold Manufacture

It was noted that the addition of the ethanol solutions to the plotting solution had no effect on the optimum plotting parameters found in §2.4.1.1.1. The resulting scaffold geometry appeared to be very similar to that of the optimised PCL scaffold, as described in §2.4.1.1.1 (see **Figure 2.2e**).

5.5.2.2. hMSC Reaction to $1,25(OH)_2D_3$

During preliminary experiments, it was determined that PI was not a suitable stain for accurate cell counts for the experiments described in §5.4.3. This was because the nuclei were not distinctively stained. In contrast, DAPI was thought to be sufficient for accurate cell counts to be performed (see **Figure 5.9**).

Positive ALP staining of the hMSCs, prepared as described in §5.4.3.2 and §5.4.4, was observed in each group tested. Differences in staining between the groups were observed (see **Figure 5.10**). However, it was again necessary to quantify the area of staining through image analysis using ImageJ. For each patient, a range of images from the OST media (–ve ALP control) and the 10 nM $1,25(OH)_2D_3$ group (+ve ALP control). The threshold was selected such that areas judged to be ALP +ve were included, whereas areas of ALP –ve shadow were excluded.

Similarly, a range of DAPI images were examined for each patient. Both the threshold and the size range were adjusted such that all visually identified cells were counted, and all objects identified as artefacts were excluded. Randomly chosen manual cell counts, from the DAPI stained images, showed a mean deviation from the automated ImageJ counts of 0.70±0.13%.

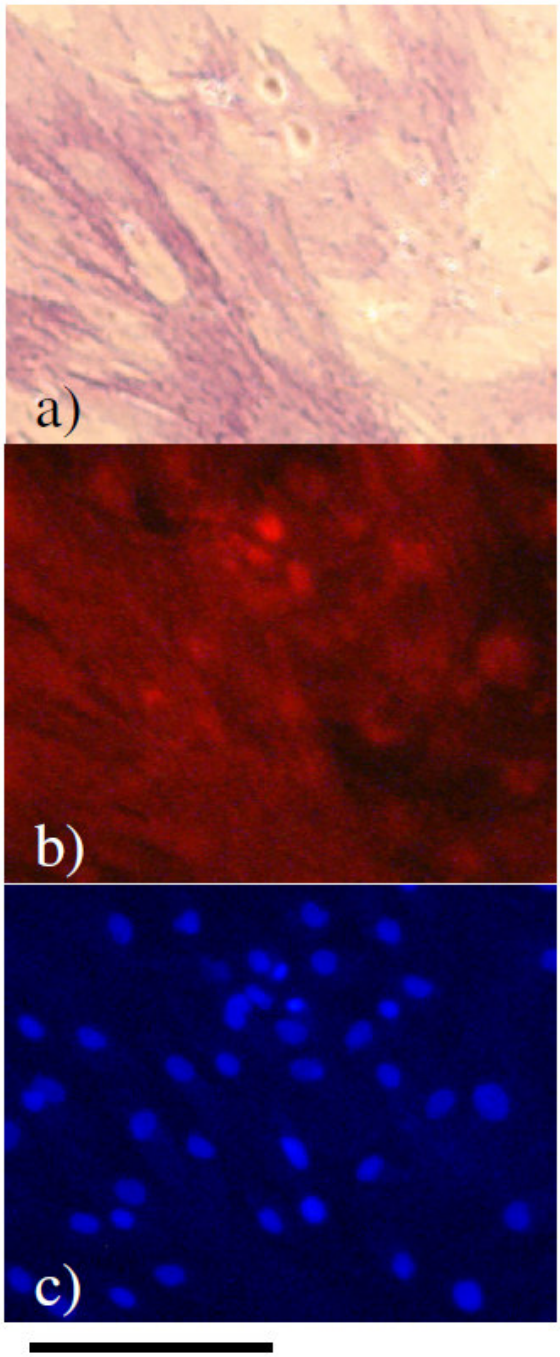

Figure 5.9: hMSC cells stained for ALP and with PI and DAPI.

A representative field of view of hMSCs treated with OST media, photographed at × 10 magnification. In this case the media was supplemented with $1,25(OH)_2D_3$ at 10 nM. The hMSC patient number was 544. Figure a) shows a bright-field view of the ALP staining. Figures b) and c) show PI and DAPI staining respectively. The bar represents 50 µm.

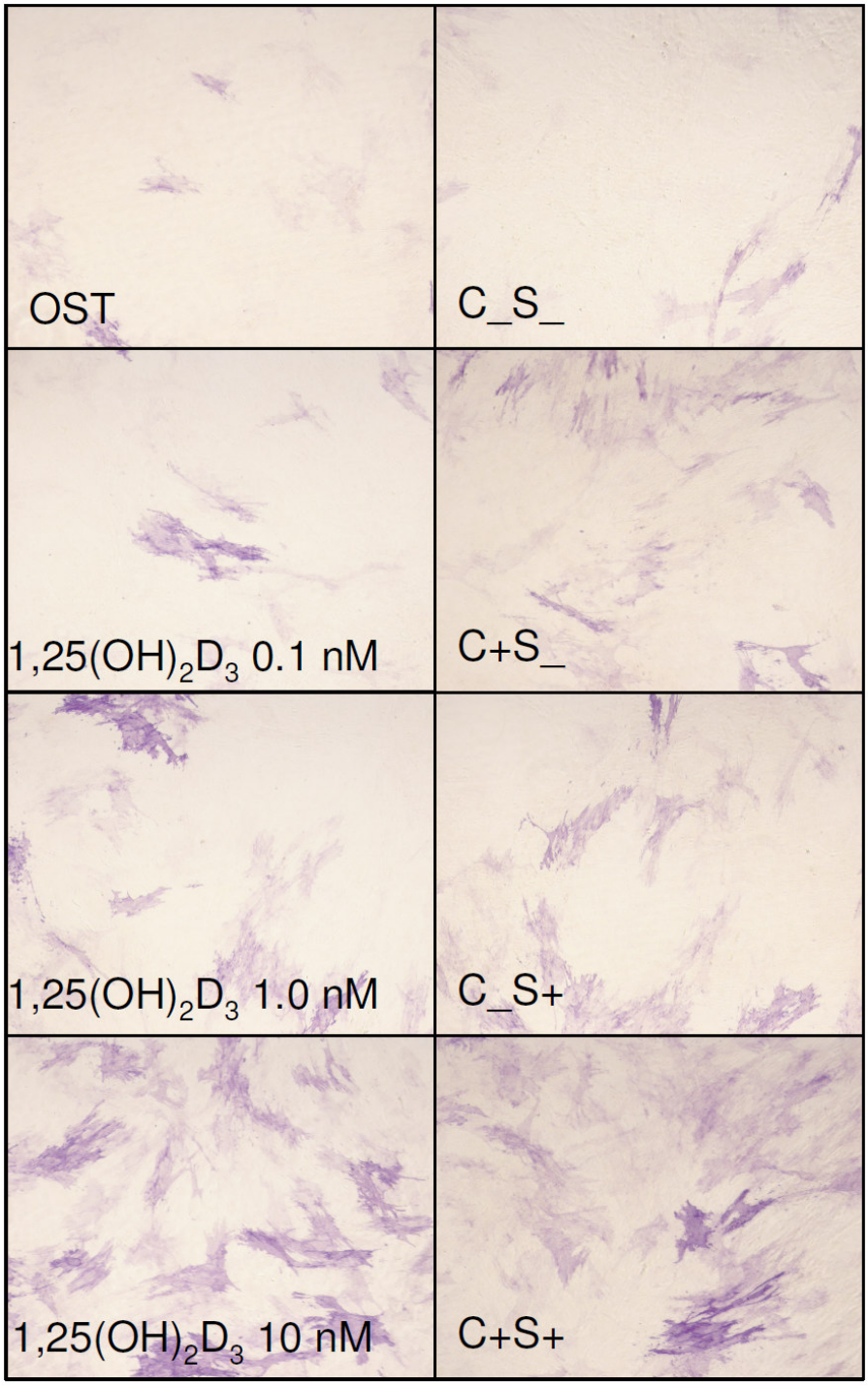

Figure 5.10: ALP staining for the $1,25(OH)_2D_3$ release experiments.

Bright-field images of hMSCs stained for ALP in response to various test media and scaffolds. These representative images were taken at × 10 magnification, of patient 544. The bar represents 100 µm.

It was observed that ALP staining, whether normalised or not, was significantly increased for the 10 nM $1,25(OH)_2D_3$ group compared to the OST media control, for all the hMSC patients tested (see **Figure 5.11a** and **Figure 5.13a**). Although there was little obvious pattern to the data on the cell densities, the highest $1,25(OH)_2D_3$ concentration was associated with a significant increase in the cell counts compared to the OST media control for two of the three patients (see **Figure 5.12a**).

For the $Coat_{1,25(OH)2D3}Scaff_{ethanol}$ and $Coat_{1,25(OH)2D3}Scaff_{1,25(OH)2D3}$ groups, significant increases in both the area of ALP staining (133±20% and 361±43% average increases respectively) and normalised ALP expression (115±28% and 303±76% average increases respectively) were calculated for all hMSC patients compared to the $Coat_{ethanol}Scaff_{ethanol}$ control ($p < 0.01$) (see **Figure 5.11b** and **Figure 5.13b**). Similarly the $Coat_{ethanol}Scaff_{1,25(OH)2D3}$ scaffolds were associated with elevated ALP staining and normalised ALP staining (96±37% and 69±25% average increases respectively)) for two of the three patients ($p < 0.01$). It was also observed that normalised ALP expression was significantly increased for the $Coat_{1,25(OH)2D3}Scaff_{1,25(OH)2D3}$ scaffolds compared to either delivery system alone, for two of the three patients ($p < 0.01$) (see **Figure 5.13b**).

The $Coat_{1,25(OH)2D3}Scaff_{1,25(OH)2D3}$ scaffolds were also associated with a statistically significant increase in the cell density, compared to the $Coat_{ethanol}Scaff_{ethanol}$ control, for two hMSC patients ($p < 0.01$) (see **Figure 5.12b**). The average increase was 23±11%. No other obvious trend in the cell density data was observed.

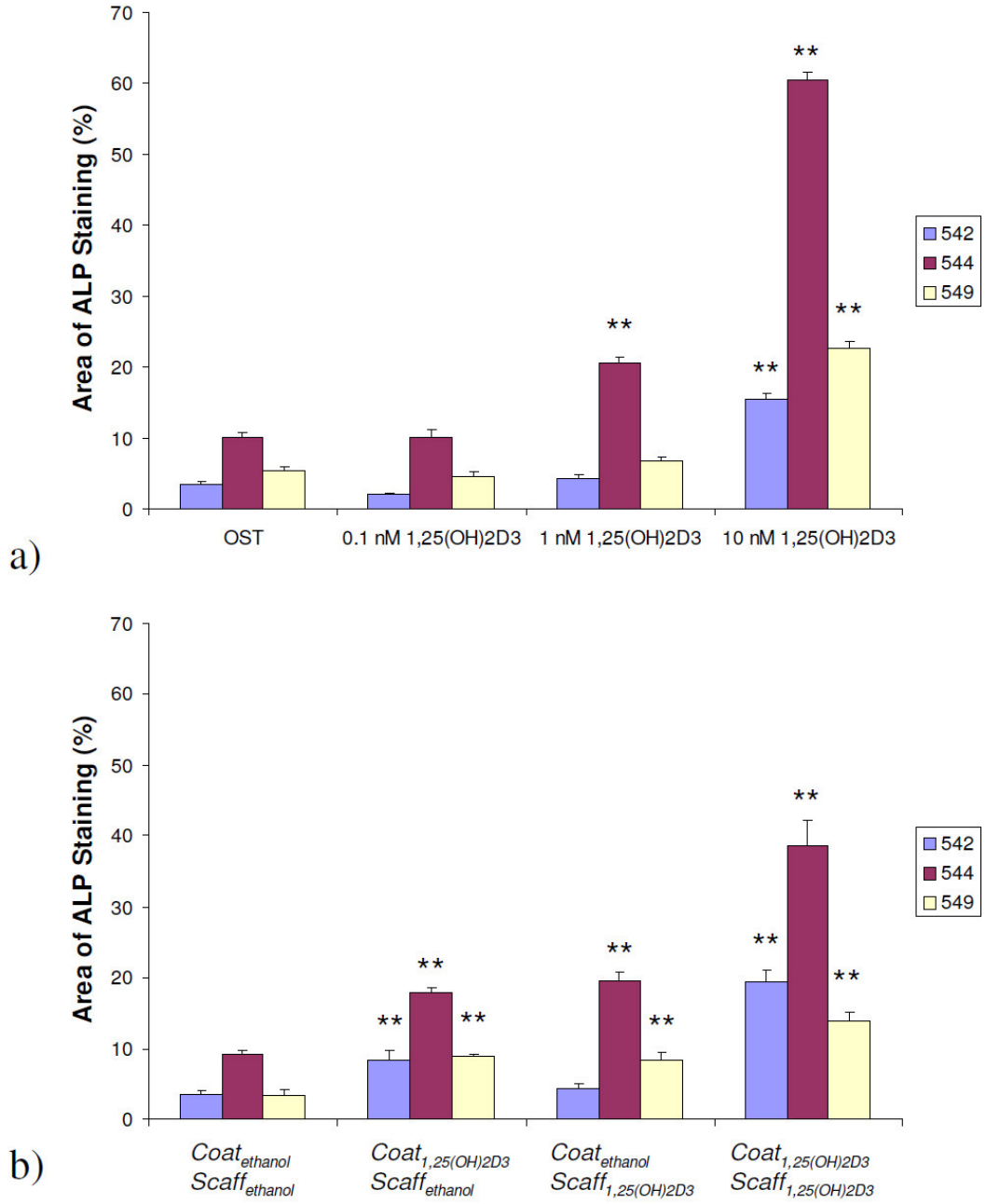

Figure 5.11: Areas of ALP staining of hMSCs.

The mean areas of +ve ALP staining of hMSCs. Figure a) shows the data for the cells exposed to $1,25(OH)_2D_3$ and other test media, with no scaffold present. * and ** denote $p < 0.05$ and 0.01 respectively, compared to the base OST media. Figure b) shows the data for the cells exposed to the test scaffolds in OST media. * and ** denote $p < 0.05$ and 0.01 respectively, compared to the control $Coat_{ethanol}Scaff_{ethanol}$ group. The error bars represent the SEM, n = 6 in each case.

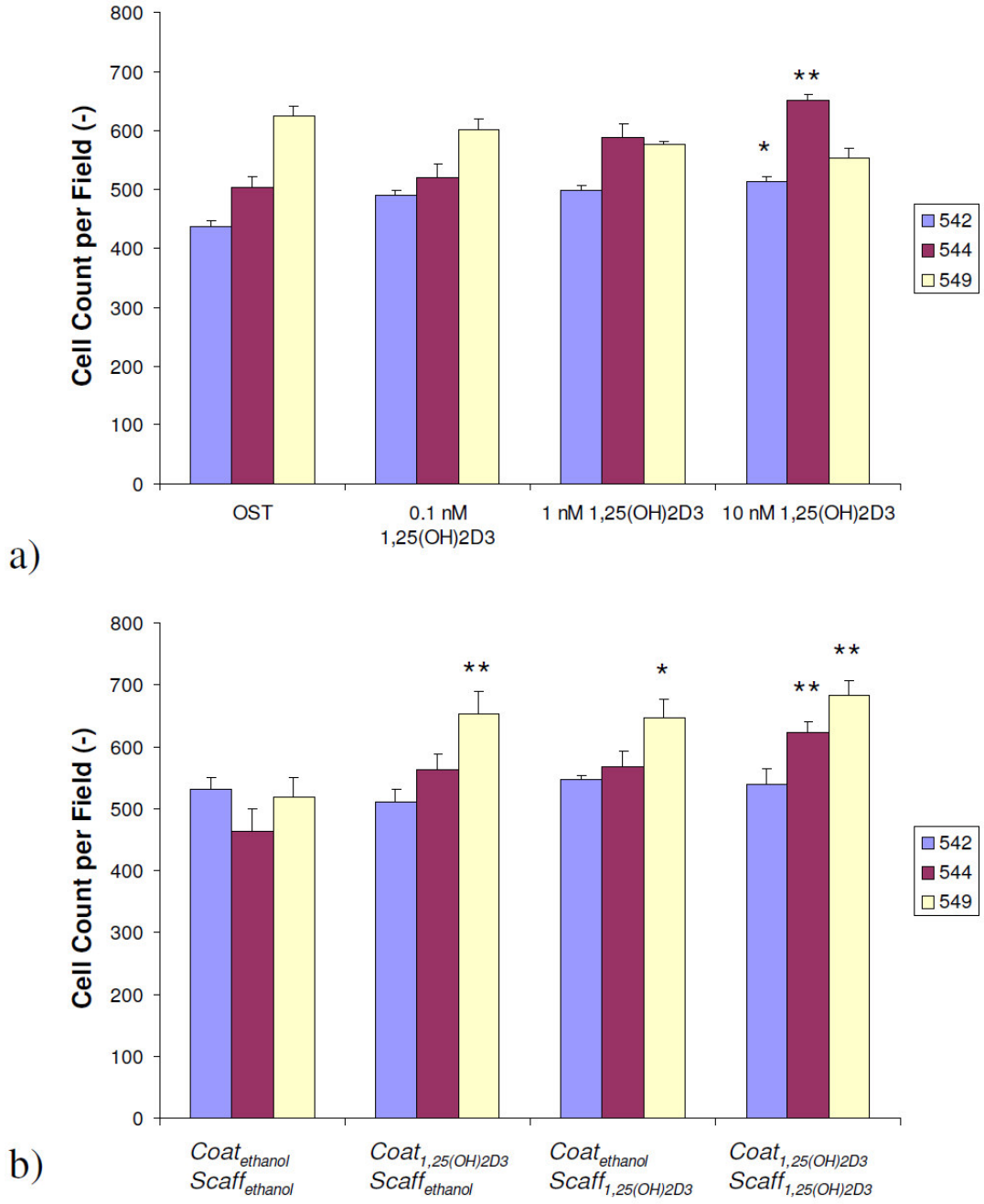

Figure 5.12: Cell counts of hMSCs.

The mean cell densities of hMSCs. Figure a) shows the data for the cells exposed to $1,25(OH)_2D_3$ and other test media, with no scaffold present. * and ** denote $p < 0.05$ and 0.01 respectively, compared to the base OST media. Figure b) shows the data for the cells exposed to the test scaffolds in OST media. * and ** denote $p < 0.05$ and 0.01 respectively, compared to the control $Coat_{ethanol}Scaff_{ethanol}$ group. The error bars represent the SEM, n = 6 in each case.

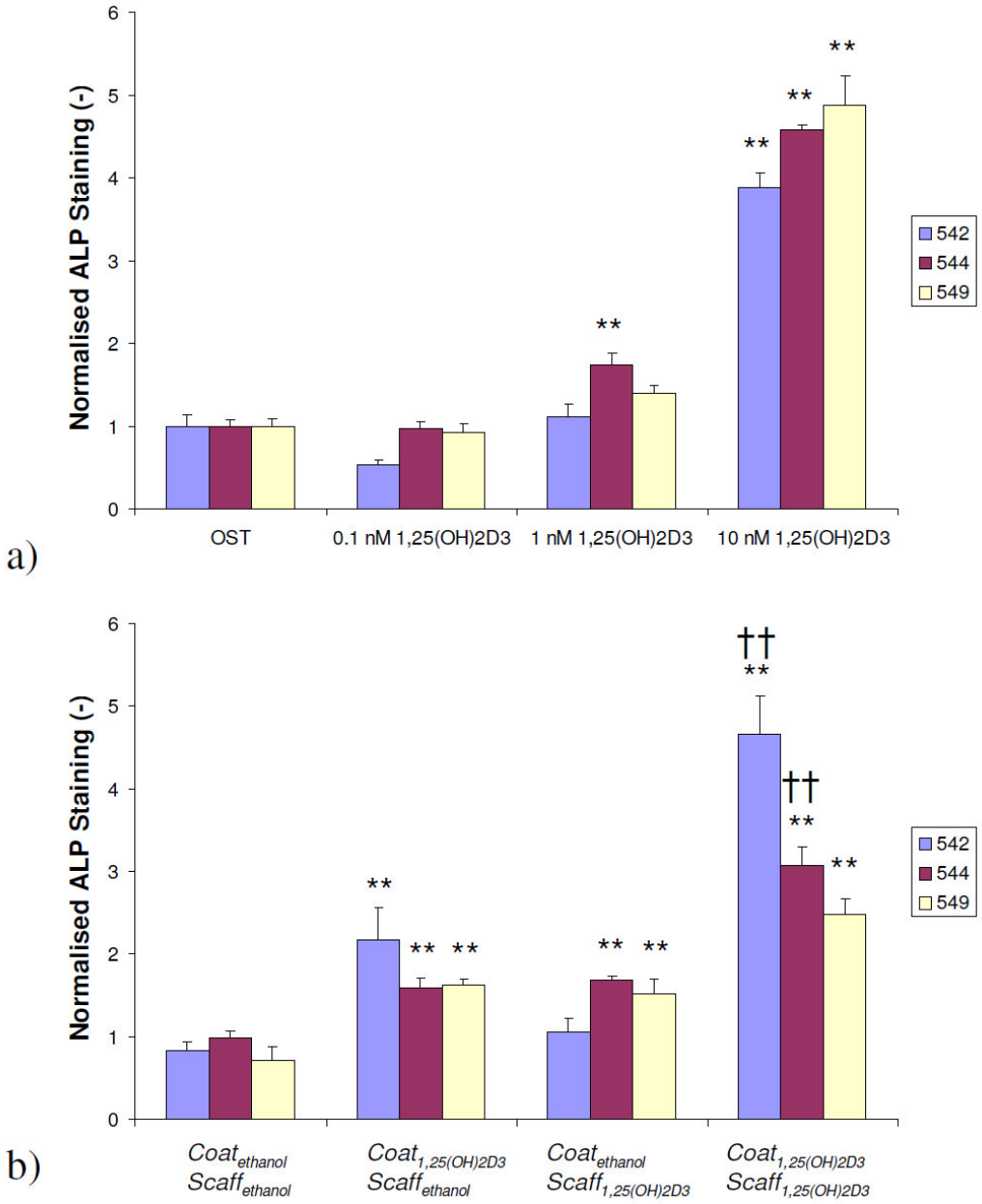

Figure 5.13: Normalised areas of ALP staining of hMSCs.

The mean areas of +ve ALP staining of hMSCs per cell, normalised against the OST group. Figure a) shows the data for the cells exposed to $1,25(OH)_2D_3$ and other test media, with no scaffold present. * and ** denote $p < 0.05$ and 0.01 respectively, compared to the base OST media. Figure b) shows the data for the cells exposed to the test scaffolds in OST media. * and ** denote $p < 0.05$ and 0.01 respectively, compared to the control $Coat_{ethanol}Scaff_{ethanol}$ group. †† denotes $p < 0.01$ compared to both the $Coat_{1,25(OH)2D3}Scaff_{ethanol}$ and $Coat_{ethanol}Scaff_{1,25(OH)2D3}$ groups. The error bars represent the SEM, n = 6 in each case.

5.6. Discussion

5.6.1. Rational for Normalisation of ALP staining

Common practice in previous studies has been to couple ALP assays with methods of determining cell numbers (Holtorf *et al.*, 2005; Dadsetan *et al.*, 2008; Bjerre *et al.*, 2008). This was because ALP expression per cell was thought to yield more information, as it was capable of distinguishing between low or moderate expression of ALP by a large number of cells, and high ALP expression by a smaller cell population. Therefore, the area of ALP staining was normalised by the number of cells present in that field.

The data on ALP staining divided by the cell counts per field, were then normalised to the control group for each hMSC patient. There were three main reasons for this. First, in an effort to reduce the effects of patient variability on the data. As can be seen in **Figure 5.6a**, patient variability in the control media group was evident. This reduction in patient variability also made trends in the data more apparent. Second, this reduced potential variability in the ALP staining solution, which was made up in different batches for the different test patients. Third, this reduced the potential for variability in the light conditions between batches, as the brightness of the microscope bulb was not precisely calibrated. Potentially, this could have introduced variability between test patients since the image analysis was based on colour brightness. The resulting normalised data are displayed in **Figure 5.8**.

5.6.2. rhBMP-7 Release

The purposes of the experiments involving rhBMP-7 described in this chapter were two-fold. First: to find the optimum growth factor dose for hMSC osteogenic differentiation. Second: to ascertain whether the rhBMP-7 released from the scaffolds was bioactive, and thereby assess the feasibility of delivering growth factors and other water-soluble active factors from such scaffolds.

The optimum dose of rhBMP-7 for the induction of osteogenic differentiation of hMSCs is unclear from the literature. Currently, the majority of *in vitro* studies have

been conducted using mouse or rat MSCs, however the response of these cells to rhBMP-7 may differ from that of human MSCs. For example, Diefenderfer *et al.* (2003) found that ALP activity was increased by factors of 3 and 8 times for rat and mouse MSCs respectively when cultured in media containing rhBMP-2 (100 ng/ml) for 6 days. In contrast, no significant change in ALP activity was observed for hMSCs. Therefore, the optimum concentration for humans cannot be deduced from these studies. Nevertheless, there is broad agreement that MSC expression of ALP, an early marker for osteogenic differentiation, is increased in response to rhBMP-7 in the range 10 – 100 ng/ml (Knippenberg *et al.*, 2006; Edgar *et al.*, 2007; Tsiridis *et al.*, 2007). Normalised ALP expression was therefore used as the main outcome measure for these studies.

For these experiments, OS media, as previously described by Tremoleda *et al.* (2008) and Sottile *et al.* (2003), was used as a positive control for ALP staining. This media contained dexamethasone, which is known to stimulate osteogenic differentiation of hMSCs (Beresford *et al.*, 1994; Jorgensen *et al.*, 2004b; Kotobuki *et al.*, 2005). Ascorbic acid, another component of OS media, is thought to support both the proliferation and osteogenic differentiation of hMSCs at concentrations of 50 μM and above (Choi *et al.*, 2008). β-glycerophosphate is also commonly added to osteogenic media, as a substrate for matrix mineralisation, usually at a concentration of 10 mM (Maniatopoulos *et al.*, 1988; Noble *et al.*, 1995; Tremoleda *et al.*, 2008).

OS media without dexamethasone was used as the base media for the rhBMP-7 studies. The OS-D media was thought capable of supporting osteogenic differentiation, without stimulating ALP activity directly. A similar media was used by Knippenberg *et al.* (2006) to study the osteogenic effects of both rhBMP-2 and -7. It was decided to analyse the ALP expression of the hMSCs after 14 days, as previous studies have found that *in vitro* ALP reaches a maximum at approximately this time point, before decreasing again as the hMSCs differentiate further (Edgar *et al.*, 2007; Santoni *et al.*, 2007; Fisher and Reddi, 2003; Liao *et al.*, 2008).

It was found that the area of ALP staining, as well as the normalised ALP expression, was statistically significantly higher for the OS media compared to the OS-D control for all of the patients tested (see **Figure 5.6a** and **Figure 5.8a**). This indicated that the hMSCs from each patient were capable of osteogenic differentiation.

Both the ALP and normalised ALP expression were found to be statistically significantly increased for at least two patients at each concentration of rhBMP-7 (see **Figure 5.6a** and **Figure 5.8a**) although the actual sizes of the increases were often small. Although normalising the area of ALP staining yielded more consistent results between patients, no consistent optimum rhBMP-7 concentration was found. Instead, each rhBMP-7 concentration tested appeared to have similar potential to stimulate ALP staining. This might indicate that the optimum concentration range of rhBMP-7 is relatively broad compared to other growth factors. For example and by way of contrast, the optimum concentration range of TGF-β1 for inducing motility in epithelial cells is only between 1 and 2 ng/ml (Kutz *et al.*, 2001).

From the data collected as shown in Chapter 4, the mean PCL (M_n 42,500) scaffold mass was found to be 19.6±1.0 mg. Therefore the mean quarter scaffold mass was thought to be 4.90±0.25 mg. The theoretical sum of the release of rhBMP-7 per unit scaffold mass was found to be 3540±45 ng/g and 119±4 ng/g for the $Coat_{BMP\ 1.25}Scaff_{PBS}$ and $Coat_{PBS}Scaff_{BMP\ 1.25}$ scaffolds respectively. Although potentially this may be an underestimate due to degradation of rhBMP-7 in the release media. The maximum theoretical loading in the scaffolds was 12.5±1.0 µg/g and 710±6 ng/g.

Therefore the hMSCs may have been exposed to concentrations in the media as high as 153±15 ng/ml and 8.7±0.5 ng/ml for the $Coat_{BMP\ 1.25}Scaff_{PBS}$ and $Coat_{PBS}Scaff_{BMP\ 1.25}$ scaffolds respectively, although the release in the bulk media may be as low as 43±3 ng/ml and 1.46±0.09 ng/ml at the end of the first 3 days. The latter values assume that there was no difference in the release profiles of rhBMP-7 between the OS-D media and the bovine serum albumin/PBS solutions. This assumption may not hold due to the degradation of the active form of rhBMP-7 once released. The bioactive form of BMP-7 consists of a dimer of two of two identical monomer units,

held together by a single disulphide bond (Griffith *et al.*, 1996). Although little is known about the breakdown of rhBMP-7 in growth media, disulphide bonds are known to be susceptible to cleavage either chemically (in reducing environments) or by enzymes (Stryer, 1995). The *in vivo* clearance rate is also thought to be rapid (Bishop and Einhorn, 2007).

The release of rhBMP-7 from the $Coat_{BMP\ 1.25}Scaff_{PBS}$ and $Coat_{BMP\ 0.63}Scaff_{PBS}$ scaffolds may have been in the range of concentrations found to stimulate ALP staining. Since ALP and normalised ALP expression was elevated for two out of three test patients, it is likely that a proportion of the rhBMP-7 released from the $Coat_{BMP\ 1.25}Scaff_{PBS}$ and $Coat_{BMP\ 0.63}Scaff_{PBS}$ scaffolds was bioactive (see **Figure 5.6b** and **Figure 5.8b**). Interestingly, there was little difference in the ALP expression between the $Coat_{BMP\ 1.25}Scaff_{PBS}$ and $Coat_{BMP\ 0.63}Scaff_{PBS}$ scaffold groups. It is likely that this was due to the broad range of rhBMP-7 concentrations able to induce a similar osteogenic response (see **Figure 5.6a** and **Figure 5.8a**). Hence the assay was not able to distinguish between the different concentrations of growth factor released. This may, in part, be as a result of the assay measuring the area of ALP staining rather than ALP activity.

The release from the scaffold coatings ($Coat_{BMP\ 1.25}$ and $Coat_{BMP\ 0.63}$) may have been comparable to some of the test concentrations used, theoretically as high as 153±15 ng/ml and 76.5 ±8 ng/ml, for the high and low doses respectively. However, this release is unlikely to have been sustained for as long as the test concentrations. Nevertheless, previous studies have found that treatments as short as 15 min with concentrations of rhBMP-7 and rhBMP-2 as low as 10 ng/ml, have been found to influence the differentiation of MSCs (Knippenberg *et al.*, 2006). It should also be noted that the cells may have experienced concentrations of rhBMP-7 higher than the bulk media concentrations reported above. This is because, although the scaffolds were not in physical contact with the cells, the scaffolds may have been relatively close to the cells as they were at the bottom of the wells. Since the distance was relatively short, the cells are likely to have experienced higher concentrations than the bulk media concentrations. Also, since a non-linear relationship between

increases in normalised ALP staining and rhBMP-7 concentration, it is feasible that lower concentrations than the 5 ng/ml or high rhBMP-7 doses sustained for a short period of time, could be capable of causing ALP staining comparable to that achieved between 5 and 50 ng/ml sustained for 14 days.

Unfortunately, the data from Chapter 4 would imply that the release of rhBMP-7 from the $Coat_{PBS}Scaff_{BMP\ 1.25}$ and $Coat_{PBS}Scaff_{BMP\ 0.63}$ scaffolds may have been below the range of growth factors concentrations tested. This assumes that no degradation of rhBMP-7 occurred in the ELISA release media, although the maximum theoretical release from the scaffolds of 8.7±0.5 ng/ml and 4.4±0.3 ng/ml respectively. This was calculated from the methylene blue encapsulation efficiency of PCL (M_n 42,500) scaffolds which was found to be 71±6% in Chapter 4. Therefore it is uncertain whether the lack of significant increases in the normalised ALP staining was caused by the release being too low to affect the hMSCs, or whether the rhBMP-7 released was no longer bioactive (see **Figure 5.6b** and **Figure 5.8b**).

It is interesting that the $Coat_{PBS}Scaff_{BMP\ 1.25}$ scaffolds were associated with a significant decrease in cell density (see **Figure 5.7b**). This was in contrast to the rhBMP-7 test concentrations, where only a slight decrease in cell numbers was observed at 20 ng/ml (see **Figure 5.7a**). While it is possible that a decrease in cell density occurs as a result of a low rhBMP-7 dose, it is perhaps more likely that this is a Type-I statistical error. Alternatively, the decrease in cell numbers, possibly as a result of reduced proliferation, and reduced ALP staining, may indicate that the cells in this group were more differentiated than the cells in the other scaffold groups. For many adult cell types, proliferation is thought to be poorly compatible with differentiation (Xia *et al.*, 2006), this is also thought to be the case for the osteoblastic lineage (Stein *et al.*, 2004). In addition, while high ALP activity is a marker of early osteoblastic differentiation, it is known to decrease as differentiation progresses (Stein *et al.*, 2004; Zaidi, 2007).

From these data, it would seem that release of rhBMP-7 from the $Coat_{BMP\ 1.25}Scaff_{PBS}$ and $Coat_{BMP\ 0.63}Scaff_{PBS}$ scaffolds was sufficient to affect cells not in direct contact

with the scaffolds, whereas the release from the $Coat_{PBS}Scaff_{BMP\ 1.25}$ and $Coat_{PBS}Scaff_{BMP\ 0.63}$ scaffolds was not.

However, as discussed in §1.2.6.1, how the growth factors are presented to the target cells is extremely important. Cells on tissue culture plastic will obviously experience a different environment to those seeded directly onto the scaffolds. This is both in terms of cell-scaffold surface interaction, as well as the growth factor concentration the cells experience. Therefore the scaffolds with the highest rhBMP-7 loadings, $Coat_{BMP\ 1.25}Scaff_{PBS}$ and $Coat_{PBS}Scaff_{BMP\ 1.25}$, were subjected to further testing as described in Chapter 6 and Chapter 7.

5.6.3. $1,25(OH)_2D_3$ Release

As discussed previously in §1.2.4.2, $1,25(OH)_2D_3$ has been considered as a potential compound of interest for bone regenerative medicine, particularly in combination with an isoform of transforming growth factor-β (TGF-β) (Bosetti *et al.*, 2007). However, $1,25(OH)_2D_3$ can easily be delivered systemically to patients. Indeed the normal serum concentration range of $1,25(OH)_2D_3$ is 80 – 150 nM (Heaney, 2004): an order of magnitude higher than the highest concentration tested in the studies described in this chapter. In adults, it is thought this concentration can be maintained by the daily consumption of 5 – 15 µg (IOM, 1997), though it is recommended that healthy adults should avoid regular daily consumption of more than 250 µg (Hathcock *et al.*, 2007).

Therefore the clinical advantages of the local delivery of $1,25(OH)_2D_3$ from scaffolds may be limited, although the short term exposure of cells on the scaffolds to $1,25(OH)_2D_3$ may prove to be advantageous, particularly pre-implantation. However, it was thought that $1,25(OH)_2D_3$ could act as a model drug for the lipid-soluble active factors of interest in bone regenerative medicine. For example, many cathepsin K inhibitors are hydrophobic (Wang *et al.*, 2004).

The purposes of the experiments involving $1,25(OH)_2D_3$ in this chapter, were to assess the feasibility of releasing lipid-soluble active factors, and to determine

whether the coating and encapsulating delivery systems were mutually compatible in this case. For these studies, rhTGF-β3 was added to OS media as the base media because isoforms of TGF-β, at 10 ng/ml, have been found to inhibit ALP expression. However, on the addition of $1,25(OH)_2D_3$, hMSC ALP expression was synergistically enhanced (Liu *et al.*, 1999).

Interestingly, for the cells grown in OST media, PI did not stain the cell nuclei distinctively (see **Figure 5.9b**). This was in contrast to the distinct staining observed in the experiments using OS-D (see **Figure 5.5b**). However, DAPI was able to stain the nuclei distinctly (see **Figure 5.9c**). Since PI stains both deoxyribonucleic acid (DNA) and ribonucleic acid (RNA), while DAPI stains only DNA (Suzuki *et al.*, 1997), it is possible that the cytoplasm of the cells in OST media contained more RNA than those in OS-D. Images of the cells stained with DAPI were therefore used to perform the cell counts for these experiments.

It was found that both ALP and normalised ALP expression were significantly increased for the 10 nM $1,25(OH)_2D_3$ groups, for each hMSC patient, compared to the OST control (see **Figure 5.11a** and **Figure 5.13a**). The increase in normalised ALP expression, for these groups, was found to be both greater and more consistent between patients than that for the experiments involving rhBMP-7 (see **Figure 5.8a** and **Figure 5.13a**). Hence, it was thought that the test for $1,25(OH)_2D_3$ was more sensitive than that for rhBMP-7.

Unlike the studies involving rhBMP-7, the release profile of $1,25(OH)_2D_3$ from the scaffolds was unknown. The maximum possible release from the $Coat_{1,25(OH)2D3}Scaff_{ethanol}$ scaffolds was therefore derived from the data in Chapter 4. It was previously found that the mean methylene blue content per unit mass of the coated scaffolds was 64.9±5.0 μg/g. Since the concentration of methylene blue in the coating was 50 μg/ml, the volume of collagen solution coated per gram of scaffold was calculated to be 1.3±0.1 ml/g. The mean quarter scaffold mass was 4.90±0.25 mg. Therefore the mean volume of coating per quarter sheet was 6.4±0.6 μl. Since the concentration of $1,25(OH)_2D_3$ in the coating solution was 3.6 μM, the

$1,25(OH)_2D_3$ content of the quarter scaffolds was 23±2 pmoles. Hence the maximum possible concentration achievable for the $Coat_{1,25(OH)2D3}Scaff_{ethanol}$ scaffolds in 0.4 ml of media was 57.5±5.0 nM.

For the $Coat_{ethanol}Scaff_{1,25(OH)2D3}$ scaffolds, the $1,25(OH)_2D_3$ was added to the plotting solution at a final moles/mass ratio of $1,25(OH)_2D_3$ to PCL of 4.8 nmoles/g. Since the mean scaffold mass was 4.90±0.25 mg, the $1,25(OH)_2D_3$ content was calculated to be 23.5±1.2 pmoles per scaffold. Hence the maximum possible concentration achievable for the $Coat_{ethanol}Scaff_{1,25(OH)2D3}$ scaffolds in 0.4 ml of media was 58.8±3.0 nM.

Therefore the maximum potential $1,25(OH)_2D_3$ release from the $Coat_{1,25(OH)2D3}Scaff_{ethanol}$, $Coat_{ethanol}Scaff_{1,25(OH)2D3}$ and $Coat_{1,25(OH)2D3}Scaff_{1,25(OH)2D3}$ scaffolds were theoretically capable of releasing, were well above the 10 nM threshold for increasing hMSC ALP expression.

The ALP and normalised ALP expression was significantly increased for two and three of the hMSC patients for the $Coat_{ethanol}Scaff_{1,25(OH)2D3}$ and $Coat_{1,25(OH)2D3}Scaff_{ethanol}$ scaffolds respectively, compared to the OST control (see **Figure 5.11b** and **Figure 5.13b**). Although these data do not yield information of the release profile, it is likely that bioactive $1,25(OH)_2D_3$ was released from both the encapsulating and loaded-coating delivery systems. Hence, it was concluded that it was feasible to deliver lipid-soluble active factors from both of the encapsulating and collagen coating delivery systems.

Levels of ALP and normalised ALP expression were also significantly elevated in all three hMSC patients for the $Coat_{1,25(OH)2D3}Scaff_{1,25(OH)2D3}$ scaffolds, compared to the OST control. Furthermore, the normalised ALP expression was significantly increased compared to either delivery system on its own for two of three test patients (see **Figure 5.13b**). These data suggest that the two delivery systems are mutually compatible.

5.7. Conclusion

A quantitative system, based on the image analysis of ALP staining and PI cell counts, was used to assess the osteogenic potential of rhBMP-7, and the release from growth factor incorporating scaffolds. Each of the rhBMP-7 concentrations tested (5, 20, and 50 ng/ml) was found to increase the normalised area of ALP staining statistically significantly compared to the base media. This might indicate that rhBMP-7 is able to stimulate the osteogenic differentiation of hMSCs over a relatively wide range of concentrations.

The release from the $Coat_{BMP\ 1.25}Scaff_{PBS}$ and $Coat_{BMP\ 0.63}Scaff_{PBS}$ scaffolds was found to stimulate hMSC ALP staining compared to the control scaffolds. This indicated that at least a proportion of the rhBMP-7 released was bioactive. In contrast, the release from $Coat_{PBS}Scaff_{BMP\ 1.25}$ and $Coat_{PBS}Scaff_{BMP\ 0.63}$ was found not to enhance hMSC ALP staining. Either the growth factor released was not bioactive, or the dose was insufficient to influence the cells measurably.

It was thought that the cells would experience a different environment and different growth factor concentrations if the cells were seeded directly on to the scaffolds. The scaffolds incorporating rhBMP-7 were therefore tested further, as described in Chapter 6 and Chapter 7.

Image analysis of ALP staining, normalised against DAPI cell counts, was used to assess quantitatively the ability of the $Coat_{1,25(OH)2D3}Scaff_{ethanol}$, $Coat_{ethanol}Scaff_{1,25(OH)2D3}$ and $Coat_{1,25(OH)2D3}Scaff_{1,25(OH)2D3}$ scaffolds to release $1,25(OH)_2D_3$. Normalised ALP expression of the hMSCs was significantly increased for each of the $1,25(OH)_2D_3$ loaded scaffold types compared to the control scaffolds. Furthermore, ALP expression was significantly enhanced for the dual delivery scaffolds over and above that for either delivery system on its own. It was therefore concluded that the PCL scaffolds coated with collagen could be capable of releasing bioactive lipid-soluble active factors, and that both delivery systems were mutually compatible.

Chapter 6 : Cell/Scaffold Interactions

6.1. Scaffold Nomenclature

$Coat_{PBS}$	Collagen coating with PBS (rhBMP-7 control)
$Coat_{BMP\ 1.25}$	Collagen coating with rhBMP-7 (1.25 µg/ml)
$Scaff_{PBS}$	Scaffold encapsulating PBS (rhBMP-7 control)
$Scaff_{BMP\ 1.25}$	Scaffold encapsulating rhBMP-7 (1.25 µg/ml)

6.2. Abstract

Previous studies, described in the preceding chapters, have assessed the cell-compatibility of the scaffold materials, and examined the quantity and bioactivity of recombinant human bone morphogenetic protein-7 (rhBMP-7) released from the scaffolds. However, it was unknown how the clinically relevant human marrow stromal cells (hMSCs) would react to the combined stimuli, when seeded directly onto the scaffolds. This was therefore assessed in this chapter by quantifying the activity of alkaline phosphatase (ALP), the mass of calcium phosphate deposited, and the number of cells on the scaffolds.

The apparent number of cells on the scaffolds was quantified via a deoxyribonucleic acid (DNA) assay, using PicoGreen. The apparent quantity of hMSC per quarter scaffold was found to range from 1.36×10^5 and 3.60×10^5. The cells were also found to have completely spanned the majority of the scaffold pores.

The activity of ALP was assessed by quantifying the degradation of para-nitrophenylphosphate to para-nitrophenol, and normalising this against the apparent mass of DNA in the scaffold cell lysate. In the range of rhBMP-7 concentrations tested (5, 20, and 50 ng/ml), higher concentrations of the growth factor were associated with elevated activity of ALP (increased by 98±18% for 50 ng/ml on the control). Statistically significantly elevated levels of ALP activity were also found for the $Coat_{BMP\ 1.25}Scaff_{BMP\ 1.25}$ and $Coat_{PBS}Scaff_{BMP\ 1.25}$ scaffold groups for hMSCs derived from two and three patients respectively (increased by 35±10% and 39±10 on the control respectively), whereas this was the case for only one patient's cells for the $Coat_{BMP\ 1.25}Scaff_{PBS}$ scaffolds (increased be 35±14% on the control).

The apparent mass of calcium phosphate deposited on the scaffolds was quantified using the o-cresolphthalein complexone method. This was also normalised by the mass of DNA in the scaffold cell lysate. However, significant increases in calcium deposition were only observed in one of the three hMSC patients, compared to the control.

These data indicate that the osteogenic differentiation of hMSCs, although not mineralisation, was supported by the $Coat_{BMP\ 1.25}Scaff_{BMP\ 1.25}$ and $Coat_{PBS}Scaff_{BMP\ 1.25}$ scaffolds, when the cells were seeded directly onto them. It was also found that the osteogenic effect of the scaffolds was not significantly enhanced by the rhBMP-7 loaded Type-I collagen scaffold coating. This leaves a potential for the loading of different active factors in the coating delivery system for the final "product" intended for clinical use. However, this is beyond the scope of the studies described in this thesis. The potential of the scaffolds loaded with rhBMP-7 to induce osteogenic differentiation in cells seeded upon them was investigated further in Chapter 7.

6.3. Introduction

The aim of the studies described in Chapter 2 was to develop scaffolds and scaffold coatings which had geometries suitable for bone regenerative medical applications. Chapter 3 describes how the cell-compatibility of Type-I collagen coatings and poly(ε-caprolactone) (PCL) (M_n 42,500) scaffolds was assessed. In chapters 4 and 5, the release of rhBMP-7 was examined, both in terms of the quantity released, and the effect this release had on hMSCs. However, it was unknown how these cells would behave in response to being seeded directly onto the scaffolds and being exposed to the combination of stimuli described above.

As discussed in §1.1.1.5, ALP expression and matrix mineralisation are well established indicators of osteogenic differentiation. Therefore, quantifications of ALP activity and calcium deposition, normalised per unit mass of DNA, protein or scaffold, are frequently used as outcome measures for assessing the osteoinductive potential of bone regenerative medical scaffolds. ALP expression is commonly quantified using para-nitrophenylphosphate (pNPP) (Bjerre *et al.*, 2008; Liu *et al.*, 2008b; Moreau and Xu, 2009). ALP catalyses the conversion of pNPP to para-nitrophenol (pNP), the concentration of which can be determined using a colourimetric assay (see **Figure 6.1**) (Bretaudiere and Spillman, 1984).

A well established method for quantifying calcium concentrations in solution, employs o-cresolphthalein complexone (Moorehead and Biggs, 1974; Toffaletti and Kirvan, 1980). Under basic conditions, colourless o-cresolphthalein complexone reacts with calcium ions to yield Ca-cresolphthalein complexone, which is purple. Hence, the concentration of calcium can be quantified using a colourimetric assay. This technique has been used by a number of authors to quantify the deposition of calcium by cells on bone regenerative medical scaffolds (Holtorf *et al.*, 2005; Vadillo, 2009; Dadsetan *et al.*, 2008).

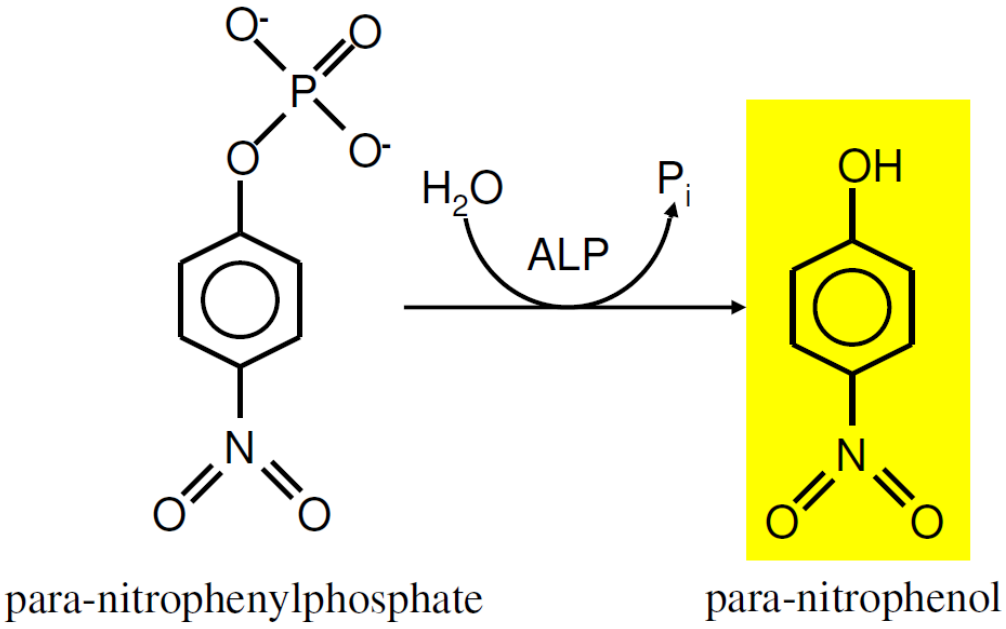

Figure 6.1: Mode of action of pNPP.

A cartoon of chemical reaction by which ALP catalysis the conversion of pNPP to pNP. The activity of ALP can therefore be assessed by calculating the rate of the reaction by quantifying the concentration of pNP. Since pNP is yellow and pNPP is colourless, a colourimetric assay can be applied.

Data obtained on ALP activity or calcium deposition, to give an accurate indication of the osteogenic differentiation of cells on scaffolds, should be normalised against the number of cells present. This may be achieved using a protein assay. However these tests are not suitable for all types of scaffolds, such as those which have a significant protein content. Alternatively, the number of cells can be found using a DNA assay.

Currently one of the most accurate DNA assays available employs PicoGreen. Assays using this fluorescent dye are capable of detecting DNA concentrations as low as 25 pg/ml: 400-fold more sensitive than using Hoechst 33258 (Singer *et al.*, 1997). PicoGreen has been successfully employed by many authors in studies involving scaffolds (Dadsetan *et al.*, 2008; Moreau and Xu, 2009; Holtorf *et al.*, 2005).

During the studies described in this chapter, the osteogenic differentiation of hMSCs on Type-I collagen coated PCL (M_n 42,500) scaffolds, loaded with rhBMP-7, was investigated. This was assessed by quantifying the ALP activity, calcium deposition, and DNA content of the scaffolds.

6.4. Materials and Methods

Unless otherwise stated, all reagents were purchased from Sigma, UK. All the techniques involving cell culture, described below, were conducted in a sterile environment, using sterilised equipment.

6.4.1. hMSC Isolation and Culture

After written consent from the patients and approval from the local ethical committee (Lothian local research ethics committee), human femoral head tissue was obtained from patients who had undergone elective arthroplasty. Tissue was collected from a total of three patients (see **Table 6.1**). The tissue samples were allocated an anonymous number based on the chronological order of the sample collection. The hMSCs were isolated and cultured as described in §3.3.1.1. The hMSCs underwent routine characterisation as described in **Appendix G**.

Table 6.1: hMSC patient details

In-House Patient Number	549	553	569
Patient Age	61	65	69
Patient Sex	Female	Female	Male

6.4.2. hMSC DNA Content

A tissue culture flask (75 cm^2) containing confluent hMSCs (passage 2) from patient 553 was washed three times in PBS, and the cells were detached from the flask using 2.5 mg/ml trypsin in phosphate buffered saline (PBS) (Invitrogen, UK) and growth media, as described in §3.3.1. The cell density of the cell suspensions was measured using a haemocytometer. After appropriate dilution with growth media, the cells were added to wells of a 48-well TC plastic plate (Corning, USA), at cell densities of 20000, 10000, 5000, 2500, 1250, and 625 cells/well (in 400 µl of media). Three wells were seeded for each cell density. The plate was then maintained in a humidified air incubator at 37°C with 5% (v/v) CO_2. After 4 hr, the media was removed by inverting the plate, and quickly blotted with a sterile dry medical wipe (Kimberly Clark, UK). The plate was then frozen at -80°C.

The following day, the plate was thawed for 30 min at 37°C and 200 µl of distilled water (dH_2O) were added to each well. The plate was then subjected to two freeze/thaw cycles of freezing at -80°C for 1 hr, and thawing at 37°C for 30 min, as previously described with minor modifications from Rago *et al.* (1990). Then 50 µl of the cell lysate from each well was transferred to the wells of a 96-well plate (Costar, USA).

DNA sodium salt from herring testes stock solution (10 mg/ml in PBS) was diluted to a concentration of 16 µg/ml in dH_2O. A calibration curve was then pipetted into the 96-well plate, by performing two-fold dilutions in dH_2O from the 16 µg/ml until

a final concentration of 250 ng/ml was reached. A blank of dH_2O was also added. The final volume in each well was 50 µl, two wells were used for each concentration.

A DNA assay using PicoGreen (Invitrogen, UK) was performed according to the manufacturer's instructions. A working solution of PicoGreen was prepared by diluting the stock solution 200-fold in TE buffer: Trizma® hydrochloride (10 mM) and ethylenediaminetetraacetic acid (1 mM) at pH7.5. After mixing, 50 µl of the PicoGreen working solution were added to each of the test wells in the 96-well plate. The plate was "tapped" to aid the mixing of the solutions and was then incubated in the dark, at room temperature, for 5 min. The fluorescence of the wells was then measured using a CytoFluor® Series 400 spectrometer, exciting at a wavelength of 485 nm and reading at 520 nm.

6.4.3. Scaffold Manufacture

A stock solution of 1 mg/ml rhBMP-7 (Stryker, USA) was diluted with PBS to a concentration of 25 µg/ml. This was added at 1% (v/v) to 25% (w/v) solutions of PCL (M_n 42,500)/dichloromethane (DCM). This yielded a final mass ratio of rhBMP-7 to PCL of 1.00 µg/g or 1.25 µg/ml for the PCL/DCM solution.

Once added, emulsions were created by vigorous manual mixing, using sterile 3 ml transfer pipettes (Fisher, UK), for approximately 30 seconds. The resulting emulsions were loaded into the syringe of the Bioplotter™. Scaffolds were then manufactured, with no plotting medium, using the optimised plotting parameters determined in §2.4.1.1.1, and then vacuum dried at 75 mbar (absolute pressure) for 60 min. These scaffolds were designated $Scaff_{BMP\ 1.25}$.

Control scaffolds were also manufactured in a similar fashion, replacing the 25 µg/ml rhBMP-7 solution with PBS. These scaffolds were designated $Scaff_{PBS}$.

All the scaffolds were immersed in IMS for 10 min before being washed with dH_2O (5 min) and PBS (Oxoid, UK) (5 min). The stock solution of rhBMP-7 (1 mg/ml) was then added to 1 mg/ml Type-I collagen in 0.1 M aqueous acetic acid, to yield a

final concentration of 1.25 µg/ml. The equivalent volume of PBS was added to a similar solution of Type-I collagen.

All the scaffolds were then immersed for 5 min in one of the collagen solutions either containing or lacking rhBMP-7. The scaffolds were designated with the prefixes $Coat_{BMP\ 1.25}$ or $Coat_{PBS}$ respectively. Afterwards, the scaffolds were removed, and allowed to air dry for 4 hr at room temperature. Once dry, the scaffolds were cut into approximately equal quarters using a scalpel. The scaffolds were then stored at -80°C.

6.4.4. hMSC Culture on Scaffolds

After the quarter scaffolds, prepared as described in §6.4.3, were thawed, they were individually placed at the bottom of the well of 48-well non-TC plastic plates (Corning, USA). Care was taken to ensure the scaffolds were flat against the bottom of the wells, and that they were held in place by the scaffolds corners' contact with the wells' sides. The number of $Coat_{PBS}Scaff_{PBS}$, $Coat_{BMP\ 1.25}Scaff_{PBS}$, $Coat_{PBS}Scaff_{BMP\ 1.25}$ and $Coat_{BMP\ 1.25}Scaff_{BMP\ 1.25}$ quarter scaffolds used for each hMSC patient was 62, 16, 16 and 16 respectively.

Tissue culture flasks (75 cm^2) containing confluent hMSCs (passage 2) from patients 549, 553, and 569 (in separate flasks), were washed three times in PBS, and the cells were detached from the flasks using 2.5 mg/ml trypsin in PBS (Invitrogen, UK) and growth media, as described in §3.3.1. The cell density of the suspensions was measured using a haemocytometer. After appropriate dilution with growth media, the cells were added to wells of the 48-well non-TC plastic plates, containing scaffolds (except for six $Coat_{PBS}Scaff_{PBS}$ scaffolds), at a density of 16,000 cells/well (in 400 µl of media). Similarly, 400 µl of growth media with no hMSCs were added to the wells containing the non-seeded scaffolds. Growth media was also added to the empty wells (400 µl/well) to reduce edge evaporation effects. The plate plan was as shown in **Figure 6.2**. The plates were then maintained in a humidified air incubator at 37°C with 5% (v/v) CO_2.

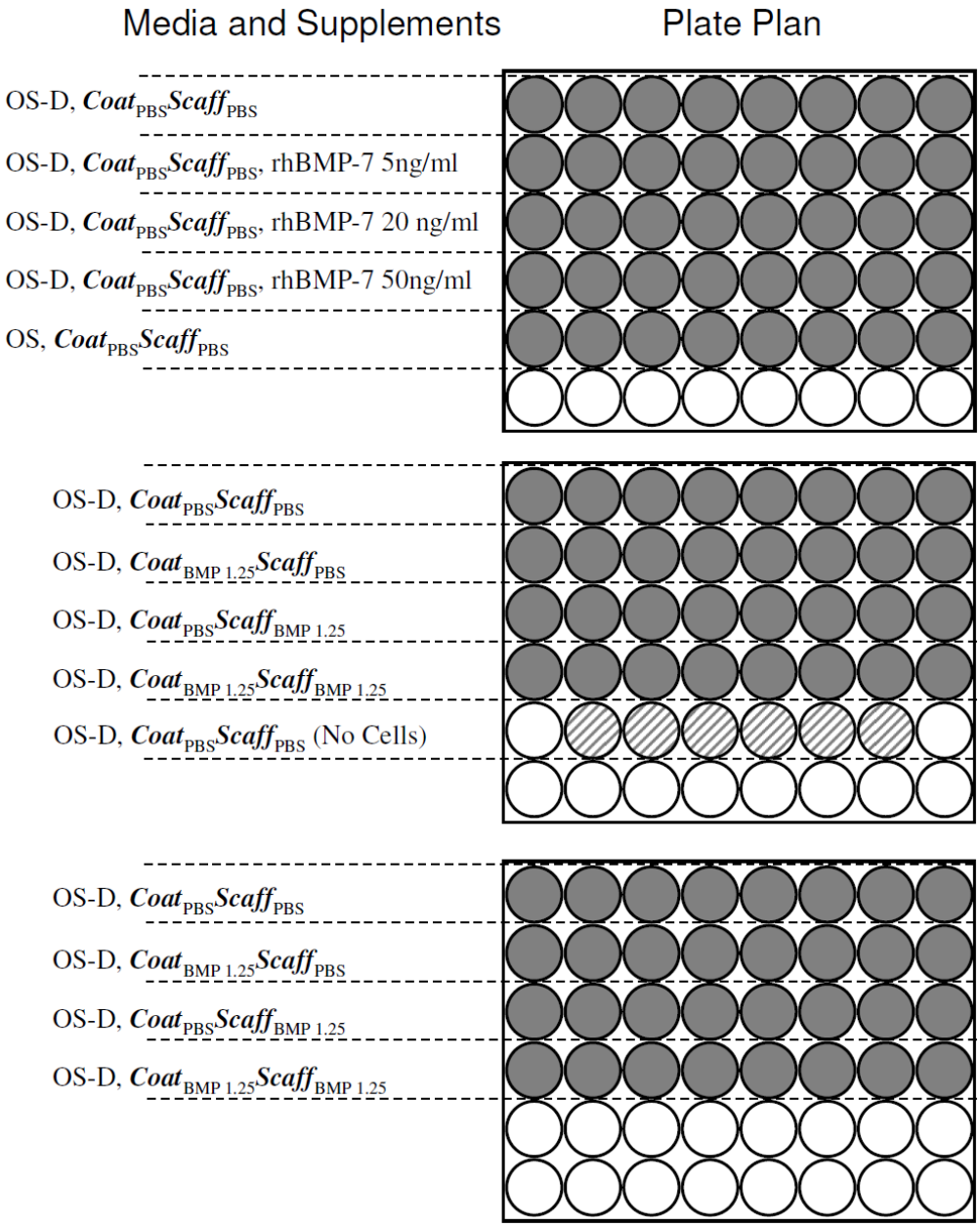

Figure 6.2: Plate plan for experiments involving hMSCs seeded onto scaffolds.

A cartoon showing the plate plan of the 48-well plates for the experiments involving hMSCs seeded onto scaffolds. The media composition, media supplements, and scaffold Type-Are indicated. The shaded wells indicate the test wells containing hMSCs, whereas the crosshatched wells indicate the test wells containing media and scaffolds without cells. The white wells indicate wells containing growth media only. This plate plan was used for each of the hMSC test patients.

The following day, all the media was changed. The media of the wells containing $Coat_{BMP\ 1.25}Scaff_{PBS}$, $Coat_{PBS}Scaff_{BMP\ 1.25}$ and $Coat_{BMP\ 1.25}Scaff_{BMP\ 1.25}$ scaffolds was replaced with OS-D media. For each patient, 16 of the wells containing $Coat_{PBS}Scaff_{PBS}$ hMSC seeded scaffolds were refreshed with OS-D media, whereas in six wells the media was replaced with either OS-D containing rhBMP-7 (5, 20 or 50 ng/ml) or OS media (see **Figure 6.2**). OS-D media was added to the wells containing the non-seeded scaffolds. The plates were then maintained in a humidified air incubator at 37°C with 5% (v/v) CO_2. The media was replaced with fresh media, of the same composition, at regular intervals three times every 7 days. After 21 days, the scaffolds were treated as follows.

Three $Coat_{PBS}Scaff_{PBS}$, $Coat_{BMP\ 1.25}Scaff_{PBS}$, $Coat_{PBS}Scaff_{BMP\ 1.25}$ and $Coat_{BMP\ 1.25}Scaff_{BMP\ 1.25}$ scaffolds, which had been cultured in OS-D, were fixed in 4% (w/v) paraformaldehyde in PBS for 10 min. The scaffolds were washed with PBS (twice) and dH_2O (once): 2 min per wash. The scaffolds were left to dry for 4 hr before being stored at 4°C. The scaffolds were then stained for ALP and with DAPI, using the protocol described in §5.4.4. They were then photographed using an upright microscope (Nikon Eclipse E800) with a mounted camera (Nikon DXM1200), and using an inverted microscope (Axio Observer, Carl Zeiss Ltd., Germany).

One $Coat_{PBS}Scaff_{PBS}$, $Coat_{BMP\ 1.25}Scaff_{PBS}$, $Coat_{PBS}Scaff_{BMP\ 1.25}$ and $Coat_{BMP\ 1.25}Scaff_{BMP\ 1.25}$ scaffold each from patient 569, which had been cultured in OS-D, were fixed overnight in 3% (w/v) gluteraldehyde in 0.1 M sodium cacodylate buffer (pH = 7.3). The $Coat_{BMP\ 1.25}Scaff_{BMP\ 1.25}$ scaffold was then prepared for examination using a scanning electron microscope as described in §6.4.5. The remaining samples were not prepared for examination.

For the remainder, the scaffolds were removed from the well and placed in individual 1.5 ml eppendorf tubes. The scaffolds were then assayed for their DNA content and either the ALP activity or calcium content, as described in §6.4.6 and §6.4.7.

6.4.5. Electron Microscope Sample Preparation

The $Coat_{BMP\ 1.25}Scaff_{BMP\ 1.25}$ scaffold was prepared for scanning electron microscopy as previously described by Leus *et al.* (2004) and Macdonald *et al.* (2008). After treatment with glutaraldehyde, the scaffold was immersed overnight in 2% (w/v) guanidine hydrochloride and 2% (w/v) tannic acid. It was subsequently post-fixed in 2% (w/v) osmium tetroxide in dH_2O for 8 hr.

The scaffold was then dehydrated in graded concentrations of acetone (50%, 70%, 90%, and 100%). This was followed by critical point drying using CO_2. After mounting on an aluminium stub, the scaffold was sputter coated with 20 nmoles of gold/palladium. Photographs of the sample were then taken using a Phillips 505 scanning electron microscope.

6.4.6. ALP/DNA Assay

For each patient, six scaffolds from the $Coat_{BMP\ 1.25}Scaff_{PBS}$, $Coat_{PBS}Scaff_{BMP\ 1.25}$ and $Coat_{BMP\ 1.25}Scaff_{BMP\ 1.25}$ groups, as well as the $Coat_{PBS}Scaff_{PBS}$ exposed to different rhBMP-7 concentrations (six scaffolds per concentration), were thawed. The scaffolds were then examined using a combined ALP/DNA assay based on that described previously by Dadsetan *et al.* (2008). After 30 min at 37°C, 200 µl of dH_2O were added to each eppendorf tube. Care was taken to immerse each scaffold completely. The tubes were frozen at -80°C for 60 min before being thawed at 37°C for 30 min. The tubes were then sonicated in a bath sonicator (KS200, Kerry Ultrasonics, UK) filled with ice water for 30 min. The freeze/thaw/sonicate cycle was then repeated.

6.4.6.1. DNA Assay

After mixing, half of the cell lysate (100 µl) was removed from the tubes. The remaining lysate, for the ALP assay, was stored at 4°C. Then 50 µl of the cell lysate extracted were added to the wells of 96-well plates. Calibration curves of known DNA concentrations was added to the plates, as described in §6.4.2. PicoGreen working solution (50 µl) was added to each of the test wells. The plates were then "tapped" to aid the mixing of the solutions.

After incubating the plates at room temperature, in the dark, for 5 min, the fluorescence of the wells was measured (excitation 485 nm, emission 520 nm). The apparent concentrations of DNA in the samples were calculated using the calibration curves. The apparent number of cells was found using the correlation between the DNA concentration and the number of cells calculated in §6.5.1.

6.4.6.2. ALP Assay

An ALP assay, with minor modifications from Modrovich (1979) and Bjerre *et al.* (2008), was applied to the cell lysate set aside as described in §6.4.6.1. Tablets of 4-nitrophenyl phosphate disodium salt hexahydrate (5 mg) were added to an aqueous solution of 16.7 mM 2-amino-2-methylpropanol and 2.2 mM magnesium chloride ($MgCl_2$) (pH 10.3). The final pNPP concentration was 50 mM.

Then 300 µl of the pNPP solution were added to each eppendorf tube. After mixing, the tubes were incubated in the dark, at room temperature. After 60 min, 100 µl of 3 M NaOH were added to each tube. The samples were diluted at a ratio of 1:1 with aqueous 10.0 mM 2-amino-2-methylpropanol, 1.32 mM $MgCl_2$ and 0.6 M NaOH. 100 µl of the samples were then added to 96-well plates.

A calibration curve of 16 concentrations of pNP, in aqueous 10.0 mM 2-amino-2-methylpropanol, 1.32 mM $MgCl_2$ and 0.6 M NaOH, was added to the 96-well plates. The starting concentration of pNP was 50 mM. A further 14 two-fold dilutions were made from the starting concentration, and a blank was included. The final volume in each well was 100 µl.

The optical densities of the wells were read using an automated 96-well plate reader set at 405 nm. The apparent concentrations of pNP were calculated for each of the samples using the calibration curves, taking the 1:1 sample dilution into account. The ALP activity was then calculated for each scaffold, by dividing the number of moles of pNP produced per hour, by the mass of DNA in the lysate for that scaffold.

6.4.7. Calcium/DNA Assay

For each patient, six scaffolds from the $Coat_{PBS}Scaff_{PBS}$, $Coat_{BMP\ 1.25}Scaff_{PBS}$, $Coat_{PBS}Scaff_{BMP\ 1.25}$ and $Coat_{BMP\ 1.25}Scaff_{BMP\ 1.25}$ groups were defrosted. They were then examined using a combined assay to assess their calcium and DNA content.

After 30 min at 37°C, 200 µl of dH_2O were added to each eppendorf. Care was taken to immerse each scaffold completely. The tubes were frozen at -80°C for 60 min before being thawed at 37°C for 30 min. The tubes were then sonicated in a bath sonicator (KS200, Kerry Ultrasonics, UK) filled with ice water for 30 min. The freeze/thaw/sonicate cycle was then repeated.

6.4.7.1. DNA Assay

The scaffolds were assayed for their DNA content, as described in §6.4.6.1.

6.4.7.2. Calcium Assay

The cell lysate which was not used for the DNA assay was transferred from the eppendorf tubes containing the scaffolds, to new tubes. A calcium assay was then performed on the scaffolds, based on the underlying chemistry described by Moorehead and Biggs (1974) and Toffaletti and Kirvan (1980). The o-cresolphthalein complexone method has been used previously to assess calcium deposition on scaffolds by Vadillo (2009), Kim *et al.* (2006), and Holtorf *et al.* (2005). Afterwards, 200 µl of 1 M hydrochloric acid (HCl) were added to each tube containing scaffolds. Similarly, 100 µl of 2 M HCl were added to each tube of cell lysate. The tubes were then incubated overnight in an orbital incubator (Stuart S150), set to 120 rpm (orbital diameter: 1.5 cm) and 37°C.

Two solutions were prepared: AMP buffer and Colour reagent. AMP buffer consisted of 15.12 % (v/v) 2-amino-2-methyl-1-propanol in dH_2O (pH 10.7). The Colour reagent was made from 0.1 mg/ml o-cresolphthalein complexone (Fluka, UK) and 1 mg/ml 8-hydroxychinolin in 6 % (v/v) aqueous HCl.

Known concentrations of dibasic calcium phosphate ($CaHPO_4$) in 1 M HCl were prepared. The highest concentration was 1.28 mg/ml, and a further eight two-fold dilutions were made. A blank of 1 M HCl was also included.

Equal quantities of AMP buffer and Colour reagent were added together. For each sample and known calcium phosphate concentration, 10 µl were added to 400 µl of the AMP buffer and Colour reagent mixture. After mixing, 100 µl of each solution were added to the wells of 96-well plates.

The optical densities of the wells were read using an automated 96-well plate reader set at 540 nm. The apparent calcium phosphate concentrations of the samples were calculated using the calibration curves. The apparent mass of calcium phosphate deposited on each scaffold was normalised by dividing by the mass of DNA in the lysate for that scaffold.

6.4.8. Statistical Analysis

All correlations derived from calibration curves using Excel 2003. All correlations, had R^2 values greater than 0.99. All other data were analysed using the statistical software package SPSS 14.0 for Windows.

The data collected for the combined ALP/DNA assay were found not to satisfy Levene's test, even after mathematical transformations. Parametric tests, such as one-way analysis of variance (ANOVA), were therefore unsuitable. Hence, the nonparametric test Kruskal-Wallis was used to test for statistical significance for each data set. The statistical significance between the groups was found using the Mann-Whitney U test (Zar, 1984; Petrie and Sabin, 2005). $p < 0.05$ was considered to be statistically significant.

All the data collected for the Calcium/DNA assay required the transformation of $\log_{10}$ to satisfy Levene's test and that of Kolmogorov-Smirnov. ANOVA was then applied, followed by the Tukey-Kramer *post hoc* test to determine the statistical differences between the groups.

The mean was used throughout, and all results are expressed as the sample means ± standard error of the mean (SEM).

6.5. Results

6.5.1. hMSC DNA Content

In the range of DNA concentrations examined, a linear relationship between the concentration and the fluorescence was found. A correlation was therefore calculated by linear regression. Unknown DNA concentrations were calculated using the resulting correlation (see **Figure 6.3a**).

Similarly, a linear relationship between the number of cells seeded per well, and the apparent DNA concentration in the cell lysate, was found (see **Figure 6.3b**). A correlation was calculated by linear regression. This correlation was used to estimate the number of cells present from apparent DNA concentrations.

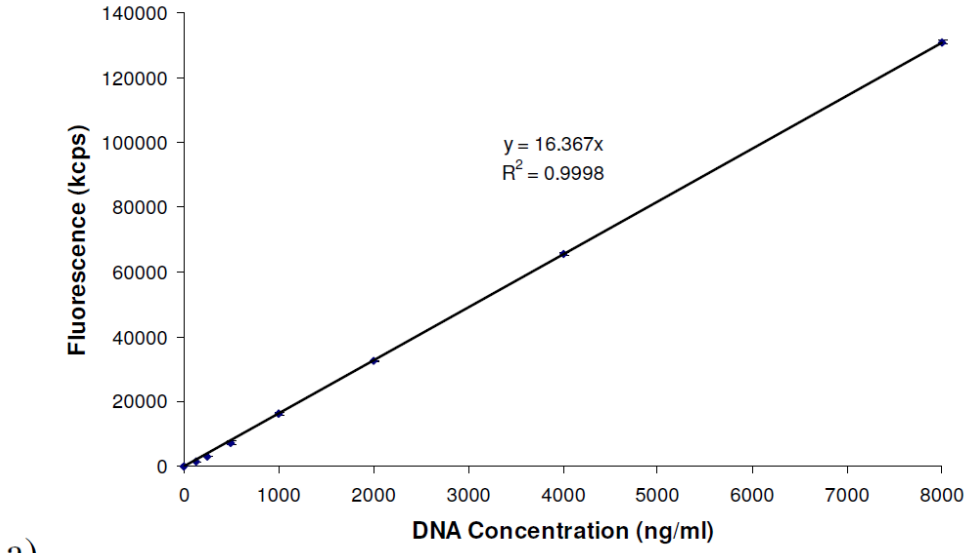

a)

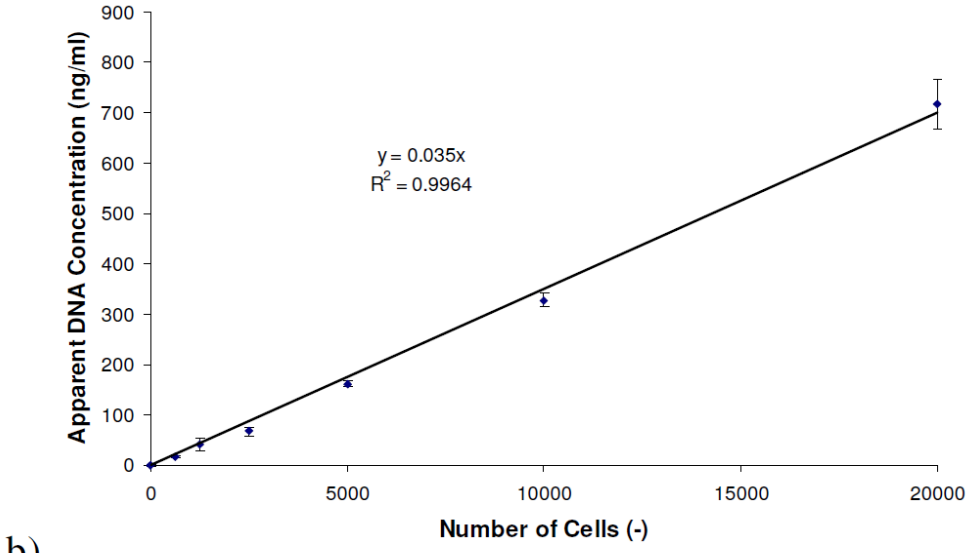

b)

Figure 6.3: DNA and Cell Calibration Curves.

Figure a) shows a calibration curve, relating DNA concentration to fluorescence. Each data point represents two repeats. The resulting correlation was used to find unknown concentrations of DNA. Figure b) shows a calibration curve, relating the number of cells to the apparent DNA concentration. Each data point represents three repeats. The resulting correlation was used to find unknown cell counts from apparent DNA concentrations.

6.5.2. ALP Activity on Scaffolds

In the range of pNP concentrations examined, a linear relationship between the concentration and the optical density at 405 nm, was found. Linear correlations were therefore calculated by linear regression. Unknown pNP concentrations were calculated using these correlations. A representative calibration curve is shown in **Figure 6.4**. As observed in the results described in §6.5.1, the DNA concentration was found to yield a linear relationship with the fluorescence. The resulting calibration curves were similar to that shown in **Figure 6.3a**.

For all hMSC patients, both pNP production and ALP activity were significantly increased for the scaffolds in OS media compared to the control scaffolds (by 165±32% and 224±42% respectively) (see **Figure 6.5a** and **c**). pNP production was elevated for the hMSCs exposed to rhBMP-7 (by 52±25% for 50 ng/ml on the control). ALP activity was also increased significantly for the hMSCs exposed to rhBMP-7 (by 98±18% for 50 ng/ml on the control). Unlike the raw pNP data, ALP activity was found to significantly increase with increasing rhBMP-7 concentrations. The ALP activity data were also found to be more consistent between different hMSC patients. Apparent pNP concentration and ALP activity were statistically significantly increased for the $Coat_{PBS}Scaff_{BMP\ 1.25}$ and $Coat_{BMP\ 1.25}Scaff_{BMP\ 1.25}$ scaffold groups for at least two patients, compared to the $Coat_{PBS}Scaff_{PBS}$ scaffolds (by 39±12% and 35±10% respectively) (see **Figure 6.5a** and **c**).

The apparent number of cells on the scaffolds was observed to decrease as the concentration of rhBMP-7 in the media was increased (by 25±5% for 50 ng/ml on the control) (see **Figure 6.5b**). The cell count was also significantly decreased for the $Coat_{PBS}Scaff_{PBS}$ scaffolds in OS media, compared to the control in OS-D, for two out of three patients (by an average of 18±4%). Although the cell counts were found to decrease in two of three patients for the $Coat_{BMP\ 1.25}Scaff_{PBS}$ scaffolds (by an average of 17±5% on the control), this trend was less pronounced for the $Coat_{PBS}Scaff_{BMP\ 1.25}$ and $Coat_{BMP\ 1.25}Scaff_{BMP\ 1.25}$ groups (by 9.5±4.2% and 4.8±3.3% on the control respectively).

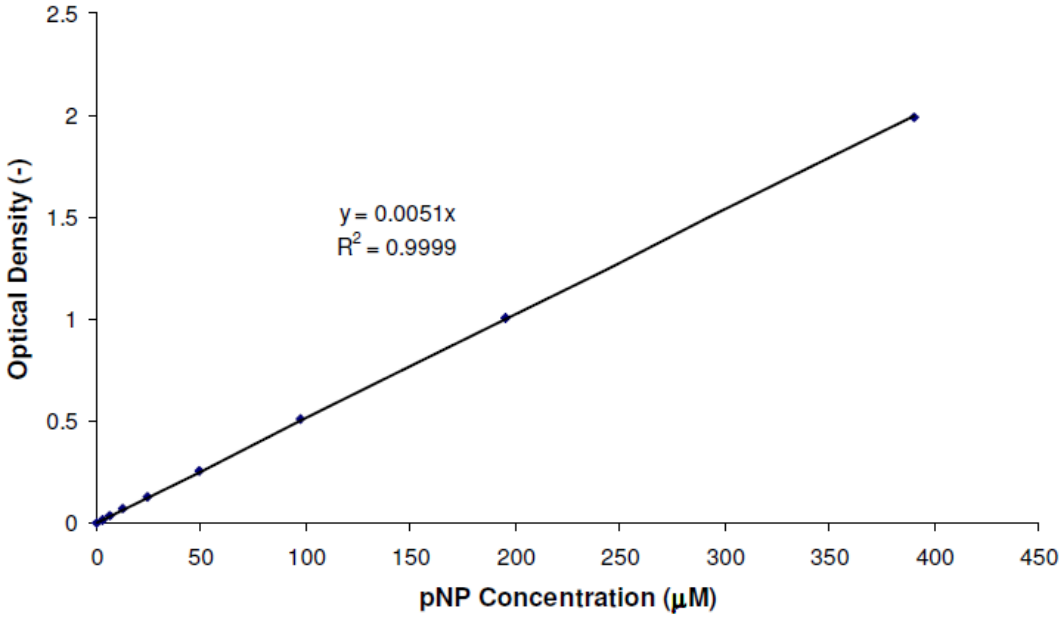

Figure 6.4: Optical density against pNP concentration.

A representative calibration curve, relating the optical density at 405 nm to the concentration of pNP. The resulting linear correlation was used to calculate unknown concentrations of pNP. Each data point represents the mean of two repeats.

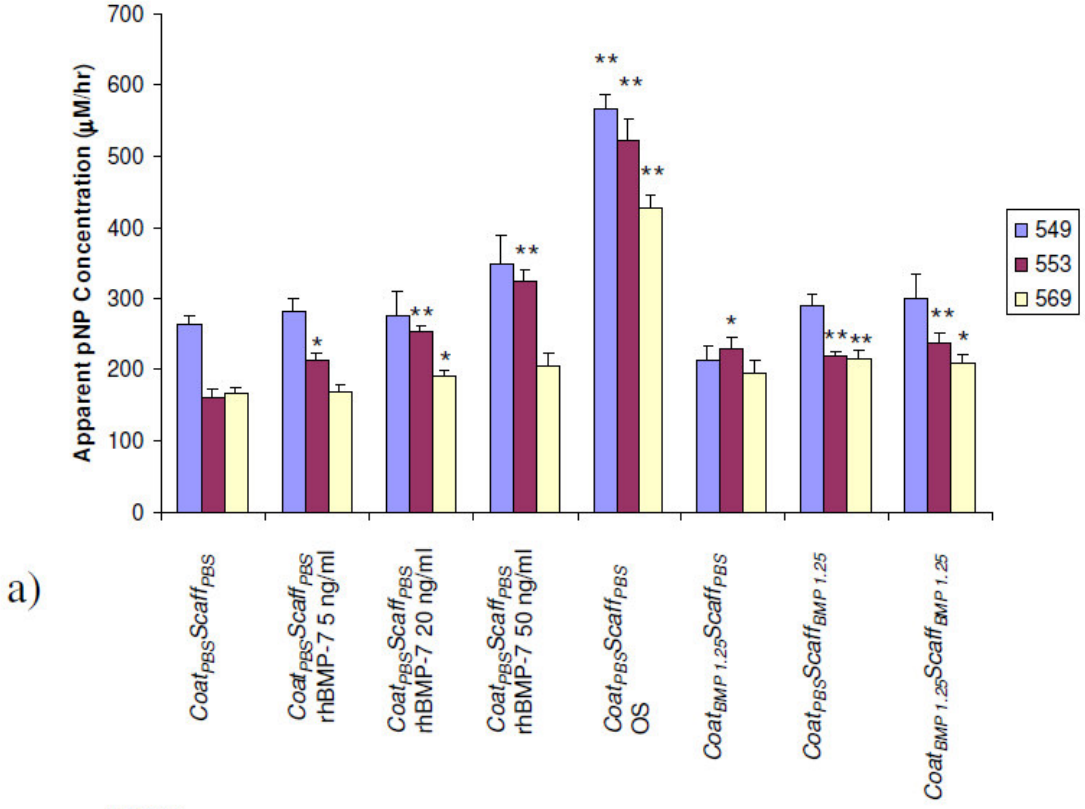
Apparent pNP Concentration (µM/hr)
700
600
500
400
300
200
100
0
549
553
569
$Coat_{PBS}Scaff_{PBS}$
$Coat_{PBS}Scaff_{PBS}$ rhBMP-7 5 ng/ml
$Coat_{PBS}Scaff_{PBS}$ rhBMP-7 20 ng/ml
$Coat_{PBS}Scaff_{PBS}$ rhBMP-7 50 ng/ml
$Coat_{PBS}Scaff_{PBS}$ OS
$Coat_{BMP\ 1.25}Scaff_{PBS}$
$Coat_{PBS}Scaff_{BMP\ 1.25}$
$Coat_{BMP\ 1.25}Scaff_{BMP\ 1.25}$

a)

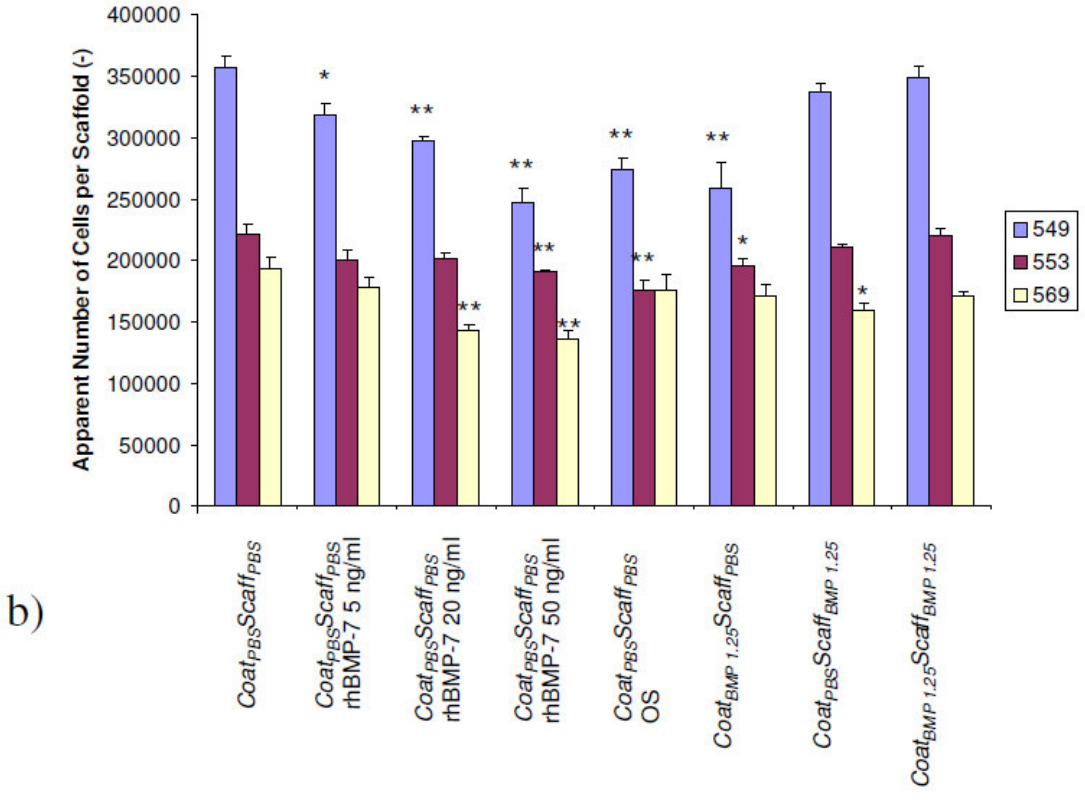
Apparent Number of Cells per Scaffold (-)
400000
350000
300000
250000
200000
150000
100000
50000
0
549
553
569
$Coat_{PBS}Scaff_{PBS}$
$Coat_{PBS}Scaff_{PBS}$ rhBMP-7 5 ng/ml
$Coat_{PBS}Scaff_{PBS}$ rhBMP-7 20 ng/ml
$Coat_{PBS}Scaff_{PBS}$ rhBMP-7 50 ng/ml
$Coat_{PBS}Scaff_{PBS}$ OS
$Coat_{BMP\ 1.25}Scaff_{PBS}$
$Coat_{PBS}Scaff_{BMP\ 1.25}$
$Coat_{BMP\ 1.25}Scaff_{BMP\ 1.25}$

b)

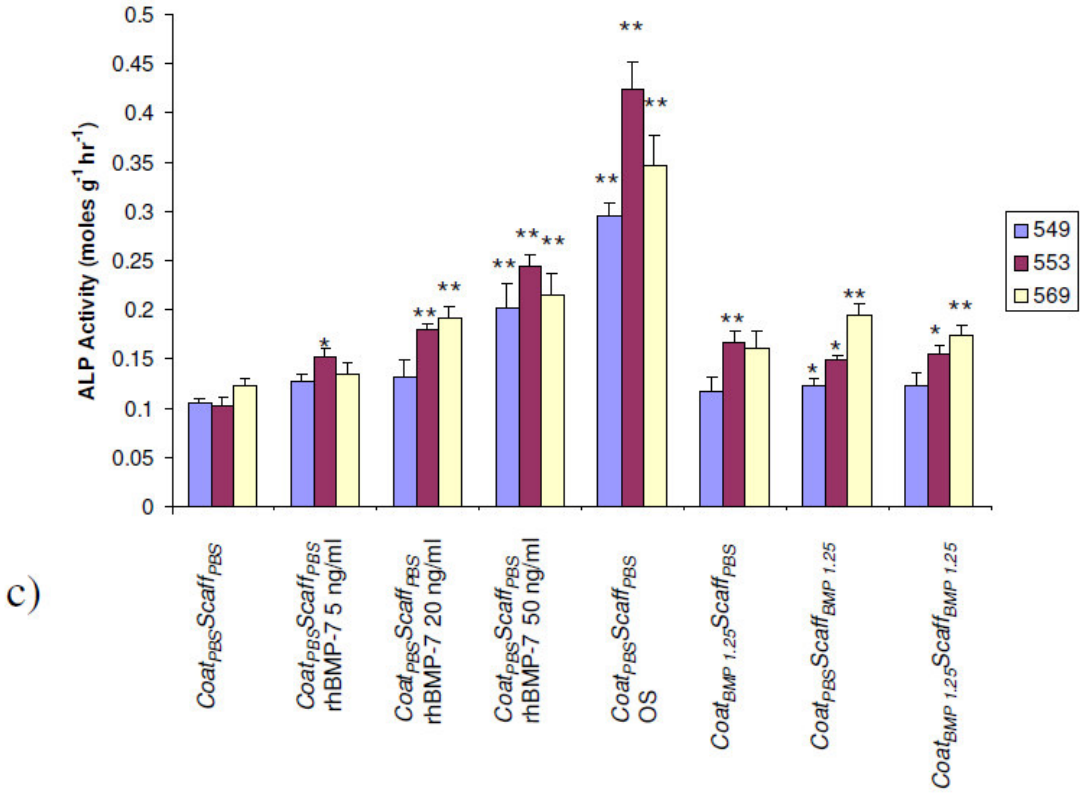

Figure 6.5: Results for the ALP/DNA assay.

The response of hMSCs seeded onto Type-I collagen coated PCL (M_n 42,500) scaffolds. Figure a) shows the apparent production of pNP, from pNPP, in the cell lysate. Figure b) shows the apparent number of cells on the scaffolds. Figure c) shows the apparent ALP activity of the cells, by normalising the pNP produced, by the mass of DNA in the cell lysate. * and ** denote $p < 0.05$ and 0.01 respectively, compared to the control $Coat_{PBS}Scaff_{PBS}$ group. The error bars represent the SEM, n = 6 in each case.

It should be noted that the concentrations of pNP and DNA for the "lysate" from the scaffolds devoid of cells, were below the detection limit of the assays. These data are therefore not shown.

6.5.3. Calcium Deposition on Scaffolds

In the range of calcium phosphate concentrations examined, a linear relationship between the concentration and the optical density at 540 nm, was found. A linear correlation was therefore calculated by linear regression. Unknown apparent calcium phosphate concentrations were calculated using this correlation (see **Figure 6.6**).

The data collected for the apparent mass of calcium phosphate were very similar, whether normalised against the mass of DNA in the cell lysate or not (see **Figure 6.7a** and **b**). Significant changes in apparent calcium phosphate levels were only observed for hMSC patient 549. For this patient, normalised apparent calcium phosphate deposition was significantly enhanced for the $Coat_{BMP\ 1.25}Scaff_{BMP\ 1.25}$ and especially the $Coat_{PBS}Scaff_{BMP\ 1.25}$ scaffold groups, compared to the $Coat_{PBS}Scaff_{PBS}$ control (by 290±140% and 1700±400% respectively). The $Coat_{BMP\ 1.25}Scaff_{PBS}$ groups were not associated with elevated calcium phosphate deposition for any of the hMSC patients tested.

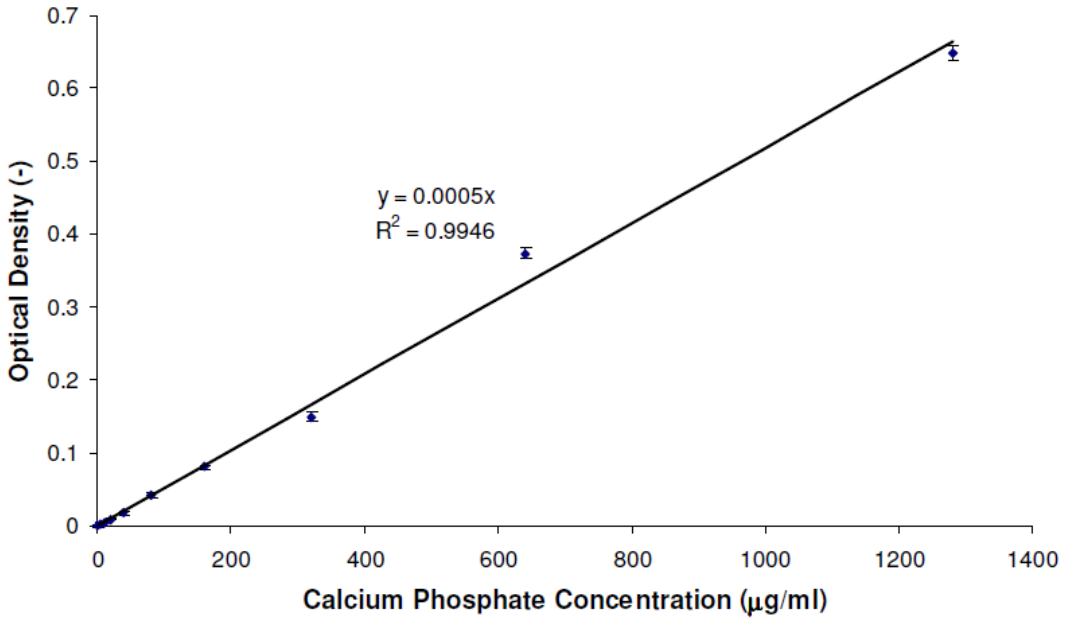

Figure 6.6: Optical density against calcium phosphate concentration.

The calibration curve, relating the optical density at 540 nm to the concentration of calcium phosphate. The resulting linear correlation was used to calculate unknown concentrations of calcium phosphate. Each data point represents the mean of two repeats.

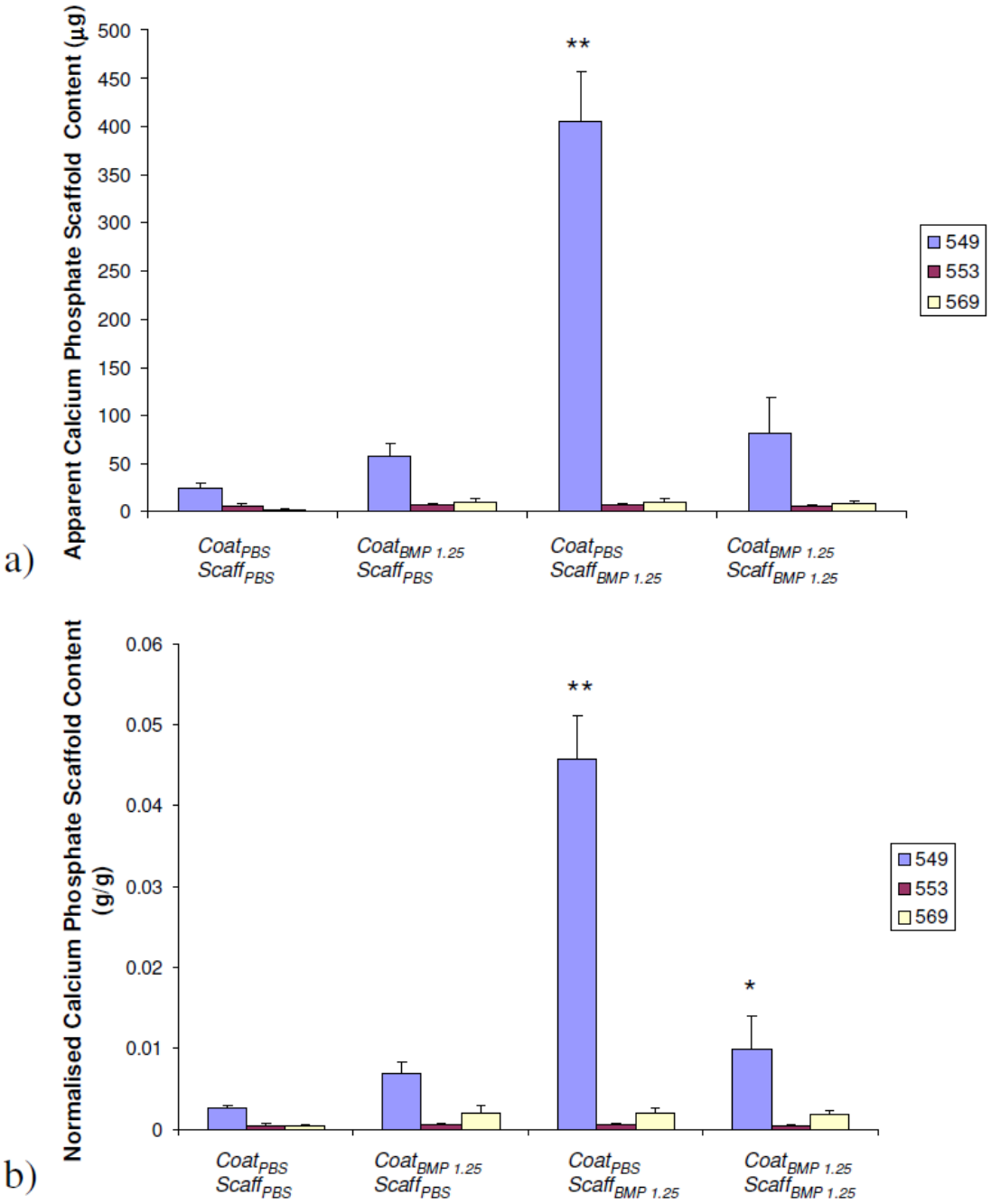

Figure 6.7: Results for the Calcium/DNA assay.

The response of hMSCs seeded onto Type-I collagen coated PCL (M_n 42,500) scaffolds. Figure a) shows the apparent deposition of calcium phosphate on the scaffolds. Figure b) shows the apparent calcium phosphate deposition, normalised against the mass of DNA in the cell lysate. * and ** denote $p < 0.05$ and 0.01 respectively, compared to the control $Coat_{PBS}Scaff_{PBS}$ group. The error bars represent the SEM, n = 6 in each case.

6.5.4. Scaffold Imaging

6.5.4.1. Electron Microscopy

Cell-like structures were observed on the surface of the $Coat_{BMP\ 1.25}Scaff_{BMP\ 1.25}$ (see **Figure 6.8a** and **b**). The morphology of the cells was observed to be rounded, and relatively few extended cell processes to the surface were observed. However, much of the scaffold's surface appeared to have been damaged by the sample preparation process (see **Figure 6.8c** and **d**). The majority of the surface was free from cell-like structures.

6.5.4.2. Light Microscopy

Using bright-field microscopy, positive ALP staining was observed on the scaffolds. This was particularly the case for the $Coat_{PBS}Scaff_{BMP\ 1.25}$ and $Coat_{BMP\ 1.25}Scaff_{BMP\ 1.25}$ groups (see **Figure 6.9**). It was noted that the positive ALP staining was observed spanning the "pores" of the scaffolds.

Using fluorescence microscopy, cell nuclei were observed to cover the surface of the scaffolds (see **Figure 6.10**). The cell density was found to be relatively high. Again cells were found to cover the span between the scaffold "pores".

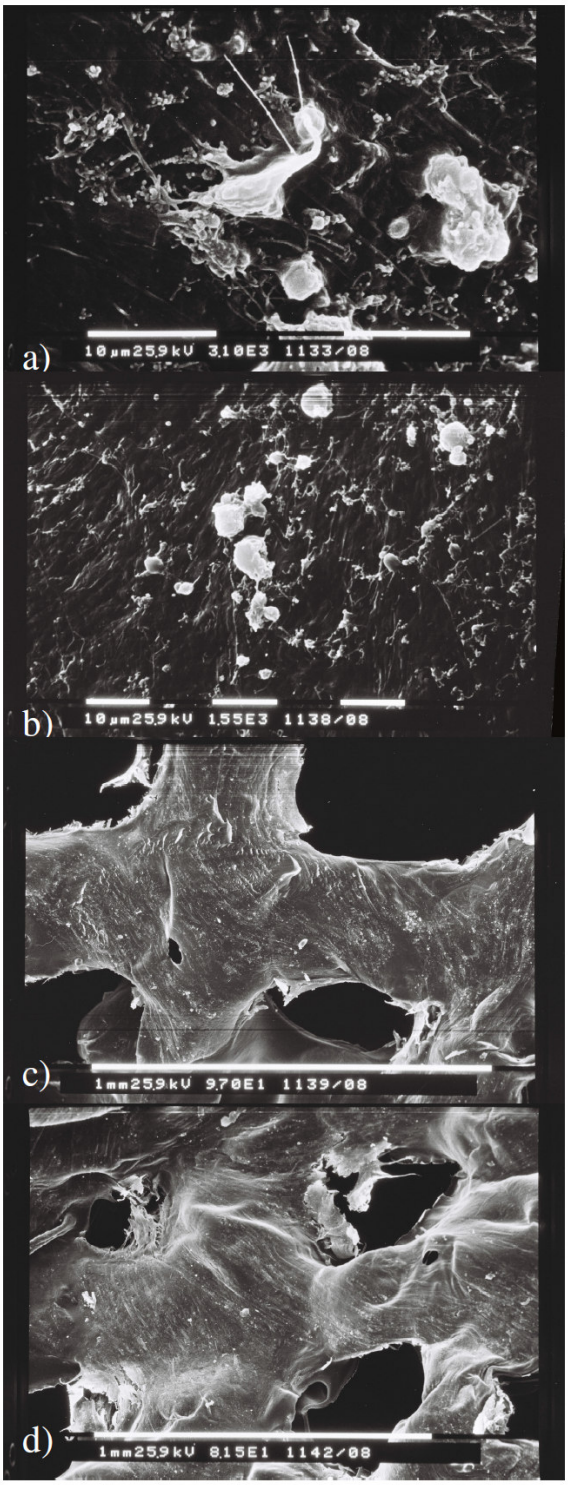

Figure 6.8: Electron microscope images of a scaffold.

Scanning electron microscope images of a $Coat_{BMP\ 1.25}Scaff_{BMP\ 1.25}$ Type-I collagen coated PCL (M_n 42,500) scaffold seeded with hMSCs from patient 569. Figures a) and b) depict high magnification images (the bars represent 10 µm). Figures c) and d) depict low magnification images (the bars represent 1 mm).

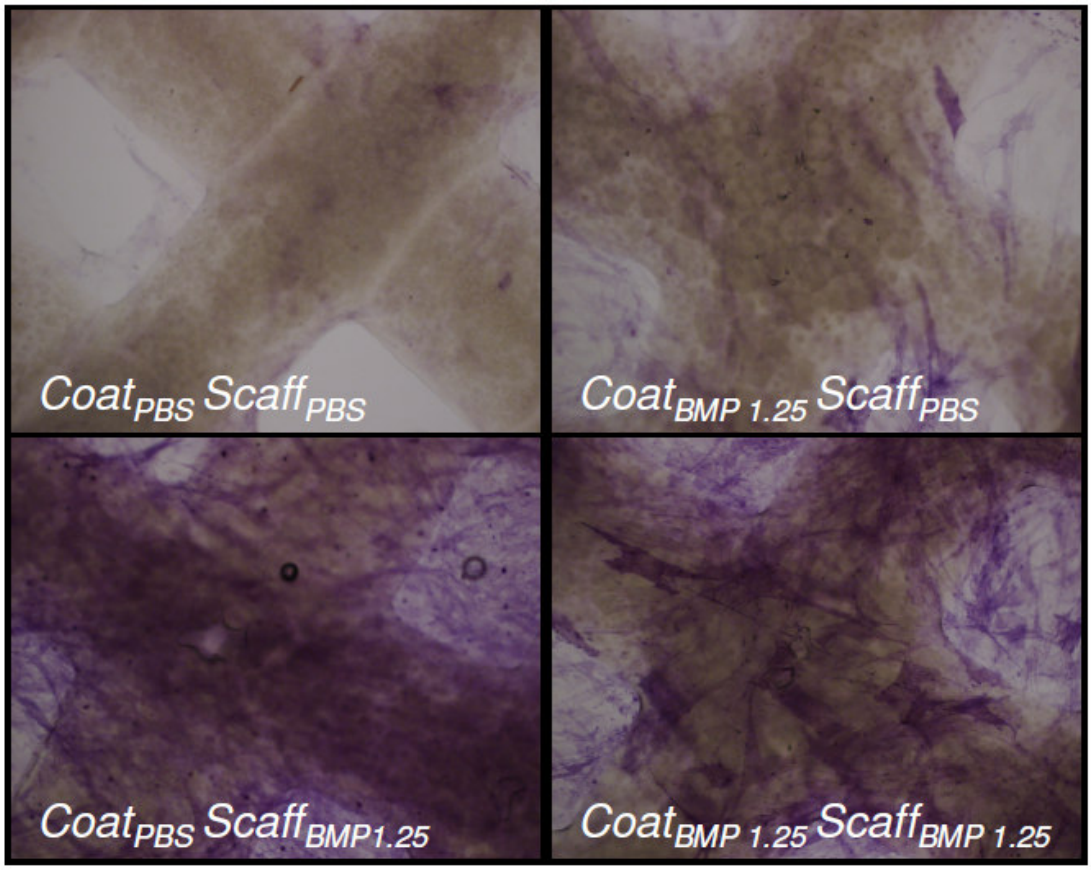

Figure 6.9: Bright-field images of ALP stained scaffolds.

Bright-field images of different Type-I collagen coated PCL (M_n 42,500) scaffolds seeded with hMSCs from patient 549, stained for ALP. The images were taken at × 10 magnification. The bar represents 500 µm.

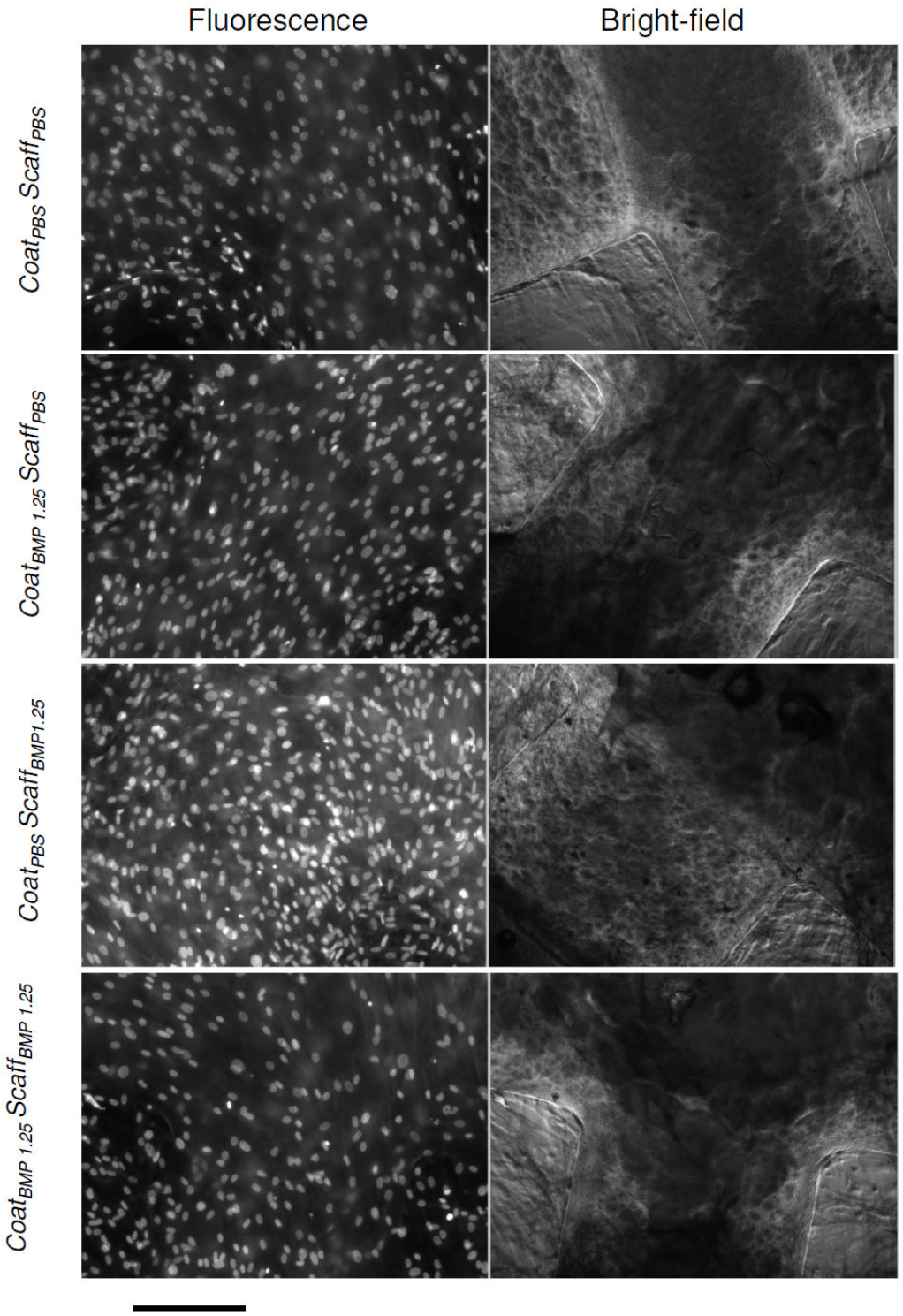

Figure 6.10: Fluorescence and bright-field images of scaffolds.

Fluorescence and corresponding bright-field images of different Type-I collagen coated PCL (M_n 42,500) scaffolds seeded with hMSCs from patient 549, and stained with DAPI. The images were taken at × 20 magnification. The bar represents 200 µm.

6.6. Discussion

The purpose of the studies described in this chapter was to assess the cell-scaffold interactions with scaffolds containing rhBMP-7. Although the studies described in previous chapters had investigated cell interactions with the Type-I collagen coating (Chapter 3), and with the rhBMP-7 released from the scaffolds (Chapter 5), the cellular response to these combined stimuli was unknown.

As discussed in §1.1.1.5, both ALP and calcium deposition are well established markers for osteogenic differentiation. These markers, along with a DNA assay to assess the number of cells per scaffold, were therefore quantitatively assessed to examine the extent of hMSC differentiation.

6.6.1. Number of hMSCs on the Scaffolds

In general, the apparent number of cells per scaffold was relatively high. For the hMSCs used in these experiments, the highest number of cells found in a confluent tissue culture flask (75 cm^2) was found to be approximately 1×10^6 (data not shown). This corresponds to an approximate cell density of 1.3×10^4 cells/cm^2. However, making the crude assumption that the surface area of the scaffolds was approximately 2 cm^2, the cell density varied from 6.8×10^4 and 1.8×10^5 cells/cm^2 on the scaffolds.

Even taking into account the likely error in the estimation of the scaffold surface area, the cell density was considerably higher than expected. However, the fluorescence images of DAPI stained cells on the scaffolds (see **Figure 6.10**) confirmed that the cell density was, indeed, high compared to TC plastic (see **Figure 3.3** and **Figure 3.11**). The results for the apparent number of cells per scaffold, displayed in **Figure 6.5b**, are therefore likely to be accurate. Coupled with the observation that the cells bridged the scaffold pores (see **Figure 6.10**), these data provide evidence that the scaffolds are relatively cell-compatible.

Meaningful comparison of the cell densities achieved with those previously reported for bone regenerative medical scaffolds is non-trivial. Many studies that quantify

cell densities fail to specify scaffold dimensions sufficiently for a fair comparison (Bjerre *et al.*, 2008; Holtorf *et al.*, 2005), use scaffolds with very different geometries (Dadsetan *et al.*, 2008), or do not report cell densities directly (Tsiridis *et al.*, 2007).

Li *et al.* (2005) seeded hMSCs at 250,000 cells/scaffold onto 1 cm^2 "mats" of electrospun PCL. The cells were cultured in media designed to induce chondrogenic differentiation. Approximately 1 µg of DNA was extracted per scaffold after 21 days, equating to approximately 140,000 cells/scaffold (using the correlation shown in **Figure 6.3b**). While the cell densities reported above (136,000 – 360,000 cells/scaffold) compare favourably with those measured by Li *et al.* (2005), the comparison is still not a fair one, as the culture conditions were different.

It was found that higher rhBMP-7 concentrations, OS media, and $Coat_{BMP\ 1.25}Scaff_{PBS}$ scaffold groups were associated with significant decreases in the apparent number of cells on the scaffolds, compared to the control (see **Figure 6.5b**). This could indicate increased differentiation of the hMSCs in these groups, as this is associated with decreased proliferation (Stein *et al.*, 2004).

6.6.2. Morphology of hMSCs on the Scaffolds

The morphology of the hMSCs on the scaffolds was to be assessed using scanning electron microscopy. However, due to the damage to the surface of the sample, accurate assessment of the cell morphology was not possible.

6.6.3. ALP Activity on Scaffolds

The purpose of examining the scaffolds using an ALP/DNA assay was to assess whether the scaffolds loaded with rhBMP-7 were capable of supporting the osteogenic differentiation of hMSCs seeded onto the scaffolds.

It should be noted that the photographic method for the assessment of the area of ALP staining, used in Chapter 5, could not be used in conjunction with scaffolds. This was because of the strong shadows cast by the scaffold struts.

It was found that the activity of ALP was significantly higher for the OS media groups compared to the $Coat_{PBS}Scaff_{PBS}$ in OS-D control, for all the hMSC patients tested (see **Figure 6.5c**). This indicated that the hMSCs from each patient were capable of osteogenic differentiation.

As was observed in Chapter 5, rhBMP-7 was associated with statistically significant increases in ALP activity for each patient (see **Figure 5.8** and **Figure 6.5a** and **c**). However, the data obtained in the current chapter were more consistent between patients, and revealed more pronounced differences between the groups than the data obtained in Chapter 5. It is possible that the ALP assay based on pNPP may be more sensitive than the photographic method, or the cells may respond differently when on the scaffolds for 21 days, rather than TC plastic for 14 days. However, there was more evidence for the latter hypothesis, as more pronounced differences in ALP staining were observed on the scaffolds than in the TC plastic wells (see **Figure 6.9** and **Figure 5.3**).

For the cells on the scaffolds, it was found that the rhBMP-7 concentration yielding the highest ALP activity was 50 ng/ml for each patient (**Figure 6.5a**). Indeed the higher the rhBMP-7 concentration, the higher was the observed ALP activity. Again this is in contrast to the data obtained in Chapter 5, where the cells were on a different substrate.

The $Coat_{BMP\ 1.25}Scaff_{BMP\ 1.25}$ and $Coat_{PBS}Scaff_{BMP\ 1.25}$ groups were associated with statistically significant increases in ALP activity, compared to the $Coat_{PBS}Scaff_{PBS}$ control scaffolds, for two and three hMSC patients respectively. These data imply not only that bioactive rhBMP-7 was released from these groups, but also that the doses were appropriate to induce a degree of osteogenic differentiation in the hMSCs. It should be noted that this is the first evidence presented in this thesis to support the hypothesis that the rhBMP-7 released from the $Coat_{PBS}Scaff_{BMP\ 1.25}$ scaffolds was bioactive.

In contrast, statistically significant increases in ALP activity were observed for only one hMSC patient for the $Coat_{BMP\ 1.25}Scaff_{PBS}$ scaffolds. Since it was known from the studies described in Chapter 5 that these scaffolds were capable of releasing bioactive rhBMP-7, this may be a result of a Type-II statistical error. It was, however, possible that the release profile of the growth factor from the scaffold coating may be unsuitable to encourage the osteogenic differentiation of the hMSCs on the scaffolds.

The ALP activity values were found to be between a factor of 10 (Bjerre *et al.*, 2008; Tsiridis *et al.*, 2007) and 10,000 (Dadsetan *et al.*, 2008; Moreau and Xu, 2009) lower compared to studies using animal MSCs or transformed hMSCs on scaffolds, cultured in osteogenic media. However, this was not a fair comparison, as the cell sources were different to the clinically relevant hMSCs used in the studies described in this chapter.

Due to the significant increases in ALP activity compared to the control scaffolds (see **Figure 6.5c**), it was concluded that the $Coat_{PBS}Scaff_{BMP\ 1.25}$ and $Coat_{BMP\ 1.25}Scaff_{BMP\ 1.25}$ scaffolds were able to support the osteogenic differentiation of primary hMSCs. Indeed the osteogenic effects of the encapsulating delivery system do not appear to be enhanced by the release of rhBMP-7 from the collagen coating. Potentially this leaves the coating delivery system available for the release of other active factors, such as VEGF, which could enhance *in vivo* bone formation, by stimulating angiogenesis. However, this is beyond the scope of the studies described in this thesis.

6.6.4. Calcium Deposition on Scaffolds

The purpose of examining the scaffolds using a calcium/DNA assay was to assess further whether the scaffolds loaded with rhBMP-7 were capable of supporting the osteogenic differentiation of hMSCs seeded onto them. This was assessed by quantifying matrix mineralisation.

The o-cresolphthalein complexone method, employed in the studies described in this chapter, was capable of quantifying calcium ions. However, it was unable to determine whether the ions detected originally formed part of calcium phosphate, let alone whether it was in the form of hydroxyapatite. Indeed, the most rigorous method of determining the presence of hydroxyapatite remains X-ray crystallography (Leventouri, 2006). Nevertheless, as discussed in §6.3, the o-cresolphthalein complexone method is commonly used to assess the mineral content of bone regenerative medical scaffolds. This may be due to its speed, simplicity, and repeatability.

Significant increases in the apparent mineral content of the scaffolds were only observed for cells from patient 549. It was noted that this patient was also associated with the lowest observed ALP activity of all the test patients. This was consistent with the cells from this patient having progressed further along the osteoblastic lineage to the point where ALP expression decreases as matrix mineralisation increases, as discussed in §1.1.1.5 (see **Figure 1.3**). However, these data do not support the hypothesis that the scaffolds loaded with rhBMP-7 were able to induce mineralisation in the hMSCs seeded on them.

It is interesting to note that $Coat_{BMP\ 1.25}Scaff_{BMP\ 1.25}$ scaffolds were associated with statistically significantly elevated levels of either ALP activity or calcium deposition in hMSCs from all the patients tested (see **Figure 6.5** and **Figure 6.7**). Taken together with the ALP studies, the data presented in the current chapter appear to support the hypothesis that $Coat_{BMP\ 1.25}Scaff_{BMP\ 1.25}$ scaffolds were able to support the osteogenic differentiation of clinically relevant hMSCs. However, it must be stressed that since calcium deposition was only significantly increased in one patient, these data do not support the hypothesis that the scaffolds loaded with rhBMP-7 were capable of increasing mineralisation in hMSCs.

Osteogenic differentiation of cells on the scaffolds was assessed with more rigour in Chapter 7. The expression of the osteogenic markers Type-I collagen, ALP,

osteopontin, osteocalcin and Runx2 was examined using quantitative reverse transcription polymerase chain reaction.

6.7. Conclusion

Combined ALP/DNA and calcium/DNA assays were used to assess whether the Type-I collagen coated PCL (M_n 42,500) scaffolds loaded with rhBMP-7, were capable of supporting the osteogenic differentiation of hMSCs, seeded onto them.

ALP activity was found to increase with increasing concentrations of rhBMP-7 in the range of concentrations tested (5, 20, and 50 ng/ml). ALP was also statistically significantly stimulated for the $Coat_{PBS}Scaff_{BMP\ 1.25}$ and $Coat_{BMP\ 1.25}Scaff_{BMP\ 1.25}$ scaffold groups. These data indicated that these scaffolds were capable of stimulating the osteogenic differentiation of hMSCs seeded onto them.

Levels of calcium deposition were only stimulated in the cells of one of the three hMSC patients tested. These data do not support the hypothesis that the rhBMP-7 loaded scaffolds tested were able to induce mineralisation in the hMSCs seeded on them.

The data collected in the studies described in this chapter suggest that the osteogenic effect of the encapsulation delivery system was not enhanced by the release from the coating. Therefore in the final "product" for clinical use, the coating delivery system might be better employed in the delivery of a different active factor.

Chapter 7 : Functional Assay

7.1. Scaffold Nomenclature

$Coat_{PBS}$	Collagen coating with PBS (rhBMP-7 control)
$Coat_{BMP\ 1.25}$	Collagen coating with rhBMP-7 (1.25 µg/ml)
$Scaff_{PBS}$	Scaffold encapsulating PBS (rhBMP-7 control)
$Scaff_{BMP\ 1.25}$	Scaffold encapsulating rhBMP-7 (1.25 µg/ml)

7.2. Abstract

The studies described in Chapter 6 investigated the reaction of human marrow stromal cells seeded onto scaffolds, loaded with recombinant human bone morphogenetic protein-7 (rhBMP-7). However this was only achieved by examining the activity of the enzyme alkaline phosphatase (ALP), and mineralisation. The current chapter describes cellular reaction to the scaffold in terms of the expression of genes associated with osteogenesis. This was done by exploring the expression of Type-I collagen (Col1), osteopontin (OP), ALP, osteocalcin (OC) and runt related transcription factor 2 (Runx2), by quantitative reverse transcription polymerase chain reaction (qRT-PCR). The cells selected for these studies were of the murine myoblast cell line C2C12.

C2C12 cells cultured on $Coat_{PBS}Scaff_{PBS}$ scaffolds, exposed to 200 ng/ml rhBMP-7 in the media, were found to upregulate OP, ALP, OC and Runx2 after 24 hr compared to the control (by 64±15%, 385±68%, 127±66%, and 76±43% respectively).

Similarly, the $Coat_{BMP\ 1.25}Scaff_{PBS}$ scaffolds, without rhBMP-7 in the media, were found to have an early osteoinductive effect on the C2C12 cells cultured on them. OP, ALP, OC and Runx2 were found to be statistically significantly up-regulated during the first 2 days only, compared to the control (*e.g.* by 44±12%, 128±42%, 60±25% and 46±25% respectively at the 24 hr mark).

The $Coat_{PBS}Scaff_{BMP\ 1.25}$ scaffolds also had an osteoinductive effect on the cells, which was more sustained than that observed for the $Coat_{BMP\ 1.25}Scaff_{PBS}$ group. While OP, ALP and Runx2 were up-regulated in the first 24 hr compared to the

control (by 38±10%, 208±82% and 72±31% respectively), statistically significant up-regulation of the late marker OC was delayed until the 48 hr mark (by 73±49%). The effect was found to be sustained until day 7, when OC and Runx2 were both statistically significantly up-regulated compared to the control (by 151±91% and 93±27% respectively).

The $Coat_{BMP\ 1.25}Scaff_{BMP\ 1.25}$ scaffolds were found to combine the early effect of the $Coat_{BMP\ 1.25}Scaff_{PBS}$ scaffolds, with the more sustained effect of the $Coat_{PBS}Scaff_{BMP\ 1.25}$ scaffolds. ALP, OC and Runx2 were all up-regulated at the 24 hr mark (by 312±56%, 329±39% and 96±25% respectively). This osteoinductive effect was sustained until day 7 when Col1, ALP and Runx2 were still up-regulated compared to the control (by 174±78%, 72±24% and 178±78% respectively).

These data suggest that the scaffolds containing rhBMP-7 have a weak osteoinductive effect on the cells seeded onto them. The different delivery systems were found to affect the cells differently. The clinical significance of this was not assessed in these studies.

7.3. Introduction

The purpose of the work described in Chapter 6 was to assess the reaction of human marrow stromal cells (hMSCs) to the scaffolds in terms of their ability to induce increased alkaline phosphatase expression and mineralisation. The purpose of the studies described in the current chapter was to assess the ability of the scaffolds to up-regulate the expression of genes associated with osteogenesis. This was achieved using quantitative reverse transcription polymerase chain reaction (qRT-PCR).

The cell type selected for these studies was the murine myoblast cell line C2C12. Though originally derived from murine muscle tissue (Yaffe and Saxel, 1977), previous studies have shown that the differentiation pathway can be shifted from myoblastic to osteoblastic in the presence of either recombinant human bone morphogenetic protein-2 (rhBMP-2) (Lee *et al.*, 1999; Katagiri *et al.*, 1994; Kim *et al.*, 2009) and -7 (rhBMP-7) (Gu *et al.*, 2004b; Yeh *et al.*, 2002; Tou *et al.*, 2003).

The genes of interest selected for the current study were; runt related transcription factor 2 (Runx2), Type 1 collagen (Col1), osteocalcin (OC), osteopontin (OP) and alkaline phosphatase (ALP). The transcription factor Runx2, also called core binding factor alpha1 (Cbfa1), has been found to be necessary for bone development in murine developmental models and is thought to be essential for osteoblastic differentiation (Komori *et al.*, 1997; Otto *et al.*, 1997). Indeed the expression of Runx2 has been described as being necessary and sufficient for osteoblast differentiation (Karsenty, 2003).

Runx2 is thought to act as a "master switch" during the commitment of mesenchymal stem cells to the osteoblastic lineage, and is expressed before the development of the osteoblastic phenotype (Ducy *et al.*, 1997). Expression of Runx2 also increases during osteoblast maturation (Banerjee *et al.*, 2001), and is present during the transdifferentiation of premuscle (C2C12) cells to the osteoblastic lineage (Lee *et al.*, 1999). It has also been found that calvarial-derived cells from mice with a mutated Runx2 locus, express ALP only weakly and lack expression of either osteopontin or osteocalcin. Examination of the skeletal system of such mice also shows a complete lack of mineralisation (Komori *et al.*, 1997). Runx2 has also been described as being the earliest transcription factor necessary for bone formation (Stein *et al.*, 2004).

Col1 expression is an early maker of osteoblastic differentiation and is first expressed by osteoprogenitor cells but not by MSCs (Liu *et al.*, 1994). Col1 is the most abundant protein in bone extracellular matrix. In both humans and mice, the gene Col1 α1(I) contains Runx2 binding sites (OSE2) in its promoter, suggesting it is up-regulated by the transcription factor Runx2 (Kern *et al.*, 2001).

The osteocalcin gene also contains a Runx2 binding site (OSE2) in its promoter (Ducy and Karsenty, 1995; Ducy *et al.*, 1997). It is one of the few genes thought to be specific to osteoblasts and odontoblasts (Desbois *et al.*, 1994). Osteocalcin is thought to play a role in mineralisation and calcium homeostasis, as well as being a marker of mature osteoblasts (Liu *et al.*, 1994).

Similarly, the osteopontin gene contains a Runx2 binding site in its promoter (Ducy *et al.*, 1997). It is thought to play a role in the anchoring of osteoclasts (Reinholt *et al.*, 1990), and serves as a marker of preosteoblasts (Liu *et al.*, 1994). OP is, however, not specific to osteoblasts, and it is also expressed in hypertrophied chondrocytes (Mark *et al.*, 1988; Nomura *et al.*, 1988).

Runx2 has also been found to up-regulate expression of ALP (Harada *et al.*, 1999), although it is possible that BMP-7 induction of ALP expression may be through the Wnt autocrine loop, as is thought to be the case with BMP-2 (Rawadi *et al.*, 2003). As previously discussed in §5.3, although ALP expression is not confined to bone tissue, it is commonly used in assays for osteogenesis. ALP mRNA expression is also a marker of immature osteoblasts, but is thought to occur later than osteopontin (Liu *et al.*, 1994).

In turn previous studies have demonstrated that rhBMP-7 increases the expression of Runx2 in C2C12 (Tou *et al.*, 2003; Gu *et al.*, 2004b). BMP-7 is thought to activate Smad1 and Smad5. This is in contrast to BMP-2 which activates Smad1, -5, and -8 (Aoki *et al.*, 2001). After BMP-7 binds to BMP receptor I or II, the receptor is thought to phosphorylate the receptor-regulated Smads (Smad-1 and -5), which in turn bind to the coSmad (Smad4) (Shen *et al.*, 2002) (see **Figure 7.1**). The resulting complex translocates to the nucleus, where it influences the expression of target genes including Dlx5, which in turn induces the expression of Runx2 (Miyama *et al.*, 1999; Lee *et al.*, 2003b).

During the studies described in this chapter, the osteogenic differentiation of C2C12 on Type-I collagen coated PCL (M_n 42,500) scaffolds, loaded with rhBMP-7, was investigated. This was achieved using qRT-PCR to quantify the up-regulation of genes associated with osteogenesis.

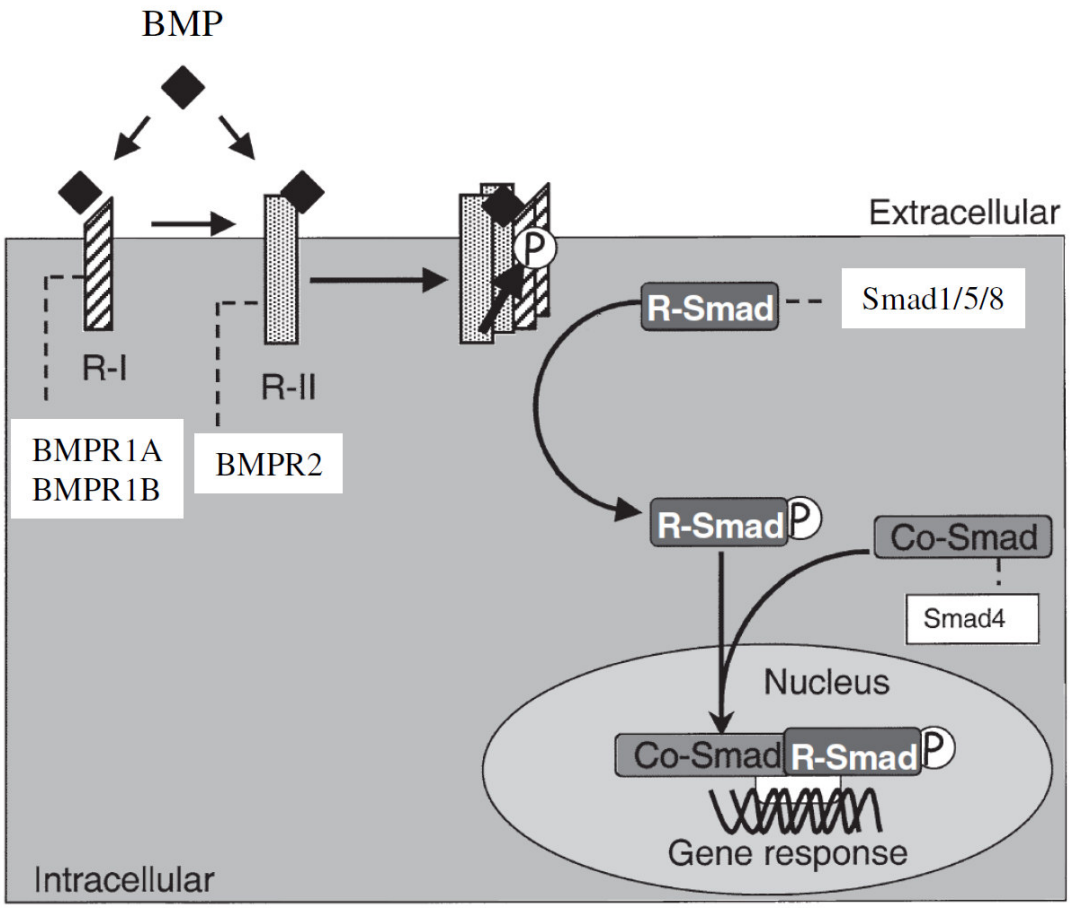

Figure 7.1: BMP Signal Transduction.

A cartoon representing BMP signal transduction. The binding of BMP-7 to BMP receptors I and II causes the phosphorylation of Smad 1 and Smad 5. These bind to Smad 4, and the resulting complex translocates to the nucleus where target genes are influenced (adapted from Roelen and Dijke (2003)).

7.4. Methods and Materials

Unless otherwise stated, all reagents were purchased from Sigma, UK. All techniques involving cell culture, described below, were conducted in a sterile environment, using sterile equipment. All consumables used during PCR procedures were certified as being RNAse free by the manufacturers.

7.4.1. C2C12 Culture

The murine myoblast cell line C2C12 (Yaffe and Saxel, 1977) was cultured as previously described by Gu *et al.*,(2004b). C2C12 cells were cultured in growth media (as described in §3.3.1), in tissue culture flasks (75 cm^2) (Corning, UK), incubated at 37°C with 5% (v/v) CO_2. The growth media was refreshed every 2 – 3 days. When the cells were 70% confluent, they were washed three times in phosphate buffered saline (PBS) (Oxoid, UK), and passaged by adding 1 ml of 2.5 mg/ml trypsin solution in PBS. After 10 min incubation at 37°C, 9 ml of growth media were added to each of the flasks. Then 1 ml of cell suspension was added to new tissue culture flasks (75 cm^2). An additional 9 ml of fresh growth media were then added to each new flask. The flasks were then incubated and refreshed with new growth media as before.

7.4.2. Primer Testing

Primers were purchased from Integrated DNA Technologies, UK. The sequences, which were obtained from previous studies, were as follows (see **Table 7.1**):

Table 7.1: Primer sequences for qPCR.

Gene	Sequence and reference
Runx2	5'-AGCCTCTTCAGCGCAGTGA-3' 5'-GTGCTCGGATCCCAAAAGAA-3' (Gu *et al.*, 2004b)
Type 1 Collagen	5'- TGCTTCTCCTGTCCCCTCTA-3' 5'- GGAAGATTTCAGGACCCACA-3' (Kim *et al.*, 2009)
Osteocalcin	5'- CTCACAGATGCCAAGCCCA-3' 5'- CCAAGGTAGCGCCGGAGTCT-3' (Capelo *et al.*, 2008)
Osteopontin	5'- TGCACCCAGATCCTATAGCC-3' 5'- TCCATCGTCATCATCATCGT-3' (Kim *et al.*, 2009)
Alkaline Phosphatase	5'- CCTAGTTATTGCCCTTTGGCC-3' 5'- TGCCTGCCCAAGAGAGAAA-3' (Gu *et al.*, 2004b)
Glyceraldehyde 3-phosphate dehydrogenase (GAPDH)	5'- ACTCCACTCACGGCAAATTC-3' 5'- TCTCCATGGTGGTGAAGACA-3' (Kim *et al.*, 2009)

7.4.2.1. RNA Extraction

It was desirable to determine a single annealing temperature suitable for all the primer pairs. A 70% confluent tissue culture flask (75 cm^2) of C2C12 cells (passage 18) was washed three times with PBS, and the cells were detached from the flask using trypsin and growth media as described in §7.4.1. The cell suspension was centrifuged (1,000 rpm for 5 min), the supernatant was discarded and the cell pellet was resuspended in 1 ml of TRIzol® Reagent (Invitrogen, UK). After 5 minutes of incubation at room temperature and mixing with a pipette, the sample was transferred

to a 1.5 ml eppendorf tube (Axygen, USA) with 200 µl of chloroform. The sample was vortexed for 15 seconds and incubated at room temperature for 3 min before centrifugation at 4°C for 15 min at 13,000 rpm (eppendorf centrifuge 5417R). The aqueous (upper) phase was carefully transferred into a new tube after which an equal volume of phenol/chloroform (1:1) was added. After vortexing for 15 seconds, the sample was centrifuged at 13,000 rpm for 3 min at room temperature.

The aqueous phase was transferred to a fresh tube with an equal volume of chloroform. After vortexing (15 seconds) the tube was again centrifuged at 13,000 rpm for 3 min at room temperature. Following the transfer of the aqueous phase to a fresh tube, an equal volume of isopropyl alcohol was added, before re-vortexing (15 seconds) and centrifugation (13,000 rpm for 50 min at 4°C).

The supernatant was removed and 800 µl of 70% ethanol were added. Following centrifugation (13,000 rpm at 4°C for 2 min) the supernatant was carefully removed, and the RNA pellet was air dried at room temperature for 5 min. The pellet was then dissolved in 50 µl of DEPC-treated water (Invitrogen, UK).

The concentrations of the RNA sample was measured using the NanoDrop™ 1000 (Thermo Scientific, UK). The 260/280 and 260/230 ratios, used to assess the purity of the nucleic acid, were recorded as 1.94 and 2.15. The RNA sample was then treated as described in §7.4.2.2.

7.4.2.2. Complementary DNA (cDNA) Synthesis

SuperScript™ III First-Strand Synthesis SuperMix for qRT-PCR (Invitrogen, UK) was used to synthesis the first strand of cDNA from the RNA templates. The reaction was set up as follows: 2X RT Reaction Mix (20 µl), RT Enzyme Mix (4 µl), RNA sample (1 µl), DEPC-treated water (15 µl).

After mixing, the reaction mixtures were incubated for 10 min at room temperature before being incubated at 50°C for 60 min then 85°C for 5 min. After cooling on ice for 5 min, 2 µl (4 U) of *E. coli* RNAse H were added before incubation at 37°C for 20 min. RT-PCR was then conducted on the sample.

7.4.2.3. RT-PCR

For each primer pair (see **Table 7.1**), 5 µl of both forward and reverse primers (10 nM) were added to 36 µl of DEPC-treated water (Invitrogen, UK). For each solution, 11.5 µl were added to fresh eppendorf tubes with 12.5 µl of Thermo-Start PCR Master Mix (Thermo Fisher Scientific) and either 1 µl of cDNA or 1 µl of DEPC-treated water (hereafter referred to as the non-template (NT) control). The reaction was then performed using an automatic DNA Thermal Cycler (Peltier Thermal Cycler, MJ Research PTC-200) at temperatures corresponding to the three steps of the reaction: denaturation, annealing and elongation. The reactions were run twice (for separate samples) using two different programs (see **Table 7.2**).

Table 7.2: Thermal cycler programs for RT-PCR.

Run 1			**Run 2**		
Temperature	**Time**	**Cycles**	**Temperature**	**Time**	**Cycles**
95°C	15 min	×1	95°C	15 min	×1
95°C	30 sec	} ×40	95°C	30 sec	} ×40
57°C	30 sec		59°C	30 sec	
72°C	15 sec		72°C	15 sec	
4°C	Forever*	×1	4°C	Forever*	×1

* The term "forever" denotes holding the samples at the specified temperature, until manual retrieval of the samples.

Afterwards, the PCR products were visualised and sized by agarose gel electrophoresis.

7.4.2.4. Agarose Gel Electrophoresis

The protocol used was previously described by Voultsiadou (2009). SeaKem GTG Agarose (FMC Bioproducts, USA) was dissolved in 100 ml of TBE Buffer (89 mM Tris Base, 89 mM Boric Acid, 2 mM EDTA) at 1.5 % (w/v). The mixture was heated in a microwave oven for approximately 2 min, until the agarose had dissolved. After cooling under running tap water, 5 µl ethidium bromide (10 mg/ml) were added prior to the gel being cast in a mould. When the gel had set, the

electrophoresis tank was filled with TBE buffer. 2.5 µl of Orange G loading dye (1% (w/v)) were added to each of the 25 µl samples prepared as described in §7.4.2.3. After vortexing, 10 µl were added per well in the gel. 100 volts were applied across the gel until the dye front had migrated two thirds from the end of the gel. Gels were visualised using a UV transilluminator (Uvidoc, UVItec, BTS-20-M). The product size was measured relative to size markers: 10 µl of Tracklt™ 100bp DNA ladders (Invitrogen) which were run alongside samples.

7.4.3. Scaffold Manufacture

Poly(ε-caprolactone) scaffolds containing or lacking rhBMP-7 (designated $Scaff_{BMP\ 1.25}$ and $Scaff_{PBS}$ respectively) were manufactured and coated with collagen either containing or lacking rhBMP-7 (designated with the prefixes $Coat_{BMP\ 1.25}$ and $Coat_{PBS}$ respectively) as described in §6.4.3.

7.4.4. C2C12 Culture on Scaffolds

After the quarter scaffolds, prepared as described in §7.4.3, were defrosted, they were individually placed at the bottom of the well of 48-well non-TC plastic plates (Corning, USA). Care was taken to ensure the scaffolds were flat against the bottom of the wells, and that they were held in place by the scaffolds corners' contact with the wells' sides. The number of $Coat_{PBS}Scaff_{PBS}$, $Coat_{BMP\ 1.25}Scaff_{PBS}$, $Coat_{PBS}Scaff_{BMP\ 1.25}$ and $Coat_{BMP\ 1.25}Scaff_{BMP\ 1.25}$ quarter scaffolds used was 27, 12, 12 and 12 respectively.

Tissue culture flasks (75 cm^2) containing 70% confluent C2C12 cells (passage 18), were washed three times in PBS, and the cells were detached from the flasks using 2.5 mg/ml trypsin in PBS (Invitrogen, UK) and growth media, as described in §3.3.1. The cell density of the suspensions was measured using a haemocytometer. The cells were centrifuged (1,000 rpm, 5 min) and resuspended in half-serum media [Dulbecco's Modified Eagle's Medium – high glucose (DMEM), supplemented with 5% (v/v) FCS (Autogen Bioclear, UK), L-glutamine (2 mM) (Gibco, UK), penicillin (100 IU/ml) and streptomycin (100 µg/ml) (Gibco, UK)], such that the final cell density was 4×10^5 cells/ml.

The cells were added to wells of the 48-well non-TC plastic plates, containing scaffolds. The cells seeded onto 12 of the $Coat_{PBS}Scaff_{PBS}$ scaffolds were supplemented with rhBMP-7 to a final concentration of 200 ng/ml. The remaining wells in the 48-well plates were filled with growth media to limit the rate of evaporation of media from the test wells. The plates were then maintained in a humidified air incubator at 37°C with 5% (v/v) CO_2.

After 4 hr, three of the $Coat_{PBS}Scaff_{PBS}$ scaffolds were removed from the wells and analysed for DNA content, as described in §7.4.6. On day 1, the media was removed from the wells, and wells were washed with PBS to remove non-adhered cells from the wells, before fresh media was added. After 24, 48 and 72 hr, three scaffolds from each group were processed as described in §7.4.5.1. On days 3 and 6, the media on the remaining scaffolds was refreshed before they were also processed as described in §7.4.5.1 after 168 hr (7 days).

7.4.5. qRT-PCR Analysis

7.4.5.1. RNA extraction from Scaffolds

The scaffolds to be processed were extracted from the wells of the 48-well plates and placed in 0.5 ml eppendorf tubes (Axygen, USA) with 200 µl TRIzol® Reagent. The samples were incubated for 5 min at room temperature. After mixing with a pipette, the liquid was extracted from the tubes and stored in fresh eppendorf tubes at -80°C.

RNA was then extracted from the samples as described in §7.4.2.1 with the modification that 40 µl of chloroform were added to each tube rather than 200 µl, since the sample volume was smaller. The RNA pellets were also resuspended in 20 µl of DEPC-treated water. 260/280 and 260/230 ratios were found using the NanoDrop™ 1000 Spectrophotometer. All the samples prepared for qRT-PCR analysis had 260/280 ratios greater than 1.80, and 260/230 ratios greater than their respective 260/280 ratios.

The cDNA was synthesised from the RNA samples as described in §7.4.2.2 with the modification that the reactions were set up as follows: 2X RT Reaction Mix (10 µl),

RT Enzyme Mix (2 µl), RNA sample (*x* µl), DEPC-treated water ([8 – x] µl). In this case, *x* was 8 µl when the RNA sample was 125 ng/µl or less, and adjusted such that 1 µg of RNA was added when the concentration was greater than 125 ng/µl. The samples were then diluted five-fold with water before storage at -80°C.

7.4.5.2. qRT-PCR

The cDNA samples described in §7.4.5.1 were analysed using qRT-PCR. Reaction mixtures were prepared for each primer pair as follows using materials from GoTaq® qPCR Master Mix kit (Promega, USA) : 39.8% Nuclease-Free Water, 55.6% GoTaq® Reaction mix, 2.2% forward primer, 2.2% reverse primer, 0.2% Reference Dye. 18 µl of the mixture was added to the wells of MicroAmp® Optical 96-well reaction plates (Applied Biosystems) along with 2 µl of cDNA samples.

The plates were subsequently analysed using a 7500 Fast Real-Time PCR System (Applied Biosystems) set to "Standard Runs" using the parameters described in **Table 7.3**. This was followed by dissociation steps. GAPDH was used as the endogenous control throughout.

Table 7.3: Thermal cycler programs for qRT-PCR.

Temperature	Time	Cycles
50°C	2 min	×1
95°C	10 min	×1
95°C	15 sec	×40
57°C	1 min	×40

The resulting data were analysed using the 7500 Fast Real-Time PCR Software 1.4.0.

7.4.6. DNA Assay

The scaffolds extracted from the wells 4 hr after cell seeding, as described in §7.4.4, were assayed for their DNA content as previously described in §6.4.6 and §6.4.6.1.

7.4.7. Statistical Analysis

All correlations were derived from calibration curves using Excel 2003. All correlations had R^2 values greater than 0.99. All other data were analysed using the statistical software package SPSS 14.0 for Windows.

Since three biological repeats were used for the qRT-PCR studies, parametric tests, such as one-way analysis of variance (ANOVA), were unsuitable. Hence, the nonparametric Kruskal-Wallis test was used to assess statistical significance for each data set. The statistical significance between the groups was found using the Mann-Whitney U test (Zar, 1984; Petrie and Sabin, 2005). $p < 0.05$ was considered to be statistically significant.

The mean was used throughout, and all results are expressed as the sample means ± standard error of the mean (SEM).

7.5. Results

7.5.1. Primer Testing

Photographs of the electrophoresis gels visualising the RT-PCR reactions run as described in §7.4.2.3 and §7.4.2.4, are shown in **Figure 7.2**. At both 57°C and 59°C, a single band of amplicons were found to have been produced for each primer pair. However, amplicons were found to be present in the NT control for the osteocalcin primer pair at 57°C (see **Figure 7.2a**). On increasing the temperature to 59°C, no bands were observed for the NT controls for any of the primer pairs (see **Figure 7.2b**). It was also found that the bands were consistent with the predicted product sizes.

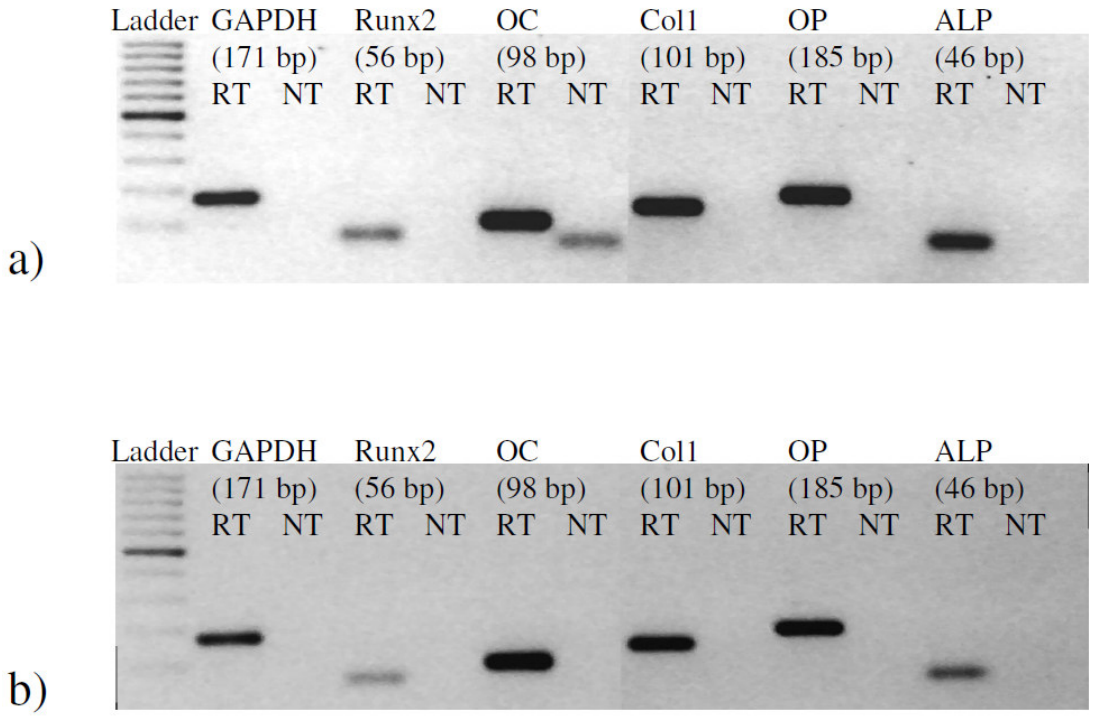

Figure 7.2: Electrophoresis Gels for Primer Testing

These figures represent electrophoresis gels, visualising the RT-PCR products derived from reaction temperatures of a) 57°C (note the presence of a band for the NT control for OC), and b) 59°C. The photographs are shown as negatives.

7.5.2. qRT-PCR Analysis

The dissociation curves for each primer pair are shown in **Figure 7.3**. For each primer pair, a single peak was observed. The melting temperature was found to be consistent between samples.

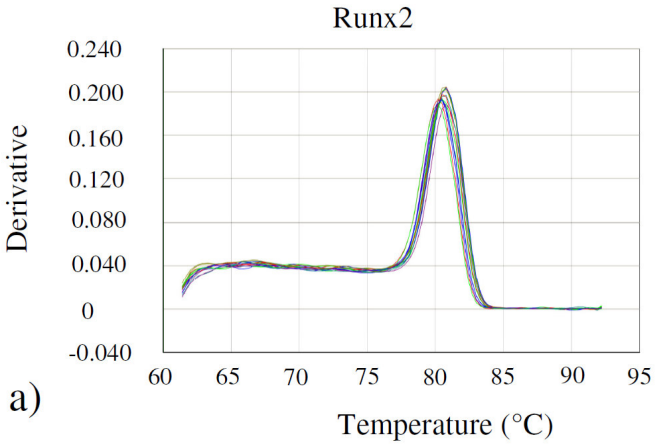
Runx2
Derivative
0.240
0.200
0.160
0.120
0.080
0.040
0
-0.040
60
65
70
75
80
85
90
95
Temperature (°C)

a)

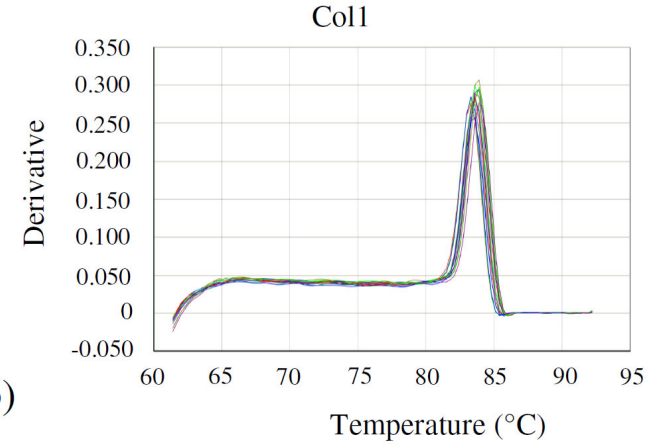
Col1
Derivative
0.350
0.300
0.250
0.200
0.150
0.100
0.050
0
-0.050
60
65
70
75
80
85
90
95
Temperature (°C)

b)

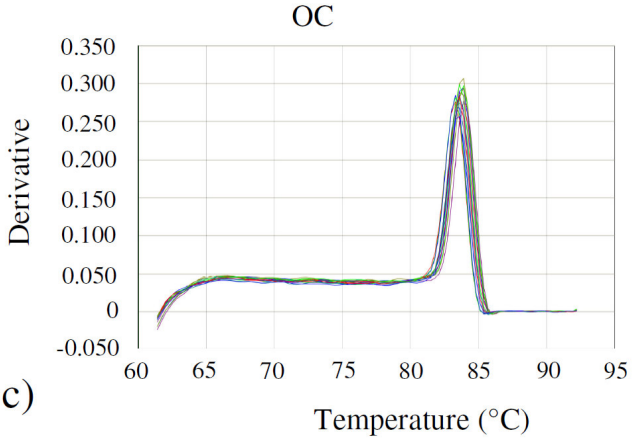
OC
Derivative
0.350
0.300
0.250
0.200
0.150
0.100
0.050
0
-0.050
60
65
70
75
80
85
90
95
Temperature (°C)

c)

d)

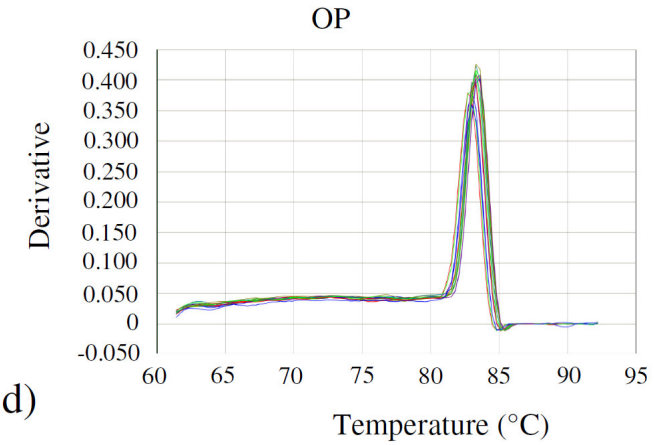
OP
Derivative
0.450
0.400
0.350
0.300
0.250
0.200
0.150
0.100
0.050
0
-0.050
60
65
70
75
80
85
90
95
Temperature (°C)

e)

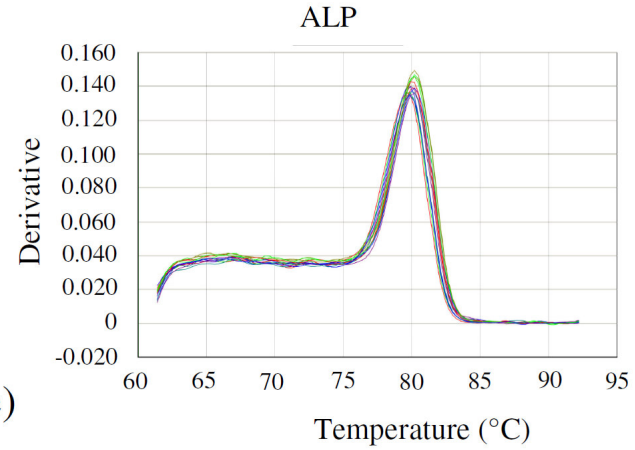
ALP
Derivative
0.160
0.140
0.120
0.100
0.080
0.060
0.040
0.020
0
-0.020
60
65
70
75
80
85
90
95
Temperature (°C)

f)

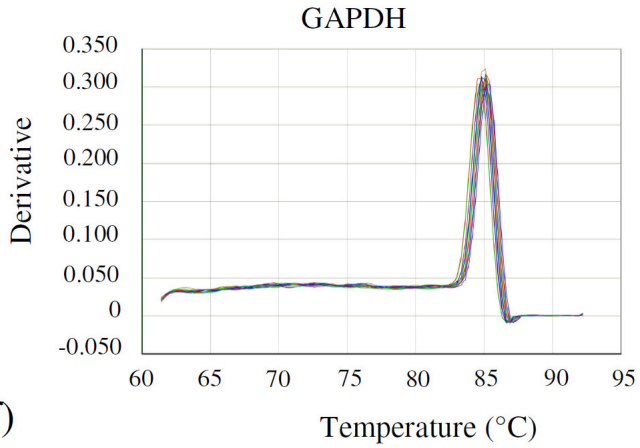
GAPDH
Derivative
0.350
0.300
0.250
0.200
0.150
0.100
0.050
0
-0.050
60
65
70
75
80
85
90
95
Temperature (°C)

Figure 7.3: Dissociation Curves

These figures represent typical dissociation curves of the amplicons produced during qRT-PCR reactions for the following target genes; a) Runx2, b) Col1, c) OC, d) OP, e) ALP, and f) GAPDH.

For Runx2, mRNA expression was statistically significantly increased compared to the $Coat_{PBS}Scaff_{PBS}$ controls in; the $Coat_{PBS}Scaff_{PBS}$ + rhBMP-7 group on day 1 (76±43%), the $Coat_{BMP\ 1.25}Scaff_{PBS}$ group on days 1 and 2 (46±25% and 19±10% respectively), the $Coat_{PBS}Scaff_{BMP\ 1.25}$ group on days 1, 2 and 7 (72±43, 28±8 and 93±27% respectively), and the $Coat_{BMP\ 1.25}Scaff_{BMP\ 1.25}$ group on days 1, 2 and 7 (96±25%, 35±13% and 178±78% respectively) (see **Figure 7.4a**). Runx2 expression in the $Coat_{PBS}Scaff_{PBS}$ group was also found to increase statistically significantly on day 3 (69±45%) and decrease on day 7 (49±7%) compared to day 1 (see **Figure 7.5a**).

Levels of mRNA expression of OC were found to be elevated statistically significantly compared to the $Coat_{PBS}Scaff_{PBS}$ controls in; the $Coat_{PBS}Scaff_{PBS}$ + rhBMP-7 group on day 1 (127±66%), the $Coat_{BMP\ 1.25}Scaff_{PBS}$ group on days 1 and 2 (60±25% and 236±98% respectively), the $Coat_{PBS}Scaff_{BMP\ 1.25}$ group on days 2 and 7 (73±49% and 151±91%) and the $Coat_{BMP\ 1.25}Scaff_{BMP\ 1.25}$ group on days 1 and 2 (329±39% and 244±67% respectively) (see **Figure 7.4b**). OC expression was also found to increase statistically significantly in the $Coat_{PBS}Scaff_{PBS}$ group on days 2, 3 and 7 compared to day 1 (287±55%, 1390±240% and 785±261% respectively) (see **Figure 7.5b**).

For ALP, mRNA expression was statistically significantly increased compared to the $Coat_{PBS}Scaff_{PBS}$ controls for; the $Coat_{PBS}Scaff_{PBS}$ + rhBMP-7 group on days 1 and 2 (385±68% and 100±36% respectively), the $Coat_{BMP\ 1.25}Scaff_{PBS}$ group on day 1 (128±42%), the $Coat_{PBS}Scaff_{BMP\ 1.25}$ group on day 1 (208±82%), and the $Coat_{BMP\ 1.25}Scaff_{BMP\ 1.25}$ group on days 1, 2 and 7 (312±56%, 82±29% and 72±24% respectively) (see **Figure 7.4c**). However it was decreased for the $Coat_{PBS}Scaff_{BMP\ 1.25}$ group on day 3 (37±13%). ALP mRNA expression was also found to increase statistically significantly for $Coat_{PBS}Scaff_{PBS}$ on days 3 and 7 compared to day 1 (490±134% and 128±32% respectively) (see **Figure 7.5c**).

OP expression was increased statistically significantly in the $Coat_{PBS}Scaff_{PBS}$ + rhBMP-7, $Coat_{BMP\ 1.25}Scaff_{PBS}$ and $Coat_{PBS}Scaff_{BMP\ 1.25}$ groups compared to the

$Coat_{PBS}Scaff_{PBS}$ control on day 1, and in the $Coat_{PBS}Scaff_{BMP\ 1.25}$ group on day 2, by 64±15%, 44±12%, 38±10% and 163±71% respectively (see **Figure 7.4d**). OP mRNA expression was also statistically significantly decreased in the $Coat_{BMP\ 1.25}Scaff_{BMP\ 1.25}$ on day 1 compared to the $Coat_{PBS}Scaff_{PBS}$ control by 40±6%.

It was found that mRNA expression of Col1 was increased statistically significantly for the $Coat_{PBS}Scaff_{BMP\ 1.25}$ and $Coat_{BMP\ 1.25}Scaff_{BMP\ 1.25}$ groups compared to the $Coat_{PBS}Scaff_{PBS}$ control on days 2 and 7 respectively by 72±29% and 174±78% (see **Figure 7.4e**). Col1 was also found to decrease statistically significantly for $Coat_{PBS}Scaff_{PBS}$ on day 7 compared to day 1 (by 86±3%) (see **Figure 7.5e**).

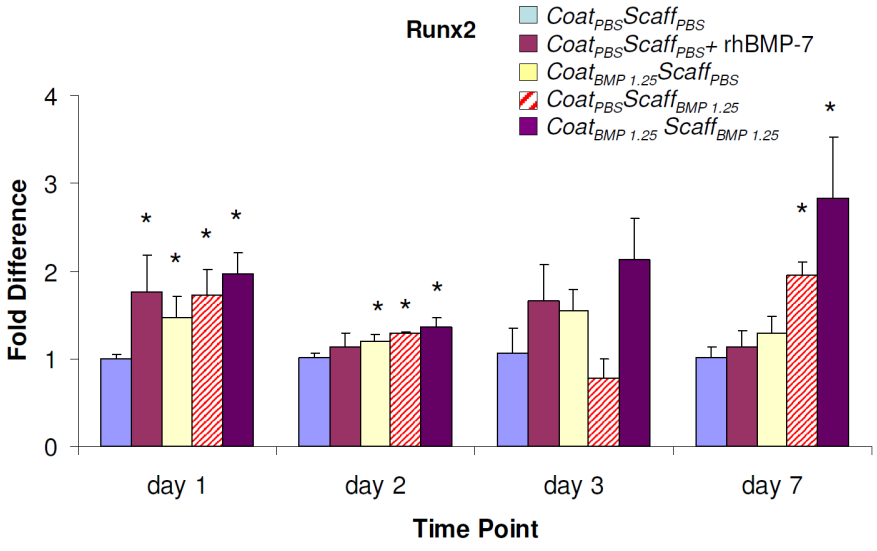
Runx2
$Coat_{PBS}Scaff_{PBS}$
$Coat_{PBS}Scaff_{PBS}$+ rhBMP-7
$Coat_{BMP\ 1.25}Scaff_{PBS}$
$Coat_{PBS}Scaff_{BMP\ 1.25}$
$Coat_{BMP\ 1.25}\ Scaff_{BMP\ 1.25}$
Fold Difference
0
1
2
3
4
day 1
day 2
day 3
day 7
Time Point

a)

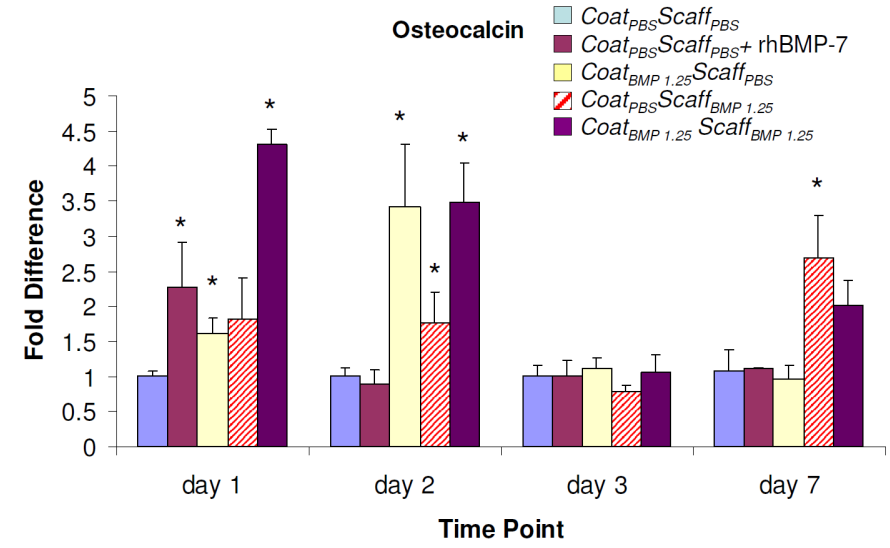
Osteocalcin
$Coat_{PBS}Scaff_{PBS}$
$Coat_{PBS}Scaff_{PBS}$+ rhBMP-7
$Coat_{BMP\ 1.25}Scaff_{PBS}$
$Coat_{PBS}Scaff_{BMP\ 1.25}$
$Coat_{BMP\ 1.25}\ Scaff_{BMP\ 1.25}$
Fold Difference
0
0.5
1
1.5
2
2.5
3
3.5
4
4.5
5
day 1
day 2
day 3
day 7
Time Point

b)

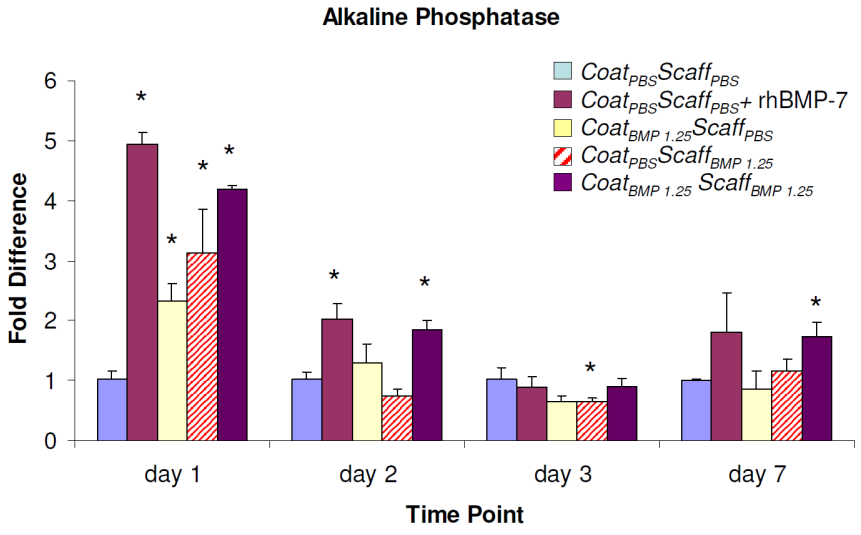
Alkaline Phosphatase
$Coat_{PBS}Scaff_{PBS}$
$Coat_{PBS}Scaff_{PBS}$+ rhBMP-7
$Coat_{BMP\ 1.25}Scaff_{PBS}$
$Coat_{PBS}Scaff_{BMP\ 1.25}$
$Coat_{BMP\ 1.25}\ Scaff_{BMP\ 1.25}$
Fold Difference
0
1
2
3
4
5
6
day 1
day 2
day 3
day 7
Time Point

c)

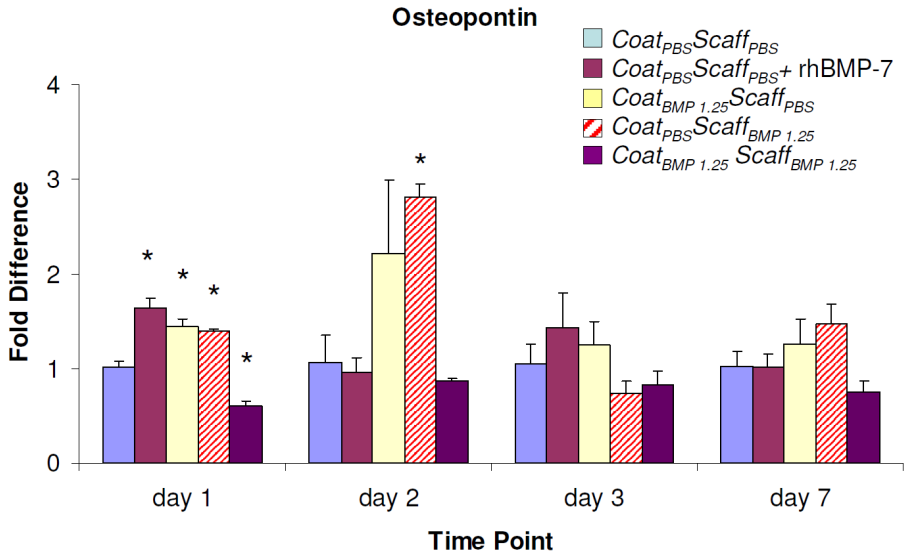

d)

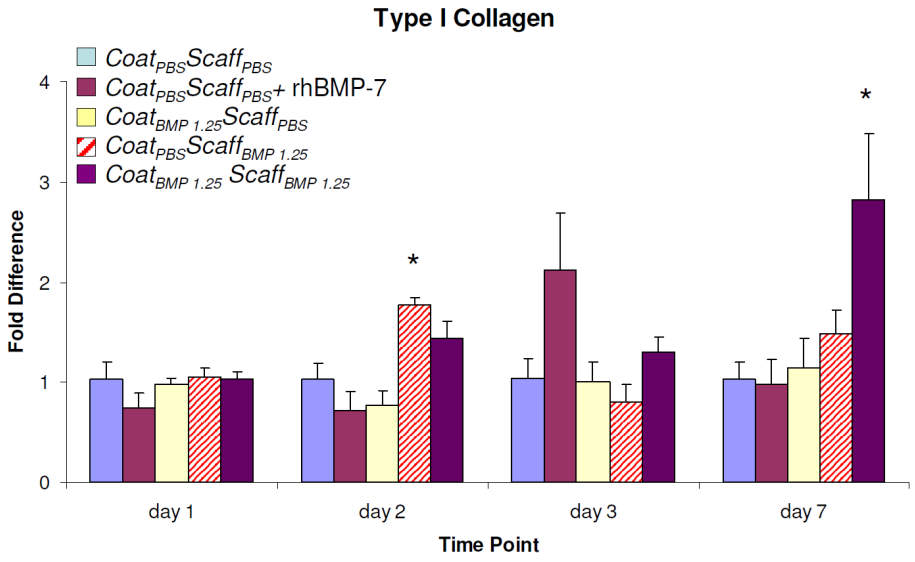

e)

Figure 7.4: Gene expression in C2C12 cells cultured on scaffolds.

These figures represent the fold change, compared to the *Coat$_{PBS}$Scaff$_{PBS}$* controls, in mRNA expression of genes associated with osteogenesis for C2C12 cells cultured on Type-I collagen coated PCL (M_n 42,500) scaffolds. The relative expression was assessed by qRT-PCR, using GAPDH as the endogenous control. The target genes were; a) Runx2, b) OC, c) ALP, d) OP, and e) Col1. * denotes $p < 0.05$ compared to the *Coat$_{PBS}$Scaff$_{PBS}$* control for the same time point. The error bars represent the SEM, n = 3 in each case.

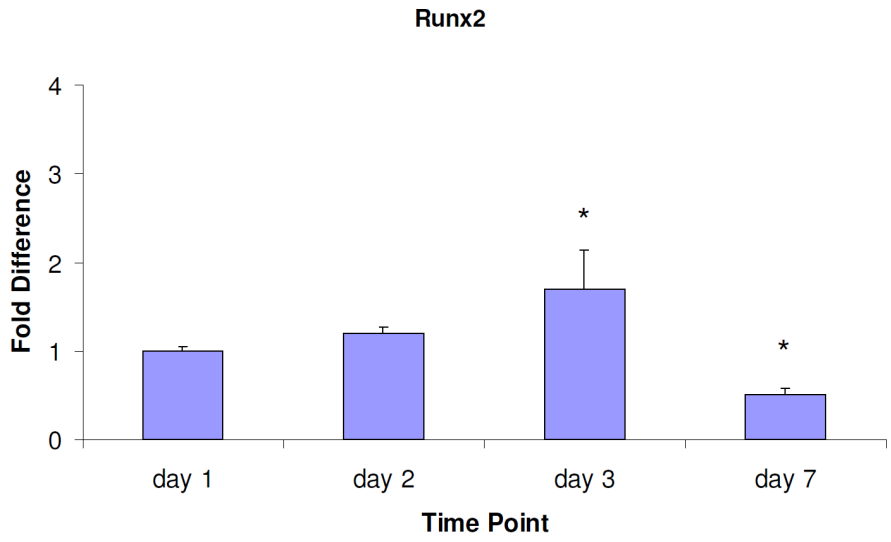
Runx2
Fold Difference
4
3
2
1
0
*
*
day 1
day 2
day 3
day 7
Time Point

a)

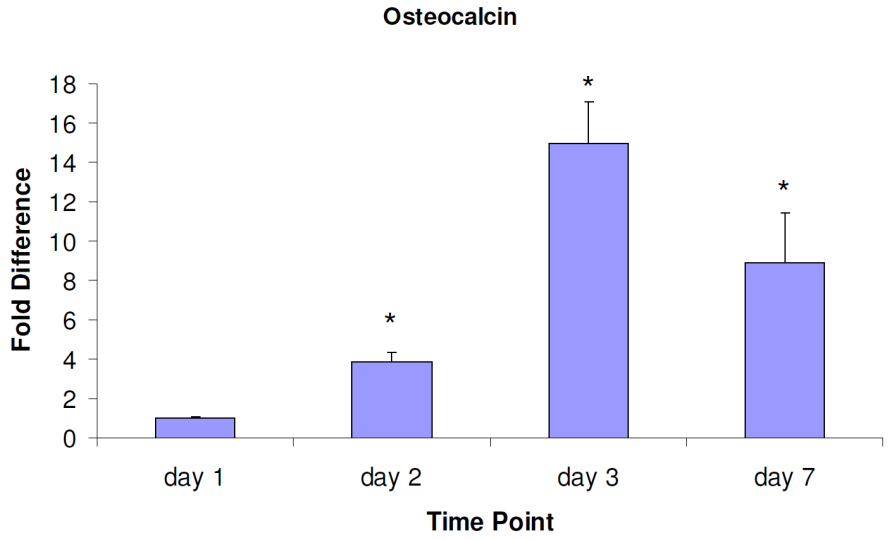
Osteocalcin
Fold Difference
18
16
14
12
10
8
6
4
2
0
*
*
*
day 1
day 2
day 3
day 7
Time Point

b)

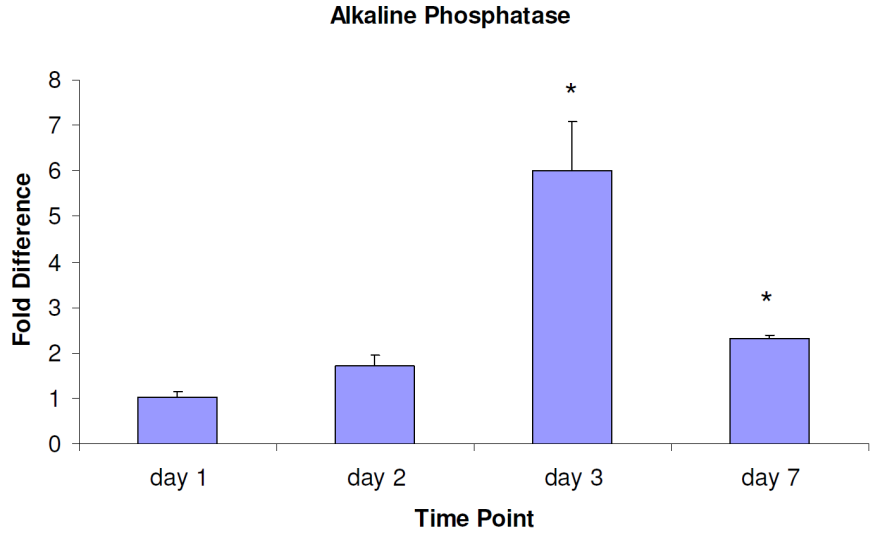
Alkaline Phosphatase
Fold Difference
8
7
6
5
4
3
2
1
0
*
*
day 1
day 2
day 3
day 7
Time Point

c)

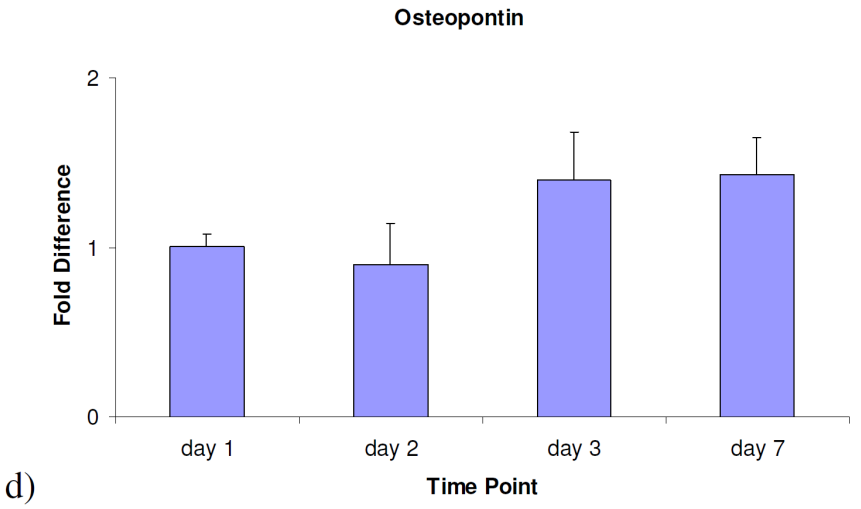

d)

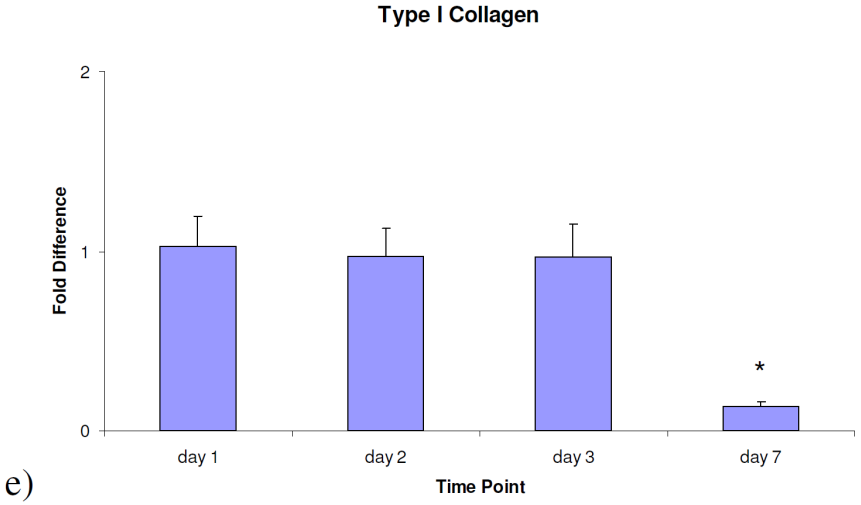

e)

Figure 7.5: Gene expression in C2C12 cells cultured on control scaffolds.

These figures represent the fold change, compared to the $Coat_{PBS}Scaff_{PBS}$ day 1 control, in mRNA expression of genes associated with osteogenesis for C2C12 cells cultured on Type-I collagen coated PCL (M_n 42,500) scaffolds. The relative expression was assessed by qRT-PCR, using GAPDH as the endogenous control. The target genes were; a) Runx2, b) OC, c) ALP, d) OP, and e) Col1. * denotes $p < 0.05$ comparing the $Coat_{PBS}Scaff_{PBS}$ controls to the $Coat_{PBS}Scaff_{PBS}$ day 1 control. The error bars represent the SEM, n = 3 in each case.

7.5.3. DNA Assay

Using calibration curves similar to those shown in **Figure 6.3a** and **Figure 6.3b**, the number of C2C12 cells successfully seeded into the $Coat_{PBS}Scaff_{PBS}$ scaffolds was 67,700±12,000 cells. This corresponds to a seeding efficiency of 42±8%.

7.6. Discussion

7.6.1. Primer Testing

By electrophoresis, it was determined that an annealing temperature of 59°C was sufficiently high for primer dimers not to form for each of the primer pairs (see **Figure 7.2b**). At 59°C, single bands were formed at approximately the same sizes as the predicted fragment lengths. Taking this evidence together with the single peaks observed for each primer pair during qRT-PCR (see **Figure 7.3**), it was concluded that the primer pairs were specific for the target genes of interest.

7.6.2. DNA Assay

A previous study investigating the differentiation of C2C12 cells using rhBMP-7, conducted by Gu *et al.*,(2004b), seeded the cells as 2×10^4 cells/cm^2 24 hr before exposure to the growth factor. The doubling time of C2C12 cells has previously been reported as being approximately 19 hr (Pisani *et al.*, 2004), hence the cell density at T0 is likely to have been approximately 4.8×10^4 cells/cm^2.

Making the crude assumption that the upper surface area of the scaffolds was 1 cm^2, the cell density at T0 used in the studies described this chapter was $(6.77 \pm 0.12) \times 10^4$ cells/cm^2 on the scaffolds. This is, therefore, comparable to the T0 cell density used in the C2C12 differentiation studies reported by Gu *et al.*,(2004b).

7.6.3. qRT-PCR Analysis

Previous studies have examined the ability of rhBMP-7 to shift the differentiation pathway from myoblastic to osteoblastic. In these studies, rhBMP-7 at 200 ng/ml in the culture media was sufficient for this shift in differentiation pathway (Gu *et al.*,

2004b; Tou *et al.*, 2003; Yeh *et al.*, 2002). Hence, this concentration of rhBMP-7 was chosen as a positive control.

Runx2 is thought to be another specific marker for osteogenesis, as this transcription factor has been described as the "master switch" for osteogenesis (see §7.3). Runx2 was found to be up-regulated statistically significantly for the rhBMP-7 positive control, in the first 24 hr period only, compared to the negative $Coat_{PBS}Scaff_{PBS}$ control (see **Figure 7.4a**). Gu *et al*. (2004b) found that Runx2 was up-regulated in C2C12 cells after 24 hr of exposure to rhBMP-7. However, the effect appeared to be damped on the $Coat_{PBS}Scaff_{PBS}$ scaffolds: 1.76±0.42 fold difference as opposed to the 5.5 fold difference observed by Gu *et al*. (2004b). Nevertheless, the observation by Gu *et al*. (2004b) that Runx2 expression in response to rhBMP-7 was transient, and peaked compared to the control at approximately the 24 hr mark, was repeated for the cells on the $Coat_{PBS}Scaff_{PBS}$ scaffolds (see **Figure 7.4a**).

A weak but nevertheless statistically significant up-regulation in Runx2 was observed for all the scaffold groups containing rhBMP-7, compared to the $Coat_{PBS}Scaff_{PBS}$ controls, on days 1 and 2 (see **Figure 7.4a**). A more sustained effect was found for the $Coat_{PBS}Scaff_{BMP\ 1.25}$ and $Coat_{BMP\ 1.25}Scaff_{BMP\ 1.25}$ groups, as statistically significant up-regulation of Runx2 was observed on day 7. This provides evidence that all the scaffold groups loaded with rhBMP-7 had an osteoinductive effect on the C2C12 cells.

It is interesting to note that Runx2 expression was increased statistically significantly in the $Coat_{PBS}Scaff_{PBS}$ control group on day 3 compared to day 1 (see **Figure 7.5a**), possibly indicating that the base $Coat_{PBS}Scaff_{PBS}$ scaffolds had a weak osteogenic effect on the C2C12 cells with no rhBMP-7 present. However, this effect appears to be relatively short-lived, as a slight but statistically significant decrease was observed on day 7. Alternatively, since these effects are relatively slight, they could have occurred as a result of Type-I statistical errors.

Osteocalcin is thought to be a specific marker of mature osteoblasts, see §7.3. OC was found to be up-regulated statistically significantly for the rhBMP-7 positive control, in the first 24 hr period only, compared to the negative $Coat_{PBS}Scaff_{PBS}$ control (see **Figure 7.4b**). Gu *et al*. (2004b) similarly found OC was up-regulated in C2C12 cells after 24 hr of exposure to rhBMP-7. However, again the effect observed in the current study (2.3±1.1 fold difference) was weaker than that observed by Gu *et al*. (2004b) (approximately 55 fold) in similar culture conditions, on tissue culture plastic. Again, it is possible that the $Coat_{PBS}Scaff_{PBS}$ scaffolds damped the effects of the rhBMP-7.

OC was up-regulated early for the $Coat_{BMP\ 1.25}Scaff_{PBS}$ and $Coat_{BMP\ 1.25}Scaff_{BMP\ 1.25}$ groups compared to the $Coat_{PBS}Scaff_{PBS}$ controls. Statistically significant increases were observed on days 1 and 2, whereas the up-regulation of OC for the $Coat_{PBS}Scaff_{BMP\ 1.25}$ group, relative to the $Coat_{PBS}Scaff_{PBS}$ controls, appeared to occur later: on days 2 and 7. Again, this provides evidence that all the scaffold groups loaded with rhBMP-7 had an osteoinductive effect on the C2C12 cells.

Again, the base $Coat_{PBS}Scaff_{PBS}$ scaffolds appeared to have a weak osteogenic effect on the C2C12 cells, as OC expression was statistically significantly increased in the $Coat_{PBS}Scaff_{PBS}$ control group on days 2, 3 and 7 compared to day 1 (see **Figure 7.4b**). No increase in OC was observed under similar culture conditions on tissue culture plastic (Katagiri *et al.*, 1994; Lee *et al.*, 1999).

As discussed above in §7.3, ALP is a marker of immature osteoblasts that is thought to be expressed later than OP. ALP was found to be up-regulated statistically significantly for the rhBMP-7 positive control, in the first and second 24 hr periods compared to the negative $Coat_{PBS}Scaff_{PBS}$ control (see **Figure 7.4c**). The trend was similar to that observed in previous studies. However, the 4.9±0.4 fold increase in ALP expression was relatively weak when compared to the 350 fold increase observed in C2C12 cells exposed to rhBMP-7 observed by Gu *et al*. (2004b).

All scaffold groups containing rhBMP-7 showed weak but statistically significant increases in ALP expression at the 24 hr mark, compared to the $Coat_{PBS}Scaff_{PBS}$ control. This effect was most sustained in the $Coat_{BMP\ 1.25}Scaff_{BMP\ 1.25}$ group, with statistically significant increases in ALP expression also occurring on days 2 and 7. Again, this provides evidence that all the scaffold groups loaded with rhBMP-7 had an osteoinductive effect on the C2C12 cells.

As with Runx2 and OC, there was a slight but statistically significant up-regulation in ALP expression on days 3 and 7 compared to the $Coat_{PBS}Scaff_{PBS}$ group, compared to day 1 (see **Figure 7.5c**). It should also be noted that previous studies have reported no significant increases in ALP expression under similar culture conditions in tissue culture plastic (Katagiri *et al.*, 1994; Lee *et al.*, 1999). Again, this provides some evidence that the base $Coat_{PBS}Scaff_{PBS}$ scaffolds may have a weak osteogenic effect on the C2C12 cells.

Osteopontin, as discussed in §7.3, is an early marker of osteogenesis. OP was found to be up-regulated statistically significantly for the rhBMP-7 positive control, in the first 24 hr period only, compared to the negative $Coat_{PBS}Scaff_{PBS}$ control (see **Figure 7.4d**). Again, few studies have examined the expression of this gene in C2C12 cells in response to rhBMP-7. However this result was consistent with the findings of previous studies where osteoblastic differentiation of C2C12 cells exposed to rhBMP-7 was observed to begin in the first 24 hrs (Gu *et al.*, 2004b).

Similarly, OP was up-regulated in the $Coat_{BMP\ 1.25}Scaff_{PBS}$ and $Coat_{PBS}Scaff_{BMP\ 1.25}$ groups. This observation is consistent with the hypothesis that these scaffolds had an osteoinductive effect on the cells. Again, it should be noted that the up-regulation of OP was relatively weak when compared to other studies such as those of Huang *et al.* (2004), where OP was up-regulated in rabbit MSCs by a factor of approximately 50-fold. Interestingly, OP was statistically significantly down-regulated in the $Coat_{BMP\ 1.25}Scaff_{BMP\ 1.25}$ compared to the $Coat_{PBS}Scaff_{PBS}$ control. It was possible that differentiation could be more advanced in this group, as OP is thought to be down-regulated as osteoblastic differentiation progresses (Stein *et al.*, 2004).

As discussed in §7.3, Col1 is an early marker of osteoblastic differentiation and is first expressed by osteoprogenitor cells. For both the positive and negative controls, no consistent trend in the data on Col1 expression was observed for days 1, 2 and 3 (see **Figure 7.4e**). However, Col1 appeared to be down-regulated in all the groups tested on day 7 (see **Figure 7.4e** and **Figure 7.5e**). Potentially, this down-regulation could be caused by the progress of osteogenic differentiation. Alternatively, the fall in Col1 expression in all the groups could be explained by the onset of myogenic differentiation. Indeed previous studies by Alexakis *et al.* (2007) found that expression of Col1 decreased as C2C12 cells underwent myogenic differentiation. Potentially this hypothesis is more likely, as C2C12 cells are known to undergo spontaneous myogenic differentiation (Yaffe and Saxel, 1977; Gu *et al.*, 2004b).

Col1 expression has been largely neglected in studies involving C2C12 cells and rhBMP-7, nevertheless Yeh *et al*. (2002) reported a weak increase in Col1 gene expression in response to rhBMP-7. However, in their case, a different substrate was used, potentially affecting the outcome.

Small, but statistically significant increases in Col1 expression were observed in the $Coat_{PBS}Scaff_{BMP\ 1.25}$ and $Coat_{BMP\ 1.25}Scaff_{BMP\ 1.25}$ groups on days 2 and 7 respectively. This provides some evidence that these scaffolds had a weak osteoinductive effect on the C2C12 cells. It should be noted, however, that this effect was relatively weak when compared to studies such as those reported by Huang *et al.* (2004) in which rabbit MSCs seeded onto PLGA scaffolds, exposed to rhBMP-2, were found to up-regulate the expression of Col1 by approximately 140 fold after 7 days.

In general, the data indicate that the $Coat_{BMP\ 1.25}Scaff_{PBS}$ group had a weak osteoinductive effect on the C2C12 cells early on, indicating that a portion of the rhBMP-7 released from the Type-I collagen coating was bioactive, and capable of having a functional effect on the C2C12 cells. ALP was found to be up-regulated on day 1, and OC and Runx2 expression was elevated on days 1 and 2. However, none of the markers were up-regulated from day 3 onwards. These observations are

consistent with the data described in §4.5.3, where the release of rhBMP-7 from the $Coat_{BMP\ 1.25}Scaff_{PBS}$ scaffolds was relatively rapid.

The weak osteoinductive effect on the C2C12 cells for the $Coat_{PBS}Scaff_{BMP\ 1.25}$ scaffolds occurred later, and was more sustained than for the $Coat_{BMP\ 1.25}Scaff_{PBS}$ scaffolds. Indeed, statistically significant up-regulation of the late osteogenic marker OC did not occur until day 2 for the $Coat_{PBS}Scaff_{BMP\ 1.25}$ group. This occurred on day 1 for the $Coat_{BMP\ 1.25}Scaff_{PBS}$ scaffolds. Additionally, Runx2 and OC were both statistically significantly upregulated on day 7, indicating a more sustained effect than the $Coat_{BMP\ 1.25}Scaff_{PBS}$ scaffolds, where no up-regulation was observed. Again, these data are consistent with that found in §4.5.3, where the release of rhBMP-7 from the $Coat_{PBS}Scaff_{BMP\ 1.25}$ scaffolds was less rapid, and relatively more sustained than for the $Coat_{BMP\ 1.25}Scaff_{PBS}$ scaffolds. These data also provide further evidence that a portion of the released rhBMP-7 was bioactive, and was capable of having a functional effect on the C2C12 cells.

The $Coat_{BMP\ 1.25}Scaff_{BMP\ 1.25}$ group combined the early effect of the $Coat_{BMP\ 1.25}Scaff_{PBS}$ scaffolds, with the more sustained effect observed for the $Coat_{PBS}Scaff_{BMP\ 1.25}$ scaffolds. Expression of Runx2, ALP and OC were all elevated at the 24 hr timepoint. However a sustained effect was also evident, as Col1, ALP and Runx2 were all statistically significantly elevated on day 7 compared to the $Coat_{PBS}Scaff_{PBS}$ control. Again, these data provide further evidence that a portion of the rhBMP-7 released from the $Coat_{BMP\ 1.25}Scaff_{BMP\ 1.25}$ was bioactive, and was capable of having a functional effect on the C2C12 cells.

Although there were differences in the osteogenic effects the rhBMP-7 loaded scaffold groups had on the C2C12 cells, the differences may not be of clinical significance and would need to be evaluated further.

7.7. Conclusion

The functional osteoinductive capacity of Type-I collagen coated PCL (M_n 42,500) scaffolds loaded with rhBMP-7 was assessed using C2C12 cells seeded onto the scaffolds, and quantified using qRT-PCR. The genes of interest were; Type-I collagen, osteopontin, alkaline phosphatase, osteocalcin and Runx2. Similar to the findings of previous studies (Gu *et al.*, 2004b; Tou *et al.*, 2003; Yeh *et al.*, 2002), rhBMP-7 was found to up-regulate the expression of genes associated with osteogenesis in C2C12 cells when cultured on base $Coat_{PBS}Scaff_{PBS}$ scaffolds.

The $Coat_{BMP\ 1.25}Scaff_{PBS}$ scaffolds had an early osteoinductive effect on the C2C12 cells, as ALP, OC and Runx2 were elevated during the first 2 days only. These data indicate that the collagen coating delivery system was suitable for the early release of bioactive growth factors, capable of having a functional effect on the cells seeded onto the scaffolds.

The data collected for the $Coat_{PBS}Scaff_{BMP\ 1.25}$ scaffolds, showed that this group was capable of a more delayed and sustained osteoinductive effect on the cells. The late osteogenic marker, OC, was only elevated after 2 days, however Runx2 and OC were both statistically significantly upregulated on day 7. These data indicate that the encapsulating delivery system was also capable of releasing bioactive growth factors which had a more sustained functional effect than the coating delivery system.

Finally, the $Coat_{BMP\ 1.25}Scaff_{BMP\ 1.25}$ group appeared to combine the early effect of the $Coat_{BMP\ 1.25}Scaff_{PBS}$ scaffolds, with the more sustained effect observed for the $Coat_{PBS}Scaff_{BMP\ 1.25}$ scaffolds. Runx2, ALP and OC were all elevated at the 24 hr mark, however after 7 days, up-regulation of Col1, ALP and Runx2 was still evident. These data provide further evidence to the findings described in Chapter 6, that the two delivery systems are mutually compatible in their ability to release bioactive growth factors. However, the difference in the effects of the two delivery systems may not be of clinical significance.

Chapter 8 : General Conclusions and Further Work

8.1. Scaffold Nomenclature

$Coat_{PBS}$	Collagen coating with PBS (rhBMP-7 control)
$Coat_{BMP\ 0.63}$	Collagen coating with low rhBMP-7 dose (0.63 µg/ml)
$Coat_{BMP\ 1.25}$	Collagen coating with high rhBMP-7 dose (1.25 µg/ml)
$Coat_{ethanol}$	Collagen coating with ethanol ($1,25(OH)_2D_3$ control)
$Coat_{1,25(OH)2D3}$	Collagen coating with $1,25(OH)_2D_3$
$Scaff_{PBS}$	Scaffold encapsulating PBS (rhBMP-7 control)
$Scaff_{BMP\ 0.63}$	Scaffold encapsulating low rhBMP-7 dose (0.63 µg/ml)
$Scaff_{BMP\ 1.25}$	Scaffold encapsulating high rhBMP-7 dose (1.25 µg/ml)
$Scaff_{ethanol}$	Scaffolds encapsulating ethanol ($1,25(OH)_2D_3$ control)
$Scaff_{1,25(OH)2D3}$	Scaffolds encapsulating $1,25(OH)_2D_3$

8.2. General Conclusions

Fracture non-unions and bone defects represent a recalcitrant problem in the field of orthopaedic surgery. Although the current gold-standard treatment, autologous bone grafting, has a relatively high success rate, the technique is not without problems. These include; limited donor bone supply and quality, and the possibility of substantial morbidity at the donor site. The emerging field of regenerative medicine may have the potential to provide an alternative treatment.

A number of growth factors, operating at different times, are believed to regulate many of the events crucial to normal bone fracture healing. Therefore the delivery, to the defect site, of both cells and multiple growth factors with different release profiles, may be required for a successful artificial bone graft substitute. However, a satisfactory delivery system for achieving this has yet to be developed. The studies described in this thesis report the development of novel scaffolds and their subsequent testing for their potential to fulfil these functions with regard to potential application in bone regenerative medicine, by testing the following thesis hypothesis: *It is possible to manufacture cell-compatible scaffolds, with sufficient porosity for the diffusion of cellular nutrients and waste products, incorporating two delivery systems, each capable of releasing a bioactive growth factor with clinically*

significantly different release profiles. It was concluded that the data reported in this thesis did not confirm the hypothesis.

A range of scaffolds was developed from poly(ε-caprolactone) (PCL) (M_n 42,500 and 80,000), poly(lactide-co-glycolide) (PLGA) and two blends of PCL (M_n 42,500) and PLGA. The scaffolds were manufactured utilising a novel modified fused deposition modelling (FDM) system, based on polymer/dichloromethane (DCM) solutions processed using a Bioplotter™. The PCL (M_n 42,500) scaffolds were found to have a pore diameter of 373±9.5 μm in the Y-direction, and 460±13 μm in the X-direction. Previous studies have found that scaffolds with pore diameters ranging from 96 – 350 μm were capable of being pervaded with fluids in bioreactor systems (Jungreuthmayer *et al.*, 2008), and Robinson *et al.* (1995) found that in the size range 100 – 350 μm, the largest pore size allowed the most bone ingrowth. Indeed, Karageorgiou and Kaplan (2005) found that pore sizes greater than 300 μm in diameter favoured vascular ingrowth and intramembranous ossification. The scaffold pore sizes were therefore thought to be suitable for bone regenerative medical applications. The remaining scaffolds were observed to possess a similar architecture. Five scaffold coatings were also developed from alginate, chitosan, Type-I collagen and Type-A gelatin. Each scaffold coating was found not to interfere with the scaffold porosity.

The scaffolds were found to be only 52±3 μm in height, whereas the strand thicknesses were found to be 444±3.5 μm and 353±9.7 μm in the X and Y-directions respectively. This means that the two-layer scaffolds were relatively flat. It was found that 3D geometry was difficult to fabricate using the process developed in §2.4.1.1.1 and §2.4.1.1.2. This was undesirable, as direct control of the complete 3D geometry was the favoured strategy (van Griensven *et al.*, 2008; Zhang and Ma, 2004), though it may not be a necessary requirement (Karp *et al.*, 2003).

The cell-compatibility of the scaffold coatings was assessed using human marrow stromal cells (hMSCs), human osteoblasts (hOBs), and MG63 cells, via a quantitative live/dead assay, based on calcein AM and PI staining. The hydrogels

alginate and chitosan were found to perform poorly compared to gelatin and collagen, both in terms of total cells counts and the proportion of dead cells present. For hMSCs, their dead rates were found to be 19.1±6.3% for alginate, 5.3±3.6% and 2.9±1.4% for chitosan crosslinked with tripolyphosphate and sodium hydroxide respectively, compared to 0.11±0.07% for Type-I collagen, and 0.15±0.13% and 0.16±0.12% for 0.1% and 0.2% gelatin respectively.

Type-I collagen was found to be the most cell-compatible coating, as it was consistently associated with higher cell counts than Type-A gelatin. In addition, Type-I collagen was thought to be a suitable coating material for bone regenerative medical scaffolds, as collagen may mediate the osteogenic response of hMSCs (Yang *et al.*, 2004; Mizuno *et al.*, 2000), and this material has also been used to release rhBMP-2 and -7 in USFDA approved devices for the treatment of fracture non-unions (Govender *et al.*, 2002; Friedlaender *et al.*, 2001).

A similar system, employing hMSCs, was used to assess the PCL (M_n 42,500) scaffolds. Vacuum drying times of 60 min or more, before the application of cells, were found to have no detectable effect on the total cell count, the proportion of cell death, or the morphology. These data support the hypothesis that the PCL (M_n 42,500) scaffolds, dried for 60 min, were cell-compatible.

Scaffolds manufactured from PCL (M_n 42,500 and 80,000), PLGA, as well as blends of PCL (M_n 42,500) and PLGA, were evaluated using the model drug methylene blue. The encapsulation efficiencies and the release profiles of methylene blue were quantitatively assessed. It was found that PCL (M_n 42,500 and 80,000) scaffolds had relatively high encapsulation efficiencies. The encapsulation efficiency of the PCL scaffolds, for both M_n 42,500 and 80,000, was calculated to be 71±6% and 71±5% respectively. The encapsulation efficiency was found to be relatively consistent, both between and within batches. This loading efficiency was found to be similar to other potential drug delivery devices (Rai *et al.*, 2005; Silva *et al.*, 2006), and superior to the PCL and PLGA microspheres studied by Cao *et al*. (1999) and the PLA scaffolds of Murphy *et al*. (2000).

The release rate of the model drug methylene blue from scaffolds manufactured from PCL (M_n 42,500) was found to be consistent between batches. This was in contrast from the release from PCL (M_n 80,000). The release rate of methylene blue from PCL (M_n 80,000) was also thought to be higher than desired.

The PLGA, and PCL/PLGA blends were found to perform poorly. The methylene blue release rates from the PCL/PLGA blends were found to be relatively inconsistent between batches and the encapsulation efficiencies of PLGA and PCL:PLGA 66:33 were also relatively low (38±10% and 57±5% respectively). The encapsulation efficiency of PCL:PLGA 33:66, although high, was found to be relatively inconsistent between batches (78±10%). PCL (M_n 42,500) scaffolds, made without plotting media, were therefore considered to be the optimum scaffold material.

The drug loading potentials, as well as model drug release profiles from collagen coatings on PCL (M_n 42,500) scaffolds, were similarly assessed. The fast methylene blue release rate, and the methylene blue content of the scaffolds, were found to be compatible with the design philosophy of this thesis: slow release from the encapsulating delivery system and fast release from the scaffold coating.

The release profiles of the growth factor human bone morphogenetic protein-7 (rhBMP-7), from both encapsulating scaffolds and loaded collagen scaffold coatings, were measured using an enzyme-linked immunosorbent assay (ELISA). As with the methylene blue results, the collagen coating was found to release rhBMP-7 at a faster rate than the encapsulating PCL (M_n 42,500) scaffolds. While this was consistent with the design philosophy of the thesis, the manner of release was not. Although, from the ELISA data, it was found that the encapsulating PCL (M_n 42,500) scaffolds, and the loaded collagen scaffold coatings, were capable of releasing detectable amounts of rhBMP-7 with different release profiles for up to 14 days, burst release from both delivery systems was observed.

Release from the collagen coating ($Coat_{BMP\ 1.25}$) in the first 24 hr represented 23±3% of the theoretical rhBMP-7 loading, although this may represent approximately 77% of the total available for release. Similarly, 12±2% of the theoretical rhBMP-7 loading capacity was released from the $Scaff_{BMP\ 1.25}$ delivery system in the first 24 hr period, although this may represent approximately 60% of the total available for release. The release of rhBMP-7 from the two delivery systems was found not to match the ideal release profile (see **Figure 1.18**). However, it was noted that scaffolds with less than ideal release profiles, may still have potential for clinical use (Wei *et al.*, 2007).

The studies quantifying rhBMP-7 release using an ELISA did not determine whether the growth factor released was bioactive. Therefore studies were undertaken to examine the bioactivity of the release from the scaffolds.

A quantitative system, based on the image analysis of alkaline phosphatase (ALP) staining and propidium iodide (PI) cell counts of hMSCs, was used to assess the osteogenic potential of rhBMP-7, and the release from growth factor incorporating scaffolds. Each of the rhBMP-7 concentrations tested (5, 20, and 50 ng/ml) was found to increase the normalised area of ALP staining statistically significantly compared to the base media for at least three of the test patients, although often the actual difference was small. This could indicate that rhBMP-7 is able to stimulate the osteogenic differentiation of hMSCs over a relatively wide range of concentrations.

The release from the $Coat_{BMP\ 1.25}Scaff_{PBS}$ and $Coat_{BMP\ 0.63}Scaff_{PBS}$ scaffolds was found to statistically significantly stimulate hMSC ALP staining compared to the control scaffolds, although the actual differences were small. This indicated that at least a proportion of the rhBMP-7 released was bioactive. In contrast, the release from $Coat_{PBS}Scaff_{BMP\ 1.25}$ and $Coat_{PBS}Scaff_{BMP\ 0.63}$ was found not to enhance hMSC ALP staining. Either the growth factor released was not bioactive, or the dose was insufficient to influence the cells measurably.

Image analysis of ALP staining, normalised against 4',6-diamino-2-phenylindole (DAPI) cell counts, was used to assess quantitatively the ability of the $Coat_{1,25(OH)2D3}Scaff_{ethanol}$, $Coat_{ethanol}Scaff_{1,25(OH)2D3}$ and $Coat_{1,25(OH)2D3}Scaff_{1,25(OH)2D3}$ scaffolds to release 1,25-dihydroxyvitamin D_3 ($1,25(OH)_2D_3$). Normalised ALP expression of the hMSCs was significantly increased for each of the $1,25(OH)_2D_3$ loaded scaffold types compared to the control scaffolds. Furthermore, ALP expression was significantly enhanced for the dual delivery scaffolds over and above that for either delivery system on its own. It was therefore concluded that the PCL scaffolds coated with collagen could be capable of releasing bioactive lipid-soluble active factors, and that both delivery systems were mutually compatible.

The cell-compatibility of the scaffold materials had previously been assessed in Chapter 3, and the quantity and bioactivity of rhBMP-7 released from the scaffolds was examined in Chapter 4 and Chapter 5. However, it was unknown how the clinically relevant hMSCs would react to the combined stimuli, when seeded directly onto the scaffolds. Combined ALP/deoxyribonucleic acid (DNA) and calcium/DNA assays were therefore used to assess whether the Type-I collagen coated PCL (M_n 42,500) scaffolds, loaded with rhBMP-7, were capable of supporting the osteogenic differentiation of hMSCs, seeded onto them.

ALP activity on the scaffolds was found to increase with increasing concentrations of rhBMP-7 in the range of concentrations tested (5, 20, and 50 ng/ml). For example, ALP activity was increased by 98±18% for 50 ng/ml of rhBMP-7 compared to the control group. ALP activity was also statistically significantly stimulated in hMSCs for the $Coat_{PBS}Scaff_{BMP\ 1.25}$ and $Coat_{BMP\ 1.25}Scaff_{BMP\ 1.25}$ scaffold groups for three and two patients out of three respectively (increased by 35±10% and 39±10 on the control respectively), whereas this was the case for only one patient's cells for the $Coat_{BMP\ 1.25}Scaff_{PBS}$ scaffolds (increased be 35±14% on the control). These data indicated that the $Coat_{PBS}Scaff_{BMP\ 1.25}$ and $Coat_{BMP\ 1.25}Scaff_{BMP\ 1.25}$ scaffolds were capable of stimulating the osteogenic differentiation of hMSCs seeded onto them.

Calcium deposition was only stimulated in the cells of one of the three hMSC patients tested. Since the osteogenic effect of the encapsulation delivery system was not enhanced by the release from the coating, in the final "product" for clinical use the coating delivery system could be better employed in the delivery of a different active factor.

The functional osteoinductive capacity of Type-I collagen coated PCL (M_n 42,500) scaffolds loaded with rhBMP-7 was assessed using C2C12 cells seeded onto the scaffolds, and quantified using qRT-PCR. The genes of interest were; Type-I collagen (Col1), osteopontin (OP), ALP, osteocalcin (OC) and Runx2. Similar to the findings of previous studies (Gu *et al.*, 2004b; Tou *et al.*, 2003; Yeh *et al.*, 2002), rhBMP-7 was found to up-regulate the expression of genes associated with osteogenesis in C2C12 cells when cultured on the control $Coat_{PBS}Scaff_{PBS}$ scaffolds. C2C12 cells cultured on $Coat_{PBS}Scaff_{PBS}$ scaffolds, exposed to 200 ng/ml rhBMP-7 in the media, were found to upregulate OP, ALP, OC and Runx2 after 24 hr compared to the control (by 64±15%, 385±68%, 127±66%, and 76±43% respectively).

The $Coat_{BMP\ 1.25}Scaff_{PBS}$ scaffolds had an early osteoinductive effect on the C2C12 cells, as ALP, OC and Runx2 were elevated during the first 2 days only, compared to the control (for example, by 44±12%, 128±42%, 60±25% and 46±25% respectively at the 24 hr mark). These data indicate that the collagen coating delivery system ($Coat_{BMP\ 1.25}$) was suitable for the early release of bioactive growth factors, capable of having a functional effect on the cells seeded onto the scaffolds.

The $Coat_{PBS}Scaff_{BMP\ 1.25}$ scaffolds also had an osteoinductive effect on the cells, which was more sustained than that observed for the $Coat_{BMP\ 1.25}Scaff_{PBS}$ group. While OP, ALP and Runx2 were up-regulated in the first 24 hr compared to the control (by 38±10%, 208±82% and 72±31% respectively), statistically significant up-regulation of the late marker OC was delayed until the 48 hr mark (by 73±49%). The effect was found to be sustained until day 7, when OC and Runx2 were both statistically significantly up-regulated compared to the control (by 151±91% and 93±27% respectively).

The $Coat_{BMP\ 1.25}Scaff_{BMP\ 1.25}$ scaffolds were found to combine the early effect of the $Coat_{BMP\ 1.25}Scaff_{PBS}$ scaffolds, with the more sustained effect of the $Coat_{PBS}Scaff_{BMP\ 1.25}$ scaffolds. ALP, OC and Runx2 were all up-regulated at the 24 hr mark (by 312±56%, 329±39% and 96±25% respectively). This osteoinductive effect was sustained until day 7 when Col1, ALP and Runx2 were still up-regulated compared to the control (by 174±78%, 72±24% and 178±78% respectively). These data provide further evidence to the findings described in Chapter 6, that the two delivery systems are mutually compatible in their ability to release bioactive growth factors.

These data suggest that the scaffolds containing rhBMP-7 have a weak osteoinductive effect on the cells seeded onto them. The different delivery systems were found to affect the cells differently. The clinical significance of this was not assessed in these studies.

8.3. Comparison with other Dual Delivery Systems

As discussed in §1.2.6.3.4, the dual delivery of growth factors with different temporal release profiles may be advantageous, yet few examples exist. At least three studies have described scaffolds with two independent delivery systems.

Ginty *et al.* (2008) used supercritical CO_2 foaming to create poly(lactic acid) scaffolds, coupled with PCL microparticles or entrapped alginate to release RNase and horseradish peroxidase as model drugs. However, unlike the scaffolds studied in this thesis, release of bioactive growth factors was not examined, neither was the cell-compatibility assessed.

Sohier *et al.* (2006) manufactured scaffolds of poly(ethylene glycol)- terephthalate (PEGT) and poly(butylene terephthalate) (PBT) with successive coatings of the same material. They achieved different release kinetics from the layers of myoglobin and lysozyme, used as model drugs. Like the studies conducted by Ginty *et al.* (2008), the cell-compatibility and their ability to release bioactive growth factors was not assessed.

Perhaps the most promising of the dual drug delivery systems was presented by Richardson *et al.* (2001). PLGA scaffolds, produced by $scCO_2$ gas foaming, and microparticles delivery systems were combined, and used to deliver bioactive VEGF and PDGF in a controlled manner. However, release from the microparticle delivery system presented, was either very similar to the release from the scaffold, or was too slow to be of clinical significance. This scaffold system has been found to stimulate angiogenesis, although it was not applied to bone regenerative medical applications. As discussed in §1.2.5.9, PLGA used in bulk, has properties which may prove to be disadvantageous for bone regenerative medical applications because of its acidic breakdown products and their self-accelerated degradation (Sokolsky-Papkov *et al.*, 2007).

Without parallel *in vivo* experiments, it is uncertain whether the scaffolds developed by Richardson *et al.* (2001), or the scaffolds developed in this thesis would be more suitable for bone regenerative medical applications. The release properties from the PLGA scaffolds developed by Richardson *et al.* (2001) are likely to be more favourable, however the Type-I collagen coated PCL scaffolds developed in this thesis may prove to be more cell-compatible and osteoinductive, as collagen may mediate the osteogenic response of hMSCs (Yang *et al.*, 2004; Mizuno *et al.*, 2000).

The lack of intrinsic 3D structure of the scaffolds developed in this thesis may prove to be disadvantageous compared to the other dual delivery scaffolds described above. Potentially, this problem could be alleviated by packing the wound site with multiple scaffolds (see §2.5.1.1.3). If future *in vivo* studies found packing to be an unsuitable solution, future work should focus on the development of intrinsic 3D geometry.

8.4. Testing of Thesis Hypothesis

The evidence reported in this thesis indicates that the Type-I collagen coated PCL (M_n 42,500) scaffolds; were cell-compatible, and had sufficient porosity to allow the adequate diffusion of cellular nutrients and waste products. Two delivery systems were developed which were capable of releasing bioactive growth. However, release

profiles may not have been clinically different from the two delivery systems. In addition, the release profile were found to deviate significantly from the ideal release profiles described in §1.4.1. It was therefore concluded that the data reported in this thesis did not confirm the thesis hypothesis.

8.5. Future Work

The studies described in this thesis employed rhBMP-7 and $1,25(OH)_2D_3$ to assess the effectiveness of the scaffolds as delivery systems. However, as discussed in §1.2.4, a number of active factors are available which have the potential to enhance the efficacy of bone regenerative medicine constructs. Future studies could examine the possibility of releasing factors to promote angiogenesis or hMSC proliferation from the scaffold coating early on, followed by the slower release of factors to encourage the osteogenic differentiation of hMSCs from the scaffold itself. The efficacy of these scaffolds could be examined using *in vivo* animal fracture non-union models, to determine the optimum growth factor combination and dose. Candidate growth factors could include; recombinant human vascular endothelial growth factor (rhVEGF) and recombinant human fibroblast growth factor-2 (rhFGF-2) in the coating, with recombinant human bone morphogenetic protein-2 (rhBMP-2) and rhBMP-7 within the scaffolds.

The manufacturing technique could be used to constrict scaffolds from synthetic polymers other than PCL and PLGA. For example PLA, or blends of PLA could be used. Potentially the use of this polymer could enhance the scaffold mechanical properties, and slow the rate of active factor release because of its semicrystaline structure at physiological temperatures (see §1.2.5.9). Blending with other synthetic polymers, or altering the monomer composition of PLA to alter the crystal structure may also present opportunities to alter the active factor release characteristics (Ginty *et al.*, 2008).

Microparticles of PLGA or another synthetic polymer could be employed as a third potential delivery system. As discussed in §1.2.6.3.3, there is scope for altering the release profiles by changing their composition and average size.

As discussed in §2.5.1.1.3, two-layer scaffolds may be sufficient to create the 3D geometry required for successful clinical application. However, direct manipulation of the 3D scaffold geometry may prove to be advantageous. Scaffold manufacture with a height greater than two layers should therefore be investigated, if future *in vivo* studies found the packing of multiple scaffold sheets to be an unsuitable solution.

The same materials used in different scaffold manufacturing techniques. For example, a freezing and freeze drying technique similar to that described by Khan *et al.* (2010) could be used. Although direct control of scaffold geometry would be lost, this could potentially be outweighed by the ability to build substantial 3D geometry.

Appendices

Appendix A

NC code program to produce two-layer scaffolds with a strand spacing of 0.80 mm in both the X and Y axes, and a Z spacing of 0.14 mm. The plotting speed is set at 140 mm/min.

N0001_(SCAFFOLD_20X20)¶N0002_G54¶N0003_(Dispensing)¶N0004_E0_0¶N0005_G00_Z106¶N0006_G00_X0_Y0¶N0007_G00_X-9.6_Y-8.8_Z1.14¶N0008_G01_Z0.14_F50¶N0009_E1_1¶N0010_G00¶N0011_G04_P400¶N0012_G01_X9.6_F140¶N0013_G01_Y-8¶N0014_G01_X-9.6¶N0015_G01_Y-7.2¶N0016_G01_X9.6¶N0017_G01_Y-6.4¶N0018_G01_X-9.6¶N0019_G01_Y-5.6¶N0020_G01_X9.6¶N0021_G01_Y-4.8¶N0022_G01_X-9.6¶N0023_G01_Y-4¶N0024_G01_X9.6¶N0025_G01_Y-3.2¶N0026_G01_X-9.6¶N0027_G01_Y-2.4¶N0028_G01_X9.6¶N0029_G01_Y-1.6¶N0030_G01_X-9.6¶N0031_G01_Y-0.8¶N0032_G01_X9.6¶N0033_G01_Y0¶N0034_G01_X-9.6¶N0035_G01_Y0.8¶N0036_G01_X9.6¶N0037_G01_Y1.6¶N0038_G01_X-9.6¶N0039_G01_Y2.4¶N0040_G01_X9.6¶N0041_G01_Y3.2¶N0042_G01_X-9.6¶N0043_G01_Y4¶N0044_G01_X9.6¶N0045_G01_Y4.8¶N0046_G01_X-9.6¶N0047_G01_Y5.6¶N0048_G01_X9.6¶N0049_G01_Y6.4¶N0050_G01_X-9.6¶N0051_G01_Y7.2¶N0052_G01_X9.6¶N0053_G01_Y8¶N0054_G01_X-9.6¶N0055_G01_Y8.8¶N0056_G01_X9.6¶N0057_G01_Z0.28¶N0058_G01_X8.8_Y9.6¶N0059_G01_Y-9.6¶N0060_G01_X8¶N0061_G01_Y9.6¶N0062_G01_X7.2¶N0063_G01_Y-9.6¶N0064_G01_X6.4¶N0065_G01_Y9.6¶N0066_G01_X5.6¶N0067_G01_Y-9.6¶N0068_G01_X4.8¶N0069_G01_Y9.6¶N0070_G01_X4¶N0071_G01_Y-9.6¶N0072_G01_X3.2¶N0073_G01_Y9.6¶N0074_G01_X2.4¶N0075_G01_Y-9.6¶N0076_G01_X1.6¶N0077_G01_Y9.6¶N0078_G01_X0.8¶N0079_G01_Y-9.6¶N0080_G01_X0¶N0081_G01_Y9.6¶N0082_G01_X-0.8¶N0083_G01_Y-9.6¶N0084_G01_X-1.6¶N0085_G01_Y9.6¶N0086_G01_X-2.4¶N0087_G01_Y-9.6¶N0088_G01_X-3.2¶N0089_G01_Y9.6¶N0090_G01_X-4¶N0091_G01_Y-9.6¶N0092_G01_X-4.8¶N0093_G01_Y9.6¶N0094_G01_X-5.6¶N0095_G01_Y-9.6¶N0096_G01_X-6.4¶N0097_G01_Y9.6¶N0098_G01_X-7.2¶N0099_G01_Y-9.6¶N0100_G01_X-8¶N0101_G01_Y9.6¶N0102_G01_X-8.8¶N0103_G01_Y-9.6¶N0104_E1_0¶N0105_G01_Z1.28_F2¶N0106_M30

Appendix B

NC code program to produce two-layer scaffolds with a strand spacing of 1.00 mm in both the X and Y axes, and a Z spacing of 0.14 mm. The plotting speed is set at 560 mm/min.

N0001_(SCAFFOLD_20X20)¶N0002_G54¶N0003_(Dispensing)¶N0004_E0_0¶N0005_G00_Z106¶N0006_G00_X0_Y0¶N0007_G00_X-9.5_Y-8.5_Z1.14¶N0008_G01_Z0.14_F50¶N0009_E1_1¶N0010_G00¶N0011_G04_P400¶N0012_G01_X9.5_F560¶N0013_G01_Y-7.5¶N0014_G01_X-9.5¶N0015_G01_Y-6.5¶N0016_G01_X9.5¶N0017_G01_Y-5.5¶N0018_G01_X-9.5¶N0019_G01_Y-4.5¶N0020_G01_X9.5¶N0021_G01_Y-3.5¶N0022_G01_X-9.5¶N0023_G01_Y-2.5¶N0024_G01_X9.5¶N0025_G01_Y-1.5¶N0026_G01_X-9.5¶N0027_G01_Y-0.5¶N0028_G01_X9.5¶N0029_G01_Y0.5¶N0030_G01_X-9.5¶N0031_G01_Y1.5¶N0032_G01_X9.5¶N0033_G01_Y2.5¶N0034_G01_X-9.5¶N0035_G01_Y3.5¶N0036_G01_X9.5¶N0037_G01_Y4.5¶N0038_G01_X-9.5¶N0039_G01_Y5.5¶N0040_G01_X9.5¶N0041_G01_Y6.5¶N0042_G01_X-9.5¶N0043_G01_Y7.5¶N0044_G01_X9.5¶N0045_G01_Y8.5¶N0046_G01_X-9.5¶N0047_G01_Z0.28¶N0048_G01_X-8.5_Y9.5¶N0049_G01_Y-9.5¶N0050_G01_X-7.5¶N0051_G01_Y9.5¶N0052_G01_X-6.5¶N0053_G01_Y-9.5¶N0054_G01_X-5.5¶N0055_G01_Y9.5¶N0056_G01_X-4.5¶N0057_G01_Y-9.5¶N0058_G01_X-3.5¶N0059_G01_Y9.5¶N0060_G01_X-2.5¶N0061_G01_Y-9.5¶N0062_G01_X-1.5¶N0063_G01_Y9.5¶N0064_G01_X-0.5¶N0065_G01_Y-9.5¶N0066_G01_X0.5¶N0067_G01_Y9.5¶N0068_G01_X1.5¶N0069_G01_Y-9.5¶N0070_G01_X2.5¶N0071_G01_Y9.5¶N0072_G01_X0.5¶N0073_G01_Y-9.5¶N0074_G01_X4.5¶N0075_G01_Y9.5¶N0076_G01_X5.5¶N0077_G01_Y-9.5¶N0078_G01_X6.5¶N0079_G01_Y9.5¶N0080_G01_X7.5¶N0081_G01_Y-9.5¶N0082_G01_X8.5¶N0083_G01_Y9.5¶N0084_E1_0¶N0085_G01_Z3.34_F2¶N0086_M30

Appendix C

NC code program to produce 16-layer scaffolds with a strand spacing of 0.80 mm in both the X and Y axes, and a Z spacing of 0.14 mm. The plotting speed is set at 140 mm/min.

N0001_(SCAFFOLD_20X20)¶N0002_G54¶N0003_(Dispensing)¶N0004_E0_0¶N0005_G00_Z106¶N0006_G00_X0_Y0¶N0007_G00_X-9.6_Y-8.8_Z1.14¶N0008_G01_Z0.14_F50¶N0009_E1_1¶N0010_G00¶N0011_G04_P400¶N0012_G01_X9.6_F140¶N0013_G01_Y-8¶N0014_G01_X-9.6¶N0015_G01_Y-7.2¶N0016_G01_X9.6¶N0017_G01_Y-6.4¶N0018_G01_X-9.6¶N0019_G01_Y-5.6¶N0020_G01_X9.6¶N0021_G01_Y-4.8¶N0022_G01_X-9.6¶N0023_G01_Y-4¶N0024_G01_X9.6¶N0025_G01_Y-3.2¶N0026_G01_X-9.6¶N0027_G01_Y-2.4¶N0028_G01_X9.6¶N0029_G01_Y-1.6¶N0030_G01_X-9.6¶N0031_G01_Y-0.8¶N0032_G01_X9.6¶N0033_G01_Y0¶N0034_G01_X-9.6¶N0035_G01_Y0.8¶N0036_G01_X9.6¶N0037_G01_Y1.6¶N0038_G01_X-9.6¶N0039_G01_Y2.4¶N0040_G01_X9.6¶N0041_G01_Y3.2¶N0042_G01_X-9.6¶N0043_G01_Y4¶N0044_G01_X9.6¶N0045_G01_Y4.8¶N0046_G01_X-9.6¶N0047_G01_Y5.6¶N0048_G01_X9.6¶N0049_G01_Y6.4¶N0050_G01_X-9.6¶N0051_G01_Y7.2¶N0052_G01_X9.6¶N0053_G01_Y8¶N0054_G01_X-9.6¶N0055_G01_Y8.8¶N0056_G01_X9.6¶N0057_G01_Z0.28¶N0058_G01_X8.8_Y9.6¶N0059_G01_Y-9.6_F110¶N0060_G01_X8¶N0061_G01_Y9.6¶N0062_G01_X7.2¶N0063_G01_Y-9.6¶N0064_G01_X6.4¶N0065_G01_Y9.6¶N0066_G01_X5.6¶N0067_G01_Y-9.6¶N0068_G01_X4.8¶N0069_G01_Y9.6¶N0070_G01_X4¶N0071_G01_Y-9.6¶N0072_G01_X3.2¶N0073_G01_Y9.6¶N0074_G01_X2.4¶N0075_G01_Y-9.6¶N0076_G01_X1.6¶N0077_G01_Y9.6¶N0078_G01_X0.8¶N0079_G01_Y-9.6¶N0080_G01_X0¶N0081_G01_Y9.6¶N0082_G01_X-0.8¶N0083_G01_Y-9.6¶N0084_G01_X-1.6¶N0085_G01_Y9.6¶N0086_G01_X-2.4¶N0087_G01_Y-9.6¶N0088_G01_X-3.2¶N0089_G01_Y9.6¶N0090_G01_X-4¶N0091_G01_Y-9.6¶N0092_G01_X-4.8¶N0093_G01_Y9.6¶N0094_G01_X-5.6¶N0095_G01_Y-9.6¶N0096_G01_X-6.4¶N0097_G01_Y9.6¶N0098_G01_X-7.2¶N0099_G01_Y-9.6¶N0100_G01_X-8¶N0101_G01_Y9.6¶N0102_G01_X-8.8¶N0103_G01_Y-9.6¶N0104_E1_0¶N0105_G01_Z0.32_F0.28¶N0106_E1_1¶N0106_G01_Y9.6_F11

0¶N0107_G01_X-8¶N0108_G01_Y-9.6¶N0109_G01_X-
7.2¶N0110_G01_Y9.6¶N0111_G01_X-6.4¶N0112_G01_Y-9.6¶N0113_G01_X-
5.6¶N0114_G01_Y9.6¶N0115_G01_X-4.8¶N0116_G01_Y-9.6¶N0117_G01_X-4
N0118_G01_Y9.6¶N0119_G01_X-3.2¶N0120_G01_Y-9.6¶N0121_G01_X-
2.4¶N0122_G01_Y9.6¶N0123_G01_X-1.6¶N0124_G01_Y-9.6¶N0125_G01_X-
0.8¶N0126_G01_Y9.6¶N0127_G01_X0¶N0128_G01_Y-
9.6¶N0129_G01_X0.8¶N0130_G01_Y9.6¶N0131_G01_X1.6¶N0132_G01_Y-
9.6¶N0133_G01_X2.4¶N0134_G01_Y9.6¶N0135_G01_X3.2¶N0136_G01_Y-
9.6¶N0137_G01_X4¶N0138_G01_Y9.6¶N0139_G01_X4.8¶N0140_G01_Y-
9.6¶N0141_G01_X5.6¶N0142_G01_Y9.6¶N0143_G01_X6.4¶N0144_G01_Y-
9.6¶N0145_G01_X7.2¶N0146_G01_Y9.6¶N0147_G01_X8¶N0148_G01_Y-
9.6¶N0149_G01_X8.8¶N0150_G01_Y9.6¶N0151_G01_Z0.56¶N0152_G01_X9.6_
Y8.8¶N0153_G01_X-
9.6¶N0154_G01_Y8¶N0155_G01_X9.6¶N0156_G01_Y7.2¶N0157_G01_X-
9.6¶N0158_G01_Y6.4¶N0159_G01_X9.6¶N0160_G01_Y5.6¶N0161_G01_X-
9.6¶N0162_G01_Y4.8¶N0163_G01_X9.6¶N0164_G01_Y4¶N0165_G01_X-
9.6¶N0166_G01_Y3.2¶N0167_G01_X9.6¶N0168_G01_Y2.4¶N0169_G01_X-
9.6¶N0170_G01_Y1.6¶N0171_G01_X9.6¶N0172_G01_Y0.8¶N0173_G01_X-
9.6¶N0174_G01_Y0¶N0175_G01_X9.6¶N0176_G01_Y-0.8¶N0177_G01_X-
9.6¶N0178_G01_Y-1.6¶N0179_G01_X9.6¶N0180_G01_Y-2.4¶N0181_G01_X-
9.6¶N0182_G01_Y-3.2¶N0183_G01_X9.6¶N0184_G01_Y-4¶N0185_G01_X-
9.6¶N0186_G01_Y-4.8¶N0187_G01_X9.6¶N0188_G01_Y-5.6¶N0189_G01_X-
9.6¶N0190_G01_Y-6.4¶N0191_G01_X9.6¶N0192_G01_Y-7.2¶N0193_G01_X-
9.6¶N0194_G01_Y-8¶N0195_G01_X9.6¶N0196_G01_Y-8.8¶N0197_G01_X-
9.6¶N0198_E1_0¶N0199_G01_Z0.6_F0.28¶N0200_E1_1¶N0201_G01_X9.6_F110
¶N0202_G01_Y-8¶N0203_G01_X-9.6¶N0204_G01_Y-
7.2¶N0205_G01_X9.6¶N0206_G01_Y-6.4¶N0207_G01_X-9.6¶N0208_G01_Y-
5.6¶N0209_G01_X9.6¶N0210_G01_Y-4.8¶N0211_G01_X-9.6¶N0212_G01_Y-
4¶N0213_G01_X9.6¶N0214_G01_Y-3.2¶N0215_G01_X-9.6¶N0216_G01_Y-
2.4¶N0217_G01_X9.6¶N0218_G01_Y-1.6¶N0219_G01_X-9.6¶N0220_G01_Y-
0.8¶N0221_G01_X9.6¶N0222_G01_Y0¶N0223_G01_X-
9.6¶N0224_G01_Y0.8¶N0225_G01_X9.6¶N0226_G01_Y1.6¶N0227_G01_X-

9.6¶N0228_G01_Y2.4¶N0229_G01_X9.6¶N0230_G01_Y3.2¶N0231_G01_X-
9.6¶N0232_G01_Y4¶N0233_G01_X9.6¶N0234_G01_Y4.8¶N0235_G01_X-
9.6¶N0236_G01_Y5.6¶N0237_G01_X9.6¶N0238_G01_Y6.4¶N0239_G01_X-
9.6¶N0240_G01_Y7.2¶N0241_G01_X9.6¶N0242_G01_Y8¶N0243_G01_X-
9.6¶N0244_G01_Y8.8¶N0245_G01_X9.6¶N0246_G01_Z0.84¶N0247_G01_X8.8_
Y9.6¶N0248_G01_Y-
9.6¶N0249_G01_X8¶N0250_G01_Y9.6¶N0251_G01_X7.2¶N0252_G01_Y-
9.6¶N0253_G01_X6.4¶N0254_G01_Y9.6¶N0255_G01_X5.6¶N0256_G01_Y-
9.6¶N0257_G01_X4.8¶N0258_G01_Y9.6¶N0259_G01_X4¶N0260_G01_Y-
9.6¶N0261_G01_X3.2¶N0262_G01_Y9.6¶N0263_G01_X2.4¶N0264_G01_Y-
9.6¶N0265_G01_X1.6¶N0266_G01_Y9.6¶N0267_G01_X0.8¶N0268_G01_Y-
9.6¶N0269_G01_X0¶N0270_G01_Y9.6¶N0271_G01_X-0.8¶N0272_G01_Y-
9.6¶N0273_G01_X-1.6¶N0274_G01_Y9.6¶N0275_G01_X-2.4¶N0276_G01_Y-
9.6¶N0277_G01_X-3.2¶N0278_G01_Y9.6¶N0279_G01_X-4¶N0280_G01_Y-
9.6¶N0281_G01_X-4.8¶N0282_G01_Y9.6¶N0283_G01_X-5.6¶N0284_G01_Y-
9.6¶N0285_G01_X-6.4¶N0286_G01_Y9.6¶N0287_G01_X-7.2¶N0288_G01_Y-
9.6¶N0289_G01_X-8¶N0290_G01_Y9.6¶N0291_G01_X-8.8¶N0292_G01_Y-
9.6¶N0293_E1_0¶N0294_G01_Z0.88_F0.28¶N0295_E1_1¶N0295_G01_Y9.6_F11
0¶N0296_G01_X-8¶N0297_G01_Y-9.6¶N0298_G01_X-
7.2¶N0299_G01_Y9.6¶N0300_G01_X-6.4¶N0301_G01_Y-9.6¶N0302_G01_X-
5.6¶N0303_G01_Y9.6¶N0304_G01_X-4.8¶N0305_G01_Y-9.6¶N0306_G01_X-
4¶N0307_G01_Y9.6¶N0308_G01_X-3.2¶N0309_G01_Y-9.6¶N0310_G01_X-
2.4¶N0311_G01_Y9.6¶N0312_G01_X-1.6¶N0313_G01_Y-9.6¶N0314_G01_X-
0.8¶N0315_G01_Y9.6¶N0316_G01_X0¶N0317_G01_Y-
9.6¶N0318_G01_X0.8¶N0319_G01_Y9.6¶N0320_G01_X1.6¶N0321_G01_Y-
9.6¶N0322_G01_X2.4¶N0323_G01_Y9.6¶N0324_G01_X3.2¶N0325_G01_Y-
9.6¶N0326_G01_X4¶N0327_G01_Y9.6¶N0328_G01_X4.8¶N0329_G01_Y-
9.6¶N0330_G01_X5.6¶N0331_G01_Y9.6¶N0332_G01_X6.4¶N0333_G01_Y-
9.6¶N0334_G01_X7.2¶N0335_G01_Y9.6¶N0336_G01_X8¶N0337_G01_Y-
9.6¶N0338_G01_X8.8¶N0339_G01_Y9.6¶N0340_G01_Z1.12¶N0341_G01_X9.6_
Y8.8¶N0342_G01_X-
9.6¶N0343_G01_Y8¶N0344_G01_X9.6¶N0345_G01_Y7.2¶N0346_G01_X-

9.6¶N0347_G01_Y6.4¶N0348_G01_X9.6¶N0349_G01_Y5.6¶N0350_G01_X-
9.6¶N0351_G01_Y4.8¶N0352_G01_X9.6¶N0353_G01_Y4¶N0354_G01_X-
9.6¶N0355_G01_Y3.2¶N0356_G01_X9.6¶N0357_G01_Y2.4¶N0358_G01_X-
9.6¶N0359_G01_Y1.6¶N0360_G01_X9.6¶N0361_G01_Y0.8¶N0362_G01_X-
9.6¶N0363_G01_Y0¶N0364_G01_X9.6¶N0365_G01_Y-0.8¶N0366_G01_X-
9.6¶N0367_G01_Y-1.6¶N0368_G01_X9.6¶N0369_G01_Y-2.4¶N0370_G01_X-
9.6¶N0371_G01_Y-3.2¶N0372_G01_X9.6¶N0373_G01_Y-4¶N0374_G01_X-
9.6¶N0375_G01_Y-4.8¶N0376_G01_X9.6¶N0377_G01_Y-5.6¶N0378_G01_X-
9.6¶N0379_G01_Y-6.4¶N0380_G01_X9.6¶N0381_G01_Y-7.2¶N0382_G01_X-
9.6¶N0383_G01_Y-8¶N0384_G01_X9.6¶N0385_G01_Y-8.8¶N0386_G01_X-
9.6¶N0387_E1_0¶N0388_G01_Z1.16_F0.28¶N0389_E1_1¶N0390_G01_X9.6_F11
0¶N0391_G01_Y-8¶N0392_G01_X-9.6¶N0393_G01_Y-
7.2¶N0394_G01_X9.6¶N0395_G01_Y-6.4¶N0396_G01_X-9.6¶N0397_G01_Y-
5.6¶N0398_G01_X9.6¶N0399_G01_Y-4.8¶N0400_G01_X-9.6¶N0401_G01_Y-
4¶N0402_G01_X9.6¶N0403_G01_Y-3.2¶N0404_G01_X-9.6¶N0405_G01_Y-
2.4¶N0406_G01_X9.6¶N0407_G01_Y-1.6¶N0408_G01_X-9.6¶N0409_G01_Y-
0.8¶N0410_G01_X9.6¶N0411_G01_Y0¶N0412_G01_X-
9.6¶N0413_G01_Y0.8¶N0414_G01_X9.6¶N0415_G01_Y1.6¶N0416_G01_X-
9.6¶N0417_G01_Y2.4¶N0418_G01_X9.6¶N0419_G01_Y3.2¶N0420_G01_X-
9.6¶N0421_G01_Y4¶N0422_G01_X9.6¶N0423_G01_Y4.8¶N0424_G01_X-
9.6¶N0425_G01_Y5.6¶N0426_G01_X9.6¶N0427_G01_Y6.4¶N0428_G01_X-
9.6¶N0429_G01_Y7.2¶N0430_G01_X9.6¶N0431_G01_Y8¶N0432_G01_X-
9.6¶N0433_G01_Y8.8¶N0434_G01_X9.6¶N0435_G01_Z1.4¶N0436_G01_X8.8_Y
9.6¶N0437_G01_Y-
9.6¶N0438_G01_X8¶N0439_G01_Y9.6¶N0440_G01_X7.2¶N0441_G01_Y-
9.6¶N0442_G01_X6.4¶N0443_G01_Y9.6¶N0444_G01_X5.6¶N0445_G01_Y-
9.6¶N0446_G01_X4.8¶N0447_G01_Y9.6¶N0448_G01_X4¶N0449_G01_Y-
9.6¶N0450_G01_X3.2¶N0451_G01_Y9.6¶N0452_G01_X2.4¶N0453_G01_Y-
9.6¶N0454_G01_X1.6¶N0455_G01_Y9.6¶N0456_G01_X0.8¶N0457_G01_Y-
9.6¶N0458_G01_X0¶N0459_G01_Y9.6¶N0460_G01_X-0.8¶N0461_G01_Y-
9.6¶N0462_G01_X-1.6¶N0463_G01_Y9.6¶N0464_G01_X-2.4¶N0465_G01_Y-
9.6¶N0466_G01_X-3.2¶N0467_G01_Y9.6¶N0468_G01_X-4¶N0469_G01_Y-

9.6¶N0470_G01_X-4.8¶N0471_G01_Y9.6¶N0472_G01_X-5.6¶N0473_G01_Y-
9.6¶N0474_G01_X-6.4¶N0475_G01_Y9.6¶N0476_G01_X-7.2¶N0477_G01_Y-
9.6¶N0478_G01_X-8¶N0479_G01_Y9.6¶N0480_G01_X-8.8¶N0481_G01_Y-
9.6¶N0482_E1_0¶N0483_G01_Z1.44_F0.28¶N0484_E1_1¶N0485_G01_Y9.6_F11
0¶N0486_G01_X-8¶N0487_G01_Y-9.6¶N0488_G01_X-
7.2¶N0489_G01_Y9.6¶N0490_G01_X-6.4¶N0491_G01_Y-9.6¶N0492_G01_X-
5.6¶N0493_G01_Y9.6¶N0494_G01_X-4.8¶N0495_G01_Y-9.6¶N0496_G01_X-
4¶N0497_G01_Y9.6¶N0498_G01_X-3.2¶N0499_G01_Y-9.6¶N0500_G01_X-
2.4¶N0501_G01_Y9.6¶N0502_G01_X-1.6¶N0503_G01_Y-9.6¶N0504_G01_X-
0.8¶N0505_G01_Y9.6¶N0506_G01_X0¶N0507_G01_Y-
9.6¶N0508_G01_X0.8¶N0509_G01_Y9.6¶N0510_G01_X1.6¶N0511_G01_Y-
9.6¶N0512_G01_X2.4¶N0513_G01_Y9.6¶N0514_G01_X3.2¶N0515_G01_Y-
9.6¶N0516_G01_X4¶N0517_G01_Y9.6¶N0518_G01_X4.8¶N0519_G01_Y-
9.6¶N0520_G01_X5.6¶N0521_G01_Y9.6¶N0522_G01_X6.4¶N0523_G01_Y-
9.6¶N0524_G01_X7.2¶N0525_G01_Y9.6¶N0526_G01_X8¶N0527_G01_Y-
9.6¶N0528_G01_X8.8¶N0529_G01_Y9.6¶N0530_G01_Z1.68¶N0531_G01_X9.6_
Y8.8¶N0532_G01_X-
9.6¶N0533_G01_Y8¶N0534_G01_X9.6¶N0535_G01_Y7.2¶N0536_G01_X-
9.6¶N0537_G01_Y6.4¶N0538_G01_X9.6¶N0539_G01_Y5.6¶N0540_G01_X-
9.6¶N0541_G01_Y4.8¶N0542_G01_X9.6¶N0543_G01_Y4¶N0544_G01_X-
9.6¶N0545_G01_Y3.2¶N0546_G01_X9.6¶N0547_G01_Y2.4¶N0548_G01_X-
9.6¶N0549_G01_Y1.6¶N0550_G01_X9.6¶N0551_G01_Y0.8¶N0552_G01_X-
9.6¶N0553_G01_Y0¶N0554_G01_X9.6¶N0555_G01_Y-0.8¶N0556_G01_X-
9.6¶N0557_G01_Y-1.6¶N0558_G01_X9.6¶N0559_G01_Y-2.4¶N0560_G01_X-
9.6¶N0561_G01_Y-3.2¶N0562_G01_X9.6¶N0563_G01_Y-4¶N0564_G01_X-
9.6¶N0565_G01_Y-4.8¶N0566_G01_X9.6¶N0567_G01_Y-5.6¶N0568_G01_X-
9.6¶N0569_G01_Y-6.4¶N0570_G01_X9.6¶N0571_G01_Y-7.2¶N0572_G01_X-
9.6¶N0573_G01_Y-8¶N0574_G01_X9.6¶N0575_G01_Y-8.8¶N0576_G01_X-
9.6¶N0577_E1_0¶N0578_G01_Z1.72_F0.28¶N0579_E1_1¶N0580_G01_X9.6_F11
0¶N0581_G01_Y-8¶N0582_G01_X-9.6¶N0583_G01_Y-
7.2¶N0584_G01_X9.6¶N0585_G01_Y-6.4¶N0586_G01_X-9.6¶N0587_G01_Y-
5.6¶N0588_G01_X9.6¶N0589_G01_Y-4.8¶N0590_G01_X-9.6¶N0591_G01_Y-

4¶N0592_G01_X9.6¶N0593_G01_Y-3.2¶N0594_G01_X-9.6¶N0595_G01_Y-
2.4¶N0596_G01_X9.6¶N0597_G01_Y-1.6¶N0598_G01_X-9.6¶N0599_G01_Y-
0.8¶N0600_G01_X9.6¶N0601_G01_Y0¶N0602_G01_X-
9.6¶N0603_G01_Y0.8¶N0604_G01_X9.6¶N0605_G01_Y1.6¶N0606_G01_X-
9.6¶N0607_G01_Y2.4¶N0608_G01_X9.6¶N0609_G01_Y3.2¶N0610_G01_X-
9.6¶N0611_G01_Y4¶N0612_G01_X9.6¶N0613_G01_Y4.8¶N0614_G01_X-
9.6¶N0615_G01_Y5.6¶N0616_G01_X9.6¶N0617_G01_Y6.4¶N0618_G01_X-
9.6¶N0619_G01_Y7.2¶N0620_G01_X9.6¶N0621_G01_Y8¶N0622_G01_X-
9.6¶N0623_G01_Y8.8¶N0624_G01_X9.6¶N0625_G01_Z1.96¶N0626_G01_X8.8_
Y9.6¶N0627_G01_Y-
9.6¶N0628_G01_X8¶N0629_G01_Y9.6¶N0630_G01_X7.2¶N0631_G01_Y-
9.6¶N0632_G01_X6.4¶N0633_G01_Y9.6¶N0634_G01_X5.6¶N0635_G01_Y-
9.6¶N0636_G01_X4.8¶N0637_G01_Y9.6¶N0638_G01_X4¶N0639_G01_Y-
9.6¶N0640_G01_X3.2¶N0641_G01_Y9.6¶N0642_G01_X2.4¶N0643_G01_Y-
9.6¶N0644_G01_X1.6¶N0645_G01_Y9.6¶N0646_G01_X0.8¶N0647_G01_Y-
9.6¶N0648_G01_X0¶N0649_G01_Y9.6¶N0650_G01_X-0.8¶N0651_G01_Y-
9.6¶N0652_G01_X-1.6¶N0653_G01_Y9.6¶N0654_G01_X-2.4¶N0655_G01_Y-
9.6¶N0656_G01_X-3.2¶N0657_G01_Y9.6¶N0658_G01_X-4¶N0659_G01_Y-
9.6¶N0660_G01_X-4.8¶N0661_G01_Y9.6¶N0662_G01_X-5.6¶N0663_G01_Y-
9.6¶N0664_G01_X-6.4¶N0665_G01_Y9.6¶N0666_G01_X-7.2¶N0667_G01_Y-
9.6¶N0668_G01_X-8¶N0669_G01_Y9.6¶N0670_G01_X-8.8¶N0671_G01_-
9.6¶N0672_E1_0¶N0673_G01_Z2_F0.28¶N0674_E1_1¶N0675_G01_Y9.6_F110¶N
0676_G01_X-8¶N0677_G01_Y-9.6¶N0678_G01_X-
7.2¶N0679_G01_Y9.6¶N0680_G01_X-6.4¶N0681_G01_Y-9.6¶N0682_G01_X-
5.6¶N0683_G01_Y9.6¶N0684_G01_X-4.8¶N0685_G01_Y-9.6¶N0686_G01_X-
4¶N0687_G01_Y9.6¶N0688_G01_X-3.2¶N0689_G01_Y-9.6¶N0690_G01_X-
2.4¶N0691_G01_Y9.6¶N0692_G01_X-1.6¶N0693_G01_Y-9.6¶N0694_G01_X-
0.8¶N0695_G01_Y9.6¶N0696_G01_X0¶N0697_G01_Y-
9.6¶N0698_G01_X0.8¶N0699_G01_Y9.6¶N0700_G01_X1.6¶N0701_G01_Y-
9.6¶N0702_G01_X2.4¶N0703_G01_Y9.6¶N0704_G01_X3.2¶N0705_G01_Y-
9.6¶N0706_G01_X4¶N0707_G01_Y9.6¶N0708_G01_X4.8¶N0709_G01_Y-
9.6¶N0710_G01_X5.6¶N0711_G01_Y9.6¶N0712_G01_X6.4¶N0713_G01_Y-

9.6¶N0714_G01_X7.2¶N0715_G01_Y9.6¶N0716_G01_X8¶N0717_G01_Y-
9.6¶N0718_G01_X8.8¶N0719_G01_Y9.6¶N0720_G01_Z2.24¶N0721_G01_X9.6_
Y8.8¶N0722_G01_X-
9.6¶N0723_G01_Y8¶N0724_G01_X9.6¶N0725_G01_Y7.2¶N0726_G01_X-
9.6¶N0727_G01_Y6.4¶N0728_G01_X9.6¶N0729_G01_Y5.6¶N0730_G01_X-
9.6¶N0731_G01_Y4.8¶N0732_G01_X9.6¶N0733_G01_Y4¶N0734_G01_X-
9.6¶N0735_G01_Y3.2¶N0736_G01_X9.6¶N0737_G01_Y2.4¶N0738_G01_X-
9.6¶N0739_G01_Y1.6¶N0740_G01_X9.6¶N0741_G01_Y0.8¶N0742_G01_X-
9.6¶N0743_G01_Y0¶N0744_G01_X9.6¶N0745_G01_Y-0.8¶N0746_G01_X-
9.6¶N0747_G01_Y-1.6¶N0748_G01_X9.6¶N0749_G01_Y-2.4¶N0750_G01_X-
9.6¶N0751_G01_Y-3.2¶N0752_G01_X9.6¶N0753_G01_Y-4¶N0754_G01_X-
9.6¶N0755_G01_Y-4.8¶N0756_G01_X9.6¶N0757_G01_Y-5.6¶N0758_G01_X-
9.6¶N0759_G01_Y-6.4¶N0760_G01_X9.6¶N0761_G01_Y-7.2¶N0762_G01_X-
9.6¶N0763_G01_Y-8¶N0764_G01_X9.6¶N0765_G01_Y-8.8¶N0766_G01_X-
9.6¶N0767_E1_0¶N0768_G01_Z3.34_F2¶N0769_M30

Appendix D

NC code program to produce two-layer scaffolds with a strand spacing of 1.60 mm in both the X and Y axes, and a Z spacing of 0.14 mm. The plotting speed is set at 168 mm/min.

N0001_(SCAFFOLD_20X20)N0002_G54¶N0003_(Dispensing)¶N0004_E0_0¶N0005_00_Z106¶N0006_G00_X0_Y0¶N0007_G00_X-9.6_Y-8.8_Z1.14¶N0008_G01_Z0.14_F50¶N0009_E1_1¶N0010_G00¶N0011_G04_P400¶N0012_G01_X9.6_F168¶N0013_G01_Y-7.2¶N0014_G01_X-9.6¶N0015_G01_Y-5.6¶N0016_G01_X9.6¶N0017_G01_Y-4¶N0018_G01_X-9.6¶N0019_G01_Y-2.4¶N0020_G01_X9.6¶N0021_G01_Y-0.8¶N0022_G01_X-9.6¶N0023_G01_Y0.8¶N0024_G01_X9.6¶N0025_G01_Y2.4¶N0026_G01_X-9.6¶N0027_G01_Y4¶N0028_G01_X9.6¶N0029_G01_Y5.6¶N0030_G01_X-9.6¶N0031_G01_Y7.2¶N0032_G01_X9.6¶N0033_G01_Y8.8¶N0034_G01_X9.6¶N0035_G01_Z0.28¶N0036_G01_X-8.8_Y9.6¶N0037_G01_Y-9.6¶N0038_G01_X-7.2¶N0039_G01_Y9.6¶N0040_G01_X-5.6¶N0041_G01_Y-9.6¶N0042_G01_X-4¶N0043_G01_Y9.6¶N0044_G01_X-2.4¶N0045_G01_Y-9.6¶N0046_G01_X-0.8¶N0047_G01_Y9.6¶N0048_G01_X0.8¶N0049_G01_Y-9.6¶N0050_G01_X2.4¶N0051_G01_Y9.6¶N0052_G01_X4¶N0053_G01_Y-9.6¶N0054_G01_X5.6¶N0055_G01_Y9.6¶N0056_G01_X7.2¶N0057_G01_Y-9.6¶N0058_G01_X8.8¶N0059_G01_Y9.6¶N0060_E1_0¶N0061_G01_Z3.34_F2¶N0062_M30

Appendix E

ImageJ macro program for the automated batch counting of PI +ve cells.

```
macro "Batch Measure" {
   requires("1.33n");
   dir = getDirectory("Choose a Directory ");
   list = getFileList(dir);
   start = getTime();
   setBatchMode(true);
   for (i=0; i<list.length; i++) {
      path = dir+list[i];
      showProgress(i, list.length);
      if (!endsWith(path,"/")) open(path);
      if (nImages>=1) {
run("8-bit");
setAutoThreshold();
//run("Threshold...");
setThreshold(set lower bound, set upper bound);
run("Convert to Mask");
run("Analyze Particles...", "size=set lower bound cell size-infinity circularity=0.00-
1.00 show=Nothing display summarize");
          close();
      }
   }
 //print((getTime()-start)/1000);
}
```

Appendix F

ImageJ macro program for the automated batch calculation of the area of +ve ALP staining.

```
macro "Batch Measure" {
   requires("1.33n");
   dir = getDirectory("Choose a Directory ");
   list = getFileList(dir);
   start = getTime();
   setBatchMode(true);
   for (i=0; i<list.length; i++) {
      path = dir+list[i];
      showProgress(i, list.length);
      if (!endsWith(path,"/")) open(path);
      if (nImages>=1) {
run("RGB Split");
close();
setAutoThreshold();
//run("Threshold...");
setThreshold(set lower bound, set upper bound);
run("Threshold", "thresholded remaining black");
run("Analyze Particles...", "size=0.00004-44.44 circularity=0.00-1.00 bins=200
show=Nothing display summarize");
          close();
      }
   }
 //print((getTime()-start)/1000);
}
```

Appendix G: hMSC Characterisation

G.1. Abstract

This appendix describes the characterisation procedure for the cells isolated from human femoral heads. Routine characterisation involved osteogenic, chondrogenic and adipogenic differentiation of the cells. This was assessed by von Kossa, Safranin O and Oil Red-O staining respectively. Weak positive staining was observed after 14 days while strongly positive staining was observed after 21 days.

In cells from one patient (652), this differentiation was further investigated using reverse transcription polymerase chain reaction (RT-PCR) by examining the expression of Runx2, PPARγ2 and Col2A1. Expression of these markers for osteogenesis, chondrogenesis and adipogenesis was observed on days 14 and 21, after exposure to differentiation media.

From the routine staining evidence, and the data from patient 652, it was concluded that the cultured cells were capable of undergoing osteogenic, chondrogenic and adipogenic differentiation, *in vitro*.

Cells from three patients (514, 523 and 531), were examined for two markers associated with MSCs: CD105 and Stro-1. The cells were found to be 92±1% and 30±5% positive for CD105 and Stro-1 respectively. This compared favourably with previous studies characterising MSCs.

Only very limited evidence was presented that multipotent cells were present in the cell cultures, therefore the term “Mesenchymal Stem Cells” was thought to be inappropriate. However, it was concluded that the term “Marrow Stromal Cells” was appropriate for these cell populations.

G.2. Introduction

In recent years, there has been much interest in the study of human marrow stromal cells (hMSCs), also termed mesenchymal stem cells and marrow stromal cells. This is primarily because of their potential for use in regenerative medical applications, as discussed in §1.2.3.3. In the past, a variety of different protocols have been used to characterise hMSCs. The majority of these stress the importance of both plastic-adhesion and the ability to undergo osteogenic, chondrogenic and adipogenic differentiation (Pittenger *et al.*, 1999; Baddoo *et al.*, 2003; Dominici *et al.*, 2006). The identification of surface markers is also thought to be important, however since there is a lack of a specific marker for MSCs (Horwitz *et al.*, 2005), there is debate regarding the markers for which it is most important to test.

A common source of contamination in MSC cultures are cells of haematopoietic origin. CD105 is thought to be expressed by MSCs, but not cells of the haematopoietic lineage (Haynesworth *et al.*, 1992b), furthermore CD105 expression is thought to disappear upon differentiation (Barry *et al.*, 1999; Goussetis *et al.*, 2005). CD105, also called endoglin, is thought to form part of the TGF-β signalling system (Cheifetz *et al.*, 1992). It is, however, not specific to MSCs, as it has also been detected in endothelial cells (Gougos and Letarte, 1990). Nevertheless, in conjunction with other markers, CD105 has been widely used in characterisation processes for MSCs (Keating, 2006; Liu *et al.*, 2008a; Kotobuki *et al.*, 2005; Harting *et al.*, 2008; Meinel *et al.*, 2004).

Simmons and Torok-Strob (1991) first identified an association between Stro-1 and fibroblast colony-forming cells (CFU-F) in human bone marrow. The osteogenic potential of bone marrow aspirates, selected for Stro-1, was assessed by Gronthos *et al*. (1994). After culture in osteogenic media, 90% of the cells in the colonies were found to be positive for alkaline phosphatase (ALP). Similarly, Howard *et al*. (2002) found enriching for Stro-1 from bone marrow aspirates, led to a 300% increase in the ratio of CFU-F isolated. The Stro-1 positive fraction also showed increased ALP activity over unselected marrow cell cultures. In addition, Stewart *et al*. (1999)

found Stro-1 to be characteristic of relatively undifferentiated cells capable of osteoblastic differentiation. Stro-1 has, therefore, been used to characterise MSCs in previous studies (Wang *et al.*, 2003; Tuli *et al.*, 2003; Coipeau *et al.*, 2009; Zhang *et al.*, 2009).

The aim of the studies described in this appendix was to characterise hMSCs, prepared as described in preceding chapters of this thesis. To achieve this, the ability of the cells to undergo osteogenic, chondrogenic and adipogenic differentiation, was assessed. The presence of the markers CD105 and Stro-1 was also examined using flow cytometry.

G.3. Materials and Methods

Unless otherwise stated, all reagents were purchased from Sigma, UK.

G.3.1. Cell Culture

G.3.1.1. Human MSC Isolation and Culture

After written consent from the patients and approval from the local ethical committee (Lothian local research ethics committee), human femoral head tissue was obtained from patients who had undergone elective arthroplasty. In addition to routine characterisation, tissue was collected from four patients (see **Table G.1**). The tissue samples were allocated an anonymous number based on the chronological order of the sample collection. It should be noted that the patient numbers for routine characterisation are not listed below.

Table G.1: hMSC patient details for non-routine characterisation.

In-House Patient Number	514	523	531	652
Patient Age	60	57	58	57
Patient Sex	Male	Female	Female	Female

The samples were stored at 4°C in sterile phosphate buffered saline (PBS) (Oxoid, UK) directly after surgery. The hMSCs were isolated from the samples and cultured as described above in §3.3.1.1.

G.3.2. Human MSC Differentiation

The experiments described in sections §G.3.2.1, §G.3.2.4 and §G.3.2.5 were conducted by Miss Kate Cameron.

G.3.2.1. Differentiation Protocol for Patient 652

The media referred to as "osteogenic media" was identical to the OS media described in §5.4.2.2. "Chondrogenic media" consisted of Dulbecco's Modified Eagle's Medium – high glucose (DMEM), supplemented with L-glutamine (2 mM) (Gibco, UK), penicillin (100 IU/ml), streptomycin (100 µg/ml) (Gibco, UK), dexamethasone (100 nM), L-ascorbic acid-2-phosphate (50 µg/ml), sodium pyruvate (1 mM), proline (40 µM), TGF-β3 (10 ng/ml), insulin (6 µg/ml) transferrin (6 µg/ml) and bovine serum albumin (1.25 mg/ml). "Adipogenic media" consisted of growth media (as described in §3.3.1) supplemented with dexamethasone (1 µM), 3-isobutyl-1-methylxanthine (0.5 mM), insulin (1 µg/ml), and indomethacin (0.1 mM).

Tissue culture flasks (75 cm^2) containing confluent hMSCs (passage 3) from patient 652, were washed three times in PBS, and the cells were detached from the flasks using trypsin solution (2.5 mg/ml) in PBS (Invitrogen, UK) and growth media, as described in §3.3.1. The cell density of the suspensions was measured using a haemocytometer. After appropriate dilution with growth media, the cells were added to wells of 12-well treated tissue culture (TC) plastic plates (Corning, USA) at a density of 2×10^4 cells/well (in 2 ml of media). The plates were then maintained in a humidified air incubator at 37°C with 5% (v/v) CO_2, for 3 days, to become confluent.

Afterwards, the culture media was replaced with osteogenic media, chondrogenic media or adipogenic media. The cells were maintained in a humidified air incubator at 37°C with 5% (v/v) CO_2, and the media was refreshed at regular intervals three times every 7 days. After 7, 14 and 21 days, three wells of cells were fixed with paraformaldehype as described in §3.3.4.1. TRIzol® Reagent (Invitrogen, UK) was added to a further three wells per time point (200 µl/well). After 5 min of incubation at room temperature and mixing by repeated aspiration, RNA was extracted from the

samples as described in §7.4.2.1 and complimentary DNA was synthesised as described in §7.4.2.2, and stored at -80°C.

The fixed cells were stained as described below in §G.3.2.3. RT-PCR was used to analyse the cDNA samples, as described below in §G.3.2.5.

G.3.2.2. Routine Differentiation Protocol

Routine characterisation of hMSCs cultured in the laboratory was conducted by Dr Nusrat Khan. The cells were cultured and exposed to osteogenic, chondrogenic and adipogenic media as described in §G.3.2.1. These cells were subsequently fixed and stained using the von Kossa technique, and stained using Safranin O and Oil Red-O as described below in §G.3.2.3.

G.3.2.3. Staining

The fixed cells were stained as previously described by Tremoleda *et al.* (2008). Mineralisation was identified using the von Kossa technique (Bills *et al.*, 1971). Three wells of cells per time point were incubated in 0.5% (w/v) silver nitrate under strong light for 1 hr at room temperature. Following a 5 min wash with dH_2O, the cells were incubated in 5% (w/v) sodium thiosulphate for 5 min at room temperature. The cells were then washed twice with dH_2O, before 200 µl of dH_2O were added to the wells.

Proteoglycan production was indicated using Safranin O staining (Rosenberg, 1971) of three wells per time point. The cells were washed with dH_2O and incubated in Safranin O solution (0.5% (w/v) in 0.1 M sodium acetate buffer pH 4.6) for 10 min at room temperature. Following washing with dH_2O, the cells were dehydrated with 95% ethyl alcohol, absolute ethyl alcohol and xylene (using 2 changes each, 2 min in each solution). The cells were mounted using Pertex non-aqueous mountant.

Adipogenesis was identified using Oil Red-O staining (Pittenger *et al.*, 1999) of three wells per time point. The cells were first covered with 60% (v/v) isopropanol for 3 min and then with 3 mg/ml Oil Red-O (3 parts of 5 mg/ml Oil Red-O to 2 parts

dH_2O) for 10 min. The cells were then washed twice with dH_2O, before 200 µl of dH_2O were added to the wells.

The plates were then photographed using a mounted camera (Nikon, DXM1200) on an inverted microscope (Nikon, Eclipse TS 100) set for bright-field at × 10 magnification.

G.3.2.4. Positive control for RT-PCR

Bone chips were prepared from the femoral head from patient 652 as described in §3.3.1.2. RNA was then extracted as previously described by Voultsiadou (2009). Bone chips attached to both adipose and cartilage tissue were selected, and the sample was pulverised in liquid nitrogen using a mortar and pestle. The homogenised sample was suspended in TRIzol® Reagent and allowed to incubate at room temperature for 5 min before being centrifuged (2 min at 13,000 rpm (eppendorf centrifuge 5417R)) to remove any debris. The supernatant was transferred to a new eppendorf tube. The RNA was extracted from the sample as described in §7.4.2.1 and complimentary DNA was synthesised as described in §7.4.2.2. The sample was stored at -80°C.

G.3.2.5. RT-PCR

RT-PCR was used to analyse the cDNA samples described in §G.3.2.1 and G.3.2.4. The samples were processed and visualised on agarose gels using the general procedure described in §7.4.2.3 and §7.4.2.4, substituting the primers for the human genes PPARγ2, Runx2, Type-II Collagen, and GAPDH. The latter acting as a housekeeping gene to confirm equal loading. The primer sequences, annealing temperatures and cycle numbers used are shown in **Table G.2**.

Table G.2: Primer sequences for PCR

Gene	Temperature	Number of cycles	Sequence and Fragment Size
PPARγ2	50.0°C	40	5'-AAACTCTGGGAGATTCTCCT-3' 5'-TCTTGTGAATGGAATGTCTT-3' (Sottile *et al.*, 2002)
Runx2	57.5°C	35	5'-CCGCACGACAACCGCACCAT-3' 5'-CGCTCCGGCCTACAAATCTC-3' (Kozhevnikova *et al.*, 2008)
Type-II Collagen	55.0°C	40	5'-GAAACCATCAATGGTGGCTT C-3' 5'-CGATAACAGTCTTGCCCCA C-3' (designed in-house)
GAPDH	55.0°C	35	5'-TGTTGCCATCAATGACCCCTT-3' 5'-CTCCACGACGTACTCAGCG-3' (designed in-house)

G.3.3. Flow Cytometry

The experiments described in this section were conducted by Dr Aimee Reynolds and Mrs Kay Samuel.

Tissue culture flasks (75 cm^2) containing confluent hMSCs from patients 514 (passage 5), 523 (passage 3) and 531 (passage 4) (in separate flasks), were washed three times in PBS, and the cells were detached from the flasks using trypsin solution (2.5 mg/ml) in PBS (Invitrogen, UK) and growth media, as described in §3.3.1. The cell density was measured using a haemocytometer. The cell suspensions were centrifuged (1,000 rpm for 5 min), the supernatant was discarded and the cell pellets were resuspended in FACS-PBS (PBS supplemented with 0.1% BSA and 0.1% sodium azide) to a final cell density of 1×10^7 cells/ml. Aliquots of 1 x 10^6 cells were incubated for 40 min at 4°C with optimum concentration (determined by titration), of primary antibody to STRO-1 (mouse IgM) (BioLegend) or CD105-APC

(mouse IgG) (BioLegend). The cells were washed twice to remove unbound antibody and resuspended in 100 µl FACS-PBS. Binding of primary antibody was detected using optimum concentration (determined by titration) of appropriate isotype specific fluorochrome labelled secondary antibody: anti-mouse IgM-PE and anti-mouse IgG-PE (Jackson Labs).

After incubation for 40 min at 4°C, the cells were washed twice and finally resuspended in 250 µl. Unstained cells and cells labelled with secondary antibody alone were included as controls. Dead and apoptotic cells, and debris were excluded from analysis using an electronic 'live' gate on forward scatter and side scatter parameters. Data for 5,000 - 100,000 'live' events were acquired for each sample using a FACSCaliber cytometer equipped with 488nm and 633nm lasers and analysed using CellQuest software (Becton Dickinson).

G.4. Results

G.4.1. Human MSC Differentiation

G.4.1.1. Staining

Negative staining was observed for all samples at day 7 for each staining technique (see **Figure G.1**). Weak positive von Kossa, Safranin O, and Oil Red-O staining was observed after 14 days for the cells cultured in osteogenic, chondrogenic and adipogenic media respectively. Stronger positive staining was routinely observed after 21 days for each treatment group (see **Figure G.1**).

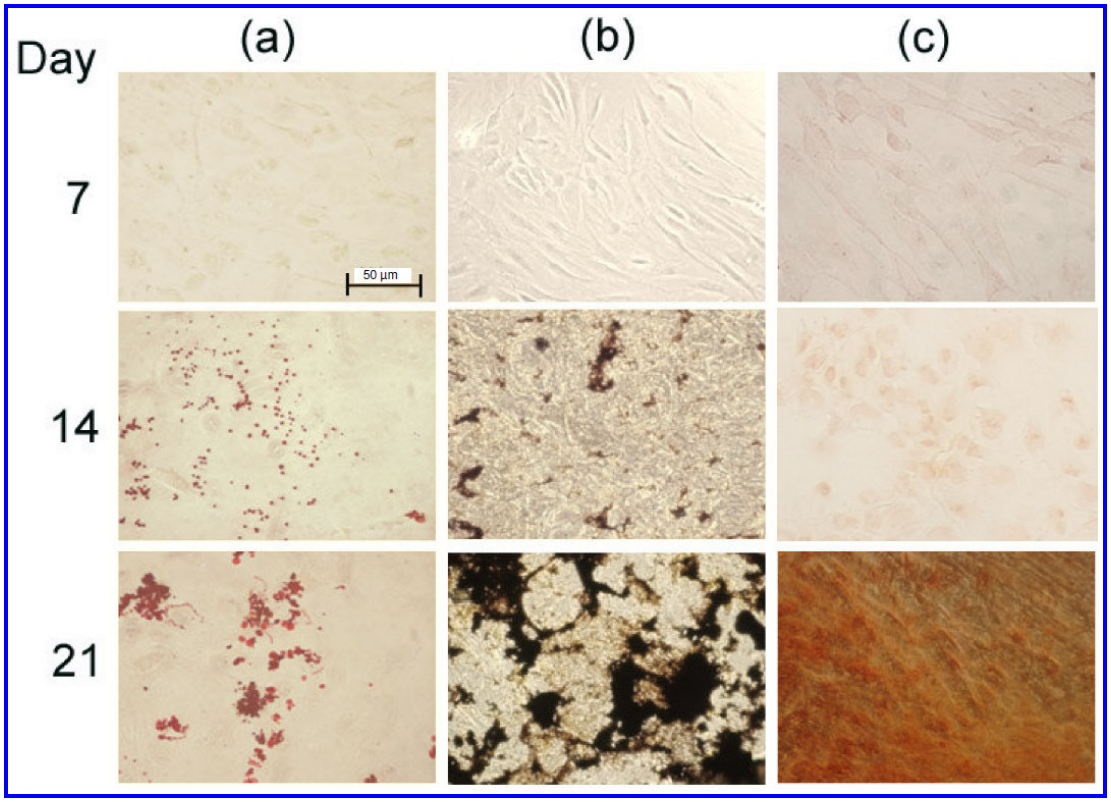

Figure G.1: hMSC Staining for Differentiation.

Bright-field images of hMSCs. The figures represent a) hMSCs cultured in adipogenic media stained with Oil Red-O, b) hMSCs cultured in osteogenic media stained using the von Kossa technique and, c) hMSCs cultured in chondrogenic media and stained using Safranin O. These representative images were taken at × 20 magnification, of tissue from a representative patient (patient 652). The bar represents 50 µm.

G.4.1.2. RT-PCR

For each primer pair, single bands were observed in the electrophoresis gels for the positive control. These bands had approximately the number of base pairs predicted (see **Table G.2**). PPARγ2 expression for the cells treated with adipogenic media, was not evident at day 7 but was observed on days 14 and 21 (see **Figure G.2**). PPARγ2 expression appeared to be higher on day 21 than day 14.

Runx2 expression was not found on day 7 in the cells cultured in osteogenic media (see **Figure G.2**). Runx2 was up-regulated on days 14 and 21, with expression on day 14 being the higher of the two time points.

Again, Type-II collagen alpha 1 (Col2A1) expression was not found on day 7 in the cells cultured in chondrogenic media (see **Figure G.2**). Col2A1 expression was evident on days 14 and 21. Expression was observed to be higher on day 21 than day 14.

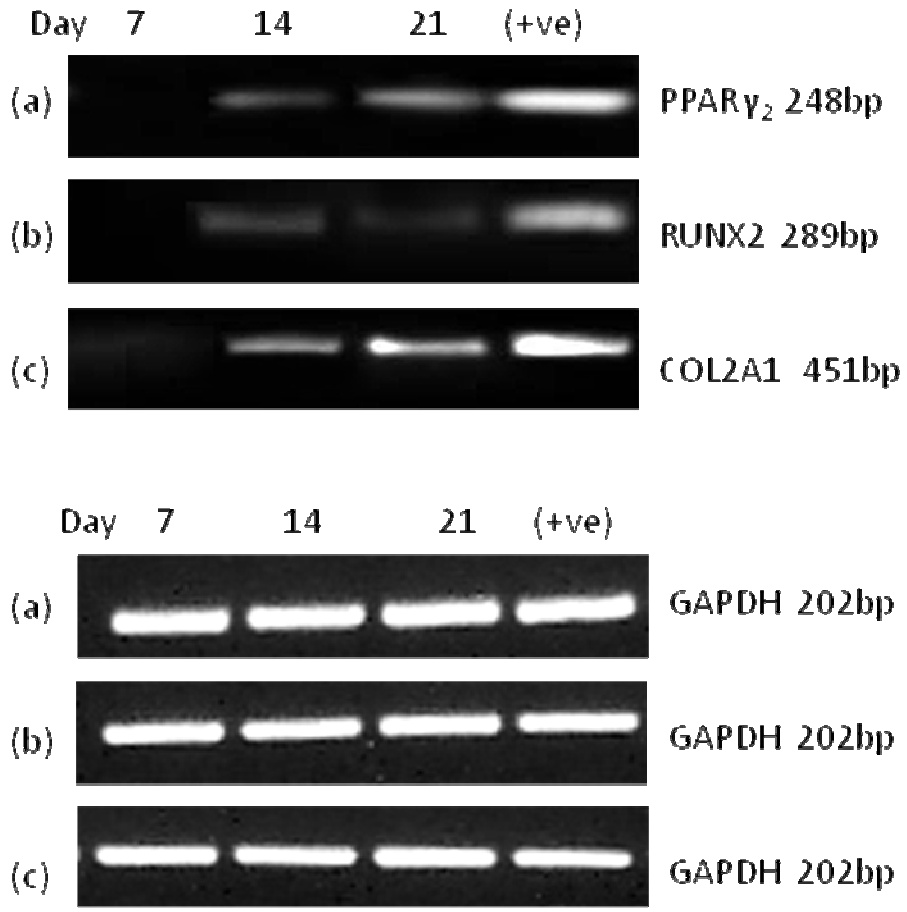

Figure G.2: Electrophoresis Gels for RT-PCR of differentiated hMSCs.

These figures represent electrophoresis gels, visualising the RT-PCR products for hMSCs exposed to a) adipogenic media, b) osteogenic media, and c) chondrogenic media. The genes of interest, and the time points are as indicated.

G.4.2. Flow Cytometry

Data plots were derived from flow cytometry, see **Figure G.3**. It was found that 92±1% of the live cells were CD105 positive, and 30±5% were Stro-1 positive.

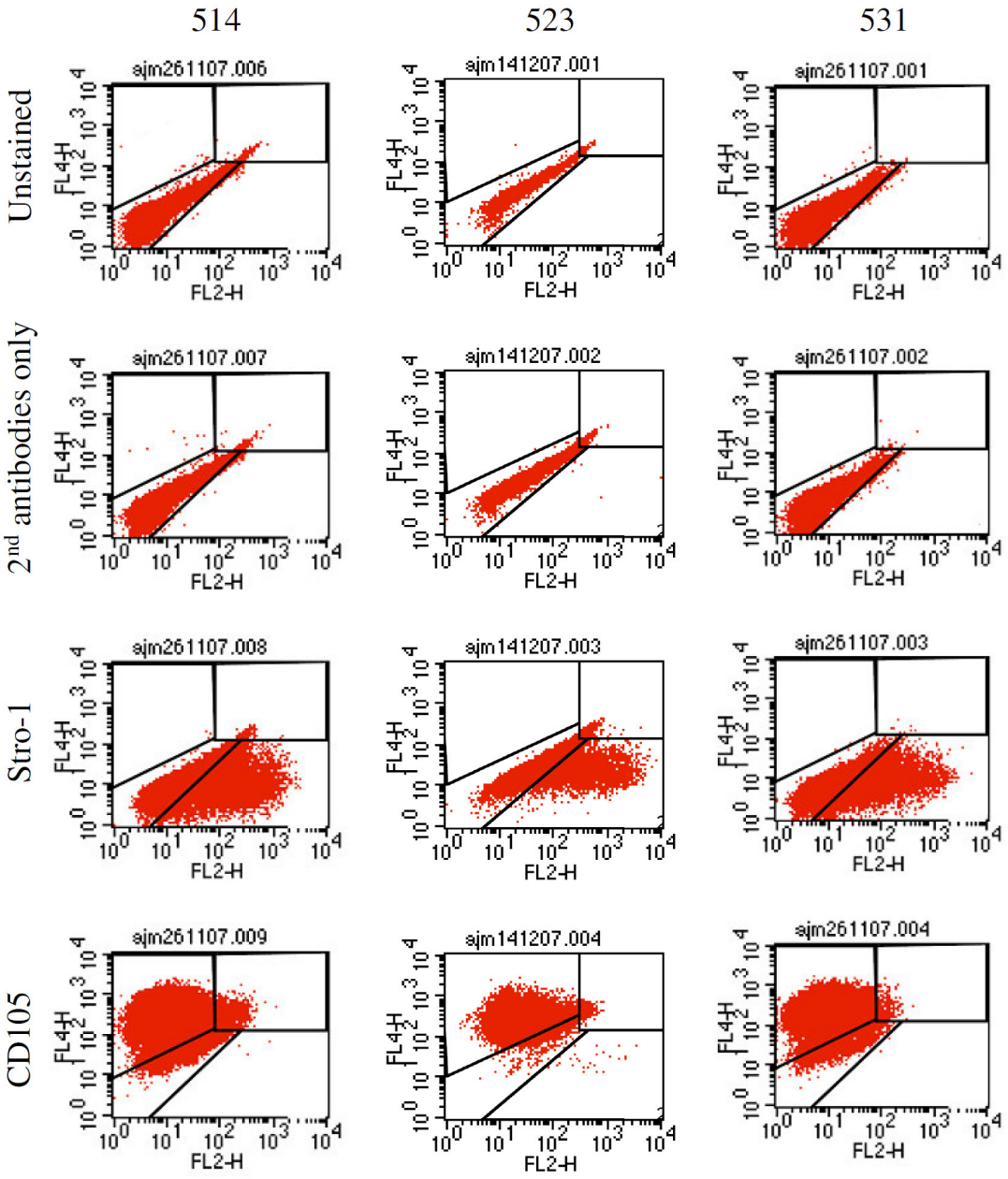

Figure G.3: Graphs of flow cytometry.

These figures represent data plots collected using flow cytometry for hMSCs from each of the three patients tested.

G.5. Discussion

G.5.1. Differentiation

As discussed in §5.6.2, the OS media used in the current study is known to induce hMSCs to undergo osteogenic differentiation. Mineralisation, as determined by staining using the von Kossa technique, is a widely used indicator of osteogenesis (Howard *et al.*, 2002; Kim *et al.*, 2005; Tremoleda *et al.*, 2008).

Mineralisation was routinely observed after 21 days of exposure to osteogenic media (see **Figure G.1**). This implies that at least a subpopulation of the hMSCs cultured was capable of osteogenic differentiation.

The chondrogenic media used during these studies, has been shown previously to induce chondrogenic differentiation in hMSCs (Pittenger *et al.*, 2002). Positive Safranin O staining is a widely accepted method of detecting chondrogenic differentiation (Rosenberg, 1971; Kim *et al.*, 2005; Tremoleda *et al.*, 2008).

Consistently positive Safranin O staining was observed after 21 days of exposure to chondrogenic media (see **Figure G.1**). This provides evidence that at least a subpopulation of the hMSCs cultured was capable of chondrogenic differentiation.

Again, the adipogenic media used in the studies described above has previously been shown to stimulate the adipogenic differentiation of hMSCs (Pittenger *et al.*, 2002). Positive Oil Red-O staining is often used to identify adipogenic differentiation (Asahina *et al.*, 1996; Pittenger *et al.*, 1999; Tremoleda *et al.*, 2008).

Positive Oil Red-O staining was routinely observed after 21 days of exposure to adipogenic differentiation (see **Figure G.1**). Again, this would provide evidence that at least a subpopulation of the hMSCs cultures was capable of adipogenic differentiation. Hence it was concluded that, consistently, cells were present in the hMSC cultures which were capable of osteogenesis, chondrogenesis and adipogenesis.

G.5.2. Morphology

The cells isolated were also found to have fibroblastic morphology similar to that described for CFU-F (Gronthos *et al.*, 1994). The cells were also found to be within the 20 – 150 µm diameter size range reported for MSCs cultured *in vitro* (Curran *et al.*, 2006; Noth *et al.*, 2002; Salasznyk *et al.*, 2004; Liu *et al.*, 2003; Hong *et al.*, 2005; Santiago *et al.*, 2009; Sengers *et al.*, 2010).

G.5.3. RT-PCR

For one patient (652), the differentiation process was examined further. As previously discussed in §7.3, Runx2 is thought to act as the "master switch" for osteogenic differentiation. Similarly, the adipocyte specific transcription factor PPARγ2 is thought to stimulate adipogenesis in MSCs and to inhibit osteogenesis (Lecka-Czernik *et al.*, 2002), hence PPARγ2 expression is used widely as an indicator of adipogenic differentiation (Duque and Rivas, 2007; Kim *et al.*, 2007b; Shang *et al.*, 2007).

Unlike Runx2 and PPARγ2, Col2A1 is not a transcription factor, instead this gene codes for a structural protein. Type-II collagen forms a high proportion of the extracellular matrix of articular cartilage (Herbage *et al.*, 1977). Therefore, Col2A1 has become a widely used marker for chondrogenesis (Kawakami *et al.*, 2005; Dickhut *et al.*, 2008; Zimmermann *et al.*, 2008).

The up-regulation of these markers of MSC differentiation (see **Figure G.2**), gives further evidence, at least in the case of patient 652, that at least a subpopulation of the cells cultured was able to undergo osteogenic, chondrogenic and adipogenic differentiation. In addition, this presents some evidence that the cultures were in a relatively undifferentiated state before day 7, implying the presence of multipotent cells. However, it should be emphasised that these data relate to one patient only, and do not indicate if this was consistent for cells derived using the isolation procedure described in §3.3.1.1.

G.5.4. Flow Cytometry

Relatively high numbers of hMSCs isolated using the technique described in §3.3.1.1, were found to be CD105 positive (see **Figure G.3**). Levels recorded in the studies described above (92±1%) were comparable to those found by Liu *et al.* (2008a) (approximately 97%), and superior to those found by Sakaguchi *et al.* (2004) (74±41%) and Meinel *et al.* 2004 (approximately 87%). CD105 is thought to be expressed by MSCs, but not by cells of the haematopoietic lineage (Haynesworth *et al.*, 1992b), furthermore CD105 expression is thought to disappear upon differentiation (Barry *et al.*, 1999; Goussetis *et al.*, 2005). Therefore, if present, cells of the haematopoietic lineage represented a maximum of 8% of the cultured cells.

Similarly, relatively high numbers of hMSCs were positive for Stro-1 (see **Figure G.3**). The 30±5% recorded in the studies described above was found to be higher than that reported by Zhand *et al.* (2009) (10.4%) and Howard *et al.* (2002) (7.12±3.78% before Stro-1 positive cells were actively selected for), and was found to be comparable to levels reported by Stenderup *et al*. (2001) (27%). As discussed in §G.2, Stro-1 positive cells are associated with relatively undifferentiated cells, capable of osteoblastic differentiation.

These data, particularly for Stro-1, represent evidence that at least a subpopulation of the cultured cells was CFU-F, capable of osteogenic differentiation.

G.5.5. Cell Classification

The cell isolation procedure used for the studies described above, has been widely used by previous authors to extract hMSCs (Tremoleda *et al.*, 2008; Gronthos *et al.*, 1998; Gundle *et al.*, 1995).

The routine characterisation procedure for the hMSCs indicates that, consistently, a proportion of the cells was able to undergo osteogenic, chondrogenic and adipogenic differentiation. It should be noted, however, that evidence was not presented that the populations of progenitor cells for the three lineages represented the same population. Whether multipotent MSCs were present, or whether the cultures

contained a mixture of committed progenitor cells, was unclear. However, this is true of previous studies (Owen, 1988; Pittenger *et al.*, 1999; Digirolamo *et al.*, 1999; Kemp *et al.*, 2005). Indeed, in a given MSC population cultured *in vitro*, the frequency of multipotent cells may be low, with most cells being bi- or indeed uni-potent (Digirolamo, 1999 #1051).

For studies designed to examine the cell biology of MSCs in detail, a collection of markers must be examined (Kemp *et al.*, 2005; Dominici *et al.*, 2006). The cells should not express haematopoietic markers such as CD34, CD45 and CD14 nor endothelial cell markers such as CD24, CD31 and VWF (Kemp *et al.*, 2005; Pittenger *et al.*, 1999; Prockop, 1997; Majumdar *et al.*, 1998). The cells should also express the adhesion molecule CD90 (Rege and Hagood, 2006; Campioni *et al.*, 2008), CD105 which is part of the TGF-β signalling system (see §G.2), and the marker for non-haematopoietic stromal cells, CD73 (Haynesworth *et al.*, 1992b).

However, many studies focussing on scaffolds for bone regenerative medical applications, or the osteogenic differentiation of the cells, use MSC characterisation procedures similar to, or less rigorous than, those utilised in the studies described in this appendix (Tremoleda *et al.*, 2008; Porter *et al.*, 2009; Tsiridis *et al.*, 2007; Moreau and Xu, 2009; Edgar *et al.*, 2007; Knippenberg *et al.*, 2006). Since only very limited evidence was presented that a subpopulation of the cells was multipotent, the term “Mesenchymal Stem Cells” was thought to be inappropriate for the cells cultured (Horwitz *et al.*, 2005). However, the characterisation procedure described above was thought sufficient to term the cultured cells “Marrow Stromal Cells”.

G.6. Conclusions

The studies described in this appendix aimed to characterise the cells isolated from primary human tissue. The ability of the cells to undergo osteogenic, chondrogenic and adipogenic differentiation was assessed using von Kossa, Safranin-O and Oil Red-O staining. Positive staining for these three differentiation pathways was routinely found to be positive by the 21st day after exposure to differentiation media. For one patient, expression of genes characteristic of osteogenic, chondrogenic and adipogenic differentiation was also observed.

The cells were also examined for markers associated with MSCs: CD105 and Stro-1. The expression of these markers was found to be consistently high, relative to previous studies.

Although only very limited evidence was presented that multipotent cells were present in the cell cultures, it was concluded that the term “Marrow Stromal Cells” was appropriate for these cell populations.

References

Achilli, M. and Mantovani, D. (2010). Tailoring Mechanical Properties of Collagen-Based Scaffolds for Vascular Tissue Engineering: The Effects of pH, Temperature and Ionic Strength on Gelation. *Polymers*. **2**(4): 664-680.

Adhirajan, N., Shanmugasundaram, N., Shanmuganathan, S. and Babu, M. (2009). Functionally modified gelatin microspheres impregnated collagen scaffold as novel wound dressing to attenuate the proteases and bacterial growth. *Eur J Pharm Sci*. **36**(2-3): 235-245.

Ahlmann, E., Patzakis, M., Roidis, N., Shepherd, L. and Holtom, P. (2002). Comparison of anterior and posterior iliac crest bone grafts in terms of harvest-site morbidity and functional outcomes. *J Bone Joint Surg Am*. **84-A**(5): 716-720.

Ahn, S., Montero, M., Odell, D., Roundy, S. and Wright, P. (2002). Anisotropic material properties of fused deposition modelling ABS. *Rapid Prototyping*. **8**(4): 248-257.

Alemdaroglu, C., Degim, Z., Celebi, N., Zor, F., Ozturk, S. and Erdogan, D. (2006). An investigation on burn wound healing in rats with chitosan gel formulation containing epidermal growth factor. *Burns*. **32**(3): 319-327.

Alexakis, C., Partridge, T. and Bou-Gharios, G. (2007). Implication of the satellite cell in dystrophic muscle fibrosis: a self-perpetuating mechanism of collagen overproduction. *Am J Physiol Cell Physiol*. **293**(2): C661-669.

Allen, M.R., Hock, J.M. and Burr, D.B. (2004). Periosteum: biology, regulation, and response to osteoporosis therapies. *Bone*. **35**(5): 1003-1012.

Alliston, T., Choy, L., Ducy, P., Karsenty, G. and Derynck, R. (2001). TGF-beta-induced repression of CBFA1 by Smad3 decreases cbfa1 and osteocalcin expression and inhibits osteoblast differentiation. *Embo J*. **20**(9): 2254-2272.

Amaral, M., Dias, A.G., Gomes, P.S., Lopes, M.A., Silva, R.F., Santos, J.D. and Fernandes, M.H. (2008). Nanocrystalline diamond: In vitro biocompatibility assessment by MG63 and human bone marrow cells cultures. *J Biomed Mater Res A*. **87**(1): 91-99.

Andersen, T.L., Sondergaard, T.E., Skorzynska, K.E., Plesner, T., Plesner, T.L., Hauge, E. and Delaisse, J.-M. (2008). A physical mechanism for coupling bone resorption and formation in adult human bone. *Bone*. **42**(Supplement 1): S42-S42.

Andrew, J.G., Hoyland, J.A., Freemont, A.J. and Marsh, D.R. (1995). Platelet-derived growth factor expression in normally healing human fractures. *Bone*. **16**(4): 455-460.

Ang, T.H., Sultana, F.S.A., Hutmacher, D.W., Wong, Y.S., Fuh, J.Y.H., Mo, X.M., Loh, H.T., Burdet, E. and Teoh, S.H. (2002). Fabrication of 3D chitosan-hydroxyapatite scaffolds using a robotic dispensing system. *Mater. Sci. Eng., C*. **20**: 35-42.

Antonov, E.N., Bagratashvili, V.N., Whitaker, M.J., Barry, J.J., Shakesheff, K.M., Konovalov, A.N., Popov, V.K. and Howdle, S.M. (2004). Three-Dimensional Bioactive and Biodegradable Scaffolds Fabricated by Surface-Selective Laser Sintering. *Adv Mater Deerfield*. **17**(3): 327-330.

Aoki, H., Fujii, M., Imamura, T., Yagi, K., Takehara, K., Kato, M. and Miyazono, K. (2001). Synergistic effects of different bone morphogenetic protein type I receptors on alkaline phosphatase induction. *J Cell Sci*. **114**(Pt 8): 1483-1489.

Arrington, E.D., Smith, W.J., Chambers, H.G., Bucknell, A.L. and Davino, N.A. (1996). Complications of iliac crest bone graft harvesting. *Clin Orthop Relat Res*. **329**: 300-309.

Asahina, I., Sampath, T.K. and Hauschka, P.V. (1996). Human Osteogenic Protein-1 Induces Chondroblastic, Osteoblastic, and/or Adipocytic Differentiation of Clonal Murine Target Cells. *Exp Cell Res*. **222**(1): 38-47.

Aspenberg, P., Albrektsson, T. and Thorngren, K.G. (1989). Local application of growth-factor IGF-1 to healing bone. Experiments with a titanium chamber in rabbits. *Acta Orthop Scand*. **60**(5): 607-610.

Atala, A. and Lanza, R.P. (2002). *Methods of tissue engineering*. ed., Academic, London.

Aubin, J.E., Liu, F., Malaval, L. and Gupta, A.K. (1995). Osteoblast and chondroblast differentiation. *Bone*. **17**(2 Suppl): 77S-83S.

Aubin, J.E. and Turksen, K. (1996). Monoclonal antibodies as tools for studying the osteoblast lineage. *Microsc Res Tech*. **33**(2): 128-140.

Augst, A.D., Kong, H.J. and Mooney, D.J. (2006). Alginate hydrogels as biomaterials. *Macromol Biosci*. **6**(8): 623-633.

Babensee, J.E., McIntire, L.V. and Mikos, A.G. (2000). Growth factor delivery for tissue engineering. *Pharm Res*. **17**(5): 497-504.

Babhulkar, S., Pande, K. and Babhulkar, S. (2005). Nonunion of the diaphysis of long bones. *Clin Orthop Relat Res*. **431**: 50-56.

Baddoo, M., Hill, K., Wilkinson, R., Gaupp, D., Hughes, C., Kopen, G.C. and Phinney, D.G. (2003). Characterization of mesenchymal stem cells isolated from murine bone marrow by negative selection. *J Cell Biochem*. **89**(6): 1235-1249.

Bae, H.W., Zhao, L., Kanim, L.E., Wong, P., Delamarter, R.B. and Dawson, E.G. (2006). Intervariability and intravariability of bone morphogenetic proteins in commercially available demineralized bone matrix products. *Spine*. **31**(12): 1299-1306; discussion 1307-1298.

Bai, C.B., Auerbach, W., Lee, J.S., Stephen, D. and Joyner, A.L. (2002). Gli2, but not Gli1, is required for initial Shh signaling and ectopic activation of the Shh pathway. *Development*. **129**(20): 4753-4761.

Bak, B., Jorgensen, P.H. and Andreassen, T.T. (1990). Dose response of growth hormone on fracture healing in the rat. *Acta Orthop Scand*. **61**(1): 54-57.

Baker, M. (2008). FDA to vet embryonic stem cells' safety. *Nature*. **452**(7188): 670.

Banerjee, C., Javed, A., Choi, J.Y., Green, J., Rosen, V., van Wijnen, A.J., Stein, J.L., Lian, J.B. and Stein, G.S. (2001). Differential regulation of the two principal Runx2/Cbfa1 n-terminal isoforms in response to bone morphogenetic protein-2 during development of the osteoblast phenotype. *Endocrinology*. **142**(9): 4026-4039.

Banfi, A., Muraglia, A., Dozin, B., Mastrogiacomo, M., Cancedda, R. and Quarto, R. (2000). Proliferation kinetics and differentiation potential of ex vivo expanded human bone marrow stromal cells: Implications for their use in cell therapy. *Exp Hematol*. **28**(6): 707-715.

Baron, R. (1996). Anatomy and ultrastructure of bone. In: *Primer on the metabolic bone diseases and disorders of mineral metabolism*), Lippincott-Raven, New York, pp. 3-10.

Baron, R., Neff, L., Tran Van, P., Nefussi, J.R. and Vignery, A. (1986). Kinetic and cytochemical identification of osteoclast precursors and their differentiation into multinucleated osteoclasts. *Am J Pathol*. **122**(2): 363-378.

Barron, M., Franklin, L., Woodall, J., Jr., Wingerter, S., Benghuzzi, H. and Tucci, M. (2007). Comparison of osteoconductive materials on MG63 osteoblast cell function. *Biomed Sci Instrum*. **43**: 248-253.

Barron, V. and Pandit, A. (2003). Chapter 13: Combinatorial Approaches in Tissue Engineering: Progenitor Cells, Scaffolds, and Growth Factors. In: *Topics in Tissue Engineering* (N. Ashammakhi and P. Ferretti, eds.), University of Oulu, Vol. 1, pp. 1 - 21.

Barry, F., Boynton, R., Murphy, M., Haynesworth, S. and Zaia, J. (2001). The SH-3 and SH-4 antibodies recognize distinct epitopes on CD73 from human mesenchymal stem cells. *Biochem Biophys Res Commun*. **289**(2): 519-524.

Barry, F.P., Boynton, R.E., Haynesworth, S., Murphy, J.M. and Zaia, J. (1999). The monoclonal antibody SH-2, raised against human mesenchymal stem cells,

recognizes an epitope on endoglin (CD105). *Biochem Biophys Res Commun*. **265**(1): 134-139.

Bauer, T.W. and Muschler, G.F. (2000). Bone graft materials. An overview of the basic science. *Clin Orthop Relat Res*. **371**: 10-27.

Baylink, D.J., Finkelman, R.D. and Mohan, S. (1993). Growth factors to stimulate bone formation. *J Bone Miner Res*. **8 Suppl 2**: S565-572.

Behrens, J., Jerchow, B.A., Wurtele, M., Grimm, J., Asbrand, C., Wirtz, R., Kuhl, M., Wedlich, D. and Birchmeier, W. (1998). Functional interaction of an axin homolog, conductin, with beta-catenin, APC, and GSK3beta. *Science*. **280**(5363): 596-599.

Benoit, D.S., Tripodi, M.C., Blanchette, J.O., Langer, S.J., Leinwand, L.A. and Anseth, K.S. (2007). Integrin-linked kinase production prevents anoikis in human mesenchymal stem cells. *J Biomed Mater Res A*. **81**(2): 259-268.

Beresford, J.N., Joyner, C.J., Devlin, C. and Triffitt, J.T. (1994). The effects of dexamethasone and 1,25-dihydroxyvitamin D3 on osteogenic differentiation of human marrow stromal cells in vitro. *Arch Oral Biol*. **39**(11): 941-947.

Berger, J., Reist, M., Mayer, J.M., Felt, O. and Gurny, R. (2004a). Structure and interactions in chitosan hydrogels formed by complexation or aggregation for biomedical applications. *Eur J Pharm Biopharm*. **57**(1): 35-52.

Berger, J., Reist, M., Mayer, J.M., Felt, O., Peppas, N.A. and Gurny, R. (2004b). Structure and interactions in covalently and ionically crosslinked chitosan hydrogels for biomedical applications. *Eur J Pharm Biopharm*. **57**(1): 19-34.

Bernard, G.W. (1969). The ultrastructural interface of bone crystals and organic matrix in woven and lamellar endochondral bone. *J Dent Res*. **48**(5): 781-788.

Bernardo, M.E., Zaffaroni, N., Novara, F., Cometa, A.M., Avanzini, M.A., Moretta, A., Montagna, D., Maccario, R., Villa, R., Daidone, M.G., Zuffardi, O. and Locatelli, F. (2007). Human bone marrow derived mesenchymal stem cells do not undergo transformation after long-term in vitro culture and do not exhibit telomere maintenance mechanisms. *Cancer Res*. **67**(19): 9142-9149.

Bessa, P.C., Casal, M. and Reis, R.L. (2008). Bone morphogenetic proteins in tissue engineering: the road from the laboratory to the clinic, part I (basic concepts). *J Tissue Eng Regen Med*. **2**(1): 1-13.

Bhanot, P., Brink, M., Samos, C.H., Hsieh, J.C., Wang, Y., Macke, J.P., Andrew, D., Nathans, J. and Nusse, R. (1996). A new member of the frizzled family from Drosophila functions as a Wingless receptor. *Nature*. **382**(6588): 225-230.

Bianco, P., Riminucci, M., Silvestrini, G., Bonucci, E., Termine, J.D., Fisher, L.W. and Robey, P.G. (1993). Localization of bone sialoprotein (BSP) to Golgi and post-Golgi secretory structures in osteoblasts and to discrete sites in early bone matrix. *J Histochem Cytochem*. **41**(2): 193-203.

Bianco, P. and Robey, P.G. (2000). Marrow stromal stem cells. *J. Clin. Invest.* **105**(12): 1663-1668.

Bielby, R., Jones, E. and McGonagle, D. (2007). The role of mesenchymal stem cells in maintenance and repair of bone. *Injury*. **38**(1, Supplement 1): S26-S32.

Bigi, A., Bracci, B., Cojazzi, G., Panzavolta, S. and Roveri, N. (1998). Drawn gelatin films with improved mechanical properties. *Biomaterials*. **19**(24): 2335-2340.

Bigi, A., Cojazzi, G., Panzavolta, S., Rubini, K. and Roveri, N. (2001). Mechanical and thermal properties of gelatin films at different degrees of glutaraldehyde crosslinking. *Biomaterials*. **22**(8): 763-768.

Bigi, A., Panzavolta, S. and Rubini, K. (2004). Relationship between triple-helix content and mechanical properties of gelatin films. *Biomaterials*. **25**(25): 5675-5680.

Bikle, D.D. and Halloran, B.P. (1999). The response of bone to unloading. *J Bone Miner Metab*. **17**(4): 233-244.

Billiau, A., Edy, V.G., Heremans, H., Van Damme, J., Desmyter, J., Georgiades, J.A. and De Somer, P. (1977). Human interferon: mass production in a newly established cell line, MG-63. *Antimicrob Agents Chemother*. **12**(1): 11-15.

Bills, C.E., Eisenberg, H. and Pallante, S.L. (1971). Complexes of organic acids with calcium phosphate: the von Kossa stain as a clue to the composition of bone mineral. *Johns Hopkins Med J*. **128**(4): 194-207.

Bishop, G.B. and Einhorn, T.A. (2007). Current and future clinical applications of bone morphogenetic proteins in orthopaedic trauma surgery. *Int Orthop*. **31**(6): 721-727.

Bjerre, L., Bünger, C.E., Kassem, M. and Mygind, T. (2008). Flow perfusion culture of human mesenchymal stem cells on silicate-substituted tricalcium phosphate scaffolds. *Biomaterials*. **29**(17): 2616-2627.

Blaine, M.G. (1947). Experimental observations on absorbable alginate products in surgery. *Ann Surg*. **125**(102-114).

Blanco, D. and Alonso, M.J. (1998). Protein encapsulation and release from poly(lactide-co-glycolide) microspheres: effect of the protein and polymer properties and of the co-encapsulation of surfactants. *Eur J Pharm Biopharm*. **45**(3): 285-294.

Bland, R., Worker, C.A., Noble, B.S., Eyre, L.J., Bujalska, I.J., Sheppard, M.C., Stewart, P.M. and Hewison, M. (1999). Characterization of 11β-hydroxysteroid dehydrogenase activity and corticosteroid receptor expression in human osteosarcoma cell lines. *J Endocrinol*. **161**(3): 455-464.

Bodde, E.W., Boerman, O.C., Russel, F.G., Mikos, A.G., Spauwen, P.H. and Jansen, J.A. (2008). The kinetic and biological activity of different loaded rhBMP-2 calcium phosphate cement implants in rats. *J Biomed Mater Res A*. **87**(3): 780-791.

Bolander, M.E. (1992). Regulation of fracture repair by growth factors. *Proc Soc Exp Biol Med*. **200**(2): 165-170.

Bortner, C.D. and Cidlowski, J.A. (2003). Uncoupling cell shrinkage from apoptosis reveals that Na+ influx is required for volume loss during programmed cell death. *J Biol Chem*. **278**(40): 39176-39184.

Bosetti, M., Boccafoschi, F., Leigheb, M. and Cannas, M.F. (2007). Effect of different growth factors on human osteoblasts activities: a possible application in bone regeneration for tissue engineering. *Biomol Eng*. **24**(6): 613-618.

Bosetti, M. and Cannas, M. (2005). The effect of bioactive glasses on bone marrow stromal cells differentiation. *Biomaterials*. **26**(18): 3873-3879.

Bostrom, M.P. (1998). Expression of bone morphogenetic proteins in fracture healing. *Clin Orthop Relat Res*. (355 Suppl): S116-123.

Bouillon, R., Bischoff-Ferrari, H. and Willett, W. (2008). Vitamin D and Health: Perspectives From Mice and Man. *Journal of Bone and Mineral Research*. **23**(7): 974-979.

Boutahar, N., Guignandon, A., Vico, L. and Lafage-Proust, M.H. (2004). Mechanical strain on osteoblasts activates autophosphorylation of focal adhesion kinase and proline-rich tyrosine kinase 2 tyrosine sites involved in ERK activation. *J Biol Chem*. **279**(29): 30588-30599.

Boyle, W.J., Simonet, W.S. and Lacey, D.L. (2003). Osteoclast differentiation and activation. *Nature*. **423**(6937): 337-342.

Brandao-Burch, A., Utting, J.C., Orriss, I.R. and Arnett, T.R. (2005). Acidosis inhibits bone formation by osteoblasts in vitro by preventing mineralization. *Calcif Tissue Int*. **77**(3): 167-174.

Bretaudiere, J. and Spillman, T. (1984). Alkaline phosphatases. In: *Methods of Enzymatic Analysis* (H. Bergmeyer, ed), Verlag Chemica, Weinheim, Germany, Vol. 4, pp. 75-92.

Brighton, C.T. and Hunt, R.M. (1986a). Histochemical localization of calcium in the fracture callus with potassium pyroantimonate. Possible role of chondrocyte mitochondrial calcium in callus calcification. *J Bone Joint Surg Am*. **68**(5): 703-715.

Brighton, C.T. and Hunt, R.M. (1986b). Ultrastructure of electrically induced osteogenesis in the rabbit medullary canal. *J Orthop Res*. **4**(1): 27-36.

Brighton, C.T. and Hunt, R.M. (1991). Early histological and ultrastructural changes in medullary fracture callus. *J Bone Joint Surg Am*. **73**(6): 832-847.

Brighton, C.T., Sugioka, Y. and Hunt, R.M. (1973). Cytoplasmic structures of epiphyseal plate chondrocytes. Quantitative evaluation using electron micrographs of rat costochondral junctions with special reference to the fate of hypertrophic cells. *J Bone Joint Surg Am*. **55**(4): 771-784.

Brodsky, B. and Ramshaw, J.A. (1997). The collagen triple-helix structure. *Matrix Biol*. **15**(8-9): 545-554.

Brown, P.D., Wakefield, L.M., Levinson, A.D. and Sporn, M.B. (1990). Physicochemical activation of recombinant latent transforming growth factor-beta's 1, 2, and 3. *Growth Factors*. **3**(1): 35-43.

Bucholz, R.W., Carlton, A. and Holmes, R. (1989). Interporous hydroxyapatite as a bone graft substitute in tibial plateau fractures. *Clin Orthop Relat Res*. (240): 53-62.

Bucholz, R.W., Carlton, A. and Holmes, R.E. (1987). Hydroxyapatite and tricalcium phosphate bone graft substitutes. *Orthop Clin North Am*. **18**(2): 323-334.

Buck, B.E. and Malinin, T.I. (1994). Human bone and tissue allografts. Preparation and safety. *Clin Orthop Relat Res*. **303**: 8-17.

Burr, D.B., Schaffler, M.B., Yang, K.H., Lukoschek, M., Sivaneri, N., Blaha, J.D. and Radin, E.L. (1989). Skeletal change in response to altered strain environments: is woven bone a response to elevated strain? *Bone*. **10**(3): 223-233.

Calalb, M.B., Polte, T.R. and Hanks, S.K. (1995). Tyrosine phosphorylation of focal adhesion kinase at sites in the catalytic domain regulates kinase activity: a role for Src family kinases. *Mol Cell Biol*. **15**(2): 954-963.

Campioni, D., Lanza, F., Moretti, S., Ferrari, L. and Cuneo, A. (2008). Loss of Thy-1 (CD90) antigen expression on mesenchymal stromal cells from hematologic malignancies is induced by in vitro angiogenic stimuli and is associated with peculiar functional and phenotypic characteristics. *Cytotherapy*. **10**(1): 69-82.

Campioni, D., Moretti, S., Ferrari, L., Punturieri, M., Castoldi, G.L. and Lanza, F. (2006). Immunophenotypic heterogeneity of bone marrow-derived mesenchymal stromal cells from patients with hematologic disorders: correlation with bone marrow microenvironment. *Haematologica*. **91**(3): 364-368.

Campioni, D., Rizzo, R., Stignani, M., Melchiorri, L., Ferrari, L., Moretti, S., Russo, A., Bagnara, G.P., Bonsi, L., Alviano, F., Lanzoni, G., Cuneo, A., Baricordi, O.R. and Lanza, F. (2009). A decreased positivity for CD90 on human mesenchymal stromal cells (MSCs) is associated with a loss of immunosuppressive activity by MSCs. *Cytometry B Clin Cytom*. **76**(3): 225-230.

Canalis, E., McCarthy, T.L. and Centrella, M. (1989). Effects of platelet-derived growth factor on bone formation in vitro. *J Cell Physiol*. **140**(3): 530-537.

Canty, E.G. and Kadler, K.E. (2005). Procollagen trafficking, processing and fibrillogenesis. *J Cell Sci*. **118**(Pt 7): 1341-1353.

Cao, X. and Shoichet, M.S. (1999). Delivering neuroactive molecules from biodegradable microspheres for application in central nervous system disorders. *Biomaterials*. **20**(4): 329-339.

Capelo, L.P., Beber, E.H., Huang, S.A., Zorn, T.M., Bianco, A.C. and Gouveia, C.H. (2008). Deiodinase-mediated thyroid hormone inactivation minimizes thyroid hormone signaling in the early development of fetal skeleton. *Bone*. **43**(5): 921-930.

Carano, R.A. and Filvaroff, E.H. (2003). Angiogenesis and bone repair. *Drug Discov Today*. **8**(21): 980-989.

Carinci, F., Palmieri, A., Martinelli, M., Perrotti, V., Piattelli, A., Brunelli, G., Arlotti, M. and Pezzetti, F. (2007). Genetic portrait of osteoblast-like cells cultured on PerioGlas. *J Oral Implantol*. **33**(6): 327-333.

Carinci, F., Pezzetti, F., Volinia, S., Francioso, F., Arcelli, D., Farina, E. and Piattelli, A. (2004). Zirconium oxide: analysis of MG63 osteoblast-like cell response by means of a microarray technology. *Biomaterials*. **25**(2): 215-228.

Carmeliet, P. and Jain, R.K. (2000). Angiogenesis in cancer and other diseases. *Nature*. **407**(6801): 249-257.

Carpenter, J.E., Hipp, J.A., Gerhart, T.N., Rudman, C.G., Hayes, W.C. and Trippel, S.B. (1992). Failure of growth hormone to alter the biomechanics of fracture-healing in a rabbit model. *J Bone Joint Surg Am*. **74**(3): 359-367.

Carrier, R.L., Papadaki, M., Rupnick, M., Schoen, F.J., Bursac, N., Langer, R., Freed, L.E. and Vunjak-Novakovic, G. (1999). Cardiac tissue engineering: cell seeding, cultivation parameters, and tissue construct characterization. *Biotechnol Bioeng*. **64**(5): 580-589.

Carter, D.H., Sloan, P. and Aaron, J.E. (1991). Immunolocalization of collagen types I and III, tenascin, and fibronectin in intramembranous bone. *J Histochem Cytochem*. **39**(5): 599-606.

Carter, D.R., Van Der Meulen, M.C. and Beaupre, G.S. (1996). Mechanical factors in bone growth and development. *Bone*. **18**(1 Suppl): 5S-10S.

Cartmell, S. (2008). Controlled release scaffolds for bone tissue engineering. *J Pharm Sci*.

Castro-Malaspina, H., Gay, R.E., Resnick, G., Kapoor, N., Meyers, P., Chiarieri, D., McKenzie, S., Broxmeyer, H.E. and Moore, M.A. (1980). Characterization of human bone marrow fibroblast colony-forming cells (CFU-F) and their progeny. *Blood*. **56**(2): 289-301.

Chandrasekhar, S. and Harvey, A.K. (1996). Modulation of PDGF mediated osteoblast chemotaxis by leukemia inhibitory factor (LIF). *J Cell Physiol*. **169**(3): 481-490.

Chapman, J.A. (1989). The regulation of size and form in the assembly of collagen fibrils in vivo. *Biopolymers*. **28**(8): 1367-1382.

Chapman, M.W., Bucholz, R. and Cornell, C. (1997). Treatment of acute fractures with a collagen-calcium phosphate graft material. A randomized clinical trial. *J Bone Joint Surg Am*. **79**(4): 495-502.

Chaudhary, L.R. and Avioli, L.V. (1997). Activation of extracellular signal-regulated kinases 1 and 2 (ERK1 and ERK2) by FGF-2 and PDGF-BB in normal human osteoblastic and bone marrow stromal cells: differences in mobility and in-gel renaturation of ERK1 in human, rat, and mouse osteoblastic cells. *Biochem Biophys Res Commun*. **238**(1): 134-139.

Cheifetz, S., Bellon, T., Cales, C., Vera, S., Bernabeu, C., Massague, J. and Letarte, M. (1992). Endoglin is a component of the transforming growth factor-beta receptor system in human endothelial cells. *J Biol Chem*. **267**(27): 19027-19030.

Chen, B., Lin, H., Wang, J., Zhao, Y., Wang, B., Zhao, W., Sun, W. and Dai, J. (2007). Homogeneous osteogenesis and bone regeneration by demineralized bone matrix loading with collagen-targeting bone morphogenetic protein-2. *Biomaterials*. **28**(6): 1027-1035.

Chen, R.R. and Mooney, D.J. (2003). Polymeric growth factor delivery strategies for tissue engineering. *Pharm Res*. **20**(8): 1103-1112.

Chen, T.L., Bates, R.L., Dudley, A., Hammonds, R.G., Jr. and Amento, E.P. (1991). Bone morphogenetic protein-2b stimulation of growth and osteogenic phenotypes in rat osteoblast-like cells: comparison with TGF-beta 1. *J Bone Miner Res*. **6**(12): 1387-1393.

Chen, Y., Cho, M.R., Mak, A.F., Li, J.S., Wang, M. and Sun, S. (2008). Morphology and adhesion of mesenchymal stem cells on PLLA, apatite and apatite/collagen surfaces. *J Mater Sci Mater Med*. **19**(7): 2563-2567.

Cheng, H., Jiang, W., Phillips, F.M., Haydon, R.C., Peng, Y., Zhou, L., Luu, H.H., An, N., Breyer, B., Vanichakarn, P., Szatkowski, J.P., Park, J.Y. and He, T.C. (2003a). Osteogenic activity of the fourteen types of human bone morphogenetic proteins (BMPs). *J Bone Joint Surg Am*. **85-A**(8): 1544-1552.

Cheng, S.L., Shao, J.S., Charlton-Kachigian, N., Loewy, A.P. and Towler, D.A. (2003b). MSX2 promotes osteogenesis and suppresses adipogenic differentiation of multipotent mesenchymal progenitors. *J Biol Chem*. **278**(46): 45969-45977.

Cho, T.J., Gerstenfeld, L.C. and Einhorn, T.A. (2002). Differential temporal expression of members of the transforming growth factor beta superfamily during murine fracture healing. *J Bone Miner Res*. **17**(3): 513-520.

Choi, K.-M., Seo, Y.-K., Yoon, H.-H., Song, K.-Y., Kwon, S.-Y., Lee, H.-S. and Park, J.-K. (2008). Effect of ascorbic acid on bone marrow-derived mesenchymal stem cell proliferation and differentiation. *J Biosci Bioeng*. **105**(6): 586-594.

Choi, N.W., Cabodi, M., Held, B., Gleghorn, J.P., Bonassar, L.J. and Stroock, A.D. (2007). Microfluidic scaffolds for tissue engineering. *Nat Mater*. **6**(11): 908-915.

Chow, J.W., Wilson, A.J., Chambers, T.J. and Fox, S.W. (1998). Mechanical loading stimulates bone formation by reactivation of bone lining cells in 13-week-old rats. *J Bone Miner Res*. **13**(11): 1760-1767.

Chuang, P.T. and McMahon, A.P. (1999). Vertebrate Hedgehog signalling modulated by induction of a Hedgehog-binding protein. *Nature*. **397**(6720): 617-621.

Civin, C.I., Banquerigo, M.L., Strauss, L.C. and Loken, M.R. (1987). Antigenic analysis of hematopoiesis. VI. Flow cytometric characterization of My-10-positive progenitor cells in normal human bone marrow. *Exp Hematol*. **15**(1): 10-17.

Civin, C.I., Strauss, L.C., Brovall, C., Fackler, M.J., Schwartz, J.F. and Shaper, J.H. (1984). Antigenic analysis of hematopoiesis. III. A hematopoietic progenitor cell surface antigen defined by a monoclonal antibody raised against KG-1a cells. *J Immunol*. **133**(1): 157-165.

Claffey, K.P., Abrams, K., Shih, S.C., Brown, L.F., Mullen, A. and Keough, M. (2001). Fibroblast growth factor 2 activation of stromal cell vascular endothelial growth factor expression and angiogenesis. *Lab Invest*. **81**(1): 61-75.

Clancey, G.J. and Hansen, S.T., Jr. (1978). Open fractures of the tibia: a review of one hundred and two cases. *J Bone Joint Surg Am*. **60**(1): 118-122.

Clancey, G.J., Winquist, R.A. and Hansen, S.T., Jr. (1982). Nonunion of the tibia treated with Kuntscher intramedullary nailing. *Clin Orthop Relat Res*. (167): 191-196.

Clark, A.H. and Ross-Murphy, S.B. (1987). Structural and mechanical properties of biopolymer gels. *Adv Polym Sci*. **83**: 57-192.

Coipeau, P., Rosset, P., Langonne, A., Gaillard, J., Delorme, B., Rico, A., Domenech, J., Charbord, P. and Sensebe, L. (2009). Impaired differentiation potential of human trabecular bone mesenchymal stromal cells from elderly patients. *Cytotherapy*. **11**(5): 584-594.

Cole, C.G.B. (2000). Gelatin. In: *Encyclopedia of Food Science and Technology* (F. Francis, ed), John Wiley & Sons, New York, NY, pp. 1183-1188.

Collins, T.J. (2007). ImageJ for microscopy. *Biotechniques*. **43**(1 Suppl): 25-30.

Colvin, J.S., Feldman, B., Nadeau, J.H., Goldfarb, M. and Ornitz, D.M. (1999). Genomic organization and embryonic expression of the mouse fibroblast growth factor 9 gene. *Dev Dyn*. **216**(1): 72-88.

Cooke, A.M. (1955). Osteoporosis. *Lancet*. **268**(6870): 877-882.

Cove, J.A., Lhowe, D.W., Jupiter, J.B. and Siliski, J.M. (1997). The management of femoral diaphyseal nonunions. *J Orthop Trauma*. **11**(7): 513-520.

Cowles, E.A., Brailey, L.L. and Gronowicz, G.A. (2000). Integrin-mediated signaling regulates AP-1 transcription factors and proliferation in osteoblasts. *J Biomed Mater Res*. **52**(4): 725-737.

Coxon, A., Rieu, P., Barkalow, F.J., Askari, S., Sharpe, A.H., von Andrian, U.H., Arnaout, M.A. and Mayadas, T.N. (1996). A novel role for the β2 integrin CD11b/CD18 in neutrophil apoptosis: a homeostatic mechanism in inflammation. *Immunity*. **5**(6): 653-666.

Curran, J.M., Chen, R. and Hunt, J.A. (2005). Controlling the phenotype and function of mesenchymal stem cells in vitro by adhesion to silane-modified clean glass surfaces. *Biomaterials*. **26**(34): 7057-7067.

Curran, J.M., Chen, R. and Hunt, J.A. (2006). The guidance of human mesenchymal stem cell differentiation in vitro by controlled modifications to the cell substrate. *Biomaterials*. **27**(27): 4783-4793.

Dadsetan, M., Hefferan, T.E., Szatkowski, J.P., Mishra, P.K., Macura, S.I., Lu, L. and Yaszemski, M.J. (2008). Effect of hydrogel porosity on marrow stromal cell phenotypic expression. *Biomaterials*. **29**(14): 2193-2202.

Dalby, M.J., Di Silvio, L., Gurav, N., Annaz, B., Kayser, M.V. and Bonfield, W. (2002). Optimizing HAPEX topography influences osteoblast response. *Tissue Eng*. **8**(3): 453-467.

Daniels, D.L. and Weis, W.I. (2005). Beta-catenin directly displaces Groucho/TLE repressors from Tcf/Lef in Wnt-mediated transcription activation. *Nat Struct Mol Biol*. **12**(4): 364-371.

Davis, G.E. (1992). Affinity of integrins for damaged extracellular matrix: alpha v beta 3 binds to denatured collagen type I through RGD sites. *Biochem Biophys Res Commun*. **182**(3): 1025-1031.

Dawson, E., Mapili, G., Erickson, K., Taqvi, S. and Roy, K. (2008). Biomaterials for stem cell differentiation. *Adv Drug Deliver Rev*. **60**(2): 215-228.

Dawson, J.I. and Oreffo, R.O. (2008). Bridging the regeneration gap: stem cells, biomaterials and clinical translation in bone tissue engineering. *Arch Biochem Biophys*. **473**(2): 124-131.

Day, T.F., Guo, X., Garrett-Beal, L. and Yang, Y. (2005). Wnt/beta-catenin signaling in mesenchymal progenitors controls osteoblast and chondrocyte differentiation during vertebrate skeletogenesis. *Dev Cell*. **8**(5): 739-750.

Day, T.F. and Yang, Y. (2008). Wnt and hedgehog signaling pathways in bone development. *J Bone Joint Surg Am*. **90 Suppl 1**: 19-24.

De Long, W.G., Jr., Einhorn, T.A., Koval, K., McKee, M., Smith, W., Sanders, R. and Watson, T. (2007). Bone grafts and bone graft substitutes in orthopaedic trauma surgery. A critical analysis. *J Bone Joint Surg Am*. **89**(3): 649-658.

De, S. and Robinson, D. (2003). Polymer relationships during preparation of chitosan-alginate and poly-l-lysine-alginate nanospheres. *J Control Release*. **89**(1): 101-112.

Deckers, M.M., van Bezooijen, R.L., van der Horst, G., Hoogendam, J., van Der Bent, C., Papapoulos, S.E. and Lowik, C.W. (2002). Bone morphogenetic proteins stimulate angiogenesis through osteoblast-derived vascular endothelial growth factor A. *Endocrinology*. **143**(4): 1545-1553.

DeFail, A.J., Chu, C.R., Izzo, N. and Marra, K.G. (2006). Controlled release of bioactive TGF-β1 from microspheres embedded within biodegradable hydrogels. *Biomaterials*. **27**(8): 1579-1585.

Delgado, A., Evora, C. and Llabres, M. (1996). Optimization of 7-day release (in vitro) from DL-PLA methadone microspheres. *Int J Pharm*. **134**(1-2): 203-211.

Dempster, D.W., Lian, J.B. and Goldring, S.R. (2006). Chapter 2. Anatomy and Functions of the Adult Skeleton. In: *Primer on the Metabolic Bone Diseases and Disorders of Mineral Metabolism*), Lippincott-Raven, New York, Vol. 6, pp. 7-11.

Deng, C., Wynshaw-Boris, A., Zhou, F., Kuo, A. and Leder, P. (1996). Fibroblast growth factor receptor 3 is a negative regulator of bone growth. *Cell*. **84**(6): 911-921.

Desbois, C., Hogue, D.A. and Karsenty, G. (1994). The mouse osteocalcin gene cluster contains three genes with two separate spatial and temporal patterns of expression. *J Biol Chem*. **269**(2): 1183-1190.

Dhanikula, A.B. and Panchagnula, R. (2004). Development and characterization of biodegradable chitosan films for local delivery of Paclitaxel. *Aaps J*. **6**(3): e27.

Di Martino, A., Sittinger, M. and Risbud, M.V. (2005). Chitosan: A versatile biopolymer for orthopaedic tissue-engineering. *Biomaterials*. **26**(30): 5983-5990.

Dickhut, A., Gottwald, E., Steck, E., Heisel, C. and Richter, W. (2008). Chondrogenesis of mesenchymal stem cells in gel-like biomaterials in vitro and in vivo. *Front Biosci*. **13**: 4517-4528.

Dickson, K., Katzman, S., Delgado, E. and Contreras, D. (1994). Delayed unions and nonunions of open tibial fractures. Correlation with arteriography results. *Clin Orthop Relat Res*. **302**: 189-193.

Diefenderfer, D.L., Osyczka, A.M., Reilly, G.C. and Leboy, P.S. (2003). BMP responsiveness in human mesenchymal stem cells. *Connect Tissue Res*. **44** (Suppl 1): 305-311.

Digirolamo, C.M., Stokes, D., Colter, D., Phinney, D.G., Class, R. and Prockop, D.J. (1999). Propagation and senescence of human marrow stromal cells in culture: a simple colony-forming assay identifies samples with the greatest potential to propagate and differentiate. *Br J Haematol*. **107**(2): 275-281.

Dimitriou, R., Dahabreh, Z., Katsoulis, E., Matthews, S.J., Branfoot, T. and Giannoudis, P.V. (2005). Application of recombinant BMP-7 on persistent upper and lower limb non-unions. *Injury*. **36 Suppl 4**: S51-59.

Ding, Z.M., Babensee, J.E., Simon, S.I., Lu, H., Perrard, J.L., Bullard, D.C., Dai, X.Y., Bromley, S.K., Dustin, M.L., Entman, M.L., Smith, C.W. and Ballantyne, C.M. (1999). Relative contribution of LFA-1 and Mac-1 to neutrophil adhesion and migration. *J Immunol*. **163**(9): 5029-5038.

Dodig, M., Tadic, T., Kronenberg, M.S., Dacic, S., Liu, Y.H., Maxson, R., Rowe, D.W. and Lichtler, A.C. (1999). Ectopic Msx2 overexpression inhibits and Msx2 antisense stimulates calvarial osteoblast differentiation. *Dev Biol*. **209**(2): 298-307.

Dominici, M., Le Blanc, K., Mueller, I., Slaper-Cortenbach, I., Marini, F., Krause, D., Deans, R., Keating, A., Prockop, D. and Horwitz, E. (2006). Minimal criteria for defining multipotent mesenchymal stromal cells. The International Society for Cellular Therapy position statement. *Cytotherapy*. **8**(4): 315-317.

Donaldson, L.J., Reckless, I.P., Scholes, S., Mindell, J.S. and Shelton, N.J. (2008). The epidemiology of fractures in England. *J Epidemiol Community Health*. **62**(2): 174-180.

Donati, D., Di Bella, C., Col Angeli, M., Bianchi, G. and Mercuri, M. (2005). The use of massive bone allografts in bone tumour surgery of the limb. *Curr Orthopaed*. **19**(5): 393-399.

Donati, D., Di Bella, C., Lucarelli, E., Dozza, B., Frisoni, T., Aldini, N.N. and Giardino, R. (2008). OP-1 application in bone allograft integration: preliminary results in sheep experimental surgery. *Injury*. **39 Suppl 2**: S65-72.

Doonan, F. and Cotter, T.G. (2008). Morphological assessment of apoptosis. *Methods*. **44**(3): 200-204.

Dorea, H.C., McLaughlin, R.M., Cantwell, H.D., Read, R., Armbrust, L., Pool, R., Roush, J.K. and Boyle, C. (2005). Evaluation of healing in feline femoral defects filled with cancellous autograft, cancellous allograft or Bioglass. *Vet Comp Orthop Traumatol*. **18**(3): 157-168.

Doucet, C., Ernou, I., Zhang, Y., Llense, J.R., Begot, L., Holy, X. and Lataillade, J.J. (2005). Platelet lysates promote mesenchymal stem cell expansion: a safety substitute for animal serum in cell-based therapy applications. *J Cell Physiol*. **205**(2): 228-236.

Douglas, T., Hempel, U., Mietrach, C., Viola, M., Vigetti, D., Heinemann, S., Bierbaum, S., Scharnweber, D. and Worch, H. (2008). Influence of collagen-fibril-based coatings containing decorin and biglycan on osteoblast behavior. *J Biomed Mater Res A*. **84**(3): 805-816.

Drury, J.L. and Mooney, D.J. (2003). Hydrogels for tissue engineering: scaffold design variables and applications. *Biomaterials*. **24**(24): 4337-4351.

Ducy, P. and Karsenty, G. (1995). Two distinct osteoblast-specific cis-acting elements control expression of a mouse osteocalcin gene. *Mol Cell Biol*. **15**(4): 1858-1869.

Ducy, P., Schinke, T. and Karsenty, G. (2000). The osteoblast: a sophisticated fibroblast under central surveillance. *Science*. **289**(5484): 1501-1504.

Ducy, P., Zhang, R., Geoffroy, V., Ridall, A.L. and Karsenty, G. (1997). Osf2/Cbfa1: a transcriptional activator of osteoblast differentiation. *Cell*. **89**(5): 747-754.

Duque, G. and Rivas, D. (2007). Alendronate has an anabolic effect on bone through the differentiation of mesenchymal stem cells. *J Bone Miner Res*. **22**(10): 1603-1611.

Eckardt, H., Ding, M., Lind, M., Hansen, E.S., Christensen, K.S. and Hvid, I. (2005). Recombinant human vascular endothelial growth factor enhances bone healing in an experimental nonunion model. *J Bone Joint Surg Br*. **87**(10): 1434-1438.

Edgar, C.M., Chakravarthy, V., Barnes, G., Kakar, S., Gerstenfeld, L.C. and Einhorn, T.A. (2007). Autogenous regulation of a network of bone morphogenetic proteins (BMPs) mediates the osteogenic differentiation in murine marrow stromal cells. *Bone*. **40**(5): 1389-1398.

Einhorn, T.A. (1996). The bone organ system: Form and function. In: *Osteoporosis* (R. Marcus, D. Feldman and J. Kelsey, eds.), Academic Press, California, pp. 3-21.

Einhorn, T.A. (1998). The cell and molecular biology of fracture healing. *Clin Orthop Relat Res*. (355 Suppl): S7-21.

Einhorn, T.A., Majeska, R.J., Rush, E.B., Levine, P.M. and Horowitz, M.C. (1995). The expression of cytokine activity by fracture callus. *J Bone Miner Res*. **10**(8): 1272-1281.

Eisenmann, D.M. (2005). Wnt signaling. *WormBook*. 1-17.

Elisseeff, J., McIntosh, W., Fu, K., Blunk, T. and Langer, R. (2001). Controlled-release of IGF-I and TGF-β1 in a photopolymerizing hydrogel for cartilage tissue engineering. *Journal of Orthopaedic Research*. **19**(6): 1098-1104.

Ellis, D.L. and Yannas, I.V. (1996). Recent advances in tissue synthesis in vivo by use of collagen-glycosaminoglycan copolymers. *Biomaterials*. **17**(3): 291-299.

Engelberg, I. and Kohn, J. (1991). Physico-mechanical properties of degradable polymers used in medical applications: a comparative study. *Biomaterials*. **12**(3): 292-304.

Enneking, W.F. and Mindell, E.R. (1991). Observations on massive retrieved human allografts. *J Bone Joint Surg Am*. **73**(8): 1123-1142.

Evans, M.J. and Kaufman, M.H. (1981). Establishment in culture of pluripotential cells from mouse embryos. *Nature*. **292**(5819): 154-156.

Fedorovich, N.E., De Wijn, J.R., Verbout, A.J., Alblas, J. and Dhert, W.J. (2008). Three-dimensional fiber deposition of cell-laden, viable, patterned constructs for bone tissue printing. *Tissue Eng Part A*. **14**(1): 127-133.

Felsenfeld, A.J. and Rodriguez, M. (1999). Phosphorus, regulation of plasma calcium, and secondary hyperparathyroidism: a hypothesis to integrate a historical and modern perspective. *J Am Soc Nephrol*. **10**(4): 878-890.

Fernandez, N.J. and Kidney, B.A. (2007). Alkaline phosphatase: beyond the liver. *Vet Clin Pathol*. **36**(3): 223-233.

Fick, A. (1855). On liquid diffusion. *Phil Mag and J Sci*. **10**: 31-39.

Fiedler, J., Roderer, G., Gunther, K.P. and Brenner, R.E. (2002). BMP-2, BMP-4, and PDGF-bb stimulate chemotactic migration of primary human mesenchymal progenitor cells. *J Cell Biochem*. **87**(3): 305-312.

Finkemeier, C.G. (2002). Bone-grafting and bone-graft substitutes. *J Bone Joint Surg Am*. **84-A**(3): 454-464.

Finkemeier, C.G. and Chapman, M.W. (2002). Treatment of femoral diaphyseal nonunions. *Clin Orthop Relat Res*. **398**: 223-234.

Fisher, J.P. and Reddi, A.H. (2003). Chapter 5: Functional Tissue Engineering of Bone: Signals and Scaffolds. In: *Topics in Tissue Engineering* (N. Ashammakhi and P. Ferretti, eds.), University of Oulu, Vol. 1, pp. 1 - 29.

Forsyth, K.D., Chua, K.Y., Talbot, V. and Thomas, W.R. (1993). Expression of the leukocyte common antigen CD45 by endothelium. *J Immunol*. **150**(8 Pt 1): 3471-3477.

Fox, S.W. and Lovibond, A.C. (2005). Current insights into the role of transforming growth factor-beta in bone resorption. *Mol Cell Endocrinol*. **243**(1-2): 19-26.

Fredenberg, S., Reslow, M. and Axelsson, A. (2005). Measurement of protein diffusion through poly(D,L-lactide-Co-glycolide). *Pharm Dev Technol*. **10**(2): 299-307.

Friedenstein, A.J., Chailakhyan, R.K. and Gerasimov, U.V. (1987). Bone marrow osteogenic stem cells: in vitro cultivation and transplantation in diffusion chambers. *Cell Tissue Kinet*. **20**(3): 263-272.

Friedlaender, G.E., Perry, C.R., Cole, J.D., Cook, S.D., Cierny, G., Muschler, G.F., Zych, G.A., Calhoun, J.H., LaForte, A.J. and Yin, S. (2001). Osteogenic protein-1 (bone morphogenetic protein-7) in the treatment of tibial nonunions. *J Bone Joint Surg Am*. **83-A Suppl 1**(Pt 2): S151-S158.

Frölke, J.P.M. and Patka, P. (2007). Definition and classification of fracture non-unions. *Injury*. **38**(Supplement 2): S19-S22.

Frost, H.M. (1969). Tetracycline-based histological analysis of bone remodeling. *Calcif Tissue Res*. **3**(3): 211-237.

Furumatsu, T., Ozaki, T. and Asahara, H. (2009). Smad3 activates the Sox9-dependent transcription on chromatin. *Int J Biochem Cell Biol*. **41**(5): 1198-1204.

Furumatsu, T., Tsuda, M., Taniguchi, N., Tajima, Y. and Asahara, H. (2005). Smad3 induces chondrogenesis through the activation of SOX9 via CREB-binding protein/p300 recruitment. *J Biol Chem*. **280**(9): 8343-8350.

Gallagher, J.A. (2003). Human Osteoblast Culture. In: *Bone Research Protocols* (M. P. Helfrich and S. H. Ralston, eds.), Humana Press, Totowa, NJ, Vol. 80.

Gao, J., Zoller, K.E., Ginsberg, M.H., Brugge, J.S. and Shattil, S.J. (1997). Regulation of the pp72syk protein tyrosine kinase by platelet integrin alpha IIb beta 3. *Embo J*. **16**(21): 6414-6425.

Garrigue-Antar, L., Barbieux, I., Lieubeau, B., Boisteau, O. and Gregoire, M. (1995). Optimisation of CCL64-based bioassay for TGF-β. *J Immunol Methods*. **186**(2): 267-274.

Gaston, M.S. and Simpson, A.H. (2007). Inhibition of fracture healing. *J Bone Joint Surg Br*. **89**(12): 1553-1560.

Geissler, U., Hempel, U., Wolf, C., Scharnweber, D., Worch, H. and Wenzel, K. (2000). Collagen type I-coating of Ti6Al4V promotes adhesion of osteoblasts. *J Biomed Mater Res*. **51**(4): 752-760.

Giacomello, E., Neumayer, J., Colombatti, A. and Perris, R. (1999). Centrifugal assay for fluorescence-based cell adhesion adapted to the analysis of ex vivo cells and capable of determining relative binding strengths. *Biotechniques*. **26**(4): 758-762, 764-756.

Gilding, D.K. and Reed, A.M. (1979). Biodegradable polymers for use in surgery--polyglycolic/poly(actic acid) homo- and copolymers: 1. *Polymer*. **20**(12): 1459-1464.

Gilmore, P.T., Falabella, R. and Laurence, R.L. (1980). Polymer/Polymer Diffusion. 2. Effect of Temperature and Molecular Weight on Macromolecular Diffusion in Blends of Poly(vinyl chloride) and Poly(ε-caprolactone). *Macromolecules*. **13**(4): 880-883.

Ginty, P.J., Barry, J.J.A., White, L.J., Howdle, S.M. and Shakesheff, K.M. (2008). Controlling protein release from scaffolds using polymer blends and composites. *Eur J Pharm Biopharm*. **68**(1): 82-89.

Glass, D.A., 2nd, Bialek, P., Ahn, J.D., Starbuck, M., Patel, M.S., Clevers, H., Taketo, M.M., Long, F., McMahon, A.P., Lang, R.A. and Karsenty, G. (2005). Canonical Wnt signaling in differentiated osteoblasts controls osteoclast differentiation. *Dev Cell*. **8**(5): 751-764.

Goel, A., Sangwan, S.S., Siwach, R.C. and Ali, A.M. (2005). Percutaneous bone marrow grafting for the treatment of tibial non-union. *Injury*. **36**(1): 203-206.

Goldberg, V.M. and Stevenson, S. (1987). Natural history of autografts and allografts. *Clin Orthop Relat Res*. **225**: 7-16.

Goodell, M.A., Brose, K., Paradis, G., Conner, A.S. and Mulligan, R.C. (1996). Isolation and functional properties of murine hematopoietic stem cells that are replicating in vivo. *J Exp Med*. **183**(4): 1797-1806.

Goodhill, G.J. (1997). Diffusion in axon guidance. *Eur J Neurosci*. **9**(7): 1414-1421.

Goodrich, L.V., Johnson, R.L., Milenkovic, L., McMahon, J.A. and Scott, M.P. (1996). Conservation of the hedgehog/patched signaling pathway from flies to mice: induction of a mouse patched gene by Hedgehog. *Genes Dev*. **10**(3): 301-312.

Goodwin, C.J., Braden, M., Downes, S. and Marshall, N.J. (1998). Release of bioactive human growth hormone from a biodegradable material: poly(epsilon-caprolactone). *J Biomed Mater Res.* **40**(2): 204-213.

Gougos, A. and Letarte, M. (1990). Primary structure of endoglin, an RGD-containing glycoprotein of human endothelial cells. *J Biol Chem*. **265**(15): 8361-8364.

Goulet, J.A., Senunas, L.E., DeSilva, G.L. and Greenfield, M.L. (1997). Autogenous iliac crest bone graft. Complications and functional assessment. *Clin Orthop Relat Res*. **339**: 76-81.

Goumans, M.J., Valdimarsdottir, G., Itoh, S., Rosendahl, A., Sideras, P. and ten Dijke, P. (2002). Balancing the activation state of the endothelium via two distinct TGF-beta type I receptors. *Embo J*. **21**(7): 1743-1753.

Goussetis, E., Spiropoulos, A., Theodosaki, M., Paterakis, G., Peristeri, I., Kitra, V., Petrakou, E., Soldatou, A. and Graphakos, S. (2005). Culture of bone marrow CD105+ cells allows rapid selection of pure BM-stromal cells for chimerism studies in patients undergoing allogeneic bone marrow transplantation. *Bone Marrow Transplant*. **36**(6): 557-559.

Govender, S., Csimma, C., Genant, H.K., Valentin-Opran, A., Amit, Y., Arbel, R., Aro, H., Atar, D., Bishay, M., Borner, M.G., Chiron, P., Choong, P., Cinats, J., Courtenay, B., Feibel, R., Geulette, B., Gravel, C., Haas, N., Raschke, M., Hammacher, E., van der Velde, D., Hardy, P., Holt, M., Josten, C., Ketterl, R.L., Lindeque, B., Lob, G., Mathevon, H., McCoy, G., Marsh, D., Miller, R., Munting, E., Oevre, S., Nordsletten, L., Patel, A., Pohl, A., Rennie, W., Reynders, P., Rommens, P.M., Rondia, J., Rossouw, W.C., Daneel, P.J., Ruff, S., Ruter, A., Santavirta, S., Schildhauer, T.A., Gekle, C., Schnettler, R., Segal, D., Seiler, H., Snowdowne, R.B., Stapert, J., Taglang, G., Verdonk, R., Vogels, L., Weckbach, A., Wentzensen, A. and Wisniewski, T. (2002). Recombinant human bone morphogenetic protein-2 for treatment of open tibial fractures: a prospective, controlled, randomized study of four hundred and fifty patients. *J Bone Joint Surg Am*. **84-A**(12): 2123-2134.

Gregory, C.A., Prockop, D.J. and Spees, J.L. (2005). Non-hematopoietic bone marrow stem cells: molecular control of expansion and differentiation. *Exp Cell Res*. **306**(2): 330-335.

Griffith, D.L., Keck, P.C., Sampath, T.K., Rueger, D.C. and Carlson, W.D. (1996). Three-dimensional structure of recombinant human osteogenic protein 1: structural paradigm for the transforming growth factor beta superfamily. *Proc Natl Acad Sci U S A*. **93**(2): 878-883.

Gronthos, S., Graves, S.E., Ohta, S. and Simmons, P.J. (1994). The STRO-1+ fraction of adult human bone marrow contains the osteogenic precursors. *Blood*. **84**(12): 4164-4173.

Gronthos, S., Graves, S.E. and Simmons, P.J. (1998). Isolation, purification and *in vitro* manipulation of human marrow stromal precursor cells. In: *Marrow stromal cell culture* (J. N. Beresford and M. E. Owen, eds.), Cambridge University Press, Cambridge, UK, pp. 26-42.

Gu, F., Amsden, B. and Neufeld, R. (2004a). Sustained delivery of vascular endothelial growth factor with alginate beads. *J Control Release*. **96**(3): 463-472.

Gu, K., Zhang, L., Jin, T. and Rutherford, R.B. (2004b). Identification of potential modifiers of Runx2/Cbfa1 activity in C2C12 cells in response to bone morphogenetic protein-7. *Cells Tissues Organs*. **176**(1-3): 28-40.

Guha, S.C. and Poole, M.D. (1983). Stress fracture of the iliac bone with subfascial femoral neuropathy: unusual complications at a bone graft donor site: case report. *Br J Plast Surg*. **36**(3): 305-306.

Guicheux, J., Lemonnier, J., Ghayor, C., Suzuki, A., Palmer, G. and Caverzasio, J. (2003). Activation of p38 mitogen-activated protein kinase and c-Jun-NH2-terminal kinase by BMP-2 and their implication in the stimulation of osteoblastic cell differentiation. *J Bone Miner Res*. **18**(11): 2060-2068.

Gundle, R., Joyner, C.J. and Triffitt, J.T. (1995). Human bone tissue formation in diffusion chamber culture in vivo by bone-derived cells and marrow stromal fibroblastic cells. *Bone*. **16**(6): 597-601.

Gupta, A., Dixit, A., Sales, K.M., Winslet, M.C. and Seifalian, A.M. (2006). Tissue engineering of small intestine--current status. *Biomacromolecules*. **7**(10): 2701-2709.

Habraken, W.J., Wolke, J.G., Mikos, A.G. and Jansen, J.A. (2008). PLGA microsphere/calcium phosphate cement composites for tissue engineering: in vitro release and degradation characteristics. *J Biomater Sci Polym Ed*. **19**(9): 1171-1188.

Hall, M.B., Vallerand, W.P., Thompson, D. and Hartley, G. (1991). Comparative anatomic study of anterior and posterior iliac crests as donor sites. *J Oral Maxillofac Surg*. **49**(6): 560-563.

Hamada, F., Tomoyasu, Y., Takatsu, Y., Nakamura, M., Nagai, S., Suzuki, A., Fujita, F., Shibuya, H., Toyoshima, K., Ueno, N. and Akiyama, T. (1999). Negative regulation of Wingless signaling by D-axin, a Drosophila homolog of axin. *Science*. **283**(5408): 1739-1742.

Hanks, S.K., Calalb, M.B., Harper, M.C. and Patel, S.K. (1992). Focal adhesion protein-tyrosine kinase phosphorylated in response to cell attachment to fibronectin. *Proc Natl Acad Sci U S A*. **89**(18): 8487-8491.

Harada, H., Tagashira, S., Fujiwara, M., Ogawa, S., Katsumata, T., Yamaguchi, A., Komori, T. and Nakatsuka, M. (1999). Cbfa1 isoforms exert functional differences in osteoblast differentiation. *J Biol Chem*. **274**(11): 6972-6978.

Harada, S. and Rodan, G.A. (2003). Control of osteoblast function and regulation of bone mass. *Nature*. **423**(6937): 349-355.

Harting, M., Jimenez, F., Pati, S., Baumgartner, J. and Cox, C., Jr. (2008). Immunophenotype characterization of rat mesenchymal stromal cells. *Cytotherapy*. **10**(3): 243-253.

Hathcock, J.N., Shao, A., Vieth, R. and Heaney, R. (2007). Risk assessment for vitamin D. *Am J Clin Nutr*. **85**(1): 6-18.

Hathcock, K.S., Hirano, H., Murakami, S. and Hodes, R.J. (1992). CD45 expression by B cells. Expression of different CD45 isoforms by subpopulations of activated B cells. *J Immunol*. **149**(7): 2286-2294.

Hauge, E.M., Qvesel, D., Eriksen, E.F., Mosekilde, L. and Melsen, F. (2001). Cancellous bone remodeling occurs in specialized compartments lined by cells expressing osteoblastic markers. *J Bone Miner Res*. **16**(9): 1575-1582.

Hawke, M. and Jahn, A.F. (1975). Bone formation in the normal human otic capsule. *Arch Otolaryngol*. **101**(8): 462-464.

Hay, E., Faucheu, C., Suc-Royer, I., Touitou, R., Stiot, V., Vayssiere, B., Baron, R., Roman-Roman, S. and Rawadi, G. (2005). Interaction between LRP5 and Frat1 mediates the activation of the Wnt canonical pathway. *J Biol Chem*. **280**(14): 13616-13623.

Hay, E., Lemonnier, J., Modrowski, D., Lomri, A., Lasmoles, F. and Marie, P.J. (2000). N- and E-cadherin mediate early human calvaria osteoblast differentiation promoted by bone morphogenetic protein-2. *J Cell Physiol*. **183**(1): 117-128.

Haynesworth, S.E., Barer, M.A. and Caplan, A.I. (1992a). Cell surface antigens on human marrow-derived mesenchymal cells are detected by monoclonal antibodies. *Bone*. **13**(1): 69-80.

Haynesworth, S.E., Goshima, J., Goldberg, V.M. and Caplan, A.I. (1992b). Characterization of cells with osteogenic potential from human marrow. *Bone*. **13**(1): 81-88.

Heaney, R.P. (2004). Functional indices of vitamin D status and ramifications of vitamin D deficiency. *Am J Clin Nutr*. **80**(6 Suppl): 1706S-1709S.

Helseth, D.L., Jr. and Veis, A. (1981). Collagen self-assembly in vitro. Differentiating specific telopeptide-dependent interactions using selective enzyme modification and the addition of free amino telopeptide. *J Biol Chem*. **256**(14): 7118-7128.

Hench, L., Splinter, R. and Allen, W. (1971). Bonding mechanisms at the interface of ceramic prosthetic materials. *J Biomed Mater Res*. **2**: 117 -141.

Henry, T.D., Annex, B.H., McKendall, G.R., Azrin, M.A., Lopez, J.J., Giordano, F.J., Shah, P.K., Willerson, J.T., Benza, R.L., Berman, D.S., Gibson, C.M., Bajamonde, A., Rundle, A.C., Fine, J. and McCluskey, E.R. (2003). The VIVA trial: Vascular endothelial growth factor in Ischemia for Vascular Angiogenesis. *Circulation*. **107**(10): 1359-1365.

Herbage, D., Bouillet, J. and Bernengo, J.C. (1977). Biochemical and physiochemical characterization of pepsin-solubilized type-II collagen from bovine articular cartilage. *Biochem J*. **161**(2): 303-312.

Heremans, H., Billiau, A., Cassiman, J.J., Mulier, J.C. and de Somer, P. (1978). In vitro cultivation of human tumor tissues. II. Morphological and virological characterization of three cell lines. *Oncology*. **35**(6): 246-252.

Hernigou, P., Poignard, A., Beaujean, F. and Rouard, H. (2005). Percutaneous autologous bone-marrow grafting for nonunions. Influence of the number and concentration of progenitor cells. *J Bone Joint Surg Am*. **87**(7): 1430-1437.

Hill, P.A. (1998). Bone remodelling. *Br J Orthod*. **25**(2): 101-107.

Hill, T.P., Spater, D., Taketo, M.M., Birchmeier, W. and Hartmann, C. (2005). Canonical Wnt/beta-catenin signaling prevents osteoblasts from differentiating into chondrocytes. *Dev Cell*. **8**(5): 727-738.

Hillam, R.A. and Skerry, T.M. (1995). Inhibition of bone resorption and stimulation of formation by mechanical loading of the modeling rat ulna in vivo. *J Bone Miner Res*. **10**(5): 683-689.

Hirano, S., Tsuchida, H. and Nagao, N. (1989). N-acetylation in chitosan and the rate of its enzymic hydrolysis. *Biomaterials*. **10**(8): 574-576.

Ho, M.H., Wang, D.M., Hsieh, H.J., Liu, H.C., Hsien, T.Y., Lai, J.Y. and Hou, L.T. (2005). Preparation and characterization of RGD-immobilized chitosan scaffolds. *Biomaterials*. **26**(16): 3197-3206.

Ho, M.L., Fu, Y.C., Wang, G.J., Chen, H.T., Chang, J.K., Tsai, T.H. and Wang, C.K. (2008). Controlled release carrier of BSA made by W/O/W emulsion method containing PLGA and hydroxyapatite. *J Control Release*. **128**(2): 142-148.

Hoemann, C.D., El-Gabalawy, H. and McKee, M.D. (2008). In vitro osteogenesis assays: Influence of the primary cell source on alkaline phosphatase activity and mineralization. *Pathol Biol (Paris)*. **In Press**.

Hofmann, H., Fietzek, P.P. and Kuhn, K. (1980). Comparative analysis of the sequences of the three collagen chains alpha 1(I), alpha 2 and alpha 1(III) Functional and genetic aspects. *J Mol Biol*. **141**(3): 293-314.

Holland, T.A., Tabata, Y. and Mikos, A.G. (2003). In vitro release of transforming growth factor-β1 from gelatin microparticles encapsulated in biodegradable, injectable oligo(poly(ethylene glycol) fumarate) hydrogels. *J Control Release*. **91**(3): 299-313.

Holleville, N., Mateos, S., Bontoux, M., Bollerot, K. and Monsoro-Burq, A.H. (2007). Dlx5 drives Runx2 expression and osteogenic differentiation in developing cranial suture mesenchyme. *Dev Biol*. **304**(2): 860-874.

Hollinger, J.O., Brekke, J., Gruskin, E. and Lee, D. (1996). Role of bone substitutes. *Clin Orthop Relat Res*. (324): 55-65.

Holtorf, H.L., Datta, N., Jansen, J.A. and Mikos, A.G. (2005). Scaffold mesh size affects the osteoblastic differentiation of seeded marrow stromal cells cultured in a flow perfusion bioreactor. *J Biomed Mater Res A*. **74**(2): 171-180.

Hong, L., Peptan, I., Clark, P. and Mao, J.J. (2005). Ex vivo adipose tissue engineering by human marrow stromal cell seeded gelatin sponge. *Ann Biomed Eng*. **33**(4): 511-517.

Horwitz, E.M., Le Blanc, K., Dominici, M., Mueller, I., Slaper-Cortenbach, I., Marini, F.C., Deans, R.J., Krause, D.S. and Keating, A. (2005). Clarification of the nomenclature for MSC: The International Society for Cellular Therapy position statement. *Cytotherapy*. **7**(5): 393-395.

Hosokawa, R., Urata, M., Han, J., Zehnaly, A., Bringas, P., Jr., Nonaka, K. and Chai, Y. (2007). TGF-beta mediated Msx2 expression controls occipital somites-derived caudal region of skull development. *Dev Biol*. **310**(1): 140-153.

Hosono, K., Nishida, Y., Knudson, W., Knudson, C.B., Naruse, T., Suzuki, Y. and Ishiguro, N. (2007). Hyaluronan oligosaccharides inhibit tumorigenicity of osteosarcoma cell lines MG-63 and LM-8 in vitro and in vivo via perturbation of hyaluronan-rich pericellular matrix of the cells. *Am J Pathol*. **171**(1): 274-286.

Hosseinkhani, H., Hosseinkhani, M., Khademhosseini, A. and Kobayashi, H. (2007). Bone regeneration through controlled release of bone morphogenetic protein-2 from 3-D tissue engineered nano-scaffold. *J Control Release*. **117**(3): 380-386.

Howard, D., Buttery, L.D., Shakesheff, K.M. and Roberts, S.J. (2008). Tissue engineering: strategies, stem cells and scaffolds. *J Anat*. **213**(1): 66-72.

Howard, D., Partridge, K., Yang, X., Clarke, N.M., Okubo, Y., Bessho, K., Howdle, S.M., Shakesheff, K.M. and Oreffo, R.O. (2002). Immunoselection and adenoviral genetic modulation of human osteoprogenitors: in vivo bone formation on PLA scaffold. *Biochem Biophys Res Commun*. **299**(2): 208-215.

Howdle, S.M., Watson, M.S., Whitaker, M.J., Popov, V.K., Davies, M.C., Mandel, F.S., Wang, J.D. and Shakesheff, K.M. (2001). Supercritical fluid mixing: preparation of thermally sensitive polymer composites containing bioactive materials. *Chem Commun*. **1**(1): 109-110.

Hu, H., Hilton, M.J., Tu, X., Yu, K., Ornitz, D.M. and Long, F. (2005). Sequential roles of Hedgehog and Wnt signaling in osteoblast development. *Development*. **132**(1): 49-60.

Huang, W., Carlsen, B., Wulur, I., Rudkin, G., Ishida, K., Wu, B., Yamaguchi, D.T. and Miller, T.A. (2004). BMP-2 exerts differential effects on differentiation of rabbit bone marrow stromal cells grown in two-dimensional and three-dimensional systems and is required for in vitro bone formation in a PLGA scaffold. *Exp Cell Res*. **299**(2): 325-334.

Huang, W., Yang, S., Shao, J. and Li, Y.P. (2007). Signaling and transcriptional regulation in osteoblast commitment and differentiation. *Front Biosci*. **12**: 3068-3092.

Hughes, D.E., Wright, K.R., Uy, H.L., Sasaki, A., Yoneda, T., Roodman, G.D., Mundy, G.R. and Boyce, B.F. (1995). Bisphosphonates promote apoptosis in murine osteoclasts in vitro and in vivo. *J Bone Miner Res*. **10**(10): 1478-1487.

Hunter, W.L., Machan, L.S. and Arsenault, A.L. (1998). *Anti-angiogenic compositions and methods of use*. USPTO: Patent No. **5716981**.

Hurley, M.M., Marcello, K., Abreu, C. and Kessler, M. (1996). Signal transduction by basic fibroblast growth factor in rat osteoblastic Py1a cells. *J Bone Miner Res*. **11**(9): 1256-1263.

Husheem, M., Nyman, J.K., Vaaraniemi, J., Vaananen, H.K. and Hentunen, T.A. (2005). Characterization of circulating human osteoclast progenitors: development of in vitro resorption assay. *Calcif Tissue Int*. **76**(3): 222-230.

Hutmacher, D.W. (2000). Scaffolds in tissue engineering bone and cartilage. *Biomaterials*. **21**(24): 2529-2543.

Hutmacher, D.W., Schantz, T., Zein, I., Hg, K.W., Teoh, S.H. and Tan, K.C. (2001). Mechanical properties and cell cultural response of polycaprolactone scaffolds designed and fabricated via fused deposition modeling. *J Biomed Mater Res.* **55**(2): 203-216.

Hutmacher, D.W., Sittinger, M. and Risbud, M.V. (2004). Scaffold-based tissue engineering: rationale for computer-aided design and solid free-form fabrication systems. *Trends Biotechnol*. **22**(7): 354-362.

Ichida, F., Nishimura, R., Hata, K., Matsubara, T., Ikeda, F., Hisada, K., Yatani, H., Cao, X., Komori, T., Yamaguchi, A. and Yoneda, T. (2004). Reciprocal roles of MSX2 in regulation of osteoblast and adipocyte differentiation. *J Biol Chem*. **279**(32): 34015-34022.

Ignatius, A.A. and Claes, L.E. (1996). In vitro biocompatibility of bioresorbable polymers: poly(L, DL-lactide) and poly(L-lactide-co-glycolide). *Biomaterials*. **17**(8): 831-839.

IOM. (1997). Dietary Reference Intake. In: US National Academy of Sciences. Institute of Medicine, Washinton, D.C., USA

Ishihara, M., Obara, K., Ishizuka, T., Fujita, M., Sato, M., Masuoka, K., Saito, Y., Yura, H., Matsui, T., Hattori, H., Kikuchi, M. and Kurita, A. (2003). Controlled release of fibroblast growth factors and heparin from photocrosslinked chitosan hydrogels and subsequent effect on in vivo vascularization. *J Biomed Mater Res A*. **64**(3): 551-559.

Itano, N., Atsumi, F., Sawai, T., Yamada, Y., Miyaishi, O., Senga, T., Hamaguchi, M. and Kimata, K. (2002). Abnormal accumulation of hyaluronan matrix diminishes contact inhibition of cell growth and promotes cell migration. *Proc Natl Acad Sci U S A*. **99**(6): 3609-3614.

Itoh, F., Asao, H., Sugamura, K., Heldin, C.H., ten Dijke, P. and Itoh, S. (2001a). Promoting bone morphogenetic protein signaling through negative regulation of inhibitory Smads. *Embo J*. **20**(15): 4132-4142.

Itoh, K., Krupnik, V.E. and Sokol, S.Y. (1998). Axis determination in Xenopus involves biochemical interactions of axin, glycogen synthase kinase 3 and beta-catenin. *Curr Biol*. **8**(10): 591-594.

Itoh, S., Kikuchi, M., Takakuda, K., Koyama, Y., Matsumoto, H.N., Ichinose, S., Tanaka, J., Kawauchi, T. and Shinomiya, K. (2001b). The biocompatibility and osteoconductive activity of a novel hydroxyapatite/collagen composite biomaterial, and its function as a carrier of rhBMP-2. *J Biomed Mater Res*. **54**(3): 445-453.

Jacob, A.L., Smith, C., Partanen, J. and Ornitz, D.M. (2006). Fibroblast growth factor receptor 1 signaling in the osteo-chondrogenic cell lineage regulates sequential steps of osteoblast maturation. *Dev Biol*. **296**(2): 315-328.

Jaklenec, A., Hinckfuss, A., Bilgen, B., Ciombor, D.M., Aaron, R. and Mathiowitz, E. (2008). Sequential release of bioactive IGF-I and TGF-beta 1 from PLGA microsphere-based scaffolds. *Biomaterials*. **29**(10): 1518-1525.

Jarcho, M. (1981). Calcium phosphate ceramics as hard tissue prosthetics. *Clin Orthop Relat Res*. **157**: 259-278.

Jell, G. and Stevens, M.M. (2006). Gene activation by bioactive glasses. *J Mater Sci Mater Med*. **17**(11): 997-1002.

Jin, E.J., Park, J.H., Lee, S.Y., Chun, J.S., Bang, O.S. and Kang, S.S. (2006). Wnt-5a is involved in TGF-beta3-stimulated chondrogenic differentiation of chick wing bud mesenchymal cells. *Int J Biochem Cell Biol*. **38**(2): 183-195.

Johnson, B.D., Beebe, D.J. and Crone, W.C. (2004). Effects of swelling on the mechanical properties of a pH-sensitive hydrogel for use in microfluidic devices. *Materials Science and Engineering: C*. **24**(4): 575-581.

Jordan, K.M. and Cooper, C. (2002). Epidemiology of osteoporosis. *Best Pract Res Clin Rheumatol*. **16**(5): 795-806.

Jorgensen, C., Gordeladze, J. and Noel, D. (2004a). Tissue engineering through autologous mesenchymal stem cells. *Curr Opin Biotechnol*. **15**(5): 406-410.

Jorgensen, N.R., Henriksen, Z., Sorensen, O.H. and Civitelli, R. (2004b). Dexamethasone, BMP-2, and 1,25-dihydroxyvitamin D enhance a more differentiated osteoblast phenotype: validation of an in vitro model for human bone marrow-derived primary osteoblasts. *Steroids*. **69**(4): 219-226.

Jungreuthmayer, C., Donahue, S.W., Jaasma, M.J., Al-Munajjed, A.A., Zanghellini, J., Kelly, D.J. and O'Brien, F.J. (2008). A Comparative Study of Shear Stresses in Collagen-Glycosaminoglycan and Calcium Phosphate Scaffolds in Bone Tissue-Engineering Bioreactors. *Tissue Eng Part A*.

Kaigler, D., Krebsbach, P.H., Polverini, P.J. and Mooney, D.J. (2003). Role of vascular endothelial growth factor in bone marrow stromal cell modulation of endothelial cells. *Tissue Eng*. **9**(1): 95-103.

Kamakura, S., Nakajo, S., Suzuki, O. and Sasano, Y. (2004). New scaffold for recombinant human bone morphogenetic protein-2. *J Biomed Mater Res A*. **71**(2): 299-307.

Kanczler, J.M., Barry, J., Ginty, P., Howdle, S.M., Shakesheff, K.M. and Oreffo, R.O. (2007). Supercritical carbon dioxide generated vascular endothelial growth factor encapsulated poly(DL-lactic acid) scaffolds induce angiogenesis in vitro. *Biochem Biophys Res Commun*. **352**(1): 135-141.

Kang, J.S., Alliston, T., Delston, R. and Derynck, R. (2005). Repression of Runx2 function by TGF-beta through recruitment of class II histone deacetylases by Smad3. *Embo J*. **24**(14): 2543-2555.

Kang, Q., Sun, M.H., Cheng, H., Peng, Y., Montag, A.G., Deyrup, A.T., Jiang, W., Luu, H.H., Luo, J., Szatkowski, J.P., Vanichakarn, P., Park, J.Y., Li, Y., Haydon, R.C. and He, T.C. (2004). Characterization of the distinct orthotopic bone-forming activity of 14 BMPs using recombinant adenovirus-mediated gene delivery. *Gene Ther*. **11**(17): 1312-1320.

Kapur, S., Baylink, D.J. and Lau, K.H. (2003). Fluid flow shear stress stimulates human osteoblast proliferation and differentiation through multiple interacting and competing signal transduction pathways. *Bone*. **32**(3): 241-251.

Karageorgiou, V. and Kaplan, D. (2005). Porosity of 3D biomaterial scaffolds and osteogenesis. *Biomaterials*. **26**(27): 5474-5491.

Karp, J.M., Shoichet, M.S. and Davies, J.E. (2003). Bone formation on two-dimensional poly(DL-lactide-co-glycolide) (PLGA) films and three-dimensional PLGA tissue engineering scaffolds in vitro. *J Biomed Mater Res A*. **64**(2): 388-396.

Karsenty, G. (2003). The complexities of skeletal biology. *Nature*. **423**(6937): 316-318.

Katagiri, T., Yamaguchi, A., Komaki, M., Abe, E., Takahashi, N., Ikeda, T., Rosen, V., Wozney, J.M., Fujisawa-Sehara, A. and Suda, T. (1994). Bone morphogenetic protein-2 converts the differentiation pathway of C2C12 myoblasts into the osteoblast lineage. *J Cell Biol*. **127**(6 Pt 1): 1755-1766.

Kato, T., Kawaguchi, H., Hanada, K., Aoyama, I., Hiyama, Y., Nakamura, T., Kuzutani, K., Tamura, M., Kurokawa, T. and Nakamura, K. (1998). Single local injection of recombinant fibroblast growth factor-2 stimulates healing of segmental bone defects in rabbits. *J Orthop Res*. **16**(6): 654-659.

Katz, F.E., Tindle, R., Sutherland, D.R. and Greaves, M.F. (1985). Identification of a membrane glycoprotein associated with haemopoietic progenitor cells. *Leuk Res*. **9**(2): 191-198.

Kawakami, Y., Tsuda, M., Takahashi, S., Taniguchi, N., Esteban, C.R., Zemmyo, M., Furumatsu, T., Lotz, M., Belmonte, J.C. and Asahara, H. (2005). Transcriptional coactivator PGC-1alpha regulates chondrogenesis via association with Sox9. *Proc Natl Acad Sci U S A*. **102**(7): 2414-2419.

Keating, A. (2006). Mesenchymal stromal cells. *Curr Opin Hematol*. **13**(6): 419-425.

Keaveny, T.M. and Yeh, O.C. (2002). Architecture and trabecular bone - toward an improved understanding of the biomechanical effects of age, sex and osteoporosis. *J Musculoskelet Neuronal Interact*. **2**(3): 205-208.

Kells, A.F., Coats, S.R., Schwartz, H.S. and Hoover, R.L. (1995). TGF-beta and PDGF act synergistically in affecting the growth of human osteoblast-enriched cultures. *Connect Tissue Res*. **31**(2): 117-124.

Kemp, K.C., Hows, J. and Donaldson, C. (2005). Bone marrow-derived mesenchymal stem cells. *Leuk Lymphoma*. **46**(11): 1531-1544.

Kempen, D.H., Lu, L., Hefferan, T.E., Creemers, L.B., Maran, A., Classic, K.L., Dhert, W.J. and Yaszemski, M.J. (2008). Retention of in vitro and in vivo BMP-2 bioactivities in sustained delivery vehicles for bone tissue engineering. *Biomaterials*. **29**(22): 3245-3252.

Kemshead, J.T., Ritter, M.A., Cotmore, S.F. and Greaves, M.F. (1982). Human Thy-1: expression on the cell surface of neuronal and glial cells. *Brain Res*. **236**(2): 451-461.

Keramaris, N.C., Calori, G.M., Nikolaou, V.S., Schemitsch, E.H. and Giannoudis, P.V. (2008). Fracture vascularity and bone healing: A systematic review of the role of VEGF. *Injury*. **39**(Supplement 2): S45-S57.

Kern, B., Shen, J., Starbuck, M. and Karsenty, G. (2001). Cbfa1 contributes to the osteoblast-specific expression of type I collagen genes. *J Biol Chem*. **276**(10): 7101-7107.

Khalil, S., Nam, J. and Sun, W. (2005). Multi-nozzle deposition for construction of 3D biopolymer tissue scaffolds. *Rapid Prototyping Journal*. **11**: 9-17.

Khan, F., Tare, R.S., Kanczler, J.M., Oreffo, R.O. and Bradley, M. (2010). Strategies for cell manipulation and skeletal tissue engineering using high-throughput polymer blend formulation and microarray techniques. *Biomaterials*. **31**(8): 2216-2228.

Kim, H., Kim, H.W. and Suh, H. (2003a). Sustained release of ascorbate-2-phosphate and dexamethasone from porous PLGA scaffolds for bone tissue engineering using mesenchymal stem cells. *Biomaterials*. **24**(25): 4671-4679.

Kim, H., Suh, H., Jo, S.A., Kim, H.W., Lee, J.M., Kim, E.H., Reinwald, Y., Park, S.H., Min, B.H. and Jo, I. (2005). In vivo bone formation by human marrow stromal cells in biodegradable scaffolds that release dexamethasone and ascorbate-2-phosphate. *Biochem Biophys Res Commun*. **332**(4): 1053-1060.

Kim, H.D. and Valentini, R.F. (2002). Retention and activity of BMP-2 in hyaluronic acid-based scaffolds *in vitro*. *J Biomed Mater Res*. **59**(3): 573-584.

Kim, H.J., Kim, J.H., Bae, S.C., Choi, J.Y., Kim, H.J. and Ryoo, H.M. (2003b). The protein kinase C pathway plays a central role in the fibroblast growth factor-stimulated expression and transactivation activity of Runx2. *J Biol Chem*. **278**(1): 319-326.

Kim, I.S., Song, Y.M., Cho, T.H., Kim, J.Y., Weber, F.E. and Hwang, S.J. (2009). Synergistic action of static stretching and BMP-2 stimulation in the osteoblast differentiation of C2C12 myoblasts. *J Biomech*. **42**(16): 2721-2727.

Kim, J.H., Kim, S.M., Kim, J.H., Kwon, K.J. and Park, Y.W. (2008). Effect of Type I Collagen on Hydroxyapatite and Tricalcium Phosphate Mixtures in Rat Calvarial Bony Defects. *J. Kor. Oral Maxillofac. Surg*. **34**(1): 36-48.

Kim, S., Hyung, K., Surendran, S., Han, C., Lee, S., Choi, H., Choi, Y., Lee, K., Rhie, J. and Ahn, S. (2006). Bone Morphogenic Protein-2 (BMP-2) Immobilized Biodegradable Scaffolds for Bone Tissue Engineering. *Macromol Res*. **14**(5): 565-572.

Kim, S.E., Park, J.H., Cho, Y.W., Chung, H., Jeong, S.Y., Lee, E.B. and Kwon, I.C. (2003c). Porous chitosan scaffold containing microspheres loaded with transforming growth factor-β1: Implications for cartilage tissue engineering. *J Control Release*. **91**(3): 365-374.

Kim, S.S., Ahn, K.M., Park, M.S., Lee, J.H., Choi, C.Y. and Kim, B.S. (2007a). A poly(lactide-co-glycolide)/hydroxyapatite composite scaffold with enhanced osteoconductivity. *J Biomed Mater Res A*. **80**(1): 206-215.

Kim, T.H. and Park, T.G. (2004). Critical effect of freezing/freeze-drying on sustained release of FITC-dextran encapsulated within PLGA microspheres. *Int J Pharm*. **271**(1-2): 207-214.

Kim, W.K., Meliton, V., Amantea, C.M., Hahn, T.J. and Parhami, F. (2007b). 20(S)-hydroxycholesterol inhibits PPARgamma expression and adipogenic differentiation of bone marrow stromal cells through a hedgehog-dependent mechanism. *J Bone Miner Res*. **22**(11): 1711-1719.

Kim, Y.J., Lee, M.H., Wozney, J.M., Cho, J.Y. and Ryoo, H.M. (2004). Bone morphogenetic protein-2-induced alkaline phosphatase expression is stimulated by Dlx5 and repressed by Msx2. *J Biol Chem*. **279**(49): 50773-50780.

Kincade, P.W. (1987). Experimental models for understanding B lymphocyte formation. *Adv Immunol*. **41**: 181-267.

Kleinheinz, J., Stratmann, U., Joos, U. and Wiesmann, H.P. (2005). VEGF-activated angiogenesis during bone regeneration. *J Oral Maxillofac Surg*. **63**(9): 1310-1316.

Kloen, P., Di Paola, M., Borens, O., Richmond, J., Perino, G., Helfet, D.L. and Goumans, M.J. (2003). BMP signaling components are expressed in human fracture callus. *Bone*. **33**(3): 362-371.

Knight, C.G., Morton, L.F., Peachey, A.R., Tuckwell, D.S., Farndale, R.W. and Barnes, M.J. (2000). The collagen-binding A-domains of integrins $\alpha_1\beta_1$ and $\alpha_2\beta_1$ recognize the same specific amino acid sequence, GFOGER, in native (triple-helical) collagens. *J Biol Chem*. **275**(1): 35-40.

Knippenberg, M., Helder, M.N., Zandieh Doulabi, B., Wuisman, P.I.J.M. and Klein-Nulend, J. (2006). Osteogenesis versus chondrogenesis by BMP-2 and BMP-7 in adipose stem cells. *Biochem Bioph Res Co*. **342**(3): 902-908.

Kobayashi, K., Nomoto, Y., Suzuki, T., Tada, Y., Miyake, M., Hazama, A., Kanemaru, S., Nakamura, T. and Omori, K. (2006). Effect of fibroblasts on tracheal epithelial regeneration in vitro. *Tissue Eng*. **12**(9): 2619-2628.

Komori, T., Yagi, H., Nomura, S., Yamaguchi, A., Sasaki, K., Deguchi, K., Shimizu, Y., Bronson, R.T., Gao, Y.H., Inada, M., Sato, M., Okamoto, R., Kitamura, Y., Yoshiki, S. and Kishimoto, T. (1997). Targeted disruption of Cbfa1 results in a complete lack of bone formation owing to maturational arrest of osteoblasts. *Cell*. **89**(5): 755-764.

Komura, M., Komura, H., Kanamori, Y., Tanaka, Y., Suzuki, K., Sugiyama, M., Nakahara, S., Kawashima, H., Hatanaka, A., Hoshi, K., Ikada, Y., Tabata, Y. and Iwanaka, T. (2008). An animal model study for tissue-engineered trachea fabricated from a biodegradable scaffold using chondrocytes to augment repair of tracheal stenosis. *J Pediatr Surg*. **43**(12): 2141-2146.

Kon, T., Cho, T.J., Aizawa, T., Yamazaki, M., Nooh, N., Graves, D., Gerstenfeld, L.C. and Einhorn, T.A. (2001). Expression of osteoprotegerin, receptor activator of NF-kappaB ligand (osteoprotegerin ligand) and related proinflammatory cytokines during fracture healing. *J Bone Miner Res*. **16**(6): 1004-1014.

Kotobuki, N., Hirose, M., Machida, H., Katou, Y., Muraki, K., Takakura, Y. and Ohgushi, H. (2005). Viability and osteogenic potential of cryopreserved human bone marrow-derived mesenchymal cells. *Tissue Eng*. **11**(5-6): 663-673.

Kozawa, O., Tokuda, H., Matsuno, H. and Uematsu, T. (1999). Involvement of p38 mitogen-activated protein kinase in basic fibroblast growth factor-induced interleukin-6 synthesis in osteoblasts. *J Cell Biochem*. **74**(3): 479-485.

Kozhevnikova, M.N., Mikaelian, A.S., Paiushina, O.V. and Starostin, V.I. (2008). [Comparative characterization of mesenchymal bone marrow stromal cells at early and late stages of culturing]. *Izv Akad Nauk Ser Biol*. (2): 156-162.

Krishnan, V., Moore, T.L., Ma, Y.L., Helvering, L.M., Frolik, C.A., Valasek, K.M., Ducy, P. and Geiser, A.G. (2003). Parathyroid hormone bone anabolic action requires Cbfa1/Runx2-dependent signaling. *Mol Endocrinol*. **17**(3): 423-435.

Kurihara, N., Chenu, C., Miller, M., Civin, C. and Roodman, G.D. (1990). Identification of committed mononuclear precursors for osteoclast-like cells formed in long term human marrow cultures. *Endocrinology*. **126**(5): 2733-2741.

Kutz, S.M., Hordines, J., McKeown-Longo, P.J. and Higgins, P.J. (2001). TGF-beta1-induced PAI-1 gene expression requires MEK activity and cell-to-substrate adhesion. *J Cell Sci*. **114**(Pt 21): 3905-3914.

Kuznetsov, S.A., Krebsbach, P.H., Satomura, K., Kerr, J., Riminucci, M., Benayahu, D. and Robey, P.G. (1997). Single-colony derived strains of human marrow stromal fibroblasts form bone after transplantation in vivo. *J Bone Miner Res*. **12**(9): 1335-1347.

Lacey, D.L., Timms, E., Tan, H.L., Kelley, M.J., Dunstan, C.R., Burgess, T., Elliott, R., Colombero, A., Elliott, G., Scully, S., Hsu, H., Sullivan, J., Hawkins, N., Davy, E., Capparelli, C., Eli, A., Qian, Y.X., Kaufman, S., Sarosi, I., Shalhoub, V., Senaldi, G., Guo, J., Delaney, J. and Boyle, W.J. (1998). Osteoprotegerin ligand is a cytokine that regulates osteoclast differentiation and activation. *Cell*. **93**(2): 165-176.

Lai, C.F., Chaudhary, L., Fausto, A., Halstead, L.R., Ory, D.S., Avioli, L.V. and Cheng, S.L. (2001). Erk is essential for growth, differentiation, integrin expression, and cell function in human osteoblastic cells. *J Biol Chem*. **276**(17): 14443-14450.

Lai, C.F. and Cheng, S.L. (2002). Signal transductions induced by bone morphogenetic protein-2 and transforming growth factor-beta in normal human osteoblastic cells. *J Biol Chem*. **277**(18): 15514-15522.

Landers, R., Hübner, U., Schmelzeisen, R. and Mülhaupt, R. (2002). Rapid prototyping of scaffolds derived from thermoreversible hydrogels and tailored for applications in tissue engineering. *Biomaterials*. **23**(23): 4437-4447.

Lange, C., Cakiroglu, F., Spiess, A.N., Cappallo-Obermann, H., Dierlamm, J. and Zander, A.R. (2007). Accelerated and safe expansion of human mesenchymal stromal cells in animal serum-free medium for transplantation and regenerative medicine. *J Cell Physiol*. **213**(1): 18-26.

Langer, R. and Vacanti, J.P. (1993). Tissue Engineering. *Science*. **260**(5110): 920-926.

LaVelle, D. (1998). Delayed union and non-union of fractures. In: *Campbell's operative orthopaedics* (T. Canale, ed), Mosby, St. Louis, pp. 2579-2629.

Lavik, E. and Langer, R. (2004). Tissue engineering: current state and perspectives. *Appl Microbiol Biotechnol*. **65**(1): 1-8.

Lazennec, G. and Jorgensen, C. (2008). Concise review: adult multipotent stromal cells and cancer: risk or benefit? *Stem Cells*. **26**(6): 1387-1394.

Lecka-Czernik, B., Moerman, E.J., Grant, D.F., Lehmann, J.M., Manolagas, S.C. and Jilka, R.L. (2002). Divergent effects of selective peroxisome proliferator-activated receptor-gamma 2 ligands on adipocyte versus osteoblast differentiation. *Endocrinology*. **143**(6): 2376-2384.

Leclerc, E., Corlu, A., Griscom, L., Baudoin, R. and Legallais, C. (2006). Guidance of liver and kidney organotypic cultures inside rectangular silicone microchannels. *Biomaterials*. **27**(22): 4109-4119.

Lee, C.H., Singla, A. and Lee, Y. (2001). Biomedical applications of collagen. *Int J Pharm*. **221**(1-2): 1-22.

Lee, G.H. and Barlow, J.W. (1994). Selective laser sintering of calcium phosphate powders. In: Solid Freeform Fabrication Symposium, Austin, TX, p. 191-197

Lee, J., Kim, S., Kwon, I., Ahn, H., Cho, H., Lee, S., Kim, H., Seong, S. and Lee, M. (2004a). Effects of a Chitosan Scaffold Containing TGF-β1 Encapsulated Chitosan Microspheres on In Vitro Chondrocyte Culture. *Artificial Organs*. **28**(9): 829-839.

Lee, J.E., Kim, K.E., Kwon, I.C., Ahn, H.J., Lee, S.H., Cho, H., Kim, H.J., Seong, S.C. and Lee, M.C. (2004b). Effects of the controlled-released TGF-β1 from chitosan microspheres on chondrocytes cultured in a collagen/chitosan/glycosaminoglycan scaffold. *Biomaterials*. **25**(18): 4163-4173.

Lee, J.Y., Seol, Y.J., Kim, K.H., Lee, Y.M., Park, Y.J., Rhyu, I.C., Chung, C.P. and Lee, S.J. (2004c). Transforming Growth Factor (TGF)-β1 Releasing Tricalcium Phosphate/Chitosan Microgranules as Bone Substitutes. *Pharmaceutical Research*. **21**(10).

Lee, K.Y. and Mooney, D.J. (2001). Hydrogels for tissue engineering. *Chem Rev*. **101**(7): 1869-1879.

Lee, K.Y., Peters, M.C. and Mooney, D.J. (2003a). Comparison of vascular endothelial growth factor and basic fibroblast growth factor on angiogenesis in SCID mice. *J Control Release*. **87**(1-3): 49-56.

Lee, M., Chen, T.T., Iruela-Arispe, M.L., Wu, B.M. and Dunn, J.C.Y. (2007). Modulation of protein delivery from modular polymer scaffolds. *Biomaterials*. **28**(10): 1862-1870.

Lee, M.H., Javed, A., Kim, H.J., Shin, H.I., Gutierrez, S., Choi, J.Y., Rosen, V., Stein, J.L., van Wijnen, A.J., Stein, G.S., Lian, J.B. and Ryoo, H.M. (1999). Transient upregulation of CBFA1 in response to bone morphogenetic protein-2 and transforming growth factor beta1 in C2C12 myogenic cells coincides with suppression of the myogenic phenotype but is not sufficient for osteoblast differentiation. *J Cell Biochem*. **73**(1): 114-125.

Lee, M.H., Kim, Y.J., Kim, H.J., Park, H.D., Kang, A.R., Kyung, H.M., Sung, J.H., Wozney, J.M., Kim, H.J. and Ryoo, H.M. (2003b). BMP-2-induced Runx2 expression is mediated by Dlx5, and TGF-beta 1 opposes the BMP-2-induced osteoblast differentiation by suppression of Dlx5 expression. *J Biol Chem*. **278**(36): 34387-34394.

Lee, M.H., Kwon, T.G., Park, H.S., Wozney, J.M. and Ryoo, H.M. (2003c). BMP-2-induced Osterix expression is mediated by Dlx5 but is independent of Runx2. *Biochem Biophys Res Commun*. **309**(3): 689-694.

Lee, M.Y., Finn, H.A., Lazda, V.A., Thistlethwaite, J.R., Jr. and Simon, M.A. (1997a). Bone allografts are immunogenic and may preclude subsequent organ transplants. *Clin Orthop Relat Res*. **340**: 215-219.

Lee, Y.M., Kim, S.S. and Kim, S.H. (1997b). Synthesis and properties of poly(ethylene glycol) macromer/beta-chitosan hydrogels. *J Mater Sci Mater Med*. **8**(9): 537-541.

Leenslag, J.W., Pennings, A.J., Bos, R.R., Rozema, F.R. and Boering, G. (1987). Resorbable materials of poly(L-lactide). VI. Plates and screws for internal fracture fixation. *Biomaterials*. **8**(1): 70-73.

Lefrancois, L. and Goodman, T. (1987). Developmental sequence of T200 antigen modifications in murine T cells. *J Immunol*. **139**(11): 3718-3724.

Leong, K.F., Cheah, C.M. and Chua, C.K. (2003). Solid freeform fabrication of three-dimensional scaffolds for engineering replacement tissues and organs. *Biomaterials*. **24**(13): 2363-2378.

Lepperdinger, G., Brunauer, R., Jamnig, A., Laschober, G. and Kassem, M. (2008). Controversial issue: Is it safe to employ mesenchymal stem cells in cell-based therapies? *Exp Gerontol*. **43**(11): 1018-1023.

Leung, L., Chan, C., Baek, S. and Naguib, H. (2008). Comparison of morphology and mechanical properties of PLGA bioscaffolds. *Biomed Mater*. **3**(2): 25006.

Leus, K., Macdonald, A.A., Goodall, G., Veitch, D., Mitchell, S. and Bauwens, L. (2004). Light and scanning electron microscopy of the cardiac gland region of the stomach of the babirusa (Babyrousa babyrussa--Suidae, Mammalia). *C R Biol*. **327**(8): 735-743.

Levenberg, S., Golub, J.S., Amit, M., Itskovitz-Eldor, J. and Langer, R. (2002). Endothelial cells derived from human embryonic stem cells. *Proc Natl Acad Sci U S A*. **99**(7): 4391-4396.

Levenberg, S., Huang, N.F., Lavik, E., Rogers, A.B., Itskovitz-Eldor, J. and Langer, R. (2003). Differentiation of human embryonic stem cells on three-dimensional polymer scaffolds. *Proc Natl Acad Sci U S A*. **100**(22): 12741-12746.

Leventouri, T. (2006). Synthetic and biological hydroxyapatites: crystal structure questions. *Biomaterials*. **27**(18): 3339-3342.

Li, C., Vepari, C., Jin, H.J., Kim, H.J. and Kaplan, D.L. (2006a). Electrospun silk-BMP-2 scaffolds for bone tissue engineering. *Biomaterials*. **27**(16): 3115-3124.

Li, J., Sarosi, I., Cattley, R.C., Pretorius, J., Asuncion, F., Grisanti, M., Morony, S., Adamu, S., Geng, Z., Qiu, W., Kostenuik, P., Lacey, D.L., Simonet, W.S., Bolon, B., Qian, X., Shalhoub, V., Ominsky, M.S., Zhu Ke, H., Li, X. and Richards, W.G. (2006b). Dkk1-mediated inhibition of Wnt signaling in bone results in osteopenia. *Bone*. **39**(4): 754-766.

Li, J.P., de Wijn, J.R., Van Blitterswijk, C.A. and de Groot, K. (2006c). Porous Ti6Al4V scaffold directly fabricating by rapid prototyping: Preparation and in vitro experiment. *Biomaterials*. **27**(8): 1223-1235.

Li, W.J., Tuli, R., Okafor, C., Derfoul, A., Danielson, K.G., Hall, D.J. and Tuan, R.S. (2005). A three-dimensional nanofibrous scaffold for cartilage tissue engineering using human mesenchymal stem cells. *Biomaterials*. **26**(6): 599-609.

Liao, C.J., Chen, C.F., Chen, J.H., Chiang, S.F., Lin, Y.J. and Chang, K.Y. (2002). Fabrication of porous biodegradable polymer scaffolds using a solvent merging/particulate leaching method. *J Biomed Mater Res*. **59**(4): 676-681.

Liao, S., Chan, C.K. and Ramakrishna, S. (2008). Stem cells and biomimetic materials strategies for tissue engineering. *Mater. Sci. Eng., C*. **28**(8): 1189-1202.

Lichtenfels, R., Biddison, W.E., Schulz, H., Vogt, A.B. and Martin, R. (1994). CARE-LASS (calcein-release-assay), an improved fluorescence-based test system to measure cytotoxic T lymphocyte activity. *J Immunol Methods*. **172**(2): 227-239.

Lieberman, J.R., Daluiski, A. and Einhorn, T.A. (2002). The role of growth factors in the repair of bone. Biology and clinical applications. *J Bone Joint Surg Am*. **84-A**(6): 1032-1044.

Liebschner, M. and Wettergreen, M. (2003). Chapter 6: Optimization of Bone Scaffold Engineering for Load Bearing Applications. In: *Topics in Tissue Engineering* (N. Ashammakhi and P. Ferretti, eds.), University of Oulu, Vol. 1, pp. 1 - 39.

Lincks, J., Boyan, B.D., Blanchard, C.R., Lohmann, C.H., Liu, Y., Cochran, D.L., Dean, D.D. and Schwartz, Z. (1998). Response of MG63 osteoblast-like cells to titanium and titanium alloy is dependent on surface roughness and composition. *Biomaterials*. **19**(23): 2219-2232.

Lindsey, R.W., Wood, G.W., Sadasivian, K.K., Stubbs, H.A. and Block, J.E. (2006). Grafting long bone fractures with demineralized bone matrix putty enriched with bone marrow: pilot findings. *Orthopedics*. **29**(10): 939-941.

Linhart, W., Peters, F., Lehmann, W., Schwarz, K., Schilling, A.F., Amling, M., Rueger, J.M. and Epple, M. (2001). Biologically and chemically optimized composites of carbonated apatite and polyglycolide as bone substitution materials. *J Biomed Mater Res*. **54**(2): 162-171.

Link, D.P., van den Dolder, J., van den Beucken, J.J., Wolke, J.G., Mikos, A.G. and Jansen, J.A. (2008). Bone response and mechanical strength of rabbit femoral defects filled with injectable CaP cements containing TGF-[beta]1 loaded gelatin microparticles. *Biomaterials*. **29**(6): 675-682.

Liu, F., Akiyama, Y., Tai, S., Maruyama, K., Kawaguchi, Y., Muramatsu, K. and Yamaguchi, K. (2008a). Changes in the expression of CD106, osteogenic genes, and transcription factors involved in the osteogenic differentiation of human bone marrow mesenchymal stem cells. *J Bone Miner Metab*. **26**(4): 312-320.

Liu, F., Malaval, L., Gupta, A.K. and Aubin, J.E. (1994). Simultaneous detection of multiple bone-related mRNAs and protein expression during osteoblast differentiation: polymerase chain reaction and immunocytochemical studies at the single cell level. *Dev Biol*. **166**(1): 220-234.

Liu, G., Shu, C., Cui, L., Liu, W. and Cao, Y. (2008b). Tissue-engineered bone formation with cryopreserved human bone marrow mesenchymal stem cells. *Cryobiology*. **56**(3): 209-215.

Liu, H., Fan, H., Cui, Y., Chen, Y., Yao, K. and Goh, J.C. (2007). Effects of the controlled-released basic fibroblast growth factor from chitosan-gelatin microspheres on human fibroblasts cultured on a chitosan-gelatin scaffold. *Biomacromolecules*. **8**(5): 1446-1455.

Liu, H., Lee, Y.W. and Dean, M.F. (1998). Re-expression of differentiated proteoglycan phenotype by dedifferentiated human chondrocytes during culture in alginate beads. *Biochim Biophys Acta*. **1425**(3): 505-515.

Liu, P., Oyajobi, B.O., Russell, R.G. and Scutt, A. (1999). Regulation of osteogenic differentiation of human bone marrow stromal cells: interaction between transforming growth factor-beta and 1,25(OH)(2) vitamin D(3) In vitro. *Calcif Tissue Int*. **65**(2): 173-180.

Liu, Y., Song, J., Liu, W., Wan, Y., Chen, X. and Hu, C. (2003). Growth and differentiation of rat bone marrow stromal cells: does 5-azacytidine trigger their cardiomyogenic differentiation? *Cardiovasc Res*. **58**(2): 460-468.

Liu, Z., Xu, J., Colvin, J.S. and Ornitz, D.M. (2002). Coordination of chondrogenesis and osteogenesis by fibroblast growth factor 18. *Genes Dev*. **16**(7): 859-869.

Longobardi, L., O'Rear, L., Aakula, S., Johnstone, B., Shimer, K., Chytil, A., Horton, W.A., Moses, H.L. and Spagnoli, A. (2006). Effect of IGF-I in the chondrogenesis of bone marrow mesenchymal stem cells in the presence or absence of TGF-beta signaling. *J Bone Miner Res*. **21**(4): 626-636.

Luo, G., Hofmann, C., Bronckers, A.L., Sohocki, M., Bradley, A. and Karsenty, G. (1995). BMP-7 is an inducer of nephrogenesis, and is also required for eye development and skeletal patterning. *Genes Dev*. **9**(22): 2808-2820.

Luong-Van, E., Grondahl, L., Nurcombe, V. and Cool, S. (2007). In vitro biocompatibility and bioactivity of microencapsulated heparan sulfate. *Biomaterials*. **28**(12): 2127-2136.

Ma, G., Song, C., Sun, H., Yang, J. and Leng, X. (2006). A biodegradable levonorgestrel-releasing implant made of PCL/F68 compound as tested in rats and dogs. *Contraception*. **74**(2): 141-147.

Macchiarini, P., Jungebluth, P., Go, T., Asnaghi, M.A., Rees, L.E., Cogan, T.A., Dodson, A., Martorell, J., Bellini, S., Parnigotto, P.P., Dickinson, S.C., Hollander, A.P., Mantero, S., Conconi, M.T. and Birchall, M.A. (2008). Clinical transplantation of a tissue-engineered airway. *The Lancet*. **373**(9655): 2023-2030.

Macdonald, A.A., Mitchell, S., Signorella, A. and Leus, K. (2008). Ultrastructural characterization of the epithelium that constitutes the cardiac gland epithelial 'honeycomb' in the stomach of the babirusa (Babyrousa babyrussa). *C R Biol*. **331**(1): 32-41.

Majumdar, M.K., Thiede, M.A., Mosca, J.D., Moorman, M. and Gerson, S.L. (1998). Phenotypic and functional comparison of cultures of marrow-derived mesenchymal stem cells (MSCs) and stromal cells. *J Cell Physiol*. **176**(1): 57-66.

Makino, T., Hak, D.J., Hazelwood, S.J., Curtiss, S. and Reddi, A.H. (2005). Prevention of atrophic nonunion development by recombinant human bone morphogenetic protein-7. *J Orthop Res*. **23**(3): 632-638.

Malda, J., Woodfield, T.B., van der Vloodt, F., Wilson, C., Martens, D.E., Tramper, J., van Blitterswijk, C.A. and Riesle, J. (2005). The effect of PEGT/PBT scaffold architecture on the composition of tissue engineered cartilage. *Biomaterials*. **26**(1): 63-72.

Maniatopoulos, C., Sodek, J. and Melcher, A.H. (1988). Bone formation in vitro by stromal cells obtained from bone marrow of young adult rats. *Cell Tissue Res*. **254**(2): 317-330.

Mansilla, E., Marin, G.H., Drago, H., Sturla, F., Salas, E., Gardiner, C., Bossi, S., Lamonega, R., Guzman, A., Nunez, A., Gil, M.A., Piccinelli, G., Ibar, R. and Soratti, C. (2006). Bloodstream cells phenotypically identical to human mesenchymal bone marrow stem cells circulate in large amounts under the influence of acute large skin damage: new evidence for their use in regenerative medicine. *Transplant Proc*. **38**(3): 967-969.

Mao, B., Wu, W., Davidson, G., Marhold, J., Li, M., Mechler, B.M., Delius, H., Hoppe, D., Stannek, P., Walter, C., Glinka, A. and Niehrs, C. (2002). Kremen proteins are Dickkopf receptors that regulate Wnt/beta-catenin signalling. *Nature*. **417**(6889): 664-667.

Mao, J., Wang, J., Liu, B., Pan, W., Farr, G.H., 3rd, Flynn, C., Yuan, H., Takada, S., Kimelman, D., Li, L. and Wu, D. (2001). Low-density lipoprotein receptor-related protein-5 binds to Axin and regulates the canonical Wnt signaling pathway. *Mol Cell*. **7**(4): 801-809.

Mao, J.S., Cui, Y.L., Wang, X.H., Sun, Y., Yin, Y.J., Zhao, H.M. and De Yao, K. (2004). A preliminary study on chitosan and gelatin polyelectrolyte complex cytocompatibility by cell cycle and apoptosis analysis. *Biomaterials*. **25**(18): 3973-3981.

Marie, P.J. (2002). Role of N-cadherin in bone formation. *J Cell Physiol*. **190**(3): 297-305.

Marie, P.J. (2008). Transcription factors controlling osteoblastogenesis. *Arch Biochem Biophys*. **473**(2): 98-105.

Marigo, V., Davey, R.A., Zuo, Y., Cunningham, J.M. and Tabin, C.J. (1996). Biochemical evidence that patched is the Hedgehog receptor. *Nature*. **384**(6605): 176-179.

Mark, M.P., Butler, W.T., Prince, C.W., Finkelman, R.D. and Ruch, J.V. (1988). Developmental expression of 44-kDa bone phosphoprotein (osteopontin) and bone gamma-carboxyglutamic acid (Gla)-containing protein (osteocalcin) in calcifying tissues of rat. *Differentiation*. **37**(2): 123-136.

Marra, K.G., Szem, J.W., Kumta, P.N., DiMilla, P.A. and Weiss, L.E. (1999). In vitro analysis of biodegradable polymer blend/hydroxyapatite composites for bone tissue engineering. *J Biomed Mater Res*. **47**(3): 324-335.

Marsh, J.L. (2006). Principles of bone grafting: non-union, delayed union. *Surgery (Oxford)*. **24**(6): 207-210.

Martin, A.J., Tremoleda, J.L., Vadillo, P.T., Khan, N., Mann, V. and Noble, B.S. (2008). An osteogenic scaffold carrier for the delivery of human marrow stromal cells to a murine calvarial defect. In: Bone Research Society, Manchester, UK

Martin, C., Winet, H. and Bao, J.Y. (1996). Acidity near eroding polylactide-polyglycolide in vitro and in vivo in rabbit tibial bone chambers. *Biomaterials*. **17**(24): 2373-2380.

Martin, G.R. (1981). Isolation of a pluripotent cell line from early mouse embryos cultured in medium conditioned by teratocarcinoma stem cells. *Proc Natl Acad Sci U S A*. **78**(12): 7634-7638.

Martins, M.J., Negrao, M.R. and Hipolito-Reis, C. (2001). Alkaline phosphatase from rat liver and kidney is differentially modulated. *Clin Biochem*. **34**(6): 463-468.

Martinsen, A., Skjåk-Bræk, G., Smidsrød, O., Zanetti, F. and Paoletti, S. (1991). Comparison of different methods for determination of molecular weight and molecular weight distribution of alginates. *Carbohydr Polym*. **15**(2): 171-193.

Mason, D.Y., van Noesel, C.J., Cordell, J.L., Comans-Bitter, W.M., Micklem, K., Tse, A.G., van Lier, R.A. and van Dongen, J.J. (1992). The B29 and mb-1 polypeptides are differentially expressed during human B cell differentiation. *Eur J Immunol*. **22**(10): 2753-2756.

Masson, N.M., Currie, I.S., Terrace, J.D., Garden, O.J., Parks, R.W. and Ross, J.A. (2006). Hepatic progenitor cells in human fetal liver express the oval cell marker Thy-1. *Am J Physiol Gastrointest Liver Physiol*. **291**(1): G45-54.

Mathieu, L.M., Mueller, T.L., Bourban, P.E., Pioletti, D.P., Muller, R. and Manson, J.A. (2006). Architecture and properties of anisotropic polymer composite scaffolds for bone tissue engineering. *Biomaterials*. **27**(6): 905-916.

Matsubara, T., Kida, K., Yamaguchi, A., Hata, K., Ichida, F., Meguro, H., Aburatani, H., Nishimura, R. and Yoneda, T. (2008). BMP2 regulates Osterix through Msx2 and Runx2 during osteoblast differentiation. *J Biol Chem*. **283**(43): 29119-29125.

Mattioli-Belmonte, M., Gigante, A., Muzzarelli, R.A., Politano, R., De Benedittis, A., Specchia, N., Buffa, A., Biagini, G. and Greco, F. (1999). N,N-dicarboxymethyl chitosan as delivery agent for bone morphogenetic protein in the repair of articular cartilage. *Med Biol Eng Comput*. **37**(1): 130-134.

Mauney, J.R., Kirker-Head, C., Abrahamson, L., Gronowicz, G., Volloch, V. and Kaplan, D.L. (2006). Matrix-mediated retention of in vitro osteogenic differentiation potential and in vivo bone-forming capacity by human adult bone marrow-derived mesenchymal stem cells during ex vivo expansion. *J Biomed Mater Res A*. **79**(3): 464-475.

McCarthy, T.L., Chang, W.Z., Liu, Y. and Centrella, M. (2003). Runx2 integrates estrogen activity in osteoblasts. *J Biol Chem*. **278**(44): 43121-43129.

McCulloch, C.A., Strugurescu, M., Hughes, F., Melcher, A.H. and Aubin, J.E. (1991). Osteogenic progenitor cells in rat bone marrow stromal populations exhibit self-renewal in culture. *Blood*. **77**(9): 1906-1911.

McKeague, A.L., Wilson, D.J. and Nelson, J. (2003). Staurosporine-induced apoptosis and hydrogen peroxide-induced necrosis in two human breast cell lines. *Br J Cancer*. **88**(1): 125-131.

McKee, M. (2000). Aseptic non-union. In: *AO-Principles of fracture management* (T. Ruedi and W. Murphy, eds.), Georg Thieme Verlag, Stuttgart and New York, pp. 748-762.

McKibbin, B. (1978). The biology of fracture healing in long bones. *J Bone Joint Surg Br*. **60-B**(2): 150-162.

Meager, A. (1991). Assays for transforming growth factor β. *J Immunol Methods*. **141**(1): 1-14.

Meinel, L., Karageorgiou, V., Fajardo, R., Snyder, B., Shinde-Patil, V., Zichner, L., Kaplan, D., Langer, R. and Vunjak-Novakovic, G. (2004). Bone tissue engineering using human mesenchymal stem cells: effects of scaffold material and medium flow. *Ann Biomed Eng*. **32**(1): 112-122.

Mendelson, K. and Schoen, F.J. (2006). Heart valve tissue engineering: concepts, approaches, progress, and challenges. *Ann Biomed Eng*. **34**(12): 1799-1819.

Middleton, J.C. and Tipton, A.J. (2000). Synthetic biodegradable polymers as orthopedic devices. *Biomaterials*. **21**(23): 2335-2346.

Mierisch, C.M., Cohen, S.B., Jordan, L.C., Robertson, P.G., Balian, G. and Diduch, D.R. (2002). Transforming growth factor-β in calcium alginate beads for the treatment of articular cartilage defects in the rabbit. *Arthroscopy*. **18**(8): 892-900.

Miller, E.D., Fisher, G.W., Weiss, L.E., Walker, L.M. and Campbell, P.G. (2006). Dose-dependent cell growth in response to concentration modulated patterns of FGF-2 printed on fibrin. *Biomaterials*. **27**(10): 2213-2221.

Miller, Z., Fuchs, M.B. and Arcan, M. (2002). Trabecular bone adaptation with an orthotropic material model. *J Biomech*. **35**(2): 247-256.

Miura, M., Miura, Y., Padilla-Nash, H.M., Molinolo, A.A., Fu, B., Patel, V., Seo, B.M., Sonoyama, W., Zheng, J.J., Baker, C.C., Chen, W., Ried, T. and Shi, S. (2006). Accumulated chromosomal instability in murine bone marrow mesenchymal stem cells leads to malignant transformation. *Stem Cells*. **24**(4): 1095-1103.

Miyama, K., Yamada, G., Yamamoto, T.S., Takagi, C., Miyado, K., Sakai, M., Ueno, N. and Shibuya, H. (1999). A BMP-inducible gene, dlx5, regulates osteoblast differentiation and mesoderm induction. *Dev Biol*. **208**(1): 123-133.

Miyanishi, K., Trindade, M.C., Lindsey, D.P., Beaupre, G.S., Carter, D.R., Goodman, S.B., Schurman, D.J. and Smith, R.L. (2006). Dose- and time-dependent effects of cyclic hydrostatic pressure on transforming growth factor-beta3-induced chondrogenesis by adult human mesenchymal stem cells in vitro. *Tissue Eng*. **12**(8): 2253-2262.

Mizuno, M., Fujisawa, R. and Kuboki, Y. (2000). Type I collagen-induced osteoblastic differentiation of bone-marrow cells mediated by collagen-alpha2beta1 integrin interaction. *J Cell Physiol*. **184**(2): 207-213.

Modrovich, I. (1979). *Stabilized liquid phosphate containing diagnostic compositions and method of preparing same*. USPTO: Patent No. **4132598**.

Moioli, E.K., Hong, L., Guardado, J., Clark, P.A. and Mao, J.J. (2006). Sustained release of TGF-β3 from PLGA microspheres and its effect on early osteogenic differentiation of human mesenchymal stem cells. *Tissue Engineering*. **12**(3): 537-546.

Montero, A., Okada, Y., Tomita, M., Ito, M., Tsurukami, H., Nakamura, T., Doetschman, T., Coffin, J.D. and Hurley, M.M. (2000). Disruption of the fibroblast growth factor-2 gene results in decreased bone mass and bone formation. *J Clin Invest*. **105**(8): 1085-1093.

Mooney, D.J., Baldwin, D.F., Suh, N.P., Vacanti, J.P. and Langer, R. (1996). Novel approach to fabricate porous sponges of poly(D,L-lactic-co-glycolic acid) without the use of organic solvents. *Biomaterials*. **17**(14): 1417-1422.

Moorehead, W.R. and Biggs, H.G. (1974). 2-Amino-2-methyl-1-propanol as the alkalizing agent in an improved continuous-flow cresolphthalein complexone procedure for calcium in serum. *Clin Chem*. **20**(11): 1458-1460.

Moreau, J.L. and Xu, H.H. (2009). Mesenchymal stem cell proliferation and differentiation on an injectable calcium phosphate-chitosan composite scaffold. *Biomaterials*. **30**(14): 2675-2682.

Morvan, F., Boulukos, K., Clement-Lacroix, P., Roman Roman, S., Suc-Royer, I., Vayssiere, B., Ammann, P., Martin, P., Pinho, S., Pognonec, P., Mollat, P., Niehrs, C., Baron, R. and Rawadi, G. (2006). Deletion of a single allele of the Dkk1 gene leads to an increase in bone formation and bone mass. *J Bone Miner Res*. **21**(6): 934-945.

Mumper, R.J., Huffman, A.S., Puolakkainen, P.A., Bouchard, L.S. and Gombotz, W.R. (1994). Calcium-alginate beads for the oral delivery of transforming growth

factor-β1 (TGF-β1): stabilization of TGF-β1 by the addition of polyacrylic acid within acid-treated beads. *J Control Release*. **30**(3): 241-251.

Muraglia, A., Cancedda, R. and Quarto, R. (2000). Clonal mesenchymal progenitors from human bone marrow differentiate in vitro according to a hierarchical model. *J Cell Sci*. **113 (Pt 7)**: 1161-1166.

Murphy, W.L., Peters, M.C., Kohn, D.H. and Mooney, D.J. (2000). Sustained release of vascular endothelial growth factor from mineralized poly(lactide-co-glycolide) scaffolds for tissue engineering. *Biomaterials*. **21**(24): 2521-2527.

Nadler, L.M., Anderson, K.C., Marti, G., Bates, M., Park, E., Daley, J.F. and Schlossman, S.F. (1983). B4, a human B lymphocyte-associated antigen expressed on normal, mitogen-activated, and malignant B lymphocytes. *J Immunol*. **131**(1): 244-250.

Nakamura, T., Hara, Y., Tagawa, M., Tamura, M., Yuge, T., Fukuda, H. and Nigi, H. (1998). Recombinant human basic fibroblast growth factor accelerates fracture healing by enhancing callus remodeling in experimental dog tibial fracture. *J Bone Miner Res*. **13**(6): 942-949.

Nakashima, K., Zhou, X., Kunkel, G., Zhang, Z., Deng, J.M., Behringer, R.R. and de Crombrugghe, B. (2002). The novel zinc finger-containing transcription factor osterix is required for osteoblast differentiation and bone formation. *Cell*. **108**(1): 17-29.

Nam, Y.S. and Park, T.G. (1999). Porous biodegradable polymeric scaffolds prepared by thermally induced phase separation. *J Biomed Mater Res*. **47**(1): 8-17.

Neri, S., Mariani, E., Meneghetti, A., Cattini, L. and Facchini, A. (2001). Calcein-acetyoxymethyl cytotoxicity assay: standardization of a method allowing additional analyses on recovered effector cells and supernatants. *Clin Diagn Lab Immunol*. **8**(6): 1131-1135.

Ng, K.W., Khor, H.L. and Hutmacher, D.W. (2004). In vitro characterization of natural and synthetic dermal matrices cultured with human dermal fibroblasts. *Biomaterials*. **25**(14): 2807-2818.

NHS (2008). *Transplant Activity in the UK*ed., National Health Service (UK Transplant), Bristol.

Nie, H., Soh, B.W., Fu, Y.C. and Wang, C.H. (2008). Three-dimensional fibrous PLGA/HAp composite scaffold for BMP-2 delivery. *Biotechnol Bioeng*. **99**(1): 223-234.

Nikolaou, V.S. and Tsiridis, E. (2007). (i) Pathways and signalling molecules. *Curr Orthopaed*. **21**(4): 249-257.

Noble, B.S. (2008). The osteocyte lineage. *Arch Biochem Biophys*. **473**(2): 106-111.

Noble, B.S., Dean, V., Loveridge, N. and Thomson, B.M. (1995). Dextran sulfate promotes the rapid aggregation of porcine bone-marrow stromal cells. *Bone*. **17**(4): 375-382.

Noble, B.S., Peet, N., Stevens, H.Y., Brabbs, A., Mosley, J.R., Reilly, G.C., Reeve, J., Skerry, T.M. and Lanyon, L.E. (2003). Mechanical loading: biphasic osteocyte survival and targeting of osteoclasts for bone destruction in rat cortical bone. *Am J Physiol Cell Physiol*. **284**(4): C934-943.

Nomura, S., Wills, A.J., Edwards, D.R., Heath, J.K. and Hogan, B.L. (1988). Developmental expression of 2ar (osteopontin) and SPARC (osteonectin) RNA as revealed by in situ hybridization. *J Cell Biol*. **106**(2): 441-450.

Noshi, T., Yoshikawa, T., Ikeuchi, M., Dohi, Y., Ohgushi, H., Horiuchi, K., Sugimura, M., Ichijima, K. and Yonemasu, K. (2000). Enhancement of the in vivo osteogenic potential of marrow/hydroxyapatite composites by bovine bone morphogenetic protein. *J Biomed Mater Res*. **52**(4): 621-630.

Noth, U., Osyczka, A.M., Tuli, R., Hickok, N.J., Danielson, K.G. and Tuan, R.S. (2002). Multilineage mesenchymal differentiation potential of human trabecular bone-derived cells. *J Orthop Res*. **20**(5): 1060-1069.

O'Neil, M.J. (2006). *The Merck index: an encyclopedia of chemicals, drugs, and biologicals*. 14th ed., Merck, Whitehouse Station, NJ.

Oest, M.E., Dupont, K.M., Kong, H.J., Mooney, D.J. and Guldberg, R.E. (2007). Quantitative assessment of scaffold and growth factor-mediated repair of critically sized bone defects. *J Orthop Res*. **25**(7): 941-950.

Ogden, J.A., Hempton, R.J. and Southwick, W.O. (1975). Development of the tibial tuberosity. *Anat Rec*. **182**(4): 431-445.

Ohbayashi, N., Shibayama, M., Kurotaki, Y., Imanishi, M., Fujimori, T., Itoh, N. and Takada, S. (2002). FGF18 is required for normal cell proliferation and differentiation during osteogenesis and chondrogenesis. *Genes Dev*. **16**(7): 870-879.

Okita, K., Ichisaka, T. and Yamanaka, S. (2007). Generation of germline-competent induced pluripotent stem cells. *Nature*. **448**(7151): 313-317.

Oldham, J.B., Lu, L., Zhu, X., Porter, B.D., Hefferan, T.E., Larson, D.R., Currier, B.L., Mikos, A.G. and Yaszemski, M.J. (2000). Biological activity of rhBMP-2 released from PLGA microspheres. *J Biomech Eng*. **122**(3): 289-292.

Olson, S. and Hahn, D. (2006). Surgical treatment of non-unions: A case for internal fixation. *Injury*. **37**(8): 681 - 690.

Osyczka, A.M., Diefenderfer, D.L., Bhargave, G. and Leboy, P.S. (2004). Different effects of BMP-2 on marrow stromal cells from human and rat bone. *Cells Tissues Organs*. **176**(1-3): 109-119.

Otto, F., Thornell, A.P., Crompton, T., Denzel, A., Gilmour, K.C., Rosewell, I.R., Stamp, G.W., Beddington, R.S., Mundlos, S., Olsen, B.R., Selby, P.B. and Owen, M.J. (1997). Cbfa1, a candidate gene for cleidocranial dysplasia syndrome, is essential for osteoblast differentiation and bone development. *Cell*. **89**(5): 765-771.

Owen, M. (1988). Marrow stromal stem cells. *J Cell Sci Suppl*. **10**: 63-76.

Paley, D., Catagni, M.A., Argnani, F., Villa, A., Benedetti, G.B. and Cattaneo, R. (1989). Ilizarov treatment of tibial nonunions with bone loss. *Clin Orthop Relat Res*. **241**: 146-165.

Paley, D. and Maar, D.C. (2000). Ilizarov bone transport treatment for tibial defects. *J Orthop Trauma*. **14**(2): 76-85.

Palma, P.F., Baggio, G.L., Spada, C., Silva, R.D., Ferreira, S.I. and Treitinger, A. (2008). Evaluation of annexin V and Calcein-AM as markers of mononuclear cell apoptosis during human immunodeficiency virus infection. *Braz J Infect Dis*. **12**(2): 108-114.

Panagakos, F.S. (1993). Insulin-like growth factors-I and -II stimulate chemotaxis of osteoblasts isolated from fetal rat calvaria. *Biochimie*. **75**(11): 991-994.

Panagiotis, M. (2005). Classification of non-union. *Injury*. **36**(4, Supplement 1): S30-S37.

Panseri, S., Cunha, C., Lowery, J., Del Carro, U., Taraballi, F., Amadio, S., Vescovi, A. and Gelain, F. (2008). Electrospun micro- and nanofiber tubes for functional nervous regeneration in sciatic nerve transections. *BMC Biotechnol*. **8**: 39.

Papadopoulos, N.G., Dedoussis, G.V., Spanakos, G., Gritzapis, A.D., Baxevanis, C.N. and Papamichail, M. (1994). An improved fluorescence assay for the determination of lymphocyte-mediated cytotoxicity using flow cytometry. *J Immunol Methods*. **177**(1-2): 101-111.

Park, A., Wu, B. and Griffith, L.G. (1998). Integration of surface modification and 3D fabrication techniques to prepare patterned poly(L-lactide) substrates allowing regionally selective cell adhesion. *J Biomater Sci Polym Ed*. **9**(2): 89-110.

Park, I.H., Zhao, R., West, J.A., Yabuuchi, A., Huo, H., Ince, T.A., Lerou, P.H., Lensch, M.W. and Daley, G.Q. (2008). Reprogramming of human somatic cells to pluripotency with defined factors. *Nature*. **451**(7175): 141-146.

Parker, J., Brunner, G., Von den Hoff, J., Maltha, J. and Jansen, J. (2002). Release of Bioactive Transforming Growth Factor ß3 from Microtextured Polymer Surfaces in Vitro and in Vivo. *Tissue Engineering*. **8**(5): 853-861.

Partridge, K., Yang, X., Clarke, N.M.P., Okubo, Y., Bessho, K., Sebald, W., Howdle, S.M., Shakesheff, K.M. and Oreffo, R.O.C. (2002). Adenoviral BMP-2 Gene Transfer in Mesenchymal Stem Cells: In Vitro and in Vivo Bone Formation on Biodegradable Polymer Scaffolds. *Biochem Bioph Res Co*. **292**(1): 144-152.

Patel, Z.S., Young, S., Tabata, Y., Jansen, J.A., Wong, M.E. and Mikos, A.G. (2008). Dual delivery of an angiogenic and an osteogenic growth factor for bone regeneration in a critical size defect model. *Bone*. **43**(5): 931-940.

Patil, S.D., Papadmitrakopoulos, F. and Burgess, D.J. (2007). Concurrent delivery of dexamethasone and VEGF for localized inflammation control and angiogenesis. *J Control Release*. **117**(1): 68-79.

Paul, W. and Sharma, C.P. (2007). Effect of calcium, zinc and magnesium on the attachment and spreading of osteoblast like cells onto ceramic matrices. *J Mater Sci Mater Med*. **18**(5): 699-703.

Pead, M.J., Skerry, T.M. and Lanyon, L.E. (1988). Direct transformation from quiescence to bone formation in the adult periosteum following a single brief period of bone loading. *J Bone Miner Res*. **3**(6): 647-656.

Pen, A., Moreno, M.J., Durocher, Y., Deb-Rinker, P. and Stanimirovic, D.B. (2008). Glioblastoma-secreted factors induce IGFBP7 and angiogenesis by modulating Smad-2-dependent TGF-beta signaling. *Oncogene*. **27**(54): 6834-6844.

Peng, H., Wright, V., Usas, A., Gearhart, B., Shen, H.C., Cummins, J. and Huard, J. (2002). Synergistic enhancement of bone formation and healing by stem cell-expressed VEGF and bone morphogenetic protein-4. *J Clin Invest*. **110**(6): 751-759.

Perets, A., Baruch, Y., Weisbuch, F., Shoshany, G., Neufeld, G. and Cohen, S. (2003). Enhancing the vascularization of three-dimensional porous alginate scaffolds by incorporating controlled release basic fibroblast growth factor microspheres. *J Biomed Mater Res A*. **65**(4): 489-497.

Perka, C., Spitzer, R.S., Lindenhayn, K., Sittinger, M. and Schultz, O. (2000). Matrix-mixed culture: new methodology for chondrocyte culture and preparation of cartilage transplants. *J Biomed Mater Res*. **49**(3): 305-311.

Perry, R.H., Green, D.W. and Maloney, J.O. (1997). *Perry's Chemical Engineers' Handbook*. 7th ed., McGraw-Hill, Sydney.

Perumal, V. and Roberts, C.S. (2007). (ii) Factors contributing to non-union of fractures. *Curr Orthopaed*. **21**(4): 258-261.

Peter, B., Gauthier, O., Laib, S., Bujoli, B., Guicheux, J., Janvier, P., van Lenthe, G.H., Muller, R., Zambelli, P.Y., Bouler, J.M. and Pioletti, D.P. (2006). Local delivery of bisphosphonate from coated orthopedic implants increases implants mechanical stability in osteoporotic rats. *J Biomed Mater Res A*. **76**(1): 133-143.

Peters, K., Ornitz, D., Werner, S. and Williams, L. (1993). Unique expression pattern of the FGF receptor 3 gene during mouse organogenesis. *Dev Biol*. **155**(2): 423-430.

Peters, K.G., Werner, S., Chen, G. and Williams, L.T. (1992). Two FGF receptor genes are differentially expressed in epithelial and mesenchymal tissues during limb formation and organogenesis in the mouse. *Development*. **114**(1): 233-243.

Petit-Zeman, S. (2001). Regenerative medicine. *Nat Biotechnol*. **19**(3): 201-206.

Petrie, A. and Sabin, C. (2005). *Medical statistics at a glance*. 2nd ed., Blackwell, Malden, MA.

Pezron, I., Djabourov, M. and Leblond, J. (1991). Conformation of gelatin chains in aqueous solutions: 1. A light and small-angle neutron scattering study. *Polymer*. **32**(17): 3201-3210.

Phieffer, L.S. and Goulet, J.A. (2006). Delayed unions of the tibia. *J Bone Joint Surg Am*. **88**(1): 205-216.

Philipson, B. (1965). Composition of Cement Lines in Bone. *J Histochem Cytochem*. **13**: 270-281.

Phillips, A.M. (2005). Overview of the fracture healing cascade. *Injury*. **36**(3, Supplement 1): S5-S7.

Phillips, F.M., Turner, A.S., Seim, H.B., 3rd, MacLeay, J., Toth, C.A., Pierce, A.R. and Wheeler, D.L. (2006a). In vivo BMP-7 (OP-1) enhancement of osteoporotic vertebral bodies in an ovine model. *Spine J*. **6**(5): 500-506.

Phillips, G.O., Wedlock, D.J. and Williams, P.A. (1990). *Gums and stabilisers for the food industry 5 (Gums and Stabilisers for the Food Industry)*ed., Oxford University Press

Phillips, J.E., Hutmacher, D.W., Guldberg, R.E. and Garcia, A.J. (2006b). Mineralization capacity of Runx2/Cbfa1-genetically engineered fibroblasts is scaffold dependent. *Biomaterials*. **27**(32): 5535-5545.

Piez, K.A. (1984). Molecular and aggregate structures of collagens. In: *Extracellular Matrix Biochemistry* (K. A. Piez and A. H. Reddi, eds.), Elsevier, New York, pp. 1-39.

Pisani, D.F., Cabane, C., Derijard, B. and Dechesne, C.A. (2004). The topoisomerase 1-interacting protein BTBD1 is essential for muscle cell differentiation. *Cell Death Differ*. **11**(11): 1157-1165.

Pitt, C.G., Andrady, A.L., Bao, Y.T. and Samuel, N.K.P. (1987). Estimation of rate of diffusion in polymers. In: *Controlled-release technology : pharmaceutical applications* (P. I. Lee and W. R. Good, eds.), American Chemical Society, Washington, DC.

Pitt, C.G., Chasalow, F.I., Hibionada, Y.M., Klimas, D.M. and Schindler, A. (1981). Aliphatic polyesters 1. The degradation of poly(ε-caprolactone) *in vivo*. *J Appl Polym Sci*. **26**: 3779-3787.

Pitt, C.G., Hendren, R.W., Schindler, A. and Woodward, S.C. (1984). The enzymatic surface erosion of aliphatic polyesters. *J Control Release*. **1**(1): 3-14.

Pittenger, M.F., Flake, A.M. and Deans, R.J. (2002). Stem Cell Culture: Mesenchymal Stem Cells from Bone Marrow. In: *Methods of Tissue Engineering* (A. Atala and R. P. Lanza, eds.), Academic Press, San Diego, pp. 461-469.

Pittenger, M.F., Mackay, A.M., Beck, S.C., Jaiswal, R.K., Douglas, R., Mosca, J.D., Moorman, M.A., Simonetti, D.W., Craig, S. and Marshak, D.R. (1999). Multilineage potential of adult human mesenchymal stem cells. *Science*. **284**(5411): 143-147.

Pollack, A. (2009). F.D.A. Approves a Stem Cell Trial. *The New York Times*. (23rd January): B1.

Porter, J.R., Henson, A. and Popat, K.C. (2009). Biodegradable poly(epsilon-caprolactone) nanowires for bone tissue engineering applications. *Biomaterials*. **30**(5): 780-788.

Premaraj, S., Mundy, B.L., Morgan, D., Winnard, P.L., Mooney, M.P. and Moursi, A.M. (2006). Sustained delivery of bioactive cytokine using a dense collagen gel vehicle: Collagen gel delivery of bioactive cytokine. *Arch Oral Biol*. **51**(4): 325-333.

Prisell, P.T., Edwall, D., Lindblad, J.B., Levinovitz, A. and Norstedt, G. (1993). Expression of insulin-like growth factors during bone induction in rat. *Calcif Tissue Int*. **53**(3): 201-205.

Prockop, D.J. (1997). Marrow stromal cells as stem cells for nonhematopoietic tissues. *Science*. **276**(5309): 71-74.

Quaglia, F. (2008). Bioinspired tissue engineering: The great promise of protein delivery technologies. *Int J Pharm*. **364**(2): 281-297.

Radomsky, M.L., Aufdemorte, T.B., Swain, L.D., Fox, W.C., Spiro, R.C. and Poser, J.W. (1999). Novel formulation of fibroblast growth factor-2 in a hyaluronan gel accelerates fracture healing in nonhuman primates. *J Orthop Res*. **17**(4): 607-614.

Radomsky, M.L., Thompson, A.Y., Spiro, R.C. and Poser, J.W. (1998). Potential role of fibroblast growth factor in enhancement of fracture healing. *Clin Orthop Relat Res*. (355 Suppl): S283-293.

Rago, R., Mitchen, J. and Wilding, G. (1990). DNA fluorometric assay in 96-well tissue culture plates using Hoechst 33258 after cell lysis by freezing in distilled water. *Anal Biochem*. **191**(1): 31-34.

Rai, B., Teoh, S.H., Ho, K.H., Hutmacher, D.W., Cao, T., Chen, F. and Yacob, K. (2004). The effect of rhBMP-2 on canine osteoblasts seeded onto 3D bioactive polycaprolactone scaffolds. *Biomaterials*. **25**(24): 5499-5506.

Rai, B., Teoh, S.H., Hutmacher, D.W., Cao, T. and Ho, K.H. (2005). Novel PCL-based honeycomb scaffolds as drug delivery systems for rhBMP-2. *Biomaterials*. **26**(17): 3739-3748.

Rajan, N., Habermehl, J., Cote, M.F., Doillon, C.J. and Mantovani, D. (2006). Preparation of ready-to-use, storable and reconstituted type I collagen from rat tail tendon for tissue engineering applications. *Nat Protoc*. **1**(6): 2753-2758.

Rawadi, G., Vayssiere, B., Dunn, F., Baron, R. and Roman-Roman, S. (2003). BMP-2 controls alkaline phosphatase expression and osteoblast mineralization by a Wnt autocrine loop. *J Bone Miner Res*. **18**(10): 1842-1853.

Razzaque, M.S., Soegiarto, D.W., Chang, D., Long, F. and Lanske, B. (2005). Conditional deletion of Indian hedgehog from collagen type 2alpha1-expressing cells results in abnormal endochondral bone formation. *J Pathol*. **207**(4): 453-461.

Reed, A.A., Joyner, C.J., Isefuku, S., Brownlow, H.C. and Simpson, A.H. (2003). Vascularity in a new model of atrophic nonunion. *J Bone Joint Surg Br*. **85**(4): 604-610.

Reed, A.A.C., Joyner, C.J., Brownlow, H.C. and Simpson, A.H.R.W. (2002). Human atrophic fracture non-unions are not avascular. *J Orthop Res*. **20**(3): 593-599.

Reed, A.M. and Gilding, D.K. (1981). Biodegradable polymers for use in surgery -- poly(glycolic)/poly(Iactic acid) homo and copolymers: 2. In vitro degradation. *Polymer*. **22**(4): 494-498.

Rees, D.A. (1981). Polysaccharide shapes and their interactions - some recent advances. *Pure Appl Chem*. **53**: 1-14.

Rees, D.A. and Welsh, E.J. (1977). Secondary and Tertiary Structure of Polysaccharides in Solutions and Gels. *Angew Chem Int Ed Engl*. **16**(4): 214-224.

Rege, T.A. and Hagood, J.S. (2006). Thy-1 as a regulator of cell-cell and cell-matrix interactions in axon regeneration, apoptosis, adhesion, migration, cancer, and fibrosis. *Faseb J*. **20**(8): 1045-1054.

Reinholt, F.P., Hultenby, K., Oldberg, A. and Heinegard, D. (1990). Osteopontin--a possible anchor of osteoclasts to bone. *Proc Natl Acad Sci U S A*. **87**(12): 4473-4475.

Richardson, T.P., Peters, M.C., Ennett, A.B. and Mooney, D.J. (2001). Polymeric system for dual growth factor delivery. *Nat Biotechnol*. **19**(11): 1029-1034.

Ringe, J., Kaps, C., Burmester, G.R. and Sittinger, M. (2002). Stem cells for regenerative medicine: advances in the engineering of tissues and organs. *Naturwissenschaften*. **89**(8): 338-351.

Risbud, M.V., Karamuk, E., Moser, R. and Mayer, J. (2002). Hydrogel-coated textile scaffolds as three-dimensional growth support for human umbilical vein endothelial cells (HUVECs): possibilities as coculture system in liver tissue engineering. *Cell Transplant*. **11**(4): 369-377.

Ritger, P.L. and Peppas, N.A. (1987a). A simple equation for description of solute release I. Fickian and non-fickian release from non-swellable devices in the form of slabs, spheres, cylinders or discs. *J Control Release*. **5**(1): 23-36.

Ritger, P.L. and Peppas, N.A. (1987b). A simple equation for description of solute release II. Fickian and anomalous release from swellable devices. *J Control Release*. **5**(1): 37-42.

Robey, P.G., Young, M.F., Flanders, K.C., Roche, N.S., Kondaiah, P., Reddi, A.H., Termine, J.D., Sporn, M.B. and Roberts, A.B. (1987). Osteoblasts synthesize and respond to transforming growth factor-type beta (TGF-beta) in vitro. *J Cell Biol*. **105**(1): 457-463.

Robinson, B.P., Hollinger, J.O., Szachowicz, E.H. and Brekke, J. (1995). Calvarial bone repair with porous D,L-polylactide. *Otolaryngol Head Neck Surg*. **112**(6): 707-713.

Robinson, J., Sieff, C., Delia, D., Edwards, P.A. and Greaves, M. (1981). Expression of cell-surface HLA-DR, HLA-ABC and glycophorin during erythroid differentiation. *Nature*. **289**(5793): 68-71.

Roden, M.M., Lee, K.H., Panelli, M.C. and Marincola, F.M. (1999). A novel cytolysis assay using fluorescent labeling and quantitative fluorescent scanning technology. *J Immunol Methods*. **226**(1-2): 29-41.

Rodriguez, L.V., Alfonso, Z., Zhang, R., Leung, J., Wu, B. and Ignarro, L.J. (2006). Clonogenic multipotent stem cells in human adipose tissue differentiate into functional smooth muscle cells. *Proc Natl Acad Sci U S A*. **103**(32): 12167-12172.

Roelen, B.A. and Dijke, P. (2003). Controlling mesenchymal stem cell differentiation by TGFβ family members. *J Orthop Sci*. **8**(5): 740-748.

Rosenberg, L. (1971). Chemical basis for the histological use of safranin O in the study of articular cartilage. *J Bone Joint Surg Am.* **53**(1): 69-82.

Ross-Murphy, S.B. (1992). Structure and rheology of gelatin gels: recent progress. *Polymer*. **33**(12): 2622-2627.

Ruhe, P.Q., Hedberg, E.L., Padron, N.T., Spauwen, P.H., Jansen, J.A. and Mikos, A.G. (2003). rhBMP-2 release from injectable poly(DL-lactic-co-glycolic acid)/calcium-phosphate cement composites. *J Bone Joint Surg Am.* **85-A Suppl 3**: 75-81.

Ryoo, H.-M., Lee, M.-H. and Kim, Y.-J. (2006). Critical molecular switches involved in BMP-2-induced osteogenic differentiation of mesenchymal cells. *Gene*. **366**(1): 51-57.

Sacchetti, B., Funari, A., Michienzi, S., Di Cesare, S., Piersanti, S., Saggio, I., Tagliafico, E., Ferrari, S., Robey, P.G., Riminucci, M. and Bianco, P. (2007). Self-renewing osteoprogenitors in bone marrow sinusoids can organize a hematopoietic microenvironment. *Cell*. **131**(2): 324-336.

Sakaguchi, Y., Sekiya, I., Yagishita, K., Ichinose, S., Shinomiya, K. and Muneta, T. (2004). Suspended cells from trabecular bone by collagenase digestion become virtually identical to mesenchymal stem cells obtained from marrow aspirates. *Blood*. **104**(9): 2728-2735.

Sakou, T. (1998). Bone morphogenetic proteins: from basic studies to clinical approaches. *Bone*. **22**(6): 591-603.

Salasznyk, R.M., Williams, W.A., Boskey, A., Batorsky, A. and Plopper, G.E. (2004). Adhesion to Vitronectin and Collagen I Promotes Osteogenic Differentiation of Human Mesenchymal Stem Cells. *J Biomed Biotechnol*. **2004**(1): 24-34.

Salazar, K.D., Lankford, S.M. and Brody, A.R. (2009). Mesenchymal stem cells produce Wnt isoforms and TGF-beta1 that mediate proliferation and procollagen expression by lung fibroblasts. *Am J Physiol Lung Cell Mol Physiol*. **297**(5): L1002-1011.

Salgado, A.J., Oliveira, J.T., Pedro, A.J. and Reis, R.L. (2006). Adult stem cells in bone and cartilage tissue engineering. *Curr Stem Cell Res Ther.* **1**(3): 345-364.

Salic, A., Lee, E., Mayer, L. and Kirschner, M.W. (2000). Control of beta-catenin stability: reconstitution of the cytoplasmic steps of the wnt pathway in Xenopus egg extracts. *Mol Cell*. **5**(3): 523-532.

Sanchez-Ramos, J., Song, S., Cardozo-Pelaez, F., Hazzi, C., Stedeford, T., Willing, A., Freeman, T.B., Saporta, S., Janssen, W., Patel, N., Cooper, D.R. and Sanberg,

P.R. (2000). Adult bone marrow stromal cells differentiate into neural cells in vitro. *Exp Neurol*. **164**(2): 247-256.

Sandeman, S.R., Allen, M.C., Liu, C., Faragher, R.G. and Lloyd, A.W. (2000). Human keratocyte migration into collagen gels declines with in vitro ageing. *Mech Ageing Dev*. **119**(3): 149-157.

Sandler, S.I. (1999). *Chemical and engineering thermodynamics*. 3rd ed., Wiley, New York.

Santiago, J.A., Pogemiller, R. and Ogle, B.M. (2009). Heterogeneous differentiation of human mesenchymal stem cells in response to extended culture in extracellular matrices. *Tissue Eng Part A*. **15**(12): 3911-3922.

Santoni, B.G., Pluhar, G.E., Motta, T. and Wheeler, D.L. (2007). Hollow calcium phosphate microcarriers for bone regeneration: in vitro osteoproduction and ex vivo mechanical assessment. *Biomed Mater Eng*. **17**(5): 277-289.

Sarugaser, R., Lickorish, D., Baksh, D., Hosseini, M.M. and Davies, J.E. (2005). Human umbilical cord perivascular (HUCPV) cells: a source of mesenchymal progenitors. *Stem Cells*. **23**(2): 220-229.

Satokata, I., Ma, L., Ohshima, H., Bei, M., Woo, I., Nishizawa, K., Maeda, T., Takano, Y., Uchiyama, M., Heaney, S., Peters, H., Tang, Z., Maxson, R. and Maas, R. (2000). Msx2 deficiency in mice causes pleiotropic defects in bone growth and ectodermal organ formation. *Nat Genet*. **24**(4): 391-395.

Schildhauer, T.A., Bauer, T.W., Josten, C. and Muhr, G. (2000). Open reduction and augmentation of internal fixation with an injectable skeletal cement for the treatment of complex calcaneal fractures. *J Orthop Trauma*. **14**(5): 309-317.

Schlaepfer, D.D., Hanks, S.K., Hunter, T. and van der Geer, P. (1994). Integrin-mediated signal transduction linked to Ras pathway by GRB2 binding to focal adhesion kinase. *Nature*. **372**(6508): 786-791.

Schmidt, C., Pommerenke, H., Durr, F., Nebe, B. and Rychly, J. (1998). Mechanical stressing of integrin receptors induces enhanced tyrosine phosphorylation of cytoskeletally anchored proteins. *J Biol Chem*. **273**(9): 5081-5085.

Schmoekel, H.G., Weber, F.E., Schense, J.C., Gratz, K.W., Schawalder, P. and Hubbell, J.A. (2005). Bone repair with a form of BMP-2 engineered for incorporation into fibrin cell ingrowth matrices. *Biotechnol Bioeng*. **89**(3): 253-262.

Schuh, J., Fanslow, W., Gombotz, W.R. and Wee, S. (1996). Intranasal localization and antibody response to polycation-coated ova-encapsulated alginate microbeads. *Vet Pathol*. **33**(5): 581.

Schumann, R.R., Rietschel, E.T. and Loppnow, H. (1994). The role of CD14 and lipopolysaccharide-binding protein (LBP) in the activation of different cell types by endotoxin. *Med Microbiol Immunol*. **183**(6): 279-297.

Seal, B.L., Otero, T.C. and Panitch, A. (2001). Polymeric biomaterials for tissue and organ regeneration. *Mat Sci Eng R*. **34**: 147-230.

Seitz, H., Rieder, W., Irsen, S., Leukers, B. and Tille, C. (2005). Three-dimensional printing of porous ceramic scaffolds for bone tissue engineering. *J Biomed Mater Res B Appl Biomater*. **74**(2): 782-788.

Semenov, M., Tamai, K. and He, X. (2005). SOST is a ligand for LRP5/LRP6 and a Wnt signaling inhibitor. *J Biol Chem*. **280**(29): 26770-26775.

Sen, M.K. and Miclau, T. (2007). Autologous iliac crest bone graft: should it still be the gold standard for treating nonunions? *Injury*. **38** (Suppl 1): S75-80.

Sengers, B.G., Dawson, J.I. and Oreffo, R.O. (2010). Characterisation of human bone marrow stromal cell heterogeneity for skeletal regeneration strategies using a two-stage colony assay and computational modelling. *Bone*. **46**(2): 496-503.

Serrano, M.C., Pagani, R., Vallet-Regi, M., Pena, J., Ramila, A., Izquierdo, I. and Portoles, M.T. (2004). In vitro biocompatibility assessment of poly(epsilon-caprolactone) films using L929 mouse fibroblasts. *Biomaterials*. **25**(25): 5603-5611.

Sgouras, D. and Duncan, R. (1990). Methods for evaluation of biocompatibility of soluble synthetic polymers which have potential for biomedial use: 1-use of the tetrazolium-based colorimetric assay (MTT) as a preliminary screen for evaluation of cytotoxicity. *J. Mater. Sci. Mater. Med.* **1**: 61-68.

Shamblott, M.J., Axelman, J., Wang, S., Bugg, E.M., Littlefield, J.W., Donovan, P.J., Blumenthal, P.D., Huggins, G.R. and Gearhart, J.D. (1998). Derivation of pluripotent stem cells from cultured human primordial germ cells. *Proc Natl Acad Sci U S A*. **95**(23): 13726-13731.

Shang, Y.C., Zhang, C., Wang, S.H., Xiong, F., Zhao, C.P., Peng, F.N., Feng, S.W., Yu, M.J., Li, M.S. and Zhang, Y.N. (2007). Activated beta-catenin induces myogenesis and inhibits adipogenesis in BM-derived mesenchymal stromal cells. *Cytotherapy*. **9**(7): 667-681.

Shapiro, F., Holtrop, M.E. and Glimcher, M.J. (1977). Organization and cellular biology of the perichondrial ossification groove of ranvier: a morphological study in rabbits. *J Bone Joint Surg Am*. **59**(6): 703-723.

Shen, Z.J., Nakamoto, T., Tsuji, K., Nifuji, A., Miyazono, K., Komori, T., Hirai, H. and Noda, M. (2002). Negative regulation of bone morphogenetic protein/Smad signaling by Cas-interacting zinc finger protein in osteoblasts. *J Biol Chem*. **277**(33): 29840-29846.

Shin, M., Abukawa, H., Troulis, M.J. and Vacanti, J.P. (2008). Development of a biodegradable scaffold with interconnected pores by heat fusion and its application to bone tissue engineering. *J Biomed Mater Res A*. **84**(3): 702-709.

Shive, M.S. and Anderson, J.M. (1997). Biodegradation and biocompatibility of PLA and PLGA microspheres. *Adv Drug Deliv Rev*. **28**(1): 5-24.

Shu, X.Z. and Zhu, K.J. (2002). Controlled drug release properties of ionically cross-linked chitosan beads: the influence of anion structure. *Int J Pharm*. **233**(1-2): 217-225.

Sieuwerts, S., de Bok, F.A., Mols, E., de vos, W.M. and Vlieg, J.E. (2008). A simple and fast method for determining colony forming units. *Lett Appl Microbiol*. **47**(4): 275-278.

Sikavitsas, V.I., Temenoff, J.S. and Mikos, A.G. (2001). Biomaterials and bone mechanotransduction. *Biomaterials*. **22**(19): 2581-2593.

Silva, C.M., Ribeiro, A.J., Figueiredo, I.V., Goncalves, A.R. and Veiga, F. (2006). Alginate microspheres prepared by internal gelation: Development and effect on insulin stability. *International Journal of Pharmaceutics*. **311**(1-2): 1-10.

Silver, F.H., Freeman, J.W. and Seehra, G.P. (2003). Collagen self-assembly and the development of tendon mechanical properties. *J Biomech*. **36**(10): 1529-1553.

Simmons, C.A., Alsberg, E., Hsiong, S., Kim, W.J. and Mooney, D.J. (2004). Dual growth factor delivery and controlled scaffold degradation enhance in vivo bone formation by transplanted bone marrow stromal cells. *Bone*. **35**(2): 562-569.

Simmons, P.J. and Torok-Storb, B. (1991). Identification of stromal cell precursors in human bone marrow by a novel monoclonal antibody, STRO-1. *Blood*. **78**(1): 55-62.

Simon, L.D., Stella, V.J., Charman, W.N. and Charman, S.A. (1999). Mechanisms controlling diffusion and release of model proteins through and from partially esterified hyaluronic acid membranes. *J Control Release*. **61**(3): 267-279.

Simpson, A.H., Mills, L. and Noble, B. (2006). The role of growth factors and related agents in accelerating fracture healing. *J Bone Joint Surg Br*. **88**(6): 701-705.

Singer, V.L., Jones, L.J., Yue, S.T. and Haugland, R.P. (1997). Characterization of PicoGreen reagent and development of a fluorescence-based solution assay for double-stranded DNA quantitation. *Anal Biochem*. **249**(2): 228-238.

Smidsrød, O. (1973). The relative extension of alginates having different chemical composition. *Carbohyd Res*. **27**: 107-118.

Smith, A.G. (2001). Embryo-derived stem cells: of mice and men. *Annu Rev Cell Dev Biol*. **17**: 435-462.

Smith, E. and Frenkel, B. (2005). Glucocorticoids inhibit the transcriptional activity of LEF/TCF in differentiating osteoblasts in a glycogen synthase kinase-3beta-dependent and -independent manner. *J Biol Chem*. **280**(3): 2388-2394.

Sodian, R., Lemke, T., Fritsche, C., Hoerstrup, S.P., Fu, P., Potapov, E.V., Hausmann, H. and Hetzer, R. (2002). Tissue-engineering bioreactors: a new combined cell-seeding and perfusion system for vascular tissue engineering. *Tissue Eng*. **8**(5): 863-870.

Sohier, J., Vlugt, T.J., Cabrol, N., Van Blitterswijk, C., de Groot, K. and Bezemer, J.M. (2006). Dual release of proteins from porous polymeric scaffolds. *J Control Release*. **111**(1-2): 95-106.

Sokolsky-Papkov, M., Agashi, K., Olaye, A., Shakesheff, K. and Domb, A.J. (2007). Polymer carriers for drug delivery in tissue engineering. *Adv Drug Deliver Rev*. **59**(4-5): 187-206.

Solovjov, D.A., Pluskota, E. and Plow, E.F. (2005). Distinct roles for the alpha and beta subunits in the functions of integrin alphaMbeta2. *J Biol Chem*. **280**(2): 1336-1345.

Sommerfeldt, D.W. and Rubin, C.T. (2001). Biology of bone and how it orchestrates the form and function of the skeleton. *Eur Spine J*. **10 Suppl 2**: S86-95.

Song, B., Estrada, K.D. and Lyons, K.M. (2009). Smad signaling in skeletal development and regeneration. *Cytokine Growth Factor Rev*. **20**(5-6): 379-388.

Song, L. and Tuan, R.S. (2004). Transdifferentiation potential of human mesenchymal stem cells derived from bone marrow. *Faseb J*. **18**(9): 980-982.

Sottile, V., Halleux, C., Bassilana, F., Keller, H. and Seuwen, K. (2002). Stem cell characteristics of human trabecular bone-derived cells. *Bone*. **30**(5): 699-704.

Sottile, V., Thomson, A. and McWhir, J. (2003). In vitro osteogenic differentiation of human ES cells. *Cloning Stem Cells*. **5**(2): 149-155.

Spickett, G.P., Brandon, M.R., Mason, D.W., Williams, A.F. and Woollett, G.R. (1983). MRC OX-22, a monoclonal antibody that labels a new subset of T lymphocytes and reacts with the high molecular weight form of the leukocyte-common antigen. *J Exp Med*. **158**(3): 795-810.

Springer, I.N.G., Acil, Y., Kuchenbecker, S., Bolte, H., Warnke, P.H., Abboud, M., Wiltfang, J. and Terheyden, H. (2005). Bone graft versus BMP-7 in a critical size defect--Cranioplasty in a growing infant model. *Bone*. **37**(4): 563-569.

Srouji, S., Blumenfeld, I., Rachmiel, A. and Livne, E. (2004). Bone defect repair in rat tibia by TGF-beta1 and IGF-1 released from hydrogel scaffold. *Cell Tissue Bank*. **5**(4): 223-230.

St-Jacques, B., Hammerschmidt, M. and McMahon, A.P. (1999). Indian hedgehog signaling regulates proliferation and differentiation of chondrocytes and is essential for bone formation. *Genes Dev*. **13**(16): 2072-2086.

Stein, G.S., Lian, J.B., van Wijnen, A.J., Stein, J.L., Montecino, M., Javed, A., Zaidi, S.K., Young, D.W., Choi, J.Y. and Pockwinse, S.M. (2004). Runx2 control of organization, assembly and activity of the regulatory machinery for skeletal gene expression. *Oncogene*. **23**(24): 4315-4329.

Stenderup, K., Justesen, J., Eriksen, E.F., Rattan, S.I. and Kassem, M. (2001). Number and proliferative capacity of osteogenic stem cells are maintained during aging and in patients with osteoporosis. *J Bone Miner Res*. **16**(6): 1120-1129.

Stewart, K., Walsh, S., Screen, J., Jefferiss, C.M., Chainey, J., Jordan, G.R. and Beresford, J.N. (1999). Further characterization of cells expressing STRO-1 in cultures of adult human bone marrow stromal cells. *J Bone Miner Res*. **14**(8): 1345-1356.

Stoch, S.A. and Wagner, J.A. (2008). Cathepsin K inhibitors: a novel target for osteoporosis therapy. *Clin Pharmacol Ther*. **83**(1): 172-176.

Stock, U.A. and Vacanti, J.P. (2001). Tissue engineering: current state and prospects. *Annu Rev Med*. **52**: 443-451.

Stone, D.M., Hynes, M., Armanini, M., Swanson, T.A., Gu, Q., Johnson, R.L., Scott, M.P., Pennica, D., Goddard, A., Phillips, H., Noll, M., Hooper, J.E., de Sauvage, F. and Rosenthal, A. (1996). The tumour-suppressor gene patched encodes a candidate receptor for Sonic hedgehog. *Nature*. **384**(6605): 129-134.

Street, J., Winter, D., Wang, J.H., Wakai, A., McGuinness, A. and Redmond, H.P. (2000). Is human fracture hematoma inherently angiogenic? *Clin Orthop Relat Res*. (378): 224-237.

Stryer, L. (1995). *Biochemistry*. 4th ed., W.H. Freeman, New York.

Sudres, M., Norol, F., Trenado, A., Gregoire, S., Charlotte, F., Levacher, B., Lataillade, J.J., Bourin, P., Holy, X., Vernant, J.P., Klatzmann, D. and Cohen, J.L. (2006). Bone marrow mesenchymal stem cells suppress lymphocyte proliferation in vitro but fail to prevent graft-versus-host disease in mice. *J Immunol*. **176**(12): 7761-7767.

Sumner, D.R., Turner, T.M., Purchio, A.F., Gombotz, W.R., Urban, R.M. and Galante, J.O. (1995). Enhancement of bone ingrowth by transforming growth factor-beta. *J Bone Joint Surg Am*. **77**(8): 1135-1147.

Sung, H.J., Meredith, C., Johnson, C. and Galis, Z.S. (2004). The effect of scaffold degradation rate on three-dimensional cell growth and angiogenesis. *Biomaterials*. **25**(26): 5735-5742.

Suzuki, T., Fujikura, K., Higashiyama, T. and Takata, K. (1997). DNA staining for fluorescence and laser confocal microscopy. *J Histochem Cytochem*. **45**(1): 49-53.

Szivek, J.A., Margolis, D.S., Garrison, B.K., Nelson, E., Vaidyanathan, R.K. and DeYoung, D.W. (2005). TGF-beta1-enhanced TCP-coated sensate scaffolds can detect bone bonding. *J Biomed Mater Res B Appl Biomater*. **73**(1): 43-53.

Tabata, Y., Nagano, A. and Ikada, Y. (1999). Biodegradation of hydrogel carrier incorporating fibroblast growth factor. *Tissue Eng*. **5**(2): 127-138.

Tadic, T., Dodig, M., Erceg, I., Marijanovic, I., Mina, M., Kalajzic, Z., Velonis, D., Kronenberg, M.S., Kosher, R.A., Ferrari, D. and Lichtler, A.C. (2002). Overexpression of Dlx5 in chicken calvarial cells accelerates osteoblastic differentiation. *J Bone Miner Res*. **17**(6): 1008-1014.

Taipale, J., Cooper, M.K., Maiti, T. and Beachy, P.A. (2002). Patched acts catalytically to suppress the activity of Smoothened. *Nature*. **418**(6900): 892-897.

Takagishi, Y., Kawakami, T., Hara, Y., Shinkai, M., Takezawa, T. and Nagamune, T. (2006). Bone-like tissue formation by three-dimensional culture of MG63 osteosarcoma cells in gelatin hydrogels using calcium-enriched medium. *Tissue Eng*. **12**(4): 927-937.

Takahashi, K. and Yamanaka, S. (2006). Induction of pluripotent stem cells from mouse embryonic and adult fibroblast cultures by defined factors. *Cell*. **126**(4): 663-676.

Tamai, K., Zeng, X., Liu, C., Zhang, X., Harada, Y., Chang, Z. and He, X. (2004). A mechanism for Wnt coreceptor activation. *Mol Cell*. **13**(1): 149-156.

Tang, Q.O., Shakib, K., Heliotis, M., Tsiridis, E., Mantalaris, A., Ripamonti, U. and Tsiridis, E. (2009). TGF-beta3: A potential biological therapy for enhancing chondrogenesis. *Expert Opin Biol Ther*. **9**(6): 689-701.

Tang, Z.G., Callaghan, J.T. and Hunt, J.A. (2005). The physical properties and response of osteoblasts to solution cast films of PLGA doped polycaprolactone. *Biomaterials*. **26**(33): 6618-6624.

Tanzer, M., Karabasz, D., Krygier, J.J., Cohen, R. and Bobyn, J.D. (2005). The Otto Aufranc Award: bone augmentation around and within porous implants by local bisphosphonate elution. *Clin Orthop Relat Res*. **441**: 30-39.

Tedder, T.F. and Isaacs, C.M. (1989). Isolation of cDNAs encoding the CD19 antigen of human and mouse B lymphocytes. A new member of the immunoglobulin superfamily. *J Immunol*. **143**(2): 712-717.

Teo, W.E. and Ramakrishna, S. (2006). A review on electrospinning design and nanofibre assemblies. *Nanotechnology*. **17**(14): R89-R106.

Thaller, S.R., Dart, A. and Tesluk, H. (1993). The effects of insulin-like growth factor-1 on critical-size calvarial defects in Sprague-Dawley rats. *Ann Plast Surg*. **31**(5): 429-433.

Thomson, J.A., Itskovitz-Eldor, J., Shapiro, S.S., Waknitz, M.A., Swiergiel, J.J., Marshall, V.S. and Jones, J.M. (1998). Embryonic stem cell lines derived from human blastocysts. *Science*. **282**(5391): 1145-1147.

Thorp, B.H., Anderson, I. and Jakowlew, S.B. (1992). Transforming growth factor-beta 1, -beta 2 and -beta 3 in cartilage and bone cells during endochondral ossification in the chick. *Development*. **114**(4): 907-911.

Tiedeman, J.J., Garvin, K.L., Kile, T.A. and Connolly, J.F. (1995). The role of a composite, demineralized bone matrix and bone marrow in the treatment of osseous defects. *Orthopedics*. **18**(12): 1153-1158.

Tobias, P.S. and Ulevitch, R.J. (1993). Lipopolysaccharide binding protein and CD14 in LPS dependent macrophage activation. *Immunobiology*. **187**(3-5): 227-232.

Toffaletti, J. and Kirvan, K. (1980). Spectrophotometric micro method for measurement of dialyzable calcium by use of cresolphthalein complexone and continuous-flow analysis. *Clin Chem*. **26**(11): 1562-1565.

Tokuda, H., Kozawa, O. and Uematsu, T. (2000). Basic fibroblast growth factor stimulates vascular endothelial growth factor release in osteoblasts: divergent regulation by p42/p44 mitogen-activated protein kinase and p38 mitogen-activated protein kinase. *J Bone Miner Res*. **15**(12): 2371-2379.

Tolwinski, N.S., Wehrli, M., Rives, A., Erdeniz, N., DiNardo, S. and Wieschaus, E. (2003). Wg/Wnt signal can be transmitted through arrow/LRP5,6 and Axin independently of Zw3/Gsk3beta activity. *Dev Cell*. **4**(3): 407-418.

Tolwinski, N.S. and Wieschaus, E. (2004). A nuclear function for armadillo/beta-catenin. *PLoS Biol*. **2**(4): E95.

Toma, C., Pittenger, M.F., Cahill, K.S., Byrne, B.J. and Kessler, P.D. (2002). Human mesenchymal stem cells differentiate to a cardiomyocyte phenotype in the adult murine heart. *Circulation*. **105**(1): 93-98.

Tou, L., Quibria, N. and Alexander, J.M. (2003). Transcriptional regulation of the human Runx2/Cbfa1 gene promoter by bone morphogenetic protein-7. *Mol Cell Endocrinol*. **205**(1-2): 121-129.

Tremoleda, J.L., Forsyth, N.R., Khan, N.S., Wojtacha, D., Christodoulou, I., Tye, B.J., Racey, S.N., Collishaw, S., Sottile, V., Thomson, A.J., Simpson, A.H.W.R., Noble, B.S. and Mcwhir, J. (2008). Bone tissue formation from human embryonic stem cells in vivo. *Cloning Stem Cells*. **10**(1): 119-131.

Tsiridis, E., Ali, Z., Bhalla, A., Heliotis, M., Gurav, N., Deb, S. and DiSilvio, L. (2007). In vitro and in vivo optimization of impaction allografting by demineralization and addition of rh-OP-1. *J Orthop Res*. **25**(11): 1425-1437.

Tsiridis, E., Bhalla, A., Ali, Z., Gurav, N., Heliotis, M., Deb, S. and DiSilvio, L. (2006). Enhancing the osteoinductive properties of hydroxyapatite by the addition of human mesenchymal stem cells, and recombinant human osteogenic protein-1 (BMP-7) in vitro. *Injury*. **37**(3, Supplement 1): S25-S32.

Tu, J., Bolla, S., Barr, J., Miedema, J., Li, X. and Jasti, B. (2005). Alginate microparticles prepared by spray-coagulation method: Preparation, drug loading and release characterization. *Int J Pharm*. **303**(1-2): 171-181.

Tuli, R., Tuli, S., Nandi, S., Wang, M.L., Alexander, P.G., Haleem-Smith, H., Hozack, W.J., Manner, P.A., Danielson, K.G. and Tuan, R.S. (2003). Characterization of multipotential mesenchymal progenitor cells derived from human trabecular bone. *Stem Cells*. **21**(6): 681-693.

Turner, C.H. (1992). Functional determinants of bone structure: Beyond Wolff's law of bone transformation. *Bone*. **13**(6): 403-409.

Tylzanowski, P., Verschueren, K., Huylebroeck, D. and Luyten, F.P. (2001). Smad-interacting protein 1 is a repressor of liver/bone/kidney alkaline phosphatase transcription in bone morphogenetic protein-induced osteogenic differentiation of C2C12 cells. *J Biol Chem*. **276**(43): 40001-40007.

Udagawa, N., Takahashi, N., Akatsu, T., Tanaka, H., Sasaki, T., Nishihara, T., Koga, T., Martin, T.J. and Suda, T. (1990). Origin of osteoclasts: mature monocytes and macrophages are capable of differentiating into osteoclasts under a suitable microenvironment prepared by bone marrow-derived stromal cells. *Proc Natl Acad Sci U S A*. **87**(18): 7260-7264.

Ueda, H., Hong, L., Yamamoto, M., Shigeno, K., Inoue, M., Toba, T., Yoshitani, M., Nakamura, T., Tabata, Y. and Shimizu, Y. (2002). Use of collagen sponge incorporating transforming growth factor-beta1 to promote bone repair in skull defects in rabbits. *Biomaterials*. **23**(4): 1003-1010.

Ueng, S.W., Wei, F.C. and Shih, C.H. (1999). Management of femoral diaphyseal infected nonunion with antibiotic beads local therapy, external skeletal fixation, and staged bone grafting. *J Trauma*. **46**(1): 97-103.

Ulsamer, A., Ortuno, M.J., Ruiz, S., Susperregui, A.R., Osses, N., Rosa, J.L. and Ventura, F. (2008). BMP-2 induces Osterix expression through up-regulation of Dlx5 and its phosphorylation by p38. *J Biol Chem*. **283**(7): 3816-3826.

Unger, F., Wittmar, M. and Kissel, T. (2007). Branched polyesters based on poly[vinyl-3-(dialkylamino)alkylcarbamate-co-vinyl acetate-co-vinyl alcohol]-graft-poly(d,l-lactide-co-glycolide): effects of polymer structure on cytotoxicity. *Biomaterials*. **28**(9): 1610-1619.

Unger, R.E., Huang, Q., Peters, K., Protzer, D., Paul, D. and Kirkpatrick, C.J. (2005). Growth of human cells on polyethersulfone (PES) hollow fiber membranes. *Biomaterials*. **26**(14): 1877-1884.

Urist, M.R. (1965). Bone: formation by autoinduction. *Science*. **150**(698): 893-899.

USFDA. (1988). Guidance document for the preparation of investigational device exemptions and pre-market approval applications for bone growth stimulator devices. In. United States Food and Drug Administration, Rockville, MD

USFDA. (2001). H010002 OP-1™ Implant. In. United States Food and Drug Administration, Rockville, MD

USFDA. (2003). H020008 OP-1™ Putty. In. United States Food and Drug Administration, Rockville, MD

USFDA. (2004). P000054 INFUSE® Bone Graft. In. United States Food and Drug Administration, Rockville, MD

USFDA. (2006). K053538 Phytacare® Alginate Hydrogel. In. United States Food and Drug Administration, Rockville, MD

USFDA. (2008). K080879 Bioretec ActivaPin™. In. United States Food and Drug Administration, Rockville, MD

USFDA. (2009). K090026 ChitoGause™. In. United States Food and Drug Administration, Rockville, MD

Vaananen, H.K. and Laitala-Leinonen, T. (2008). Osteoclast lineage and function. *Arch Biochem Biophys*. **473**(2): 132-138.

Vadillo, P.T. (2009). *Scaffolds for bone repair using computer aided design and manufacture*. PhD Thesis In: Clinical and Surgical Sciences. University of Edinburgh, Edinburgh.

Vail, N.K., Beaman, J.J., Bourell, D.L., Marcus, H.L. and Barlow, J.W. (1994). Development of a poly(methyl methacrylate-co-n-butyl methacrylate) copolymer binder system. *J Appl Polym Sci*. **52**(6): 789-812.

van Beek, E., Lowik, C., van der Pluijm, G. and Papapoulos, S. (1999). The role of geranylgeranylation in bone resorption and its suppression by bisphosphonates in fetal bone explants in vitro: A clue to the mechanism of action of nitrogen-containing bisphosphonates. *J Bone Miner Res*. **14**(5): 722-729.

van Griensven, M., Diederichs, S., Roeker, S., Boehm, S., Peterbauer, A., Wolbank, S., Riechers, D., Stahl, F. and Kasper, C. (2008). Mechanical Strain Using 2D and 3D Bioreactors Induces Osteogenesis: Implications for Bone Tissue Engineering. *Adv Biochem Eng Biotechnol*.

van Luyn, M.J., van Wachem, P.B., Olde Damink, L.H., Dijkstra, P.J., Feijen, J. and Nieuwenhuis, P. (1992). Secondary cytotoxicity of cross-linked dermal sheep collagens during repeated exposure to human fibroblasts. *Biomaterials*. **13**(14): 1017-1024.

Vance, A. (2010). 3-D Printing Spurs a Manufacturing Revolution. *The New York Times*. (13th September): A1.

VandeVord, P.J., Matthew, H.W., DeSilva, S.P., Mayton, L., Wu, B. and Wooley, P.H. (2002). Evaluation of the biocompatibility of a chitosan scaffold in mice. *J Biomed Mater Res*. **59**(3): 585-590.

Vaquette, C., Frochot, C., Rahouadj, R. and Wang, X. (2008). An innovative method to obtain porous PLLA scaffolds with highly spherical and interconnected pores. *J Biomed Mater Res B Appl Biomater*. **86**(1): 9-17.

Vehof, J.W., Fisher, J.P., Dean, D., van der Waerden, J.P., Spauwen, P.H., Mikos, A.G. and Jansen, J.A. (2002). Bone formation in transforming growth factor beta-1-coated porous poly(propylene fumarate) scaffolds. *J Biomed Mater Res*. **60**(2): 241-251.

Velazco, A., Whitesides, T.E., Jr. and Fleming, L.L. (1983). Open fractures of the tibia treated with the Lottes nail. *J Bone Joint Surg Am*. **65**(7): 879-885.

Verborgt, O., Gibson, G.J. and Schaffler, M.B. (2000). Loss of osteocyte integrity in association with microdamage and bone remodeling after fatigue in vivo. *J Bone Miner Res*. **15**(1): 60-67.

Verhasselt, V., Buelens, C., Willems, F., De Groote, D., Haeffner-Cavaillon, N. and Goldman, M. (1997). Bacterial lipopolysaccharide stimulates the production of cytokines and the expression of costimulatory molecules by human peripheral blood dendritic cells: evidence for a soluble CD14-dependent pathway. *J Immunol*. **158**(6): 2919-2925.

Vitagliano, L., Nemethy, G., Zagari, A. and Scheraga, H.A. (1995). Structure of the type I collagen molecule based on conformational energy computations: the triple-stranded helix and the N-terminal telopeptide. *J Mol Biol*. **247**(1): 69-80.

Voultsiadou, A. (2009). *Anabolic Treatment and Bone Cell Viability*. PhD Thesis In: Clinical and Surgical Sciences. University of Edinburgh, Edinburgh.

Wada, R., Hyon, S.-H. and Ikada, Y. (1995). Kinetics of diffusion-mediated drug release enhanced by matrix degradation. *J Control Release*. **37**(1-2): 151-160.

Wang, D. and Bromme, D. (2005). Drug delivery strategies for cathepsin inhibitors in joint diseases. *Expert Opin Drug Deliv*. **2**(6): 1015-1028.

Wang, D., Li, W., Pechar, M., Kopeckova, P., Bromme, D. and Kopecek, J. (2004). Cathepsin K inhibitor-polymer conjugates: potential drugs for the treatment of osteoporosis and rheumatoid arthritis. *Int J Pharm*. **277**(1-2): 73-79.

Wang, L., Li, Y., Zuo, Y., Zhang, L., Zou, Q., Cheng, L. and Jiang, H. (2009a). Porous bioactive scaffold of aliphatic polyurethane and hydroxyapatite for tissue regeneration. *Biomed Mater*. **4**(2): 25003.

Wang, M.L., Tuli, R., Manner, P.A., Sharkey, P.F., Hall, D.J. and Tuan, R.S. (2003). Direct and indirect induction of apoptosis in human mesenchymal stem cells in response to titanium particles. *J Orthop Res*. **21**(4): 697-707.

Wang, X., Wenk, E., Zhang, X., Meinel, L., Vunjak-Novakovic, G. and Kaplan, D.L. (2009b). Growth factor gradients via microsphere delivery in biopolymer scaffolds for osteochondral tissue engineering. *J Control Release*. **134**(2): 81-90.

Wang, X.M., Terasaki, P.I., Rankin, G.W., Jr., Chia, D., Zhong, H.P. and Hardy, S. (1993). A new microcellular cytotoxicity test based on calcein AM release. *Hum Immunol*. **37**(4): 264-270.

Wang, Y., Wang, M., Abarbanell, A.M., Weil, B.R., Herrmann, J.L., Tan, J., Novotny, N.M., Coffey, A.C. and Meldrum, D.R. (2009c). MEK mediates the novel cross talk between TNFR2 and TGF-EGFR in enhancing vascular endothelial growth factor (VEGF) secretion from human mesenchymal stem cells. *Surgery*. **146**(2): 198-205.

Ward, W.G., Gautreaux, M.D., Lippert, D.C. and Boles, C. (2008). HLA sensitization and allograft bone graft incorporation. *Clin Orthop Relat Res*. **466**(8): 1837-1848.

Watanabe, J., Eriguchi, T. and Ishihara, K. (2002). Cell adhesion and morphology in porous scaffold based on enantiomeric poly(lactic acid) graft-type phospholipid polymers. *Biomacromolecules*. **3**(6): 1375-1383.

Waugh, A., Grant, A., Chambers, G., Ross, J.S. and Wilson, K.J.W. (2006). *Ross and Wilson anatomy and physiology in health and illness*. 10th ed., Churchill Livingstone, Edinburgh, UK.

Weadock, K.S., Wolff, D. and Silver, F.H. (1987). Diffusivity of 125I-labelled macromolecules through collagen: mechanism of diffusion and effect of adsorption. *Biomaterials*. **8**(2): 105-112.

Weber, B. and Cech, O. (1976). *Pseudarthrosis, Pathology, Biomechanics, Therapy, Results*ed., Hans Huber, Bern.

Wee, S. and Gombotz, W.R. (1998). Protein release from alginate matrices. *Adv Drug Deliv Rev*. **31**(3): 267-285.

Wehrli, M., Dougan, S.T., Caldwell, K., O'Keefe, L., Schwartz, S., Vaizel-Ohayon, D., Schejter, E., Tomlinson, A. and DiNardo, S. (2000). arrow encodes an LDL-receptor-related protein essential for Wingless signalling. *Nature*. **407**(6803): 527-530.

Wei, G., Jin, Q., Giannobile, W.V. and Ma, P.X. (2006). Nano-fibrous scaffold for controlled delivery of recombinant human PDGF-BB. *J Control Release*. **112**(1): 103-110.

Wei, G., Jin, Q., Giannobile, W.V. and Ma, P.X. (2007). The enhancement of osteogenesis by nano-fibrous scaffolds incorporating rhBMP-7 nanospheres. *Biomaterials*. **28**(12): 2087-2096.

Wei, G., Pettway, G.J., McCauley, L.K. and Ma, P.X. (2004). The release profiles and bioactivity of parathyroid hormone from poly(lactic-co-glycolic acid) microspheres. *Biomaterials*. **25**(2): 345-352.

Weiner, S., Traub, W. and Wagner, H.D. (1999). Lamellar bone: structure-function relations. *J Struct Biol*. **126**(3): 241-255.

Weiner, S. and Wagner, H.D. (1998). The Material Bone: Structure-Mechanical Function Relations. *Annu. Rev. Mater. Sci.* **28**: 271-298.

Weng, Y.S., Lin, H.Y., Hsiang, Y.J., Hsieh, C.T. and Li, W.T. (2003). The effects of different growth factors on human bone marrow stromal cells differentiating into hepatocyte-like cells. *Adv Exp Med Biol*. **534**: 119-128.

West, J.L., Chowdhury, S.M., Sawhney, A.S., Pathak, C.P., Dunn, R.C. and Hubbell, J.A. (1996). Efficacy of adhesion barriers. Resorbable hydrogel, oxidized regenerated cellulose and hyaluronic acid. *J Reprod Med*. **41**(3): 149-154.

Westerhuis, R.J., van Bezooijen, R.L. and Kloen, P. (2005). Use of bone morphogenetic proteins in traumatology. *Injury*. **36**(12): 1405-1412.

Wildemann, B., Kadow-Romacker, A., Haas, N.P. and Schmidmaier, G. (2007). Quantification of various growth factors in different demineralized bone matrix preparations. *J Biomed Mater Res A*. **81**(2): 437-442.

Wilkie, A.O., Tang, Z., Elanko, N., Walsh, S., Twigg, S.R., Hurst, J.A., Wall, S.A., Chrzanowska, K.H. and Maxson, R.E., Jr. (2000). Functional haploinsufficiency of the human homeobox gene MSX2 causes defects in skull ossification. *Nat Genet*. **24**(4): 387-390.

Williams, D.F. (2008). On the mechanisms of biocompatibility. *Biomaterials*. **29**(20): 2941-2953.

Williams, J.M., Adewunmi, A., Schek, R.M., Flanagan, C.L., Krebsbach, P.H., Feinberg, S.E., Hollister, S.J. and Das, S. (2005). Bone tissue engineering using polycaprolactone scaffolds fabricated via selective laser sintering. *Biomaterials*. **26**(23): 4817-4827.

Wolff, J. (1892). Das Gesetz der Transformation der Knochen. In: (A. Hirchwald, ed), (An English translation of this monograph has been published by Springer-Verlag in 1986), Berlin.

Woo, B.H., Fink, B.F., Page, R., Schrier, J.A., Jo, Y.W., Jiang, G., DeLuca, M., Vasconez, H.C. and DeLuca, P.P. (2001). Enhancement of bone growth by sustained delivery of recombinant human bone morphogenetic protein-2 in a polymeric matrix. *Pharm Res*. **18**(12): 1747-1753.

Woodward, S.C., Brewer, P.S., Moatamed, F., Schindler, A. and Pitt, C.G. (1985). The intracellular degradation of poly(ε-caprolactone). *J Biomed Mater Res*. **19**: 437-444.

Wraighte, P.J. and Scammell, B.E. (2006). Principles of fracture healing. *Surgery (Oxford)*. **24**(6): 198-207.

Wu, B.M., Borland, S.W., Giordano, R.A., Cima, L.G., Sachs, E.M. and Cima, M.J. (1996). Solid free-form fabrication of drug delivery devices. *J Control Release*. **40**(1-2): 77-87.

Xia, K., Xue, H., Dong, D., Zhu, S., Wang, J., Zhang, Q., Hou, L., Chen, H., Tao, R., Huang, Z., Fu, Z., Chen, Y.G. and Han, J.D. (2006). Identification of the proliferation/differentiation switch in the cellular network of multicellular organisms. *PLoS Comput Biol*. **2**(11): e145.

Xiao, G., Jiang, D., Gopalakrishnan, R. and Franceschi, R.T. (2002). Fibroblast growth factor 2 induction of the osteocalcin gene requires MAPK activity and phosphorylation of the osteoblast transcription factor, Cbfa1/Runx2. *J Biol Chem*. **277**(39): 36181-36187.

Yaffe, D. and Saxel, O. (1977). Serial passaging and differentiation of myogenic cells isolated from dystrophic mouse muscle. *Nature*. **270**(5639): 725-727.

Yamaoka, H., Asato, H., Ogasawara, T., Nishizawa, S., Takahashi, T., Nakatsuka, T., Koshima, I., Nakamura, K., Kawaguchi, H., Chung, U.I., Takato, T. and Hoshi, K. (2006). Cartilage tissue engineering using human auricular chondrocytes embedded in different hydrogel materials. *J Biomed Mater Res A*. **78**(1): 1-11.

Yamashita, Y., Hooker, S.W., Jiang, H., Laurent, A.B., Resta, R., Khare, K., Coe, A., Kincade, P.W. and Thompson, L.F. (1998). CD73 expression and fyn-dependent signaling on murine lymphocytes. *Eur J Immunol*. **28**(10): 2981-2990.

Yan, S., Xiaoqiang, L., Shuiping, L., Xiumei, M. and Ramakrishna, S. (2009). Controlled release of dual drugs from emulsion electrospun nanofibrous mats. *Colloids Surf B Biointerfaces*. **73**(2): 376-381.

Yang-Snyder, J., Miller, J.R., Brown, J.D., Lai, C.J. and Moon, R.T. (1996). A frizzled homolog functions in a vertebrate Wnt signaling pathway. *Curr Biol*. **6**(10): 1302-1306.

Yang, J., Park, S.B., Yoon, H.-G., Huh, Y.M. and Haam, S. (2006). Preparation of poly ε-caprolactone nanoparticles containing magnetite for magnetic drug carrier. *Int J Pharm*. **324**(2): 185-190.

Yang, X., Chen, L., Xu, X., Li, C., Huang, C. and Deng, C.X. (2001). TGF-beta/Smad3 signals repress chondrocyte hypertrophic differentiation and are required for maintaining articular cartilage. *J Cell Biol*. **153**(1): 35-46.

Yang, X.B., Whitaker, M.J., Sebald, W., Clarke, N., Howdle, S.M., Shakesheff, K.M. and Oreffo, R.O. (2004). Human osteoprogenitor bone formation using encapsulated bone morphogenetic protein 2 in porous polymer scaffolds. *Tissue Eng*. **10**(7-8): 1037-1045.

Yasuda, H., Shima, N., Nakagawa, N., Yamaguchi, K., Kinosaki, M., Mochizuki, S., Tomoyasu, A., Yano, K., Goto, M., Murakami, A., Tsuda, E., Morinaga, T., Higashio, K., Udagawa, N., Takahashi, N. and Suda, T. (1998). Osteoclast differentiation factor is a ligand for osteoprotegerin/osteoclastogenesis-inhibitory factor and is identical to TRANCE/RANKL. *Proc Natl Acad Sci U S A*. **95**(7): 3597-3602.

Yeh, L.C., Tsai, A.D. and Lee, J.C. (2002). Osteogenic protein-1 (OP-1, BMP-7) induces osteoblastic cell differentiation of the pluripotent mesenchymal cell line C2C12. *J Cell Biochem*. **87**(3): 292-304.

Yoon, K., Buenaga, R. and Rodan, G.A. (1987). Tissue specificity and developmental expression of rat osteopontin. *Biochem Biophys Res Commun*. **148**(3): 1129-1136.

Yoon, S.J., Park, K.S., Kim, M.S., Rhee, J.M., Khang, G. and Lee, H.B. (2007). Repair of diaphyseal bone defects with calcitriol-loaded PLGA scaffolds and marrow stromal cells. *Tissue Eng*. **13**(5): 1125-1133.

Yoshimoto, H., Shin, Y.M., Terai, H. and Vacanti, J.P. (2003). A biodegradable nanofiber scaffold by electrospinning and its potential for bone tissue engineering. *Biomaterials*. **24**(12): 2077-2082.

Younger, E.M. and Chapman, M.W. (1989). Morbidity at bone graft donor sites. *J Orthop Trauma*. **3**(3): 192-195.

Yu, H.B., Shen, G.F. and Wei, F.C. (2007). Effect of cryopreservation on the immunogenicity of osteoblasts. *Transplant Proc*. **39**(10): 3030-3031.

Zaidi, M. (2007). Skeletal remodeling in health and disease. *Nat Med*. **13**(7): 791-801.

Zaman, M.H. (2007). Understanding the molecular basis for differential binding of integrins to collagen and gelatin. *Biophys J*. **92**(2): L17-19.

Zar, J.H. (1984). *Biostatistical analysis*. 2nd ed., Prentice-Hall, Englewood Cliffs; London.

Zein, I., Hutmacher, D.W., Tan, K.C. and Teoh, S.H. (2002). Fused deposition modeling of novel scaffold architectures for tissue engineering applications. *Biomaterials*. **23**(4): 1169-1185.

Zhang, C. (2010). Transcriptional regulation of bone formation by the osteoblast-specific transcription factor Osx. *J Orthop Surg Res*. **5**: 37.

Zhang, C., Cho, K., Huang, Y., Lyons, J.P., Zhou, X., Sinha, K., McCrea, P.D. and de Crombrugghe, B. (2008). Inhibition of Wnt signaling by the osteoblast-specific transcription factor Osterix. *Proc Natl Acad Sci U S A*. **105**(19): 6936-6941.

Zhang, H. and Bradley, A. (1996). Mice deficient for BMP2 are nonviable and have defects in amnion/chorion and cardiac development. *Development*. **122**(10): 2977-2986.

Zhang, J., Li, W., Sanders, M.A., Sumpio, B.E., Panja, A. and Basson, M.D. (2003a). Regulation of the intestinal epithelial response to cyclic strain by extracellular matrix proteins. *Faseb J*. **17**(8): 926-928.

Zhang, R. and Ma, P.X. (2004). Biomimetic polymer/apatite composite scaffolds for mineralized tissue engineering. *Macromol Biosci*. **4**(2): 100-111.

Zhang, Y., Ni, M., Zhang, M. and Ratner, B. (2003b). Calcium phosphate-chitosan composite scaffolds for bone tissue engineering. *Tissue Eng*. **9**(2): 337-345.

Zhang, Z.Y., Teoh, S.H., Chong, M.S., Schantz, J.T., Fisk, N.M., Choolani, M.A. and Chan, J. (2009). Superior osteogenic capacity for bone tissue engineering of fetal compared with perinatal and adult mesenchymal stem cells. *Stem Cells*. **27**(1): 126-137.

Zhou, Y.S., Liu, Y.S. and Tan, J.G. (2006). Is 1, 25-dihydroxyvitamin D3 an ideal substitute for dexamethasone for inducing osteogenic differentiation of human adipose tissue-derived stromal cells in vitro? *Chin Med J (Engl)*. **119**(15): 1278-1286.

Zhu, W., Kim, J., Cheng, C., Rawlins, B.A., Boachie-Adjei, O., Crystal, R.G. and Hidaka, C. (2006). Noggin regulation of bone morphogenetic protein (BMP) 2/7 heterodimer activity in vitro. *Bone*. **39**(1): 61-71.

Zhu, X.H., Wang, C.H. and Tong, Y.W. (2008). In vitro characterization of hepatocyte growth factor release from PHBV/PLGA microsphere scaffold. *J Biomed Mater Res A*.

Ziegler, J., Mayr-Wohlfart, U., Kessler, S., Breitig, D. and Gunther, K.P. (2002). Adsorption and release properties of growth factors from biodegradable implants. *J Biomed Mater Res*. **59**(3): 422-428.

Zimmermann, P., Boeuf, S., Dickhut, A., Boehmer, S., Olek, S. and Richter, W. (2008). Correlation of COL10A1 induction during chondrogenesis of mesenchymal stem cells with demethylation of two CpG sites in the COL10A1 promoter. *Arthritis Rheum*. **58**(9): 2743-2753.

Zisa, D., Shabbir, A., Suzuki, G. and Lee, T. (2009). Vascular endothelial growth factor (VEGF) as a key therapeutic trophic factor in bone marrow mesenchymal stem cell-mediated cardiac repair. *Biochem Biophys Res Commun*. **390**(3): 834-838.

Zuk, P.A., Zhu, M., Ashjian, P., De Ugarte, D.A., Huang, J.I., Mizuno, H., Alfonso, Z.C., Fraser, J.K., Benhaim, P. and Hedrick, M.H. (2002). Human adipose tissue is a source of multipotent stem cells. *Mol Biol Cell*. **13**(12): 4279-4295.